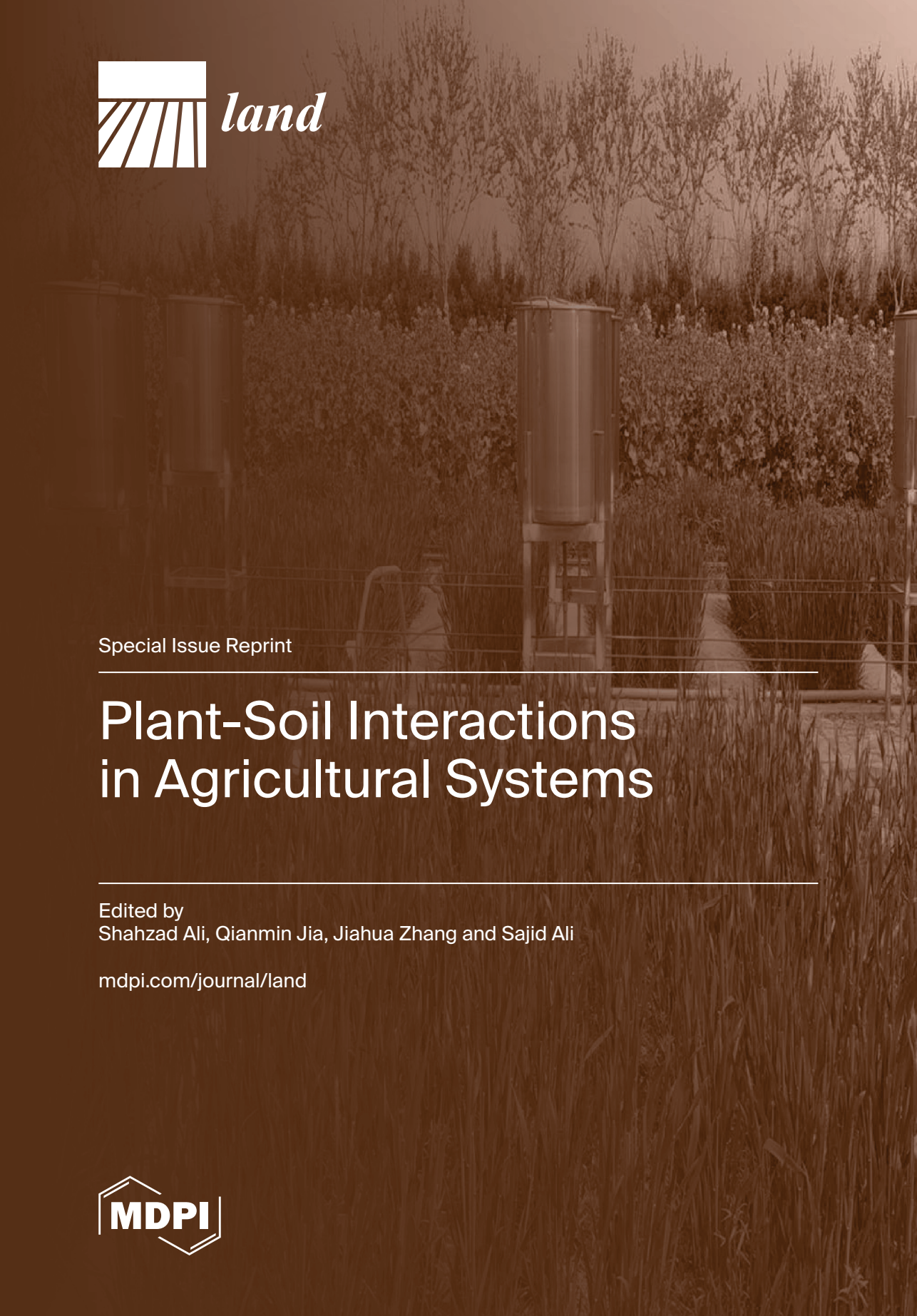

land

Special Issue Reprint

Plant-Soil Interactions in Agricultural Systems

Edited by
Shahzad Ali, Qianmin Jia, Jiahua Zhang and Sajid Ali

mdpi.com/journal/land

MDPI

Plant-Soil Interactions in Agricultural Systems

Plant-Soil Interactions in Agricultural Systems

Guest Editors

Shahzad Ali
Qianmin Jia
Jiahua Zhang
Sajid Ali

MDPI

Basel • Beijing • Wuhan • Barcelona • Belgrade • Novi Sad • Cluj • Manchester

Guest Editors
Shahzad Ali
Hazara University
Mansehra
Pakistan

Qianmin Jia
Lanzhou University
Lanzhou
China

Jiahua Zhang
Chinese Academy of
Sciences (CAS)
Beijing China

Sajid Ali
Hazara University
Mansehra
Pakistan

Editorial Office
MDPI AG
Grosspeteranlage 5
4052 Basel, Switzerland

This is a reprint of the Special Issue, published open access by the journal *Land* (ISSN 2073-445X), freely accessible at: https://www.mdpi.com/journal/land/special_issues/QVQP73ZNVR.

For citation purposes, cite each article independently as indicated on the article page online and as indicated below:

Lastname, A.A.; Lastname, B.B. Article Title. *Journal Name* **Year**, *Volume Number*, Page Range.

ISBN 978-3-7258-2963-7 (Hbk)
ISBN 978-3-7258-2964-4 (PDF)
https://doi.org/10.3390/books978-3-7258-2964-4

Cover image courtesy of Shahzad Ali

Contents

About the Editors

Shahzad Ali

Dr. Ali (male) is a lecturer and doctoral supervisor. Dr. Ali completed his Ph.D. in China (Northwest A&F University) and his first postdoctoral fellowship at Qingdao University (remote sensing, climate change, and big data analysis), while he completed his second postdoctoral fellowship at Zhejiang Normal University (global change ecology) and worked at Lanzhou University as a Young Talent Researcher (2020). Dr. Shahzad Ali is currently working as a lecturer at Hazara University Mansehra, where he has been working since 2020. His research mainly focuses on water-saving practices and theory of crops, crop cultivation and dry-land farming systems, the dynamics of soil–plant–livestock interactions under rain-fed conditions, agricultural water management, grassland grazing management, remote sensing climate change and big data analysis, the Maxent Model, and GIS. He has expertise in the areas of agronomy, crop cultivation, dry-land farming systems, remote sensing, climate change, big data analysis, grassland and grazing practices, GIS, and the Maxent Model. Dr. Shahzad Ali has won four research grants (PKR 10 million). He has published research outputs with total citations of +3600 (H-index = 33).

Qianmin Jia

Prof. Dr. Jia (male) is a professor and doctoral supervisor. He graduated from Northwest A&F University with a Ph.D. degree. He is mainly engaged in research on forage cultivation and utilization and has published 74 papers in mainstream international and domestic journals in this field, among which he has been the first or corresponding author for articles published in *Field Crops Research*, *Journal of Cleaner Production*, *Agricultural Water Management*, *Soil and Tillage Research*, and *Acta Pratacultural Sinica*. He has published 41 papers in international and domestic mainstream journals such as *Acta Agronomica Sinica*, 16 SCI papers (11 papers in Zone 1 of the Chinese Academy of Sciences), and 3 articles that have been selected as highly cited papers of academic importance. As the first contributor, he has registered one international patent and one invention patent, four utility model patents, and two computer software copyrights. He has also received RMB 70,000 for transformative achievements in research.

Jiahua Zhang

Prof. Dr. Jiahua received his Ph.D. degree in cartography and remote sensing from the Institute of Remote Sensing Applications, Chinese Academy of Sciences (CAS), Beijing, China, in 1998. From 1999 to 2001, he was a postdoctoral researcher with the National Institute for Environmental Studies, Japan. Since 2002, he has been a professor with the Chinese Academy of Meteorological Sciences. Since 2012, he has been a full professor at the Institute of Remote Sensing and Digital Earth, CAS. Since 2017, he also has been a professor at Qingdao University, China. He has published more than 150 peer-reviewed articles, 30 international conferences articles, and 6 books. His current research interests include remote sensing and geosciences, environment and disaster monitoring, image processing, and pollution remote sensing.

Sajid Ali

Prof. Dr. Ali acquired a PhD in Molecular Plant Breeding and Population Genetics, Biotechnology and Population Biology, from Paris-XI University, Paris, France. Dr. Ali has completed one postdoctorate fellowship in Population Genetics from Aarhus University, Denmark, and another from CIRAD-INRA-SupAgro University, Montpellier, in crop and pathogen population genomics. He has expertise in crop and pathogen population dynamics at the spatial and temporal scales, along with in-depth knowledge of the genetics, breeding, and ecological consequences of resistance gene deployment. Dr. Ali is a member of a strong research group, started at the University of Agriculture, Peshawar, and now based at Hazara University, Mansehra, Pakistan, which is focused on understanding crop and pathogen diversity and population structure in the context of invasion and adaptation. The research work conducted in collaboration with other internationally recognized research groups has enabled Dr. Ali to generate substantial results with global importance on wheat rust population biology. Dr. Ali has earned several research grants from international donors such as the European Research Council-EU, CIMMYT-USDA-USA, JIC-UK, ANU, Australia, and HEC-Pakistan. Dr. Ali's work on crop improvement contributed to the development of the wheat variety "Ghanimat-e-IBGE", the Brassica varieties "Dalai" and "Rokhana", and the Common Bean variety "Himalaya-1". The group collaborates extensively with research groups at the international (e.g., in Australia, Denmark, Canada, France, Mexico, and the UK), regional (e.g., in China, Nepal, Bhutan, Iran, and Afghanistan), and national levels. Dr. Ali has been awarded a Research Productivity Award twice (in 2016 and 2017) and the Fakhre-Peshawar Award (2019). The council of the Pakistan Academy of Sciences has awarded Dr. Ali the Gold Medal 2024 in Agricultural Sciences.

land

MDPI

Article

Effects of Organic and Inorganic Fertilizers on Soil Nutrient Conditions in Rice Fields with Varying Soil Fertility

Guozhu Ma [1,2,*], Shenghai Cheng [1,2], Wenli He [1,2], Yixuan Dong [3], Shaowu Qi [2,4,*], Naimei Tu [3] and Weixu Tao [1,2]

[1] College of Tropical Crops, Hainan University, No. 58 Renmin Avenue, Meilan District, Haikou 570228, China; 21220951310008@hainanu.edu.cn (S.C.); 21220951310024@hainanu.edu.cn (W.H.); 20095131210069@hainanu.edu.cn (W.T.)
[2] National Technology Innovation Center for Saline Tolerant Rice, No. 736 Yuanda 2nd Road, Furong District, Changsha 410125, China
[3] College of Agriculture, Hunan Agricultural University, No. 1 Nongda Road, Furong District, Changsha 410127, China
[4] Hunan Academy of Agricultural Sciences, No. 892 Yuanda 2nd Road, Furong District, Changsha 410125, China
* Correspondence: student@hhrrc.ac.cn (G.M.); qishaowu@hhrrc.ac.cn (S.Q.)

Abstract: The majority of crop-growing areas in China have low or medium fertility levels, which limits the yield of crops grown in those areas. Fertilizer application can improve soil quality, but the effects of such treatments vary depending on the base soil fertility. However, the specific differences associated with the application of different fertilizer types to soils of varying fertility levels have yet to be clearly delineated. Here, the influences of several fertilizer types on physical, chemical, and biological soil indicators were assessed in rice fields in the red soil area of Hunan Province with varying base fertility levels: Hehua (low fertility), Dahu (medium fertility), and Longfu (high fertility). Four treatments were applied to these fields: no fertilizer, standard fertilizer, 60% chemical fertilizer + 40% organic fertilizer, and 100% chemical fertilizer. Across the three sites and treatment groups, the largest increases in total nitrogen and phosphorus contents were in Hehua and Longfu, respectively. Soil organic matter content increased most significantly in Hehua. Application of any type of fertilizer increased the total and fast-acting nutrient content in the low-yielding fields, whereas organic fertilizers increased the nutrient content and soil biological indicators more than chemical fertilizer alone did; the effect of organic fertilizer application on the combined enzyme activity of the soil was also higher than that of chemical fertilizers alone. Overall, these experiments provide a theoretical basis and technical support for rational fertilizer application and improvement of Hunan's red soil quality based on the natural soil fertility levels.

Keywords: base fertility; soil nutrients; enzyme activity; fertilizer application patterns

Citation: Ma, G.; Cheng, S.; He, W.; Dong, Y.; Qi, S.; Tu, N.; Tao, W. Effects of Organic and Inorganic Fertilizers on Soil Nutrient Conditions in Rice Fields with Varying Soil Fertility. *Land* **2023**, *12*, 1026. https://doi.org/10.3390/land12051026

Academic Editors: Shahzad Ali, Qianmin Jia, Jiahua Zhang and Sajid Ali

Received: 11 April 2023
Revised: 1 May 2023
Accepted: 5 May 2023
Published: 7 May 2023

1. Introduction

Soil fertility is a fundamental parameter that determines the reproductive growth capacity, yield, and nutritional value of crop plants. In China, low- and medium-yielding fields account for ~67% of the total arable land area [1]. Improving soil quality in such fields to increase grain crop yields is an effective method of increasing food security and promoting the strategy of promoting the Chinese strategic national initiative of agricultural land and technique development [2]. Soil productivity, fertilizer application techniques, and soil improvement technology vary among areas with different base soil fertility rates [3]. Developing standard protocols for reasonable fertilizer application and soil improvement technology based on local soil fertility is, therefore, of great significance in rice production [4].

Rice-growing soils are influenced by the anthropogenic management practices associated with rice-based cropping systems [5]. These management practices affect parameters

including soil capacitance, which affects the water-holding capacity and solute migration of a soil [6]. Soils with low capacitance and high porosity are conducive to root growth, aboveground tissue growth and development, and biomass accumulation, all of which can somewhat improve yield [7]. Li et al. [8] concluded that medium-, high-, and ultra-high-yielding fields generally have lower capacity than low-yielding fields and that soil porosity is highest in ultra-high-yielding fields, lower in high-yielding fields, and lowest in low-yielding fields. Soil management practices can also affect soil aggregate abundance. The number of aggregates reflects the ability of soil to supply and store nutrients [9]. The rate of soil aggregate destruction is correlated with organic matter content (i.e., high organic matter content is associated with low rates of aggregate destruction) [10,11]. High-yield, fertile soils generally have high organic matter content and low aggregate destruction rates [12]. In general, the responses of medium- and low-fertility soils to nitrogen fertilizers are more pronounced, whereas high-fertility soils have weaker responses. This is primarily due to differences in the chemical stability of agglomerates, which arise from the combined effects of salt solution concentrations and fertility levels [13].

Nitrogen (N) is a key nutrient required for crop growth and development. Soluble N is generally higher in high- and medium-fertility soils than in low-fertility soils. Tao et al. [14] showed that high-yield soils have relatively high levels of organic matter and alkaline nitrogen. Soil organic matter can be increased to promote soil total nitrogen and alkaline nitrogen fixation [15]. Shengxian et al. [5] concluded that soil organic matter, total N, available phosphorus content, and nutrients are highest in high-yielding rice soils, lower in medium-yielding rice soils, and lowest in low-yielding rice soils. However, Rui [16] determined that the main differences in soil performance are associated with variations in total N, organic matter, and fast-acting potassium content but not soil pH or available phosphorus content. Rui concluded that the discrepancies between their results and those of Shengxian et al. occurred because the two studies used soils with different textures and physical properties. Overall, low-fertility soils tend to have significantly lower cation exchange capacity, organic matter contents, and clay particle contents than high-fertility soils [17].

Previous studies have addressed the biological properties of soils with different fertility levels. For example, soil microbial carbon (C) is an important indicator of soil microbiological properties [18]. As soil fertility levels increase, soil microbial C and N levels increase accordingly [19]. One of the most important indicators of soil fertility is enzyme activity, which reflects the level of biological activity and the capacity for nutrient transformation, transport, and metabolism [20]. Soil enzymes are secreted by microorganisms, living plants, and animals, and they are released in the decomposition of plant and animal residues [21]. In high-fertility soil, increased N application is associated with an initial decrease, then an increase in peroxidase activity, whereas the opposite pattern is observed in medium-fertility soil. The level of N supply can indirectly reflect the level of urease activity, which is highly correlated with alkaline N levels [22]. Compared to medium-N conditions, under high-N conditions, increases in alkaline N content are associated with consistent or decreased urease activity, indicating that N fertilizer application affects urease [23]. Ye Xie Feng et al. [24] showed that tilling green manure significantly increased the enzymatic activity and fertility level of soil, and the highest enzymatic activity and fertility level was achieved when the tilling volume was 22,500–30,000 kg/hm^2. In low-fertility soils, the number and activity of microorganisms in the soil sink significantly increased with organic–inorganic application, which had a significant effect on improving soil fertility [25]. Liu et al. [26] showed that the long-term combined application of chemical fertilizers and pig manure could improve phosphatase activity in the soil, and the application of organic fertilizers could improve the soil structure and fertility. Similarly, when the straw application rate was 11,250 kg/hm^2, the number of fungi, bacteria, and actinomycetes and the activities of invertase and cellulase in the soil increased the most, and when the straw application rate was 7500 kg/hm^2, soil alkaline urease, phosphatase activity, and alkaline nitrogen content increased significantly [27].

At present, the responses of rice soils with different base fertility levels to varied fertilizer treatments are unknown. As discussed above, prior results suggest that the effects of fertilization are highly dependent on soil properties at the physical, chemical, and biological levels. Thus, appropriate measures for soil quality improvement will depend on local soil conditions. Here, we examined these phenomena by using rice fields in the red soil areas of Hunan with variations in soil fertility. After assessing the base fertility levels and physicochemical and biological properties of three fields, we tested four fertilization treatments to clarify their effects on soil quality. Overall, the results of this study provide valuable new information regarding the efficiency of fertilizer application in soils with varying fertility levels and lay the foundation for improved rice cultivation technologies in eastern Hunan.

2. Materials and Methods

2.1. Test Materials and Sites

The rice variety 'Shenliangyou 5814' was obtained from Hunan Yahwa Seed Co. No. 11, Yangao Road, Lugu Hi-Tech Development Zone, Changsha City, Hunan Province, China and used in all experiments in this study. The first trial site was located in Baitang Village, Longfu Town, Liuyang City, in the eastern hilly region of Hunan Province (28°25′38.2″ N, 113°24′26.2″ E). The second was located in Niu Shi Ling Village, Hehua Office (28°034823.1″ N, 113°41′08.8″ E), and the third was located in Shuxiang Village, Dahu Town (28°52′35.1″ N, 113°54′09.5″ E). Each location contained a long-term soil fertility monitoring site established in 2013. The soil sampling time for this test was 2018. The soil at each site was red loam, and the tillage system was mono-annual.

2.2. Experimental Design

Four fertilizer treatments were tested at each site: no fertilizer (T1); standard fertilizer, which comprised 95% chemical fertilizer and 5% pig manure (T2); 60% chemical fertilizer + 40% organic fertilizer (T3); 100% chemical fertilizer (T4) (Table 1). Each treatment plot was 24 m^2 (6 × 4 m), arranged with a fully randomized design, and there were three biological replicates per treatment. Each experimental plot was constructed with field ridges (20 cm wide and 30 cm high) and wrapped with plastic film to prevent fertilizer and water infiltration between the plots, and each plot was single-rowed and single-irrigated. Other field management practices were consistent with those of the local one-season rice cropping system, including weed, pest, and disease control. The water management of the whole reproductive period was based on shallow water transplanting, inch water rejuvenation, shallow water tillering, sufficient seedlings for sunning, inch water for spike, and wet and strong seeds. The tested inorganic fertilizers were urea (46% N), calcium superphosphate (12% P_2O_5), and potassium chloride (60% K_2O); the organic fertilizers were pig manure (0.6% N, 0.4% P_2O_5, and 0.44% K_2O), zoysia (0.4% N, 0.1% P_2O_5, and 0.3% K_2O), and rice straw (0.6% N, 0.3% P_2O_5, and 1.1% K_2O) (Table 1). Organic fertilizers and inorganic phosphorus fertilizer were applied as base fertilizers. The inorganic N and K fertilizers were applied in stages: 50% base fertilizer, 30% at the tillering stage, and 20% at the spike stage.

Table 1. Fertilizer treatments that were applied at each test site. All measurements are in kg/hm^2.

Treatment Group Name	Treatment Group Description	Inorganic Fertilizer			Organic Fertilizer			Total		
		N	P_2O_5	K_2O	Pig Manure	Zoysia	Rice Straw	N	P_2O_5	K_2O
T1	No fertilizer	-	-	-	-	-	-	-	-	-
T2	Standard fertilizer	171.0	69.0	113.4	1500	-	-	180	75	120
T3	40% organic fertilizer	108.0	51.6	42.6	-	12,600	3600	180	75	120
T4	100% chemical fertilizer	180.0	75.0	120.0	-	-	-	180	75	120

2.3. Soil Property Measurements

Soil samples were collected at a depth of 0 to 20 cm at the tiller bloom stages, pregnancy spike stages, tassel stages, waxing stages, and maturity stages of rice. A five-point sampling method was used to extract the whole soil layer at each collection timepoint. All samples were dried at room temperature and then passed through 20- and 60-mesh sieves. Soil capacity was determined by using the ring knife method [28]. Basic soil nutrient indicators (total N, total phosphorus, organic matter content, available phosphorus, alkaline decomposition N, and pH) were determined with conventional analytical methods, as described in the Soil Agrochemical Analysis Methods [29] (Table 2). Urease activity was determined with the indophenol blue colorimetric method [30] and expressed in mg of ammoniacal N (NH_3-N) per g of soil after 24 h of incubation at 37 °C ($mg{\cdot}g^{-1}{\cdot}d^{-1}$). Phosphatase activity was determined by using the colorimetric method with sodium phenyl phosphate and expressed in mg of p-aminophenol per g of soil after 1 h of incubation at 37 °C ($mg{\cdot}g^{-1}{\cdot}h^{-1}$) [30]. Sucrose activity was determined with the 3,5 dinitro salicylic acid method and expressed in mg of glucose per g of soil after 24 h incubation at 37 °C ($mg{\cdot}g^{-1}{\cdot}d^{-1}$) [30].

Table 2. Basic rice soil chemical properties.

Sample Site	pH	Organic Matter (g/kg)	Total Nitrogen (g/kg)	Total Phosphorus (g/kg)	Total Potassium (g/kg)	Available Nitrogen (mg/kg)	Available Phosphorus (mg/kg)	Available Potassium (mg/kg)
Hehua	6.45	11.55	0.75	0.60	13.55	84.82	4.12	68.21
Dahu	5.65	25.45	1.35	0.84	8.03	155.38	3.63	72.34
Longfu	5.92	28.21	1.82	0.35	8.60	150.04	12.85	60.31

2.4. Combined Soil Fertility Values

Soil fertility was calculated by using the Nemero index method. The first step was the calculation of the partition fertility factor $\boldsymbol{IFI_i}$:

$$\boldsymbol{IFI_i} = \begin{cases} X/X_a & X \le X_a \\ 1 + (X - X_a)/(X_c - X_a) & X_a < X \le X_c \\ 2 + (X - X_c)/(X_P - X_c) & X_{C^C} < X \le X_P \\ 3 & X > X_P \end{cases}$$

where $\boldsymbol{IFI_i}$ is the fertility factor; X is the measured value of a given property; X_a and X_P are the lower and upper grading criteria, respectively (Table 3); X_c is between the lower and upper ends of the attribute value grading scale such that $X_a < X_c < X_P$.

Table 3. Grading standards for soil properties. The criteria were consistent with those set forth in the Second National Soil Census.

Grade	Organic Matter (g/kg)	Nitrogen Alkali Digestion (mg/kg)	Fast-Acting Potassium (mg/kg)	Effective Phosphorus (mg/kg)
X_a	10	60	40	3
X_c	20	120	100	10
X_P	30	180	150	20

The second step was the calculation of the combined soil fertility by using the Nemero formula as follows:

$$\mathrm{IFI} = \sqrt{\frac{\left(\mathrm{IFI_i\,Average}\right)^2 + \left(\mathrm{Minimum}\right)^2}{2}} \times \left(\frac{\mathrm{n}-1}{\mathrm{n}}\right)$$

where IFI is the combined soil fertility; IFIi average and IFIi minimum are the mean and minimum fertility values for a given soil attribute, respectively; n is the number of evaluation indicators.

2.5. Soil Enzyme Activity Composite Index

A combined soil enzyme activity index, GMea, was used:

$$\mathrm{GMea} = \sqrt[3]{\mathrm{Inv} \times \mathrm{Ure} \times \mathrm{Acp}}$$

where Inv is the sucrase activity, Ure is the urease activity, and Acp is the acid phosphatase activity.

2.6. Statistical Analysis

Statistical analyses were conducted in SPSS v23. Differences between treatment groups were assessed with analysis of variance (ANOVA) and considered statistically significant at $p < 0.05$. Graphs were generated in Excel 2016.

3. Results

3.1. Effects of Fertilizer Treatments on Rice Soil Physical Properties

We first assessed the effects of fertilizer application on the physical soil properties at the three sample sites. In the four treatments, the application of chemical fertilizers and organic fertilizers could reduce soil bulk density and increase soil porosity (Table 4). There were no significant differences in soil bulk density or soil porosity between the treatment groups at any of the sites. However, there were site-specific differences between these parameters; the soil at Longfu was denser and had higher porosity than the soil from Dahu, which, in turn, had higher density and porosity than the soil from Hehua. Soil with a bulk density of <0.9 g/cm^3 was considered to be too loose, whereas soil with a capacity of 1.0–1.2 g/cm^3 was considered to have a suitable texture for crop growth [31]. Therefore, Hehua soils from all treatment groups were too loose; all Dahu samples were suitable, except for the T1 samples; all Longfu samples were suitable.

Table 4. Effects of fertilizer treatment on rice soil bulk density and porosity.

Treatment Group	Soil Capacity (g/cm^3)			Soil Porosity (%)		
	Hehua	Dahu	Longfu	Hehua	Dahu	Longfu
T1	0.99 ± 0.090 a	0.79 ± 0.075 a	1.19 ± 0.069 a	62.56 ± 0.090 a	58.83 ± 0.075 a	58.84 ± 0.069 a
T2	1.02 ± 0.044 a	1.09 ± 0.121 a	1.09 ± 0.045 a	61.55 ± 0.044 a	57.95 ± 0.121 a	60.25 ± 0.045 a
T3	1.05 ± 0.080 a	1.11 ± 0.069 a	1.05 ± 0.053 a	60.50 ± 0.080 a	57.14 ± 0.069 a	59.64 ± 0.053 a
T4	0.93 ± 0.065 a	1.14 ± 0.088 a	1.07 ± 0.066 a	64.74 ± 0.065 a	54.94 ± 0.088 a	57.39 ± 0.066 a

Lowercase letters within a column indicate statistically significant groups at $p < 0.05$ (analysis of variance (ANOVA)).

3.2. Effects of Fertilizer Treatments on Rice Soil Nutrients

We next analyzed the effects of each fertilizer treatment on the chemical properties of each site. Across all treatments, Longfu generally had the highest total N and organic matter contents, whereas Dahu had the highest total phosphorus content (Table 5). The differences in total N and organic matter content were not significant between Hehua and Longfu. In the Hehua samples, the total N and organic matter contents were 10.13–14.47% and 11.54–19.07% higher, respectively, in the T4 treatment compared to the other treatments, and the total phosphorus content was 12.66–30.88% higher in the T3 treatment than in the other treatments. In Dahu samples, the total N, total phosphorus, and organic matter contents were significantly higher in the T3 treatment than in the control. In the Longfu samples, the total N, total phosphorus, and organic matter contents were 10.38–10.99%, 11.54–38.10%, and 0.33–7.59% higher, respectively, in the T2 treatment than in the other treatments.

Table 5. Effects of fertilizer treatment on total nutrients in rice soil at the three sites.

Sample Site	Treatment Group	Total Nitrogen (g/kg)	Total Phosphorus (g/kg)	Organic Matter (g/kg)
Hehua	T1	0.76 ± 0.085 a	0.68 ± 0.005 c	11.85 ± 1.075 a
	T2	0.79 ± 0.034 a	0.79 ± 0.020 b	12.35 ± 1.553 a
	T3	0.77 ± 0.046 a	0.89 ± 0.050 a	12.62 ± 2.775 a
	T4	0.87 ± 0.040 a	0.75 ± 0.015 b	14.11 ± 2.259 a
Dahu	T1	1.00 ± 0.097 b	0.92 ± 0.005 c	24.90 ± 3.030 b
	T2	1.36 ± 0.119 a	0.95 ± 0.011 b	27.03 ± 1.235 ab
	T3	1.37 ± 0.149 a	0.98 ± 0.016 a	28.96 ± 0.325 a
	T4	1.36 ± 0.048 a	0.94 ± 0.007 b	26.21 ± 0.729 ab
Longfu	T1	1.82 ± 0.048 a	0.42 ± 0.005 d	28.47 ± 0.620 a
	T2	2.02 ± 0.188 a	0.58 ± 0.002 a	30.63 ± 1.156 a
	T3	1.83 ± 0.511 a	0.52 ± 0.005 b	30.53 ± 1.590 a
	T4	1.83 ± 0.118 a	0.46 ± 0.005 c	30.37 ± 4.468 a

Lowercase letters within a column indicate statistically significant groups at $p < 0.05$ (ANOVA).

The alkaline N content was highest in the Longfu samples and lowest in the Hehua samples, with those from Dahu falling in the middle (Table 6). The maximum alkaline N content in the Hehua samples occurred at the tiller bloom stage, then gradually decreased as the fertile period progressed. The available phosphorus content was highest in Dahu and lowest in the Longfu samples; Hehua and Dahu reached the maximum available phosphorus levels at the tiller bloom and pregnancy spike stages, respectively. At maturity, both the Longfu and Dahu samples had significantly higher alkaline N content in all treatment groups than the Hehua samples did (by 73.6–142.8 mg/kg and 45.47–64.63 mg/kg, respectively).

Table 6. Effects of fertilizer treatment on fast-acting nutrient content in rice soil.

Sample Site	Nutrient Indicator (mg/kg)	Treatment Group	Tiller Bloom	Pregnancy Spike	Tassel	Waxing	Maturity
Hehua	Alkaline nitrogen content	T1	94.03 ± 0.404 c	83.07 ± 0.808 c	97.98 ± 3.453 b	77.70 ± 0.926 b	83.90 ± 3.245 b
		T2	114.33 ± 1.070 b	100.57 ± 8.697 a	98.58 ± 4.041 b	91.00 ± 8.231 a	104.53 ± 4.351 a
		T3	117.37 ± 0.404 a	95.55 ± 1.750 ab	106.87 ± 1.125 a	86.30 ± 1.424 ab	90.77 ± 1.762 ab
		T4	116.43 ± 1.070 a	90.53 ± 0.808 bc	102.62 ± 2.671 ab	82.48 ± 4.829 ab	90.07 ± 5.300 ab
	Effective phosphorus	T1	2.33 ± 0.858 d	6.49 ± 3.250 b	7.95 ± 1.032 c	7.68 ± 2.575 d	5.87 ± 2.730 c
		T2	4.97 ± 1.741 c	9.47 ± 1.487 a	12.17 ± 4.763 b	12.04 ± 0.991 b	12.18 ± 2.951 a
		T3	7.97 ± 1.983 b	9.73 ± 2.988 a	14.09 ± 6.157 a	13.86 ± 4.814 a	11.81 ± 1.247 a
		T4	8.52 ± 0.744 a	9.10 ± 3.481 a	15.25 ± 2.543 a	10.42 ± 2.730 c	9.37 ± 0.991 b
Dahu	Alkaline nitrogen content	T1	133.01 ± 7.000 c	104.07 ± 8.640 c	149.92 ± 14.534 c	125.07 ± 4.554 c	157.50 ± 2.425 c
		T2	175.11 ± 7.000 b	162.40 ± 1.852 b	173.25 ± 3.654 b	212.68 ± 4.057 a	205.10 ± 0.700 b
		T3	189.23 ± 0.001 b	196.00 ± 3.051 a	204.35 ± 13.376 a	204.98 ± 3.909 a	233.57 ± 8.015 a
		T4	217.63 ± 13.301 a	191.33 ± 2.650 a	221.78 ± 2.627 a	161.82 ± 1.654 b	218.40 ± 4.850 ab
	Effective phosphorus	T1	1.44 ± 2.623 c	2.66 ± 1.593 d	4.18 ± 1.741 d	2.86 ± 2.064 d	3.22 ± 0.496 d
		T2	3.39 ± 1.032 a	11.71 ± 4.157 a	9.66 ± 3.574 a	12.01 ± 2.818 a	13.56 ± 3.516 a
		T3	4.21 ± 3.469 a	9.50 ± 0.572 b	7.52 ± 1.247 b	7.45 ± 1.032 b	8.08 ± 1.311 b
		T4	2.33 ± 1.487 b	5.70 ± 2.760 c	4.64 ± 1.359 c	4.11 ± 2.160 c	5.63 ± 1.593 c
Longfu	Alkaline nitrogen content	T1	143.80 ± 2.211 c	142.63 ± 1.779 b	151.67 ± 9.812 b	132.07 ± 5.658 a	142.57 ± 6.274 b
		T2	150.73 ± 3.523 b	146.07 ± 10.200 b	163.10 ± 2.145 ab	143.97 ± 2.458 a	150.97 ± 4.102 ab
		T3	157.97 ± 5.064 a	148.63 ± 0.809 ab	187.017 ± 4.700 a	145.83 ± 2.977 a	155.40 ± 0.700 a
		T4	146.17 ± 1.070 c	157.03 ± 2.139 a	151.73 ± 2.357 b	148.17 ± 2.6501 a	152.83 ± 6.870 a
	Effective phosphorus	T1	10.39 ± 1.741 b	20.11 ± 8.058 b	19.08 ± 2.271 c	18.29 ± 7.027 b	17.36 ± 3.300 c
		T2	11.78 ± 4.965 b	20.93 ± 0.572 b	19.61 ± 4.989 bc	18.78 ± 3.095 b	18.78 ± 3.469 b
		T3	14.32 ± 1.787 a	25.33 ± 1.314 a	22.16 ± 1.983 a	17.36 ± 2.904 b	21.66 ± 0.858 a
		T4	11.32 ± 5.253 b	20.64 ± 2.904 b	20.24 ± 0.572 b	21.85 ± 2.976 a	18.42 ± 3.753 bc

Lowercase letters within a column indicate statistically significant groups at $p < 0.05$ (ANOVA).

3.3. Effects of Fertilizer Treatment on Combined Soil Fertility Values

We next analyzed site-specific and treatment-induced differences in soil fertility. Consistently, the IFI values were higher for Longfu and Dahu than for the Hehua samples. Furthermore, as expected, the IFI values were higher in all fertilized treatment groups (T2–T4) than in the control (T1) at each site (Figure 1). Overall, the Longfu T2 samples had the highest IFI (1.85), followed by Dahu T3 (1.80). In the Hehua samples, the highest IFI

value was in T4, followed by T2, then T3; Longfu had the highest IFI value in T2, followed by T3, then T4; Dahu had the highest IFI value in T3, followed by T4, then T2.

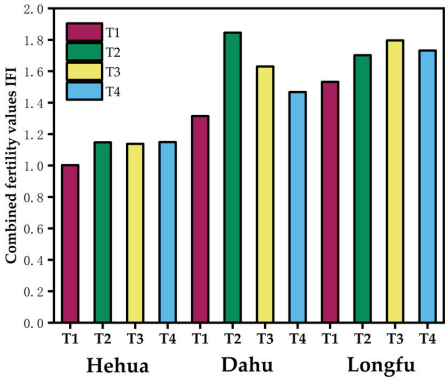

Figure 1. Combined soil fertility values in samples collected from the Hehua, Longfu, and Dahu sites. T1, no fertilizer; T2, standard fertilizer; T3, 40% organic fertilizer; T4, 100% chemical fertilizer.

3.4. Effects of Fertilizer Treatment on Enzyme Activity in Rice Soil

To establish the effects of different types of fertilizer treatment on rice soil enzymes, we quantified the activities of three key nutrient cycling enzymes: urease, acid phosphatase, and sucrase.

3.4.1. Urease

At the maturity stage, the urease activity was highest in Longfu and lowest in the Hehua samples overall (Figure 2). In the soil collected from Hehua, the T4 samples had the highest urease activity in the early stages of fertility; at the tiller bloom stage, the urease activity was 9.43%, 1.52%, and 1.80% higher in T4 compared to the T1–T3 samples, respectively, and at the pregnancy spike stage, the urease activity was 25.4%, 12.5%, and 1.82% higher in T4 than in the T1–T3 samples, respectively. At later growth stages, the T2 and T3 treatments had higher urease activity. Specifically, at the tassel and waxing stages, the highest urease activities were found in the T3 samples (0.62 $mg \cdot g^{-1} \cdot d^{-1}$) and in the T2 samples (0.72 $mg \cdot g^{-1} \cdot d^{-1}$), respectively. At the maturity stage, the T3 treatment had the highest activity at 0.57 $mg \cdot g^{-1} \cdot d^{-1}$; this was higher than in the T1, T2, and T4 samples by 31.18%, 10.26%, and 22.35%, respectively.

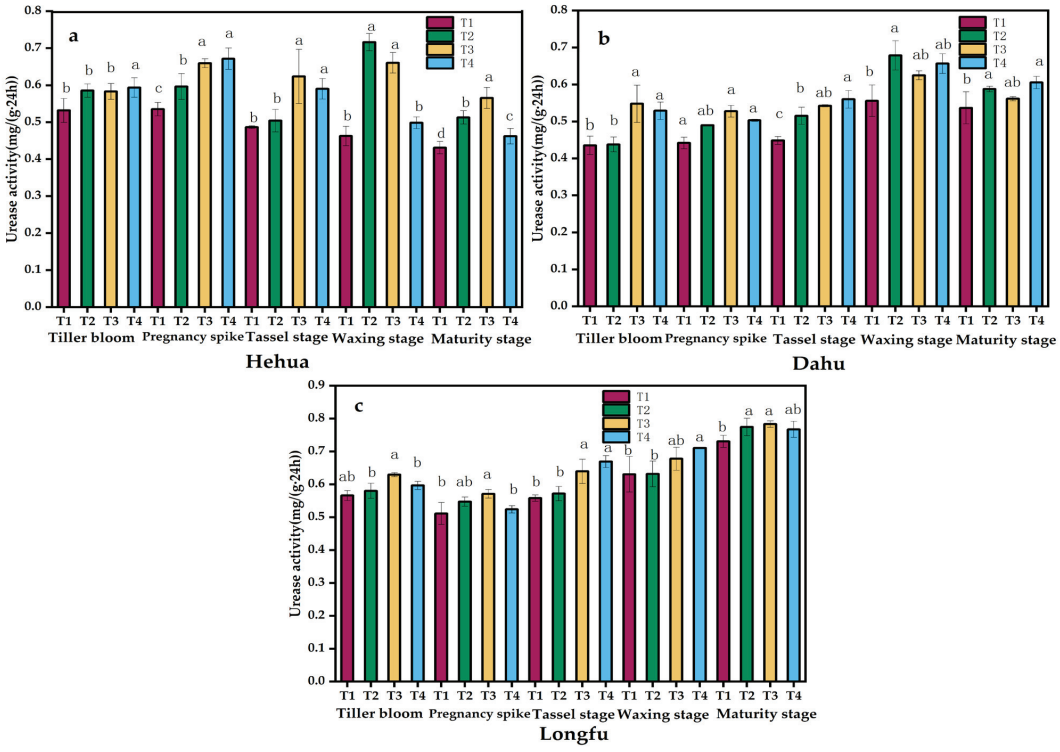

Figure 2. At each reproductive stage of rice development (**a**) is Urease activity in soil samples collected from Hehua; (**b**) is Urease activity in soil samples collected from Dahu; (**c**) is Urease activity in soil samples collected from Longfu. T1, no fertilizer; T2, standard fertilizer; T3, 40% organic fertilizer; T4, 100% chemical fertilizer. Lowercase letters above each bar indicate statistically significant groups at $p < 0.05$ (analysis of variance (ANOVA)).

In the soil collected from Dahu, the urease activity was highest in the T3 samples. At the tillering stage, the urease activity was 25.84% higher in the T3 than the T1 samples; at the pregnancy spike stage, it was 19.40% higher in the T3 samples than in the T1 samples. At the tassel stage, the urease activity was highest in the T4 treatment (0.56 $mg \cdot g^{-1} \cdot d^{-1}$). At the waxing stage, the urease activity was highest in the T2 samples (0.68 $mg \cdot g^{-1} \cdot d^{-1}$, which was a maximum of 22.10% higher than in the other treatment groups). At the maturity stage, the T4 samples had the highest urease activity, which was 12.78%, 2.99%, and 7.82% higher than in the T1, T2, and T3 samples, respectively.

In the soil collected from Longfu, the overall urease activity in the T3 samples remained high across the developmental stages. The urease activity was highest in the T3 samples at the tiller bloom and pregnancy spike stages, then highest in the T4 samples at the tassel and waxing stages. At the maturity stage, the T3 samples again had the highest urease activity (0.78 $mg \cdot g^{-1} \cdot d^{-1}$); this was 7.20%, 1.13%, and 2.07% higher than in the T1, T2, and T4 samples, respectively.

3.4.2. Acid Phosphatase

Consistently with the urease activity, the acid phosphatase activity at the maturity stage was highest in the soil collected from Longfu and lowest in the Hehua samples (Figure 3). In the soil collected from Hehua, the acid phosphatase activity was significantly higher in T4 than in the other samples at the early stages of fertility (the tillering, pregnancy spike, and tasseling stages). At the waxing stage, the T2 samples had 15.42%, 10.83%,

and 12.62% higher activity than the T1, T3, and T4 samples, but the differences were not significant. At the maturity stage, the acid phosphatase activity was highest in the T3 samples (0.56 mg·g^{-1}·h^{-1}).

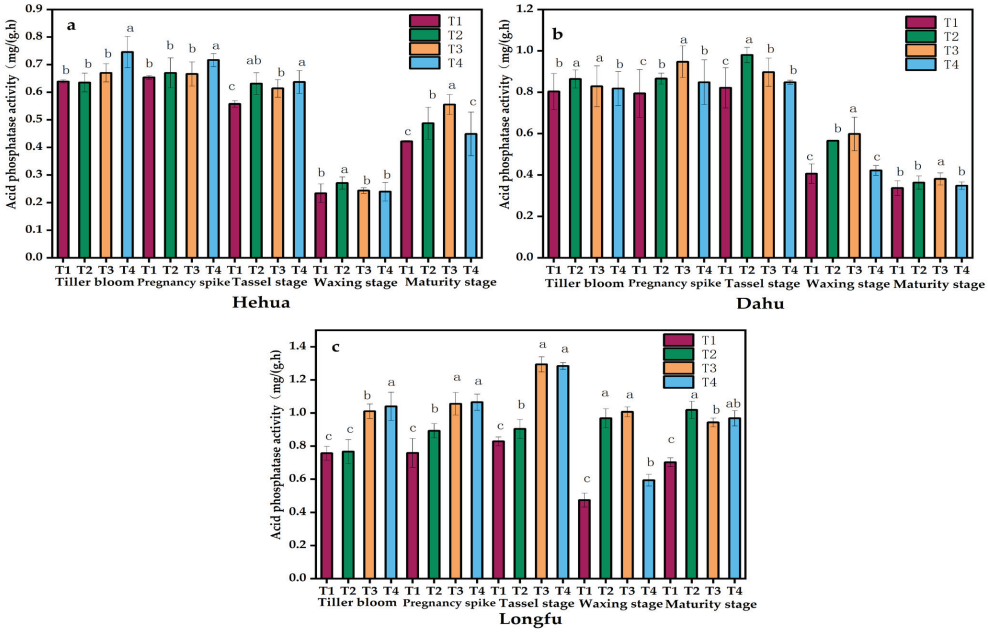

Figure 3. At each reproductive stage of rice development (**a**) is acid phosphatase activity in soil samples collected from Hehua; (**b**) is acid phosphatase activity in soil samples collected from Dahu; (**c**) is acid phosphatase activity in soil samples collected from Longfu. T1, no fertilizer; T2, standard fertilizer; T3, 40% organic fertilizer; T4, 100% chemical fertilizer. Lowercase letters above each bar indicate statistically significant groups at $p < 0.05$ (ANOVA).

In the soil collected from Dahu, the acid phosphatase activity remained high in the T2 and T3 samples across the growth stages, but the differences between treatment groups at maturity were not significant. At the tillering stage, the acid phosphatase activity was highest in the T2 group. At the pregnancy spike, waxing, and maturity stages, the T3 samples had the highest activity. In particular, the T3 samples were up to 47.63%, 6.13%, 42.21% higher than the T1, T2, and T4 samples at the waxing stage. At the tasseling stage, the acid phosphatase activity was highest in the T2 samples (0.98 mg·g^{-1}·h^{-1}), which was 19.34%, 9.28%, and 15.53% higher than in the T1, T3, and T4 samples, respectively.

In the soil collected from Longfu, the acid phosphatase activity was significantly higher in the T3 and T4 groups than in the T1 and T2 treatments at the early stages of fertility. For example, the acid phosphatase activity was 37.41% and 40.95% higher in the T4 sample than in the T1 sample at the tiller bloom and pregnancy spike stages, respectively. At the tassel stage, the T3 samples had the highest acid phosphatase activity at 1.29 mg·g^{-1}·h^{-1}, which was 55.63%, 42.62%, and 0.44% higher than those of the T1, T2, and T4 samples, respectively. At the waxing stage, the acid phosphatase activity was higher in the T3 samples by 112.97%, 4.29%, and 69.92% than in the T1, T2, and T4 samples, respectively. At the maturity stage, the T2 samples had the highest activity at 1.02 mg·g^{-1}·h^{-1}; this was 45.11%,8.14%, and 5.32% higher than in the T1, T3, and T4 samples.

3.4.3. Sucrase

Overall, the sucrase activity at the maturity stage was highest in Longfu, lower in Dahu, and lowest in Hehua. All three fertilizer application regimens significantly improved the soil sucrase activity compared to the corresponding controls (Figure 4). In the samples collected from Hehua, the sucrase activity remained high in the early stages, then significantly decreased in the later stages. This was likely due to adequate nutrition in the early stages provided by the basal application of fertilizer, followed by nutrient depletion in the later stages due to the poor base soil quality. The sucrase activity generally peaked at the pregnancy spike stage. However, in the T2 treatment group, the sucrase activity was higher at the tiller bloom, tassel, and maturity stages. At the pregnancy spike stage, the sucrase activity was 41.93%, 5.88%, and 24.80% higher in the T4 treatment (30.38 $mg \cdot g^{-1} \cdot d^{-1}$) than in the T1, T2, and T4 samples. At the waxing stage, the T3 samples had the highest sucrase activity at 14.31 $mg \cdot g^{-1} \cdot d^{-1}$, which was 35.34%, 23.34%, and 25.36% higher than in the T1, T2, and T4 samples, respectively.

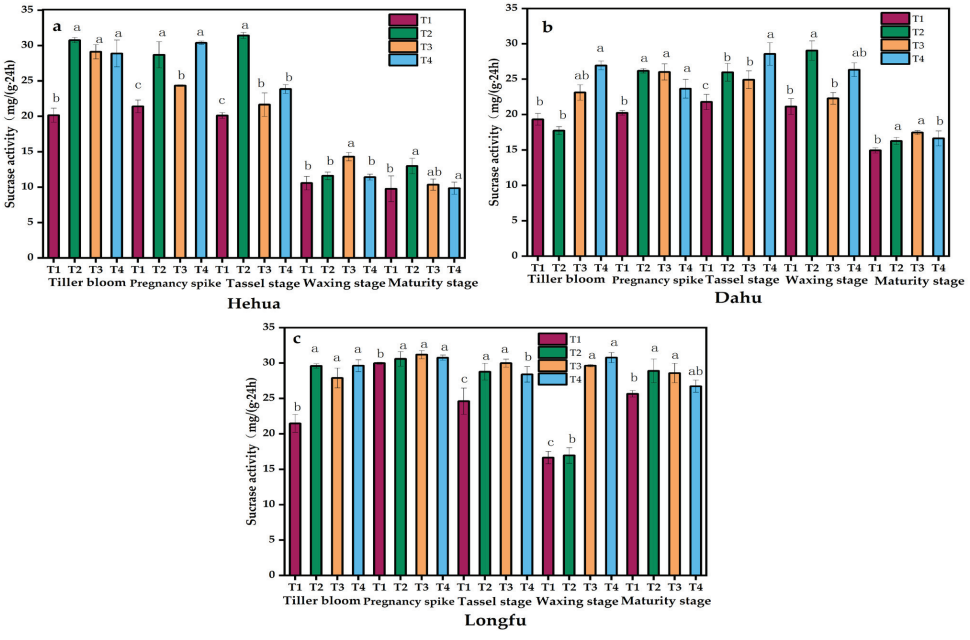

Figure 4. At each reproductive stage of rice development (**a**) is sucrase activity in soil samples collected from Hehua; (**b**) is sucrase activity in soil samples collected from Dahu; (**c**) is sucrase activity in soil samples collected from Longfu. T1, no fertilizer; T2, standard fertilizer; T3, 40% organic fertilizer; T4, 100% chemical fertilizer. Lowercase letters above each bar indicate statistically significant groups at $p < 0.05$ (ANOVA).

In soil collected from Dahu, the sucrase activity was highest in the T4 samples at the tillering and milking stages. During the pregnancy spike and waxing stages, the T2 samples had the highest sucrase activity. At the maturity stage, the highest sucrase activity was found in the T3 samples (17.45 $mg \cdot g^{-1} \cdot d^{-1}$); this was 16.80%, 7.25%, and 4.87% higher than in the T1, T2, and T4 samples, respectively.

In soil collected from Longfu, there were no significant differences in sucrase activity between treatments in the early growth stages. In the later stages, the differences between the T2, T3, and T4 treatments were significant, although the differences between the T2 and T3 treatments were only significant at the waxing stage. Across all treatment groups,

the sucrase activity was highest at the pregnancy spike stage, but the differences between treatments were not significant at that timepoint.

3.4.4. Combined Soil Enzyme Activity Index

A combined soil enzyme activity index (GMea) was used to assess the overall key enzyme activity in each soil sample. The GMea was higher in the Longfu and Dahu samples than in the Hehua samples; furthermore, it was higher for all three fertilizer treatment groups compared to the control (Figure 5). The GMea values for the Longfu and Dahu samples were 0.67–0.77 and 0.87–1.15 higher, respectively, than for the Hehua samples. Among the Hehua samples, the GMea was highest in T2, followed by T3 and then T4, and it was lowest in the T1 samples; for Longfu and Dahu, the GMea was higher in T3 than in T2, but it remained the lowest in T1 and second-lowest in T4.

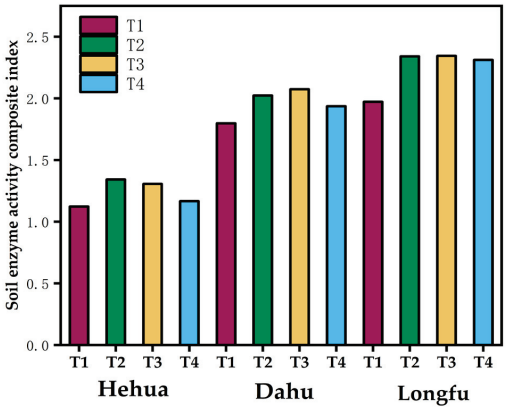

Figure 5. Comprehensive enzyme activity index values in soil samples collected from Hehua, Longfu, and Dahu at each reproductive stage of rice development. T1, no fertilizer; T2, standard fertilizer; T3, 40% organic fertilizer; T4, 100% chemical fertilizer.

3.4.5. Analysis of Simple Interactions between Location and Treatment with Indicators

In Figure 6, one can see that the T2, T3, and T4 treatments had interactive benefits in Hehua, Dahu, and Longfu.

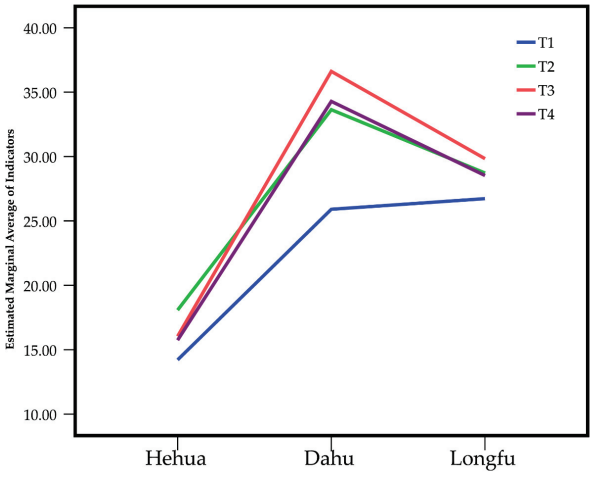

Figure 6. Analysis of the mutual benefits among the treatment sites of Hehua, Dahu, and Longfu. T1, no fertilizer; T2, standard fertilizer; T3, 40% organic fertilizer; T4, 100% chemical fertilizer. The indicators were total N, total P, organic matter, alkaline nitrogen at maturity, active phosphorus at maturity, phosphatase at maturity, urease at maturity, and sucrase at maturity.

Analysis of Simple Interactions between Location and Metrics

As can be seen in Figure 7, the relevant indicators had significant differences in the interaction benefits for Hehua, Dahu, and Longfu, with Dahu being the highest and Hehua being the lowest.

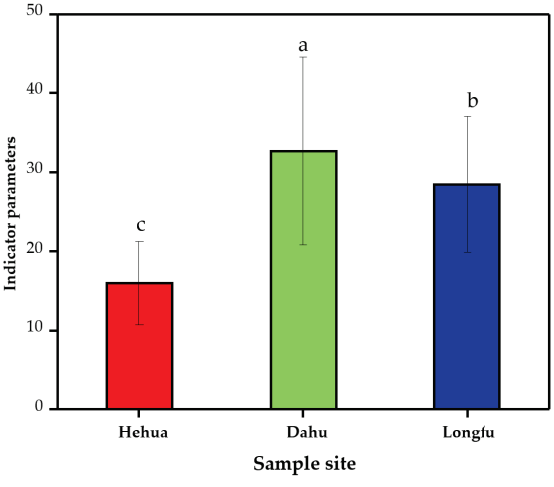

Figure 7. Analysis of the interaction benefits of each indicator on Hehua, Dahu, and Longfu. The indicators were total N, total P, organic matter, alkaline nitrogen at maturity, active phosphorus at maturity, phosphatase at maturity, urease at maturity, and sucrase at maturity. Lowercase letters above each bar indicate statistically significant groups at $p < 0.05$ (ANOVA).

Analysis of Simple Interactions between Treatments and Metrics

As can be learned from Figure 8, there were also large differences in the mutual benefits between the treatments and the indicators, with treatments T2 and T3 with organic

fertilizer being significantly higher than treatment T1 without fertilizer and treatment T4 with chemical fertilizer only.

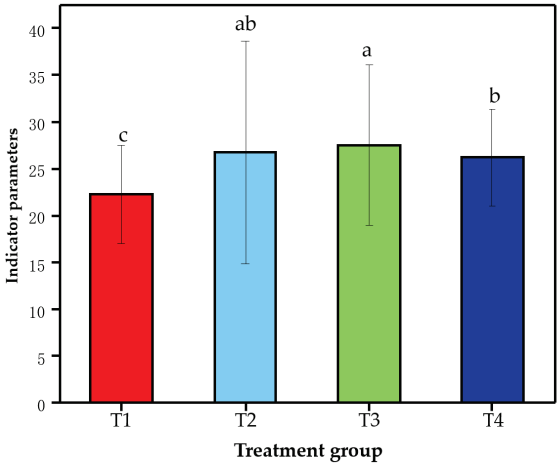

Figure 8. Analysis of the benefits of interactions between treatments and metrics. T1, no fertilizer; T2, standard fertilizer; T3, 40% organic fertilizer; T4, 100% chemical fertilizer. The indicators were total N, total P, organic matter, alkaline nitrogen at maturity, active phosphorus at maturity, phosphatase at maturity, urease at maturity, and sucrase at maturity. Lowercase letters above each bar indicate statistically significant groups at $p < 0.05$ (ANOVA).

4. Discussion

Long-term application of organic fertilizer significantly increases soil organic matter, total N, and total phosphorus compared with untreated soil [32]. Similarly, organic matter, total N, and available phosphorus levels are increased in soil treated with purely chemical fertilizer treatment or a non-organic fertilizer combination compared to untreated soil [33]. In the present study, we found varying degrees of increases in soil organic matter, total N, and total phosphorus content in three soil collection sites treated with different fertilizer types compared to untreated soil (Table 5). The largest increases in total N and organic matter content occurred at the Hehua site in the sample treated with 100% chemical fertilizer (Table 5). However, all three soil nutrient indicators (total N, available phosphorus, and organic matter content) were also increased in the Hehua and Longfu plots that were treated with 40% organic fertilizer or standard fertilizer, the latter of which included 5% pig manure (Table 5). In low-fertility fields, chemical fertilizers were shown to directly and effectively improve soil fertility. However, the inorganic N contained in chemical fertilizers decomposes quickly and is easily lost, whereas the N contained in organic fertilizers decomposes slowly and is more easily retained in the soil [34]. Therefore, in the long term, combined organic and inorganic fertilization is an effective measure in fields with varying fertility levels.

One of the key parameters assessed in this study was the decomposed alkaline N content in each soil sample. At the maturity stage, in the Hehua samples, the 40% organic (T3), standard (T2), and chemical (T4) fertilizer treatments were associated with 23.24%, 7.01%, and 6.19% increases in decomposed alkaline N compared to untreated soil; in Dahu, the T3, T2, and T4 treatments were associated with decomposed alkaline N increases of 32.00%, 50.32%, and 40.56%, respectively, and in Longfu, the same treatments were associated with increases of 0.62%, 3.57%, and 1.86%, respectively (Table 6). In Hehua, the standard treatment containing 5% pig manure (T2) significantly increased the decomposed alkaline N content compared to the 40% organic fertilizer (T3) treatment. In contrast, the highest alkaline N increases were obtained in Dahu and Longfu soil treated with 40%

organic fertilizer (Table 6). Organic fertilizers, particularly pig manure, reduce organic N mineralization [35,36]. Soil alkaline N content is also closely related to water content and heat conditions. For example, a previous study showed that soil alkaline N content was decreased by 17.84% after flooding [37]. The increases in alkaline N as a result of fertilizer addition were lower in Longfu than in Hehua, which was likely because the Longfu rice field was flooded during the rice maturity phase.

Overall, the organic matter content was lower in the standard fertilizer than in the 40% organic fertilizer treatment, the latter of which included zoysia and rice straw. However, the rate and total amount of organic matter decomposition in the 40% organic treatment was low in the short term. This was in contrast to the high rate of manure decomposition, which facilitates rapid uptake of nutrients by low-fertility rice fields. The slower decomposition of the T3 treatment could result in organic matter accumulation in low-yielding fields (Table 5). In contrast, in medium- and high-fertility fields, the base soil contains a higher abundance of microorganisms with increased species diversity, which promotes the fast decomposition of organic matter. Thus, the application of 40% organic fertilizer would be the most appropriate for fields with higher base fertility levels, and standard fertilizer treatment would be a better option for low-yielding fields.

The available phosphorus content was higher in all fertilized samples than in the control samples, and the organic and standard fertilizer treatments were associated with higher phosphorus content than the 100% chemical fertilizer treatment (Table 6). Generally, fertilizer application increases the total soil phosphorus content, although phosphorus is easily fixed by soil sorption [38]. Compared with chemical fertilizers, organic fertilizers increase levels of highly mobile organic phosphorus, which, in turn, increases the accumulation of active-state phosphorus and, thus, of effective soil phosphorus [39]. This may be because organic fertilizer decomposition produces substances that occupy some of the adsorption sites on the surfaces of iron and aluminum oxides, thus reducing soil adsorption of phosphorus and increasing the amount of active phosphorus in the soil [40]. Organic manure and pig manure mixed with inorganic fertilizer were shown here to improve soil nutrient utilization and enzyme activity, consistently with the findings of Zhao et al. [41].

Soil enzymes are closely related to soil microorganisms and play an important role in catalytic reactions for organic matter decomposition and nutrient cycling [42]. Fertilizer application affects the abundance, species diversity, and metabolic processes of soil microorganisms, which, in turn, alter the levels of soil enzyme activity [43]. Here, the Dahu and Longfu sites were found to have higher urease activity than the Hehua samples did, which may have been due to the base N content of the soils (Figure 2). Across all three sites, urease activity was higher in the soils treated with 40% organic fertilizer or standard fertilizer than in those treated with 100% chemical fertilizer or no fertilizer (Figure 2). This was similar to the results of Deng et al. [44]. On the one hand, exogenous enzymes may be contained in organic fertilizers, which create a good living environment for soil microorganisms and are conducive to the improvement of soil enzyme activities. On the other hand, the application of organic matter increases organic nitrogen, provides abundant energy substances, and enhances the metabolic activities of animals, plants, and microorganisms in the soil, thereby increasing enzyme activities [45–47]. Obviously, the response of the urease activity to organic fertilizers was greater than that to chemical fertilizers, and the soil acid phosphatase activity (Figure 3), sucrase activity (Figure 4), and urease activity (Figure 2) in the three lands were similar.

Soil phosphatase accelerates the rate at which organic phosphorus is dephosphorylated; its activity directly affects the decomposition, conversion, and biological effectiveness of soil organic phosphorus [48]. Long-term application of chemical fertilizers in combination with pig manure may increase soil phosphatase activity [26]. Soil sucrase is associated with carbon cycling in the soil and can be used as a marker of a soil's ability to decompose and utilize organic carbon [49]. Numerous studies have shown that organic and inorganic fertilizer application can effectively increase soil sucrase activity [48]. In addition to directly measuring urease, phosphatase, and sucrase activity, we also assessed soil enzyme activity

by using a comprehensive indicator of soil biological quality, GMea [20]. Overall, GMea was significantly higher in the fertilized samples than in the control samples, as expected. Furthermore, GMea was higher in samples treated with 40% organic fertilizer or 5% pig manure than in those treated with 100% chemical fertilizer (Figure 5). As discussed above, this may have been because organic matter input promoted soil microbe growth and reproduction, increasing the activity of key enzymes in the soil. However, few types of organic fertilizers were tested in the present study; future research should include additional types of organic fertilizers to determine their effects on soil enzymatic activity.

5. Conclusions

Experiments testing three types of organic and inorganic fertilizer treatments revealed varying effects on soil parameters in rice fields with different base fertility levels. In Hehua, 100% chemical fertilizer application significantly increased the soil nutrient contents. Plant matter was determined to be a suboptimal fertilizer for low-fertility soils due to the slow rate of decomposition; in such conditions, a relatively high volume of fertilizer should be applied to compensate for the poor soil quality, and the proportion of inorganic fertilizer should be high. In Dahu and Longfu, where organic fertilizer cultivation was more effective due to the higher base soil fertility, the proportion of organic fertilizer could be increased, although the optimal materials and rates require further testing and optimization. Furthermore, the total amount of fertilizer applied to high-fertility fields should be reduced to decrease investment costs, improve fertilizer utilization, and minimize environmental pollution. Overall, the results of this study support the application of organic fertilizer in combination with inorganic fertilizer as an effective measure for the improvement of soil quality in low- and medium-yielding fields. Our findings serve as a valuable guide for rational and economical improvement of soil conditions in fields with a range of yield levels, ultimately promoting increased crop yield and food security.

Author Contributions: Conceptualization, G.M. and Y.D.; methodology, S.C.; software, W.T.; validation, G.M., S.C. and W.H.; formal analysis, S.Q. and N.T.; investigation, W.H.; resources G.M.; data curation, Y.D.; writing—original draft preparation, G.M. and S.C.; writing—review and editing, G.M.; visualization, G.M.; supervision, G.M.; project administration, S.Q.; funding acquisition, G.M. All authors have read and agreed to the published version of the manuscript.

Funding: Major Science and Technology Program of Hainan Province (No. ZDKJ202001).

Data Availability Statement: Data will be made available upon personal request.

Conflicts of Interest: The authors declare no conflict of interest.

References

1. Zhou, J. An overview of soil quality changes and sustainable use of arable land resources in China. *Proc. Chin. Acad. Sci.* **2015**, *30*, 459–467.
2. Shen, R.; Wang, C.; Sun, B. Soil science and technology in the implementation of the strategy of "hiding grain in the land and hiding grain in technology". *Proc. Chin. Acad. Sci.* **2018**, *33*, 135–144. [CrossRef]
3. Lu, Y.; Liao, Y.; Nie, J.; Zhou, X.; Xie, J.; Yang, Z. Effect of continuous fertilizer application on changes in base ground strength and soil nutrients in paddy soils with different fertility. *Chin. Agric. Sci.* **2016**, *49*, 4169–4178.
4. Zhang, S.; Nie, L. Application of arable land strength evaluation results to guide scientific fertilization of rice. *Mod. Agric.* **2018**, *462*, 18–21.
5. Zheng, S.; Liao, Y.; Yang, Z.; Xie, J.; Nie, J.; Wu, X.; Xiang, Y. Fertility characteristics of rice soils with different productivity in double-season rice growing areas in Hunan. *J. Plant Nutr. Fertil.* **2011**, *17*, 1108–1121.
6. Pang, D.; Chen, J.; Tang, Y.; Yin, Y.; Yang, D.; Cui, Z.; Zheng, M.; Li, Y.; Wang, Z. Effects of maize straw return method and nitrogen fertilizer treatment on soil physicochemical properties and winter wheat yield. *J. Crop Sci.* **2016**, *42*, 1689–1699.
7. Wang, Y.; Li, H.; Han, Y.; Zhang, H.; Tan, J. Study on soil fertility differences between ultra-high yielding and high yielding fields in tidal soils. *N. China J. Agric.* **2012**, *27*, 197–201.
8. Guo, L.; Zheng, C.; Cao, C.; Dang, H.; Ma, J.; Li, K. Effects of soil fertility and fertilization measures on the ground power contribution and soil capacity of winter wheat-summer corn yield. *Hebei Agric. Sci.* **2016**, *20*, 29–33.
9. Le Bissonnais, Y. Aggregate stability and assessment of soil crustability and erodibility: I. Theory and methodology. *Eur. J. Soil Sci.* **2016**, *67*, 11–21. [CrossRef]

10. Yang, X.-M.; Wander, M.M. Temporal changes in dry aggregate size and stability: Tillage and crop effects on a silty loam Mollisol in Illinois. *Soil Tillage Res.* **1998**, *49*, 173–183. [CrossRef]
11. Jiang, C.; He, Y.; Liu, X.; Chen, P.; Wang, Y.; Li, H. Effects of long-term organic fertilizer application on the structure and stability of dryland red soil agglomerates. *J. Soil Sci.* **2010**, *47*, 715–722.
12. Liang, Y.; Yuan, Y.; Han, X.; Li, L.; Zou, W.; Ren, J.; Li, G. Effect of chemical fertilizers with different doses of organic fertilizers on the distribution of organic carbon and humic acid in black soil agglomerates. *J. Plant Nutr. Fertil.* **2016**, *22*, 9.
13. Xu, S.; Wang, Y.; Wang, H.; Zhu, F.; Ran, Y.; Chen, J. Stability of soil aggregates at different fertility levels and their response to nitrogen fertilizer salt solutions. *J. Plant Nutr. Fertil.* **2012**, *18*, 1135–1143.
14. Liang, T.; Liao, D.; Chen, X.; Wang, S.; Fu, D.; Chen, X.; Shi, X. Effect of basal ground level on nutrient use efficiency of rice fields in Chongqing. *Chin. Agric. Sci.* **2018**, *51*, 3106–3116.
15. Liang, B.; Yang, X.; Murphy, D.V.; He, X.; Zhou, J. Fate of 15 N-labeled fertilizer in soils under dryland agriculture after 19 years of different fertilizations. *Biol. Fertil. Soils* **2013**, *49*, 977–986. [CrossRef]
16. Li, R. Influence of Different Base Landraces on Rce Yield and Fertilizer Use Efficiency. Master's Thesis, Huazhong Agricultural University, Wuhan, China, 2011.
17. Li, M.; Zhang, X. Soil fertility evaluation of different soil configurations and analysis of the relationship between soil fertility and capacitance. *Soil Bull.* **2011**, *42*, 1420–1427. [CrossRef]
18. Álvaro-Fuentes, J.; Morell, F.J.; Madejón, E.; Lampurlanés, J.; Arrúe, J.L.; Cantero-Martínez, C. Soil biochemical properties in a semiarid Mediterranean agroecosystem as affected by long-term tillage and N fertilization. *Soil Tillage Res.* **2013**, *129*, 69–74. [CrossRef]
19. Xue, J.; Gao, Y.; Wang, J.; Fu, S.; Zhu, F. Exploration of soil microbial carbon and nitrogen as soil fertility indicators. *Soil Bull.* **2007**, *2*, 247–250. [CrossRef]
20. García-Ruiz, R.; Ochoa, V.; Hinojosa, M.B.; Carreira, J.A. Suitability of enzyme activities for the monitoring of soil quality improvement in organic agricultural systems. *Soil Biol. Biochem.* **2008**, *40*, 2137–2145. [CrossRef]
21. Wang, N.; Wang, S.; Gao, Q.; Zhao, L.; Tian, T.; Zhang, J. Effect of nitrogen application level on microbiological properties of soils with different fertility. *J. Soil Water Conserv.* **2014**, *28*, 148–152+167. [CrossRef]
22. Qiu, L.; Liu, J.; Wang, Y.; Sun, H.; He, W. Study on the relationship between soil enzyme activity and soil fertility. *J. Plant Nutr. Fertil.* **2004**, *18*, 277–280.
23. Song, Y.; Lv, X.; Chen, W. Response of soil alkaline nitrogen and urease activity to different nitrogen levels in rice. *North Rice* **2010**, *40*, 8–12. [CrossRef]
24. Ye, X.; Yang, C.; Li, Z.; Jing, H. Effect of green manure on soil enzyme activity and soil fertility of tobacco planting. *J. Plant Nutr. Fertil.* **2013**, *19*, 445–454.
25. Hu, C.C.; Cao, C.P.; Ye, Z.N.; Wu, W.L. Effect of different soil fertilization measures on microbial biomass carbon in low fertility farmland. *J. Ecol.* **2006**, *03*, 808–814.
26. Liu, Z.; Rong, Q.; Zhou, W.; Liang, G. Effects of inorganic and organic amendment on soil chemical properties, enzyme activities, microbial community and soil quality in yellow clayey soil. *PLoS ONE* **2017**, *12*, e0172767. [CrossRef]
27. Yan, H.; Yu, Z.; Wang, X.; Li, C.; Zhao, L.; Ji, M.; Wang, L. Dynamic characteristics of soil microorganisms, enzymes and fast-acting nutrients under rototill-based maize straw return conditions. *J. Soil Water Conserv.* **2018**, *32*, 276–282. [CrossRef]
28. Yuan, J.-K.; Zhou, Y. Accurate determination of soil bulk and porosity by improved ring knife method using soil extraction auger. *Chin. Hortic. Abstr.* **2014**, *30*, 2.
29. Bao, S. *Soil Agrochemical Analysis*, 3rd ed.; China Agricultural Press: Beijing, China, 2000.
30. Guan, S.-Y. *Soil Enzymes and Their Research Methods*; Agricultural Press: Beijing, China, 1986.
31. Lv, Y. *Soil Science*; China Agricultural Press: Beijing, China, 2006.
32. Liu, X.; Lu, R.; Dai, P.-B.; Ni, Z.; Chen, D. Effects of long-term fertilizer and organic fertilizer application on rice yield and soil fertility. *Zhejiang Agric. Sci.* **2018**, *59*, 694–697. [CrossRef]
33. Liu, Y.; Li, Y.; Zhang, Y.; Zhang, W.; Huang, X.; Jiang, T. Effect of long-term different fertilization treatments on physicochemical properties of loamy rice soils. *Jiangsu Agric. Sci.* **2017**, *45*, 5.
34. Richter, J.; Roelcke, M. The N-cycle as determined by intensive agriculture–examples from central Europe and China. *Nutr. Cycl. Agroecosyst.* **2000**, *57*, 33–46. [CrossRef]
35. Bernal, M.; Sanchez-Monedero, M.; Paredes, C.; Roig, A. Carbon mineralization from organic wastes at different composting stages during their incubation with soil. *Agric. Ecosyst. Environ.* **1998**, *69*, 175–189. [CrossRef]
36. Preusch, P.; Adler, P.; Sikora, L.; Tworkoski, T. Nitrogen and phosphorus availability in composted and uncomposted poultry litter. *J. Environ. Qual.* **2002**, *31*, 2051–2057. [CrossRef]
37. Yang, J.W.; Tang, G.M.; Li, R.Z.; Yuan, X.; Yuan, H.; Jiang, S. Simulation study on soil-surface water nitrogen and phosphorus migration characteristics in flooded agricultural fields. *J. Irrig. Drain.* **2018**, *037*, 71–77.
38. Wang, B.; Li, J.; Ren, Y.; Xin, J.; Hao, X.; Ma, Y.; Ma, X. Validation of a soil phosphorus accumulation model in the wheat–maize rotation production areas of China. *Field Crops Res.* **2015**, *178*, 42–48. [CrossRef]
39. Reddy, D.D.; Rao, A.S.; Rupa, T. Effects of continuous use of cattle manure and fertilizer phosphorus on crop yields and soil organic phosphorus in a Vertisol. *Bioresour. Technol.* **2000**, *75*, 113–118. [CrossRef]

40. Wang, S.; Liang, X.; Chen, Y.; Luo, Q.; Liang, W.; Li, S.; Huang, C.; Li, Z.; Wan, L.; Li, W. Phosphorus loss potential and phosphatase activity under phosphorus fertilization in long-term paddy wetland agroecosystems. *Soil Sci. Soc. Am. J.* **2012**, *76*, 161–167. [CrossRef]
41. Zhao, J.; Ni, T.; Li, J.; Lu, Q.; Fang, Z.; Huang, Q.; Zhang, R.; Li, R.; Shen, B.; Shen, Q. Effects of organic–inorganic compound fertilizer with reduced chemical fertilizer application on crop yields, soil biological activity and bacterial community structure in a rice–wheat cropping system. *Appl. Soil Ecol.* **2016**, *99*, 1–12. [CrossRef]
42. Allison, V.; Condron, L.; Peltzer, D.; Richardson, S.; Turner, B. Changes in enzyme activities and soil microbial community composition along carbon and nutrient gradients at the Franz Josef chronosequence, New Zealand. *Soil Biol. Biochem.* **2007**, *39*, 1770–1781. [CrossRef]
43. Vepsäläinen, M.; Kukkonen, S.; Vestberg, M.; Sirviö, H.; Niemi, R.M. Application of soil enzyme activity test kit in a field experiment. *Soil Biol. Biochem.* **2001**, *33*, 1665–1672. [CrossRef]
44. Deng, X.; Chen, M.; Wu, C.; Li, Q. Effect of different fertilization patterns on soil enzyme activity in pepper-winter melon crop rotation. *Jiangsu Agric. Sci.* **2018**, *46*, 4.
45. Lee, J. Effect of application methods of organic fertilizer on growth, soil chemical properties and microbial densities in organic bulb onion production. *Sci. Hortic.* **2010**, *124*, 299–305. [CrossRef]
46. Liu, E.; Yan, C.; Mei, X.; He, W.; Bing, S.H.; Ding, L.; Liu, Q.; Liu, S.; Fan, T. Long-term effect of chemical fertilizer, straw, and manure on soil chemical and biological properties in northwest China. *Geoderma* **2010**, *158*, 173–180. [CrossRef]
47. Li, J.; Xin, X.; Li, J.; Yu, X.; Wu, J.; Han, Y. Effect of long-term locational fertilization on soil enzyme activity under maize-soybean crop rotation. *J. Shenyang Agric. Univ.* **2015**, *46*, 7.
48. Song, Y.; Yu, J.; Chen, S.; Xiao, C.; Li, Y.; Su, X.; Ding, F. Effect of chemical fertilizer reduction with bio-organic fertilizer on the growth and soil microbial and enzyme activities of oilseed rape. *J. Soil Water Conserv.* **2018**, *32*, 9.
49. Wan, Z.; Song, C. Characteristics of enzyme activity distribution in Little Leaf Chapter wetland and its relationship with active organic carbon characterization index. *Wetl. Sci.* **2008**, *26*, 2282–2290.

land

MDPI

Article

Cultivation and Nitrogen Management Practices Effect on Soil Carbon Fractions, Greenhouse Gas Emissions, and Maize Production under Dry-Land Farming System

Honglei Ren [1,*], Shengjun Xu [2], Fengyi Zhang [1], Mingming Sun [1] and Ruiping Zhang [1]

[1] Heilongjiang Academy of Agriculture Sciences, Harbin 150086, China; openai@haas.cn (F.Z.); riyue@haas.cn (M.S.); xinhui@haas.cn (R.Z.)
[2] Gansu Academy of Agricultural Sciences, Lanzhou 730070, China; xusj1001@gsagr.cn
* Correspondence: midou@haas.cn

Abstract: Effective nitrogen management practices by using two cultivation techniques can improve corn productivity and soil carbon components such as soil carbon storage, microbial biomass carbon (MBC), carbon management index (CMI), and water-soluble carbon (WSC). It is essential to ensure the long-term protection of dry-land agricultural systems. However, excessive application of nitrogen fertilizer reduces the efficiency of nitrogen use and also leads to increased greenhouse gas emissions from farming soil and several other ecological problems. Therefore, we conducted field trials under two planting methods during 2019–2020: P: plastic mulching ridges; F: traditional flat planting with nitrogen management practices, i.e., 0: no nitrogen fertilizer; FN: a common nitrogen fertilizer rate for farmers of 290 kg ha^{-1}; ON: optimal nitrogen application rate of 230 kg ha^{-1}; $_{ON75\%+DCD}$: 25% reduction in optimal nitrogen fertilizer rate + dicyandiamide; $_{ON75\%+NC}$: 25% reduction in optimal nitrogen rate + nano-carbon. The results showed that compared to other treatments, the $_{PON75\%+DCD}$ treatment significantly increased soil water storage, water use efficiency (WUE), and nitrogen use efficiency (NUE) because total evapotranspiration (ET) and GHG were reduced. Under the $P_{ON75\%+DCD}$ or $P_{ON75\%+NC}$, the soil carbon storage significantly (50% or 47%) increased. The $P_{ON75\%+DCD}$ treatment is more effective in improving MBC, CMI, and WSC, although it increases gaseous carbon emissions more than all other treatments. Compared with FFN, under the $P_{ON75\%+DCD}$ treatment, the overall CH_4, N_2O, and CO_2 emissions are all reduced. Under the $P_{ON75\%+DCD}$ treatment, the area scale GWP (52.7%), yield scale GWP (90.3%), biomass yield (22.7%), WUE (42.6%), NUE (80.0%), and grain yield (32.1%) significantly increased compared with F_{FN}, which might offset the negative ecological impacts connected with climate change. The $P_{ON75\%+DCD}$ treatment can have obvious benefits in terms of increasing yield and reducing emissions. It can be recommended to ensure future food security and optimal planting and nitrogen management practices in response to climate change.

Keywords: nitrogen management; global warming potential; soil carbon fractions; nitrogen use efficiency; farming techniques; maize production

Citation: Ren, H.; Xu, S.; Zhang, F.; Sun, M.; Zhang, R. Cultivation and Nitrogen Management Practices Effect on Soil Carbon Fractions, Greenhouse Gas Emissions, and Maize Production under Dry-Land Farming System. *Land* **2023**, *12*, 1306. https://doi.org/10.3390/land12071306

Academic Editor: Shahzad Ali

Received: 29 May 2023
Revised: 26 June 2023
Accepted: 26 June 2023
Published: 28 June 2023

1. Introduction

Plastic mulching under the ridge furrow rainfall harvesting method (P) is expanding rapidly to increase rain-fed maize production in semi-arid regions [1]. From 2013 to 2019, the global demand for plastic film mulching is expected to increase by 7.6% [2]. The soil and root respiration contribute approximately 20%, 12%, and 60% of CO_2, CH_4, and N_2O emissions [3]. The global carbon cycle is affected by global warming, which distorts the function and structure of ecosystems [4]. It is estimated that 65% of total N_2O emissions come from soil [5], and nitrogen application accounts for 36% of direct N_2O emissions from global agricultural soils [6]. In China, by 2020, reducing nitrogen input and improving water management may reduce 17% of the total greenhouse gas emissions, mainly from wheat, corn, and rice [7].

Plastic film mulching (PFM) is usually used to improve soil water storage, decrease nitrogen loss caused by leaching, provide favorable conditions for soil biological activities, and control weeds [8,9]. However, the excessive use of inorganic fertilizers in China has increased ecological problems [10], which have little influence on crop yields but have caused major nitrogen losses into the atmosphere [11]. Northwest China is an irrigated area, and numerous growers use more irrigation with unnecessary nitrogen supplies in order to raise crop production [12]. These approaches have caused severe water and nutrient deficiencies [13], decreased crop production and NUE [14], and improved the risk of GHGI [15,16]. Reducing agricultural carbon dioxide emissions can be attained by improving soil carbon sequestration [17]. Smart fertilizer management practices are essential for SOC storage [18]. Sufficient nutrients in the soil can increase biomass yield and SOC [12]. Thus, it is vital to launch more effective fertilizer management practices to use less fertilizer to increase crop yields and reduce environmental pollution.

Among various greenhouse-gas reduction strategies, fertilizers that improve NUE, such as slow-release fertilizers, can effectively reduce nitrogen loss [19]. The use of slow-release fertilizers can suspend the exchange of ammonium (NH_4^+) to nitrate (NO_3^-) by preventing nitrifying bacteria activity [20], thereby increasing the efficiency of N use, reducing N_2O emissions, and maintaining or improving crop Production [21,22]. As global warming intensifies, reducing N_2O emissions from agricultural soils has attracted great attention [23]. Dicyandiamide (DCD) is a highly effective nitrification inhibitor [24]. Nie et al. [25] report that the addition of DCD combined with an optimized nitrogen fertilizer rate significantly reduced N_2O flux emissions by 67.3–83.8%. Nanocarbon (NC) is a new type of fertilizer synergist. Compared with urea alone, nanocarbon (NC) added to urea can increase crop production, increase nitrogen use efficiency, and reduce nitrogen loss [26]. Nanocarbon is a modified carbon with non-conductive properties and low ignition points. NC can screen poisonous gases and is currently widely used in new fertilizer research fields aimed at increasing crop yields and fertilizer utilization [10]. However, it is not clear whether nanocarbons can also provide greenhouse gas emission reduction potential, especially when compared to DCD.

Numerous researchers have focused on the effects of the separate application of NI and irrigation on greenhouse gas intensity and maize yields [27,28]. The current study aims at: (a) Estimating greenhouse gas emissions in the form of CH_4, CO_2, N_2O, and GWP under different fertilizer management practices; (b) Estimating SOC and microbial activities in relation to GHG emissions. (c) determine the most adaptable N management practices that provide high and stable SOC, nitrogen use efficiency, and rain-fed maize production while decreasing greenhouse gas emissions.

2. Materials and Methods

2.1. Site Location

The field trial was carried out in the 2019 and 2020 years at the Gansu Academy of Agricultural Sciences. The experimental sites are located at 103°41′17.49″ E, 36°06′3.31″ N, and 467 m asl. The rainfall from July to September exceeds 60%. The rainfall in the growing season from 2019 to 2020 was between 279 and 265 mm (Figure 1). Table 1 indicates the soil chemical properties at a depth of 20 cm. The top 0–15 cm of soil on the research site is Eum-Orthrosols (Chinese Soil Taxonomy).

Table 1. The chemical properties of experimental site's soil layer (0–15 cm).

Year	pH	SOM (g kg^{-1})	TP (g kg^{-1})	TK (g kg^{-1})	AP (mg kg^{-1})	AK (mg kg^{-1})
2019	8.24	13.67	1.07	18.21	21.05	159.22
2020	8.08	15.33	1.03	16.34	18.89	164.65

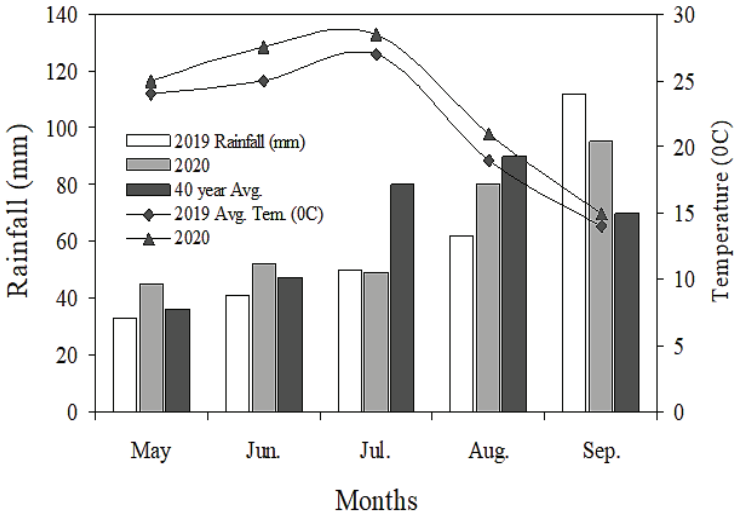

Figure 1. Monthly rainfall distribution during the maize-growing seasons.

2.2. Experimental Design

A randomized completely block design were used having three replications. The area of each plot is 60 m^2 (20 × 3 m^2). The following ten treatments and two cultivation practices P: plastic film mulching on ridges; F: traditional flat planting with five different nitrogen management practices $_0$: no N fertilizer; $_{FN}$: farmers common N rate is 290 kg ha^{-1}; $_{ON}$: optimal N rate is 230 kg ha^{-1}; $_{ON75\%+DCD}$: 25% reduction in optimal N rate + dicyandiamide (DCD) is applied at a rate of 5% of the total applied N (*w*/*w*); $_{ON75\%+NC}$: 25% reduction in optimal N rate + nano-carbon (NC) is applied at 0.3% (*w*/*w*) of the total applied fertilizer. The furrow is 60 cm wide and 15 cm high. Plant population of 75,000 ha^{-1} of Dafeng 30 maize cultivar; planting time is 10 May 2019, and 9 May 2020. The corn was harvested on 10 September 2019 and 8 September 2020. In 2019–2020, weeds will be controlled by hand. The recommended doses of P and K at 90 and 60 kg ha^{-1} apply one day before sowing. During both growing seasons, irrigation was not supplied, conventional tillage practices were used for soil flow, and weeds were controlled manually.

2.3. Sampling and Measurements

2.3.1. Soil Water Storage (mm)

Soil water storage (SWS) was determined by the following formula.

$$SWS = C \times \rho \times H \times 10 \quad (1)$$

C is the soil gravimetric moisture content (%); ρ is the bulk density (g cm^{-3}); and H is the soil depth (0–120 cm).

2.3.2. Analysis of Gas Sampling

A cylindrical opaque chamber (inner diameter 25 cm × 20 cm height) was used. Each plot was repeated three times, and the bottom chamber was buried in the inner soil 20 cm deep. An electric fan is fixed to mix the gas. From 0 to 30 min after closing the chamber, use a 30 mL air-tight syringe to collect the gas sample with the help of a gas chromatograph equipped. A gas chromatograph equipped with an HP-PLOT Q capillary column was used to quantify the concentration of three gases (N_2O, CH_4, and CO_2). A flame ionization detector (FID) with a methanizer was used to analyze CH_4 and CO_2 concentrations, while the concentration of N_2O was analyzed by the Ni electron capture detector.

As emission rates were determined by the equation below:

$$\text{Gas emission rate } (\text{mgm}^{-2}\text{h}^{-1}) = \Delta c/\Delta \text{t} \times \text{V/A} \times \rho \times 273/\text{T} \quad (2)$$

where Δc/Δt is the difference of gas concentration between 0 and 30 min, V is the volume, A is the area, ρ is the density, and T is the absolute temperature.

The seasonal gas fluxes were determined by the equation below:

$$\text{Seasonal flux } (\text{kgha}^{-1}) = \sum_{i}^{n} (R_i \times D_i) \quad (3)$$

where R is the daily gas emission rate and D is the number of days between the *i*th sampling interval.

The net GWP was determined by the equation below:

$$\begin{aligned} \text{Net GWP } (\text{kgCO}_2\text{-eq ha}^{-1}) \quad &= \text{CH}_4 \text{ flux } 28 \\ &+ \text{N}_2\text{O flux } 265 - \Delta SOC 44/12 \end{aligned} \quad (4)$$

The greenhouse gas intensity (GHGI) was determined using the net GWP per maize grain yield [3]:

$$\text{CHGI}(\text{kgCO}_2\text{-eq kg}^{-1} \text{ grain}) = \text{NetCWP/grain yield} \quad (5)$$

2.3.3. Global Warming Potential

The GWP for area and yield scale of income is determined by [29]:

$$\begin{aligned} \text{Area} - \text{scaled GWP} = \quad & 28 \times \text{CH}_4(\text{kgha}^{-1}\text{yr}^{-1}) \\ & +265 \times \text{N}_2\text{O}(\text{kghal}^{-1}\text{yr}^{-1}) \end{aligned} \quad (6)$$

The yield-scaled GWP was then calculated as the ratio between the area-scaled GWP and grain yield [29].

2.3.4. Soil Carbon Fraction Analysis

Soil MBC is determined by using a modified chloroform fumigation extraction method [30]. The mineralizable carbon (RMC) content was determined after extraction with 0.5 M K_2SO_4 [31], and then the soil extract was wet digested with dichromate [32]. The acid hydrolyzed carbohydrate carbon (AHC) is determined by taking the equivalent weight of 2 g of soil extracted with 20 mL of 1.5 M sulfuric acid (H_2SO_4) for 24 h with regular shaking and filtering through a glass fiber filter according to the procedure of [33]. The water-soluble carbohydrate carbon (WSC) content is determined by [34]. The ninhydrin reactive nitrogen (NRN) in 20-g soil samples was extracted with 0.5 M potassium sulfate (K_2SO_4) and estimated colorimetrically after mixing the soil extracts with ninhydrin [35].

2.3.5. Soil Carbon Storage, Carbon Management Index

The carbon management index (CMI) was calculated by using a reference sample value according to the procedure of Blair et al. [36]. Based on changes in between the reference and sample sites of the total carbon content, a carbon pool index (CPI) was determined by Liu et al. [37]. CPI = [sample TC/TC of reference soil].

Based on the changes in the C lability (L) = $KMnO_4$-C/TC-$KMnO_4$-C, the lability index was determined.

$$\text{LI} = [\text{sample L/reference L}]$$

$$\text{CMI} = \text{CPI} \times \text{LI} \times 100.$$

Carbon equivalent emissions (CEE) and carbon efficiency ratios (CER) were calculated using the following equations:

$$CEE = GWP \times 12/44$$

$$CER = \text{grain yield (in terms of carbon) of the maize/CEE}$$

The 43% carbon concentration in the grain was found.

2.3.6. Biomass and Maize Production

Biomass and grain yield of maize were measured at 6 m^2 area and hand harvested from each plot.

$$WUE = Y/ET \quad (7)$$

where WUE (kg ha^{-1} mm^{-1}) is the water use efficiency, Y is the grain yield, and ET is the evapotranspiration.

Nitrogen use efficiency (NUE kg kg^{-1}) was calculated by Wang et al. [38].

$$NUE = GY/N \text{ uptake} \times 100\% \quad (8)$$

2.3.7. Statistical Analysis

Data and interactions were analyzed using an analysis of variance (ANOVA) and Analytical Software (statistic 8.1/2008/statsoft/Tulsa, OK, USA). To calculate the probability levels of P (0.05), the LSD (least significant difference) test was used.

3. Results

3.1. SWS and ET

Changes in rainfall, maize water utilization, and soil evaporation have led to reduced soil water storage (SWS) at different maize growth stages (Figure 2). In our research work, SWS showed non-significant differences among all treatments at 30 days after planting (DAP). The water consumption of maize improves the growth of plants. $P_{ON75\%+DCD}$ treatment can reduce drought and ensure the successful growth of plants. In the $P_{ON75\%+DCD}$ treatment, the SWS of maize was considerably higher than in the $F_{ON75\%+DCD}$ treatment. Start with 60–80 DAP; compared to 30 DAP, the trend of SWS for each treatment is significantly enhanced. At 100 DAP, the average data of two years shows that, compared with $F_{ON75\%+DCD}$ and $F_{ON75\%+NC}$, the SWS under the $P_{ON75\%+DCD}$ treatment is significantly the largest. The different cultivations of $_{ON75\%+DCD}$ and $_{ON75\%+NC}$ nitrogen application treatments had the largest SWS, but compared with all other treatments, the difference was considerable at various corn stages. The change in SWS was not significant between $P_{ON75\%+NC}$ and $F_{ON75\%+DCD}$ treatments at 120–140 DAP.

The corn ET is positively correlated with rainfall and nitrogen management practices. Compared with FFN and PFN treatments, $P_{ON75\%+DCD}$ and $P_{ON75\%+NC}$ treatments with different nitrogen management measures resulted in lower total ET due to high soil evaporation. The results indicated that ET at $P_{ON75\%+NC}$ treatment is considerably lower than at $F_{ON75\%+DCD}$ and $F_{ON75\%+NC}$ treatment, respectively. Regardless of the cultivation method, the $_{ON75\%+DCD}$ treatment significantly reduced 10.1% compared to the FN treatment. Compared with $F_{ON75\%+DCD}$ treatment, $P_{ON75\%+DCD}$ treatment significantly reduced ET by 7.0%, and $P_{ON75\%+NC}$ treatment significantly reduced ET by 22.8% compared with FFN treatment.

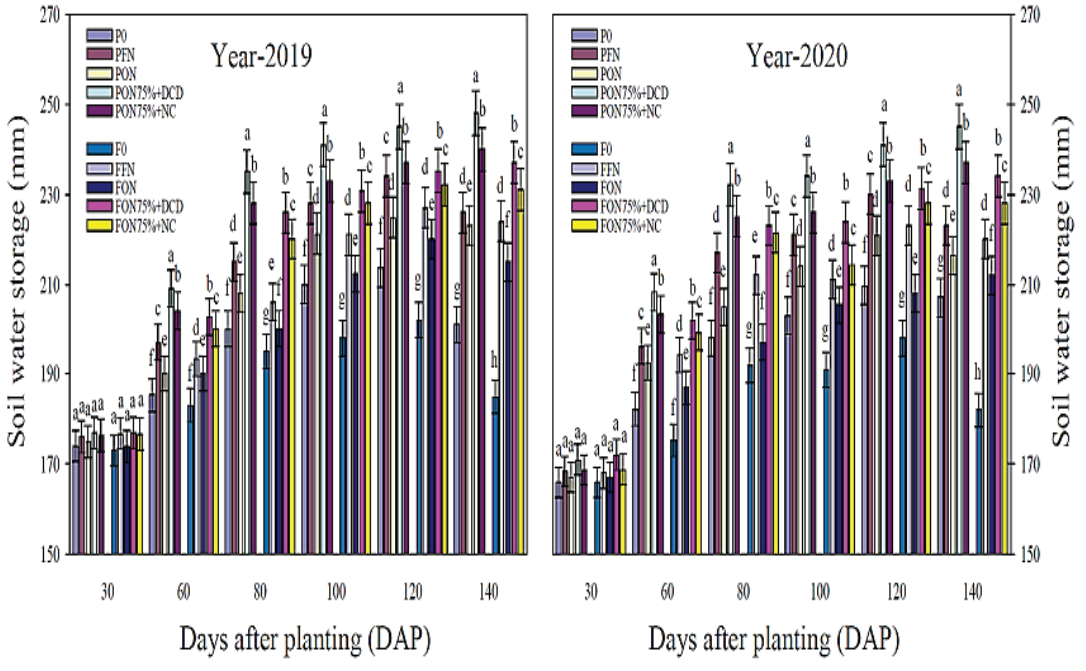

Figure 2. Effects of farming and nitrogen management practices on soil water storage at the depth of 0–120 cm soil layers at different growth stages of maize during 2019 and 2020. Vertical bars represent the LSD at $p = 0.05$ ($n = 3$).

3.2. Soil Carbon Fractions

The MBC ranges from 113.7 to 414.6 mg kg^{-1} (Table 2). Under the $P_{ON75\%+DCD}$ treatment, the MBC was significantly higher (400.3 mg kg^{-1}) compared to the rest of all treatments. The application of $P_{ON75\%+DCD}$ treatment showed a significant increase of 67% in MBC (Table 2). Compared with other treatments, the $P_{ON75\%+DCD}$ treatment considerably improved the TC content (5.08 g kg^{-1}) (Table 3). The content of easily mineralizable carbon (RMC) was the highest in the plots treated with $P_{ON75\%+DCD}$ and $P_{ON75\%+NC}$ (177.7–137.9 mg kg^{-1}) and the lowest under the F_0 treatment (25.5 mg kg^{-1}). The WSC and AHC vary considerably under different cultivation and nitrogen management practices, ranging from 6.8 to 45.4 mg C kg^{-1} and 320.9 to 583.2 mg C kg^{-1}. The CMI was considerably improved by 31.2%, 10.2%, 11.4%, 10.8%, 10.8%, and 13.4% under the treatments of P_0, P_{FN}, P_{ON}, $P_{ON75\%+DCD}$, and $P_{ON75\%+NC}$, which was higher than that of F_0 and F_{FN}, F_{ON}, $F_{ON75\%+DCD}$, and $F_{ON75\%+NC}$ treatments. Under different cultivation and nitrogen management measures, the total N, C:N ratio, NH_4^+-N, NO_3^--N, and NRN have a significant impact (Tables 2 and 3). It was found that the total N under the $P_{ON75\%+DCD}$ and $P_{ON75\%+NC}$ treatments was significantly higher (0.61–0.57 g kg^{-1}) than that of all other treatments. Compared with the $F_{ON75\%+DCD}$ and $F_{ON75\%+NC}$ treatments, the C:N ratio was significantly higher (8.55–8.37) under the $P_{ON75\%+DCD}$ and $P_{ON75\%+NC}$ treatments. There were three peaks of NH_4^+-N and NO_3^--N in at various growth stages during the two-year field study. The NO_3^--N under F_0 treatment was considerably lower compared to the rest of all treatments (Figure 3). Under the treatments of $P_{ON75\%+DCD}$ and $P_{ON75\%+NC}$, (NO_3^--N) significantly increased compared with P_{FN} and F_{FN} treatments. Compared with F_0, the NH_4^+-N of all other treatments was considerably improved, whereas the NH_4^+-N of the $P_{ON75\%+DCD}$ and $P_{ON75\%+NC}$ treatments did not change significantly under the two cultivation methods (Figure 4). Different cultivation and nitrogen management measures at each growth stage have a significant impact on the NH_4^+-N content.

Table 2. Soil carbon fractions and carbon management index at 0–15 cm soil depth under different cultivation and nitrogen management practices during 2019–2020 maize growing seasons.

Treatments	MBC (mg kg^{-1})	RMC (mg kg^{-1})	WSC (mg kg^{-1})	AHC (mg kg^{-1})	CMI
2019					
P_0	171.0 g	32.2 f	8.1 f	369.8 e	88.9 e
P_{FN}	289.5 c	102.3 c	27.5 d	474.2 c	119.2 c
P_{ON}	285.1 c	77.3 d	26.3 d	456.5 c	109.5 c
$P_{ON75\%+DCD}$	386.1 a	168.9 a	44.7 a	564.7 a	142.3 a
$P_{ON75\%+NC}$	311.7 b	130.8 b	31.0 c	506.0 b	128.6 b
F_0	113.0 h	22.2 g	6.2 g	296.4 f	62.3 f
F_{FN}	213.8 e	70.7 d	24.5 e	381.5 e	105.7 d
F_{ON}	199.2 f	55.9 e	23.7 e	370.9 e	95.8 e
$F_{ON75\%+DCD}$	300.6 b	116.3 b	40.8 b	453.8 c	125.3 b
$F_{ON75\%+NC}$	240.2 d	88.6	27.2 d	404.9 d	109.9 c
2020					
P_0	190.4 g	35.5 f	8.8 f	394.2 f	97.8 e
P_{FN}	314.7 d	112.9 c	28.6 d	505.2 c	123.7 c
P_{ON}	313.8 d	84.5 d	27.2 d	485.0 d	114.1 c
$P_{ON75\%+DCD}$	414.6 a	186.5 a	46.0 a	601.7 a	147.9 a
$P_{ON75\%+NC}$	335.5 c	144.9 b	32.2 c	539.7 b	134.8 b
F_0	151.7 h	28.8 f	7.5 f	345.3 g	80.1 f
F_{FN}	264.2 f	91.8 d	26.5 d	443.3 e	114.7 c
F_{ON}	256.5 f	70.2 e	25.4 e	428.0 e	105.0 d
$F_{ON75\%+DCD}$	357.6 b	151.4 b	43.4 b	527.8 b	136.6 b
$F_{ON75\%+NC}$	287.9 e	116.7 c	29.7 c	472.3 d	122.4 c

Values are given as means, and different lowercase letters indicate significant differences at $p \leq 0.05$ levels.

Table 3. Soil nitrogen fractions and total carbon to total nitrogen ratio at 0–15 cm soil depth under different cultivation and nitrogen management practices during 2019–2020 maize growing seasons.

Treatments	TC (g kg^{-1})	TN (g kg^{-1})	TC:TN	NRN (μg g^{-1} Soil)	CEE (kg C ha^{-1})	CER
2019						
P_0	2.42 c	0.47 b	5.1 f	3.3 e	1846 e	0.82 c
P_{FN}	3.85 b	0.54 a	7.1 b	7.4 b	2395 b	0.94 b
P_{ON}	3.29 b	0.51 a	6.4 c	6.9 c	2149 d	0.90 b
$P_{ON75\%+DCD}$	4.97 a	0.62 a	8.0 a	10.5 a	2614 a	1.01 a
$P_{ON75\%+NC}$	4.74 a	0.57 a	8.3 a	8.8 b	2334 b	0.95 b
F_0	1.74 d	0.43 b	4.1 g	3.1 e	1584 f	0.73 d
F_{FN}	3.18 b	0.46 b	6.9 d	4.9 d	2171 d	0.82 c
F_{ON}	2.61 c	0.45 b	5.9 e	4.8 d	2144 d	0.81 c
$F_{ON75\%+DCD}$	4.29 a	0.52 a	8.3 a	7.4 b	2376 b	0.92 b
$F_{ON75\%+NC}$	4.06 a	0.49 b	8.4 a	6.4 c	2258 b	0.84 c
2020						
P_0	2.64 d	0.51 a	5.2 d	5.4 d	1502 f	0.80 b
P_{FN}	4.08 b	0.54 a	7.6 b	7.2 c	2190 d	0.91 a
P_{ON}	3.51 c	0.53 a	6.7 c	7.1 c	2108 d	0.88 b
$P_{ON75\%+DCD}$	5.19 a	0.60 a	8.7 a	9.7 a	2682 a	0.97 a
$P_{ON75\%+NC}$	4.96 b	0.57 a	8.8 a	8.7 b	2471 b	0.93 a
F_0	2.19 d	0.47 b	4.7 d	3.9 e	1404 g	0.69 c
F_{FN}	3.63 c	0.51 a	7.1 b	6.5 c	2093 e	0.80 b
F_{ON}	3.06 c	0.49 b	6.2 c	6.3 c	2010 e	0.77 c
$F_{ON75\%+DCD}$	4.74 b	0.58 a	8.2 a	9.2 a	2284 c	0.87 b
$F_{ON75\%+NC}$	4.51 b	0.54 a	8.4 a	8.0 b	2173 d	0.82 b

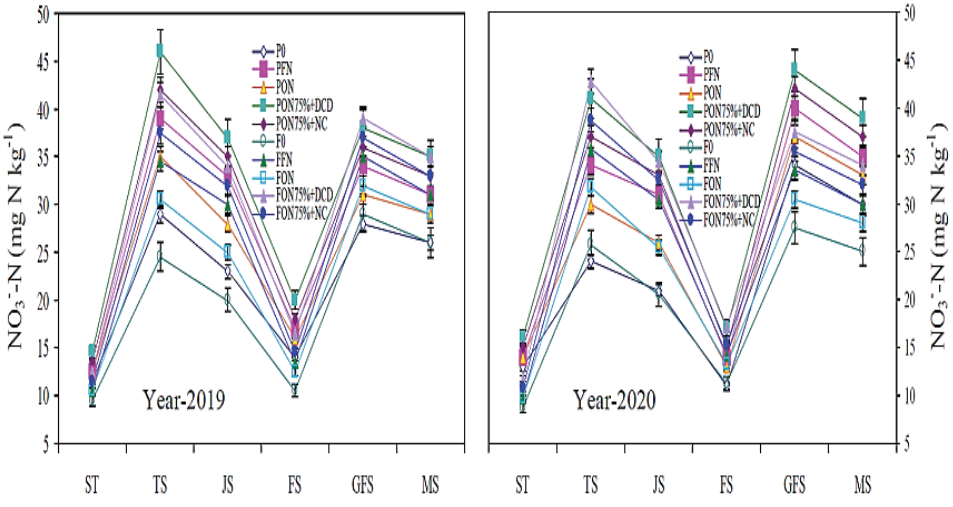

Figure 3. Effects of farming and nitrogen management practices on NO_3^--N contents. The vertical bars represent the standard error of the mean (n = 3).

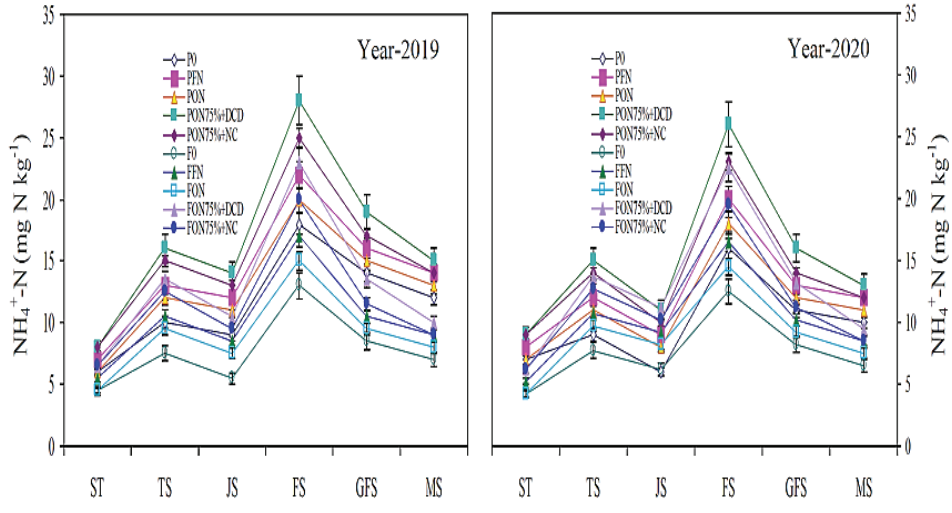

Figure 4. Effects of farming and nitrogen management practices on NH_4^+-N contents.

3.3. Greenhouse Gas Emissions

Field research found that CO_2 emissions were positive and experienced three fluctuations (Figure 5). Regardless of the different planting and nitrogen management methods, CO_2 is at its minimum during the sowing period, increases significantly during the flowering period, and reaches its highest during the grain filling period. Compared with FFN treatment, $P_{ON75\%+DCD}$ and $P_{ON75\%+NC}$ considerably changed CO_2, while the emissions of $F_{ON75\%+DCD}$ treatments were considerably higher than $F_{ON75\%+NC}$. Compared with P_0, CH_4 was considerably lower compared with the rest of the treatments, while the CH_4 of $_{ON75\%+DCD}$ and $_{ON75\%+NC}$ did not change considerably under the two cultivation methods (Figure 6). Different cultivation and nitrogen management practices apply to all growth stages. There were two peaks of N_2O during the jointing and flowering periods. The N_2O at F_0 is significantly lower than the rest of all treatments (Figure 7). Under $P_{ON75\%+DCD}$ and $P_{ON75\%+NC}$ treatments, N_2O emissions are significantly higher than those of PFN and

FFN treatments. Under different cultivation and nitrogen management measures, N_2O emissions at different growth stages have a significant impact.

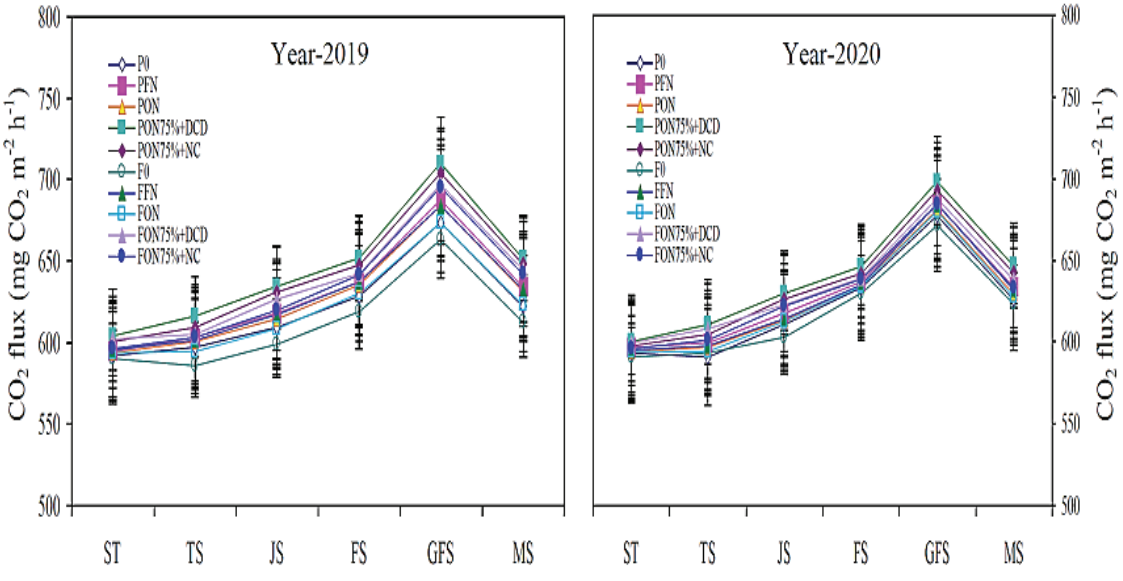

Figure 5. Effects of farming and nitrogen management practices on CO_2 emissions.

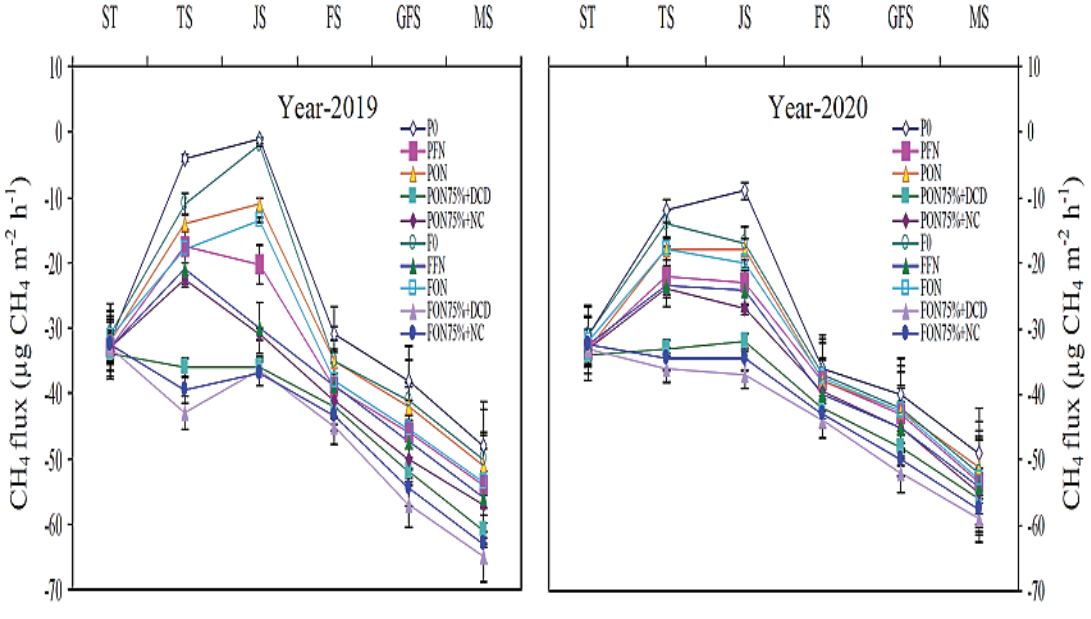

Figure 6. Effects of farming and nitrogen management practices on CH_4 emissions.

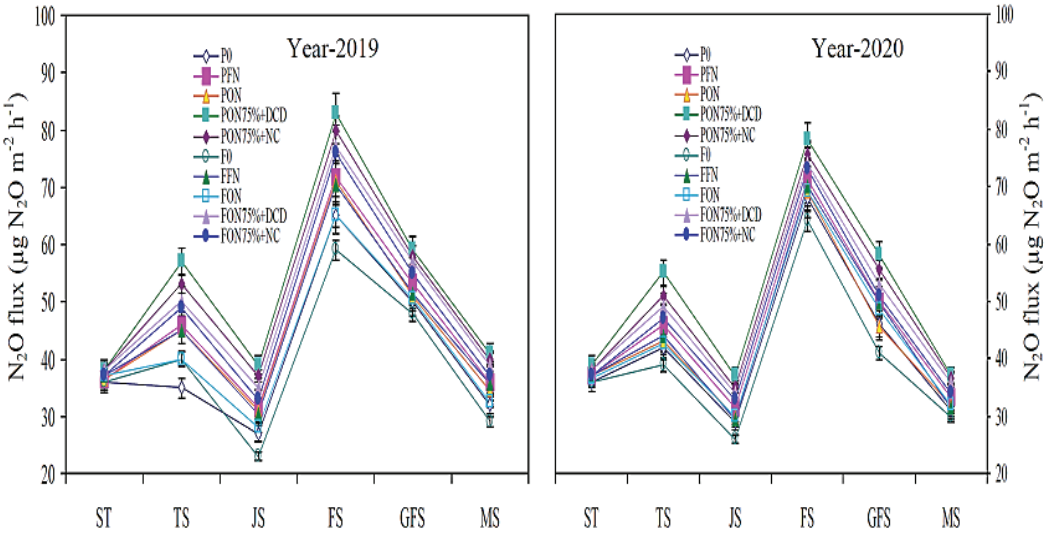

Figure 7. Effects of farming and nitrogen management practices on N_2O emissions.

3.4. GWP, GHGI, and CEE

Under different cultivation and nitrogen management practices, the effects of $P_{ON75\%+DCD}$ treatments on GHGI are different, which shows the net GWP per grain yield (Table 4). Under $P_{ON75\%+DCD}$ and $P_{ON75\%+NC,}$ GHGI was significantly reduced because of the substantial increase in corn production. This enhancement in GHGI is regularly influenced by soil carbon pool depletion rather than improved greenhouse gas emissions. Net GWP is determined by considering the GWP of N_2O and CH_4 and changes in SOC. The net GWP largely depends on the depletion of the soil carbon pool and different cultivation and nitrogen management practices. Under the $P_{ON75\%+DCD}$, the net GWP is 19.1–19.0 Mg CO_2 eq. ha^{-1}, adding 17.2–17.5 and 1.7–1.6 Mg CO_2-eq. ha^{-1}) for soil carbon depletion and N_2O (Table 4). Compared with the P_{FN} and F_{FN} treatments, the $P_{ON75\%+DCD}$ considerably improved the net GWP, which was mostly due to the significant increase in soil carbon pool consumption. The lowest CEE was measured in F_0 treatment (1494 kg C ha^{-1}). Under different cultivation and nitrogen management measures, the maximum CEE (2648 kg C ha^{-1}) was measured under the $P_{ON75\%+DCD}$ treatment.

3.5. Area and Yield-Scaled GWP

GWP shows that there are considerable differences between different cultivation and nitrogen application measures (Table 5). Under the $P_{ON75\%+DCD}$ and $P_{ON75\%+NC}$ treatments, the regional scale GWP in 2019–2020 is significantly higher than all other treatments. The mean value of the area scale GWP of P_0, P_{FN}, P_{ON}, $P_{ON75\%+DCD}$, $P_{ON75\%+NC}$, F_{FN}, F_{ON}, $F_{ON75\%+DCD}$, and $F_{ON75\%+NC}$ has increased by 33.5% and 55.7%, 50.5%, 65.5%, 62.6%, 27.1%, 18.9%, 54.0%, and 49.3%, compared with F_0 treatment. The GWP indicated significant variation between various cultivation and nitrogen application measures (Table 5). During the two-year study, $P_{ON75\%+DCD}$ produced considerable maximum-scale GWP production compared to all other processes. The average value of the data indicated that the output scale GWP of P_{FN}, P_{ON}, $P_{ON75\%+DCD}$, $P_{ON75\%+NC}$, F_{FN}, F_{ON}, $F_{ON75\%+DCD}$, and $F_{ON75\%+NC}$ treatments increased by 26.7%, 86.9%, 73.8%, 94.4%, 82.5%, 8.3%, 47.6%, 79.2%, and 74.9% when compared with F_0 treatment.

Table 4. Characteristics of seasonal greenhouse gas fluxes, GWP, and GHGI in maize cropping fields under different treatments [a] during 2019–2020 growing seasons.

Treatments	GHG Flux (kg ha^{-1})			GWP (kg CO_2-eq ha^{-1})				GHGI
	CH_4	N_2O	NECB	CH_4	N_20	NECB	Net	(kg CO_2-eq kg^{-1} Grain)
2019								
P_0	1.0 d	4.5 b	−2482 i	21.3 f	1334 e	−8998 f	10,591 g	0.9 d
P_{FN}	1.8 c	5.2 a	−3833 e	37.3 e	1471 d	−13,955 d	15,604 e	1.9 c
P_{ON}	1.2 c	4.7 b	−3605 f	26.3 f	1431 d	−12,915 e	15,057 e	1.6 c
$P_{ON75\%+DCD}$	2.7 a	5.7 a	−4743 a	63.3 c	1707 a	−17,290 a	19,165 a	2.0 b
$P_{ON75\%+NC}$	2.2 b	5.5 a	−4665 b	48.3 d	1633 b	−17,003 a	18,750 b	1.8
F_0	1.6 c	4.3 b	−1129 j	42.3 d	1289 f	−4040 g	5944 h	1.2 c
F_{FN}	2.4 b	4.8 b	−3550 g	61.6 c	1409 d	−13,117 d	14,673 f	2.b
F_{ON}	2.1 b	4.5 b	−3324 h	45.9 d	1349 e	−12,086 e	13,787 g	1.6 c
$F_{ON75\%+DCD}$	3.3 a	5.1 a	−4135 c	84.1 a	1558 c	−15,060 b	17,054 c	3.3 a
$F_{ON75\%+NC}$	2.9 a	4.9 b	−4034 d	72.9 b	1528 c	−14,688 c	16,476 d	2.4 b
2020								
P_0	1.1 c	3.8 c	−2431 i	21.9	1158 e	−8821 h	10,270 f	1.0 e
P_{FN}	1.5 c	4.5 b	−3700 e	32.0	1349 c	−13,477 e	15,036 c	1.9 d
P_{ON}	1.3 c	4.1 b	−3497 g	31.2	1230 d	−12,728 f	14,993 d	1.5 d
$P_{ON75\%+DCD}$	2.4 b	5.8 a	−4822 a	64.5	1695 a	−17,578 a	19,279 a	2.4 c
$P_{ON75\%+NC}$	2.1 b	5.4 a	−4658 b	51.3	1621 a	−16,988 b	19,029 a	2.0 c
F_0	1.4 c	3.7 c	−1161 j	33.6	1111 e	−4165 i	5913 g	1.7 d
F_{FN}	3.3 a	4.2 b	−3598 f	83.0	1278 d	−13,102 e	14,400 d	3.0 b
F_{ON}	1.7 c	4.0 b	−3043 h	43.4	1218 d	−11,056 g	12,517 e	2.4 c
$F_{ON75\%+DCD}$	3.9 a	4.9 b	−4128 c	98.0	1546 b	−15,045 c	17,033 b	4.5 a
$F_{ON75\%+NC}$	3.6 a	4.5 b	−3933 d	90.5	1356 c	−14,317 d	15,898 c	3.1 b

Table 5. Effects of different treatments [a] on area and yield-scaled GWP, biomass yield, grain yield, evapotranspiration (ET), water use efficiency (WUE), and nitrogen use efficiency (NUE) of maize during 2019–2020 growing seasons.

Treatments	Area-Sealed GWP (kg CO_2-eq ha^{-1})	Yield-Sealed GWP (kg CO_2-eq kg^{-1})	Biomass Yield (t ha^{-1})	Grain Yield (t ha^{-1})	ET (mm)	WUE (kg ha^{-1} mm^{-1})	NUE (kg kg^{-1})
2019							
P_0	170.9 f	0.05 e	14.5 e	6.8 e	274.5 e	24.8 b	--
P_{FN}	242.7 d	0.13 d	16.7 c	9.2 b	409.0 a	22.5 c	8.28 e
P_{ON}	221.4 e	0.17 d	16.0 c	7.8 d	339.6 d	23.0 c	4.35 f
$P_{ON75\%+DCD}$	308.9 a	0.76 a	19.9 a	11.1 a	382.3 b	29.0 a	24.93 a
$P_{ON75\%+NC}$	294.4 b	0.28 c	18.3 b	9.9 b	373.7 b	26.5 b	17.97 c
F_0	129.4 h	0.03 e	12.7 g	6.1 f	328.4 d	18.6 d	--
F_{FN}	150.2 g	0.04 e	14.4 e	7.3 d	436.9 a	16.7 e	4.14 f
F_{ON}	148.4 g	0.06 e	13.5 f	6.9 e	361.3 c	19.1 d	3.48 f
$F_{ON75\%+DCD}$	275.8 c	0.44 b	16.7 c	9.8 b	378.6 b	25.9 b	21.45 b
$F_{ON75\%+NC}$	231.4 d	0.21 c	15.3 d	8.3 c	364.9 c	22.7 c	12.75 d
2020							
P_0	160.3 f	0.10 d	15.1 f	6.4 f	251.5 e	25.4 b	--
P_{FN}	262.4 c	0.71 b	17.6 c	9.3 c	452.6 a	20.5 c	10.00 e
P_{ON}	230.3 d	0.25 c	15.8 e	7.7 e	342.2 c	22.5 c	5.65 g
$P_{ON75\%+DCD}$	339.8 a	1.19 a	20.7 a	11.3 a	405.7 b	27.9 a	28.41 a
$P_{ON75\%+NC}$	303.8 b	0.35 c	19.0 b	10.7 b	386.0 b	27.7 a	24.93 b
F_0	94.3 h	0.08 d	14.4 g	6.0 g	292.2 d	20.5 c	--
F_{FN}	156.8 f	0.15 d	17.0 c	7.9 e	495.9 a	15.9 e	6.55 g
F_{ON}	127.3 g	0.09 d	16.3 d	6.9 f	388.1 b	17.8 d	3.91 h
$F_{ON75\%+DCD}$	211.0 e	0.23 c	17.4 c	9.8 c	464.4 a	21.1 c	22.03 c
$F_{ON75\%+NC}$	209.6 e	0.35 c	16.5 d	8.4 d	448.6 a	18.8 d	14.17 d

3.6. Resources Use Efficiencies, Carbon Efficiency Ratio (CER), and Maize Production

During 2019–2020, different cultivation and nitrogen management practices have considerably enhanced biomass and grain yield, as well as CER and resource use efficiencies (Table 5). Compared with the F_0 treatment, the $P_{ON75\%+DCD}$ treatment significantly enhanced (41.0%) the biomass yield. The mean biomass yield was significantly enhanced in the P_0, P_{FN}, P_{ON}, $P_{ON75\%+DCD}$, $P_{ON75\%+NC}$, F_{FN}, F_{ON}, $F_{ON75\%+DCD}$, and $F_{ON75\%+NC}$ treatments by 2.8%, 19.1%, 10.4%, 41.0%, 29.5%, 5.9%, 14.7%, 13.5%, and 14.6% compared to that of the F_0 treatment. The CER was the maximum (0.99) in the $P_{ON75\%+DCD}$ treatment, followed by the $P_{ON75\%+NC}$ treatment (0.94), and then under the P_{FN} treatment (0.93). The lowest (0.71) CER was recorded in the F_0 treatment. Compared with the F_0, the mean grain yield with P_0, P_{FN}, P_{ON}, $P_{ON75\%+DCD}$, $P_{ON75\%+NC}$, F_{FN}, F_{ON}, $F_{ON75\%+DCD}$, and $F_{ON75\%+NC}$ treatments was significantly increased by 0.8%, 39.1%, 16.5%, 68.4%, 54.9%, 11.3%, 25.6%, 36.1%, and 27.0%, respectively (Table 5). The data showed that WUE with P_0, P_{FN}, P_{ON}, $P_{ON75\%+DCD}$, $P_{ON75\%+NC}$, F_{FN}, F_{ON}, $F_{ON75\%+DCD}$, and $F_{ON75\%+NC}$ treatments were considerably improved by 34.8%, 15.6%, 22.1%, 52.7%, 45.6%, 5.9%, 17.2%, 17.7%, and 1.1%, compared with F_0 treatment. While the NUE with P_{FN}, P_{ON}, $P_{ON75\%+DCD}$, and $P_{ON75\%+NC}$ treatments were significantly enhanced by 41.5%, 26.1%, 18.5%, and 37.2%, respectively, compared with F_{FN}, F_{ON}, $F_{ON75\%+DCD}$, and $F_{ON75\%+NC}$.

4. Discussion

4.1. Effects of N management Practices on ET and SWS

Mulching with different nitrogen management practices is usually used as a useful cultivation technique to enhance rain-fed maize yields by increasing soil moisture conditions [10]. In contrast, mulching with different nitrogen management measures significantly increased greenhouse gas emissions [24] and consumed soil carbon pools [39,40]. The use of plastic mulching and different nitrogen management measures to enhance crop production is still under debate. $P_{ON75\%+DCD}$ treatment can decrease drought. In the $P_{ON75\%+DCD}$ treatment, the SWS of maize was considerably higher than in the $F_{ON75\%+DCD}$ treatment. A number of studies have shown that nitrogen application can increase soil absorption of water and nitrogen content [41]. Unnecessary fertilizer use may lead to high water efficiency [11]. There is a positive correlation between crop yield and field evapotranspiration [5]. Ma et al. [42] revealed a considerable improvement in the ET due to low N supply and high soil water availability. In our research, we found that compared with F_{FN} and P_{FN} treatments, $P_{ON75\%+DCD}$ and $P_{ON75\%+NC}$ treatments with different nitrogen management measures resulted in lower total ET due to maximum soil evaporation. Oenema et al. [43] reported that, compared to the control plot, the plastic film with a low N level maintained maximum water conditions with a low total ET.

4.2. Effects of N management Practices on Greenhouse Gas Emissions

Changes in soil water storage and humidity conditions caused by mulching affected soil microbial populations and activities [44], the mineralization process [27], and soil absorption of CH_4 [45]. Regarding the CH_4 emission under the cover of plastic film, Tan et al. [46] all believe that plastic film covering reduces CH_4 absorption or increases CH_4 emissions. However, in our research, corn fields are used as sinks for CH_4 emissions. Soil carbon has a greater role in regulating the CO_2 flux from the soil and other climatic factors that favor microbial processes [47]. The increase in temperature under the film cover can stimulate microbial activity, thereby accelerating organic matter decomposition [48,49], which explains the increase in CO_2 flux. Compared with the F_{FN} treatment, the CO_2 emissions of the $F_{ON75\%+DCD}$ and $F_{ON75\%+NC}$ treatments were significantly greater. The N_2O emission is significantly lower under the F_0 treatment. Under the $P_{ON75\%+DCD}$ and $P_{ON75\%+NC}$ treatments, the N_2O emissions are significantly increased compared to the P_{FN} and F_{FN} treatments, which is consistent with the findings of Ma et al. [18]. Li et al. [50] also pointed out that DCD is more effective in suppressing early N_2O emissions from paddy

fields. Other studies report that adding DCD to nitrogen fertilizer cannot only reduce soil N_2O emissions by 39% [51] but also significantly reduce N_2O emissions from rice fields [50].

4.3. Effects of N management Practices on GWP, GHGI, and CMI

The MBC ranges from 113.7 to 414.6 mg kg^{-1}. Under the $P_{ON75\%+DCD}$ treatment, the accumulation of MBC was significantly higher (400.3 mg kg^{-1}) compared to other treatments. Compared with F_0 treatment, the application of $P_{ON75\%+DCD}$ treatment showed a significant increase of 67% in MBC, respectively. Compared to other treatments, the $P_{ON75\%+DCD}$ treatment considerably improved the TC content (5.08 g kg^{-1}). The content of easily mineralizable carbon (RMC) was the highest in the plots treated with $P_{ON75\%+DCD}$ and $P_{ON75\%+NC}$ (177.7–137.9 mg kg^{-1}) and the lowest under the F_0 treatment (25.5 mg kg^{-1}). The microbial biomass in the soil is often dynamic when nutrient utilization is limited [52]. In this case, with the enhancement of SOC mineralization, the net soil carbon loss increases. Due to the limited availability of nitrogen and net immobilization, straw with a high C:N ratio tends to slowly decompose [53]. It was found that the total N under the $P_{ON75\%+DCD}$ and $P_{ON75\%+NC}$ treatments was significantly higher (0.61–0.57 g kg^{-1}) than that of all other treatments. Compared with the $F_{ON75\%+DCD}$ and $F_{ON75\%+NC}$ treatments, the C:N ratio was significantly higher (8.55–8.37) under the $P_{ON75\%+DCD}$ and $P_{ON75\%+NC}$ treatments. A single or combined application of inorganic fertilizers may produce more unstable carbon, which can be used as a source of nutrients [29]. The CMI was considerably improved by 31.2%, 10.2%, 11.4%, 10.8%, 10.8%, and 13.4% under the treatments of P_0, P_{FN}, P_{ON}, $P_{ON75\%+DCD}$, and $P_{ON75\%+NC}$, which was higher than that of F_0, F_{FN}, F_{ON}, $F_{ON75\%+DCD}$, and $F_{ON75\%+NC}$ treatments. These planting method data are similar to those reported by Whitbread et al. [54].

4.4. Effects of N management Practices on Resource Use Efficiency and Maize Production

The (NO_3^--N) under F_0 treatment was significantly lower than all other treatments. Under the treatments of $P_{ON75\%+DCD}$ and $P_{ON75\%+NC}$, (NO_3^--N) significantly increased compared with PFN and FFN treatments. Compared with F0, the NH_4^+-N of all other treatments was significantly increased, while the NH_4^+-N of the $P_{ON75\%+DCD}$ and $P_{ON75\%+NC}$ treatments had no significant changes under the two cultivation methods. This may be due to the inhibitory effect of DCD on ammonia-oxidizing bacteria and related enzymes, effectively delaying the oxidation process of NH_4^+-N to NO_3^--N [37,55]. By adjusting the rapid conversion of soil nitrogen and maintaining a high soil NH_4^+-N, the accumulation and leaching loss of NO_3^--N can be effectively reduced, and N_2O emissions can be reduced [56]. Considering that nitrogen management practices and mulching films are widely used in arid regions [57]. The GWP data on the agricultural system can provide information on the impact of agricultural practices on climate change [3]. In our research, the treatments of $P_{ON75\%+DCD}$ and $P_{ON75\%+NC}$ with mulching film significantly reduced GHGI compared to traditional flat-land cultivation because the yield of corn was greatly increased. GHGI is a potential barometer to compare the impact of global warming on agricultural management and crop yields [48]. This increase in GHGI is mainly due to the massive consumption of soil carbon storage rather than an improvement in GHGI. Current research has indicated that improving crop yields can effectively reduce GHGI [58]. Compared with the P_{FN} and F_{FN} treatments, the $P_{ON75\%+DCD}$ treatment improved the net GWP, which was mainly due to the significant increase in soil carbon pool consumption. Current research has shown that increasing corn yield can decrease GHGI [49].

Compared with the F_0 treatment, the $P_{ON75\%+DCD}$ treatment significantly increased (41.0%) biomass yield. Plastic mulching with reasonable nitrogen application effectively utilizes rainfall; therefore, compared with flat planting, it increases grain yield with a higher WUE [59]. Compared with F_0 treatment, the average grain yield of P_0, P_{FN}, P_{ON}, $P_{ON75\%+DCD}$, $P_{ON75\%+NC}$, F_{FN}, F_{ON}, $F_{ON75\%+DCD}$, and $F_{ON75\%+NC}$ treatments was significantly increased by 0.8%, 39.1%, 16.5%, 68.4%, 54.9%, 11.3%, 25.6%, 36.1%, and 27.0%. WUE shows the link between water use and crop productivity. Liu et al. [37] also investigated

that the optimum fertilizers under plastic mulching increased grain yield and reduced the ET; therefore, the rainwater with high WUE and NUE was effectively used. Soil fertility status considerably affects resource utilization efficiencies. Low N levels result in higher NUE, while high N levels result in lower NUE [60]. Taking into account the impact on greenhouse gas emission reduction, corn yield response, and greenhouse gas emission factors, $P_{ON75\%+DCD}$ treatment can be suggested as the preferred cultivation and nitrogen management practice for increasing yield and coping with climate change.

5. Conclusions

In a semi-arid agricultural ecosystem, the application of plastic mulch under the ridge cropping system reduces the optimal N + dicyandiamide by 25%, resulting in soil carbon buildup and increased corn yield. The results showed that compared to other treatments, $P_{ON75\%+DCD}$ significantly increased SWS, WUE, and NUE because the total ET and GHG emissions were reduced. Under $P_{ON75\%+DCD}$ or $P_{ON75\%+NC}$, the soil carbon storage significantly increased. The $P_{ON75\%+DCD}$ treatment is more effective in improving MBC, CMI, and WSC, although it increases gaseous carbon emissions more than all other treatments. Compared with FFN, under the $P_{ON75\%+DCD}$ treatment, the overall CH_4, N_2O, and CO_2 emissions are all reduced. Under the $P_{ON75\%+DCD}$ treatment, the area scale GWP (52.7%), yield scale GWP (90.3%), biomass yield (22.7%), WUE (42.6%), NUE (80.0%), and grain yield (32.1%) are improved instead of FFN, which might offset the negative ecological impacts. The $P_{ON75\%+DCD}$ treatment can bring obvious benefits in terms of increasing yield, reducing global warming, and maintaining soil health.

Author Contributions: H.R. conceived and designed the experiments. H.R., S.X., F.Z., M.S. and R.Z. performed the experiments. H.R. and S.X. analyzed the data and wrote the manuscript. All authors have read and agreed to the published version of the manuscript.

Funding: Scientific Research Business Expenses of Heilongjiang Scientific Research Institutes (Grant No. CZKYF2022-1-B024; Grant No. CZKYF2022-1-C008).

Data Availability Statement: Data will be available upon personal request.

Conflicts of Interest: The authors declare no conflict of interest.

References

1. Sintim, H.Y.; Flury, M. Is biodegradable plastic mulch the solution to agriculture's plastic problem? *Environ. Sci. Technol.* **2017**, *51*, 1068–1069. [CrossRef] [PubMed]
2. Brodhagen, M.; Goldberger, J.R.; Hayes, D.G.; Inglis, D.A.; Marsh, T.L.; Miles, C. Policy considerations for limiting unintended residual plastic in agricultural soils. *Environ. Sci. Pol.* **2017**, *69*, 81–84. [CrossRef]
3. IPCC. Technical summary. In *Climate Change: The Physical Science Basis. Contribution of Working Group 1 to the Forth Assessment Report of the Inter-Governmental Panel on Climate Change*; Solomon, S., Qin, D., Manning, M., Chen, Z., Marquis, M., Averyt, K.B., Tignor, M., Miller, H.L., Eds.; Cambridge University Press: Cambridge, UK, 2007.
4. Adhikari, R.; Bristow, K.L.; Casey, P.S.; Freischmidt, G.; Hornbuckle, J.W.; Adhikari, B. Preformed and sprayable polymeric mulch film to improve agricultural water use efficiency. *Agric. Water Manag.* **2016**, *169*, 1–13. [CrossRef]
5. Chen, H.; Zhao, Y.; Feng, H.; Liu, J.; Si, B.; Feng, H.; Zhang, A.; Chen, J.; Cheng, G.; Sun, B.; et al. Effects of straw and plastic film mulching on greenhouse gas emissions in Loess Plateau, China: A field study of 2 consecutive wheat-maize rotation cycles. *Sci. Total Environ.* **2017**, *579*, 814–824. [CrossRef] [PubMed]
6. Huang, S.; Lv, W.; Bloszies, S.; Shi, Q.; Pan, X.; Zeng, Y. Effects of fertilizer management practices on yield-scaled ammonia emissions from croplands in China: A meta-analysis. *Field Crops Res.* **2016**, *192*, 118–125. [CrossRef]
7. Ju, X.; Zhang, C. Nitrogen cycling and environmental impacts in upland agri- cultural soils in North China: A review. *J. Integr. Agric.* **2017**, *16*, 2848–2862. [CrossRef]
8. Ju, X.; Xing, G.X.; Chen, X.P.; Zhang, S.L.; Zhang, L.J.; Liu, X.J.; Cui, Z.L.; Yin, B.; Christie, P.; Zhu, Z.L.; et al. Reducing environmental risk by improving N man- agement in intensive Chinese agricultural systems. *Proc. Natl. Acad. Sci. USA* **2009**, *106*, 3041–3046. [CrossRef]
9. Ma, Z.; Gao, X.; Tenuta, M.; Kuang, W.; Gui, D.; Zeng, F. Urea fertigation sources affect nitrous oxide emission from a drip-fertigated cotton field in northwestern China. *Agric. Ecosyst. Environ.* **2018**, *265*, 22–30. [CrossRef]
10. Lee, J.G.; Hwang, H.Y.; Park, M.H.; Kim, P.J. Depletion of soil organic carbon stocks are larger under plastic film mulching for maize. *Eur. J. Soil. Sci.* **2019**, *70*, 807–818. [CrossRef]

11. Purakayastha, T.J.; Rudrappa, L.; Singh, D.; Swarup, A.; Bhadraray, S. Long-term impact of fertilizers on soil organic carbon pools and sequestration rates in maize–wheat–cowpea cropping system. *Geoderma* **2008**, *144*, 370–378. [CrossRef]
12. Ju, X.; Gu, B.; Wu, Y.; Galloway, J.N. Reducing China's fertilizer use by increasing farm size. *Glob Environ. Chang. Part A* **2016**, *41*, 26–32. [CrossRef]
13. Xiong, Z.Q.; Xing, G.X.; Tsuruta, H.; Shen, G.Y.; Shi, S.L.; Du, L.J. Measurement of nitrous oxide emissions from two rice-based cropping systems in China. *Nutr. Cycl. Agroe* **2002**, *64*, 125–133. [CrossRef]
14. Bhattacharyya, T.; Pal, D.K.; Easter, M.; Batjes, N.H.; Milne, E.; Gajbhiye, K.S.; Chandran, P.; Ray, S.K.; Mandal, C.; Paustian, K.; et al. Modeled soil organic carbon stocks and changes in the Indo-Gangetic Plains, India from 1980 to 2030. *Agric. Ecosyst. Environ.* **2007**, *122*, 84–94. [CrossRef]
15. Chen, J.; Wang, P.; Ma, Z.; Lyu, X.; Liu, T.; Siddique, K.H.M. Optimum water and nitrogen supply regulates root distribution and produces high grain yields in spring wheat (*Triticum aestivum* L.) under permanent raised bed tillage in arid northwest China. *Soil Tillage Res.* **2018**, *181*, 117–126. [CrossRef]
16. Zhou, J.; Li, B.; Xia, L.; Fan, C.; Xiong, Z. Organic-substitute strategies reduced carbon and reactive nitrogen footprints and gained net ecosystem economic benefit for intensive vegetable production. *J. Clean. Prod.* **2019**, *225*, 984–994. [CrossRef]
17. Gong, W.; Yan, X.Y.; Wang, J.Y.; Hu, T.X.; Gong, Y.B. Long-term manuring and fertilization effects on soil organic carbon pools under a wheat–maize cropping system in North China Plain. *Plant Soil* **2009**, *314*, 67–76. [CrossRef]
18. Ma, Z.; Chen, J.; Lyu, X.; Liu, L.; Siddique, K.H.M. Distribution of soil carbon and grain yield of spring wheat under a permanent raised bed planting system in an arid area of northwest China. *Soil Tillage Res.* **2016**, *163*, 274–281. [CrossRef]
19. Bhatia, A.; Sasmal, S.; Jain, N.; Pathak, H.; Kumar, R.; Singh, A. Mitigating nitrous oxide emission from soil under conventional and no-tillage in wheat using nitrification inhibitors. *Agric. Ecosyst. Environ.* **2010**, *136*, 247–253. [CrossRef]
20. Chalk, P.M.; Craswell, E.T.; Polidoro, J.C.; Chen, D. Fate and efficiency of 15N- labelled slow- and controlled-release fertilizers. *Nutr. Cycl. Agroecosyst.* **2015**, *102*, 167–178. [CrossRef]
21. Asing, J.; Saggar, S.; Singh, J.; Bolan, N.S. Assessment of nitrogen losses from urea and an organic manure with and without nitrification inhibitor, dicyandiamide, applied to lettuce under glasshouse conditions. *Aust. J. Soil Res.* **2008**, *46*, 535–541. [CrossRef]
22. Huang, J.X.; Chen, Y.Q.; Liu, W.R.; Zheng, H.B.; Sui, P.; Li, Y.Y.; Shi, X.P.; Nie, S.W.; Gao, W.S. Effect on net greenhouse gases emission under different conservation tillages in Jilin province. *Sci. Agric. Sin.* **2011**, *44*, 2935–2942. (In Chinese)
23. Abalos, D.; Sanz-Cobena, A.; Garcia-Torres, L.; van Groenigen, J.W.; Vallejo, A. Role of maize stover incorporation on nitrogen oxide emissions in a non-irrigated Mediterranean barley field. *Plant Soil* **2013**, *364*, 357–371. [CrossRef]
24. Liu, J.; Zhu, L.; Luo, S.; Bu, L.; Chen, X.; Yue, S.; Li, S. Response of nitrous oxide emission to soil mulching and nitrogen fertilization in semi-arid farmland. *Agric. Ecosyst. Environ.* **2014**, *188*, 20–28. [CrossRef]
25. Nie, W.J.; Li, B.W.; Guo, Y.J.; Wang, X.M.; Han, X.L. Effects of nitrogen fertilizer and DCD application on ammonia volatilization and nitrous oxide emission from soil with cucumber growing in greenhouse. *Acta Sci. Circumstantiae* **2012**, *32*, 2500–2508. (In Chinese)
26. Wiesmeier, M.; Urbanski, L.; Hobley, E.; Lang, B.; von Lützow, M.; Marin-Spiotta, E.; van Wesemael, B.; Rabot, E.; Lie, M.; Garcia-Franco, N.; et al. Soil organic carbon storage as a key function of soils—A review of drivers and indicators at various scales. *Geoderma* **2019**, *333*, 149–162. [CrossRef]
27. Wang, Z.; Wang, Z.; Luo, Y.; Zhan, Y.N.; Meng, Y.L.; Zhou, Z.G. Biochar increases 15N fertilizer retention and indigenous soil N uptake in a cotton-barley rotation system. *Geoderma.* **2020**, *357*, 113944. [CrossRef]
28. Linquist, B.A.; Liu, L.; van Kessel, C.; van Groenigen, K.J. Enhanced efficiency nitrogen fertilizers for rice systems: Meta-analysis of yield and nitrogen uptake. *Field Crops Res.* **2013**, *154*, 246–254. [CrossRef]
29. Bayer, C.; Gomes, J.; Zanatta, J.A.; Vieira, F.C.B.; Piccolo, M.D.C.; Dieckow, J.; Six, J. Soil nitrous oxide emissions as affected by long-term tillage, cropping systems and nitrogen fertilization in Southern Brazil. *Soil Tillage Res.* **2015**, *146*, 213–222. [CrossRef]
30. Vance, E.D.; Brookes, P.C.; Jenkinson, D.S. An extraction method for measuring soil microbial biomass carbon. *Soil. Biol. Bioch* **1987**, *19*, 703–707. [CrossRef]
31. Inubushi, K.; Brookes, P.C.; Jenkinson, D.S. Soil microbial biomass C, N and ninhydrin-N in aerobic and anaerobic soils measured by fumigation-extraction method. *Soil Biol. Bioch.* **1991**, *23*, 737–741. [CrossRef]
32. Witt, C.; Gaunt, J.L.; Galicia, C.C.; Ottow, J.C.G.; Neue, H.U. A rapid chloro- form fumigation–extraction method for measuring soil microbial biomass carbon and nitrogen in flooded rice soils. *Biol. Fertil. Soils* **2000**, *30*, 510–519. [CrossRef]
33. Angers, D.A.; Mehuys, G.R. Effect of cropping on carbohydrate content and water-stable aggregation of a clay soil. *Canadian J. Soil Sci.* **1989**, *69*, 373–380. [CrossRef]
34. Badalucco, L.; Grego, S.; Dell'Orco, S.; Nannipieri, P. Effect of liming on some chemical, biochemical, and microbiological properties of acid soils under spruce (*Picea abies* L.). *Biol. Fertil. Soils* **1992**, *14*, 76–83. [CrossRef]
35. Haynes, R.J.; Swift, R.S. Stability of soil aggregates in relation to organic constituents and soil water content. *J. Soil Sci.* **1990**, *41*, 73–83. [CrossRef]
36. Blair, G.J.; Lefroy, R.D.B.; Lisle, L. Soil carbon fractions based on their degree of oxidation, and the development of a carbon management index for agricultural systems. *Aust. J. Agric. Res.* **1995**, *46*, 1459–1466. [CrossRef]
37. Liu, Y.; Li, Y.; Peng, Z.; Wang, Y.; Ma, S.; Guo, L.; Lin, E.; Han, X. Effects of different nitrogen fertilizer management practices on wheat yields and N2O emissions from wheat fields in North China. *J. Integr. Agric.* **2015**, *14*, 1184–1191. [CrossRef]

38. Wang, Z.; Zhang, W.; Peng, Z.; Beebout, S.S.; Liu, L.; Yang, J.; Zhang, J. Grain yield, water and nitrogen use efficiencies of rice as influenced by irrigation regimes and their interaction with nitrogen rates. *Field Crops Res.* **2016**, *193*, 54–69. [CrossRef]
39. Fan, X.; Zhang, J.; Wu, P. Water and nitrogen use efficiency of lowland Rice in ground covering rice production system in South China. *J. Plant. Nutr.* **2002**, *25*, 1855–1862. [CrossRef]
40. Guo, Y.J.; Di, H.J.; Cameron, K.C.; Li, B.; Podolyan, A.; Moir, J.L.; Monaghan, R.M.; Smith, L.C.; O'Callaghan, M.; Bowatte, S.; et al. Effect of 7-year application of anitrification inhibitor, dicyandiamide (DCD), on soil microbial biomass, protease and deaminase activities, and the abundance of bacteria and archaea in pasture soils. *J. Soils Sediments* **2013**, *13*, 753–759. [CrossRef]
41. Kumar, A.; Nayak, A.K.; Mohanty, S.; Das, B.S. Greenhouse gas emission from direct seeded paddy fields under different soil water potentials in Eastern India. *Agric. Ecosyst. Environ.* **2016**, *228*, 111–123. [CrossRef]
42. Ma, Y.C.; Kong, X.W.; Yang, B.; Zhang, X.L.; Yan, X.Y.; Yang, J.C.; Xiong, Z.Q. Net global warming potential and greenhouse gas intensity of annual rice–wheat rota-tions with integrated soil–crop system management. *Agric. Ecosyst. Environ.* **2013**, *164*, 209–219. [CrossRef]
43. Oenema, O.; Wrage, N.; Velthof, G.L.; Groenigen, J.W.; Dolfing, J.; Kuikman, P.J. Trends in global nitrous oxide emissions from animal production systems. *Nutr. Cycl. Agroecosyst.* **2005**, *72*, 51–65. [CrossRef]
44. Yagioka, A.; Komatsuzaki, M.; Kaneko, N.; Ueno, H. Effect of no-tillage with weed cover mulching versus conventional tillage on global warming potential and nitrate leaching. *Agric. Ecosyst. Environ.* **2015**, *200*, 42–53. [CrossRef]
45. Singh, K.P.; Ghoshal, N.; Singh, S. Soil carbon dioxide flux, carbon seques- tration and crop productivity in a tropical dryland agroecosystem: Influence of organic inputs of varying resource quality. *Appl. Soil Ecol.* **2009**, *42*, 243–253. [CrossRef]
46. Tan, Y.; Xu, C.; Liu, D.; Wu, W.; Lal, R.; Meng, F. Effects of optimized N fertilization on greenhouse gas emission and crop production in the North China Plain. *Field Crops Res.* **2017**, *205*, 135–146. [CrossRef]
47. Ding, W.X.; Yu, H.Y.; Cai, Z.C. Impact of urease and nitrification inhibitors on nitrous oxide emissions from fluvo- aquic soil in the North China Plain. *Biol. Fertil. Soils* **2011**, *47*, 91–99. [CrossRef]
48. Cuello, J.P.; Hwang, H.Y.; Gutierrez, J.; Kim, S.Y.; Kim, P.J. Impact of plastic film mulching on increasing greenhouse gas emissions in temperate upland soil during maize cultivation. *Appl. Soil Ecol.* **2015**, *91*, 48–57. [CrossRef]
49. Lam, S.K.; Chen, D.; Norton, R.; Armstrong, R.; Mosier, A.R. Influence of elevated atmospheric carbon dioxide and supplementary irrigation on greenhouse gas emis- sions from a spring wheat crop in southern Australia. *J. Agric. Sci.* **2013**, *151*, 201–208. [CrossRef]
50. Li, Q.; Li, H.; Zhang, L.; Zhang, S.; Chen, Y. Mulching improves yield and water-use efficiency of potato cropping in China: A meta-analysis. *F. Crop. Res.* **2018**, *221*, 50–60. [CrossRef]
51. Li, F.M.; Song, Q.H.; Jemba, P.K.; Shi, Y.C. Dynamics of soil microbial biomass C and soil fertility in cropland mulched with plastic film in a semiarid agro-ecosystem. *Soil Biol. Bioch.* **2004**, *36*, 1893–1902. [CrossRef]
52. Fontaine, S.; Bardoux, G.; Abbadie, L.; Mariotti, A. Carbon input to soil may decrease soil carbon content. *Ecol. Lett.* **2004**, *7*, 314–320. [CrossRef]
53. Khalil, M.I.; Boeckx, P.; Rosenani, A.B.; Cleemput, O.V. Nitrogen transformations and emission of greenhouse gases from three acid soils of humid tropics amended with N sources and moisture regime. II. Nitrous oxide and methane fluxes. *Commun. Soil Sci. Plant Anal.* **2001**, *32*, 2909–2924. [CrossRef]
54. Whitbread, A.M.; Lefroy, R.D.B.; Blair, G.J. A survey of the impact of cropping on soil physical and chemical properties in north-western New South Wales. *Aust. J. Soil Res.* **1998**, *36*, 669–681. [CrossRef]
55. Di, H.J.; Cameron, K.C.; Shen, J.P.; He, J.Z.; Winefield, C.S. Alysimeter study of nitrate leaching from grazed grassland as affected by a nitrification inhibitor, dicyandiamide, and relationships with ammonia oxidizing bacteria and archaea. *Soil Use Manag.* **2009**, *25*, 454–461. [CrossRef]
56. Manna, M.C.; Swarup, A.; Wanjari, R.H.; Ravankar, H.N. Long-term effect of NPK fertiliser and manure on soil fertility and a sorghum–wheat farming system. *Aust. J. Exp. Agric.* **2007**, *47*, 700–711. [CrossRef]
57. Gaihre, Y.K.; Singh, U.; Islam, S.M.; Huda, A.; Islam, M.R.; Satter, M.A.; Sanabria j Islam, M.R.; Shah, A.L. Impacts of urea deep placement on nitrous oxide and nitric oxide emissions from rice fields in Bangladesh. *Geoderma.* **2015**, *259*, 370–379. [CrossRef]
58. Abdallah, M.; Osborne, B.; Lanigan, G.; Forristal, D.; Williams, M.; Smith, P.; Jones, M.B. Conservation tillage systems: A review of its consequences for greenhouse gas emissions. *Soil Use Manag.* **2013**, *29*, 199–209. [CrossRef]
59. Ren, X.L.; Jia, Z.K.; Chen, X.L. Rainfall concentration for increasing corn production under semiarid climate. *Agric. Water Manag.* **2008**, *95*, 1293–1302. [CrossRef]
60. Hu, N.; Wang, B.; Gu, Z.; Tao, B.; Zhang, Z.; Hu, S.; Zhu, L.; Meng, Y. Effects of different straw returning modes on greenhouse gas emissions and crop yields in a rice–wheat rotation system. *Agric. Ecosyst. Environ.* **2016**, *223*, 115–122. [CrossRef]

land

MDPI

Article

Salicylic Acid and Pyraclostrobin Can Mitigate Salinity Stress and Improve Anti-Oxidative Enzyme Activities, Photosynthesis, and Soybean Production under Saline–Alkali Regions

Honglei Ren [1,†], Xueyang Wang [1,†], Fengyi Zhang [1], Kezhen Zhao [1], Xiulin Liu [1], Rongqiang Yuan [1], Changjun Zhou [2], Jidong Yu [2], Jidao Du [3], Bixian Zhang [1,*] and Jiajun Wang [1,*]

[1] Soybean Research Institute, Northeastern Precocious Soybean Scientific Observation Station of Ministry of Agriculture and Rural Affairs, Heilongjiang Academy of Agriculture Sciences, Harbin Branch of National Soybean Improvement Center, Harbin 150086, China; midou@haas.cn (H.R.); hljsnkywxy@163.com (X.W.); ddszhangfy2019@163.com (F.Z.); zhaokz928@163.com (K.Z.); liuxiulin1002@126.com (X.L.); yrq18846121189@163.com (R.Y.)

[2] Daqing Branch of Heilongjiang Academy of Agricultural Sciences, Daqing 163316, China; andazhouchangjun@163.com (C.Z.); yujidong666@126.com (J.Y.)

[3] Key Laboratory of Soybean Mechanized Production, Ministry of Agriculture and Rural Affairs, College of Agriculture, Heilongjiang Bayi Agricultural University, Daqing 163319, China; djdbynd@163.com

* Correspondence: hljsnkyzbx@163.com (B.Z.); junjiawang@163.com (J.W.)

† These authors contributed equally to this work.

Abstract: Soybean is a widespread crop in semi-arid regions of China, where soil salinity often increases and has a significant harmful impact on production, which will be a huge challenge in the coming years. Salicylic acid (SA) and pyraclostrobin are strobilurin-based bactericides (PBF). Under rainfall-harvesting conditions in covered ridges, the exogenous application of SA and PBF can improve the growth performance of soybeans, thereby reducing the adverse effects of soil salinity. The objectives of this research are to evaluate the potential effects of SA and PBF on soybean growth in two different regions, Harbin and Daqing. A two-year study was performed with the following four treatments: HCK: Harbin location with control; SA1+PBF1: salicylic acid (5 mL L^{-1}) with pyraclostrobin (3 mL L^{-1}); SA2+PBF2: salicylic acid (10 mL L^{-1}) with pyraclostrobin (6 mL L^{-1}); DCK: Daqing location with control. The results showed that in the Harbin region, SA2+PBF2 treatment reduced the evapotranspiration (ET) rate, increased soil water storage (SWS) during branching and flowering stages, and achieved a maximum photosynthesis rate. Moreover, this improvement is due to the reduction of MDA and oxidative damage in soybean at various growth stages. At different growth stages, the treatment of Harbin soybean with SA2+PBF2 significantly increased the activity of CAT, POD, SOD, and SP, while the content of MDA, H_2O_2, and O_2^- also decreased significantly. In the treatment of SA2+PBF2 in Harbin, the scavenging ability of free H_2O_2 and O_2^- was higher, and the activity of antioxidant enzymes was better. This was due to a worse level of lipid-peroxidation which successfully protected the photosynthesis mechanism and considerably increased water use efficiency (WUE) (46.3%) and grain yield (57.5%). Therefore, using plastic mulch with SA2+PBF2 treatment can be an effective water-saving management strategy, improving anti-oxidant enzyme activities, photosynthesis, and soybean production.

Keywords: soil salinity; salicylic acid; anti-oxidant metabolism; photosynthesis; reactive oxygen species; soybean production

Citation: Ren, H.; Wang, X.; Zhang, F.; Zhao, K.; Liu, X.; Yuan, R.; Zhou, C.; Yu, J.; Du, J.; Zhang, B.; et al. Salicylic Acid and Pyraclostrobin Can Mitigate Salinity Stress and Improve Anti-Oxidative Enzyme Activities, Photosynthesis, and Soybean Production under Saline–Alkali Regions. *Land* **2023**, *12*, 1319. https://doi.org/10.3390/land12071319

Academic Editors: Shahzad Ali, Qianmin Jia, Jiahua Zhang and Sajid Ali

Received: 13 June 2023
Revised: 24 June 2023
Accepted: 25 June 2023
Published: 30 June 2023

1. Introduction

High salinity is one of the key non-biotic stresses that leads to the decline of agricultural production [1]. Given the cultivation of soybeans in the dry-land farming systems, this issue is particularly important [2]. By 2050, 50% of farming land may be affected by salinity [3]. Especially, the threat of salinization has an impact on the soil in coastal agricultural areas [4].

However, the increase in the salinity of arable land may affect the sustainable food supply of the world population [5]. Soybean is the world's most essential oilseed crop and a significant component of worldwide food security [6]. The shortage of water resources, high soil salinity, evaporation rate, and low soil fertility status has severely restricted the improvement of the dryland farming systems [7]. A ridge and furrow rainfall-harvesting system with plastic mulching can effectively raise SWS and reduce salt content and is widely used to promote soybean production and WUE [8,9]. Plastic mulching is also appropriate for improving the photosynthesis and yield of soybean in the saline–alkali regions [10].

Salinity is harmful to soybean because it causes negative physiological, biochemical, and morphological effects and can lead to a decrease in crop production [3]. The plant growth reduction caused by salinity is mostly determined by the following aspects: (i) the increase of osmotic pressure of the culture medium reduces the ability of plants to absorb water [11]; (ii) the toxicity level of excessive ions on plant cells [12]; and (iii) ionic imbalances that affect plant nutritional status and affect biochemical and metabolic components linked to planting development [13]. Plants have developed an inherent defense mechanism, including limitations on the absorption of toxic ions, stomatal regulation to sustain water status under salt stress, and enzymatic and non-enzymatic antioxidants [14]. Salt stress and other environmental stresses can raise the production of ROS, leading to oxidative stress in plant cells [15]. ROS has high cytotoxicity and can react with different biological molecules, leading to DNA mutations, lipid peroxidation, protein denaturation, and death of cell [16]. ROS elimination can be attained by activating the antioxidant mechanism [17]. Although defense mechanisms may be compromised by severe salinity stress, plants may be adversely affected by salinity-induced damage.

We use some strategies for using biostimulants that can improve the biochemical processes of plants under stress [18]. Due to the relationship in many aspects of plant physiological responses to salt and water stress, it is assumed that pyraclostrobin-based fungicides (PBF) can reduce the destructive effects of salinity [19]. These natural molecules are produced by a group of fungi belonging to the phylum basidiomycota, which is a pathogen of wood decay in certain tree species [20]. The bactericidal effect is achieved by blocking the outer electron transport to inhibit the mitochondrial respiration of some agricultural crop pathogenic fungi [21]. In recent years, several studies have proven that crop protection products based on astragalus have complementary biological stimulator properties, which can reduce water demand and alleviate non-biotic stress [22]. In fact, after the application of these pyraclostrobin-based fungicides (PBF), changes in plant metabolism have been observed, including an increase in ABA production and the activation of oxidative stress enzymes [23], which may increase WUE and photosynthesis under salt stress [24,25].

Many growth regulators, including hormones that have been used to activate plants, seem to be promising technologies for reducing salt toxicity and improving plant yield [16,26]. SA is an important phenolic compound and a growth regulator that plays a unique role in plants' various biochemical processes [27,28]. SA can also reduce lipid peroxidation and improve plant resistance to salt stress [29]. Drought and salt stress can promote the production of ROS, such as H_2O_2 and O_2^-, leading to chlorophyll damage [30]. Due to the increased accumulation of ROS, plant water and leaf stresses are typically linked with improved activation of oxidative stress enzymes [31]. Oxidative damage can have a negative impact on Pn and chlorophyll content [32,33]. Therefore, an approach to protect soybean from oxidative damage and delay the aging process is crucially important for its anti-oxidant metabolism [34,35].

Due to the commercial significance of soybean crops, the spread of salinity issues in several regions covered by these crops, and economic losses, there is increasing interest in finding new solutions that can alleviate the negative impact of salinity. We assume that PBF may not only have bactericidal effects but also biologically stimulating effects, which can decrease the harmful effects of salt stress on soybean. Our research objectives are as follows: (i) to examine the interaction between PBF and SA strategies in the antioxidant defense system of soybean leaves and the improvement of water use efficiency; (ii) to

determine the changes in the photosynthetic capacity and ROS detoxification system of soybean leaves under plastic film mulching.

2. Materials and Methods

2.1. Site Description

This study was conducted in Daqing, located at (125°19′16.59″ E, 46°62′5.31″ N) and 147.5 m asl, and the second site was in Harbin, located at (126°51′41.91″ E, 45°50′37.82″ N) and 174 m asl, China. The total sunshine hours were 2345.2 h yr^{-1}. Over 60% of the rainfall occurred from June to September. Rainfall during the soybean-growing season in Harbin from 2020 to 2021 was 398 mm and 351 mm, while Daqing had 510 mm and 470 mm (Figure 1). The initial physicochemical properties of the soil were determined; the soil samples were collected at a depth of 20 cm at the two experimental sites, which is shown in Table 1.

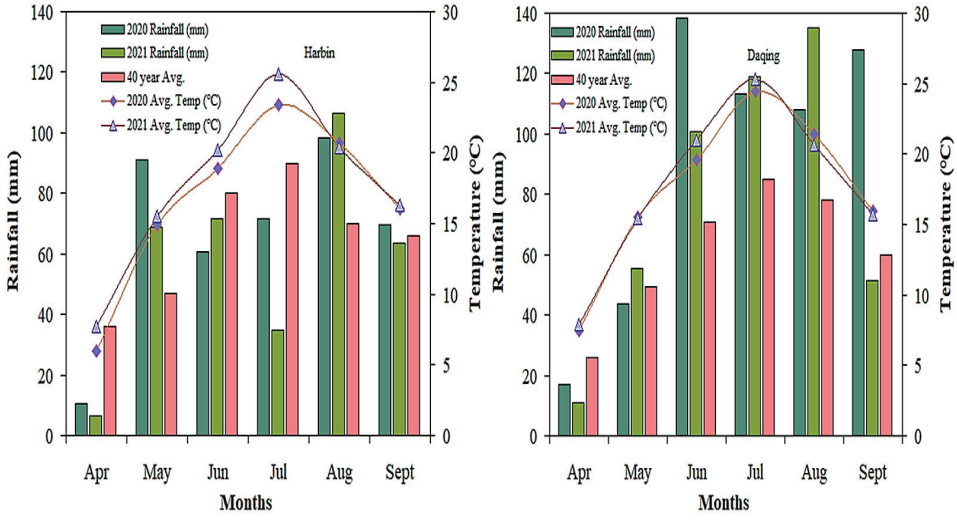

Figure 1. Precipitation distribution during 2020 and 2021 soybean-growing seasons.

Table 1. The chemical properties of experimental site of the soil layers (0–20 cm).

Location	SOM (g kg^{-1})	TN (g kg^{-1})	TP (g kg^{-1})	TK (g kg^{-1})	AN (mg kg^{-1})	AP (mg kg^{-1})	AK (mg kg^{-1})
Harbin	32.20	0.17	1.07	2.71	167.05	24.81	162.22
Daqing	29.89	0.18	1.05	2.48	135.81	23.95	116.70

2.2. Research Design

The field research was conducted in a randomized complete block design with three replications. In 2020 and 2021, we conducted field research under two experimental locations in Harbin and Daqing to study the effects of four different treatments: HCK: Harbin location with control; SA1+PBF1: salicylic acid (5 mL L^{-1}) with pyraclostrobin (3 mL L^{-1}); and SA2+PBF2: salicylic acid (10 mL L^{-1}) with pyraclostrobin (6 mL L^{-1}). Meanwhile, the Daqing location had DCK: Daqing location with control; SA1+PBF1: salicylic acid (5 mL L^{-1}) with pyraclostrobin (3 mL L^{-1}); and SA2+PBF2: salicylic acid (10 mL L^{-1}) with pyraclostrobin (6 mL L^{-1}).. Each ridge and furrow was 65 cm wide and 15 cm high. Soybeans were planted along ridges and furrows. A 1-meter wide isolation strip was set up between each plot to prevent water leakage. Heinong-531 soybean variety was planted on 17 May 2020 and harvested on 10 October 2020; the corresponding dates are 12 May and 15 October 2021. During the entire growing season, field management was carried out in

accordance with local practices. The amount of fertilizer applied during soil preparation each year was 60, 90, and 75 kg N, P_2O_5, K_2O, ha^{-1}.

2.3. Soil Water Storage (SWS)

The soil water content was calculated at the seedling, branching, flowering, grain-filling, and maturity stages during 2020 and 2021. Moisture contents of the 0–200 cm soil layers at 20 cm intervals were recorded using a TDR meter (Time-Domain Reflectometry, Germany).

The SWS was calculated by the following formula [36]:

$$SWS = C \times \rho \times H \times 10 \quad (1)$$

where C is the soil water, ρ is the bulk density, and H is the soil depth.

The ET rate was calculated by the following formula [36]:

$$ET = R + \Delta SWS \quad (2)$$

where R is the rainfall and ΔSWS is the SWS at a depth of (0–200 cm) between sowing and harvesting.

$$WUE = Y/ET \quad (3)$$

where WUE is the water use efficiency and Y is the grain yield.

2.4. Net Photosynthetic Rate (Pn)

Pn was measured using the LI Cor LI-6400XT portable photosynthesis system (LI-6400XT, LI Cor, Lincoln, NE, USA). Fully inflated leaves were measured on sunny days from 9:00 to 11:00 a.m. The CO_2 concentration in the leaf chamber was set to 380 μ mol mol^{-1}, and the photosynthetic active radiation was set to 1100 μ mol m^{-2} s^{-1}. Nine leaves of five individual plants were analyzed during the flowering, filling, and maturity stages of each treatment, with three replicates.

2.5. Antioxidant Enzyme Activities

An amount of 0.5 g of soybean leaf homogenate with midrib was removed, with 5 mL 50 mmol L^{-1} phosphate buffer (pH 7.8), 0.1mM EDTA-Na^2, and 1% insoluble PVP. The homogenate was centrifuged at 15,000× *g* for 10 min at 40 °C. After centrifugation, the upper supernatant was taken and used for enzyme determination. The SOD activity was analyzed at 560 nm according to the technology of [37]. According to Amalo et al. [38], the POD activity was calculated using guaiacol at 470 nm. The determination of CAT activity was based on the method proposed by Tan et al. [39]. The MDA content was analyzed based on the technique proposed by Zhang [40]. The Coomassie Brilliant Blue (G250) method described by Read and Northcote [41] was used to measure the soluble protein contents. The H_2O_2 and O_2^- contents were determined by the modification of the method of Elstner and Heupel [42] described by Jiang and Zhang [43]. The O_2^- content was analyzed at 530 nm, while H_2O_2 content was analyzed at 415 nm [44].

2.6. Statistical Analysis

The data were analyzed using SPSS 18.0 software. Multiple comparisons were tested using Duncan's new multiple-range test. If the F-test was significant, the mean value was evaluated by a multiple comparison test (LSD 0.05).

3. Results

3.1. Soil Water Storage (SWS) and ET Rate

Typically, significant changes in soil temperature, ET, and rainwater utilization can lead to significant differences in SWS (0–200 cm) at various growth stages (Table 2). During the two years of the seedling stage, the SWS was roughly the same without significant differences. In a two-year study, SWS varied with precipitation and different growth stages.

From the SS to BS stages in Harbin and Daqing, the average SWS (0–2 m) of SA1+PBF1 and SA2+PBF2 treatments significantly increased by 14.8%, 20.4%, 8.4%, and 5.6% compared to HCK and DCK treatments, respectively. From FS to the GFS stage, SWS gradually increases. From the GFS stage to the MS stage, the SWS trend of each treatment improved compared to the FS stage. During the GFS to MS periods, the average SWS (0–200 cm) of SA1+PBF1 and SA2+PBF2 treatments in the Harbin region significantly increased by 22.2% and 34.3% compared to HCK treatment, while the MS SWS of SA1+PBS1 and SA2+PBS2 treatments in the Daqing region considerably improved by 1.8% and 6.4% compared with DCK.

Table 2. Soil water storage (mm) at 0–200 cm soil profile at various growth stages of soybean as affected by various treatments. [a] during 2020 and 2021.

Locations	Treatments	Soil Water Storage (mm)									
		2020					2021				
		SS	BS	FS	GFS	MS	SS	BS	FS	GFS	MS
Harbin	HCK	118.5 a	123.6 b	97.7 c	101.1 d	92.0 d	114.4 a	129.7 b	89.9 c	84.9 e	122.7 c
	SA1+PBF1	119.4 a	126.1 a	104.0 b	113.4 b	116.8 b	115.5 a	132.1 a	99.8 b	101.2 b	129.7 b
	SA2+PBF2	119.9 a	127.3 a	115.3 a	125.7 a	129.7 a	116.1 a	133.2 a	110.7 a	111.7 a	141.2 a
Daqing	DCK	118.7 a	124.3 b	102.2 b	107.2 c	107.2 c	114.6 a	130.4 a	80.5 d	73.5 f	110.1 d
	SA1+PBF1	119.5 a	126.5 a	101.6 b	107.8 c	110.5 c	115.8 a	132.1 a	96.0 b	92.0 d	123.0 c
	SA2+PBF2	120.7 a	126.0 a	103.2 b	112.7 b	115.6 b	117.1 a	132.1 a	99.4 b	99.9 c	128.4 b
Analysis of variance	L	*	*	*	*	*	*	*	*	*	*
	SA	*	*	*	*	*	*	*	*	*	*
	PBF	*	*	*	*	*	*	*	*	*	*
	L × SA	ns	ns	ns	ns	ns	ns	ns	ns	ns	ns
	L × PBF	ns	ns	ns	ns	ns	ns	ns	ns	ns	ns
	SA × PBF	*	*	*	*	*	*	*	*	*	*
	L × SA × PBF	ns	ns	ns	ns	ns	ns	ns	ns	ns	ns

[a] HCK: Harbin location with control; SA1+PBF1: salicylic acid (5 mL L^{-1}) with pyraclostrobin (3 mL L^{-1}); SA2+PBF2: salicylic acid (10 mL L^{-1}) with pyraclostrobin (6 mL L^{-1}); DCK: Daqing location with control. Abbreviations are SS: seedling stage, BS: branching stage, FS: flowering stage, GFS: grain-filling stage, MS: maturity stage.

During the soybean growing season, there were significant variations in ET between different treatments. The soybean growth in the Daqing location had a high ET rate as compared with the Harbin location under different salicylic acid and pyraclostrobin levels. In 2020, the ET rate was significantly decreased at the location of Harbin with SA1+PBF1 and SA2+PBF2 treatments by 23.8% and 11.1% compared with HCK treatment, while at the Daqing location, SA1+PBF1 and SA2+PBF2 treatments had significantly decreased the ET rate by 22.4% and 9.0% compared with DCK treatment. In 2021, the ET rate was significantly decreased at the Harbin location with SA1+PBF1 and SA2+PBF2 treatments by 15.3% and 3.6% compared with HCK treatment, while at the Daqing location, SA1+PBF1 and SA2+PBF2 treatments had significantly decreased the ET rate by 16.4% and 11.3% compared with DCK treatment.

3.2. Pn Rate and SP Content

At various growth stages, the Pn and SP content of soybean leaves considerably improved with the increase of salicylic acid and pyraclostrobin levels. SP content is closely related to the Pn rate, significantly increasing the Pn rate of leaves. Due to the improvement of SWS, the SP content in soybean leaves was higher, which can maintain a higher net Pn rate (Table 3; Figure 2). During the two years of the same treatment, the Pn and SP contents of soybean leaves were considerably higher from the BS to FS stages, while they decreased considerably from the FS to GFS stages (Table 3; Figure 2). The average Pn was significantly improved at the Harbin location with SA1+PBF1 and SA2+PBF2 treatments by 36.9% and 47.9% compared with HCK treatment, while at the Daqing location, SA1+PBF1 and SA2+PBF2 treatments had 46.4% and 54.4% higher Pn compared with DCK. In a two-

year study, the Pn and SP content of SA1+PBF1 and SA2+PBF2 was considerably higher than those of HCK and DCK in the BS, FS, and GFS stages. However, with the treatment of SA1+PBF1, there was no considerable difference in Pn and SP content between the two study sites at various growth stages. In the later stage of soybean growth, both Pn and SP content was significantly affected by the levels of salicylic acid and pyraclostrobin, unlike in HCK and DCK treatments.

Table 3. The net photosynthesis rate of soybean as affected by various treatments during 2020 and 2021.

Locations	Treatments	Net Photosynthesis Rate (Pn μmol. m^{-2} s^{-1})					
		2020			2021		
		BS	FS	GFS	BS	FS	GFS
Harbin	CK	16.9 d	17.8 c	7.2 d	13.9 d	19.6 c	8.9 d
	SA1+PBF1	23.2 b	28.3 b	13.2 b	19.9 b	25.8 b	11.6 c
	SA2+PBF2	26.2 a	32.0 a	17.0 a	25.0 a	28.6 a	19.0 a
Daqing	CK	11.9 e	15.1 d	5.7 e	12.3 d	14.6 d	6.5 e
	SA1+PBF1	21.6 c	27.0 b	9.1 c	16.8 c	24.4 b	9.6 d
	SA2+PBF2	24.2 b	28.6 b	12.9 b	20.8 b	25.6 b	15.8 b
Analysis of variance	L	*	*	*	*	*	*
	SA	*	*	*	*	*	*
	PBF	*	*	*	*	*	*
	L × SA	ns	ns	ns	ns	ns	ns
	L × PBF	ns	ns	ns	ns	ns	ns
	SA × PBF	*	*	*	*	*	*
	L × SA × PBF	ns	ns	ns	ns	ns	ns

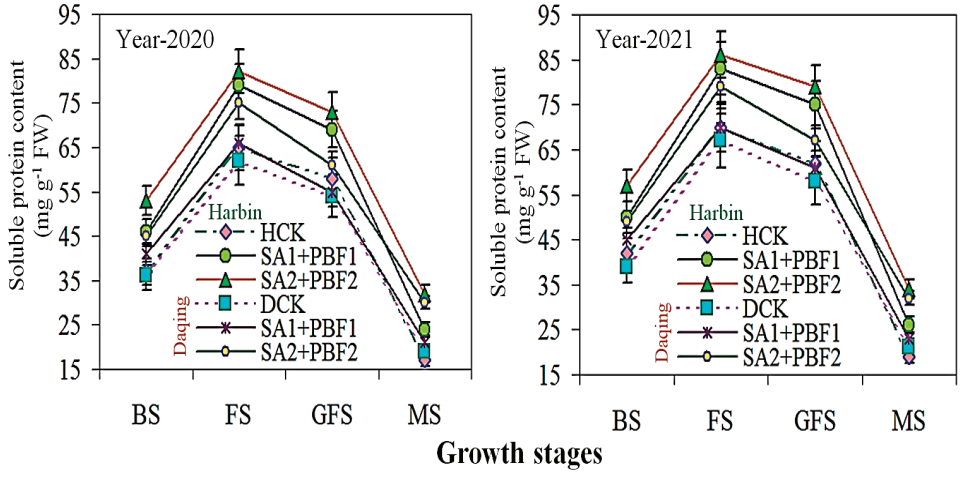

Figure 2. Effects of different treatments on soluble protein content (SP) of soybean during 2020–2021 growing seasons. Note: HCK: Harbin location with control; SA1+PBF1: salicylic acid (5 mL L^{-1}) with pyraclostrobin (3 mL L^{-1}); SA2+PBF2: salicylic acid (10 mL L^{-1}) with pyraclostrobin (6 mL L^{-1}); DCK: Daqing location with control.

3.3. Anti-Oxidative Enzyme Activities

Tables 4 and 5 and Figure 3 show that the POD, CAT, and SOD activities of soybean leaves considerably improved with increasing levels of salicylic acid and pyraclostrobin during the BS, FS, GFS, and MS stages at the research sites in Harbin and Daqing. The SA2+PBF2 treatment had the highest POD, CAT, and SOD activities in soybean leaves during the FS stage, but there was no significant difference compared to the GFS stage. Afterward, the SOD, POD, and CAT activities in soybean leaves rapidly decreased during

the MS stage. Furthermore, there were no considerable variations between the SA1+PBF1 treatments at all growth stages of soybeans at the research sites in Harbin and Daqing.

Table 4. Peroxidase (POD) activity of soybean as affected by various treatments during 2020 and 2021.

Locations	Treatments	POD Activity (U g^{-1} FW min^{-1})							
		2020				2021			
		BS	FS	GFS	MS	BS	FS	GFS	MS
Harbin	CK	93.8 e	191.2 d	135.1 e	110.1 e	96.8 e	197.2 d	141.1 e	113.0 e
	SA1+PBF1	116.0 c	314.0 b	312.8 b	159.4 c	120.0 b	326.0 b	319.4 b	166.3 c
	SA2+PBF2	140.5 a	359.7 a	330.1 a	240.0 a	144.5 a	349.7 a	336.7 a	246.9 a
Daqing	CK	93.9 e	135.5 e	127.0 f	117.1 d	99.9 d	145.5 e	133.9 f	123.3 d
	SA1+PBF1	96.9 d	191.7 d	194.1 d	157.1 c	100.9 c	203.7 d	200.7 d	164.0 c
	SA2+PBF2	136.3 b	237.1 c	228.6 c	222.6 b	140.3 a	271.1 c	235.2 c	229.5 b
Analysis of variance	L	*	*	*	*	*	*	*	*
	SA	*	*	*	*	*	*	*	*
	PBF	*	*	*	*	*	*	*	*
	L × SA	ns	ns	ns	ns	ns	ns	ns	ns
	L × PBF	ns	ns	ns	ns	ns	ns	ns	ns
	SA × PBF	*	*	*	*	*	*	*	*
	L × SA × PBF	ns	ns	ns	ns	ns	ns	ns	ns

Table 5. Catalase (CAT) activity of soybean as affected by various treatments during 2020 and 2021.

Locations	Treatments	CAT Activity (U g^{-1} FW min^{-1})							
		2020				2021			
		BS	FS	GFS	MS	BS	FS	GFS	MS
Harbin	CK	101.1 e	136.2 c	125.2 c	57.5 c	105.6 e	141.2 c	126.6 e	61.5 c
	SA1+PBF1	140.4 b	154.7 b	153.5 b	69.2 b	145.9 b	161.7 b	158.5 b	75.0 b
	SA2+PBF2	158.5 a	177.5 a	165.4 a	75.8 a	164.0 a	184.5 a	170.4 a	81.6 a
Daqing	CK	105.8 d	133.5 d	108.5 d	53.6 d	109.8 d	138.5 d	110.5 e	58.6 d
	SA1+PBF1	107.3 d	140.8 c	129.2 c	58.5 c	112.3 d	146.8 c	132.5 c	64.3 c
	SA2+PBF2	123.7 c	159.9 b	153.8 b	67.2 b	128.7 c	165.9 b	157.1 b	73.0 b
Analysis of variance	L	*	*	*	*	*	*	*	*
	SA	*	*	*	*	*	*	*	*
	PBF	*	*	*	*	*	*	*	*
	L × SA	ns	ns	ns	ns	ns	ns	ns	ns
	L × PBF	ns	ns	ns	ns	ns	ns	ns	ns
	SA × PBF	*	*	*	*	*	*	*	*
	L × SA × PBF	ns	ns	ns	ns	ns	ns	ns	ns

At the research sites in Harbin and Daqing, the POD, CAT, and SOD activities of soybean leaves considerably improved from the BS to FS stages while sharply decreasing from the GFS to MS stages at levels of salicylic acid and pyraclostrobin. At various growth stages, the effects of SA1+PBF1 and SA2+PBF2 treatments on POD, CAT, and SOD in soybean leaves were significantly greater compared with HCK and DCK treatments. At the BS, FS, GFS, and MS stages of the research sites in Harbin and Daqing, SA1+PBF1 treatment did not significantly affect the POD, CAT, and SOD of soybean leaves.

Unlike the trend of changes in POD, CAT, and SOD activities, the MDA content in soybean leaves gradually improved from the BS stage to the MS stage (Figure 4). The MDA content decreased with the increase of salicylic acid and pyraclostrobin content. Under CK treatment, the MDA content in the MS phase of DCK treatment peaked. Under the control treatment, the MDA content in the study sites of Harbin and Daqing increased sharply, respectively. The maximum antioxidant enzyme activity was recorded throughout

the soybean growth season at the research sites in Harbin and Daqing, with the lowest MDA concentration observed in the SA1+PBF1 and SA2+PBF2 treatments.

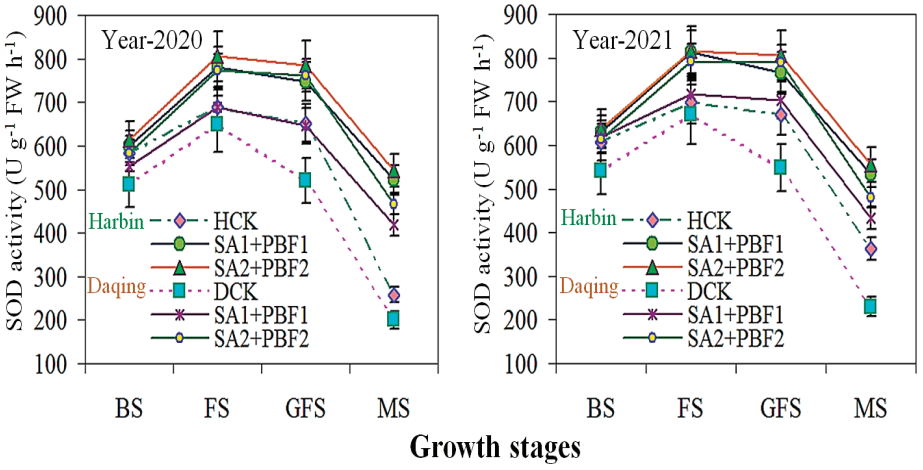

Figure 3. Effects of various treatments on superoxide dismutase activity of soybean during 2020–2021 growing seasons.

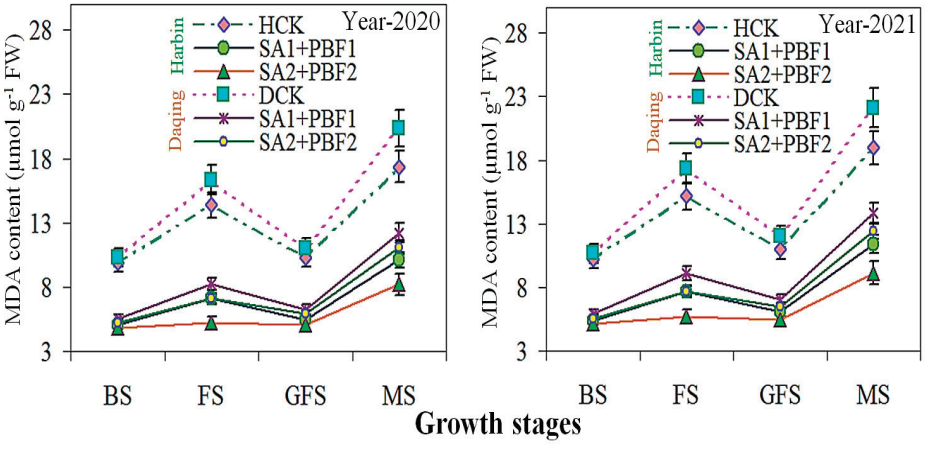

Figure 4. Effects of various treatments on malondialdehyde content of soybean during 2020–2021 growing seasons.

3.4. H_2O_2 and O_2^- Contents

Under the HCK and DCK treatments, the H_2O_2 and O_2^- of the soybean were significantly higher than that of SA1+PBF1 and SA2+PBF2 treatments throughout the soybean-growing season in both the Harbin and Daqing study locations (Figures 5 and 6). The H_2O_2 and O_2^- of soybean slowly increased from the FS to the GFS and GFS to MS stages. Furthermore, under various salicylic acid and pyraclostrobin levels, the content of H_2O_2 and O_2^- increased considerably from the GFS to MS stages. However, the average of two-year data at various growth stages of soybean indicated that in the location of Harbin, SA1+PBF1 and SA2+PBF2 treatments significantly decreased H_2O_2 by 47.3% and 28.8% compared with HCK treatment, while at the location of Daqing, SA1+PBF1 and SA2+PBF2 treatments significantly decreased H_2O_2 by 50.4% and 23.0% compared with DCK treatment. Meanwhile, the mean of O_2^- content at various growth stages of soybean showed

that in the location of Harbin, SA1+PBF1 and SA2+PBF2 treatments significantly decreased O_2^- by 53.2% and 35.6% compared with HCK treatment, while at the location of Daqing, SA1+PBF1 and SA2+PBF2 treatments significantly decreased O_2^- by 57.3% and 30.8% compared with DCK treatment. At the BS, FS, GFS, and MS stages, the soybean leaves under the HCK and DCK were considerably higher in H_2O_2 and O_2^- than in the SA1+PBF1 and SA2+PBF2 treatments. The H_2O_2 and O_2^- of the SA1+PBF1 treatment were higher compared with SA2+PBF2 in both the Harbin and Daqing study locations.

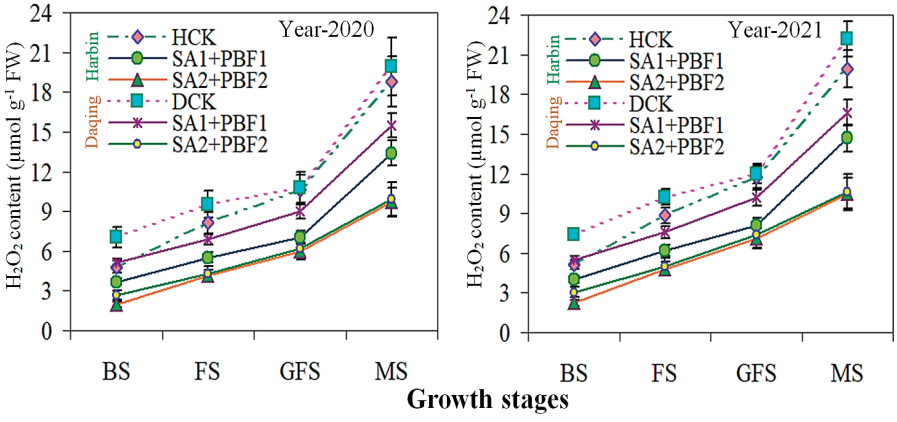

Figure 5. Effects of various treatments on hydrogen peroxide of soybean leaves during 2020–2021 growing seasons.

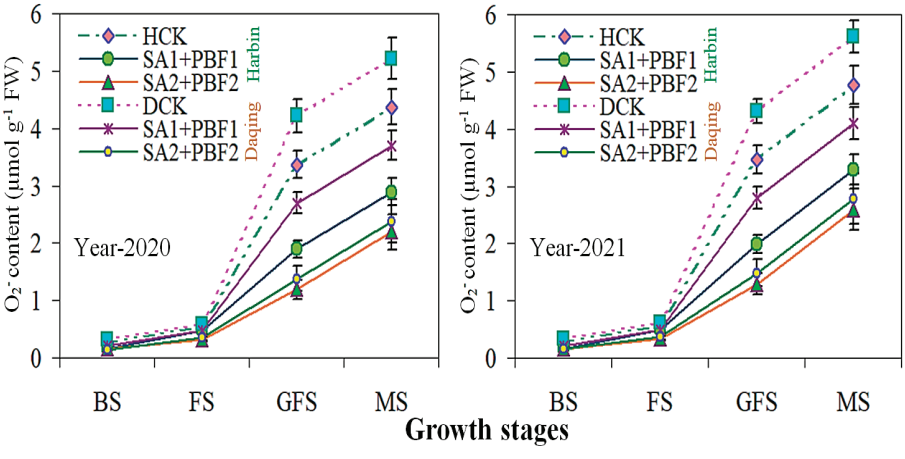

Figure 6. Effects of various treatments on superoxide radicals (O_2^-) of soybean during 2020–2021 growing seasons.

3.5. Yield and Yield Components

In both the Harbin and Daqing study locations, various salicylic acid and pyraclostrobin levels had considerable effects on grain plant^{-1}, 100-grain weight, WUE, and grain production (Table 6). In a two-year study, the results showed that compared with HCK and DCK treatments, SA2+PBF2 treatment improved SWS, Pn, and SP and reduced ET, thereby significantly improving the soybean yield under saline soil. Compared with HCK and DCK, the mean grain yield under the SA1+PBF1 and SA2+PBF2 treatments at both the Harbin and Daqing study locations improved by 29.2%, 32.1%, 28.9%, and 30.0%, while the average WUE of soybean was significantly increased by 37.1%, 43.2%, 35.5%, and

41.4%, respectively. The WUE indicated the relationship between water utilization and soybean production. Compared with all other treatments, SA2+PBF2 treatment considerably increased WUE at the Harbin study location.

Table 6. Soybean yield and yield components as affected by various treatments during 2020 and 2021.

Locations	Treatments	Soybean Yield and Yield Components									
		ET (mm)		Grains Plant^{-1}		100 Grain Weight (g)		WUE (kg mm^{-1} ha^{-1})		Grain Yield (t ha^{-1})	
		2020	2021	2020	2021	2020	2021	2020	2021	2020	2021
Harbin	CK	366.5 b	373.4 b	128 c	139 b	21.60 b	21.72 b	6.68 c	6.72 c	2.45 e	2.51 d
	SA1+PBF1	329.8 d	360.4 c	134 b	140 b	22.30 a	22.70 b	10.49 b	9.85 b	3.46 b	3.55 b
	SA2+PBF2	296.0 f	323.8 e	142 a	155 a	23.30 a	25.20 a	12.16 a	11.44 a	3.60 a	3.70 a
Daqing	CK	378.2 a	404.3 a	83 g	89 e	18.20 c	18.44 c	5.15 d	4.89 d	1.95 f	1.98 e
	SA1+PBF1	346.9 c	363.1 c	115 e	117 d	18.56 c	21.18 b	7.90 c	7.66 c	2.74 d	2.78 c
	SA2+PBF2	308.9 e	347.2 d	122 d	134 c	20.90 b	22.40 b	9.03 b	8.11 b	2.79 c	2.82 c
Analysis of variance	L	*	*	*	*	*	*	*	*	*	*
	SA	*	*	*	*	*	*	*	*	*	*
	PBF	*	*	*	*	*	*	*	*	*	*
	L × SA	ns	ns	ns	ns	ns	ns	ns	ns	ns	ns
	L × PBF	ns	ns	ns	ns	ns	ns	ns	ns	ns	ns
	SA × PBF	*	*	*	*	*	*	*	*	*	*
	L × SA × PBF	ns	ns	ns	ns	ns	ns	ns	ns	ns	ns

4. Discussion

4.1. Photosynthesis Rate Responses to Different Salicylic Acid and Pyraclostrobin

With the increase of salinity treatment levels, the degree of growth reduction was higher. Several researchers reported on the growth and biomass decline of diverse plant species under soil salinity [45,46]. Ge and Zhang [47] proposed that growth delay was an important aspect of assessing the degree of damage caused by salinity, regardless of the type of plant species. In two study years, SWS varied with precipitation and different growth stages. From the SS to BS stages, the average SWS (0–2 m) of SA1+PBF1 and SA2+PBF2 treatments was significantly increased compared to HCK and DCK treatments in Harbin and Daqing. From the FS to GFS stages, SWS gradually increased. From the GFS stage to the MS stage, the SWS trend of each treatment improved compared to the FS stage. During the GFS to MS stages, the average SWS (0–200 cm) of SA2+PBF2 treatment in the Harbin region was significantly improved compared to the HCK treatment. Plastic film mulching can considerably increase SWS capacity and WUE [48,49]. Due to the higher SWS of the soil and the acceleration of soybean development, the soybean produces the maximum production [50]. Zhang et al. [51] also studied that after the application of SA, growth increased, and the ET rate decreased under salt stress. In the presented study, the soybean growth in the Daqing location had a high ET rate compared with the Harbin location under different salicylic acid and pyraclostrobin levels. The ET rate was significantly ($p < 0.05$) decreased at the location of Harbin with SA1+PBF1 and SA2+PBF2 treatments by 23.8% and 11.1% compared with HCK treatment, while at the location of Daqing, SA1+PBF1 and SA2+PBF2 treatments had significantly decreased the ET rate by 22.4% and 9.0% compared with DCK treatment. In addition, the effect of PBF on WUE confirms that the application of PBF can considerably increase WUE [52,53].

The toxic stress indicator can affect the content of Pn and SP in leaves [54]. The decrease in Pn can be attributed to the inhibition of Pn biosynthesis induced by saline [54]. The Pn and SP content of soybean was considerably improved with the increase of salicylic acid and pyraclostrobin levels. SP content is closely related to the photosynthetic rate, significantly increasing the photosynthetic rate of leaves. Due to the improvement of SWS, the SP content in soybean leaves was higher, which can maintain a higher net Pn rate. Under salt stress, PBF can improve the Pn rate [55]. Chlorophyll contents show a vital role in energy assimilation in plants, and their levels undergo significant changes under salt stress. During two years of the same treatment, the Pn and SP content in soybean leaves

was considerably higher from the BS to FS stages, while they decreased considerably from the FS to GFS stages. Many reports indicate that PGPB and SA are effective photosynthetic regulators as they have a positive impact on the structure of leaves and chloroplasts, as well as chlorophyll content [56]. Our research results also indicate that in the late growth stage of soybeans, Pn and SP content was significantly affected at each level by salicylic acid and pyraclostrobin, unlike in HCK and DCK treatments. In many studies, it has been observed that a salt-induced complete loss of some proteins increases the synthesis of new proteins, and it is believed that newly synthesized proteins play a crucial role in salt stress tolerance [57,58]. The surge in total soluble sugar content and the increase in salinity treatment levels may be due to the accumulation of starch and sugar under salt stress [59].

4.2. Antioxidative Enzyme Activities Responses to Different Salicylic Acid and Pyraclostrobin

In order to eliminate excessive ROS production in cells, plants have developed anti-oxidant enzymes such as CAT, POD, SOD, and ascorbic acid [54]. The SA2+PBF2 treatment had the highest POD, CAT, and SOD activities in soybean leaves during the FS stage, but there was no significant difference compared to the GFS stage. Afterward, the SOD, POD, and CAT in soybean leaves rapidly decreased during the MS stage. The H_2O_2 produced in cells under stress is removed through the action of POD, CAT, and SOD enzymes [60]. The increase in ascorbic acid levels is consistent with the higher levels of POD activity after the application of PBF and SA under salt stress. The slowing down of aging is also related to the decrease in lipid peroxidation caused by reduced oxidative stress [61,62]. In our experiment, it was observed that due to the application of PBF, the activity of antioxidant enzymes increased, which will confirm the latter hypothesis. Aging is considered a process related to reactive oxygen species [63]. Furthermore, there were no significant variances between the SA1+PBF1 treatments at all growth stages of soybeans at the research sites in Harbin and Daqing. At the research sites in Harbin and Daqing, the POD, CAT, and SOD activities of soybean considerably improved from the BS to FS stages, while sharply decreasing from the GFS to MS stages at levels of salicylic acid and pyraclostrobin. Water scarcity is associated with oxidative stress caused by increased ROS accumulation [64]. The oxidative damage can have a negative impact on Pn value [65]. However, crops have developed an anti-oxidant mechanism to decrease H_2O_2 and O_2^- content [66]. The MDA decreases with the rise of salicylic acid and pyraclostrobin. The CAT and SOD increased, and reducing MDA, H_2O_2, and O_2^- production may be a vital approach under salt stress for soybean to increase chlorophyll content [64].

Under the treatment of HCK and DCK, compared with the SA1+PBF1 and SA2+PBF2 treatments in the Harbin and Daqing research sites, the H_2O_2 and O_2^- of soybean were considerably higher. The content of H_2O_2 and O_2^- in soybean gradually increases from the FS to GFS and the GFS to MS stages. The accumulation of H_2O_2 and MDA under salt stress is the result of increased ROS production [67]. SOD, POD, and CAT are key enzymes in the reactive oxygen species scavenging system that can inhibit ROS accumulation. In fact, SOD catalyzes the dismutation of H_2O_2 and O_2^-, while the other three enzymes eliminate H_2O_2 and prevent its toxicity [66]. In addition, under different levels of salicylic acid and PBF, the H_2O_2 and O_2^- significantly improved from the GFS to MS stages. At the research sites in Harbin and Daqing, compared to the SA2+PBF2 treatment, the SA1+PBF1 treatment had the highest levels of H_2O_2 and O_2^-. The salinity stress in this study resulted in a rise in H_2O_2 and MDA content. Various researchers have reported an increase in ROS production under salt stress [58,68]. The levels of MDA and H_2O_2 in plants treated with pyraclostrobin were lower than those affected by salt, indicating that PBF and SA significantly decreased lipid damage and prevented oxidative damage caused by salt stress [56].

4.3. Cultivation Systems Effect on Soil Water Storage and Soybean Production

The plastic film mulching considerably increased soybean yield, reduced ET, and effectively increased WUE [69]. Our results confirm that compared to HCK and DCK treatments, SA2+PBF2 treatment improved SWS, Pn, and SP and reduced ET, significantly

increasing soybean yield in saline–alkali soil. Compared with the HCK and DCK treatments, the grain yield of SA1+PBF1 and SA2+PBF2 treatments increased by 29.2%, 32.1%, 28.9%, and 30.0%, respectively, at the research sites in Harbin and Daqing, while the WUE of soybeans significantly improved by 37.1%, 43.2%, 35.5%, and 41.4%, respectively. However, the impact of RF systems on grain production is controversial. Previous research reported that RF systems considerably increase soybean production [63,70,71], while other studies have found that RF decreases the ET rate [72]. Our research results confirm that plastic film mulching can significantly improve water use efficiency, indicating a connection between water use and soybean production.

5. Conclusions

Salinity has become a potential risk to global agricultural productivity and food security. The research results indicate that in the Harbin region, SA2+PBF2 treatment reduced the ET rate, improved SWS during branching and grouting stages, and achieved a higher net photosynthesis rate. Moreover, this improvement is due to the reduction of oxidative damage and MDA in soybean at various growth stages. At different growth stages, the treatment of the Harbin soybean with SA2+PBF2 significantly increased the activity of SOD, POD, CAT, and SP, while the content of MDA, H_2O_2, and O_2^- also decreased considerably. Under the SA2+PBF2 in Harbin, the scavenging ability of free H_2O_2 and O_2^- was higher, and the activity of antioxidant enzymes was better. This was due to the lower level of lipid peroxidation, which efficiently secures the photosynthesis mechanism, considerably increasing WUE (46.3%) and grain yield (57.5%). These results indicate that the plastic mulch with SA2+PBF2 treatment significantly manages salt stress by improving SWS, anti-oxidant enzyme activities, photosynthesis, WUE, and soybean production to promote sustainable farming.

Author Contributions: H.R., J.W. and B.Z. conceived and designed the experiments. H.R., X.W., F.Z., K.Z., X.L., R.Y., C.Z., J.D. and J.Y. performed the experiments. H.R. and X.W. analyzed data and wrote the manuscript. All authors have read and agreed to the published version of the manuscript.

Funding: Project funded by Key R&D projects in Heilongjiang Province (Grant No. 2022ZX02B06); Key Laboratory of Soybean Mechanized Production, Ministry of Agriculture and Rural Affairs, China (Grant No. SMP202202); The National Key Research and Development Program of China (Grant No. 2022YFD1500505-1); Project of Natural Science Foundation of Heilongjiang Province (Grant No. ZD2020C009).

Institutional Review Board Statement: Not applicable.

Informed Consent Statement: Not applicable.

Data Availability Statement: Data will be available on personal request.

Conflicts of Interest: The authors declare no conflict of interest.

References

1. Chen, H.; Jingjing, L.; Afeng, Z.; Jing, C.; Gong, C.; Benhua, S.; Xiaomin, P.; Miles, D.; Bingcheng, S.; Ying, Z.; et al. Effects of straw and plastic film mulching on greenhouse gas emissions in Loess Plateau, China: A field study of 2 consecutive wheat-maize rotation cycles. *Sci. Total Environ.* **2019**, *579*, 814–824. [CrossRef]
2. Hussain, S.; Zhang, J.-H.; Zhong, C.; Zhu, L.-F.; Cao, X.-C.; Yu, S.-M.; Bohr, J.A.; Hu, J.-J.; Jin, Q.-Y. Effects of salt stress on rice growth, development characteristics, and the regulating ways: A review. *J. Integr. Agric.* **2017**, *16*, 2357–2374. [CrossRef]
3. Parihar, P.; Singh, S.; Singh, R.; Singh, V.P.; Prasad, S.M. Effect of salinity stress on plants and its tolerance strategies: A review. *Environ. Sci. Pollut. Res.* **2015**, *22*, 4056–4075. [CrossRef]
4. Boari, F.; Donadio, A.; Pace, B.; Schiattone, M.I.; Cantore, V. Kaolin improves salinity tolerance, water use efficiency and quality of tomato. *Agric. Water Manag.* **2016**, *167*, 29–37. [CrossRef]
5. Qiang, S.C.; Zhang, Y.; Fan, J.L.; Zhang, F.C.; Sun, M.; Gao, Z.Q. Combined effects of ridge–furrow ratio and urea type on grain yield and water productivity of rain-fed winter wheat on the Loess Plateau of China. *Agric. Water Manag.* **2022**, *261*, 107340. [CrossRef]
6. Scheidleger, A.; Grath, J.; Lindinger, H. Saltwater intrusion due to groundwater over-exploitation EEA inventory throughout Europe. In Proceedings of the 18th Saltwater Intrusion Meeting, Cartagena, Spain, 34 May–3 June 2004.

7. Zheng, J.; Fan, J.L.; Zhang, F.C.; Zhuang, Q.L. Evapotranspiration partitioning and water productivity of rain-fed maize under contrasting mulching conditions in Northwest China. *Agric. Water Manag.* **2021**, *243*, 106473. [CrossRef]
8. Braune, H.; Müller, J.; Diepenbrock, W. Integrating effects of leaf nitrogen, age, rank, and growth temperature into the photosynthesis-stomatal conductance model LEAFC3-N parameterised for barley (*Hordeum vulgare* L.). *Ecol. Model.* **2009**, *220*, 1599–1612. [CrossRef]
9. Polemio, M. Monitoring and Management of Karstic Coastal Groundwater in a Changing Environment (Southern Italy): A Review of a Regional Experience. *Water* **2016**, *8*, 148. [CrossRef]
10. Jamil, A.; Riaz, S.; Ashraf, M.; Foolad, M.R. Gene Expression Profiling of Plants under Salt Stress. *Crit. Rev. Plant Sci.* **2011**, *30*, 435–458. [CrossRef]
11. Choudhury, F.K.; Rivero, R.M.; Blumwald, E.; Mittler, R. Reactive oxygen species, abiotic stress and stress combination. *Plant J.* **2017**, *90*, 856–867. [CrossRef]
12. Golezani-Ghassemi, K.; Nikpour-Rashidabad, N. Seed pretreatment and salt tolerance of dill: Osmolyte accumulation, antioxidant enzymes activities and essence production. *Biocatal. Agric. Biotechnol.* **2017**, *12*, 30–35. [CrossRef]
13. Flagella, Z.; Cantore, V.; Giuliani, M.M.; Tarantino, E.; De Caro, A. Crop salt tol_erance: Physiological, yield and quality aspects. In *Recent Research Developments in Plant Biology*; Pandalai, S.G., Ed.; Iris Publishers: Francisco, CA, USA, 2002; Volume 2, pp. 155–186; ISBN 81-7736-149-X. Available online: https://fair.unifg.it/handle/11369/16900?mode=simple (accessed on 10 June 2023).
14. Munns, R.; James, R.A.; Läuchli, A. Approaches to increasing the salt tolerance of wheat and other cereals. *J. Exp. Bot.* **2006**, *57*, 1025–1043. [CrossRef]
15. Nxele, X.; Klein, A.; Ndimba, B.K. Drought and salinity stress alters ROS accumulation, water retention, and osmolyte content in sorghum plants. *S. Afr. J. Bot.* **2017**, *108*, 261–266. [CrossRef]
16. Hanin, M.; Ebel, C.; Ngom, M.; Laplaze, L.; Masmoudi, K. New Insights on Plant Salt Tolerance Mechanisms and Their Potential Use for Breeding. *Front. Plant Sci.* **2016**, *7*, 1787. [CrossRef]
17. Boari, F.; Cucci, G.; Donadio, A.; Schiattone, M.I.; Cantore, V. Kaolin influences tomato response to salinity: Physiological aspects. *Acta Agric. Scand. Sect. B Soil Plant Sci.* **2014**, *64*, 559–571. [CrossRef]
18. Caverzan, A.; Casassola, A.; Brammer, S.P. Antioxidant responses of wheat plants under stress. *Genet. Mol. Biol.* **2016**, *39*, 1–6. [CrossRef]
19. Arya, B.; Komala, B.R.; Sumalatha, N.T.; Surendra, G.M.; Gurumurthy, P.R. PGPR induced systemic tolerance in plant. *Int. J. Curr. Microbiol. App. Sci.* **2018**, *7*, 453–462.
20. Balba, H. Review of strobilurin fungicide chemicals. *J. Environ. Sci. Health Part B* **2007**, *42*, 441–451. [CrossRef]
21. Bartlett, D.; Clough, J.; Godwin, J.; Hall, A.; Hamer, M.; Parr-Dobrzanski, B. Review: The strobilurin fungicides. *Pest Manag. Sci.* **2002**, *60*, 309. [CrossRef]
22. Su, Z.; Zhang, J.; Wu, W.; Cai, D.; Lv, J.; Jiang, G.; Huang, J.; Gao, J.; Hartmann, R.; Gabriels, D. Effects of conservation tillage practices on winter wheat water-use efficiency and crop yield on the Loess Plateau, China. *Agric. Water Manag.* **2007**, *87*, 307–314. [CrossRef]
23. Nudrat, A.A.; Fahad, S.; Muhammad, A. Ascorbic acid-a potential oxidant scavenger and its role in plant development and abiotic stress tolerance. *Front. Plant Sci.* **2017**, *8*, 613.
24. Yusuf, M.; Hayat, S.; Alyemeni, M.N.; Fariduddin, Q.; Ahmad, A. Salicylic acid: Physiological roles in plants. In *Salicylic Acid*; Springer: Dordrecht, The Netherlands, 2013; pp. 15–30.
25. Liang, S.; Xu, X.; Lu, Z. Effect of azoxystrobin fungicide on the physiological and biochemical indices and ginsenoside contents of ginseng leaves. *J. Ginseng Res.* **2018**, *42*, 175–182. [CrossRef]
26. Gharbi, E.; Martinez, J.P.; Benahmed, H.; Fauconnier, M.L.; Lutts, S.; Quinet, M. Salicylic acid differently impacts ethylene and polyamine synthesis in the glycophyte *Solanum lycopersicum* and the wild-related halophyte *Solanum chilense* exposed to mild salt stress. *Physiol. Plant.* **2016**, *158*, 152–167. [CrossRef] [PubMed]
27. Baranyiova, I.; Klem, K.; Kren, J. Effect of exogenous application of growth regulators on the physiological parameters and the yield of winter wheat under drought stress. *Mendelnet* **2014**, 442–446.
28. Joshi, J.; Sharma, S.; Guruprasad, K.N. Foliar application of Pyraclostrobin fun_gicide enhances the growth, rhizobial-nodule formation and nitrogenase activity in soybean (var. JS-335). *Pestic. Biochem. Physiol.* **2014**, *114*, 61–66. [CrossRef] [PubMed]
29. Hernández, J.A.; Diaz-Vivancos, P.; Barba-Espín, G.; Clemente-Moreno, M.J. On the Role of Salicylic Acid in Plant Responses to Environmental Stresses. In *Salicylic Acid: A Multifaceted Hormone*; Springer: Singapore, 2017; pp. 17–34.
30. Irada, M.H. Photosynthetic characteristics and enzymatic antioxidant capacity of leaves from wheat cultivars exposed to drought. *Biochim. Biophys. Acta* **2012**, *1817*, 1516–1523.
31. Noreen, S.; Siddiq, A.; Hussain, K.; Ahmad, S.; Hasanuzzaman, M. Foliar application of salicylic acid with salinity stress on physiological and biochemical attributes of sunflower (*Helianthus annuus* L.) crop. *Acta Sci. Pol. Hortorum Cultus* **2017**, *16*, 57–74.
32. Ahmad, F.; Singh, A.; Kamal, A. Ameliorative effect of salicylic acid in salinity stressed Pisum sativum by improving growth parameters, activating photosynthesis and enhancing antioxidant defense system. *Biosci. Biotechnol. Res. Commun.* **2017**, *10*, 481–489. [CrossRef]
33. Miller, G.; Suzuki, N.; Ciftci-Yilmaz, S.; Mittler, R. Reactive oxygen species homeostasis and signalling during drought and salinity stresses. *Plant Cell Environ.* **2010**, *33*, 453–467. [CrossRef]

34. Fazeli, F.; Ghorbanli, M.; Niknam, V. Effect of drought on biomass, protein content, lipid peroxidation and antioxidant enzymes in two sesame cultivars. *Biol. Plant.* **2007**, *51*, 98–103. [CrossRef]
35. Nie, W.; Gong, B.; Chen, Y.; Wang, J.; Wei, M.; Shi, Q. Photosynthetic capacity, ion homeostasis and reactive oxygen metabolism were involved in exogenous salicylic acid increasing cucumber seedlings tolerance to alkaline stress. *Sci. Hortic.* **2018**, *235*, 413–423. [CrossRef]
36. Ren, X.L.; Jia, Z.K.; Chen, X.L. Rainfall concentration for increasing corn production under semiarid climate. *Agric. Water Manag.* **2008**, *95*, 1293–1302. [CrossRef]
37. Li, X.Y.; Gong, J.D. Effects of different ridge:furrow ratios and supplemental irrigation on crop production in ridge and furrow rainfall harvesting system with mulches. *Agric. Water Manag.* **2002**, *54*, 243–254. [CrossRef]
38. Amalo, K.; Chen, G.X.; Asade, K. Separate assays specific for ascorbate peroxidase and guaiacal peroxidase and for the chloroplastic and cytosolic isozymes of ascorbate peroxidase implants. *Plant Cell Physiol.* **1994**, *35*, 497–504.
39. Tan, W.; Liu, J.; Dai, T.; Jing, Q.; Cao, W.; Jiang, D. Alternations in photosynthesis and antioxidant enzyme activity in winter wheat subjected to post-anthesis water-logging. *Photosynthetica* **2008**, *46*, 21–27. [CrossRef]
40. Zhang, X.Z. *Crop Physiology Research Methods*; China Agricultural Press: Beijing, China, 1992; pp. 131–207. (In Chinese)
41. Read, S.M.; Northcote, D.H. Minimization of variation in the response to different protein of the Coomassic Blue G dye binding assay for protein. *Anal. Biochem.* **1981**, *116*, 53–64. [CrossRef] [PubMed]
42. Elstner, E.F.; Heupel, A. Inhibition of nitrite formation from hydroxyl ammonium chloride: A simple assay for superoxide dismutase. *Anal. Biochem.* **1976**, *70*, 616–620. [CrossRef] [PubMed]
43. Jiang, M.; Zhang, J. Involvement of plasma-membrane NADPH oxidase in abscisic acid- and water stress-induced antioxidant defense in leaves of maize seedlings. *Planta* **2002**, *215*, 1022–1030. [CrossRef] [PubMed]
44. Brennan, T.; Frenkel, C. Involvement of Hydrogen Peroxide in the Regulation of Senescence in Pear. *Plant Physiol.* **1977**, *59*, 411–416. [CrossRef] [PubMed]
45. Wu, G.-Q.; Liang, N.; Feng, R.-J.; Zhang, J.-J. Evaluation of salinity tolerance in seedlings of sugar beet (*Beta vulgaris* L.) cultivars using proline, soluble sugars and cation accumulation criteria. *Acta Physiol. Plant.* **2013**, *35*, 2665–2674. [CrossRef]
46. Ma, D.; Chen, L.; Qu, H.; Wang, Y.; Misselbrook, T.; Jiang, R. Impacts of plastic film mulching on crop yields, soil water, nitrate, and organic carbon in Northwestern China: A meta-analysis. *Agric. Water Manag.* **2018**, *202*, 166–173. [CrossRef] [PubMed]
47. Ge, H.; Zhang, F. Growth-Promoting Ability of Rhodopseudomonas palustris G5 and Its Effect on Induced Resistance in Cucumber Against Salt Stress. *J. Plant Growth Regul.* **2019**, *38*, 180–188. [CrossRef]
48. Li, H.Q.; Jiang, X.W. Inoculation with plant growth-promoting bacteria (PGPB) improves salt tolerance of maize seedling. *Russ. J. Plant Physiol.* **2017**, *64*, 235–241. [CrossRef]
49. Ali, S.; Xu, Y.; Ma, X.; Ahmad, I.; Kamran, M.; Dong, Z.; Cai, T.; Jia, Q.; Ren, X.; Zhang, P.; et al. Planting Patterns and Deficit Irrigation Strategies to Improve Wheat Production and Water Use Efficiency under Simulated Rainfall Conditions. *Front. Plant Sci.* **2017**, *8*, 1408. [CrossRef] [PubMed]
50. Akram, S.; Siddiqui, N.; Hussain, B.M.N.; Al Bari, A.; Mostofa, M.G.; Hossain, M.A.; Tran, L.-S.P. Exogenous Glutathione Modulates Salinity Tolerance of Soybean [*Glycine max* (L.) Merrill] at Reproductive Stage. *J. Plant Growth Regul.* **2017**, *36*, 877–888. [CrossRef]
51. Zhang, H.Z.; Guo, L.; Ye, J.; Zhang, L.; Wang, Q.; Li, F.; Zhang, X.; Cao, X.; Xu, M.; Hao, L.; et al. Responses of leaf stomatal traits and gas exchange process of cherry tomato to NaCl salinity stress. *Trans. Chin. Soc. Agric. Eng.* **2018**, *34*, 107–113.
52. Li, Z.Z.; Niu, W.; Qiao, X.W.; Ma, L.P. Anti-oxidant response of *Cucumis sativus* L. to fungicide Carbendazim. *Pestic. Biochem. Physiol.* **2007**, *89*, 54–59.
53. Giuliani, M.M.; Carucci, F.; Nardella, E.; Francavilla, M.; Ricciardi, L.; Lotti, C.; Gatta, G. Combined effects of deficit irrigation and strobilurin application on gas ex_change, yield and water use efficiency in tomato (*Solanum lycopersicum* L.). *Sci. Hortic.* **2018**, *233*, 149–158. [CrossRef]
54. Acosta-Motos, J.R.; Ortuño, M.F.; Bernal-Vicente, A.; Diaz-Vivancos, P.; Sanchez-Blanco, M.J.; Hernandez, J.A. Plant responses to salt stress: Adaptive mechanisms. *Agronomy* **2017**, *7*, 18. [CrossRef]
55. Xu, Z.; Jiang, Y.; Zhou, G. Response and adaptation of photosynthesis, respiration, and antioxidant systems to elevated CO_2 with environmental stress in plants. *Front. Plant Sci.* **2015**, *6*, 701. [CrossRef]
56. Jiang, C.; Zu, C.; Lu, D.; Zheng, Q.; Shen, J.; Wang, H.; Li, D. Effect of exogenous selenium supply on photosynthesis, Na+ accumulation and antioxidative capacity of maize (*Zea mays* L.) under salinity stress. *Sci. Rep.* **2017**, *7*, srep42039. [CrossRef] [PubMed]
57. Barickman, T.C.; Kopsell, D.; Sams, C.E. Abscisic Acid Increases Carotenoid and Chlorophyll Concentrations in Leaves and Fruit of Two Tomato Genotypes. *J. Am. Soc. Hortic. Sci.* **2014**, *139*, 261–266. [CrossRef]
58. Fariduddin, Q.; Yusuf, M.; Ahmad, I.; Ahmad, A. Brassinosteroids and their role in response of plants to abiotic stresses. *Biol. Plant* **2014**, *58*, 9–17. [CrossRef]
59. Gomathi, R.; Vasantha, S.; Shiyamala, S.; Rakkiyappan, P. Differential accumulation of salt induced proteins in contrasting sugarcane genotypes. *EJBS* **2013**, *6*, 7–11.
60. Li, H.S. *Principles and Techniques of Plant Physiological Experiment*; Higher Education Press: Beijing, China, 2000; pp. 119–120. (In Chinese)
61. Behnamnia, M.; Kalantari, M.; Rezanejad, F. Exogenous application of brassinosteroid alleviates drought-induced oxidative stress in *Lycopersicon esculentum* L. *Gen. Appl. Plant Physiol.* **2009**, *35*, 22–34.

62. Amaro, A.C.E.; Ramos, A.R.P.; Macedo, A.C.; Ono, E.O.; Rodrigues, J.D. Effects of the fungicides azoxystrobin, pyraclostrobin and boscalid on the physiology of Japanese cucumber. *Sci. Hortic.* **2018**, *228*, 66–75. [CrossRef]
63. Lum, M.S.; Hanafi, M.M.; Rafii, Y.M.; Akmar, A.S.N. Effect of drought stress on growth, proline and antioxidant enzyme activities of upland rice. *J. Anim. Plant Sci.* **2014**, *24*, 1487–1493.
64. Zhao, H.; Dai, T.; Jing, Q.; Jiang, D.; Cao, W. Leaf senescence and grain filling affected by post-anthesis high temperatures in two different wheat cultivars. *Plant Growth Regul.* **2007**, *51*, 149–158. [CrossRef]
65. Farooq, M.; Wahid, A.; Kobayashi, N.; Fujita, D.; Basra, S.M. Plant drought stress: Effects, mechanisms and management. *Agron. Sustain. Dev.* **2009**, *29*, 185–212. [CrossRef]
66. Fotelli, M.N.; Rennenberg, H.; Geßler, A. Effects of Drought on the Competitive Interference of an Early Successional Species (*Rubus fruticosus*) on Fagus sylvatica L. Seedlings: 15N Uptake and Partitioning, Responses of Amino Acids and other N Compounds. *Plant Biol.* **2002**, *4*, 311–320. [CrossRef]
67. Halo, B.A.; Khan, A.L.; Waqas, M.; Al-Harrasi, A.; Hussain, J.; Ali, L.; Lee, I.J. Endophytic bacteria (*Sphingomonas* sp. LK11) and gibberellin can improve *Solanum lycopersicum* growth and oxidative stress under salinity. *J. Plant Interact.* **2015**, *10*, 117–125. [CrossRef]
68. Chen, Y.; Liu, S.; Li, H.; Li, X.; Song, C.; Cruse, R.; Zhang, X. Effects of conservation tillage on corn and soybean yield in the humid continental climate region of Northeast China. *Soil Tillage Res.* **2011**, *115–116*, 56–61. [CrossRef]
69. Tang, Q.-X.; Li, S.-K.; Xie, R.-Z.; Zhang, J.-X.; Ren, T.-Z.; Lin, T.; Gao, S.-J. Effects of Conservation Tillage on Crop Yield: A Case Study in the Part of Typical Ecological Zones in China. *Agric. Sci. China* **2011**, *10*, 860–866. [CrossRef]
70. Sarkar, A.; Ghosh, P.K.; Pramanik, K.; Mitra, S.; Soren, T.; Pandey, S.; Mondal, M.H.; Maiti, T.K. A halotolerant *Enterobacter* sp. displaying ACC deaminase activity promotes rice seedling growth under salt stress. *Res. Microbiol.* **2018**, *169*, 20–32. [CrossRef]
71. Miao, F.; Li, Y.; Cui, S.; Jagadamma, S.; Yang, G.; Zhang, Q. Soil extracellular enzyme activities under long-term fertilization management in the croplands of China: A meta-analysis. *Nutr. Cycl. Agroecosystems* **2019**, *114*, 125–138. [CrossRef]
72. Venancio, W.S.; Tavares Rodrigues, M.A.; Begliomini, E.; de Souza, N.L. Physiological effects of strobilurin fungicides on plants. *Publ. UEPG Ciência Exatas eda Terra Ciências Agrarias Engenhairas. Ponta Grossa* **2003**, *9*, 59–68.

land

MDPI

Article

Rhizobia Inoculation Supplemented with Nitrogen Fertilization Enhances Root Nodulation, Productivity, and Nitrogen Dynamics in Soil and Black Gram (*Vigna mungo* (L.) Hepper)

Mahran Sadiq [1,2], Nasir Rahim [2], Muhammad Aamir Iqbal [3,*], Mashael Daghash Alqahtani [4], Majid Mahmood Tahir [2], Afshan Majeed [2] and Raees Ahmed [5]

[1] College of Forestry, Gansu Agricultural University, Lanzhou 730070, China; khanmahran420@gmail.com
[2] Department of Soil & Environmental Sciences, Faculty of Agriculture, University of Poonch Rawalakot, Rawalakot 12350, Pakistan; nasirrahim@upr.edu.pk (N.R.); majidmahmood@upr.edu.pk (M.M.T.); afshanmajeed@upr.edu.pk (A.M.)
[3] Department of Agronomy, Faculty of Agriculture, University of Poonch Rawalakot, Rawalakot 12350, Pakistan
[4] Department of Biology, College of Science, Princess Nourah bint Abdulrahman University, P.O. Box 84428, Riyadh 11671, Saudi Arabia; mdalqahtani@pnu.edu.sa
[5] Department of Plant Pathology, Faculty of Agriculture, University of Poonch Rawalakot, Rawalakot 12350, Pakistan; raees@upr.edu.pk
* Correspondence: aamir1801@yahoo.com

Abstract: The potential interactions of rhizobium bacteria in enhancing nodulation, nitrogen (N) fixation for boosting N availability, and the yield of black gram under a temperate environment continue to remain unexplored. Therefore, this study aimed to evaluate the agronomic performance of black gram cultivars, their yield comparisons, and shoot–grain–soil N dynamics in a prevalently rainfed farming system. Two black gram cultivars, NARC Mash-I and NARC Mash-II, were subjected to rhizobia inoculation combined with different N doses (0, 25, 50, 75, 100 kg ha^{-1}). The response variables included root nodulation, agronomic yield attributes, grain yield, shoot–grain and soil N dynamics, and biological productivity. Black gram cultivar NARC Mash-II showed the maximum nodule formation (41 per plant), while each nodule obtained 0.69 g weight in response to RI combined with 25 kg N ha^{-1}. Additionally, this combination showed the highest pods per plant and thousand grain weight, which maximized the grain yield (1777 kg ha^{-1}) and biological productivity (3007 kg ha^{-1}). In contrast, NARC Mash-I under 50 kg N recorded the highest shoot N content, while the same cultivar under 100 kg N exhibited the maximum soil N content. The correlation analyses indicated a significantly robust association among the nodule numbers, grain weight, and N contents in different plant organs. These results give mechanistic insights into plant–microbe interactions based on the eco-friendly, sustainable, and smart agricultural practice of black gram production in a temperate environment.

Keywords: pulses; phenotypic divergence; root nodulation; temperate climate; nitrogen dynamics

Citation: Sadiq, M.; Rahim, N.; Iqbal, M.A.; Alqahtani, M.D.; Tahir, M.M.; Majeed, A.; Ahmed, R. Rhizobia Inoculation Supplemented with Nitrogen Fertilization Enhances Root Nodulation, Productivity, and Nitrogen Dynamics in Soil and Black Gram (*Vigna mungo* (L.) Hepper). *Land* **2023**, *12*, 1434. https://doi.org/10.3390/land12071434

Academic Editor: Claude Hammecker

Received: 2 June 2023
Revised: 11 July 2023
Accepted: 13 July 2023
Published: 18 July 2023

1. Introduction

Declining soil fertility due to agricultural practices, unpredictable climate changes, and shortages of water and minerals is challenging for an eco-friendly modern agricultural system [1]. A gradual decrease in soil fertility has reduced the production of food crops, leading to food and nutritional insecurity for an increasing number of the population, especially in the Indo-Pak subcontinent [2]. Among the strategically crucial plant nutrients required to achieve potential crop yields, N ranks at the top as it is required by crop plants in larger quantities to attain potential vegetative growth, promote chlorophyll development, and trigger the biosynthesis of amino acids, proteins, and nucleotides [3]. However, resource-poor growers with small land holdings can ill-afford the skyrocketing cost of inorganic fertilizers to compensate for N deficiency in agricultural soils. Furthermore, a variety

of processes, especially sub-optimized N doses, cause losses of over 50% of soil-applied N fertilizers, making it a prime source of environmental pollution [4]. Interestingly, numerous studies have reported contrasting findings on N fertilization regimes for black gram under tropical and subtropical environments, including Reddy et al. [5], Rathore et al. [6], and Prasad et al. [7] who suggested 20 kg N ha^{-1}, while Marimuthu and Surendran [8] recommended 25 kg N ha^{-1}. However, Chandrasekar and Bangarusamy [9] and Ahmed et al. [10] suggested even higher quantities of N (30–55 kg ha^{-1}). Research findings are scant for temperate conditions; thus, increasing prices of N fertilizers and emerging agro-ecological pollution have renewed research interest in scouting for optimal N doses and finding biologically viable strategies to boost the crop yield and soil fertility status.

Several strategies have been applied for boosting mineral nutrition, abiotic stress tolerance, and plant impartments in soils [11–15]. In place of mineral N fertilizers, legume–rhizobium symbiosis might serve as a potent source of N and may reduce plants' N requirements and maintain crop yields as per varietal potential [16,17]. In addition, N fixed through the biological N fixation (BNF) process has the advantage of being a renewable source and there is scant probability of loss through leaching and volatilization [18]. The other associated advantage offered by rhizobia symbiosis is its potential for building up soil fertility and enhancing crop productivity in a sustainable and eco-friendly manner [4]. Previous studies have reported the positive effects of rhizobia inoculation for boosting the crop productivity of *Rhizobium trifolii* in clover, *Bradyrhizobium japonicum* in common beans, soybean, etc., *Azorhizobium caulinodans* in sesbania, *sinorhizobium/Ensifer meliloti* comb in alfalfa, and *Mesorhizobium mediterraneum* in chickpeas [4,19–21].

For sustainable legume–rhizobium symbiosis, seed inoculation must bolster root nodulation, which significantly improves N uptake and crop production [22,23]. Rhizobia participate in the BNF process in the root nodules of legumes [16], leading to the conversion of molecular N into ammonia [24]. Interestingly, non-inoculated plants are exposed to multiple rhizobia, which significantly vary in their capacity to promote nodulation and N fixation. Despite the wide abundance and effectiveness of natural rhizobia populations, maximized N fixation by legume crops has rarely been achieved. Sánchez–Navarro et al. [18] inferred that a wide array of microbiomes exist in the rhizosphere; however, rhizobium inoculation could be useful even for soils where legumes have been cultivated for many years, owing to the absence of crop-specific rhizobia [25]. It was also inferred that inoculation increased the rhizobia population in the rhizosphere, which led to enhanced N fixation by legumes in soil where there was a scarcity of crop-specific rhizobia. Additionally, it has been suggested that rhizobia must survive in soil and utilize ecological niches created by plant roots for fixing atmospheric N [26]. However, poorly fixed naturally occurring rhizobia strains may become dominant and gain an advantage over inoculated strains [27]. Therefore, Safronova et al. [28] suggested that the choice of rhizobia strains for seed inoculation must be made keeping in mind their host specificity and the microbial genera present in the rhizosphere. In order to maximize BNF, the inoculant strain must be efficient and match the desired legume variety in a growing agro-ecological zone. The adaptation of host-specific rhizobia strains to the local environment and soil conditions increases the chance of effective nodulation [26]. However, research and knowledge gaps exist pertaining to the impact of inoculation on N dynamics in the shoots and grains of legumes under temperate conditions, which necessitate conducting fresh studies.

Black gram (*Vigna mungo* (L.) Hepper) is a mash bean that is widely cultivated in the Indo-Pak sub-continent and Bangladesh [29] and ranks as the third major pulse crop of Pakistan [30]. Black gram is an excellent source of protein for human and animal nutrition. It comprises over 24% protein, 60% carbohydrates, and 1.5% fat, and finds use as whole seed and dehusked splits (cotyledons), as well as in a variety of fermented products, like dosa. Interestingly, it is subjected to fermentation with rice blends for preparing fermented steamed products and different types of roasted pancakes [31]. In black gram, the assimilated translocation to the constantly growing vegetative sinks even after the initiation of the reproductive phase considerably reduces the grain yield, owing to N

supply limitations [26]. This might be rectified by optimizing N doses and performing seed inoculation with appropriate rhizobia strains. Another serious constraint in black gram production is flower and fruit drop caused by N deficiency, which requisites conducting fresh studies on optimizing N fertilization regimes.

Thus, under a changing climate, it is of strategic pertinence to bridge the research and knowledge gaps pertaining to N dose optimization to enhance biological N fixation through the inoculation of rhizobia strains under a temperate environment. Additionally, the field testing of black gram cultivars for assessing the grain yield potential offers a bright perspective to enhance productivity and profitability. Thus, this field research tested the hypothesis that the optimization of N fertilization regimes and seed inoculation of rhizobia might increase the black gram grain yield, N dynamics, and soil fertility. Thus, the objectives of this study were to explore the genetic potential of black gram cultivars under a temperate environment through the optimization of N doses and rhizobia inoculation to enhance the nodulation properties, agronomic yield traits, and productivity, along with plant and soil N dynamics.

2. Materials and Methods

2.1. Experimental Site's Meteorological Features

The field trial was conducted during the crop growth seasons of 2019 and 2020 in the farm area of the Faculty of Agriculture, University of Poonch Rawalakot, Azad Jammu and Kashmir, Pakistan. The geographical coordinates of the study locality are depicted in Figure 1. The study site has a sub-mountainous topography of valleys, temperate climatic characteristics, and an altitude of 1633 m. The average temperature and the mean annual precipitation of the region are 15 °C and 360 mm, respectively [32]. The texture of the experimental block was silty clay loam. Pre-sowing soil sampling was performed in order to estimate the physico-chemical properties of experimental sites which exhibited a pH and electrical conductivity of 7.4 and 0.37, respectively. Additionally, the available phosphorous and N content were 2.56 mg kg^{-1} and 0.41%, respectively, while organic matter was 1.21%. Moreover, soil organic carbon, bulk density, and soil porosity were 6.38 g ka^{-1}, 1.34%, and 43%, respectively.

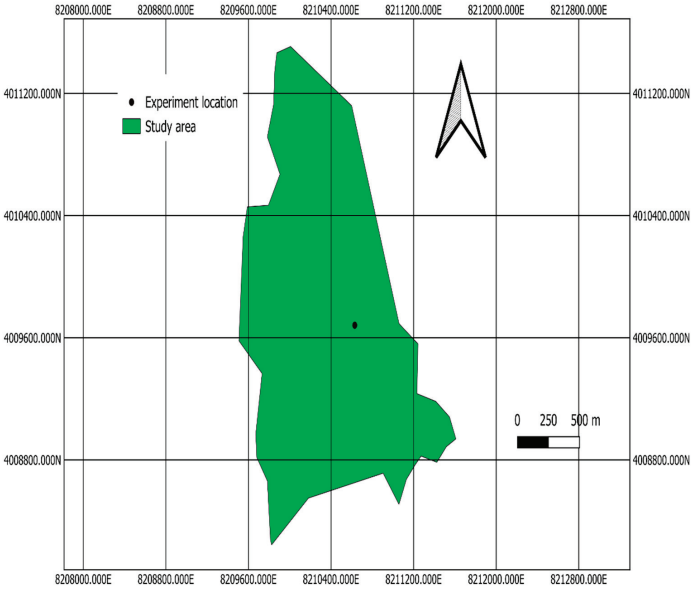

Figure 1. The trial's location (Rawalakot, Azad Kashmir, Pakistan) map prepared with the help of QGIS software (version 3.24.3, Bern, Switzerland), whereby the black point highlights the trial's location while the half-arrow is pointed toward the north direction.

2.2. Experimental Design, Rhizobia Inoculum, and Nitrogen Supplementation

The experiment was comprised of a control treatment (without inoculation and fertilization), two cultivars of black gram (V_1 = NARC Mash-I and V_2 = NARC Mash-II), and four N fertilization regimes (25, 50, 75, and 100 kg N ha^{-1}). The details of the employed treatments are presented in Table 1. The trial was conducted using a randomized complete block design (RCBD) with split plot arrangement and there were three replications. The trial was comprised of 36 experimental plots in total, while the net size of each plot was 9 m^2 (after excluding the walking paths and plot boundaries). Black gram varieties (NARC Mash-I and NARC Mash-II) were used as planting materials and their seeds were acquired from the National Agriculture Research Center (NARC), Islamabad, Pakistan. Both cultivars were bold-seeded, high-yielding, and resistant to yellow mosaic virus (YMV) and urdbean leaf crinkle virus (ULCV). These cultivars are being grown on a wide scale in the irrigated and rainfed areas of the Punjab and Sindh provinces of Pakistan [33]; however, no research-based findings are available regarding their performance under the temperate environment of the Azad Jammu and Kashmir region of Pakistan. A low soil temperature delays germination, and thus seed hydro-priming was performed by dipping the seeds into water for 12 h followed by shade drying for 5 h, as recommended by Golezani et al. [34]. The sowing was conducted on 27 and 29 April of 2019 and 2020, respectively, and harvesting was manually performed on 23 and 24 August using sickles.

Table 1. Details of treatments regarding Rhizobia inoculation and N fertilization regimes for black gram cultivars tested during the course of this study.

Treatments	Description	Abbreviation
Control (T_1)	Control [V_1 and V_2] (no inoculation, no N fertilization)	T_1V_1 and T_1V_2
N_0RI (T_2)	Inoculation [V_1 and V_2] (inoculum, no N fertilization)	T_2V_1 and T_2V_2
N_{25}RI (T_3)	25 kg N ha^{-1} + RI [V_1 and V_2]	T_3V_1 and T_3V_2
N_{50}RI (T_4)	50 kg N ha^{-1} + RI [V_1 and V_2]	T_4V_1 and T_4V_2
N_{75}RI (T_5)	75 kg N ha^{-1} + RI [V_1 and V_2]	T_5V_1 and T_5V_2
N_{100}RI (T_6)	100 kg N ha^{-1} + RI [V_1 and V_2]	T_6V_1 and T_6V_2

V_1 = NARC Mash-I, V_2 = NARC Mash-II, RI = rhizobia inoculation.

The crop was sown using 30 cm R × R and 10 cm P × P spacing (30 rows per plot). The sowing was conducted using a hand drill. The phosphorous (P = 60 kg ha^{-1}) fertilizer was applied as a basal dose in a slightly higher quantity than suggested by Qayyum et al. [30] (50 kg ha^{-1} in order to compensate for the significantly lower available P of 2.56 mg kg^{-1} of soil in all experimental plots). All agronomic management practices (e.g., land preparation, priming duration, seed rate, plot size sowing time and technique, plant–plant and row–row spacings, weeding frequency, etc.) except those employed as treatments (N dose, cultivars, and rhizobium inoculation) were kept uniform to inhibit the influence of any external factor which could have altered the treatment effects on the response variables under investigation. The seeds of black gram cultivars were inoculated with 10% brown sugar (to attain the dual purposes of thickening the solution for enhancing adherence to the grain surface and to provide an instant source of energy for microbes) solution containing the Bradyrhizobium strain of TAL-169 (2 weeks old rhizobia culture acquired from NARC, Islamabad, Pakistan). It was prepared by following the protocol of Saleem et al. [2] in such a way that the inoculum was completely stuck on the grains of the black gram [14,15]. The solution was prepared by adding sugar to water, while black gram grains were placed in a large open-top tub. The grains were mixed with the inoculant using an inoculant/grain weight ratio of 1:100, as suggested by Temprano et al. [35]. The continuous stirring of grains in the solution was performed by mixing a cup of the sugar solution at continuous intervals. The stirring was continued until the seeds were damp but not saturated by ensuring that there was no standing liquid. Once the grains were thoroughly mixed with the thick solution, the inoculant powder was gradually added. This procedure was performed using small batches of grains because a

mechanical mixer was not available for this purpose. After inoculation, grains were sown within eight hours to ensure the viability of the rhizobia.

2.3. Collection of Root Nodules and Plant Samples

In the grain filling stage, ten plants were randomly selected from the middle rows of each experimental plot and uprooted with the help of a spade. For the purpose of loosening the sticky soil from roots, plants were placed into the plastic buckets filled with water. Thereafter, soil adhering to the roots was manually removed. Subsequently, plants' roots were separated and nodules were picked from roots for data recording. In the maturity stage, plant samples from an area of one square meter were randomly harvested from all experimental plots for the estimation of different agronomical traits, including the number of pods per plant, thousand grain weight, biological and grain yields, etc.

2.4. Estimation of Physio-Chemical Parameters of the Soils

After crop harvesting, soil sampling was conducted from 0 to 15 cm and 15 to 30 cm depths, while the soil sampling points included the four corners and middle of the experimental block. Thereafter, the soil samples were thoroughly mixed and preserved in zip-lockable bags for N estimation, following the Kjeldahl method [36]. The soil organic carbon (SOC) and organic matter (SOM) were analyzed by following the standard methods [37].

2.5. Determination of Shoot and Grain N

For the estimation of the N content of the shoot and grains, 1 g of crushed matter (using mortar and pestle) was mixed with 50 mL of H_2SO_4 and 10 g of Kjeldahl Catalyst (Cu-Se) that was subsequently placed in the digestion flasks for two hrs. Thereafter, 100 mL of water was added in the flasks of each sample, which was shaken using a shaker for 10 min. Finally, all samples were put in the analyzer (Kjeltec Auto 1030 Analyzer) for N estimation [38].

2.6. Statistical Analysis

The collected data were subjected to Bartlett's test which exhibited a non-significant effect of the year, and thus data were transformed into mean values. Subsequently, the transformed data were analyzed using SPSS statistics computer software (version 17.0) by employing the analysis of variance (ANOVA) technique to measure the significant difference at $p \leq 0.05$. Additionally, two-way factor interaction (treatments $\times$ cultivars) was conducted and comparisons of means were performed using Tukey's honest significant difference (HSD) test at a 5 percent probability level [39]. Moreover, to determine the relationship among response variables, the Pearson correlation coefficient was found using the same statistical package. Furthermore, for the exploration of the multivariate variability caused by employed treatments for the grain, shoot, and soil N accumulation in the plant–soil system, principal component analysis (PCA) was employed using PAST-Paleontological Statistics [40].

3. Results

3.1. Rhizobia Inoculation Combined with N Supplementation Enhanced Root Nodulation

The nodulation potential of the black gram cultivars was evaluated in terms of number and dry weight of nodules under rhizobia inoculation (RI) and varying N fertilization regimes, while the results exhibited noticeable diversity in these traits (Table 2). Overall, the mean values of the nodulation characteristics under N doses with RI were considerably higher than for the unamended control treatment. It was revealed that the highest number of nodules per plant (41 ± 2.5) was recorded for the N_{25}RI treatment (NARC Mash-I cultivar), which remained statistically at par with N_0RI for NARC Mash-II; however, it was 32% higher than for the unamended control treatment. It was followed by N_{25}RI, which performed at par with N_{50}RI for NARC Mash-II. Likewise, the maximum nodule dry weight was recorded for NARC Mash-II in response to the treatment of N_{25}RI (0.69 ± 0.02), which was 37% higher

than for the control treatment. The minimum nodule number (27 ± 2.0) was recorded in the control treatment with the lowest nodule dry weight (0.41 ± 0.03) for NARC Mash-I, which was statistically at par with the N_{100}RI treatment. Moreover, N_{100}RI could not match the nodulation recorded by N_{75}RI, which in turn remained inferior to N_{50}RI. Furthermore, N_{50}RI exhibited significantly lower nodule numbers and dry weight than N_{25}RI. To sum up, a significant genotypic difference was recorded, because NARC Mash-I depicted the maximum number of nodules, while NARC Mash-II remained superior for nodule dry weight when inoculated with rhizobia under limited N supply.

Table 2. The variations in the root nodules of black gram cultivars under rhizobia inoculation and N fertilization regimes in a temperate climate.

	No. of Nodules per Plant			Nodule Dry Weight (g)		
Treatments	**Genotypes**		**Mean**	**Genotypes**		**Mean**
	NARC Mash-I (V_1)	**NARC Mash-II (V_2)**		**NARC Mash-I (V_1)**	**NARC Mash-II (V_2)**	
Control (T_1)	27 ± 2.0 ^{d}	29 ± 3.0 ^{cd}	28 ± 2.6 ^{C}	0.41 ± 0.03 ^{g}	0.49 ± 0.06 ^{efg}	0.44 ± 0.05 ^{E}
N_0RI (T_2)	36 ± 4.5 ^{abc}	40 ± 7.2 ^{a}	38 ± 5.5 ^{AB}	0.58 ± 0.02 ^{bcd}	0.66 ± 0.03 ^{ab}	0.62 ± 0.05 ^{AB}
N_{25}RI (T_3)	41 ± 2.5 ^{a}	39 ± 5.1 ^{ab}	40 ± 3.7 ^{A}	0.63 ± 0.03 ^{abc}	0.69 ± 0.02 ^{a}	0.66 ± 0.04 ^{A}
N_{50}RI (T_4)	35 ± 4.5 ^{abcd}	38 ± 2.5 ^{ab}	37 ± 4.5 ^{AB}	0.54 ± 0.02 ^{cde}	0.60 ± 0.03 ^{abcd}	0.57 ± 0.04 ^{BC}
N_{75}RI (T_5)	31 ± 3.0 ^{bcd}	34 ± 3.4 ^{abcd}	33 ± 3.5 ^{BC}	0.48 ± 0.03 ^{efg}	0.55 ± 0.03 ^{cde}	0.52 ± 0.04 ^{CD}
N_{100}RI (T_6)	30 ± 2.0 ^{bcd}	32 ± 3.1 ^{abcd}	32 ± 2.5 ^{C}	0.44 ± 0.06 ^{fg}	0.52 ± 0.04 ^{def}	0.48 ± 0.05 ^{DE}
Mean	33 ± 5.55 ^{B}	36 ± 5.67 ^{A}	35 ± 5.6	0.51 ± 0.08 ^{B}	0.58 ± 0.09 ^{A}	0.55 ± 0.09
CV (%)	8.247	12.430	10.043	11.874	14.513	10.058

Small and capital letters depict significant difference among treatment effects and their mean values, respectively. T_1 = control, no inoculation and fertilization, T_2 = inoculation but no fertilization, T_3 = 25 kg N ha^{-1}, T_4 = 50 kg N ha^{-1}, T_5 = 75 kg N ha^{-1}, T_6 = 100 kg N ha^{-1}, V_1 = NARC Mash-I, V_2 = NARC Mash-II, RI = rhizobia inoculation, CV = coefficient of variation.

3.2. Yield Attributes under Rhizobia Inoculation and N Fertilization Regimes

The effect of cultivars and employed treatments (rhizobia inoculation and N fertilization regimes) was significant, as depicted in Table 3. The maximum pod numbers per plant (46 ± 3.1) and thousand grain weight (62 ± 5.5) were exhibited by N_{25}RI for NARC Mash-II and were 33% and 19%, respectively, higher than for the unamended control treatment. In addition, the N_0RI and N_{50}RI treatments recorded statistically similar results in terms of pod numbers and thousand grain weight. In contrast, the minimum number of pods per plant and thousand grain weight were recorded for NARC Mash-I in the control treatment, while the N_{50}RI and N_{75}RI treatments remained statistically at par with each other (60 ± 4.5 and 59 ± 2.1, respectively) for thousand grain weight in NARC Mash-II. Likewise, NARC Mash-II in response to the N_{25}RI treatment showed the highest pod numbers and thousand grain weight; however, it remained at par with NARC Mash-I under the same treatment. In terms of the pod numbers per plant, the N_{25}RI and N_{50}RI treatments exhibited unmatched results for NARC Mash-II, while both cultivars under the control treatment recorded the minimum pod numbers and thousand grain weight.

Table 3. The grain yield attributes of black gram cultivars under rhizobia inoculation and N fertilization regimes in a temperate climate.

	No. of Pods per Plant			Thousand Grain Weight (g)		
Treatments	**Genotypes**		**Mean**	**Genotypes**		**Mean**
	NARC Mash-I (V_1)	**NARC Mash-II (V_2)**		**NARC Mash-I (V_1)**	**NARC Mash-II (V_2)**	
Control (T_1)	29 ± 4.1 ^{b}	33 ± 6.0 ^{b}	31 ± 5.0 ^{C}	47 ± 3.0 ^{c}	52 ± 2.6 ^{bc}	49 ± 3.2 ^{C}
N_0RI (T_2)	36 ± 4.5 ^{ab}	41 ± 4.7 ^{ab}	38 ± 5.1 ^{AB}	57 ± 3.5 ^{ab}	58 ± 2.0 ^{ab}	57 ± 2.6 ^{AB}

Table 3. *Cont.*

Treatments	No. of Pods per Plant			Thousand Grain Weight (g)		
	Genotypes		Mean	Genotypes		Mean
	NARC Mash-I (V_1)	NARC Mash-II (V_2)		NARC Mash-I (V_1)	NARC Mash-II (V_2)	
N_{25}RI (T_3)	40 ± 4.2^{ab}	46 ± 3.1^{a}	43 ± 4.7^{A}	61 ± 3.6^{a}	62 ± 5.5^{a}	61 ± 4.2^{A}
N_{50}RI (T_4)	35 ± 5.0^{ab}	45 ± 4.0^{a}	42 ± 7.1^{AB}	54 ± 4.5^{abc}	60 ± 4.5^{a}	58 ± 5.1^{AB}
N_{75}RI (T_5)	32 ± 3.6^{b}	42 ± 4.1^{ab}	36 ± 5.8^{ABC}	55 ± 1.5^{abc}	59 ± 2.1^{a}	59 ± 3.3^{A}
N_{100}RI (T_6)	30 ± 3.7^{b}	37 ± 5.0^{ab}	34 ± 4.7^{BC}	51 ± 3.2^{bc}	53 ± 5.0^{abc}	52 ± 4.1^{BC}
Mean	33 ± 5.17^{B}	41 ± 6.42^{A}	37 ± 6.68	54 ± 5.28^{B}	57 ± 5.32^{A}	56 ± 5.4
CV (%)	10.241	14.257	8.054	15.348	12.042	13.255

Small and capital letters depict significant difference among treatment effects and their mean values, respectively. T_1 = control, no inoculation and fertilization, T_2 = inoculation but no fertilization, T_3 = 25 kg N ha^{-1}, T_4 = 50 kg N ha^{-1}, T_5 = 75 kg N ha^{-1}, T_6 = 100 kg N ha^{-1}, V_1 = NARC Mash-I, V_2 = NARC Mash-II, RI = rhizobia inoculation, CV = coefficient of variation.

3.3. Grain and Biological Yields under Rhizobia Inoculation and N Fertilization

Black gram cultivars depicted significant diversity in terms of grains and biological yields under the influence of RI and N fertilization regimes (Table 4). All of the fertilization regimes performed superiorly over the unfertilized control treatment, especially for the NARC Mash-II cultivar. The results revealed that the maximum grain yield (1777 ± 118) and biological yield (3007 ± 105) were recorded for NARC Mash-II in response to N_{25}RI, and were 58% and 37% higher compared to the unfertilized control treatment. Interestingly, NARC Mash-II remained statistically at par with N_{25}RI, N_0RI, and N_{75}RI in terms of grain yield. In contrast, NARC Mash-II under N_{25}RI exhibited a statistically similar biological yield (3007 ± 105) as that of N_{50}RI (2893 ± 110). Among the fertilizer regimes, N_{100}RI could not perform at par to the rest of the treatments; however, it remained statistically equal to the control treatment in terms of both grain yield and biological productivity. Following the trend, the Mash-II cultivar surpassed the Mash-I cultivar under N_{25}RI by recording significantly higher grains and biological yields.

Table 4. Grain yield and biomass productivity of black gram cultivars under rhizobia inoculation and N fertilization regimes in a temperate climate.

Treatments	Grain Yield (kg ha^{-1})			Biomass Yield (kg ha^{-1})		
	Genotypes		Mean	Genotypes		Mean
	NARC Mash-I (V_1)	NARC Mash-II (V_2)		NARC Mash-I (V_1)	NARC Mash-II (V_2)	
Control (T_1)	1124 ± 72^{f}	1272 ± 80^{def}	1208 ± 114^{C}	1951 ± 83^{d}	2182 ± 193^{cd}	2066 ± 183^{D}
N_0RI (T_2)	1547 ± 112^{abcd}	1738 ± 56^{a}	1643 ± 131^{AB}	2504 ± 165^{abc}	2688 ± 200^{abc}	2596 ± 193^{B}
N_{25}RI (T_3)	1630 ± 128^{ab}	1777 ± 118^{a}	1703 ± 136^{A}	2812 ± 160^{ab}	3007 ± 105^{a}	2910 ± 162^{A}
N_{50}RI (T_4)	1430 ± 133^{bcd}	1557 ± 52^{abc}	1493 ± 115^{B}	2358 ± 190^{bcd}	2893 ± 110^{a}	2625 ± 325^{AB}
N_{75}RI (T_5)	1334 ± 66^{cdef}	1754 ± 80^{a}	1544 ± 239^{AB}	2205 ± 157^{cd}	2556 ± 256^{abc}	2381 ± 270^{BC}
N_{100}RI (T_6)	1166 ± 80^{ef}	1419 ± 160^{bcde}	1292 ± 180^{C}	2225 ± 300^{cd}	2322 ± 322^{bcd}	2273 ± 284^{CD}
Mean	1372 ± 210^{B}	1589 ± 206^{A}	1480 ± 232	2342 ± 320^{B}	2608 ± 350^{A}	2475 ± 356
CV (%)	8.235	10.249	12.346	7.438	10.025	12.342

Small and capital letters depict significant difference among treatment effects and their mean values, respectively. T_1 = control, no inoculation and fertilization, T2 = inoculation but no fertilization, T_3 = 25 kg N ha^{-1}, T_4 = 50 kg N ha^{-1}, T_5 = 75 kg N ha^{-1}, T_6 = 100 kg N ha^{-1}, V_1 = NARC Mash-I, V_2 = NARC Mash-II, RI = rhizobia inoculation, LSD = least significant difference, CV = coefficient of variation.

3.4. Nitrogen Accumulation Grains and Shoots

The findings regarding grain and shoot N content displayed significant variation among black gram cultivars and fertilization regimes (Figure 2). NARC Mash-II outperformed NARC Mash-I, especially under the fertilization regime of N_{25}RI, by recording a

47% higher grain N content than the unfertilized control treatment, while this treatment combination performed statistically at par to N_0RI (Figure 2A). In contrast, NARC Mash-I under the fertilization regime of N_{25}RI gave maximum grain N content that was 33% higher compared to the control treatment and thus, in this way, NARC Mash-II accumulated 14% higher grain N content than NARC Mash-I under N_{25}RI. Overall, all of the fertilization regimes recorded comparatively higher N content of grain compared to the unfertilized control treatment. As far as shoot N content of black gram was concerned, NARC Mash-I in response to N_{25}RI exhibited the maximum shoot N value, which was 112% higher than the control treatment (Figure 2B). Moreover, this treatment combination remained statistically non-significant compared to the same cultivar under the N_{75}RI fertilization regime. Moreover, the minimum N content of the shoot was recorded for NARC Mash-I under the unfertilized control treatment that performed statistically similarly to NARC Mash-II under no fertilization, as well as the N_{100}RI fertilization regime.

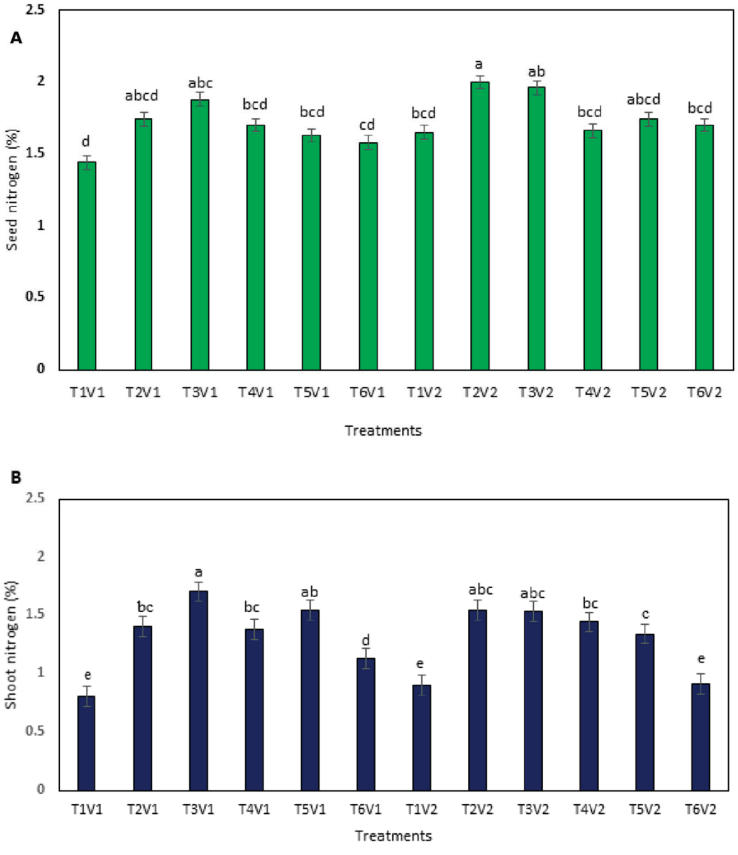

Figure 2. Content of grain nitrogen (**A**) and shoot nitrogen (**B**) of black gram cultivars supplemented with rhizobia inoculation and N fertilization in a temperate climate. Different letters on the bar column indicate significant differences at $p \leq 0.05$. All of the results are presented as mean ± SE of at least three independent replications. Here, T_1 = control, no inoculation and fertilization, T_2 = inoculation but no fertilization, T_3 = 25 kg N ha^{-1}, T_4 = 50 kg N ha^{-1}, T_5 = 75 kg N ha^{-1}, T_6 = 100 kg N ha^{-1}, V_1 = NARC Mash-I, V_2 = NARC Mash-II, RI = rhizobia inoculation.

3.5. Analysis of Soil N Dynamics

The results revealed that all of the N fertilization regimes outperformed the unfertilized control treatment in terms of soil N content (Figure 3). The maximum soil N buildup

(40% higher N compared to the unfertilized control treatment) was noted for experimental plots where NARC Mash-I was sown under the fertilization regime of N_{100}RI. It performed statistically at par with NARC Mash-II under the same fertilization regime that recorded 38% higher soil N compared to the unfertilized control treatment. Interestingly, NARC Mash-II sown in unfertilized plots remained statistically at par with the inoculated but unfertilized treatment, while NARC Mash-I and NARC Mash-II cultivars under the fertilization regimes of N_{25}RI, N_{50}RI, and N_{75}RI remained at par in terms of soil N content.

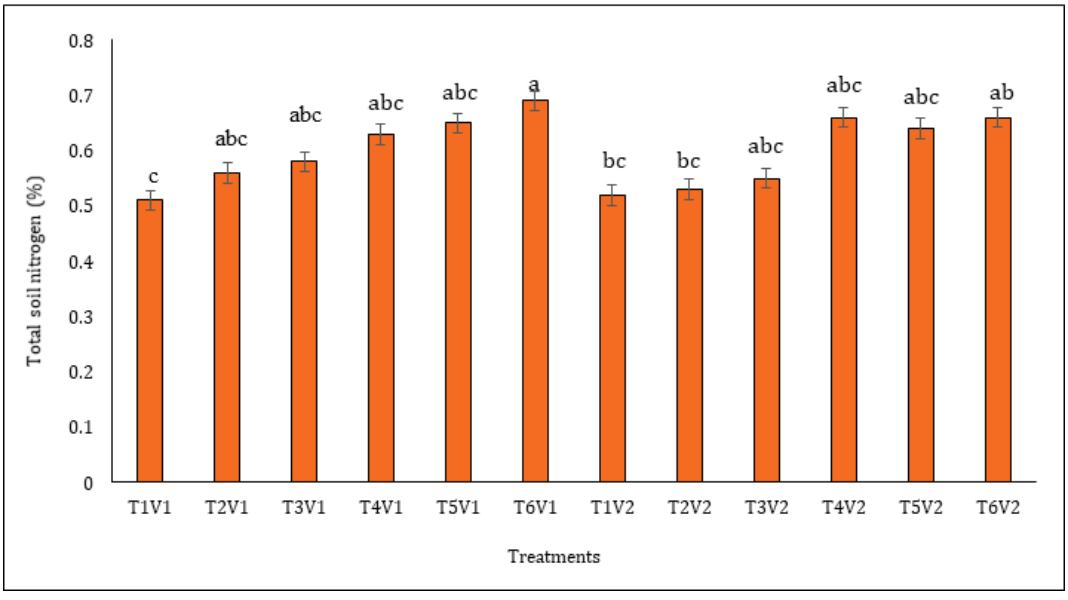

Figure 3. Accumulation of total nitrogen in soil under black gram cultivars supplemented with rhizobia inoculation and N fertilization in a temperate climate. Different letters of the bar column indicate significant differences at $p \leq 0.05$. All of the results are presented as mean ± SE of at least three independent replications. Here, T_1 = control, no inoculation and fertilization, T_2 = inoculation but no fertilization, T_3 = 25 kg N ha^{-1}, T_4 = 50 kg N ha^{-1}, T_5 = 75 kg N ha^{-1}, T_6 = 100 kg N ha^{-1}, V_1 = NARC Mash-I, V_2 = NARC Mash-II, RI = rhizobia inoculation.

3.6. Principal Component Analysis and Correlation of Different Yield Attributes

The correlation analysis indicated a highly significant association among yield attributes (number of pods per plant, thousand grain weight, etc.) with the grain yield as well as the biological yield of black gram (Table 5). Moreover, in accordance with principal component analysis (PCA), the observation point made by a combination of PC1/PC2 and PC1/PC3 depicts the general variance described by the five major components. The maximum loading was noted for the PC1 component, while the minimum loading was observed in the PC3 component for the N content of the grain, shoot, and soil. Furthermore, PC4 and PC5 were not plotted as they do not furnish any further information. Obviously, the PCA showed that the control treatments of both genotypes were less affected by the grain, shoot, and soil N accumulation in the plant–soil system in comparison with RI alone or in association with the N fertilization treatments (Figure 4A,B). Actually, the points of the control treatments found were closer compared with the other amended treatments regarding both genotypes, and also nearer to the central point of the PCA components.

Table 5. Correlation analyses of different agricultural attributes of black gram (mean values of both cultivars and years) tested under rhizobia inoculation and N fertilization regimes in a temperate climate.

	No. of Nodules per Plant	Nodule Dry Weight (g)	No. of Pods per Plant	Thousand Grain Weight (kg ha^{-1})	Grain Yield (kg ha^{-1})	Bio-Yield (kg ha^{-1})	Grain Nitrogen (%)	Shoot Nitrogen (%)
Nodule dry weight	0.768 **							
	0.000							
No. of pods per plant	0.630 **	0.714 **						
	0.000	0.000						
Thousand grain weight	0.793 **	0.724 **	0.652 **					
	0.001	0.000	0.000					
Grain yield	0.743 **	0.838 **	0.758 **	0.773 **				
	0.000	0.000	0.001	0.000				
Bio-yield	0.752 **	0.848 **	0.800 **	0.750 **	0.747 **			
	0.000	0.000	0.001	0.000	0.000			
Grain nitrogen	0.636 **	0.696 **	0.589 **	0.494 **	0.753 **	0.574 **		
	0.000	0.000	0.001	0.000	0.002	0.000		
Shoot nitrogen	0.651 **	0.682 **	0.515 **	0.672 **	0.670 **	0.627 **	0.582 **	
	0.000	0.002	0.001	0.000	0.000	0.000	0.000	
Soil nitrogen	0.054	−0.062	−0.011	−0.119	−0.076	0.037	−0.167	0.048
	0.756	0.719	0.949	0.488	0.659	0.831	0.329	0.778

** indicates highly significant association, while–sign depicts negative association.

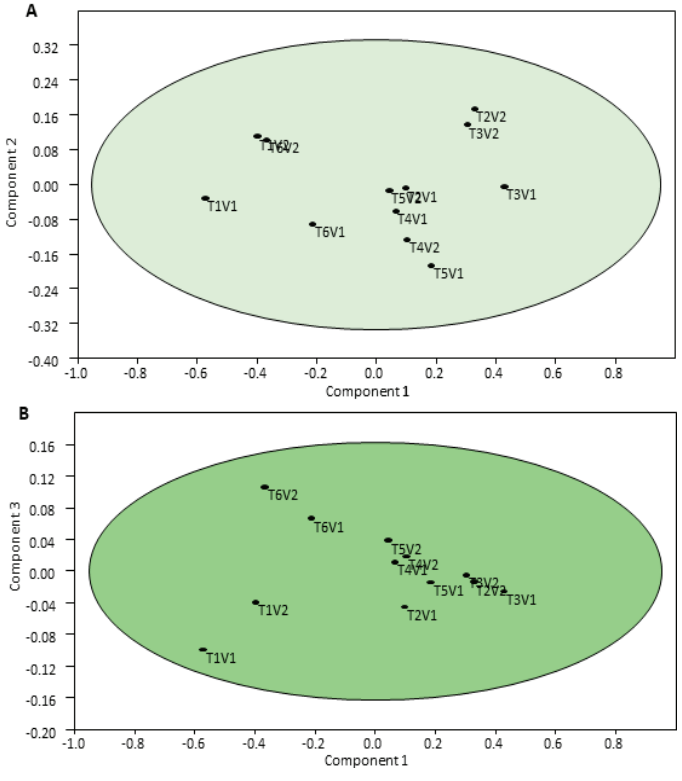

Figure 4. The principal component analysis (PCA) of black gram cultivars subjected to rhizobia inoculation (**A**) and varying N fertilization regimes (**B**) in a temperate climate. Here, T_1 = control, no inoculation and fertilization, T_2 = inoculation but no fertilization, T_3 = 25 kg N ha^{-1}, T_4 = 50 kg N ha^{-1}, T_5 = 75 kg N ha^{-1}, T_6 = 100 kg N ha^{-1}, V_1 = NARC Mash-I, V_2 = NARC Mash-II, RI = rhizobia inoculation.

4. Discussion

Increasing crop yields through microbial inoculation and N fertilizer supplementation is a biologically viable way to move toward modern agricultural production systems. The RI of leguminous crops, especially on virgin soils, constitutes a sustainable approach toward boosting crop productivity [17,20]. In this study, the RI and N fertilization regimes significantly boosted the nodulation of black gram cultivars. The RI tends to promote the grain yield of leguminous crops by boosting root nodulation, which results in the higher fixation of atmospheric N through the BNF process [41]. Similar to our findings (sole RI and N fertilization in association with RI significantly promoted black gram nodulation), it was reported that RI proved to be an eco-friendly and cost-effective technique for boosting root nodulation in mung bean, peas, and red clover [42,43]. However, a previous study suggested that RI reduces the requirement of N fertilizer due to increased N fixation in many crops [44]. Additionally, it helped to activate the response of ineffective rhizobium strains present in the soils which later on became involved in the N fixation process [45].

Interestingly, RI along with low N supply improved N fixation by producing a greater number of functional nodules [46]. In this present study, the better response of RI even without N supplementation opened a new avenue for sustainable, eco-friendly, and smart agriculture by utilizing rhizobia for promoting N fixation. In contrast, the suppression of nodulation in response to a high N dose indicates the inhibitory effects of high N content on nitrogenase activity in the root nodules. A negative correlation was found between the supplementation of N and the number of formed root nodules [47]. Robust vegetative growth was recorded as seen through higher N doses in legumes and grain crops [48]; however, nodule formation was governed by soil rhizobia population and soil N content [49]. In this study, the nodulation was influenced by RI combined with N supplementation in black gram. A number of studies reported that RI considerably improved plant growth, nutritional accumulation, and plant fitness to changing environments [9,13,50,51]. Moreover, varying genotypic potential existed among soybean cultivars, along with RI which significantly increased the nodule dry weight [52,53]. However, the nodule number could vary due to genetic potential, and agronomic management practices might impart significant influence on the nodule development of leguminous crops [54]. Likewise, it has also been inferred that genotypic divergence in black gram cultivars existed, which resulted in varying levels of nodulation in terms of the number of functional nodules along with fresh and dry weight of nodules per plant [54–57].

Legumes are the most effective crops which contribute N to soils through N fixation and ultimately improve soil fertility. Our study also reports the benefit of exogenous N supplementation and RI, which significantly enhanced the pod number per plant, thousand grain weight, grain yield, and biological biomass production in black gram cultivars. Thus, effective plant–microbe interactions, the enhancement of root nodulation, and increase in N fixation tend to improve the growth and yield attributes of black gram [58]. In contrast, the mismatching of RI with higher N doses might reduce root development and water and nutrient uptake in soils. Furthermore, RI under limited N supply tends to trigger various vital processes such as N fixation, nitrate reductase activity, the biosynthesis of crucial plant hormones such as auxins, gibberellins, and cytokinins, and the boosting of phosphate solubilization, which enhanced the legume yield [59]. In this study, shoot N status showed that the least N supply with RI significantly improved the black gram grain yield and shoot N content compared to the control treatment. It might be concluded that RI in association with reduced N doses remained effective in boosting the BNF fixation process, and ultimately, a greater concentration of N accumulated in the grains and shoots. A previous study has suggested that RI with N supplementation enhanced nitrogenase activity, which improved the total N content in plants [40]. In addition, it was also inferred that a limited supply of inorganic N fulfilled the immediate N needs of crop plants, while a slow and steady provision of N produced through the BNF process resulted in greater N content of grains. Moreover, meager N supply triggered rhizobia activity and ultimately better N accumulation was recorded in the leaves, shoots, and grains of the crops [1].

However, RI with a limited N supply increased the N content of the plant–soil system, owing to improved N absorption and higher N use efficiency [60].

Soil N content is a vital factor that determines rhizobia's ability to fix N through the BNF process. The higher doses of inorganic N with RI improved the soil N status in comparison to lower N doses, indicating that higher N doses were over and above the crop plants' requirements and remained unutilized, which led to N buildup in the soil. These results might be linked to the black gram tendency to uptake lower amounts of supplemented N, which ultimately resulted in the accumulation of higher N in the rhizosphere [53]. However, RI combined with a moderate N supply improved the total soil N contents compared to limited N doses [61,62]. Interestingly, a lower N dose with RI has been reported to increase shoot and soil N contents [60]. The Pearson correlation analysis amongst black gram nodulation, yield attributes such as number of pods per plant and their dry weight, and grain and biological yields, along with plant and soil N, indicated a stronger linear relationship, which highlights the role of these yield components in boosting the grain yield of black gram. These traits have been reported to be of great pertinence for the selection and establishment of breeding criteria to increase the grain yield of legumes. These findings are in accordance with a previous study, where it was reported that the determination of pod numbers per plant and thousand grain weight were the most crucial strategies for projecting the grain yield, because these were linearly associated with the grain yield of legumes [63,64]. Contrastingly, a greater number of pods per plant contained a lower number of grains per pod, and thus this was negatively associated with the thousand grain weight of black gram. However, our findings were supported by previous studies where the yield attributes including the pod numbers and grain weight were linearly associated with the grain yield and N content of the shoots and grains in black gram [65–68]. Moreover, shoot N increased in the presence of greater soil N content. However, the legumes' grain yield increment was directly associated with the robustness of the nodulation and amount of N fixed through the BNF process [41].

PC analysis can identify the traits that account for variation in crop yields [64–69], and thus, it may be employed for confirming the most influential response variables [70–72]. According to the PC1/PC2 combination analysis in this study, the unamended control treatment remained the least affected compared with the amended treatments for both cultivars of black gram. Furthermore, higher N doses applied with RI recorded significantly less N content in the shoots and grains of black gram. However, yield traits had a negative correlation with soil total N contents. Similarly to our findings, El-Sorady et al. [40] inferred that two PCs accounted for over 92% of the total variation among employed treatments. Likewise, our findings also remained in concurrence with the results of a previous study whereby PC analysis highlighted the major variability among the treatments [73,74]. These research findings can be of great assistance to black gram growers for boosting productivity and soil fertility in a sustainable and eco-friendly way.

5. Conclusions

The research findings provide a mechanistic insight into plant–microbe interactions and N-fertilization-based improvement in the yield attributes and grain yield of black gram. This study found that considerable yield potential variation existed among black gram cultivars which was significantly influenced by RI and different doses of N fertilization under a temperate environment. The NARC Mash-II cultivar remained superior under the N_{25}RI fertilization regime by recording significantly higher root nodulation, pod numbers per plant, and thousand grain weight than the unfertilized control treatment did. The same treatment combination outmatched the control treatment in terms of grain yield and biological yield, along with the N content of the grain, while NARC Mash-I resulted in higher N accumulation in the shoot and soil. This study further suggests that a high level of N supply (>25 kg N ha^{-1}) reduced the nodule formation and pod setting, while 25 kg N ha^{-1} combined with RI improved all of the response variables except for shoot and soil N content. This combination of cultivar (NARC Mash-II) and 25 kg N ha^{-1} combined

with RI might be recommended to growers for boosting the nodulation, N dynamics, agronomic yield attributes, and productivity of black gram. However, future research needs to focus on determining the influence of higher N doses on nodulation and soil–plant N dynamics to assess the possible negative effects of nitrate on nodule formation and root N levels.

Author Contributions: Conceptualization, M.S., N.R., M.M.T. and M.A.I.; methodology, M.S., A.M. and M.A.I.; validation, M.A.I. and R.A.; formal analysis, R.A., M.D.A. and M.A.I.; writing—original draft preparation, M.A.I., M.M.T., N.R. and R.A.; writing—review and editing, M.A.I., M.D.A. and A.M. All authors have read and agreed to the published version of the manuscript.

Funding: The authors extend their appreciation to the Princess Nourah bint Abdulrahman University Researchers Supporting Project (number PNURSP2023R355), Princess Nourah bint Abdulrahman University, Riyadh, Saudi Arabia.

Data Availability Statement: Data are available from the corresponding author upon reasonable request.

Acknowledgments: All of the authors convey the highest appreciation to the Princess Nourah bint Abdulrahman University Researchers Supporting Project (number PNURSP2023R355), Princess Nourah bint Abdulrahman University, Riyadh, Saudi Arabia.

Conflicts of Interest: The authors declare no conflict of interest.

References

1. Chattha, M.U.; Arif, W.; Khan, I.; Soufan, W.; Bilal Chattha, M.; Hassan, M.U.; Ullah, N.; Sabagh, A.E.; Qari, S.H. Mitigation of cadmium induced oxidative stress by using organic amendments to improve the growth and yield of mash beans [*Vigna mungo* (L.)]. *Agronomy* **2021**, *11*, 2152. [CrossRef]
2. Saleem, R.; Ahmad, Z.I.; Ashraf, M.; Anees, M.A.; Javed, H.I. Impact of different fertility sources intercropping on productivity of black gram. *Int. J. Biol. Biotechnol.* **2016**, *13*, 89–99.
3. Simon, Z.; Mtei, K.; Gessesse, A.; Ndakidemi, P.A. Isolation characterization of nitrogen fixing rhizobia from cultivated uncultivated soils of Northern Tanzania. *Am. J. Plant Sci.* **2014**, *5*, 4050–4067. [CrossRef]
4. Roychowdhury, R.; Banerjee, U.; Sofkova, S.; Tah, J. Organic farming for crop improvement sustainable agriculture in the Era of climate change Online. *J. Biol. Sci.* **2013**, *13*, 50–65. [CrossRef]
5. Reddy, A.; Kavitha Priya, M.S.; Reddy, D.M.; Reddy, B.R. Principal Component Analysis for Yield in blackgram (*Vigna mungo* L. Hepper) under organic and inorganic fertilizer managements. *Int. J. Plant Soil Sci.* **2021**, *33*, 26–34. [CrossRef]
6. Rathore, R.S.; Singh, R.P.; Nawange, D.D. Effect of land configuration, seed rates and fertilizer doses on growth and yield of black gram [*Vigna Mungo* (L.) Hepper]. *Legume Res.* **2010**, *33*, 274–278.
7. Prasad, J.D.; Sharma, S.K.; Amarawat, T. Effect of organic and inorganic sources of nutrients on yield and economics of blackgram (*Vigna mungo* L.) grown during kharif. *Agric. Sci. Digest.* **2015**, *35*, 224–228. [CrossRef]
8. Marimuthu, S.; Surendran, U. Effect of nutrients and plant growth regulators on growth and yield of black gram in sandy loam soils of Cauvery new delta zone, India. *Cogent Food Agri.* **2015**, *1*, 1010415. [CrossRef]
9. Chandrasekar, C.N.; Bangarusamy, U. Maximizing the yield of mungbean by foliar application of growth regulating chemicals and nutrients. *Madras Agric. J.* **2003**, *90*, 142–145.
10. Ahmed, Z.I.; Ansar, M.; Saleem, A.; Arif, Z.U.; Javed, H.I.; Saleem, R. Improvement of mash bean production under rainfed conditions by Rhizobium inoculation lower rates of starter nitrogen Pak. *J. Agric. Res.* **2012**, *25*, 154–356.
11. Rahman, M.A.; Lee, S.-H.; Ji, H.C.; Kabir, A.H.; Jones, C.S.; Lee, K.-W. Importance of mineral nutrition for mitigating aluminum toxicity in plants on acidic soils: Current status opportunities. *Int. J. Mol. Sci.* **2018**, *19*, 3073. [CrossRef]
12. Rahman, M.A.; Parvin, M.; Das, U.; Ela, E.J.; Lee, S.-H.; Lee, K.-W.; Kabir, A.H. Arbuscular mycorrhizal symbiosis mitigates iron (Fe)-deficiency retardation in alfalfa (*Medicago sativa* L.) through the enhancement of Fe accumulation sulfur-assisted antioxidant defense. *Int. J. Mol. Sci.* **2020**, *21*, 2219. [CrossRef]
13. Kabir, A.H.; Rahman, M.A.; Rahman, M.M.; Brailey-Jones, P.; Lee, K.W.; Bennetzen, J.L. Mechanistic assessment of tolerance to iron deficiency mediated by Trichoderma harzianum in soybean roots. *J. Appli. Microbiol.* **2022**, *133*, 2760–2778. [CrossRef]
14. Khan, I.; Muhammad, A.; Chattha, M.U.; Skalicky, M.; Bilal Chattha, M.; Ayub, M.A.; Anwar, M.R.; Soufan, W.; Hassan, M.U.; Rahman, M.A.; et al. Mitigation of salinity-induced oxidative damage, growth, and yield reduction in fine rice by sugarcane press mud application. *Front. Plant. Sci.* **2022**, *13*, 840900. [CrossRef]
15. Khan, Q.A.; Sardar, A.C.; Muhammad, F.; Abdul, W.; Fasih, U.H. Monitoring the role of molybdenum seed priming on productivity of mung bean (*Vigna radiata* L.). *J. Res. Ecol.* **2019**, *7*, 2417–2427.
16. Allito, B.B.; Ewusi-Mensah, N.; Logah, V. Legume-Rhizobium strain specificity enhances nutrition and nitrogen fixation in faba bean (*Vicia faba* L.). *Agronomy* **2020**, *10*, 826. [CrossRef]

17. Rahman, M.A.; Alam, I.; Kim, Y.-G.; Ahn, N.-Y.; Heo, S.-H.; Lee, D.-G.; Liu, G.; Lee, B.-H. Screening for salt-responsive proteins in two contrasting alfalfa cultivars using a comparative proteome approach. *Plant Physiol. Biochem.* **2015**, *89*, 112–122. [CrossRef] [PubMed]
18. Sánchez-Navarro, V.; Zornoza, R.; Faz, Á.; Egea-Gilabert, C.; Ros, M.; Pascual, J.A.; Fernández, J.A. Inoculation with different nitrogen-fixing bacteria and Arbuscular mycorrhiza affects grain protein content and nodule bacterial communities of a fava bean crop. *Agronomy* **2020**, *10*, 768. [CrossRef]
19. Htwe, A.Z.; Moa, S.M.; Seo, K.M.; Moe, K.; Yamakawa, T. Effects of bio-fertilizer produced from Bradyrhizobium and Streptomyces griseoflavus on plant growth, nodulation, nitrogen fixation, nutrient uptake and seed yield of mung Bean, cowpea, and soybean. *Agronomy* **2019**, *9*, 77. [CrossRef]
20. de Carvalho, R.H.; da Conceição Jesus, E.; Favero, V.O. The Co-inoculation of Rhizobium and Bradyrhizobium increases the early nodulation and development of common beans. *J. Soil. Sci. Plant Nutr.* **2020**, *20*, 860–864. [CrossRef]
21. Kebede, E. Competency of Rhizobial inoculation in sustainable agricultural production and biocontrol of plant diseases. *Front. Sustain. Food Syst.* **2021**, *5*, 728014. [CrossRef]
22. Abbas, R.N.; Arshad, M.A.; Iqbal, A.; Iqbal, M.A.; Imran, M.; Raza, A.; Chen, J.-T.; Alyemeni, M.N.; Hefft, D.I. Weeds spectrum, productivity and land-use efficiency in maize-gram intercropping systems under semi-arid environment. *Agronomy* **2021**, *11*, 1615. [CrossRef]
23. Amine-Khodja, I.R.; Boscari, A.; Riah, N.; Kechid, M.; Maougal, R.T.; Belbekri, N.; Djekoun, A. Impact of two strains of rhizobium leguminosarum on the adaptation to terminal water deficit of two cultivars *Vicia faba*. *Plants* **2022**, *11*, 515. [CrossRef] [PubMed]
24. Singh, G.; Kumar, D.; Sharma, P. Effect of organics, bio-fertilizers and crop residue application on soil microbial activity in rice-wheat and rice-wheat mung bean cropping systems in the Indo Gangetic Plains. *Cogent Geosci.* **2015**, *1*, 1085296. [CrossRef]
25. Toledo, C.B. Effect of Rhizobium inoculation on tomato (*Solanum lycopersicum* L.) Yield in protected crops. *Biol. Life Sci. Forum* **2021**, *3*, 52. [CrossRef]
26. Jalal, A.; Galindo, F.S.; Boleta, E.H.M.; Oliveira, C.E.d.S.; Reis, A.R.d.; Nogueira, T.A.R.; Moretti Neto, M.J.; Mortinho, E.S.; Fernandes, G.C.; Teixeira Filho, M.C.M. Common bean yield and zinc use efficiency in association with diazotrophic bacteria co-inoculations. *Agronomy* **2021**, *11*, 959. [CrossRef]
27. Genetu, G.; Yli-Halla, M.; Asrat, M.; Alemayehu, M. Rhizobium inoculation and chemical fertilisation improve faba bean yield and yield components in northwestern Ethiopia. *Agriculture* **2021**, *11*, 678. [CrossRef]
28. Safronova, V.; Sazanova, A.; Kuznetsova, I.; Belimov, A.; Guro, P.; Karlov, D.; Yuzikhin, O.; Chirak, E.; Verkhozina, A.; Afonin, A.; et al. Increasing the legume–rhizobia symbiotic efficiency due to the synergy between commercial strains and strains isolated from relict symbiotic systems. *Agronomy* **2021**, *11*, 1398. [CrossRef]
29. Malhi, G.S.; Rana, M.C.; Kumar, S.; Rehmani, M.I.A.; Hashem, A.; Abd_Allah, E.F. Efficacy, energy budgeting, and carbon footprints of weed management in black gram (*Vigna mungo* L.). *Sustainability* **2021**, *13*, 13239. [CrossRef]
30. Qayyum, A.; Iqbal, L.J.; Barbanti, A.; Sher, G.; Shabbir, G.; Rabbani, M.K.; Rafiq, M.N.; Tareen, M.J.; Amin, B.A. Mash bean [*Vigna mungo* (L.) Hepper] Germplasm evaluation at different ecological conditions of Pakistan. *Appl. Ecol. Environ. Res.* **2019**, *17*, 6643–6654. [CrossRef]
31. Banerjee, P.; Venugopalan, V.K.; Nath, R.; Althobaiti, Y.S.; Gaber, A.; Al-Yasi, H.; Hossain, A. Physiology growth productivity of spring–summer black gram (*Vigna mungo*, L. Hepper) as influenced by heat and moisture stresses in different dates of sowing and nutrient management conditions. *Agronomy* **2021**, *11*, 2329. [CrossRef]
32. Khaliq, A.; Muhammad Aamir Iqbal Zafar, M.; Gulzar, A. Appraising economic dimension of maize production under coherent fertilization in Azad Kashmir, Pakistan. *Custos Agronegocio* **2019**, *15*, 243–253.
33. Zia-Ul-Haq, M.; Ahmad, S.; Bukhari, S.A.; Amarowicz, R.; Ercisli, S.; Jaafar, H.Z.E. Compositional studies and biological activities of some mash bean (*Vigna mungo* (L.) Hepper) cultivars commonly consumed in Pakistan. *Biol. Res.* **2014**, *47*, 23. [CrossRef] [PubMed]
34. Golezani, K.G.; Saeid, H.B.; Ali, B.H.; Salar, F.A. Seed hydro-priming a simple way for improving mungbean performance under water stress. *Int. J. Biosci.* **2014**, *4*, 12–18. [CrossRef]
35. Temprano, F.J.; Albareda, M.; Camacho, M.; Daza, A.; Santamaría, C.; Rodríguez-Navarro, D.N. Survival of several Rhizobium/Bradyrhizobium strains on different inoculant formulations and inoculated seeds. *Int. Microbiol.* **2002**, *5*, 81–86. [CrossRef]
36. Nelson, D.W.; Sommers, L.E. Total carbon, organic carbon and organic matter. In *Methods of Soil Analysis. Part 2. Chemical and Microbiological Properties*, 2nd ed.; Page, A.L., Miller, R.H., Keeney, D.R., Eds.; Agronomy 9; American Society of Agronomy: Madison, WI, USA, 1982; pp. 539–594.
37. Apesteguia, M.; Plante, A.F.; Virto, I. Methods assessment for organic and inorganic carbon quantification in calcareous soils of the Mediterranean region. *Geoderma Reg.* **2018**, *12*, 39–48. [CrossRef]
38. Ghaemi, A.; Rahimi, A.; Banihashemi, Z. Effects of water stress and *Fusarium oxysporum* f. sp. Lycoperseci on growth (leaf area, plant height, shoot dry matter) and shoot nitrogen content of tomatoes under greenhouse conditions. *Iran Agric. Res.* **2009**, *28*, 51–62.
39. Iqbal, M.A.; Raza, R.Z.; Zafar, M.; Ali, O.M.; Ahmed, R.; Rahim, J.; Ijaz, R.; Ahmad, Z.; Bethune, B.J. Integrated fertilizers synergistically bolster temperate soybean growth, yield, and oil content. *Sustainability* **2022**, *14*, 2433. [CrossRef]

40. El-Sorady, G.A.; El-Banna, A.A.A.; Abdelghany, A.M.; Salama, E.A.A.; Ali, H.M.; Siddiqui, M.H.; Hayatu, N.G.; Paszt, L.S.; Lamlom, S.F. Response of bread wheat cultivars inoculated with azotobacter species under different nitrogen application rates. *Sustainability* **2022**, *14*, 8394. [CrossRef]
41. Thilakarathna, M.S.; Chapagain, T.; Ghimire, B.; Pudasaini, R.; Tamang, B.B.; Gurung, K.; Choi, K.; Rai, L.; Magar, S.; Bishnu, B.K.; et al. Evaluating the effectiveness of rhizobium inoculants and micronutrients as technologies for Nepalese common bean smallholder farmers in the real-world context of highly variable hillside environments and indigenous farming practices. *Agriculture* **2019**, *9*, 9010020. [CrossRef]
42. Dacko, M.; Zajac, T.; Synowiec, A.; Oleksy, A.; Klimek-Kopyra, A.; Kulig, B. New approach to determine biological and environmental factors influencing mass of a single pea (*Pisum sativum* L.) seed in Silesiaregion in Poland using a CART model. *Eur. J. Agron.* **2016**, *74*, 29–37. [CrossRef]
43. Furtak, K.; Gawryjołek, K.; Gałązka, A.; Grządziel, J. The response of red clover (*Trifolium pratense* L.) to separate mixed inoculations with Rhizobium leguminosarum Azospirillum brasilense in presence of polycyclic aromatic hydrocarbons. *Int. J. Environ. Res. Public Health* **2020**, *17*, 5751. [CrossRef] [PubMed]
44. Thilakarathna, M.S.; Raizada, M.N. A review of nutrient management studies involving finger millet in the semi-arid tropics of Asia and Africa. *Agronomy* **2015**, *5*, 262–290. [CrossRef]
45. Thilakarathna, M.S.; Raizada, M.N. Challenges in using precision agriculture to optimize symbiotic nitrogen fixation in legumes progress, limitations, and future improvements needed in diagnostic testing. *Agronomy* **2018**, *8*, 78. [CrossRef]
46. Htwe, A.Z.; Moh, S.M.; Moe, K.; Yamakawa, T. Effects of co-inoculation of Bradyrhizobium japonicum SAY3-7 and Streptomyces griseoflavus P4 on plant growth, nodulation, nitrogen fixation, nutrient uptake, and yield of soybean in a field condition. *Soil Sci. Plant Nutri.* **2018**, *64*, 222–229. [CrossRef]
47. Aung, T.T.; Tittaburt, P.; Boonkerd, N.; Herridge, D. Co-inoculation effects of Bradrhizobium japonicum Azospirillum sp on competitive nodulation rhizosphere bacterial community structures of soybean under rhizobia-established soil conditions. *Afr. J. Biotechnol.* **2013**, *12*, 2850–2862.
48. Mbarki, S.; Talbi, O.; Skalicky, M.; Vachova, P.; Hejnak, V.; Hnilicka, F.; Al-ashkar, I.; Abdelly, C.; Rahman, M.A.; El Sabagh, A.; et al. Comparison of grain sorghum and alfalfa for providing heavy metal remediation of sandy soil with different soil amendments and salt stress. *Front. Environ. Sci.* **2022**, *10*, 1022629. [CrossRef]
49. Chauhan, J.; Srivastava, J.P.; Singhal, R.K.; Soufan, W.; Dadarwal, B.K.; Mishra, U.N.; Anuragi, H.; Rahman, M.A.; Sakran, M.I.; Brestic, M.; et al. Alterations of oxidative stress indicators, antioxidant enzymes, soluble sugars, and amino acids in mustard [*Brassica juncea* (L.) Czern and Coss.] in response to varying sowing time, and field temperature. *Front. Plant. Sci.* **2022**, *13*, 875009. [CrossRef]
50. Raza, A.; Charagh, S.; García-Caparrós, P.; Rahman, M.A.; Ogwugwa, V.H.; Saeed, F.; Jin, W. Melatonin-mediated temperature stress tolerance in plants. *GM Crops Food* **2022**, *13*, 196–217. [CrossRef]
51. Raza, A.; Salehi, H.; Rahman, M.A.; Zahid, Z.; Haghjou, M.M.; Najafi-Kakavand, S.; Charagh, S.; Osman, H.S.; Albaqami, M.; Zhuang, Y.; et al. Plant hormones and neurotransmitter interactions mediate antioxidant defenses under induced oxidative stress in plants. *Front. Plant. Sci.* **2022**, *13*, 961872. [CrossRef]
52. Yamakawa, T.; Soe, K.M. Evaluation of effective Myanmar Brady-rhizobium strains isolated from Myanmar soybean and effects of co-inoculation with Streptomyces griseoflavus P4 for nitrogen fixation. *Soil Sci. Plant Nutr.* **2013**, *59*, 361–370. [CrossRef]
53. Soe, K.M.; Bhromsiri, A.; Karladee, D.; Yamakawa, T. Effects of endophytic Actinomycetes and Bradyrhizobium japonicum strains on growth, nodulation, nitrogen fixation and seed weight of soybean varieties. *Soil Sci. Plant Nutr.* **2012**, *58*, 319–325. [CrossRef]
54. Nisar, M.; Ghafoor, A.; Khan, M.R.; Ahmad, H.; Qureshi, A.S.; Ali, H. Genetic diversity geographic relationship among local exotic chickpea germplasm. *Pak. J. Bot.* **2007**, *39*, 1575–1581.
55. Hassan, H.M.; Hadifa, A.A.; El-leithy, S.A.; Batool, M.; Sherif, A.; Al-Ashkar, I.; Ueda, A.; Rahman, M.A.; Hossain, M.A.; Elsabagh, A. Variable level of genetic dominance controls important agronomic traits in rice populations under water deficit condition. *PeerJ* **2023**, *11*, e14833. [CrossRef] [PubMed]
56. Islam, M.-R.; Kamal, M.-M.; Hossain, M.-F.; Hossain, J.; Azam, M.-G.; Akhter, M.-M.; Hasan, M.-K.; Al-Ashkar, I.; Almutairi, K.-F.; Sabagh, A.-E.; et al. Drought tolerance in mung bean is associated with the genotypic divergence, regulation of proline, photosynthetic pigment and water relation. *Phyton* **2023**, *92*, 955–981. [CrossRef]
57. Zafar, S.A.; Aslam, M.; Khan, H.J.; Sarwar, S.; Rehman, R.S.; Hassan, M.; Ahmad, R.M.; Gill, R.A.; Ali, B.; Al-Ashkar, I.; et al. Estimation of genetic divergence and character association studies in local and exotic diversity panels of soybean (*Glycine max* L.) genotypes. *Phyton* **2023**, *92*, 1887–1906. [CrossRef]
58. Patra, R.K.; Pant, L.M.; Pradhan, K. Response of Soybean to Inoculation with Rhizobial Strains, Effect on Growth, Yield, N Uptake and Soil N Status. *World J. Agric. Res.* **2012**, *8*, 51–54.
59. Consentino, B.B.; Aprile, S.; Rouphael, Y.; Ntatsi, G.; De Pasquale, C.; Iapichino, G.; Alibrandi, P.; Sabatino, L. Application of PGPB combined with variable n doses affects growth, yield-related traits, n-fertilizer efficiency and nutritional status of lettuce grown under controlled condition. *Agronomy* **2022**, *12*, 236. [CrossRef]
60. Tahir, M.M.; Abbasi, M.K.; Rahim, N.; Khaliq, A.; Kazmi, M.H. Effect of Rhizobium inoculation and NP fertilization on growth, yield and nodulation of soybean (*Glycine max* L.) in the sub-humid hilly region of Rawalakot Azad Kashmir, Pakistan. *Afr. J. Biotechnol.* **2009**, *8*, 6191–6200. [CrossRef]

61. Soe, K.M.; Yamakawa, T. Low-density co-inoculation with Bradyrhizobium japonicum, S.A.Y.3.-7.; Streptomyces griseoflavus P4 promotes plant growth nitrogen fixation in soybean cultivars. *Am. J. Plant Sci.* **2016**, *7*, 1652–1661. [CrossRef]
62. Zaman, A.; Sarkar, A.S.; Sarkar, W.; Devi, P. Effect of organic inorganic sources of nutrients on productivity specific gravity processing quality of (*Solanum tuberosum*) Indian. *J. Agric. Sci.* **2011**, *81*, 1137–1142.
63. Mudasir, S.; Sofi, P.A.; Khan, M.N.; Sofi, N.R.; Dar, Z.A. Genetic diversity variability character association in local common bean (Phaseolus vulgaris L) germplasm of Kashmir Electron. *J. Plant Breed* **2012**, *3*, 883–891.
64. Yaseen, M.; Kashif, M.; Nazish, H.T.; Munir, R.; Iqbal, J.; Usman, M.; Rabbani, G. Effect of rain-fed conditions on yield of mash bean genepool by using augmented design. *J. Stat. Theory Appl.* **2022**, *21*, 186–199. [CrossRef]
65. Hakim, L. Variability correlation of agronomic characters of mung bean germplasm their utilization for variety improvement program. *Indones. J. Agric. Sci.* **2008**, *9*, 24–28. [CrossRef]
66. Konda, C.R.; Salimathand, P.H.; Mishra, M.N. Correlation and path coefficient analysis in black gram (*Vigna mungo* (L.) Hepper). *Legume Res.* **2008**, *31*, 202–205.
67. Veeramani, N.; Venkatesan, M.; Thangavel, P.; Ganesan, J. Genetic variability, heritability and genetic advance analysis in segregating generation of black gram (*Vigna mungo* (L.) Hepper). *Legume Res.* **2005**, *28*, 49–51.
68. Kumar, B.S.; Padmavathi, S.; Prakash, M.; Ganesan, J. Correlation and path analysis in black gram [*Vigna mungo* (L.) Hepper]. *Legume Res.* **2003**, *26*, 75–76.
69. Al-Suhaibani, N.; Selim, M.; Alderfasi, A.; El-Hendawy, S. Comparative performance of integrated nutrient management between composted agricultural wastes, chemical fertilizers, and biofertilizers in improving soil quantitative and qualitative properties and crop yields under arid conditions. *Agronomy* **2022**, *10*, 1503. [CrossRef]
70. Dal Cortivo, C.; Ferrari, M.; Visioli, G.; Lauro, M.; Fornasier, F.; Barion, G.; Panozzo, A.; Vamerali, T. Effects of seed-applied biofertilizers on rhizosphere biodiversity and growth of common wheat (*Triticum aestivum* L.) in the field. *Front. Plant Sci.* **2020**, *11*, 72. [CrossRef] [PubMed]
71. Lu, P.; Bainard, L.D.; Ma, B.; Liu, J. Bio-fertilizer and rotten straw amendments alter the rhizosphere bacterial community and increase oat productivity in a saline–alkaline environment. *Sci. Rep.* **2020**, *10*, 19896. [CrossRef]
72. Rathnathilaka, T.; Premarathna, M.; Madawala, S.; Pathirana, A.; Karunaratne, K.; Seneviratne, G. Biofilm biofertilizer application rapidly increases soil quality grain yield in large scale conventional rice cultivation A case study. *J. Plant. Nutr.* **2022**, *46*, 1220–1230. [CrossRef]
73. dos Santos, J.S.; dos Santos, M.L.; Conti, M.M. Comparative study of metal contents in Brazilian coffees cultivated by conventional and organic agriculture applying principal component analysis. *J. Braz. Chem. Soc.* **2010**, *21*, 1468–1476. [CrossRef]
74. Wang, X.; Xing, Y. Evaluation of the effects of irrigation and fertilization on tomato fruit yield and quality, a principal component analysis. *Sci. Rep.* **2017**, *7*, 350. [CrossRef] [PubMed]

land

MDPI

Article

Soil Bulk Density and Matric Potential Regulate Soil CO_2 Emissions by Altering Pore Characteristics and Water Content

Weiyang Gui [1], Yongliang You [2], Feng Yang [3] and Mingjun Zhang [4,*]

[1] Key Laboratory of Animal Genetics, Breeding and Reproduction in the Plateau Mountainous Region, Ministry of Education, College of Animal Science, Guizhou University, Guiyang 550025, China
[2] Dryland Farming Institute, Hebei Academy of Agricultural and Forestry Sciences, Hengshui 053000, China
[3] Guizhou Grassland Technology Experiment and Extension Station, Guiyang 550025, China
[4] Livestock and Poultry Genetic Resources Management Station of Guizhou Province, Guiyang 550025, China
* Correspondence: mingjunzhang23@163.com

Abstract: Soil pore structure and soil water content are critical regulators of microbial activity and associated carbon dioxide (CO_2) emissions. This study evaluated the impacts of soil bulk density and matric potential on carbon dioxide (CO_2) emissions through modifications of total porosity, air-filled porosity, water retention, and gas diffusivity. Soil samples were manipulated into four bulk densities (1.0, 1.1, 1.2, and 1.3 Mg m^{-3}) and ten matric potential levels (−1, −2, −3, −4, −5, −6, −7, −8, −9, and −10 kPa) in controlled soil cores. The results showed that lower bulk densities enhanced while higher densities suppressed CO_2 emissions. Similarly, wetter matric potentials decreased fluxes, but emission increased with drying. Correlation and regression analyses revealed that total porosity (r = 0.28), and gravimetric water content (r = 0.29) were strongly positively related to CO_2 emissions. In contrast, soil bulk density (r= −0.22) and matric potential (r= −0.30) were negatively correlated with emissions. The results highlight that compaction and excessive water content restrict microbial respiration and gas diffusion, reducing CO_2 emissions. Proper management of soil structure and water content is therefore essential to support soil ecological functions and associated ecosystem services.

Keywords: soil bulk density; matric potential; CO_2 emissions; pore characteristics; soil moisture content

Citation: Gui, W.; You, Y.; Yang, F.; Zhang, M. Soil Bulk Density and Matric Potential Regulate Soil CO_2 Emissions by Altering Pore Characteristics and Water Content. *Land* **2023**, *12*, 1646. https://doi.org/10.3390/land12091646

Academic Editors: Jiahua Zhang, Shahzad Ali, Sajid Ali and Qianmin Jia

Received: 24 July 2023
Revised: 15 August 2023
Accepted: 19 August 2023
Published: 22 August 2023

1. Introduction

Soil respiration, characterized by the emissions of carbon dioxide (CO_2) from the soil surface, encapsulates both plant root and microbial respiration, making it a valuable indicator of soil carbon (C) cycling [1]. Elevated atmospheric CO_2 levels, regarded as a principal greenhouse gas, not only aggravate global climate change but also manipulate the carbon stores and soil water content in terrestrial ecosystems, potentially causing escalated CO_2 emissions. This cycle suggests a positive feedback loop, thereby heightening the urgency for CO_2 emission mitigation, especially considering the growing rates of atmospheric CO_2 concentrations [2].

The emission of soil CO_2, chiefly driven by production and transportation processes, relates to the interchange of oxygen and CO_2 between soil and atmosphere. Soil respiration includes both oxygen depletion and CO_2 production [3]. Here, soil diffusivity emerges as a vital factor influencing oxygen availability and CO_2 transport from soil to the surrounding environment [4]. It is important to note that soil diffusivity is associated with both soil porosity and water content [4,5]. Various studies have proposed equations linking CO_2 and soil water content; however, these fail to express the physical force of water held in soil or soil pore connectivity and tortuosity [3,6].

Matric potential serves as a robust indicator of water availability to plant roots and microbes [3,7,8], yet many studies have overlooked soil bulk density when investigating the matric potential effect on CO_2 [9–11]. A more effective predictor of soil gas emissions like

nitrous oxide or nitrogen is relative gas diffusivity (D_p/D_o), which adjusts for variations in soil water content and soil bulk density [12–15]. However, research on this aspect in relation to soil CO_2 emission remains scant [16].

A majority of studies have calculated D_p/D_o through measuring soil porosity or water content or through model assessments due to the challenges in directly measuring soil gas diffusivity [4,5,14,17,18]. The relationship between D_p/D_o and soil porosity can vary with changes in total porosity or the continuity of soil pores due to differences in soil bulk density or water content [5,17]. Soil bulk density affects the available pore space for gas diffusion, with higher densities leading to compaction and reduced porosity [19]. Similarly, variations in water content can either fill or empty pore spaces, affecting the continuity of the pores and subsequently the gas diffusion process [15,20,21]. These changes in physical properties are essential as they govern microbial activity, nutrient cycling, and plant growth, collectively impacting the overall functionality and health of the soil ecosystem [3]. Consequently, directly measuring D_p/D_o rather than relying on empirical equations or models provides a more accurate understanding of these critical soil processes. Understanding the effects of variations in bulk density and matric potential on soil diffusivity will enhance our understanding of the control mechanisms governing soil sources and sinks of atmospheric gases.

This study aims to examine the interaction between soil bulk density and matric potential on D_p/D_o and CO_2 emissions, focusing on uncovering the underlying mechanisms in specific soil types (Ali-Perudic Argosols). By directly measuring these parameters and exploring their intricate relationships across different levels of bulk density and matric potential, the study intends to provide new insights that may have broader implications for soil management practices and climate-change-mitigation strategies. Specifically, the objective was to quantify how soil D_p/D_o and CO_2 emissions respond across a range of bulk densities and matric potentials in controlled soil cores. We hypothesized that D_p/D_o will serve as an effective indicator of soil CO_2 emissions under diverse bulk density and matric potential conditions.

2. Materials and Methods

2.1. Soil Collection, Experimental Design, and Setup

Soil was randomly sampled (0–15 cm) from Dafang County (27°23′ N, 105°52′ E; Altitude 1760 m), Bijie City, Guizhou Province (Figure 1) in June 2023 and then was air-dried. The soil carbon, nitrogen, and soil pH were measured before experimenting (Table 1). The composition of soil aggregates and particles within a depth of 0–10 cm was measured before the experiment (Table 2).

Table 1. Mean soil organic carbon (SOC, g kg^{-1}), total (TN, g kg^{-1}) and available nitrogen, total and available phosphorus (TP, AP, g kg^{-1}), and total potassium (TK, g kg^{-1}) at 0–5 and 5–10 cm in the study region.

Soil Layer (cm)	SOC ($g \cdot kg^{-1}$)	TN ($g \cdot kg^{-1}$)	Nitrate N ($mg \cdot kg^{-1}$)	Ammonium N ($mg \cdot kg^{-1}$)	TP ($g \cdot kg^{-1}$)	AP ($mg \cdot kg^{-1}$)	TK ($g \cdot kg^{-1}$)
0–5	27.05	2.82	23.14	4.95	0.80	24.08	27.75
5–10	24.46	2.59	16.83	5.06	0.66	14.99	28.79

Table 2. Basic soil aggregates and particle composition of soil depth (0–10 cm) before experiment.

Index	Soil Aggregates Composition (%)				Soil Particle Composition (%)		
					Clay	Silt	Sand
Layer (cm)	5–2 mm	2–0.25 mm	0.25–0.053 mm	<0.053 mm	<0.002 mm	0.002–0.02 mm	0.02–2 mm
0–5	0.34	0.43	0.09	0.11	24.35	61.09	14.56
5–10	0.38	0.41	0.09	0.08	26.58	60.50	12.92

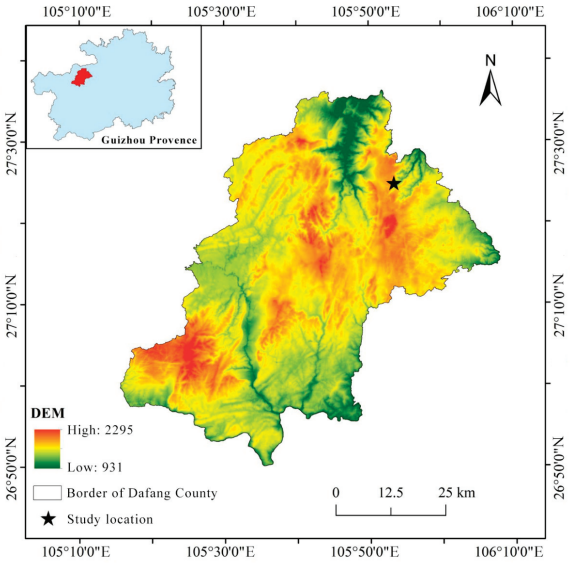

Figure 1. Study location in southeast China.

The main soil type is Ali-Perudic Argosols (APA) according to the International Society of Soil Sciences standards. After the soil was sieved ($\leq$2 mm), soil cores were made by compacting soil into stainless-steel cylinders (7.3 cm internal diameter, 7.4 cm deep) to obtain four levels of bulk density (1.0, 1.1, 1.2, and 1.3 Mg m^{-3}). Bulk density was measured using the core method, where the dry weight of a known volume of soil was determined. Each bulk density level had ten levels of matric potential (-1, -2, -3, -4, -5, -6, -7, -8, -9, and -10 kPa) measured using tensiometers at varying depths, and the entire process was replicated four times. The soil cores were preincubated for 7 days to stabilize the microbial activity [12,13].

2.2. Soil CO_2 Emissions and Relative Gas Diffusivity Measurements

To measure the soil CO_2 emissions, the soil cores were taken off the tension tables and placed into 1 L stainless-steel tins equipped with gas-tight lids pre-fitted with rubber septa. Soil CO_2 emissions were measured on days 4, 5, and 6.

According to the method of Rolston and Moldrup [20], we measured soil D_p/D_o after measuring CO_2 flux: a chamber containing a calibrated oxygen sensor was purged with a gas mixture (90% Ar and 10% N_2), while the base of the soil core was isolated from the chamber. Once the chamber oxygen concentration equaled 0%, the base of the soil core was exposed to the oxygen-free chamber atmosphere. As oxygen diffused through the soil core into the chamber, the change in oxygen concentration was recorded as a function of time over a period of 120 to 180 min. It was assumed that any error in the measured value of D_p due to oxygen consumption was negligible [20]. Regression analysis of the log-plot of relative oxygen concentration vs. time enabled D_p (oxygen diffusion coefficient in soil) to be calculated [20]. All diffusivity calculations were performed at 25 °C, and the value of D_o (oxygen diffusion coefficient in air) at 25 °C was calculated to be 0.074 m^2 h^{-1} [22].

2.3. Soil Analyses and Calculations

Soil gravimetric water content (θ_g) was measured by drying 10 g wet soil subsamples at 105 °C for 24 h. Soil air-filled porosity (ε), total porosity (φ), volumetric water content (θ_v), and water-filled pore space (*WFPS*) were calculated by using values of soil bulk density (ρ_d) (Equations (1)–(4)) while assuming a particle density (ρ_b) of 2.65 Mg m^{-3} [3].

$$\theta_v = \rho_b \times \theta_g \quad (1)$$

$$\Phi = 1 - \frac{\rho_b}{\rho_d} \quad (2)$$

$$\varepsilon = \Phi - \theta_v \quad (3)$$

$$WFPS = \frac{\theta_V}{\Phi} \quad (4)$$

2.4. Data Analyses

The effects of bulk density and matric potential on soil pore characteristics and soil CO_2 emissions were tested using analysis of variance (ANOVA) in the "agricolae" package of R version 1.3.1 [23]. Principal component analysis (PCA) was conducted to examine multivariate relationships and clustering by bulk density and observation days. Pearson's correlation analysis quantified correlation coefficients between all measured variables. Statistically significant effects were declared at $p < 0.05$. All analyses were performed in R statistical software (version 1.3.1). Prior to analysis, data normality and homogeneity of variance were confirmed using the Shapiro–Wilk test and Levene's test, respectively. Figures were constructed with the ggplot2 package in R.

3. Results

3.1. Impact of Changes in Soil Bulk Density and Matric Potential on Soil Pore Characteristics

As bulk density increased from 1.0 to 1.3 Mg m^{-3}, total porosity decreased from 0.63 to 0.52 m^3 m^{-3} (overall mean, $p < 0.01$; Figure 2). A similar decline was observed in air-filled porosity (from 0.26 to 0.07 m^3 m^{-3}) with increasing bulk density ($p < 0.01$). Conversely, volumetric water content and water-filled pore space showed an opposite trend, increasing from 0.37 to 0.46 m^3 m^{-3} and from 0.58 to 0.89 m^3 m^{-3}, respectively, as bulk density increased ($p < 0.01$). Gravimetric water content was relatively stable across the bulk densities, and the highest values (0.39 g g^{-1}) appeared with bulk density of 1.1 Mg m^{-3} ($p < 0.01$). Nonetheless, relative gas diffusivity exhibited a sharp decrease from 0.029 to 0.001 with higher bulk density ($p < 0.01$).

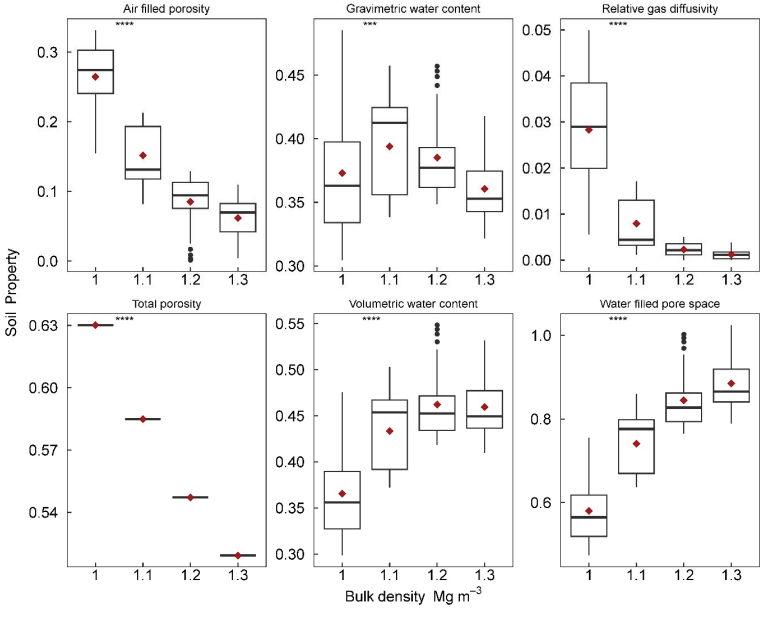

Figure 2. Soil air-filled porosity, gravimetric water content, relative gas diffusivity, total porosity, volumetric water content, and water-filled pore space in response to changes in soil bulk density.

Treatments include four levels of bulk density (1.0, 1.1, 1.2, and 1.3 Mg m^{-3}), and each bulk density has ten levels of matric potential (−1, −2, −3, −4, −5, −6, −7, −8, −9, and −10 kPa). Notes: The significance indicates the differences with *** $p < 0.001$ and **** $p < 0.0001$. Red dot indicates mean values.

Changes in the matric potential affected soil pore characteristics (Figure 3). As matric potential increased from −10 to −1 kPa, volumetric water content decreased from 0.52 to 0.38 m^3 m^{-3} ($p < 0.01$). Similarly, gravimetric water content and water-filled pore space significantly declined from 0.45 to 0.33 g g^{-1} and from 0.88 to 0.63 m^3 m^{-3}, respectively, with decreasing matric potential. In contrast, air-filled porosity increased from 0.06 to 0.19 m^3 m^{-3} with lower matric potential ($p < 0.01$), while relative gas diffusivity increased from 0.001 to 0.018 as matric potential decreased ($p < 0.01$).

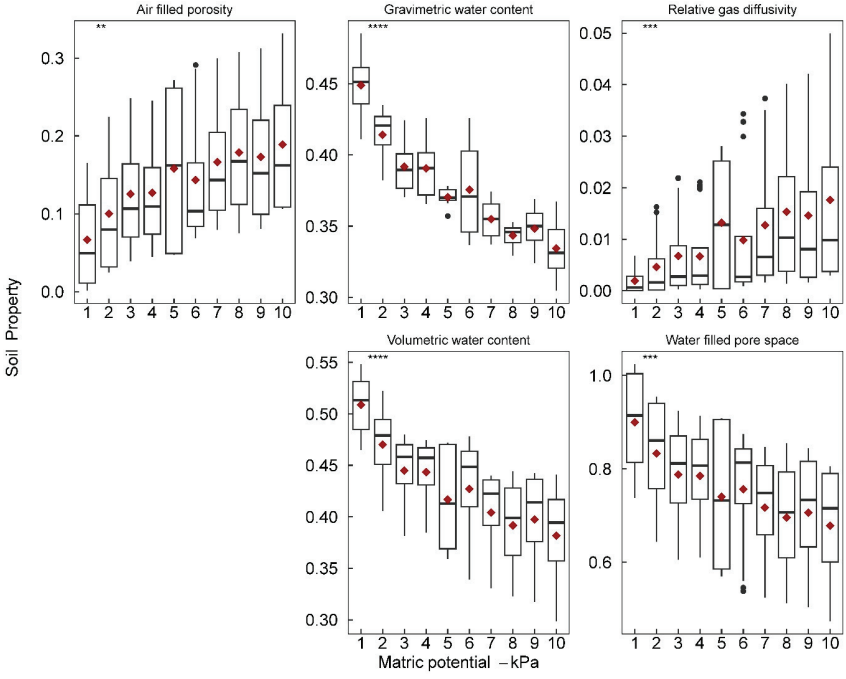

Figure 3. Soil air-filled porosity, gravimetric water content, relative gas diffusivity, total porosity, volumetric water content, and water-filled pore space in response to changes in soil matric potentials. Treatments include four levels of bulk density (1.0, 1.1, 1.2, and 1.3 Mg m^{-3}), and each bulk density has ten levels of matric potential (−1, −2, −3, −4, −5, −6, −7, −8, −9, and −10 kPa). Notes: The significance indicates the differences with ** $p < 0.01$, *** $p < 0.001$ and **** $p < 0.0001$. Red dot indicates mean values.

3.2. Soil CO_2 Emissions in Response to Changes in Soil Bulk Density and Matric Potential

Soil CO_2 emissions across varying soil bulk densities were monitored over 3 days (Figure 4). On day 4, soil CO_2 emissions ranged from 4.2 to 7.1 mol m^{-2} s^{-1} (overall mean) across the bulk densities. Soil CO_2 emissions were lowest in the bulk density treatment of 1.3 Mg m^{-3} and highest in the low-density treatment (1.0 Mg m^{-3}, $p < 0.01$). A similar trend was observed on day 5. By day 6, soil CO_2 emissions declined.

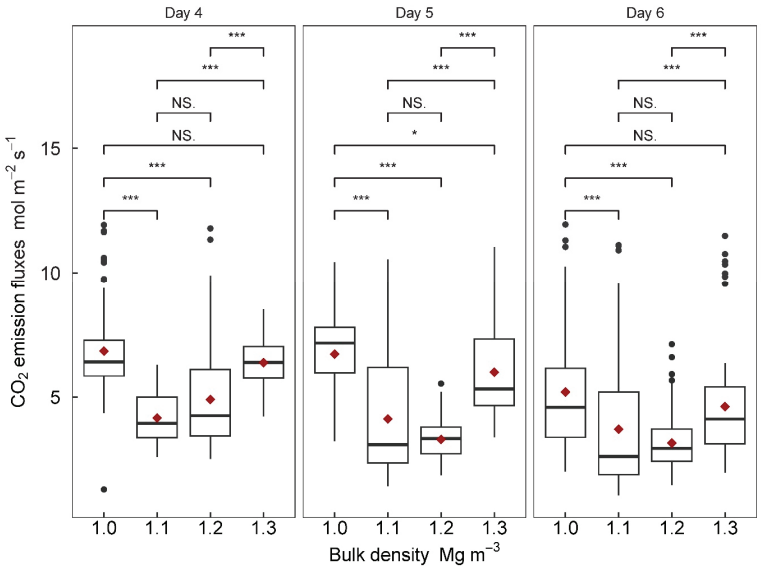

Figure 4. Soil carbon dioxide (CO_2) emissions with four levels of soil bulk density over three days. Notes: The significance indicates the differences with * $p < 0.05$ and *** $p < 0.001$. Red dot indicates mean values.

The effects of matric potential on soil CO_2 emissions were also evaluated over three days (Figure 5). On day 4, soil CO_2 emissions were lowest at −10 kPa matric potential around 4.9 mol m^{-2} s^{-1} and increased to 6.4 mol m^{-2} s^{-1} at −5 kPa matric potential. A similar trend was observed on day 5, and soil CO_2 emissions peaked at −5 kPa matric potential, with a value of 9.1 mol m^{-2} s^{-1}. By day 6, fluxes declined slightly across all matric potentials, with the decline more pronounced at low potentials (−7 to −10 kPa); however, soil CO_2 emissions peaked at −5 kPa matric potential again, with value of 10.3 mol m^{-2} s^{-1}.

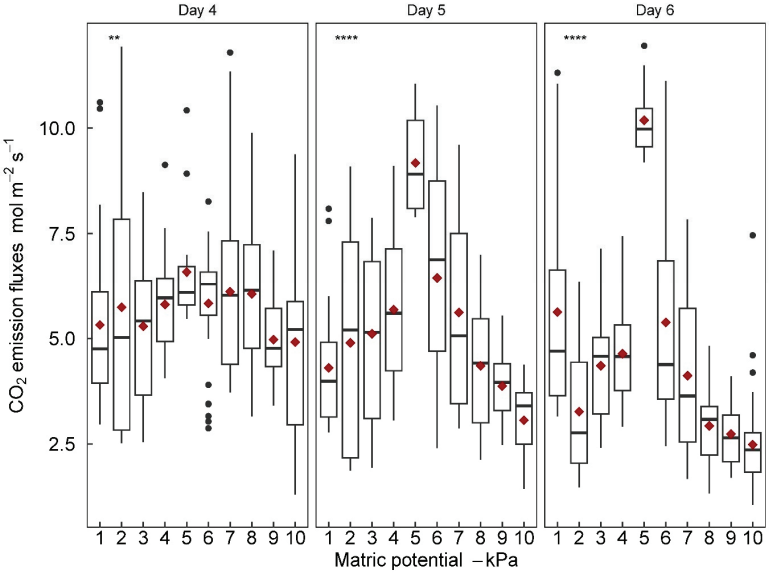

Figure 5. Soil carbon dioxide (CO_2) emissions with ten levels of soil matric potentials over three days. Notes: The significance indicates the differences with ** $p < 0.01$ and **** $p < 0.0001$. Red dot indicates mean values.

The PCA showed a slight separation of the four bulk density levels along the first principal component (44.2% variance explained; Figure 6). However, it did not present distinct clustering of the three measurement days along PC1 (43.2% variance explained).

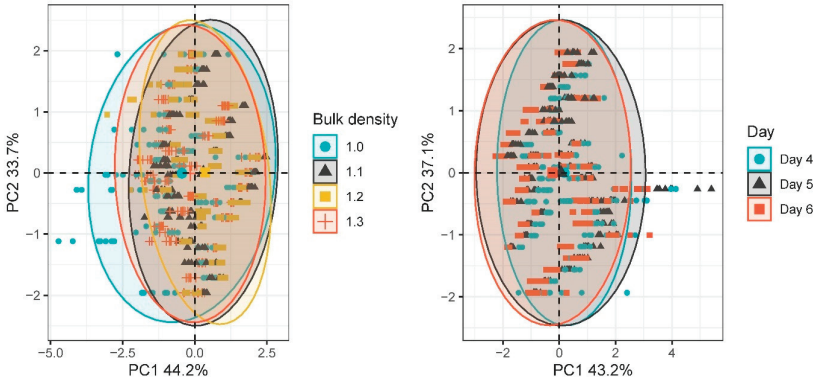

Figure 6. Principal component analysis (PCA) for soil carbon dioxide (CO_2) emissions at different bulk densities or measuring time (day). The different shapes indicate different bulk densities or measuring times, and the ellipse is the confidence interval of the distribution of variables under different treatments.

3.3. Factors Affecting Soil CO_2 Emissions in Various Bulk Densities and Matric Potentials

Distribution of soil CO_2 emissions under various soil pore characteristics was illustrated (Figure 7), and the relationships between soil CO_2 emissions and gravimetric water content and volumetric water content were significant (Table 3). Soil gravimetric water content and volumetric water content explained 43% and 36% of the variations of soil CO_2 emissions ($p < 0.01$).

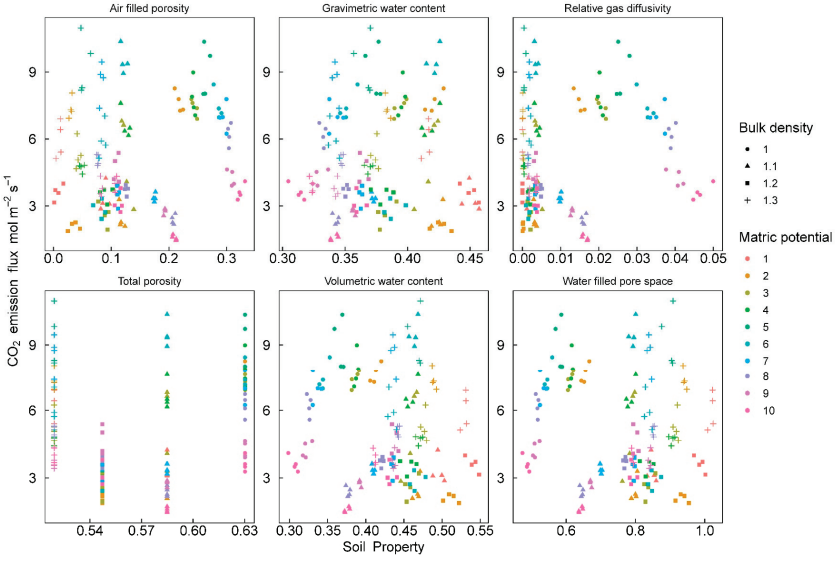

Figure 7. The desaturations of soil carbon dioxide (CO_2) emissions with air-filled porosity, gravimetric water content, relative gas diffusivity, total porosity, volumetric water content, and water-filled pore space over three days. Treatments include four levels of bulk density (1.0, 1.1, 1.2, and 1.3 Mg m^{-3}), and each bulk density has ten levels of matric potential (−1, −2, −3, −4, −5, −6, −7, −8, −9, and −10 kPa).

Table 3. The regression of soil carbon dioxide (CO_2) emissions with gravimetric water content and volumetric water content over three days.

Soil Property	Equation	R^2	*p*
Gravimetric water content	$y = 0.0009x^2 - 0.16x + 10.41$	0.43	<0.01
Volumetric water content	$y = 0.0009x^2 - 0.15x + 9.96$	0.36	<0.01

A Pearson's correlation analysis was conducted to assess relationships between the soil pore characteristics and soil CO_2 emissions (Figure 8). Significant positive correlations were observed between soil CO_2 emissions and total porosity (r = 0.28) and between soil CO_2 emissions and gravimetric water content (r = 0.29), while significant negative correlations were observed between soil CO_2 emissions and matric potential (r = −0.30) and bulk density (r = −0.22).

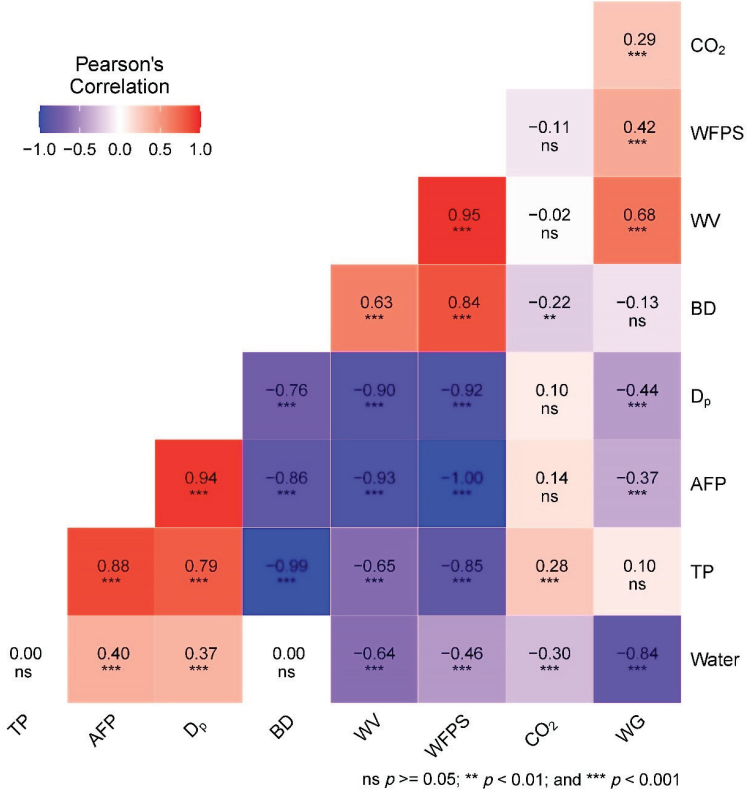

Figure 8. Correlation analysis of factors affecting soil carbon dioxide (CO_2) emissions in response to air-filled porosity (AFP), gravimetric water content (WG), relative gas diffusivity (Dp), total porosity (TP), volumetric water content (TP), and water-filled pore space (WFPS) over three days. Notes: The significance indicates the differences with ** $p < 0.01$ and *** $p < 0.001$.

4. Discussion

The observed reduction in total porosity and air-filled porosity with a rise in bulk density aligns with previous research, suggesting that greater soil compaction leaves less pore space [24–27]. This compaction is accompanied by reductions in volumetric water content and water-filled pore space, echoing the decreased overall porosity. Meanwhile, the minimal change in gravimetric water content indicates a roughly consistent total water mass, albeit one that occupies a smaller volume due to compaction. In contrast, relative gas

diffusivity sharply declines, reflecting a significant decrease in gas diffusion and transport capacity due to the reduced air-filled porosity at higher bulk densities [22,25]. These observations reinforce the significant influence of bulk density on soil pore characteristics and associated properties, underscoring the need for careful soil bulk density management to maintain optimal conditions for water availability [28], aeration, and gas diffusion.

Increased volumetric water content and water-filled pore space with decreasing matric potential can be attributed to greater water retention and the displacement of air by water as pores become more saturated at increasingly negative water potentials [29]. Similarly, the rise in gravimetric water content suggests a higher absolute water mass within the soil pores due to the greater water retention potential. Concurrently, the pronounced reduction in relative gas diffusivity reflects the decrease in air-filled porosity given that lower diffusivity corresponds to severely hampered gas diffusion through saturated pores [30]. These trends illustrate how matric potential can fundamentally alter pore water retention dynamics, aeration, and gas transport, underscoring the importance of proper irrigation management to maintain optimal matric potential for plant growth, soil ecological function, and greenhouse gas transport.

Lower soil CO_2 emissions at higher bulk densities likely reflect significantly reduced microbial activity and gas diffusion due to compaction [31,32]. The highest fluxes occur in less-compacted, low-density soils, which provide more ideal conditions for microbial processes and gas diffusion. Soil CO_2 emissions increasing over time in high-density soil suggests a chronic constraint on microbial activity and gas diffusion [24,33], with diffusion pathways gradually opening over time to release previously trapped soil CO_2. These data emphasize that soil compaction can severely reduce soil CO_2 emissions, impacting microbial respiration, carbon cycling, and climate regulation ecosystem services negatively [34–36]. Hence, maintaining sufficient soil porosity is crucial for preserving microbial function and soil health [2].

Lower fluxes under wet conditions reflect constrained diffusion and decreased oxygen availability for aerobic respiration. As soil progressively dries, diffusion pathways open, alleviating oxygen limitation and enabling higher microbial activity and soil CO_2 production [10]. The fluxes' general decline by day 6 might be due to the depletion of labile carbon substrates under the constant wetting and drying cycles, emphasizing the sensitivity of soil CO_2 emissions to soil water content and the need to balance adequate water content for microbial activity without oversaturation [10,37].

The PCA suggests that bulk density and measurement day were key factors influencing soil CO_2 emissions. The non-overlapping clusters of bulk density treatments indicate that changes in pore structure from soil compaction significantly impact gas fluxes, including reduced microbial activity and constrained diffusion [24,38]. The temporal shifts in fluxes over the days reflect the dynamic nature of microbial activity and water contents, emphasizing the critical consideration of bulk density management and monitoring timeframe in experiments and data interpretation on soil CO_2 emissions.

Positive correlations between soil CO_2 emissions and total porosity, air-filled porosity, and gas diffusivity highlight the importance of diffusion pathways and oxygen availability for aerobic microbial metabolism and gas transport [3,20,26,38]. As pores become saturated, oxygen limitation restricts soil CO_2 production and diffusion, hence the negative correlations with volumetric water content and water-filled pore space. While gravimetric water content affects respiration substrate availability, its weaker correlation indicates that physical factors enabling gas transport predominantly control it. Although the results did not fully support our hypothesis that relative gas diffusivity would correspond as an indicator of how compaction and water retention influence soil CO_2 emissions, the data suggest a threshold effect where soil CO_2 emissions changed dramatically at certain levels of compaction and matric potential (Figure 7). In our analysis, we noted that the regression coefficients (R^2) were relatively low in some instances. There are several factors that could contribute to these lower R^2 values: (1) Complex interactions: Soil properties such as bulk density and matric potential interact with each other and with other unmeasured variables

in intricate ways. This complexity may not be fully captured by the models used, leading to a lower R^2. (2) It is worth noting that a low R^2 does not necessarily mean that the model is inadequate. R^2 only explains the proportion of variance captured by the model, and in complex ecological systems, it might not be realistic to expect a very high R^2. In future studies, more sophisticated modeling techniques that can account for non-linearities, interactions, and spatial patterns might be employed to possibly increase the R^2 values. Additionally, expanding the study to include more variables or more extensive sampling might help in understanding the underlying mechanisms more accurately.

From a broader perspective, this research contributes compelling evidence that the effective management of physical structure and moisture characteristics is integral to regulating soil CO_2 emissions. The insights gained from these findings have significant implications for enhancing soil functionality and may guide agricultural practices that align with climate regulation ecosystem services. Extending this research to include studies involving different types of soils and various management practices could further enrich our understanding, as soil bulk density and matric potential effects may vary across diverse soil ecosystems. Future investigations could delve into the interactive impacts of soil biological communities, organic matter, and mineralogy on soil CO_2 emissions, as seen in conjunction with soil structure. Additionally, field monitoring of emissions across diverse management gradients, including different soil types and cultivation methods, can offer further insights into the dynamic nature of soil CO_2 emissions. This research acts as a stepping stone to a deeper understanding of the intricate relationships between soil characteristics and greenhouse gas emissions, with direct implications for climate-change-mitigation strategies. The inclusion of different soil types and management practices in future studies will provide a more comprehensive picture, enhancing our ability to develop effective strategies for various agricultural contexts.

5. Conclusions

The findings of this study, conducted on Ali-Perudic Argosols (APA), highlight the pivotal role of physical structure and soil water characteristics in the regulation of soil CO_2 emissions. Within this specific soil type, total porosity, air-filled pore space, and gas diffusivity are seen as key contributors that facilitate microbial activity and CO_2 diffusion when conditions are optimal. Nevertheless, emissions are severely limited by pore saturation and compaction, which underline the criticality of maintaining suitable soil structure and soil water content for optimal soil health and functionality. These conclusions are directed explicitly at the soil type studied, and additional research on various soil types may further generalize these findings.

Author Contributions: Conceptualization, W.G. and M.Z.; methodology, Y.Y.; software, Y.Y.; validation, W.G. and Y.Y.; formal analysis, W.G.; investigation, W.G. and Y.Y.; resources, F.Y.; data curation, F.Y.; writing—original draft preparation, W.G.; writing—review and editing, Y.Y.; visualization, W.G.; supervision, F.Y.; project administration, M.Z.; funding acquisition, M.Z. All authors have read and agreed to the published version of the manuscript.

Funding: This research was financed by the Guizhou Provincial Key Technology R&D Program (Qian Ke He Zhi Cheng (2022), Yi Ban 106; Qian Ke He Zhi Cheng (2023), Yi Ban 473; Qian Ke He Zhi Cheng (2023), Yi Ban 060).

Data Availability Statement: The data presented in this study are available on request from the corresponding author.

Conflicts of Interest: The authors declare no conflict of interest.

References

1. Raich, J.W.; Schlesinger, W.H. The global carbon dioxide flux in soil respiration and its relationship to vegetation and climate. *Tellus Ser. B-Chem. Phys. Meteorol.* **1992**, *44*, 81–99. [CrossRef]
2. Atmospheric CO_2 Growth Rates, Decadal Average Annual Growth Rates. Available online: https://gml.noaa.gov/ccgg/trends/gl_gr.html (accessed on 17 June 2023).

3. Linn, D.M.; Doran, J.W. Effect of water-filled pore space on carbon dioxide and nitrous oxide production in tilled and nontilled soils. *Soil Sci. Soc. Am. J.* **1984**, *48*, 1267–1272. [CrossRef]
4. Davidson, E.A.; Trumbore, S.E. Gas diffusivity and production of CO_2 in deep soils of the eastern Amazon. *Tellus Ser. B-Chem. Phys. Meteorol.* **1995**, *47*, 550–565. [CrossRef]
5. Millington, R.J. Gas Diffusion in Porous Media. *Science* **1959**, *130*, 100–102. [CrossRef] [PubMed]
6. Farquharson, R.; Baldock, J. Concepts in modelling N_2O emissions from land use. *Plant Soil* **2008**, *309*, 147–167. [CrossRef]
7. Liu, F.; Zhu, Q.; Wang, Y.; Lai, X.; Liao, K.; Guo, C. Storages and leaching losses of soil water dissolved CO_2 and N_2O on typical land use hillslopes in southeastern hilly area of China. *Sci. Total Environ.* **2023**, *886*, 163780. [CrossRef]
8. Vremec, M.; Forstner, V.; Herndl, M.; Collenteur, R.; Schaumberger, A.; Birk, S. Sensitivity of evapotranspiration and seepage to elevated atmospheric CO_2 from lysimeter experiments in a montane grassland. *J. Hydrol.* **2023**, *617*, 128875. [CrossRef]
9. Davidson, E.A.; Verchot, L.V.; Cattanio, J.H.; Ackerman, I.L.; Carvalho, J.E.M. Effects of soil water content on soil respiration in forests and cattle pastures of eastern Amazonia. *Biogeochemistry* **2000**, *48*, 53–69. [CrossRef]
10. Li, Z.; Cui, S.; Zhang, Q.; Xu, G.; Feng, Q.; Chen, C.; Li, Y. Optimizing Wheat Yield, Water, and Nitrogen Use Efficiency With Water and Nitrogen Inputs in China: A Synthesis and Life Cycle Assessment. *Front. Plant Sci.* **2022**, *13*, 930484. [CrossRef]
11. Orchard, V.A.; Cook, F.J. Relationship between soil respiration and soil moisture. *Soil Biol. Biochem.* **1983**, *15*, 447–453. [CrossRef]
12. Balaine, N.; Clough, T.J.; Beare, M.H.; Thomas, S.M.; Meenken, E.D. Soil gas diffusivity controls N_2O and N_2 emissions and their ratio. *Soil Sci. Soc. Am. J.* **2016**, *80*, 529–540. [CrossRef]
13. Balaine, N.; Clough, T.J.; Beare, M.H.; Thomas, S.M.; Meenken, E.D.; Ross, J.G. Changes in relative gas diffusivity explain soil nitrous oxide flux dynamics. *Soil Sci. Soc. Am. J.* **2013**, *77*, 1496–1505. [CrossRef]
14. Owens, J.; Clough, T.J.; Laubach, J.; Hunt, J.E.; Venterea, R.T.; Phillips, R.L. Nitrous oxide fluxes, soil oxygen, and denitrification potential of urine- and non-urine-treated soil under different irrigation frequencies. *J. Environ. Qual.* **2016**, *45*, 1169–1177. [CrossRef] [PubMed]
15. Rolston, D.E.; Moldrup, P. Gas Diffusivity. In *Methods of Soil Analysis: Part 4 Physical Methods*; Topp, G.C., Dane, J.H., Eds.; SSSA: Madison, WI, USA, 2002; pp. 1113–1139.
16. Räty, M.; Termonen, M.; Soinne, H.; Nikama, J.; Rasa, K.; Järvinen, M.; Lappalainen, R.; Auvinen, H.; Keskinen, R. Improving coarse-textured mineral soils with pulp and paper mill sludges: Functional considerations at laboratory scale. *Geoderma* **2023**, *438*, 116617. [CrossRef]
17. Fang, C.; Moncrieff, J.B. A model for soil CO_2 production and transport 1: Model development. *Agric. For. Meteorol.* **1999**, *95*, 225–236. [CrossRef]
18. Abeysinghe, A.M.S.N.; Lakshani, M.M.T.; Amarasinghe, U.D.H.N.; Li, Y.; Deepagoda, T.C.; Fu, W.; Fan, J.; Yang, T.; Ma, X.; Clough, T.; et al. Soil-gas diffusivity-based characterization of variably saturated agricultural topsoils. *Water* **2022**, *14*, 2900. [CrossRef]
19. Du, Y.; Guo, S.; Wang, R.; Song, X.; Ju, X. Soil pore structure mediates the effects of soil oxygen on the dynamics of greenhouse gases during wetting–drying phases. *Sci. Total Environ.* **2023**, *895*, 165192. [CrossRef]
20. Moldrup, P.; Olesen, T.; Gamst, J.; Schjønning, P.; Yamaguchi, T.; Rolston, D.E. Predicting the gas diffusion coefficient in repacked soil: Water-induced linear reduction model. *Soil Sci. Soc. Am. J.* **2000**, *64*, 1588–1594. [CrossRef]
21. Jiang, J.; Gu, K.; Xu, J.; Li, Y.; Le, Y.; Hu, J. Effect of Barometric Pressure Fluctuations on Gas Transport over Soil Surfaces. *Land* **2023**, *12*, 161. [CrossRef]
22. Currie, J.A. Gaseous diffusion in porous media Part 1. A non-steady state method. *Br. J. Appl. Phys.* **1960**, *11*, 314–317. [CrossRef]
23. Mendiburu, F.D. Statistical Procedures for Agricultural Research. R Package Version 1.3.1. 2009. Available online: https://CRAN.R-project.org/package=agricolae (accessed on 17 June 2023).
24. da Silva, T.S.; Pulido-Moncada, M.; Schmidt, M.R.; Katuwal, S.; Schlüter, S.; Köhne, J.M.; Mazurana, M.; Juhl Munkholm, L.; Levien, R. Soil pore characteristics and gas transport properties of a no-tillage system in a subtropical climate. *Geoderma* **2021**, *401*, 115222. [CrossRef]
25. Eden, M.; Schjønning, P.; Moldrup, P.; De Jonge, L.W. Compaction and rotovation effects on soil pore characteristics of a loamy sand soil with contrasting organic matter content. *Soil Use Manag.* **2011**, *27*, 340–349. [CrossRef]
26. Li, Y.; Li, Z.; Cui, S.; Jagadamma, S.; Zhang, Q. Residue retention and minimum tillage improve physical environment of the soil in croplands: A global meta-analysis. *Soil Tillage Res.* **2019**, *194*, 104292. [CrossRef]
27. Schjønning, P.; Munkholm, L.J.; Moldrup, P.; Jacobsen, O.H. Modelling soil pore characteristics from measurements of air exchange: The long-term effects of fertilization and crop rotation. *Eur. J. Soil Sci.* **2002**, *53*, 331–339. [CrossRef]
28. Qin, W.F.; Zhao, X.C.; Yang, F.; Chen, J.H.; Mo, Q.S.; Cui, S.; Chen, C.; He, S.J.; Li, Z. Impact of fertilization and grazing on soil N and enzyme activities in a karst pasture ecosystem. *Geoderma* **2023**, *437*, 116578. [CrossRef]
29. Wolf, A.B.; Vos, M.; de Boer, W.; Kowalchuk, G.A. Impact of Matric Potential and Pore Size Distribution on Growth Dynamics of Filamentous and Non-Filamentous Soil Bacteria. *PLoS ONE* **2014**, *8*, 83661. [CrossRef]
30. Killham, K.; Amato, M.; Ladd, J.N. Effect of substrate location in soil and soil pore-water regime on carbon turnover. *Soil Biol. Biochem.* **1993**, *25*, 57–62. [CrossRef]
31. Li, Y.; Clough, T.J.; Moinet, G.Y.K.; Whitehead, D. Emissions of nitrous oxide, dinitrogen and carbon dioxide from three soils amended with carbon substrates under varying soil matric potentials. *Eur. J. Soil Sci.* **2021**, *72*, 2261–2275. [CrossRef]

32. Steponavičienė, V.; Bogužas, V.; Sinkevičienė, A.; Skinulienė, L.; Vaisvalavičius, R.; Sinkevičius, A. Soil Water Capacity, Pore Size Distribution, and CO_2 Emission in Different Soil Tillage Systems and Straw Retention. *Plants* **2022**, *11*, 614. [CrossRef]
33. Neilson, J.W.; Pepper, I.L. Soil Respiration as an Index of Soil Aeration. *Soil Sci. Soc. Am. J.* **1990**, *54*, 428–432. [CrossRef]
34. Toosi, E.R.; Kravchenko, A.N.; Guber, A.K.; Rivers, M.L. Pore characteristics regulate priming and fate of carbon from plant residue. *Soil Biol. Biochem.* **2017**, *113*, 219–230. [CrossRef]
35. Torbert, H.A.; Wood, C.W. Effects of soil compaction and water-filled pore space on soil microbial activity and N losses. *Commun. Soil Sci. Plant Anal.* **1992**, *23*, 1321–1331. [CrossRef]
36. Sang, J.; Lakshani, M.M.T.; Chamindu Deepagoda, T.K.K.; Shen, Y.; Li, Y. Drying and rewetting cycles increased soil carbon dioxide rather than nitrous oxide emissions: A meta-analysis. *J. Environ. Manag.* **2022**, *324*, 116391. [CrossRef] [PubMed]
37. Cook, F.J.; Orchard, V.A. Relationships between soil respiration and soil moisture. *Soil Biol. Biochem.* **2008**, *40*, 1013–1018. [CrossRef]
38. Blagodatsky, S.; Smith, P. Soil physics meets soil biology: Towards better mechanistic prediction of greenhouse gas emissions from soil. *Soil Biol. Biochem.* **2012**, *47*, 78–92. [CrossRef]

land

MDPI

Article

Potential Mechanism of Optimal Tillage Layer Structure for Improving Maize Yield and Enhancing Root Growth in Northeast China

Hongbing Zheng [1,2], Ruiping Li [1,2], Pengxiang Sui [1,2], Hao Wang [1,2], Ying Ren [1,2], Ye Yuan [1,2], Shengtao Tian [1,2], Siqi Zhou [1,2], Wuren Liu [1,2], Yang Luo [1,2,*] and Jinyu Zheng [1,2,*]

[1] Research Institute of Agricultural Resources and Environment, Jilin Academy of Agricultural Science, Changchun 130033, China; hongbingzheng@126.com (H.Z.); ruipinghappy@126.com (R.L.); suipengxiang1990@163.com (P.S.); wanghao19810606@163.com (H.W.); renying690809@126.com (Y.R.); yuan1998e@163.com (Y.Y.); 18243397351@163.com (S.T.); 13294759741@163.com (S.Z.); liuwuren571212@163.com (W.L.)

[2] Key Laboratory of Crop Ecophysiology and Farming System in Northeast China, Ministry of Agriculture, Beijing 100125, China

* Correspondence: nkyly@163.com (Y.L.); 15844052867@163.com (J.Z.)

Abstract: A field experiment was conducted to evaluate the effect of different tillage structures on soil physical properties, soil chemical properties, maize root morphological and physiological characteristics, and yield. Four tillage structures were designed. Soil tillage plays a prominent role in agricultural sustainability. The different tillage layer structures affected soil physical properties. An enhancement in the optimal tillage layer structure improved soil structure. The MJ tillage layer structure created an improved soil structure by regulating the soil physical properties so that the soil compaction and soil bulk density would be beneficial for crop growth, increase soil water content, and adjust the soil phrase *R* value and *GSSI*. Soil nutrients are significantly affected by soil depth, with the exception of available potassium. However, soil nutrients are influenced by different tillage layer structures with soil depth. Soil nutrient responses with depth are different for MJ layer treatment compared with other tillage layer structures. Soil organic matter (SOM) is affected with an increase in depth and is significantly influenced by different tillage layer structures, except at 20–30 cm soil depth. MJ treatment increased by 10–20% compared with other tillage layer structures. In addition, QS treatment enhanced the increased pH value in soil profile compared to others. The root morphology characteristics, including root length, root ProjArea, root SurfArea, root AvgDiam, and root volume, were affected by years, depth, and the tillage layer structures. The MJ tillage layer structure enhanced root growth by improving tillage soil structure and increasing soil air and water compared with other tillage layer treatments. Specifically, the MJ layer structure significantly increased root length and root volume via deep tillage. However, the differences in root physiological properties were not significant among treatments. The root dry weight decreased with an increase in soil depth. Most of the roots were mainly distributed in a 0–40 cm soil layer. The MJ treatment enhanced the increase in root dry weight compared with others by breaking the tillage pan layer. Among the different tillage layer structures, the difference in root dry weight was smaller with an increase in soil depth. Moreover, the MJ treatment significantly improved maize yield compared with others. The yield was increased by 14.2% compared to others under MJ treatment via improvements in the soil environment. In addition, the correlation relationship was different among yield and root morphology traits, root physiology traits, soil nutrients, and soil physical traits. So, our results showed that the MJ tillage layer structure is the best tillage structure for increasing maize yield by enhancing soil nutrients, improving the soil environment and root qualities.

Keywords: tillage structures; soil physical; chemical properties; root morphology; root physiology; yield

Citation: Zheng, H.; Li, R.; Sui, P.; Wang, H.; Ren, Y.; Yuan, Y.; Tian, S.; Zhou, S.; Liu, W.; Luo, Y.; et al. Potential Mechanism of Optimal Tillage Layer Structure for Improving Maize Yield and Enhancing Root Growth in Northeast China. *Land* **2023**, *12*, 1798. https://doi.org/10.3390/land12091798

Academic Editors: Shahzad Ali, Qianmin Jia, Jiahua Zhang and Sajid Ali

Received: 30 August 2023
Revised: 6 September 2023
Accepted: 7 September 2023
Published: 16 September 2023

1. Introduction

Agriculture is important to societal development and human survival [1]. With worldwide population growth, the sustainable production of food must overcome serious challenges to guarantee the growing global food demand in the future [2]. However, China faces significant challenges in agricultural development, as its population accounts for 22% of the global population, but its arable land accounts for less than 7% of global arable land [3,4]. It is worth noting that the dry land area in Northeast China is large, accounting for approximately 21% of the country's arable land area and over 30% of the country's total grain production [3,4]. However, crop production faces many significant challenges, such as soil degradation, water and nutrient loss, low organic matter content, and fragile physical structures [5,6]. The black soil area in Northeast China is known as the "cornerstone" of maintaining crop yield and national food security in China [7].

It is necessary to take reasonable soil management measures to increase crop yield and protect or maintain soil quality [8]. The soil management system directly intervenes in the production response of crops through changes in soil physicochemical properties and root characteristics [9]. Farming is the process of physically treating soil to improve it with the help of tools [10]. The cultivation system can alter soil moisture content, temperature, aeration, and the degree of mixing of crop residues in the soil matrix, thereby affecting the physical and chemical environment of the soil [11]. This is a key soil management practice that has significant implications for seedbed preparation, root growth stimulation, weed control, soil moisture control, soil temperature control, soil compaction mitigation, soil structure improvement, soil nutrient enhancement, and the incorporation of crop residues and fertilizers [12,13]. In addition, tillage treatment plays an important role in altering soil structure and the distribution of crop residues, thereby affecting the ability of soil microorganisms to degrade soil organic matter and release crop growth nutrients [14]. Therefore, by altering soil characteristics and affecting root growth, it is believed that tillage methods are key factors in the sustainability of planting systems [15].

There are two farming methods available: conservation tillage and conventional tillage [16–18]. Although traditional tillage can loosen the soil surface, promote crop root growth, absorb soil nutrients, and increase crop yield [19], it reduces soil microbial biomass, total carbon, active carbon, total nitrogen, aggregate stability, and sand-free organic matter and increases carbon metabolism [20,21]. Protective tillage practices are divided into no tillage (no tillage), minimal tillage (minimal tillage), cover tillage, ridge tillage, and contour tillage [22]. Conservation tillage has been recognized as one of the most effective soil management measures for the sustainable development of global agriculture [23]. Conservative tillage plays an important role in improving soil structure and maintaining surface soil structure and soil physical conditions [24]. Meanwhile, conservation tillage is recommended as an effective method for maintaining soil moisture in dryland agriculture [25,26].

The purpose of soil cultivation is to prepare soil with sufficient physical conditions for plant growth [27]. Therefore, soil characteristics play an important role in the selection of tillage systems [28,29]. However, farming systems can also affect soil characteristics, including soil structure, soil compaction, soil bulk density, and crust or erosion [30]. Dal et al. [31] pointed out that the negative impact of some farming practices is that they often damage soil structure. Meanwhile, traditional farming reduces the stability of aggregates and increases their bulk density [32,33]. Compared to traditional tillage, the use of conservation tillage may lead to different soil physical properties, as the soil matrix is less disturbed [30]. Logsdon et al. [34] pointed out that when using ridge tillage or switching from traditional practices to no tillage on these or similar deep loess soils, producers do not need to worry about increased compaction. However, the soil bulk density of the corn belt under no tillage treatment was significantly higher, following the pattern of less tillage > no tillage > conventional tillage [30]. The topsoil under NT is usually cooler and wetter and has a higher bulk density (BD), thus exhibiting greater soil strength compared to CT [35]. Fabrizzi et al. [36–38] also reported that no-tillage soils typically have greater resistance and higher packing density than traditional soils to hinder root infiltration.

Soil tillage management has a significant impact on root morphology, root physiology, and root growth and development [39–42]. In addition, root growth may also be indirectly affected by changes in soil properties caused by farming systems [43–46]. By changing soil characteristics and affecting root growth, the cultivation method is a key factor in the sustainability of planting systems [47,48]. The effect of cultivation on the growth of maize roots was previously found in early growth and continued until flowering [49]. Meanwhile, the effects of soil temperature and bulk density changes caused by cultivation on plant growth are mediated by the growth and function of the root system [50]. The aims of this study were to evaluate the effect of different tillage structures on soil physical and chemical properties, determine maize root's morphological and physiological characteristics under different tillage structures, study the yield changes in different tillage layer structures, and classify the relationship yield and soil physical and chemical properties to identify the most beneficial tillage systems.

2. Materials and Methods

2.1. Site Description

The experiment was conducted during the spring maize growth seasons of 2016 and 2017 at the Gongzhuling Experimental Station of Jilin Academy of Agricultural Sciences in Jilin Province (43°45′ N and 125°01′ E). The local climate is sub-humid, with an average rainfall of 567 mm and an annual average temperature of 6.91 °C. The soil is sandy loam (36.0% sand, 24.5% silt, 39.5% clay). Jilin Province has a continental climate with a wide range of temperatures. The average temperature in Gongzhuling in 2016 was 6.68 °C, and the average temperature in 2017 was 7.05 °C. The annual precipitation values for these years were moderate (with a total precipitation of 890.8 mm in 2016 and 694.3 mm in 2017). The precipitation and temperature data are shown in Figure 1.

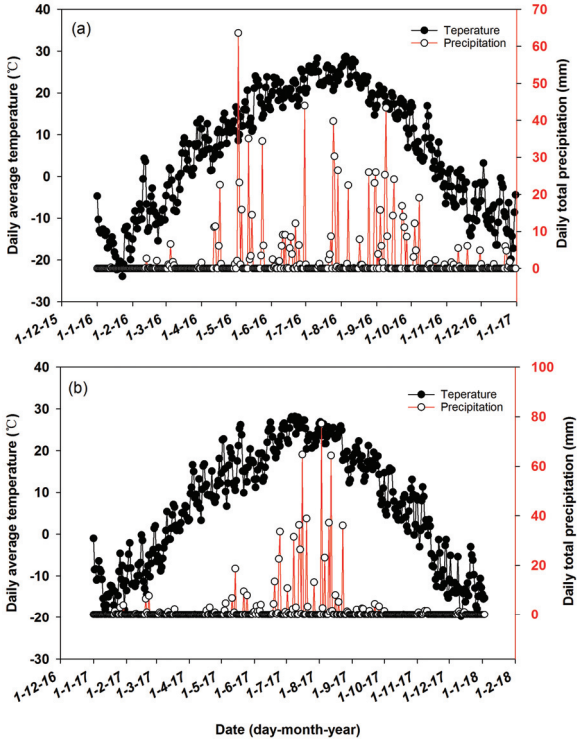

Figure 1. Precipitation and temperature at the research site in 2016 (**a**) and 2017 (**b**).

2.2. Experimental Design

The experiment was completed in Gongzhuling city, and experimental material is XY998. The experimental zone has a mid-temperate continental monsoon climate with an annual temperature of 4.5 °C and 2800 h cumulative sunshine hours. Meanwhile, the effective accumulated temperature ≥10 °C is 2860 °C d, and the frost-free period is 140 days. The annual precipitation from June to August is 567 mm. The soil type is typical medium black soil with loamy clay. The total nitrogen, total phosphorus, and total potassium contents are 0.15%, 0.05%, and 2.26%, respectively. The available nitrogen, available phosphorus, and available potassium contents are 146.36 mg/kg,13.50 mg/kg, and 152.32 mg/kg. The pH value is 6.5 in 0–20 cm soil depth.

The experiment was conducted during the 2016 and 2017 growing seasons. The experiment was conducted in Gongzhuling city and consisted of four treatments, including compaction seeding soil bed with row soil deep tillage (MJ), softy seeding soil with row soil compaction (MS), compaction seeding soil with row soil compaction (QJ), and softy seeding soil with row soil deep tillage (QS). The treatments were distributed in a completely randomized block design with four treatments and three replications. The experiment device was designed with PVC pipes that were 20 cm in height and 30 cm in diameter. Five PVC pipes that were 20 cm in length were connected by scotch tape and put into the soil according to our experimental requirements. Every treatment involved the use of 64 PVC pipe pillars. The three maize seeds were planted into the soil in a PVC soil pillar in spring. After emerging with 3 leaves, a plant of corn was kept in the PVC soil pillar, and others were cut using a knife. The plant density was 6000 plants per hectare, with 32 cm plant distance and 52 cm row distance. A total of 243 kg/hm^2 Controlled release urea was added; 92 kg/hm^2 of P_2O_5 was added, and 80 kg/hm^2 of K_2O was added, and all fertilizers were used as a base fertilizer (one-time application).

Compaction seeding soil bed with row soil deep tillage (MJ): the bulk density was 1.27–1.30 g/cm^3, and the soil compaction was 1.00–1.50 Mpa, with 11.5 cm width in the seeding zone; the bulk density was 1.00–1.10 g/cm^3, and the soil compaction was 0.10–0.50 Mpa, with 20 cm width in the subsoiling zone. Softy seeding soil with row soil compaction (MS): the bulk density was 1.00–1.10 g/cm^3, and the soil compaction was 0.10–0.50 Mpa, with 11.5 cm width in the seeding zone; the bulk density was 1.27–1.30 g/cm^3, and the soil compaction was 1.00–1.50 Mpa, with 20 cm width in the compaction row zone. Softy seeding soil with row soil compaction (MS), compaction seeding soil with row soil compaction (QJ): the soil bulk density was 1.27–1.30 g/cm^3, and the soil compaction was 1.00–1.50 Mpa, with 53 cm row distance. Softy seeding soil with row soil deep tillage (QS): the soil bulk density was 1.00–1.10 g/cm^3, and the soil compaction was 0.10–0.50 Mpa, with 53 cm row distance. The soil water content was calculated for the years 2016 and 2017. The moisture contents of the 0–60 cm soil layers were recorded at 10 cm intervals using a TDR meter.

Deep gouges (4.2 m in length × 2.6 m width × 1 m depth) were made by using a spade in order to put the PVC pipes into the soil. The soil was separated according to the tillage layers. Then, the PVC pipes were put into the deep gouges according to the different treatment types. Overall, 64 PVC soil pillars were used, along with 8 pipes that were arranged horizontally and 8 pipes that were arranged vertically. Finally, soil was returned into the PVC pipes according to the requirements of bulk density and soil compaction. The planting and fertilizer management were same as the field after freeze–thaw in spring. The experimental layout is presented in Figure 2.

Figure 2. The experimental layout.

2.3. Root Sampling

The cultivated maize PVC pipes were removed from the soil during the tasseling and silking stage (VT) of maize in 2016 and 2017, respectively. Firstly, the aboveground part of the maize plants was cut off using a knife, and then the PVC pipes were cut off at the joint of each PVC pipe using a knife. According to the height of the PVC pipe, each layer was divided into five layers. Each layer of the PVC pipes in the soil and root were collected together into a wool mesh bag over and over again and placed into a plastic bucket. The mesh bag was washed repeatedly with tap water to remove most of the soil; after rinsing, all of the dirt was cleaned from the mesh bag. Finally, the root of the mesh bag was added into a tray, and some impurities (such as sand) in the root mix were removed so that clean roots could be placed into a plastic bag. The processed names were noted with markers and put into prepared liquid nitrogen tanks to determine the root morphology and physiological indexes.

2.4. Soil Physical Parameters

Bulk density (g/cm^3) = W/V, W = oven-dry soil weight in grams, V = volume of core in cm^3; Total porosity (%) = [1 − (bulk density/particle density)] × 100, particle density = 2.65 g/cm^3; $R = \left|\sqrt{0.4 \times (X-50)^2 + (Y-25)^2 + (Z-25)^2}\right|$ X = 100 × (1 − total soil porosity), Y = 100 × soil water content rate, Z = 100 × (total soil porosity- soil water content rate); $GSSI = [(X_S - 25)X_L X_G]^{0.4769}$, X_S, X_L, and X_G were the percentage of solid, liquid, and gas phases. Soil compaction was measured by SC-900; Soil water content was measured via the aluminum box weighing method; Soil three-phase was measured using a Soil three-phrase meter (DIK1150).

2.5. Soil Nutrient Parameters

The soil samples from 0 to 10 cm, 10 to 20 cm, 20 to 30 cm, 30 to 40 cm, 40 to 50 cm, and 50 to 60 cm depth were collected to separately measure the total nitrogen (TN), total phosphorus (TP), total potassium (TK), available nitrogen (AN), phosphorus (AP), available potassium (AK), organic matter, and pH contents using a soil sampler.

2.6. Root Morphology and Physiology

We identified five morphological root traits (Root Length, Root ProjArea, Root SurfArea, Root AvgDiam, and Root Volume). All traits were measured by scanning the root system at 800 dpi using a flatbed scanner. Images were analyzed using WinRhizo Pro 2016 software (2016a, Regent Instruments, Quebec, QC, Canada). The fresh roots were put into a plastic bag and stored in liquid nitrogen tanks to maintain their activity and measure their soluble sugar, soluble protein, POD, and SOD contents in the lab.

2.7. Maize Grain Yield

On 2 October 2016 and 2017, corn was harvested manually. The corn ears of each treatment were put into net bags and brought into the laboratory. The ears were put into paper bags and placed in an oven before being dried at 80 °C to a constant weight. The corn yield was determined by manually harvesting each plot over the past two years. Grain and straw samples were air dried on the ground of the threshing field, and the yield was reported at a moisture content of 14%.

2.8. Data Analysis

The data were examined via analysis of variance, which was carried using SPSS statistical software (ver. 22.0; SPSS Inc., Chicago, IL, USA). The mean values were compared using the Least Significant Difference (LSD) test.

3. Results

3.1. Effect of Different Tillage Layer Structures on Soil Physical Properties

The effect of different tillage treatments on soil bulk density was significant at 60 cm soil depth but not at other soil layer depths in all treatments. The soil bulk density of all treatments increased with an increase in soil depth between 0 and 60 cm. The trend of change was significant from 0 to 30 cm, but was not as obvious from 30 cm to 60 cm. The top soil bulk densities of all of the treatments were significantly lower than the other soil layers in terms of soil profile depth. The soil bulk density of the QJ treatment ranged from 1.14 to 1.48 g cm^{-1}, and the average mean was 1.38 g cm^{-1} from 0 to 60 cm soil profile depth. The soil bulk density of the MS treatment ranged from 1.08 to 1.52 g cm^{-1}, and the average mean was 1.38 g cm^{-1} from 0 to 60 cm soil profile depth. The soil bulk density of the QS treatment ranged from 1.09 to 1.46 g cm^{-1}, and the average mean was 1.38 g cm^{-1} from 0 to 60 cm soil profile depth. The soil bulk density of the MJ treatment ranged from 1.16 to 1.51 g cm^{-1}, and the average mean was 1.41 g cm^{-1} from 0 to 60 cm soil profile depth (Figure 3).

The effect of different treatments on total soil porosity was significant at 0–10 cm, 10–20 cm, and 50–60 cm. However, that of other soil depths was not significant for all treatments. The change trend of all treatments decreased with the increase in soil depth. The soil porosity of the top 0–10 cm soil depth was significantly greater than the other soil layers. The total soil porosity of the QJ treatment ranged from 43.94 to 53.31%, and the average mean was 46.77% from 0 to 60 cm soil profile depth. The total soil porosity of the MS treatment ranged from 42.40 to 59.05%, and the average mean was 47.66% from 0 to 60 cm soil profile depth. The total soil porosity of the QS treatment ranged from 43.59 to 58.52%, and the average mean was 47.11% from 0 to 60 cm soil profile depth. The total soil porosity of the MJ treatment ranged from 42.91 to 55.96%, and the average mean was 46.12% from 0 to 60 cm soil profile depth (Figure 3).

The profile change of the three-phrase *R* value for all treatments was not obvious with the increase in soil depth. However, the three-phrase *R* values of all treatments were significant in the whole soil profile depth. The three-phrase *R* value of the QJ treatment ranged from 6.09 to 15.43, and the average mean was 10.41 from 0 to 60 cm soil profile depth. The three-phrase *R* value of the MS treatment ranged from 5.77 to 11.62, and the average mean was 10.84 from 0 to 60 cm soil profile depth. The three-phrase *R* value of the QS treatment ranged from 10.42 to 14.70, and the average mean was 12.56 from 0 to 60 cm soil profile depth. The three-phrase *R* value of the MJ treatment ranged from 4.46 to 12.25, and the average mean was 7.95 from 0 to 60 cm soil profile depth (Figure 3).

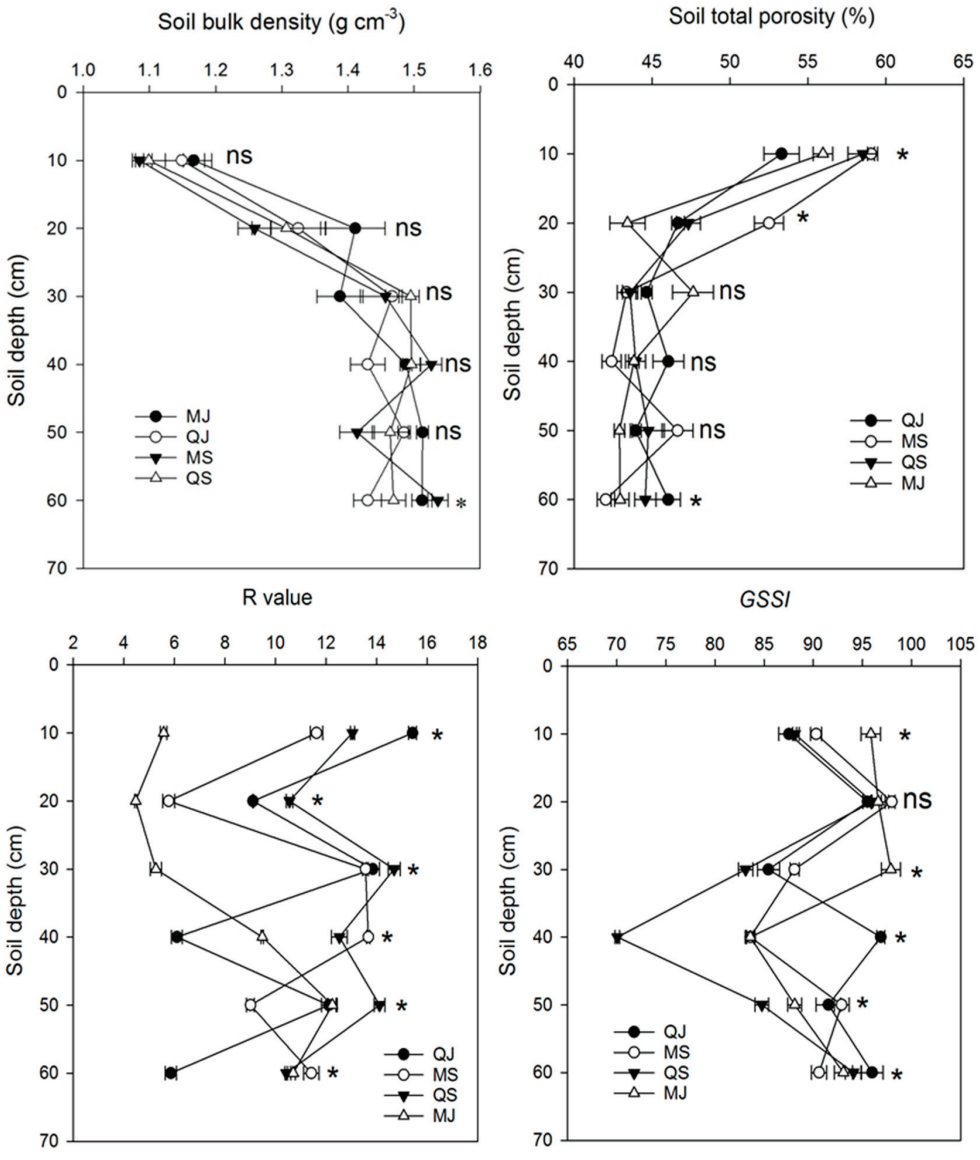

Figure 3. Means of soil bulk density, total soil porosity, *R* value, and GSSI at 0–60 cm affected by different tillage structures at the maize harvesting stage (data from 2016 to 2017). "*" was significantly different at $p < 0.05$ by a LSD test and "ns"was not significantly different at $p < 0.05$ by a LSD test.

The profile change of GSSI for all treatments was not obvious with the increase in soil depth. However, the differences in soil profile for all treatments were significant, except for the 10–20 cm soil layer. The GSSI value of the QJ treatment ranged from 85.43 to 95.99, and the average mean was 92.14 from 0 to 60 cm soil profile depth. The GSSI value of the MS treatment ranged from 83.58 to 98.00, and the average mean was 90.57 from 0 to 60 cm soil profile depth. The GSSI value of the QS treatment ranged from 83.11to 95.98, and the average mean was 86.01 from 0 to 60 cm soil profile depth. The GSSI value of the

MJ treatment ranged from 83.58 to 97.90, and the average mean was 92.52 from 0 to 60 cm soil profile depth (Figure 3).

The soil water content profile change of all treatments decreased with increasing depth (Figure 4). The difference in soil water content was significant in the whole profile depth. The soil water content of the QS treatment was significantly higher than that of the other treatments from between 0–20 cm and 50–60 cm, and the percentage increases in soil water content were 0.44–1.59%, 0.81–1.78%, 0.61–1.48%, and 0.96–1.41%, respectively. However, the MJ treatment was significantly greater than other treatments from 30 to 40 cm, and the percentage increase in soil water content was 0.49–0.94%. Nevertheless, the QJ treatment continued to have the lowest water content among all soil profiles.

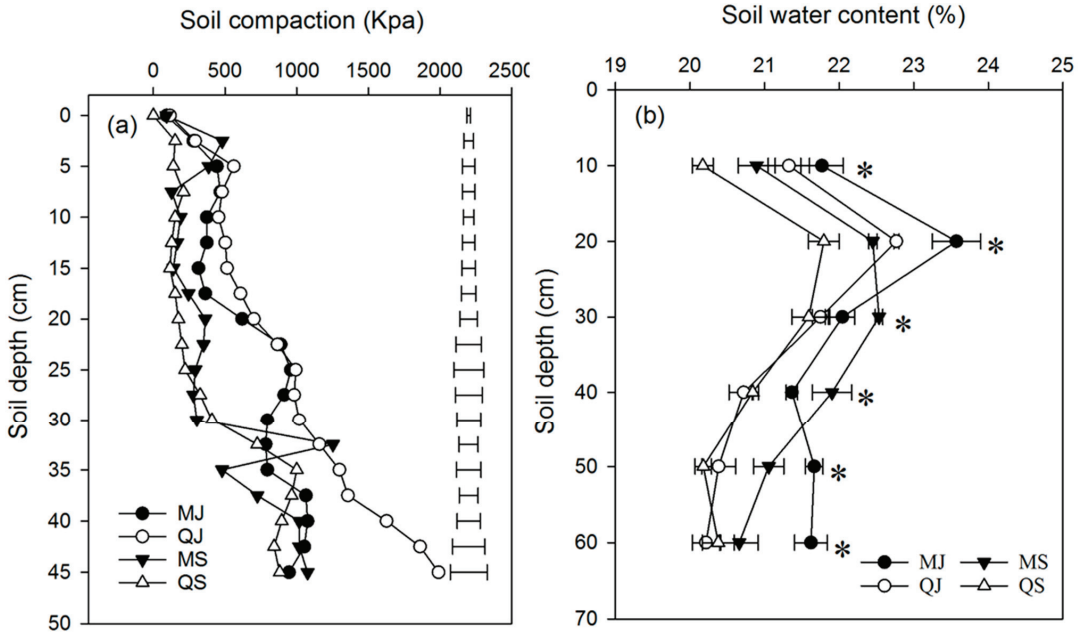

Figure 4. The soil water content (**a**) and soil compaction (**b**) profile changes in all treatments at changing depths. Horizontal bars represent ± SE in figure and * was significantly different at $p < 0.05$ by a LSD test.

Soil compaction is an important parameter of soil quality (Figure 4). Out of all of the soil profiles, the soil compaction at 0–45 cm depth increased in all four treatments. The largest increase was in the QJ treatment. Averaged across the depth of measurements, the soil compaction of the QJ treatment (914 kPa) was similar to that of the MS, QS, and MJ treatments, which had average soil compaction values of 472, 404, and 663 kPa, respectively. All treatments have similar tread at 0–35 cm. The QJ treatment continued to have greater soil compaction at 30–45 cm soil depth and increased by 27–109%, 82–170%, and 29–125% compared to MJ, MS, and QS.

3.2. Tillage's Effect on Soil Nutrients

The soil nutrient contents of the different treatments decreased with depth in all cases except for the AK treatment. The differences in contents near the surface were higher than at other soil depths, and the lowest soil nutrient concentrations were at the lower soil layers. TN concentrations decreased with the increase in soil depth. It was not significant at 0–30 cm, and it was obvious at 30 cm depth. The differences amongst treatments were significant across all soil profiles. At 0–20 cm soil depth, the TN contents of QS were

significantly higher than the other treatments. However, the lowest TN content for the QS treatment was observed at 20–30 cm and 30–40 cm. At 40–50 cm, QJ and MS were significantly higher QS and MJ, and MJ was lower than the other treatments at 50–60 cm. The value scope of the MS treatment was 0.54 g kg^{-1} to 1.19 g kg^{-1}, and the mean value was 0.95 g kg^{-1} in the whole soil profile. The value scope of the QJ treatment was 0.55 g kg^{-1} to 1.23 g kg^{-1}, and the mean value was 0.96 g kg^{-1} in the whole soil profile. The value scope of the QS treatment was 0.54 g kg^{-1} to 1.27 g kg^{-1}, and the mean value was 0.91 g kg^{-1} in the whole soil profile. The value scope of the MJ treatment was 0.52 g kg^{-1} to 1.23 g kg^{-1}, and the mean value was 0.95 g kg^{-1} in the whole soil profile. The results showed four different tillage layer structures in the order of MS > QJ = MJ > QS.

TP concentrations decreased with the increase in soil depth, and significant differences were detected in the soil profiles of the four tillage layer structures. At 0–20 cm soil depth, QS was significantly higher than the other treatments. With the increase in soil depth, the MJ was higher than the other treatments at 20–40 cm. However, the QJ was higher than the other treatments at 40–60 cm soil depth, although this difference was not significant amongst the four treatments. The value scope of the QJ treatment was 0.54 g kg^{-1} to 1.19 g kg^{-1}, and the mean value was 0.95 g kg^{-1} in the whole soil profile. The value scope of the MS treatment was 0.55 g kg^{-1} to 1.23 g kg^{-1}, and mean value was 0.96 g kg^{-1} in the whole soil profile. The value scope of the QS treatment was 0.54 g kg^{-1} to 1.27 g kg^{-1}, and the mean value was 0.91 g kg^{-1} in the whole soil profile. The value scope of the MJ treatment was 0.52 g kg^{-1} to 1.23 g kg^{-1}, and the mean value was 0.95 g kg^{-1} in the whole soil profile. The results showed four different tillage layer structures in the order of MS > QJ = MJ > QS (Figure 5).

TK concentrations decreased with the increase in soil depth, and the increasing trend was significant with depth. The differences in the different tillage layer structures were significant with depth across all soil profiles, except at 10–20 cm. At 0–10 cm soil depth, QJ and MS were significantly higher than QS and MJ. At 30–60 cm soil depth, QJ was significantly higher than the other treatments. The value scope of the QJ treatment was 0.34 g kg^{-1} to 0.48 g kg^{-1}, and the mean value was 0.41 g kg^{-1} in the whole soil profile. The value scope of the MS treatment was 0.32 g kg^{-1} to 0.50 g kg^{-1}, and the mean value was 0.42 g kg^{-1} in the whole soil profile. The value scope of the QS treatment was 0.33 g kg^{-1} to 0.47 g kg^{-1}, and the mean value was 0.41 g kg^{-1} in the whole soil profile. The value scope of the MJ treatment was 0.33 g kg^{-1} to 0.46 g kg^{-1}, and the mean value was 0.40 g kg^{-1} in the whole soil profile. The results showed that the mean values for the four tillage layer structures were similar(Figure 5).

AN concentrations decreased with the increase in soil depth. The increasing trend was not obvious from 0 cm to 30 cm soil depth but was significant from 40 cm to 60 cm (Figure 5). The difference between the four tillage layer structures was not significant at 0–20 cm. However, the difference was significant at other soil depths. At 20–30 cm soil depth, MS was significantly higher than the other treatments, and QJ was significantly higher than the other three treatments at 30–40 cm and 40–50 cm soil depth. However, MJ was significantly higher than the others at 50–60 cm soil depth. The value scope of the QJ treatment was 43.93 mg kg^{-1} to 116.75 mg kg^{-1}, and the mean value was 91.07 mg kg^{-1} in the whole soil profile. The value scope of the MS treatment was 46.01 mg kg^{-1} to 115.53 mg kg^{-1}, and the mean value was 89.99 mg kg^{-1} in the whole soil profile. The value scope of the QS treatment was 45.28 mg kg^{-1} to 116.01 mg kg^{-1}, and the mean value was 82.95 mg kg^{-1} in the whole soil profile. The results showed four different tillage layer structures in the order of QJ > MS > MS > MJ.

AP concentrations decreased with the increase in soil depth. At 0–10 cm, QS was significantly higher than the others. However, QJ was significantly higher than the others at 30–40 cm, 40–50 cm, and 50–60 cm. The value scope of the QJ treatment was 5.88 mg kg^{-1} to 16.30 mg kg^{-1}, and the mean value was 11.56 mg kg^{-1} in the whole soil profile (Figure 5). The value scope of the MS treatment was 6.17 mg kg^{-1} to 16.65 mg kg^{-1}, and the mean value was 11.16 mg kg^{-1} in the whole soil profile. The value scope of the QS treatment was

4.96 mg kg^{-1} to 17.43 mg kg^{-1}, and the mean value was 11.07 mg kg^{-1} in the whole soil profile. The value scope of the MJ treatment was 5.60 mg kg^{-1} to 16.08 mg kg^{-1}, and the mean value was 10.91 g kg^{-1} in the whole soil profile. The results showed four different tillage layer structures in the order of QJ = MS = MS > MJ.

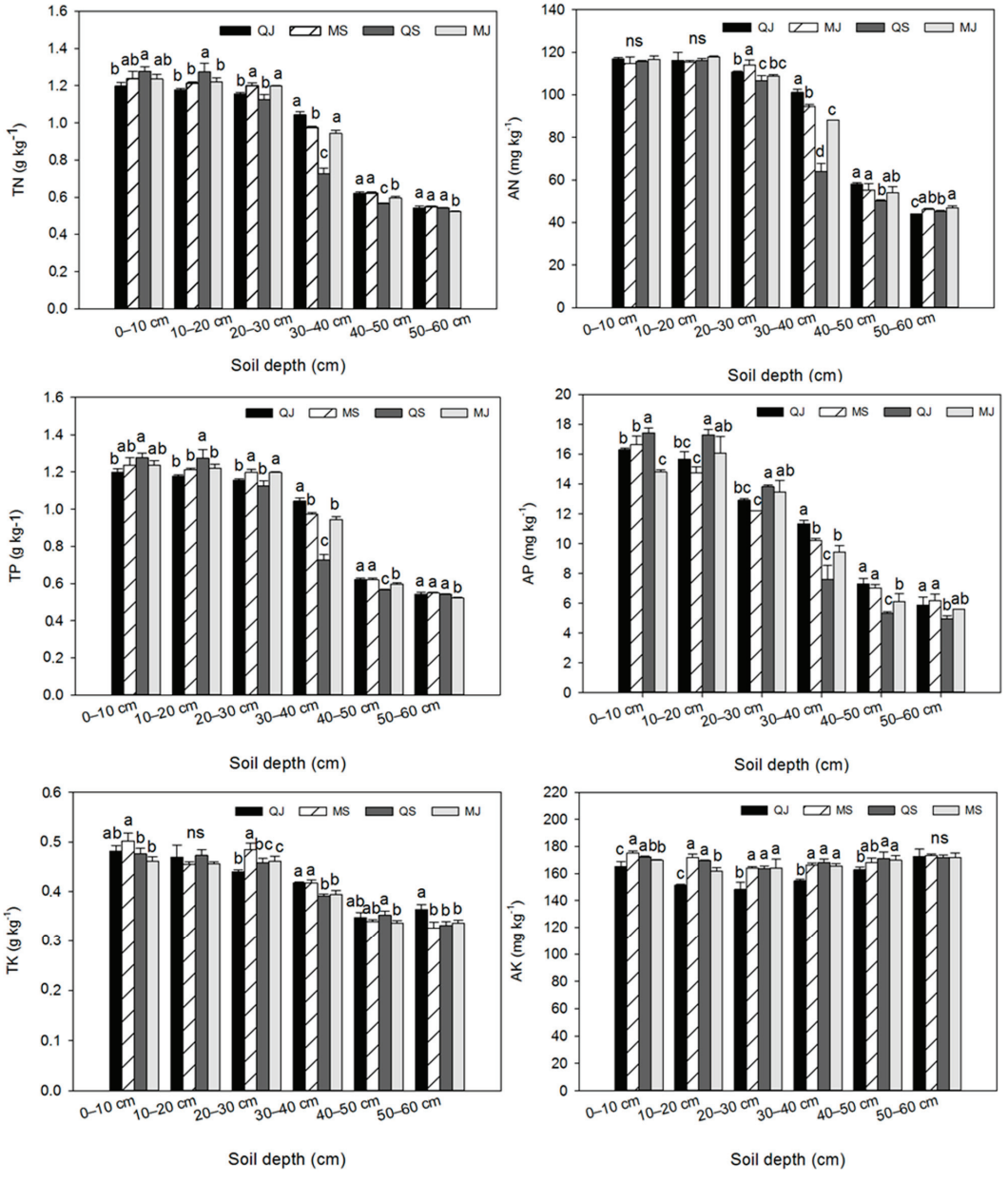

Figure 5. Tillage's effect on soil nutrient content in soil profile. Vertical bars represent ± SE and Different lowercase letters indicate significant difference among different treatments at 0.05 levels.

AK concentration was not significant with the increase in soil depth. However, the differences in the different tillage layer structures were significant in the whole soil profile except at 50–60 cm soil depth. MS was significantly higher than the other treatments at 0–10 cm, 10–20 cm, and 20–30 cm. QS was significantly higher than the other treatments at 30–40 cm and 40–50 cm. The value scope of the QJ treatment was 148.25 mg kg^{-1} to 172.58 mg kg^{-1}, and the mean value was 159.13 mg kg^{-1} in the whole soil profile. The value scope of the MS treatment was 164.04 mg kg^{-1} to 175.11 mg kg^{-1}, and the mean value was 169.75 mg kg^{-1} in the whole soil profile. The value scope of the QS treatment was 163.73 mg kg^{-1} to 172.23 mg kg^{-1}, and the mean value was 169.39 mg kg^{-1} in the whole soil profile. The value scope of the MJ treatment was 161.86 mg kg^{-1} to 171.62 mg kg^{-1}, and the mean value was 167.15 g kg^{-1} in the whole soil profile. The results showed four different tillage layer structures in the order of MS = QS> MJ> QJ (Figure 5).

The significant effects exerted by the different tillage layer structures are displayed in Figure 6. The change trend was not significant from 0 to 30 cm soil depth, and the SOM decreased significantly at 30–60 cm depth. At 10 cm soil depth, QS had a significantly higher soil organic matter concentration value than the other treatments, and the increase in SOM ranged between 3.81 and 7.20%. At 20 cm soil depth, QS had a significantly higher soil organic matter concentration value than the other treatments, and the increase in SOM ranged between 2.47 and 6.09%. At 40 cm soil depth, QJ had a significantly higher soil organic matter concentration value than the other treatments, and the increase in SOM ranged between 8.96 and 45.55%. At 50 cm soil depth, QJ had a significantly higher soil organic matter concentration value than the other treatments, and the increase in SOM ranged between 6.18 and 13.80%. At 60 cm soil depth, QS had a significantly higher soil organic matter concentration value than the other treatments, and the increase in SOM ranged between 0.78 and 8.98%.

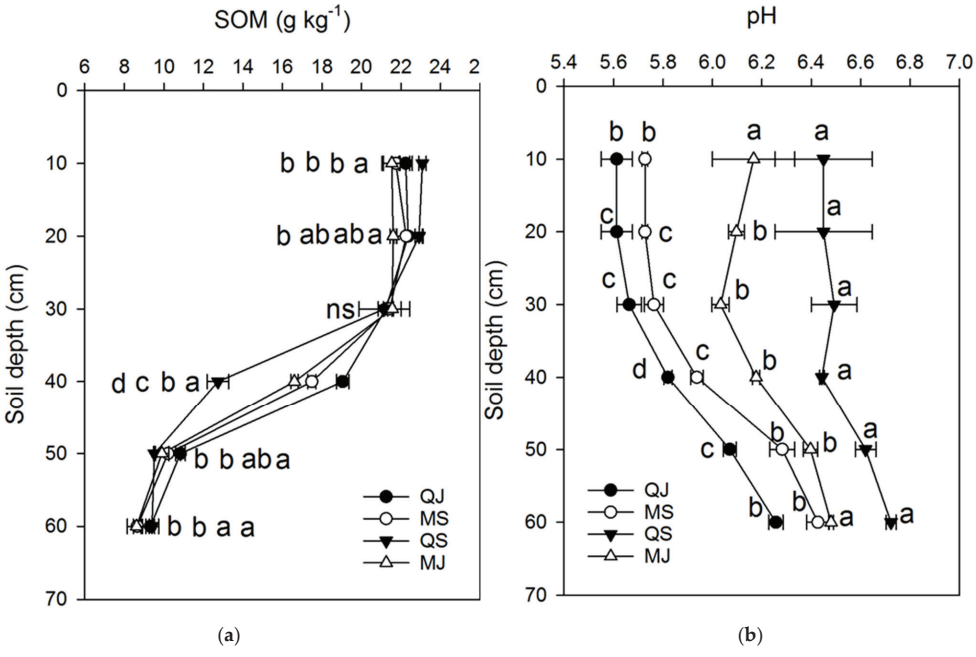

Figure 6. Tillage's effect on soil organic matter (**a**) and pH (**b**) content in soil profile. Horizontal bars represent ± SE and different lowercase letters indicate significant difference among different treatments at 0.05 levels.

Soil pH value was affected by the different tillage layer structures, and the trend of soil pH value is shown in Figure 6. The QS had a significantly higher soil pH value than the other treatments in whole soil profile. The increase in soil pH value was not obvious from 0 to 30 cm soil depth. However, the increase in soil pH value was observed to be significant at 30–60 cm soil depth. Across all soil profiles, QS had a significantly higher soil pH value than the other treatments, and the increase in soil pH value ranged between 3.75 and 14.90%.

3.3. Effect of Different Tillage Layer Structures on Root Morphology

From Table 1, it can be seen that root length, root ProjArea, root SurfArea, root AvgDiam, and root volume are all significantly affected by the year, depth, and treatments at the VT and R1 stage, respectively. In the VT stage, the root length in 2016 was significantly higher than that in 2017. The root length decreased with depth, and there were significant differences amongst the different depths. The root length of QJ and QS were significantly higher than that of MJ and MS. The root length was significantly affected by year (Y), depth (D), and treatments (T) Y×D, Y×T, D×T, and Y×D×T at 0.05 level. The root ProjArea in 2016 was significantly higher than that in 2017. The root ProjArea at 0–20 cm soil depth was significantly higher than that at other depths. The root ProjArea values of QJ, MJ, and MS were significantly higher than that of QS. The root ProjArea was significantly affected by year (Y), depth (D), and treatments (T) Y×D and Y×T (except D×T and Y×D×T) at 0.05 level. The root SurfArea in 2016 was significantly higher than that in 2017. The root SurfArea at 0–20 cm soil depth was significantly higher than that at other depths. The root SurfArea values of QJ and MJ were significantly than that of QS and MS. The root SurfArea was significantly affected by year (Y), depth (D), and treatments (T) Y×D and Y×T D×T (except Y×D×T) at 0.05 level. The root AvgDiam in 2017 was significantly higher than that in 2016. The root AvgDiam at 0–20 cm, 60–80 cm, and 80–100 cm were significantly higher than at 20–40 cm and 40–60 cm soil depths. The root AvgDiam values of MJ and MS were significantly higher than that of QJ and QS. The root AvgDiam was significantly affected by year (Y), depth (D), and treatments (T) Y×D, Y×T, D×T, and Y×D×T at 0.05 level. The root Volume in 2017 was significantly higher than that in 2016. The root Volume at 80–100 cm was significantly higher than that at other soil depths. The root Volume of MJ was significantly higher than that of the other treatments. The root Volume was significantly affected by year (Y), depth (D), and treatments (T) Y×D, Y×T, D×T, and Y×D×T at 0.05 level.

In the R1 stage, the root length in 2016 was significantly higher than that in 2017. The root length at 0–20 cm soil depth was significantly higher than that at 20–40 cm, 40–60 cm, 60–80 cm, and 80–100 cm soil depth. The root length of MS was significantly higher than that of the other treatments. The root length was significantly affected by year (Y), depth (D), and treatment (T) (except Y×D, Y×T, D×T, and Y×D×T) at 0.05 level. The root ProjArea in 2016 was considerably higher than that in 2017. The root ProjArea at 0–20 soil depth was significantly higher than that at other depths. The root ProjArea of MS was significantly higher than that of the other treatments. The root ProjArea was significantly affected by year (Y), depth (D), treatment (T), and Y×D, except Y×T, D×T, and Y×D×T at 0.05 level. The root SurfArea in 2016 was significantly higher than that in 2017. The root SurfArea at 0–20 cm soil depth was significantly higher than that at 20–40 cm, 40–60 cm, 60–80 cm, and 80–100 cm soil depth. The root SurfArea of MS was significantly higher than that of the other treatments. The root SurfArea was significantly affected by year (Y), depth (D), and treatment (T) Y×D (but not Y×T, D×T, and Y×D×T) at 0.05 level. The root AvgDiam in 2017 was significantly higher than that in 2016. The root AvgDiam at 0–20 cm and 80–100 cm was significantly higher than that at 20–40 cm, 40–60 cm, and 60–80 cm soil depth. There were no significant differences amongst the different treatments. The root SurfArea was significantly affected by year (Y), depth (D), and Y×D (except treatments (T), Y×T, D×T, and Y×D×T) at 0.05 level. The root Volume in 2016 was significantly higher than that in 2017. The root Volume at 0–20 cm soil depth was significantly higher

than that at 20–40 cm, 40–60 cm, 60–80 cm, and 80–100 cm soil depth. The root Volume values of QS and MJ were significantly higher than that of QJ and MS. The root Volume was significantly affected by year (Y), depth (D), and treatments (T) Y×D, Y×T, D×T, and Y×D×T at 0.05 level.

Table 1. Effect of tillage systems on maize roots.

		VT					R1				
		Root Length (cm)	**Root Proj. Area (cm^2)**	**Root Surf. Area (cm^2)**	**Root Avg. Diam. (mm)**	**Root Volume (cm^3)**	**Root Length (cm)**	**Root Proj. Area (cm^2)**	**Root Surf. Area (cm^2)**	**Root Avg. Diam (mm)**	**Root Volume (cm^3)**
Year (Y)	2016	1286.20 a	47.00 a	34.17 a	0.76 b	12.14 b	1385.8 a	47.51 a	35.02 a	0.75 b	44.76 a
	2017	1051.14 b	38.09 b	27.59 b	1.44 a	62.91 a	1059.5 b	38.30 b	27.63 b	1.35 a	18.40 b
Depth (D)	0–20	1512.00 a	58.47 a	42.51 a	1.27 a	42.72 b	1693.5 a	58.90 a	43.12 a	1.19 ab	43.11 a
	20–40	1105.04 b	38.91 b	28.34 b	0.72 b	23.63 c	1118.7 b	39.06 b	28.58 b	0.71 d	19.90 e
	40–60	1089.93 c	38.57 c	28.02 c	0.82 b	18.25 d	1111.0 b	39.02 b	28.51 b	0.97 c	29.89 c
	60–80	1069.63 d	38.39 cd	27.83 cd	1.42 a	41.64 b	1100.0 c	38.87 bc	28.29 c	1.03 bc	37.14 b
	80–100	1066.75 d	38.36 d	27.73 d	1.27 a	61.38 a	1089.6 d	38.69 c	28.12 d	1.36 a	27.87 d
Treatment (T)	QJ	1209.67 a	42.65 a	31.24 a	0.97 b	38.82 b	1219.2 b	42.88 b	31.31 b	1.05 a	30.87 b
	MJ	1195.24 b	42.61 a	31.04 b	1.30 a	40.63 a	1218.9 b	42.82 b	31.29 b	1.09 a	31.98 a
	MS	1072.87 c	42.42 ab	30.59 c	1.15 ab	32.38 b	1232.8 a	43.08 a	31.46 a	1.03 a	30.85 b
	QS	1196.90 b	42.49 b	30.66 c	0.99 b	38.26 c	1219.0 b	42.85 b	31.24 b	1.03 a	32.62 a
analysis of variance	Y	*	*	*	*	*	*	*	*	*	*
	D	*	*	*	*	*	*	*	*	*	*
	T	*	*	*	*	*	*	*	*	ns	*
	Y×D	*	*	*	*	*	*	*	*	*	*
	Y×T	*	*	*	*	*	ns	*	ns	ns	*
	D×T	*	ns	*	*	*	ns	ns	ns	ns	*
	Y×D×T	*	ns	ns	*	*	ns	ns	ns	ns	*

Numbers followed by the different letter were significantly different at $p < 0.05$ by a LSD test. "*" significance at the 0.05 level of probability. "ns" was not significantly different at $p < 0.05$ by a LSD test.

3.4. Tillage's Effect on Root Physiological Properties

The root physiological traits were almost affected by the stages. However, soluble sugar, soluble protein, POD, and SOD were significantly affected by the different tillage layer structures (Table 2). The soluble sugar content was significantly higher in QJ than in the other treatments and only affected by the type of treatment (not other factors). The soluble protein content was significantly higher in MS than in the other treatments and only affected by the type of treatment (not other factors). The POD content was significantly higher in MS than in the other treatments and only affected by the type of treatment (not other factors). The SOD content was significantly affected by Y×S, S×T, and Y×S×T.

Table 2. Effect of tillage on corn root physiological traits.

		Soluble Sugar %	Soluble Protein $mg \cdot g^{-1}$	POD $u \cdot g^{-1}$	SOD $u \cdot g^{-1}$
Year (Y)	2016	0.003 a	7.323 a	330.14 a	223.62 a
	2017	0.003 a	8.254 a	313.50 a	270.42 a
Stage (S)	VT	0.003 a	7.914 a	327.52 a	241.16 a
	R1	0.003 a	7.663 a	316.12 a	252.88 a
Treatment (T)	QJ	0.005 a	7.634 bc	309.13 b	251.74 a
	MJ	0.002 bc	8.503 bc	267.04 b	235.86 a
	MS	0.003 bc	11.204 a	411.24 a	260.27 a
	QS	0.001 c	3.815 c	299.86 b	240.22 a
analysis of variance	Y	ns	ns	ns	ns
	S	ns	ns	ns	ns
	T	*	*	*	ns
	Y×S	ns	ns	ns	*
	Y×T	ns	ns	ns	ns
	S×T	ns	ns	ns	*
	Y×S×T	ns	ns	ns	*

Numbers followed by the different letter were significantly different at $p < 0.05$ by a LSD test." *" Significance at the 0.05 level of probability. "ns"was not significantly different at $p < 0.05$ by a LSD test.

3.5. Tillage's Effect on Root Dry Weight and Yield

The root dry weight of different tillage layer structures decreased with the increase in soil depth in 2016 and 2017, respectively (Figure 7). The proportions of root dry weight for all treatments were 78.27% and 61.70% in 2016 and 2017, respectively. However, the differences in root dry weight were not significant among the different treatments at 10–20 cm, 20–30 cm, and 30–40 cm, respectively. The different tillage layer structures were significantly different at 50–60 cm. In 2017, the different tillage layer structures were not significant at 0–10 cm, 60–80 cm, and 80–100 cm. However, the differences were significant at 20–40 cm and 40–60 cm. At 20–40 cm soil depth, MJ and QS were significantly higher than QJ and MS. At 40–60 cm soil depth, MJ was significantly higher than other treatments. The different tillage layer structures had significant effects on grain yield across both years. The yield of the MJ treatment was significantly higher than the others in 2016 and 2017, respectively. In 2016, the yield of MJ increased by 9.04%, 23.80%, and 26.06% compared to QJ, MS, and QS, respectively (Figure 8). However, the yield of MJ increased by 11.50%, 10.10%, and 38.01% compared to QJ, MS, and QS, respectively (Figure 9).

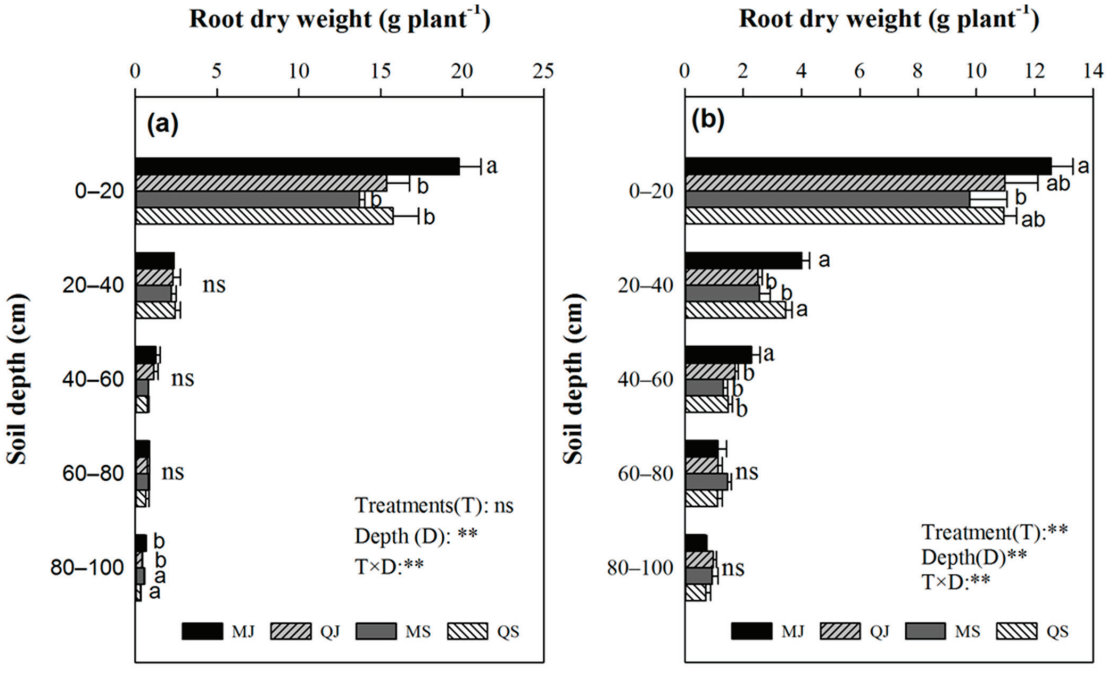

Figure 7. Tillage's effect on root dry weight (g per plant) in 2016 (**a**) and 2017 (**b**). Different lowercase letters indicate significant difference among different treatments at 0.05 levels. Horizontal bars represent ± SE. "**" significance at the 0.01 level of probability.

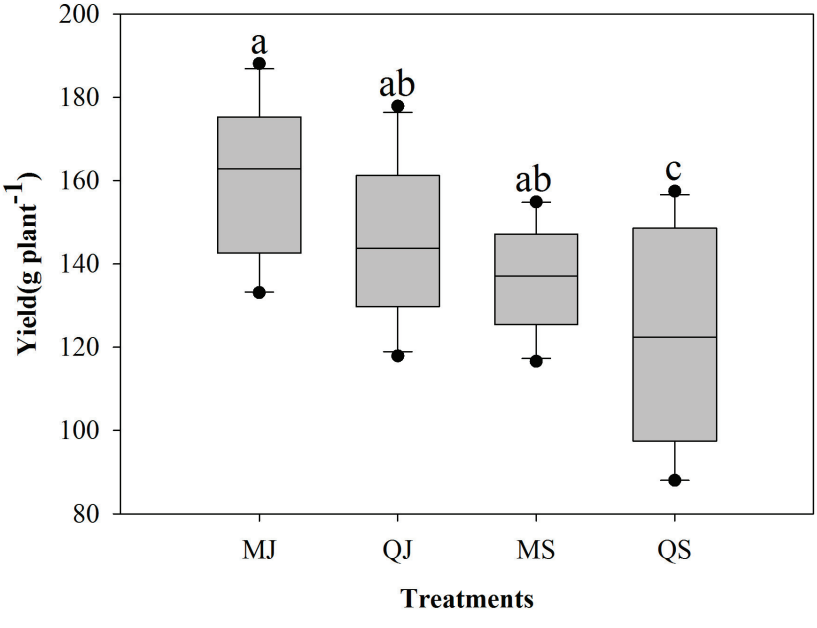

Figure 8. Effects of tillage structures on grain yield (2016–2017). Different lowercase letters on the vertical bars indicate significant difference among different treatments at 0.05 levels.

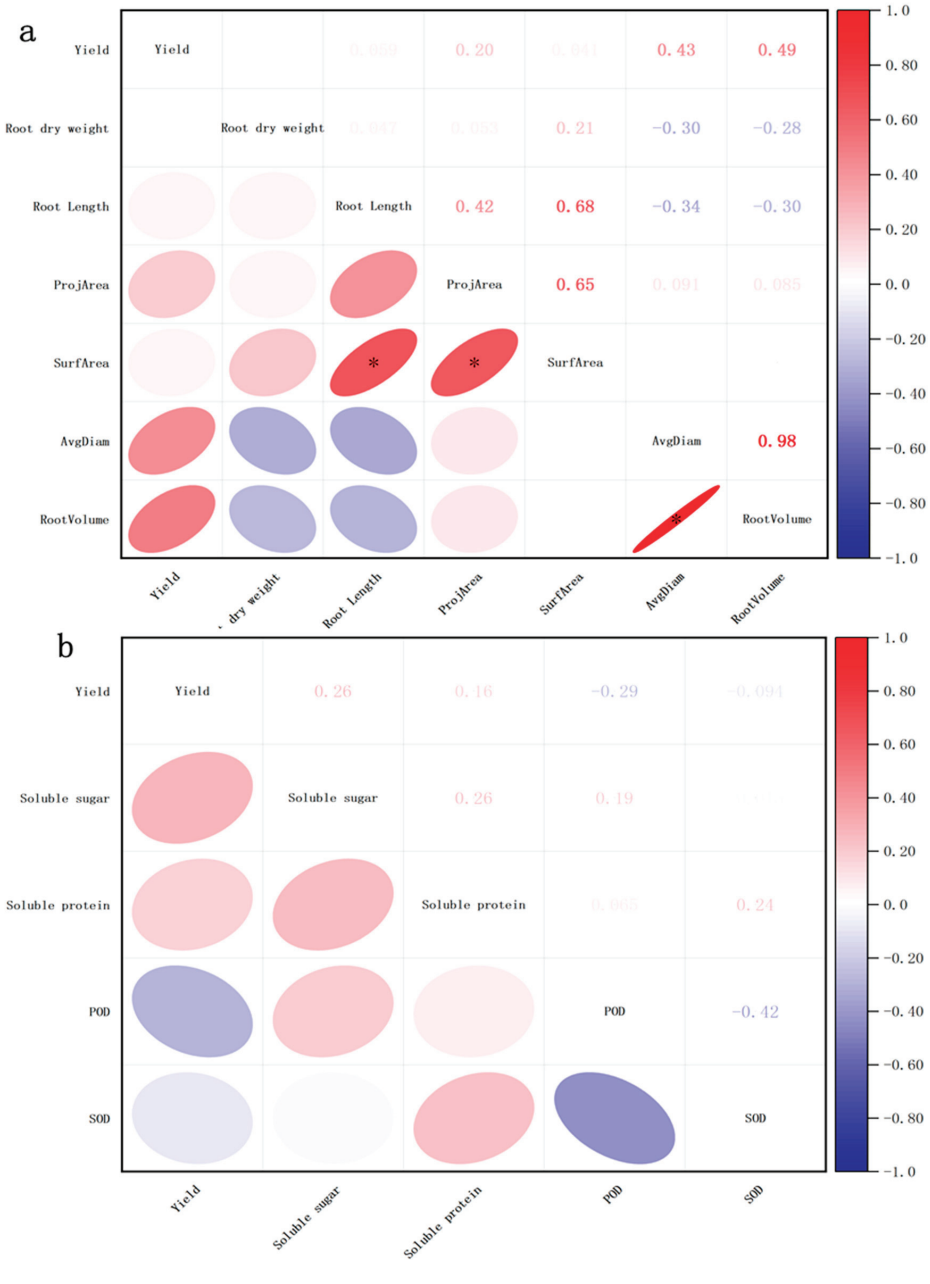

Figure 9. *Cont.*

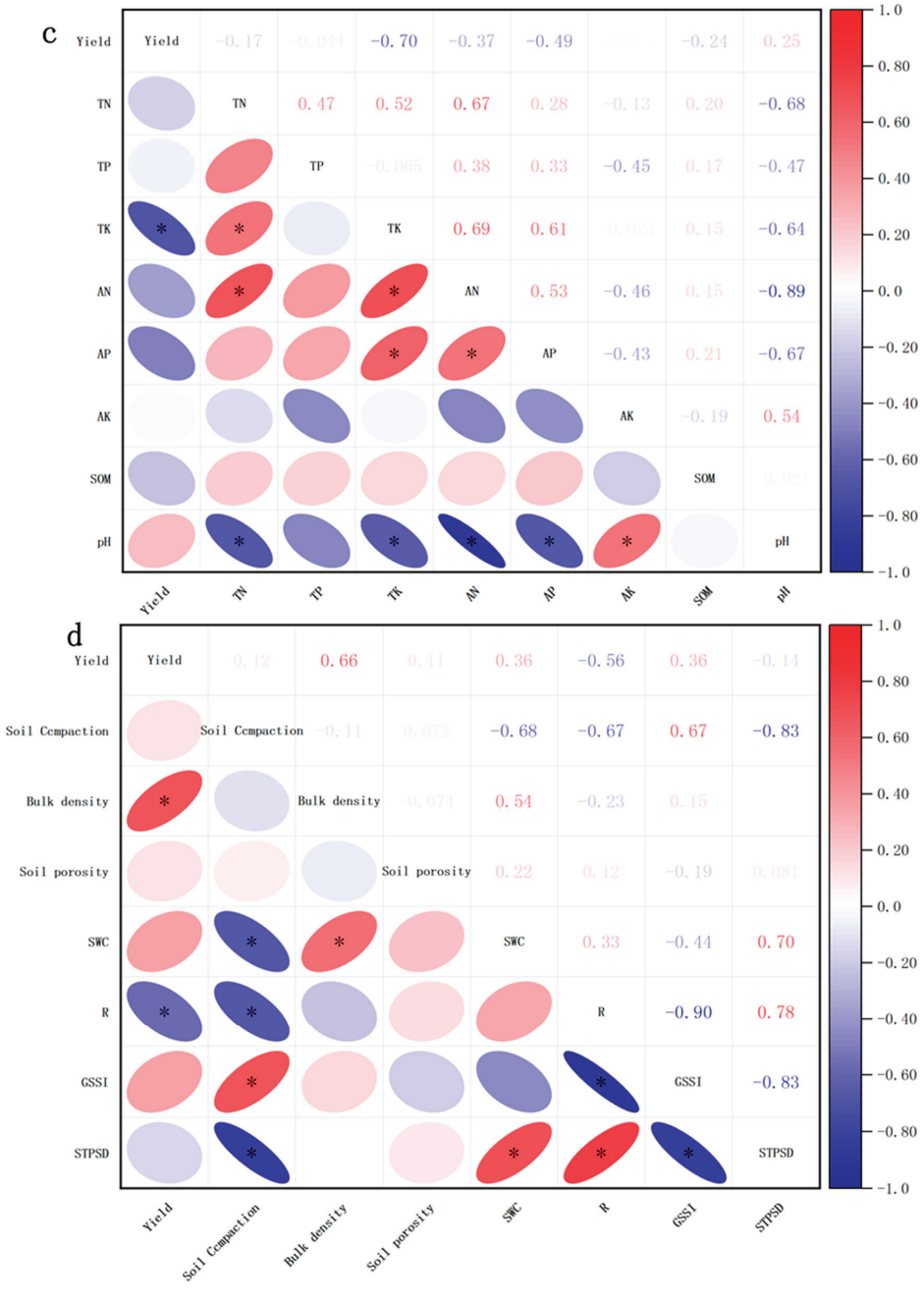

Figure 9. Relationship analysis of yield and root morphology (**a**) traits, root physiology traits (**b**), soil nutrients (**c**), and soil physical traits (**d**). "*" Significance at the 0.05 level of probability.

3.6. Correlation Analysis of Yield and Other Parameters

There was no significant correlation between the yield and morphology parameters; however, there was a significant positive correlation between the SurfArea and Root

length and ProjArea (Figure 9a). Yield was not significant with physiological parameters, including soluble sugar, soluble protein, POD, and SOD (Figure 9b). There was a significant negative correlation between the yield and TK, and yield was not correlated with other parameters, and there were different correlations among other parameters (Figure 9c). There was a positive correlation between yield and soil bulk density, and there was a negative correlation between yield and R; however, there were different correlations among the different parameters (Figure 9d).

4. Discussion

4.1. Soil Physical Properties

Improving soil physical properties is important for soil conservation and crop yield enhancement [51]. Soil physical properties are especially positively influenced by different crop rotations, cover cropping, conversation tillage systems, and chemical and organic fertilizers [52–54]. Rotation can reduce stacking density, increase soil aggregate size, and improve water retention by increasing crop residues in the soil and crop residues [10,55,56]. After tillage and harvesting operations, the soil permeability resistance, dry bulk density, and moisture content at all depths are significantly affected by tillage [57]. Aikins et al. [58] showed that after tillage and harvesting operations at a soil depth of 0–60 cm, the zero tillage system produced the highest soil permeability resistance. In addition, the bulk density (Db) of soil changes significantly with the application of different combinations of chemical and organic fertilizers [59]. Our results also proved that soil physical properties can be affected by many factors, such as different tillage layer structures. The MJ layer structure is a better tillage structure that can decrease soil bulk density and soil compaction and increase soil porosity by increasing deep tillage depth. Khurshid et al. [60] showed that Db is an inferior organic fertilizer than inorganic fertilizer. With the continuous application of inorganic and organic fertilizers, the soil particle density (Dp) of surface soil samples remains basically unchanged [61]. Meanwhile, this tillage layer can improve soil water content by enhancing the rainfall infiltration to manipulate the soil structure by improving the three-phrase soil. Our results are consistent with those published by experts in this regard. However, QJ did not significantly increase soil compaction and bulk density in our study compared to the studies of others [62,63].

4.2. Soil Nutrient Characteristics

Rotation is the cheapest and most effective method to increase crop yield and soil fertility [64]. The soil nutrient characteristics typically affected by tillage systems include pH, CEC, exchangeable cations, and total soil nitrogen [65]. Conservation tillage, especially MT, is superior to CT in soil chemical improvement [66–68]. Covering crops can protect soil from erosion, reduce N and P losses, increase soil C, reduce runoff, inhibit pests, and support animals that benefit from soil [69,70]. According to reports, the rotation of legumes and covering crops can affect soil nutrient status [71]. Due to differences in crop residues and soil organic matter mineralization rates, crop rotation and nitrogen fertilizer can affect SOC sequestration in cultivated and non-cultivated soils [72]. However, our results show that soil nutrients are significantly affected by soil depth (with the exception of available potassium). However, soil nutrients are influenced by different tillage layer structures with soil depth. Soil nutrient responses with depth are different for the MJ layer treatment compared with other tillage layer structures. Soil organic matter (SOM) values are affected with increasing depth and significantly influenced by different tillage layer structures (except at 20–30 cm soil depth). The MJ treatment increases SOM by 10–20% compared with other tillage layer structures. In addition, in our study, QS treatment more effectively enhanced the increase in the pH value of the soil profile compared to the other treatments. Covering crops is usually incorporated into the planting system as a nutritional management tool [73]. The benefits of legume-covered crops in crop rotation have long been recognized and are mainly attributed to the contribution of nitrogen to subsequent crops [74].

4.3. Root Morphological and Physiological Traits

The morphology of maize roots in the early stages of growth is influenced by tillage intensity [75]. The root system is an important component of plants, regulating many aspects of aboveground growth and development. Appropriate crop management can significantly improve the ultrastructure of root tip cells and increase root length density, and thereby increasing grain filling rate, yield, and water use efficiency [52,76]. The poor growth of roots and buds in maize seedlings may be due to the lower surface temperature of NT rather than mechanical impedance [77,78]. The increase in topsoil stacking density during NT treatment may only limit root growth to a limited extent and is more pronounced in fine-grained soil [79]. Our results show that root morphology characteristics such as root length, root ProjArea, root SurfArea, root AvgDiam, and root volume are affected according to the year, depth, and tillage layer structure. The MJ layer structure can enhance root growth by improving tillage soil structure and increasing soil air and water more effectively than other tillage layer treatments. Specifically, the MJ layer structure increased root length and root volume significantly in deep soil. However, the difference in the root physiological properties was not significant among treatments. The effect of cultivation on the growth of maize roots was previously found in early growth and persisted until flowering in our experiment [80].

The average root dry matter (RDM) of corn in the entire soil profile and growth period is affected by tillage, and there are significant differences in RDM for each soil layer under different tillage treatments [81]. Nitrogen fertilizer significantly reduced the root/shoot weight ratio, but tillage did not significantly change the root/shoot weight ratio [82]. DeFelice et al. [83] reported that tillage to 50 cm in subsoil significantly increased the dry weight of spring maize roots at soil depths of 0–80 cm, especially in deep soil [60]. Our results showed that the root dry weight decreases with increasing soil depth. Most of our roots were mainly distributed at 0–40 cm soil depth. The MJ treatment enhanced the increase in root dry weight by breaking the tillage pan layer more effectively than the others. The difference in root dry weight would have been smaller with increasing soil depth among the different tillage layer structures. In the southern and western regions, the yield of no-tillage is often higher than that of traditional tillage [63]. When maize is rotated, minimum tillage can produce the same grain yield as traditional tillage [84,85]. The MJ treatment improves maize yield significantly compared to other treatments. The yield is increased by 14.2% compared to others under The MJ treatment via improving the soil environment and soil function. So, our results show that the MJ tillage layer structure is the best tillage structure for increasing maize yield by enhancing soil nutrients, improving soil environment and root qualities. In addition, the correlation relationships were different among yield and root morphology traits, root physiology traits, soil nutrients, and soil physical traits (Figure 9).

5. Conclusions

Soil tillage plays a prominent role in agricultural sustainability. Different tillage layer structures affect soil physical properties. An enhancement in the optimal tillage layer structure improved soil structure. The MJ tillage layer structure could create better soil structures by regulating the soil physical properties, which would be beneficial for crop growth, increase soil water content, and adjust the soil phrase *R* value and *GSSI*. Soil nutrients are significantly affected by soil depth (except available potassium). However, soil nutrients are influenced by different tillage layer structures with soil depth. Soil nutrient responses with depth are different for MJ tillage layer treatment compared with other tillage layer structures. Soil organic matter (SOM) values are affected with increasing depth and significantly influenced by different tillage layer structures (except at 20–30 cm soil depth). The MJ tillage treatment increases SOM by 10–20% compared with other tillage layer structures. In addition, QS treatment enhanced the increase in pH value in the soil profile more effectively than the other treatments. Root morphology characteristics such as root length, root ProjArea, root SurfArea, root AvgDiam, and root volume are affected according

to the year, depth, and tillage layer structure. The MJ layer structure enhanced root growth by improving tillage soil structure and increasing soil air and water compared with other tillage layer treatments. Specifically, the MJ tillage layer structure significantly increased root length and root volume in deep soil. However, the difference in root physiological properties was not significant among the different treatments. Root dry weight decreases with increasing soil depth. Most of the roots were mainly distributed at 0–40 cm soil depth. MJ tillage treatment enhanced the increase in root dry weight by breaking the tillage pan layer more effectively than the others. The difference in root dry weight became smaller with increasing soil depth among the different tillage layer structures. Moreover, MJ tillage treatment significantly improved maize yield compared with the other treatments. The yield was increased by 14.2% compared to the other treatments under the MJ tillage treatment via improvements in the soil environment and soil function. So, our results show that the MJ tillage layer structure is the best tillage structure for increasing maize yield by enhancing soil nutrients, improving the soil environment and root qualities.

Author Contributions: Conceptualization, H.W. and W.L.; Methodology, S.Z. and Y.L.; Software, H.Z., R.L., P.S. and J.Z.; Validation, S.T.; Formal analysis, H.Z.; Investigation, S.T., W.L. and J.Z.; Resources, P.S., H.W. and Y.R.; Data curation, H.Z. and Y.R.; Writing—original draft, Y.L.; Writing—review and editing, R.L. and Y.Y.; Visualization, Y.Y.; Funding acquisition, S.Z. and Y.L. All authors have read and agreed to the published version of the manuscript.

Funding: This study was funded by the Chinese Academy of Sciences Strategic Pilot Technology Project (XDA28080204), the National Natural Science Foundation of China (31501248), and the National Key Technology Research and Development Program of the Ministry of Science and Technology of China (2016YFD03002).

Data Availability Statement: The data presented in this study are available on request from the first author.

Conflicts of Interest: The authors declare no conflict of interest.

References

1. Cao, Q.; Li, G.; Yang, F.; Cui, Z.; Zhang, E.; Yang, F. Eleven-year mulching and tillage practices alter the soil quality and bacterial community composition in Northeast China. *Arch. Agron. Soil Sci.* **2022**, *68*, 1274–1289. [CrossRef]
2. Ray, D.K.; Ramankutty, N.; Mueller, N.D.; West, P.C.; Foley, J.A. Recent patterns of crop yield growth and stagnation. *Nat. Commun.* **2012**, *3*, 1293. [CrossRef] [PubMed]
3. Wang, X.B.; Cai, D.X.; Hoogmoed, W.B.; Oenema, O.; Perdok, U.D. Developments in conservation tillage in rain-fed regions of North China. *Soil Tillage Res.* **2007**, *93*, 239–250. [CrossRef]
4. Sharma, A.R.; Biswas, A.K. Benefits and Limitations. In *Conservation Agriculture in India: A Paradigm Shift for Sustainable Production*; Taylor & Francis: London, UK, 2022.
5. Smil, V. Who Will Feed China? *China Q.* **1995**, *143*, 801–813. [CrossRef]
6. Liu, J.; Lu, X.S. *Study on Sustainable Development Strategy of China: Sustainable Utilization of Land Resource*; China Agricultural Press: Beijing, China, 2001.
7. da Silva, G.F.; Calonego, J.C.; Luperini, B.C.O.; Chamma, L.; Alves, E.R.; Rodrigues, S.A.; Putti, F.F.; da Silva, V.M.; de Almeida Silva, M. Soil—Plant Relationships in Soybean Cultivated under Conventional Tillage and Long-Term No-Tillage. *Agronomy* **2022**, *12*, 697. [CrossRef]
8. Basamba, T.A.; Amézquita, E.; Singh, B.R.; Rao, I.M. Effects of tillage systems on soil physical properties, root distribution and maize yield on a Colombian acid-savanna Oxisol. *Acta Agric. Scand.* **2006**, *56*, 255–262. [CrossRef]
9. Lal, R. Residue management, conservation tillage and soil restoration for mitigating greenhouse effect by CO_2 enrichment. *Soil Tillage Res.* **1997**, *43*, 81107. [CrossRef]
10. Fabrizzi, K.P.; Garc, A.F.O.; Costa, J.L.; Picone, L.I. Soil water dynamics, physical properties and corn and wheat responses to minimum and no-tillage systems in the southern pampas of argentina. *Soil Tillage Res.* **2005**, *81*, 57–69. [CrossRef]
11. Bala, M.I.; Zakharchenko, E. Which ways of soil tillage are the best for crops? In Proceedings of the Scientific-Practical Conference II International Scientific and Theoretical Conference «Science of XXI Century: Development, Main Theories and Achievements», Helsinki, Finland, 24 June 2022; Volume 1, pp. 80–82.
12. Gebhardt, M.R.; Daniel, T.C.; Schweizer, E.E.; Allmaras, R.R. Conservation Tillage. *Science* **1985**, *230*, 625–630. [CrossRef]
13. Blevins, R.L.; Smith, M.S.; Thomas, G.W.; Frye, W.W. Influence of conservation tillage on soil properties. *J. Soil Water Conserv.* **1983**, *38*, 301–305.

14. Peigné, J.; Ball, B.C.; Roger-Estrade, J.; David, C. Is conservation tillage suitable for organic farming? A review. *Soil Use Manag.* **2007**, *23*, 129–144. [CrossRef]
15. Koller, K. Techniques of soil tillage. In *Soil Tillage in Agroeco-Systems*; El Titi, A., Ed.; CRC Press: Boca Raton, FL, USA, 2003; pp. 1–25.
16. Johnson, A.M.; Hoyt, G.D. Changes to the soil environment under conservation tillage. *HortTechnology* **1999**, *9*, 380–393. [CrossRef]
17. McVay, K.A.; Radcliffe, D.E.; Hargrove, W.L. Winter legume effects on soil properties and nitrogen fertilizer requirements. *Soil Sci. Soc. Amer. J.* **1989**, *53*, 1856–1862. [CrossRef]
18. Wilson, G.F.; Lal, R.; Okigbo, B.N. Effects of cover crops on soil structure and on yield of subsequent arable crops grown under strip tillage on an eroded alfisol. *Soil Tillage Res.* **1982**, *2*, 223–250. [CrossRef]
19. Frye, W.W.; Herbek, J.H.; Blevins, R.L. Legume cover crops in production of notillage corn. In *Environmentally Sound Agriculture: Selected Papers from the 4th International Conference of the International Federation of Organic Agriculture Movements*; Praeger Scientific: Cambridge, MA, USA, 1982; pp. 179–191.
20. Aziz, I.; Mahmood, T.; Islam, K.R. Effect of long term no-till and conventional tillage practices on soil quality. *Soil Tillage Res.* **2013**, *131*, 28–35. [CrossRef]
21. Wang, W.; Yuan, J.; Gao, S.; Li, T.; Li, Y.; Vinay, N.; Mo, F.; Liao, Y.; Wen, X. Conservation tillage enhances crop productivity and decreases soil nitrogen losses in a rain-fed agroecosystem of the Loess Plateau, China. *J. Clean. Prod.* **2020**, *274*, 122854. [CrossRef]
22. Pires, L.F.; Borges JA, R.; Rosa, J.A.; Coope, M.; Heck, R.J.; Passoni, S.; Roque, W.L. Soil structure changes induced by tillage systems. *Soil Tillage Res.* **2017**, *165*, 66–79. [CrossRef]
23. Or, D.; Ghezzehei, T.A. Modeling post-tillage soil structural dynamics: A review. *Soil Tillage Res.* **2002**, *64*, 41–59. [CrossRef]
24. Vian, J.F.; Peigne, J.; Chaussod, R.; Roger-Estrade, J. Effects of four tillage systems on soil structure and soil microbial biomass in organic farming. *Soil Use Manag.* **2009**, *25*, 1–10. [CrossRef]
25. Parkhomenko, G.; Kambulov, S.; Olshevskaya, A.; Babadzhanyan, A.; Gucheva, N.; Mekhantseva, I. The tillage effect on the change of soil structure[C]//IOP Conference Series: Earth and Environmental Science. *IOP Publ.* **2019**, *403*, 012144.
26. Liu, Z.; Cao, S.; Sun, Z.; Wang, H.; Qu, S.; Lei, N.; He, J.; Dong, Q. Tillage effects on soil properties and crop yield after land reclamation. *Sci. Rep.* **2021**, *11*, 4611. [CrossRef] [PubMed]
27. Baker, J.L.; Johnson, H.P. The effect of tillage systems on pesticide in runoff from small watersheds. *Trans. ASAE* **1979**, *22*, 554–559. [CrossRef]
28. Ferreras, L.; Costa, J.; Garcia, F.; Pecorari, C. Effect of no-tillage on some soil physical properties of a structural degraded Petrocalcic Paleudoll of the southern "Pampa" of Argentina. *Soil Tillage Res.* **2000**, *54*, 31–39. [CrossRef]
29. Abascal, S.A.; Buschiazzo, D.E. Competition between wheat and weeds in two tillage and fertilization systems in the central pampas of argentina. *Agrochim. Pisa* **2005**, *49*, 1–9.
30. Zhang, Y.; Tan, C.; Wang, R.; Li, J.; Wang, X. Conservation tillage rotation enhanced soil structure and soil nutrients in long-term dryland agriculture. *Eur. J. Agron.* **2021**, *131*, 126379. [CrossRef]
31. Lal, R. Tillage and agricultural sustainability. *Soil Tillage Res.* **1991**, *20*, 133–146. [CrossRef]
32. McGarry, D. Tillage and soil compaction. In *Conservation Agriculture*; Springer: Dordrecht, The Netherlands, 2003; pp. 307–316.
33. Maurya, P.R.; Lal, R. Effects of no-tillage and ploughing on roots of maize and leguminous crops. *Exp. Agric.* **1980**, *16*, 185–193. [CrossRef]
34. Dal Ferro, N.; Sartori, L.; Simonetti, G.; Berti, A.; Morari, F. Soil macro-and microstructure as affected by different tillage systems and their effects on maize root growth. *Soil Tillage Res.* **2014**, *140*, 55–65. [CrossRef]
35. Lipiec, J.; Horn, R.; Pietrusiewicz, J.; Siczek, A. Effects of soil compaction on root elongation and anatomy of different cereal plant species. *Soil Tillage Res.* **2012**, *121*, 74–81. [CrossRef]
36. Guan, D.; Al-Kaisi, M.M.; Zhang, Y.; Duan, L.; Tan, W.; Zhang, M.; Li, Z. Tillage practices affect biomass and grain yield through regulating root growth, root-bleeding sap and nutrients uptake in summer maize. *Field Crop. Res.* **2014**, *157*, 89–97. [CrossRef]
37. Feng, X.; Hao, Y.; Latifmanesh, H.; Rattan, L.; Cao, T.; Guo, J.; Deng, A.; Song, Z.; Zhang, W. Effects of subsoiling tillage on soil properties, maize root distribution, and grain yield on mollisols of Northeastern China. *Agron. J.* **2018**, *110*, 1607–1615. [CrossRef]
38. Himmelbauer, M.L.; Sobotik, M.; Loiskandl, W. No-tillage farming, soil fertility and maize root growth. *Arch. Agron. Soil Sci.* **2012**, *58* (Suppl. 1), S151–S157. [CrossRef]
39. Zhang, Z.; Yan, L.; Wang, Y.; Ruan, R.; Xiong, P.; Peng, X.H. Bio-tillage improves soil physical properties and maize growth in a compacted Vertisol by cover crops. *Soil Sci. Soc. Am. J.* **2022**, *86*, 324–337. [CrossRef]
40. Farahani, E.; Emami, H.; Forouhar, M. Effects of tillage systems on soil organic carbon and some soil physical properties. *Land. Degrad. Dev.* **2022**, *33*, 1307–1320. [CrossRef]
41. Bhuyan, S.I.; Chakma, B.; Laskar, I. Degradation of soil physical properties due to modernization of tillage techniques: A recent man made crisis to agro-ecology in North East India. *Proc. Int. Acad. Ecol. Environ. Sci.* **2022**, *12*, 113–119.
42. Lv, L.; Gao, Z.; Liao, K.; Zhu, Q.; Zhu, J.J. Impact of conservation tillage on the distribution of soil nutrients with depth. *Soil Tillage Res.* **2023**, *225*, 105527. [CrossRef]
43. Kumar, R.; Kumar, P. Reducing and eliminating tillage in order to promote sustainable agriculture. *He Pharma Innov. J.* **2022**, *SP-11*, 183–188.
44. Upa, J. The effect of previous crop soil cultivation on the yield of grain maize and winter wheat in the drier area of southern moravia. *Rostl. Vyrob.* **2000**, *46*, 113–117.

45. Chen, S.; Yang, P.; Zhang, Y.; Dong, W.; Hu, C.; Oenema, O. Responses of cereal yields and soil carbon sequestration to four long-term tillage practices in the North China plain. *Agronomy* **2022**, *12*, 176. [CrossRef]
46. Wang, Z.; Li, S.; Vera, C.L.; Malhi, S.S. Effects of water deficit and supplemental irrigation on winter wheat growth, grain yield and quality, nutrient uptake, and residual mineral nitrogen in soil. *Commun. Soil Sci. Plant Anal.* **2015**, *36*, 1405–1419. [CrossRef]
47. Cai, L.; Guo, Z.; Zhang, J.; Liu, X. No tillage and residue mulching method on bacterial community diversity regulation in a black soil region of Northeastern China. *PLoS ONE* **2021**, *16*, e0256970. [CrossRef] [PubMed]
48. Strudley, M.W.; Green, T.R.; James, I.I. Tillage effects on soil hydraulic properties in space and time: State of the science. *Soil Tillage Res.* **2008**, *99*, 4–48. [CrossRef]
49. Hill, R.L.; Cruse, R.M. Tillage effects on bulk density and soil strength of two Mollisols. *Soil Sci. Soc. Am. J.* **1985**, *49*, 1270–1273. [CrossRef]
50. Logsdon, S.D.; Karlen, D.L. Bulk density as a soil quality indicator during conversion to no-tillage. *Soil Tillage Res.* **2004**, *78*, 143–149. [CrossRef]
51. Anderson, E.L. Corn root growth and distribution as influenced by tillage and nitrogen fertilization. *Agron. J.* **1987**, *79*, 544–549. [CrossRef]
52. Barber, S.A. Effect of tillage practice on corn (*Zea mays* L.) root distribution and morphology. *Agron. J.* **1971**, *63*, 724–726. [CrossRef]
53. Qin, R.; Noulas, C.; Herrera, J.M. Morphology and distribution of wheat and maize roots as affected by tillage systems and soil physical parameters in temperate climates: An overview. *Arch. Agron. Soil Sci.* **2018**, *64*, 747–762. [CrossRef]
54. Mosaddeghi, M.R.; Mahboubi, A.A.; Safadoust, A. Short-term effects of tillage and manure on some soil physical properties and maize root growth in a sandy loam soil in western Iran. *Soil Tillage Res.* **2009**, *104*, 173–179. [CrossRef]
55. Ji, B.; Zhao, Y.; Mu, X.; Liu, K.; Li, C. Effects of tillage on soil physical properties and root growth of maize in loam and clay in central China. *Plant Soil Environ.* **2013**, *59*, 295–302. [CrossRef]
56. Thierfelder, C.; Matemba-Mutasa, R.; Rusinamhodzi, L. Yield response of maize (*Zea mays* L.) to conservation agriculture cropping system in Southern Africa. *Soil Tillage Res.* **2015**, *146*, 230–242. [CrossRef]
57. Rashidi, M.; Keshavarzpour, F. Effect of different tillage methods on grain yield and yield components of maize (*Zea mays* L.). *Int. J. Agric. Biol.* **2007**, *9*, 274–277.
58. Aikins, S.H.M.; Afuakwa, J.J.; Owusu-Akuoko, O. Effect of four different tillage practices on maize performance under rain-fed conditions. *Agric. Biol. J. N. Am.* **2012**, *3*, 25–30. [CrossRef]
59. Hussain, I.; Olson, K.R.; Ebelhar, S.A. Impacts of tillage and no-till on production of maize and soybean on an eroded Illinois silt loam Soil. *Soil Tillage Res.* **1999**, *52*, 37–49. [CrossRef]
60. Khurshid, K.; Iqbal, M.; Arif, M.S.; Nawaz, A. Effect of tillage and mulch on soil physical properties and growth of maize. *Int. J. Agric. Biol.* **2006**, *8*, 593–596.
61. Kladivko, E.J. Tillage systems and soil ecology. *Soil Tillage Res.* **2001**, *61*, 61–76. [CrossRef]
62. Grewal, K.S.; Singh, D.; Mehta, S.C.; Singh, Y.P.; Kuhad, M.S. Effect of long-term fertilizer application on crop yields, nutrient uptake and available soil nutrients under different cropping sequences. *Crop Res.* **2000**, *20*, 426–436.
63. Haruna, S.I.; Anderson, S.H.; Udawatta, R.P.; Glark, J.J.; Phillips, N.C.; Cui, S.; Gao, Y. Improving soil physical properties through the use of cover crops: A review. *Agrosystems Geosci. Environ.* **2020**, *3*, e20105. [CrossRef]
64. Comegna, V.; Ruggiero, C.; Amato, M.; D'Anna, F.; Sommella, A.; Santini, A. Physical and hydrophysical properties of a vertic ustorthents soil of southern italy as affected by some cultivation systems. *Agric. Mediterr.* **1990**, *120*, 159–169.
65. Haynes, R.J.; Naidu, R. Influence of lime, fertilizer and manure applications on soil organic matter content and soil physical conditions: A review. *Nutr. Cycl. Agroecosystems* **1998**, *51*, 123–137. [CrossRef]
66. Toor, M.D.; Adnan, M.; Rehman, F.U.; Tahir, R.; Pareek, V. Nutrients and their importance in agriculture crop production: A review. *Ind. J. Pure App. Biosci.* **2021**, *9*, 1–6. [CrossRef]
67. Boincean, B.; Dent, D. Crop rotation. In *Farming the Black Earth*; Springer: Cham, Switzerland, 2019; pp. 89–124.
68. Malobane, M.E.; Nciizah, A.D.; Mudau, F.N.; Wakindiki, I.I.C. Tillage, crop rotation and crop residue management effects on nutrient availability in a sweet sorghum-based cropping system in marginal soils of South Africa. *Agronomy* **2020**, *10*, 776. [CrossRef]
69. Busari, M.A.; Kukal, S.S.; Kaur, A.; Bhatt, R.; Dulazi, A.A. Conservation tillage impacts on soil, crop and the environment. *Int. Soil Water Conserv. Res.* **2015**, *3*, 119–129. [CrossRef]
70. Karlen, D.L.; Hurley, E.; Andrews, S.; Cambardella, C.; Meek, M.; Duffy, M. Crop rotation effects on soil quality at three northern corn/soybean locations. *Staff. Gen. Res. Pap. Arch.* **2006**, *6*, 1–6. [CrossRef]
71. Li, F.R.; Zhao, W.Z.; Liu, J.L.; Huang, Z.G. Degraded vegetation and wind erosion influence soil carbon, nitrogen and phosphorus accumulation in sandy grasslands. *Plant Soil* **2009**, *317*, 79. [CrossRef]
72. Kaspar, T.C.; Singer, J.W. The Use of Cover Crops to Manage Soil. In *Soil Management: Building a Stable Base for Agriculture*; American Society of Agronomy, Soil Science Society of America: Madison, WI, USA, 2011; pp. 321–337.
73. Haruna, S.I.; Nkongolo, N.V. Influence of cover crop, tillage, and crop rotation management on soil nutrients. *Agriculture* **2020**, *10*, 225. [CrossRef]
74. Ruffo, M.L.; Bollero, G.A. Modeling rye and hairy vetch residue decomposition as a function of degree days and decomposition days. *Agron. J.* **2020**, *95*, 900–907. [CrossRef]
75. Smith, M.S.; Frye, W.W.; Varco, J.J. Legume winter cover crops. *Adv. Soil Sci.* **1987**, *7*, 95–139.

76. Yang, J.; Zhang, H.; Zhang, J. Root morphology and physiology in relation to the yield formation of rice. *J. Integr. Agric.* **2012**, *11*, 920–926. [CrossRef]
77. Richner, W.; Liedgens, M.; Bürgi, H.; Soldati, A.; Stamp, P. Root image analysis and interpretation. In *Root Methods*; Springer: Berlin/Heidelberg, Germany, 2000; pp. 305–341.
78. Ghuman, B.S.; Sur, H.S. Tillage and residue management effects on soil properties and yields of rainfed maize and wheat in a subhumid subtropical climate. *Soil Tillage Res.* **2001**, *58*, 1–10. [CrossRef]
79. Chassot, A. *Early Growth of Roots and Shoots of Maize as Affected by Tillage-Induced Changes in Soil Physical Properties*; ETH Zurich: Zürich, Switzerland, 2000.
80. Ren, B.; Li, X.; Dong, S.; Liu, P.; Zhao, B.; Zhang, J.W. Soil physical properties and maize root growth under different tillage systems in the North China Plain. *Crop J.* **2018**, *6*, 669–676. [CrossRef]
81. Anderson, E.L. Tillage and N fertilization effects on maize root growth and root: Shoot ratio. *Plant Soil* **1988**, *108*, 245–251. [CrossRef]
82. Cai, H.; Ma, W.; Zhang, X.; Ping, J.Q.; Yan, X.G.; Liu, J.Z.; Yuan, J.C.; Wang, L.C.; Ren, J. Effect of subsoil tillage depth on nutrient accumulation, root distribution, and grain yield in spring maize. *Crop J.* **2014**, *2*, 297–307. [CrossRef]
83. DeFelice, M.S.; Carter, P.R.; Mitchell, S.B. Influence of tillage on corn and soybean yield in the United States and Canada. *Crop Manag.* **2006**, *5*, 1–17. [CrossRef]
84. Raimbault, B.A.; Vyn, T.J. Crop rotation and tillage effects on corn growth and soil structural stability. *Agron. J.* **1991**, *83*, 979–985. [CrossRef]
85. Miao, F.; Li, Y.; Cui, S.; Jagadamma, S.; Yang, G. Soil extracellular enzyme activities under long-term fertilization management in the croplands of China: A meta-analysis. *Nutr. Cycl. Agroecosystem* **2019**, *114*, 125–138. [CrossRef]

land

MDPI

Review

Advancements in Biochar Modification for Enhanced Phosphorus Utilization in Agriculture

Nazir Ahmed [1,†], Lifang Deng [2,†], Chuan Wang [1], Zia-ul-Hassan Shah [3], Lansheng Deng [4], Yongquan Li [1], Juan Li [1], Sadaruddin Chachar [1], Zaid Chachar [5], Faisal Hayat [1], Bilquees Bozdar [3], Filza Ansari [3], Rashid Ali [3], Lin Gong [6] and Panfeng Tu [1,*]

[1] College of Horticulture and Landscape Architecture, Zhongkai University of Agriculture and Engineering, Guangzhou 510550, China; nachachar@sau.edu.pk (N.A.); wangcquanquan@163.com (C.W.); yongquanli@zhku.edu.cn (Y.L.); 13751774213@139.com (J.L.); schachar@sau.edu.pk (S.C.); maken_faisal@yahoo.com (F.H.)
[2] Institute of Biomass Engineering, South China Agricultural University, Guangzhou 510642, China; nannandeng@163.com
[3] Faculty of Crop Production, Sindh Agriculture University, Tandojam 70060, Pakistan; zhnshah@sau.edu.pk (Z.H.S.); 2k19-pd-95@student.sau.edu.pk (B.B.); 2k19-pd-122@student.sau.edu.pk (F.A.); 2k19-pd-286@student.sau.edu.pk (R.A.)
[4] College of Natural Resources and Environment, South China Agricultural University, Guangzhou 510642, China; lshdeng@scau.edu.cn
[5] College of Agriculture and Biology, Zhongkai University of Agriculture and Engineering, Guangzhou 510550, China; zs.chachar@gmail.com
[6] Dongguan Yixiang Liquid Fertilizer Co., Ltd., Dongguan 523135, China; gonglin111@126.com
* Correspondence: tupanfeng@163.com
† These authors contributed equally to this work.

Abstract: The role of modified biochar in enhancing phosphorus (P) availability is gaining attention as an environmentally friendly approach to address soil P deficiency, a global agricultural challenge. Traditional phosphatic fertilizers, while essential for crop yield, are costly and environmentally detrimental owing to P fixation and leaching. Modified biochar presents a promising alternative with improved properties such as increased porosity, surface area, and cation exchange capacity. This review delves into the variability of biochar properties based on source and production methods and how these can be optimized for effective P adsorption. By adjusting properties such as pH levels and functional groups to align with the phosphate's zero point of charge, we enhance biochar's ability to adsorb and retain P, thereby increasing its bioavailability to plants. The integration of nanotechnology and advanced characterization techniques aids in understanding the structural nuances of biochar and its interactions with phosphorus. This approach offers multiple benefits: it enables farmers to use phosphorus more efficiently, reducing the need for traditional fertilizers and thereby minimizing environmental impacts, such as greenhouse gas emissions and P leaching. This review also identifies existing research gaps and future opportunities for further biochar modifications. These findings emphasize the significant potential of modified biochar in sustainable agriculture.

Keywords: nutrient management; agro-sustainability; engineered biochar; feedstock variability; nanotechnology; characterization; artificial intelligence

Citation: Ahmed, N.; Deng, L.; Wang, C.; Shah, Z.-u.-H.; Deng, L.; Li, Y.; Li, J.; Chachar, S.; Chachar, Z.; Hayat, F.; et al. Advancements in Biochar Modification for Enhanced Phosphorus Utilization in Agriculture. *Land* **2024**, *13*, 644. https://doi.org/10.3390/land13050644

Academic Editor: Claude Hammecker

Received: 30 March 2024
Revised: 1 May 2024
Accepted: 7 May 2024
Published: 9 May 2024

1. Introduction

1.1. Background

Phosphorus (P) is universally recognized as an essential macronutrient vital for plant growth and development. Its role in various plant physiological processes, such as energy transfer, photosynthesis, and nucleic acid synthesis, is well documented [1]. It also plays a pivotal role in plant food production, as it forms a fundamental component of plant DNA, RNA, and ATP and participates in critical biochemical processes vital for plant

development and reproduction [2,3]. The significance of P in agriculture can be traced back to ancient farming practices. Animal bones, rich in P, were incorporated into the soil to bolster crop yields, thereby highlighting the vital role of P in soil fertility and plant growth. Over time, methods for enhancing soil with P have diversified. Before the late 19th century, P sources such as urine, animal manure, human excreta, bone ash, and guano (seabird droppings) were extensively utilized. Today, wastewater treatment plants and animal farms are major contributors to the production of nutrient-rich materials, including sewage sludge, effluent, manure, and animal slaughter by-products like meat and bone meal, all rich in P [4].

The global population is projected to reach 9.7 billion by 2050, placing significant pressure on agriculture to enhance productivity while ensuring food security within the constraints of limited arable land. Efficient fertilizer utilization is paramount in this context. However, the economic efficiency of mineral fertilizers has declined owing to rising prices, sometimes surpassing the cost of food production. Agriculture also faces challenges posed by global climate change driven by greenhouse gas (GHG) emissions. Finite geological resources for manufacturing fertilizers and market fluctuations in fertilizer minerals intensify competition and jeopardize food security [5]. Notably, the finite geological reserves of phosphate rock, the primary source of P fertilizer, are not considered in agricultural practices or global trade, presenting a short-sighted approach. However, phosphate rock mining underpins modern agriculture, supporting the boom in human population prosperity [6].

In modern agriculture, the reliance on phosphate fertilizers sourced from depleting non-renewable phosphate rock reserves is intensifying alongside the rapidly increasing global food demand (Figure 1). This highlights the urgent need for sustainable phosphorus (P) management strategies [6]. The direct application of P to soils often results in its fixation, primarily through chemical interactions with soil minerals like iron and aluminum oxides in acidic conditions or with calcium in alkaline soils, forming insoluble compounds that limit its availability to plants [2,7]. Such fixation reduces the efficiency of fertilizers by immobilizing a significant portion of P, making it inaccessible to plants [8] and contributing to environmental degradation. Persistent use of P-enriched fertilizers and manure leads to P accumulation in soils, which, through erosion and leaching, can affect aquatic ecosystems by promoting eutrophication [9]. Moreover, the inefficiency in P use raises concerns about the future scarcity of this finite resource [10]. Given these challenges, developing innovative strategies to enhance P availability in soils is imperative, ensuring both agricultural productivity and environmental sustainability.

1.2. P Dynamics in Soils

As illustrated in Figure 2, P dynamics in soils underscores its integral role in plant nutrition and broader agricultural sustainability. The P cycle is a complex interplay of biogeochemical processes that regulate the movement, transformation, and availability of P in terrestrial ecosystems [7]. The cycle begins by weathering primary minerals, such as apatite, releasing P into the soil system. Once present in soil, P can undergo various transformations. It can be absorbed by plants primarily as orthophosphate ions, either as $H_2PO_4^-$ in acidic soils or as HPO_4^{2-} in alkaline conditions [8]. This soil solution P serves as the direct source for plant uptake, as its reverted or fixed forms are not as accessible. However, P is not only statically held in the soil. It interacts dynamically with both organic and inorganic matter. Soil microorganisms play a role in the mineralization of organic P, converting it into inorganic forms that plants can utilize [11].

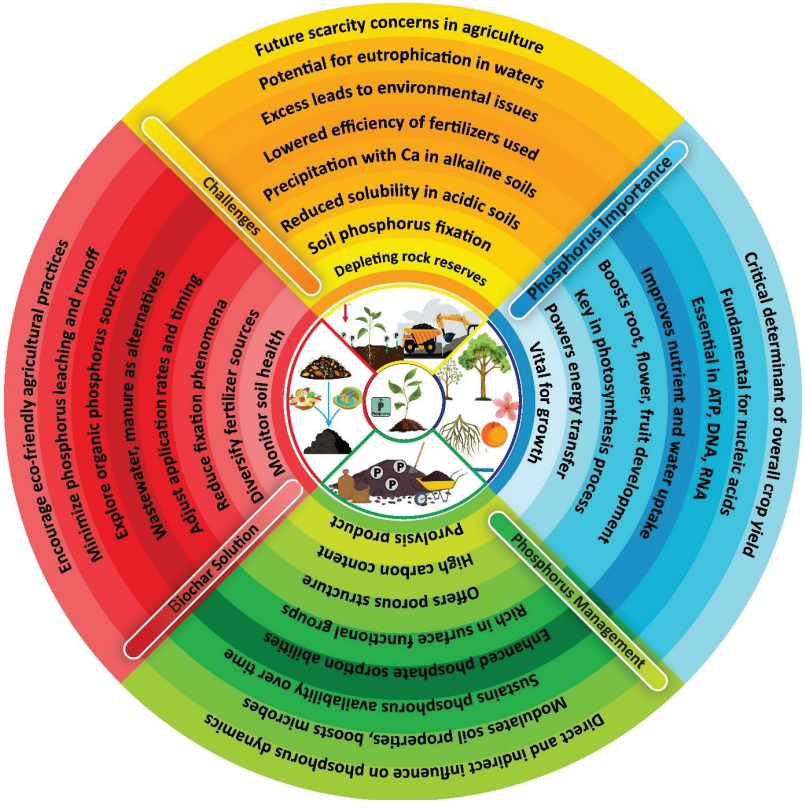

Figure 1. P in agriculture: its role, challenges in soil fixation, management strategies, and the potential of biochar.

Conversely, immobilization causes plants and microbes to take up inorganic P, converting it into organic form. Additionally, various reactions such as adsorption, desorption, dissolution, and precipitation determine the concentration of P ions in the soil solution. A significant consideration in the P-cycle is the potential for loss. Soil erosion and runoff can carry away both particulate and soluble forms of P, which can lead to aquatic eutrophication if they enter water bodies [12]. Leaching is another pathway through which soluble P might move to deeper soil layers or groundwater, rendering it unavailable to plants [13]. To counterbalance these losses and maintain soil P levels, external inputs such as compost, manure, biosolids, phosphatic fertilizers, and biochar are often incorporated [10,14]. These inputs undergo transformations, further contributing to the dynamic nature of the P cycle. Hence, adequate P availability in the soil solution must be ensured to achieve economically optimal crop yields.

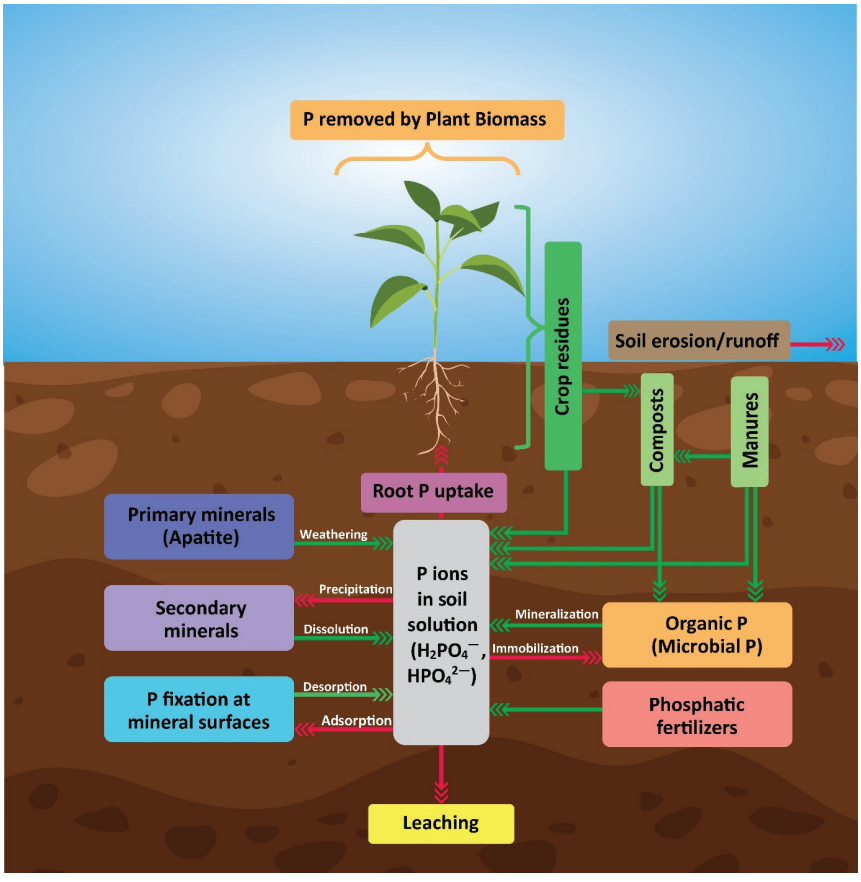

Figure 2. P dynamics in soils: a comprehensive depiction of sources, transformations, and losses that govern the availability and movement of P in terrestrial ecosystems.

1.3. Overview of Biochar and Its Role in P Management

Biochar is derived from the pyrolysis of organic materials in oxygen-limited environments. During the last few years, research on biochar has gained significant momentum in both environmental and agricultural research (Figure 1). This carbon-rich product is distinguished by its high carbon content, abundant surface functional groups, and porous structure, making it a versatile candidate for various applications [15,16]. Moreover, the potential of biochar to revolutionize P management in agriculture has come to the forefront. This versatile soil amendment possesses intrinsic properties that make it a unique solution for addressing the challenges of soil P fixation. Its highly porous structure and significant surface area, coupled with the presence of functional groups, enable biochar to effectively adsorb P [10,17,18]. Although unmodified biochar generally has low phosphate sorption capacity, mineral-rich biochar is an exception. Engineered biochar, modified with various elements, features enhanced surface characteristics such as charge, surface area, pore volume, and functionality. These modifications significantly boost its phosphate sorption capacities, turning biochar into an effective reservoir for adsorbed phosphorus, thereby ensuring prolonged availability to plants [13,17]. Additionally, certain biochars can be tailored to achieve a slow-release pattern of P, providing a sustainable source of P for plant growth [19]. The continued emphasis on research in this area underscores the potential of biochar as a sustainable solution to contemporary environmental challenges.

Furthermore, the influence of biochar on P dynamics extends beyond that of direct adsorption. It indirectly affects soil ecosystems by improving soil structure, water retention, and microbial communities (Figure 1). These enhancements foster plant nutrient uptake, increase soil nutrient availability, and promote microbial activity that assists P solubilization [20,21]. However, the efficacy of biochar as a P management tool is influenced by factors such as feedstock, pyrolysis conditions, and post-production modifications, which can significantly alter its characteristics and, consequently, its P adsorption capacity. Biochar has emerged as a pivotal solution to counter P fixation challenges in agriculture. Owing to its versatile attributes, including P adsorption, soil condition enhancement, and facilitation of microbial interactions, biochar is a potent resource for optimizing P use and reducing environmental implications. The purpose of this article is to comprehensively review recent advancements in biochar modifications aimed at enhancing phosphorus utilization in agriculture, identify the existing gaps in the research, and suggest directions for future studies.

2. Phosphorus Fixation Challenges and Impacts

2.1. Significance of Phosphorus in Crop Nutrition

P is an essential macronutrient for plant growth and development. It plays pivotal roles in various physiological processes, including photosynthesis, respiration, protein synthesis, nucleic acid formation, and energy transfer [1,2]. It is also considered integral to ATP production, which is the primary cellular energy source [22]. In addition, they contribute to the formation of phospholipids, which are essential components of cell membranes that serve as sensory interfaces and in metabolic processes [23]. The role of P in crop nutrition extends to root development, flowering, and fruiting. Adequate P levels support robust root systems, improving nutrient and water uptake [24]. Moreover, it is critical for flower and seed production during the reproductive phase and ultimately influences crop yield [25]. Despite its importance, P is often present in the soil in forms that are inaccessible to plants owing to fixation processes [7]. This limitation can lead to P deficiency in crops, resulting in stunted growth and reduced yield.

2.2. Detrimental Effects of P Fixation

P fixation in soil presents multifaceted challenges for sustainable agriculture, encompassing economic and environmental implications (Figure 1). Reduced crop productivity due to P deficiency resulting from fixation leads to stunted growth, decreased flowering, and yield decline, causing financial losses to farmers despite increased fertilizer use [26]. The economic repercussions are exacerbated by the necessity for increased fertilizer application rates to counteract P fixation, culminating in heightened farming expenditures devoid of guaranteed commensurate yield enhancements. These augmented agricultural costs place a substantial burden on farmers, primarily stemming from the escalated expenses incurred by intensified fertilizer utilization to combat P fixation. Consequently, these elevated costs pose a significant threat to the sustainability of farming operations, a concern that is particularly acute for smallholder farmers [27,28].

P fixation has profound environmental implications, notably leading to environmental degradation. It gives rise to the runoff of P into freshwater bodies, ultimately resulting in water pollution and eutrophication, thereby jeopardizing aquatic ecosystems. The excessive use of P fertilizers in response to fixation can exacerbate nutrient runoff into freshwater bodies, intensifying eutrophication, characterized by oxygen depletion, proliferation of harmful algal blooms, and loss of aquatic life [9,29]. Moreover, the production and transport of P fertilizers are associated with greenhouse gas emissions, intensifying the contribution of agriculture to global warming [9,30]. Unsustainable resource use is another outcome of P fixation. As the global reserves of rock phosphate, a primary P fertilizer source, are depleted, optimizing P use in agriculture is imperative. P fixation reduces the efficiency of applied P, necessitating more resource extraction to meet agricultural demands [10]. The degradation of soil health is a significant concern associated with P fixation. Continuous

P fertilizer application can disrupt soil microbial communities, reduce organic matter, and create secondary nutrient imbalances, ultimately compromising both soil health and productivity [29,31,32]. Addressing P fixation is imperative because these changes can degrade soil health over time, affecting resilience and overall capacity to sustain crops and ecosystems. It is essential not only to enhance crop productivity but also to mitigate its far-reaching economic, environmental, and sustainability challenges.

3. Role of Biochar in P Adsorption

3.1. Basic Mechanism of P Adsorption by Biochar

Biochar, which originates from the pyrolysis of organic materials in an oxygen-limited environment, has rapidly gained attention in the agricultural realm, particularly for its capacity to enhance soil fertility and mitigate P fixation. Understanding the mechanisms underpinning the ability of biochar to adsorb P provides insights into its multifaceted benefits and the means to tailor its production for specific agricultural needs. The fundamental mechanisms governing the capacity of biochar to adsorb P are based on its physicochemical attributes. The porous structure, extensive surface area, abundant surface groups, and mineral content of biochar play pivotal roles in its P adsorption capability [1]. The porous structure of biochar, characterized by its intricate network of pores, provides numerous sites for P adsorption, effectively capturing soluble P from soil solutions and preventing its loss or fixation. Additionally, the surface chemistry of biochar, enriched with diverse functional groups such as hydroxyl, carboxyl, and phenolic groups, actively interacts with P to form complexes that facilitate P adhesion to the biochar surface. Electrostatic interactions further enhance this process. Biochar surfaces often carry a negative charge, which attracts positively charged P species, such as $H_2PO_4^-$ and HPO_4^{2-} [33]. This electrostatic attraction facilitates the adsorption of P onto the biochar surface.

The ability of biochar to modulate soil pH, particularly in acidic soils, contributes to P availability. By increasing the soil pH to an optimal range, biochar enhances P solubility and reduces the risk of soils [34]. Ligand exchange is another significant mechanism of P adsorption, especially for biochars that undergo post-pyrolysis modifications to introduce or enhance specific surface functionalities [34]. This process involves the substitution of other ions with P ions on the biochar surface, thereby contributing to P retention (Figure 3). Furthermore, biochar has the potential to serve as a slow-release fertilizer, gradually releasing adsorbed P over time [35]. This controlled release benefits plant growth while minimizing P runoff into water bodies [33]. In addition to its role in P adsorption, biochar can effectively address soil acidity issues and improve soil health and fertility. Various types of biochar, enriched with minerals and produced at different temperatures, have been found to increase soil pH and basic cation retention, thereby promoting plant growth and yield [34]. Diverse biochar applications have been extended to the removal and recovery of P from aquatic environments, thereby contributing to eutrophication control and sustainable P reuse in agriculture. Modified biochars have demonstrated high P adsorption capacities, effectively reducing total P concentrations in water bodies and inhibiting algal growth [12]. Overall, biochar's multifaceted properties and mechanisms make it a valuable tool for managing P in agriculture, enhancing soil fertility, and mitigating the detrimental effects of P fixation.

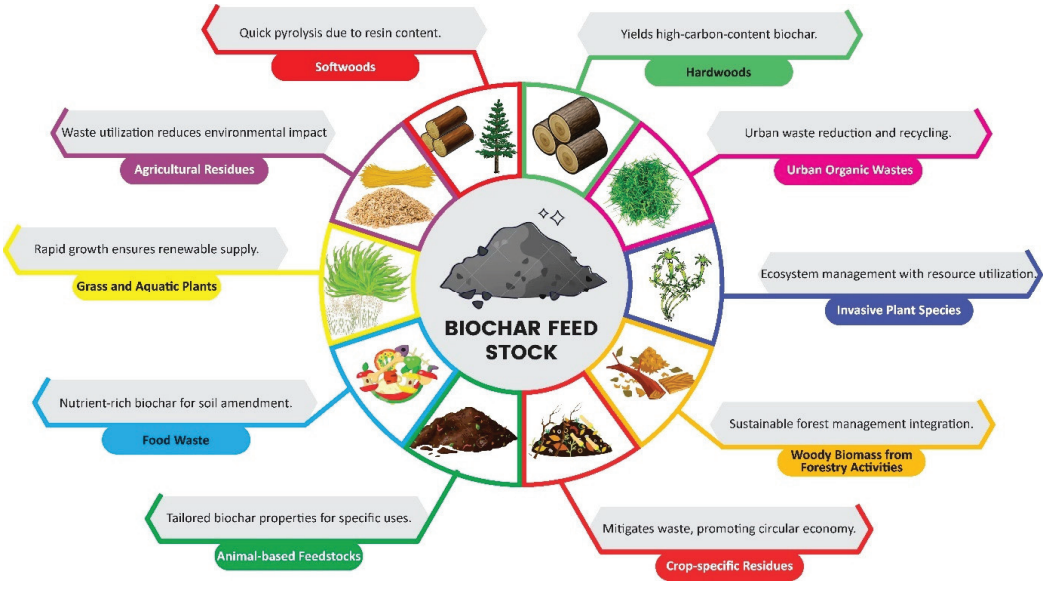

Figure 3. A visual representation of the diverse feedstocks and their unique contributions to environmentally beneficial and economically viable biochar sourcing.

3.2. Factors Influencing Adsorption and Desorption

Understanding biochar's adsorption and desorption mechanisms is essential for predicting its behavior in soil environments and optimizing its use in P management. Various factors play a role in determining the efficiency and reversibility of P binding to biochar surfaces [33,36].

Surface area and porosity: The micro-and mesoporosity of biochar significantly influence P adsorption. A higher surface area means more available sites for P to bind, with the pores acting as reservoirs, trapping P, and thereby modulating its availability to plants [1].

Surface functional groups: The chemisorption of P onto biochar is influenced by its functional groups, such as carboxylic (–COOH), hydroxyl (–OH), and phenolic (–ArOH) groups. These functional groups play pivotal roles in interactions with P ions, primarily through mechanisms such as ligand exchange and electrostatic attraction [1,37].

The pH of the system: The pH of the biochar and the surrounding environment plays a crucial role in adsorption. Typically, biochars are alkaline, making their surfaces negatively charged and thus facilitating the adsorption of positively charged ions such as Ca^{2+}, Mg^{2+}, K^{+}, and NH_{4+} [38]. Moreover, pH affects the dominant adsorption mechanism by influencing the P species and surface characteristics [1,39].

The presence of competing ions: Ions such as Cl^{-}, SO_4^{2-}, and HCO_3^{-} in contaminated water and soil can affect phosphate adsorption [40,41]. Moreover, ions such as Ca, Mg, and Al present in the soil can compete with P for available adsorption sites on biochar. These competing ions, especially SO_4^{2-} and HCO_3^{-}, can hinder the formation of calcium and magnesium phosphate, thereby affecting the adsorption efficiency [40].

Biochar mineral content: The mineral content of biochar, either inherent or introduced during pyrolysis, can aid in P adsorption. Minerals such as Ca, La, Fe, and Al can bond strongly with P, enhancing its retention capacity [42,43]. For example, biochar modified with Ca from oyster shells or La showed enhanced P adsorption capabilities over a broad pH range, demonstrating the significant influence of mineral content on the adsorption mechanism [43]. Moreover, research by Yang et al. [44] and Cui et al. [42] has emphasized that composite biochars impregnated with $FeCl_3$ or $MgCl_2$ can efficiently recover P from

wastewater. Their findings highlight the importance of mineral matching in biochar to optimize P recovery and reduce secondary pollution.

Temperature and contact time: Both the temperature of the system and the duration of contact of the biochar with P-rich solutions influence the adsorption kinetics. Elevated temperatures can accelerate adsorption, whereas extended contact times may saturate the adsorption sites [45,46].

Biochar properties are also influenced by factors such as the pyrolysis temperature and feedstock, which impact P adsorption. Utilizing biochar for P management offers ecological and agricultural benefits; however, its adsorption capabilities vary. Understanding these factors is crucial for tailoring applications to address the P challenges in agriculture and the environment.

4. Advancements in Biochar Preparation

4.1. Feedstock Variability in Biochar Production and Its Implications

The ability of biochar to adsorb P varies significantly depending on several key factors, including feedstock choice, pyrolysis conditions, and post-pyrolysis modifications. Biochar, with its distinct properties determined by feedstock and production parameters, is a multifunctional tool with the potential to reshape agricultural and environmental landscapes. Its efficacy in P adsorption and the attributes it brings into applications are deeply rooted in the type of feedstock utilized [1]. Historically rooted in a diverse array of biomass sources, ranging from animal residues to plant materials, biochar production has always been intertwined with the inherent characteristics of the chosen feedstock (Figure 3). Elements such as lignin and cellulose from these feedstocks play a pivotal role in determining the final attributes of biochar, such as surface properties and porosity [47]. For instance, hardwood-derived biochars, renowned for their high carbon content, offer enhanced soil stability and present an increased potential for long-term P retention [48].

On the other hand, biochars sourced from agricultural residues are often enriched with nutrients due to the nutrient-rich nature of the initial biomass, as indicated by Freitas et al. [14]. Notably, due to their inherent inorganic mineral content, certain feedstocks, such as rice husks and bones, pave the way for biochars with elevated P adsorption sites, optimizing their capacity to retain P [49]. In the modern context, the versatility of biochar is further demonstrated by studies such as that of Roberts et al. [50], which brought seaweed-derived biochar into the spotlight. These biochars, characterized by their low carbon yet rich essential trace element content, offer a pH spectrum from neutral to alkaline, showcasing their adaptability across varied soil types. Given the complex interplay between feedstock types and their resultant biochars, a comprehensive grasp of feedstock variability is crucial. Such an understanding aids in tailoring biochar applications, optimizing benefits, and truly harnessing its potential in both the agricultural and environmental domains.

4.2. Evolution of Pyrolysis Techniques and Their Influence on Biochar Production

Biochar, a carbon-rich product, is traditionally produced using various pyrolysis techniques. The transformation of organic materials through pyrolysis has evolved significantly, with the employed techniques profoundly affecting the properties of the resultant biochar (Table 1). Historically, biochar production has primarily relied on traditional kilns, such as simple earth mounds, pit kilns, and brick kilns, mainly used in rural areas [51]. While these kilns proved cost-effective for small-scale production, they faced challenges in terms of carbonization rate, quality, and yield and also had drawbacks related to pollution, labor intensity, and land costs. Considering the limitations of traditional kilns, innovations have led to the development of enhanced versions. These improved kilns retained the essential features of their predecessors but incorporated modifications to augment biochar yield and reduce environmental impacts, effectively bridging the gap between tradition and efficiency [51,52]. The rising scale and demand for biochar have paved the way for the advent of industrial production technologies. For large-scale operations, these systems emphasize product consistency and higher throughput. The challenges and global em-

phasis on sustainability have catalyzed the emergence of the newest pyrolysis systems, prioritizing high yields with reduced emissions. These state-of-the-art systems integrate the latest research and innovative methods, such as microwave pyrolysis, often leveraging specialized reactors for precision control. Their overarching goal is to harmoniously produce high-quality biochar while minimizing the environmental footprint and setting new standards in biochar production [53].

4.3. Advances in Pyrolysis Techniques

Pyrolysis, a notable thermochemical decomposition process, has been the focal point of research owing to its capability to convert organic materials into valuable products, primarily biochar [52]. The attributes of the resultant biochar, especially its P adsorption and desorption properties, are heavily influenced by various factors, such as the pyrolysis method employed, temperature, and residence time [54,55]. This transformation process plays an essential role in sustainable agricultural practices, particularly in efficiently managing P [56]. Among the various pyrolysis methodologies, slow pyrolysis has historically been significant. The favored method was characterized by extended residence times and temperatures ranging from 300 °C to 700 °C [57]. This method has traditionally been associated with producing biochar using basic systems such as earth mounds, pit kilns, and brick kilns, particularly in more rural settings [57]. Conversely, fast pyrolysis, characterized by elevated temperatures and rapid heating rates, took center stage, primarily producing bio-oil with biochar and syngas as secondary outputs [55].

Recent innovations have paved the way for developing more advanced pyrolysis techniques. Microwave pyrolysis is one such method that has gained traction owing to its energy efficiency and uniform heating. This approach has emerged as a favored choice for modular systems designed for efficient solid waste management [52]. Moreover, hydrothermal carbonization has been introduced to address the challenges of processing wet biomass. This technique yields hydrochars that possess a pronounced degree of carbonization compared to their counterparts derived from torrefaction, making them uniquely suitable for specific agricultural contexts [54]. Furthermore, there have been advancements beyond traditional pyrolysis. For instance, intermediate pyrolysis reactors, also referred to as converters, are being explored for the large-scale balanced production of char and bio-oil from forests and agricultural waste without the need for exhaustive preprocessing [52]. Additionally, torrefaction, another thermal treatment, augments the qualities of biomass and biochar, enhancing their fixed carbon content and energy density rendering them valuable for energy pursuits [54]. To further advance the potential of biochar, clay–biochar composites have been developed by integrating clay minerals during pyrolysis, resulting in products with superior cation exchange capacities and P retention, potentially elevating soil quality and nutrient management [58].

Elevated pyrolysis temperatures generally result in biochar with a greater surface area, porosity, and carbon content, all of which augment its P adsorption capacity [36]. However, excessively high temperatures can lead to the volatilization of essential nutrients, potentially limiting the nutrient supplementation capacity of biochar. However, they also result in reduced CEC and volatile matter due to the extensive decomposition of organic matter [47]. Such biochars, with larger surface areas, heightened porosities, and produced at higher temperatures, have properties that can notably improve P adsorption [36]. Despite high temperatures enhancing certain properties, they can also diminish the functional groups essential for P binding [45]. Thus, the quest to determine an optimal temperature to produce biochar tailored for specific applications remains at the forefront of many studies.

The residence time, categorized into slow and fast pyrolysis, is another decisive factor in determining biochar quality and yield. Characterized by temperatures ranging from 300 to 700 °C and longer residence times, slow pyrolysis predominantly produces biochar. These extended residence times can foster secondary reactions, refine the biochar structure, and influence its P retention potential [59]. This method is favorable when producing higher biochar outputs that excel in P adsorption, as demonstrated by Tenic et al. [55]. In contrast,

fast pyrolysis, with its short residence times and elevated temperatures, is geared towards maximizing bio-oil production, relegating biochar to a secondary product [53]. Biochars derived from slow pyrolysis typically exhibit a high fixed carbon content, suggesting superior stability and microbial decomposition resistance. Such biochars, especially those sourced from lignin-rich feedstocks, have been highlighted for their enhanced P adsorption capacities, implying their suitability for long-term environmental applications [53,60]. Drawing from research findings, it is evident that pyrolysis temperature and residence time, particularly in slow pyrolysis, play a central role in determining the P adsorption and desorption attributes of biochar. The choice of these production parameters significantly shapes the physicochemical properties of biochar. Additionally, sourcing biochar from P-rich feedstocks accentuates its critical role in the ecological P cycle. Mastering these production nuances ensures that biochar remains a pivotal tool for sustainable P management.

Table 1. Comparison of traditional and modified biochar characteristics.

Property/ Characteristic	Traditional Biochar	Modified Biochar	Impact on P Adsorption	P Adsorption by Modified Biochar	Experimental Conditions	References
Porosity	Low to moderate	Enhanced, due to specific modification techniques	Higher porosity can increase the surface area available for P adsorption	620 mg g^{-1}	Phosphate solutions	[61,62]
Surface Area (m^2/g)	Typically <300	Can exceed 1000, depending on the modification technique	A larger surface area provides more adsorption sites, increasing P retention	10.4 mg g^{-1}	P-containing wastewater	[63,64]
pH	Generally alkaline, but variable (6–9)	Can be fine-tuned to desired values using specific precursors or post-treatment methods	pH close to phosphate's zero point of charge (pH_zpc) can enhance P adsorption	95.2 mg g^{-1}	River sediment-water	[12,61]
Cation Exchange Capacity (CEC)	Moderate	Enhanced due to the addition of functional groups or mineral phases	Higher CEC can lead to better P retention by promoting ion exchange	28–29 mg g^{-1}	Phosphate solutions	[65]
Presence of Functional Groups	Limited presence of hydroxyl, carboxyl, and phenolic groups	Enriched with specific functional groups post-modification	Functional groups play a crucial role in P binding, especially hydroxyl groups	24.7 mg g^{-1}	Phosphate solutions	[35]
Stability in Soil	Moderate	Enhanced, especially if cross-linked or treated with minerals	Stable biochars persist longer in soil, providing sustained P management	Reduced P runoff from soil; greater microaggregate stability.	Temperate Agricultural Soil	[66]
Hydrophobicity	Often high due to carbon-rich nature	Can be adjusted using post-treatments	Lower hydrophobicity may promote aqueous interactions and P adsorption	56.12 mg g^{-1}	Phosphate solution	[67,68]
Metal Content	It depends on the biomass source	It can be enriched if treated with metal solutions	Metals can act as bridges for P, enhancing its adsorption onto biochar through ligand exchange and electrostatic attraction	19.66 mg g^{-1}	Phosphate solution	[64,69]

Comparison of the properties and characteristics of traditional and modified biochars and their implications for P adsorption. The table provides an overview of how specific modifications in biochar can enhance its efficiency in P management.

5. Modification and Characterization

5.1. Biochar Modification Techniques

Post-pyrolysis modification of biochar can significantly boost its ability to adsorb P. Utilizing activation agents such as steam or carbon dioxide augments the biochar's surface area and microporosity. The integration of nanoparticles, metalloids, and alterations in functional groups further optimized P retention capabilities (Figure 4). Modern enhancements in biochar modification techniques are paving the way for improved performance of this carbon-rich material, particularly in agricultural and environmental contexts. By tailoring the properties of biochar to fit specific needs, its efficacy in nutrient and water retention and contaminant immobilization is greatly amplified.

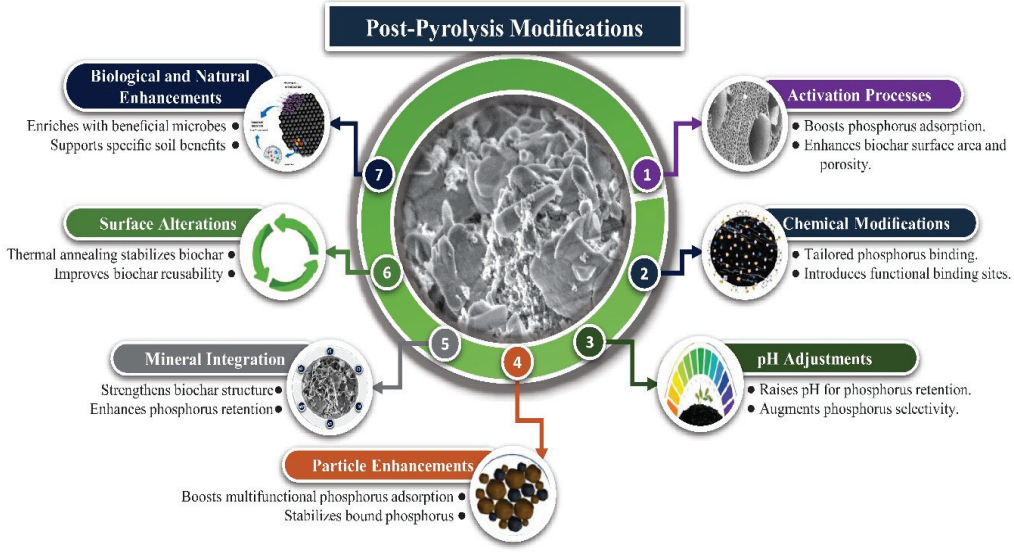

Figure 4. A comprehensive overview of post-pyrolysis modifications for biochar: enhancing structure, functionality, and P retention capabilities.

5.2. Functional Groups in Biochar

Biochar has garnered increasing attention for environmental applications, especially because of its rich functional groups that play a vital role in adsorption and pollutant remediation. Among these alkaline functional groups, predominantly hydroxyl (–OH) and carboxylate ($–COO^-$) groups are essential for their pronounced influence on P adsorption and retention of other ions [70,71]. The abundance and density of these alkaline functional groups on the biochar surfaces varied significantly depending on the feedstock and pyrolysis conditions. For example, a higher pyrolysis temperature often leads to the formation of more aromatic structures, thereby reducing the density of these functional groups. However, moderate pyrolysis temperatures may enhance the concentration of alkaline functional groups and optimize P adsorption [72]. The influence of different temperatures and carrier gases on biochar yields and properties revealed that higher temperatures result in fewer functional groups and a more significant surface area [72]. Modification of post-production processes, such as chemical activation or functionalization, can further introduce or enhance alkaline functional groups (Figure 4). Chemical treatments using strong alkalis, such as KOH or NaOH, can considerably increase the number of hydroxyl and carboxylate groups [71,73]. Owing to its tailored functionalities, biochar has emerged as a promising material for remedying soils laden with heavy metals, reducing phosphorous fixation, and improving soil properties [74]. The application of novel biochar materials, such as ball-milled P-loaded biochar (BPBCs) prepared by combined ball milling and P loading,

has been observed to enhance soil properties and increase soil nutrient concentrations. BPBCs also help reduce soil alkalization and promote plant growth in coastal saline-alkali soils [70]. Moreover, these electrostatic interactions, driven by the negative charges of the alkaline functional groups, ensure P retention on the biochar surface, thereby providing a solution for reducing water pollution [75].

Chemical modifications, such as the introduction of Mg, Ca, K, Fe, Zn, or Al, can also enhance the affinity of biochar for P (Figure 4). Moreover, modification of biochar through processes such as Mg impregnation can further enhance its adsorption capacity for P. For instance, hardwood biochar modified with Mg exhibited a 34% increase in its adsorption capacity, making it a promising candidate for phosphate recovery and subsequent slow-release fertilizer applications [76]. One notable breakthrough is chemical activation, in which biochar is treated with activating agents such as potassium hydroxide (KOH), phosphoric acid (H_3PO_4), or zinc chloride ($ZnCl_2$). This treatment significantly increases biochar's surface area and porosity, thus improving its adsorption capabilities, particularly for heavy metals, organic pollutants, and essential nutrients such as P [77]. Furthermore, iron oxides are recognized for their strong affinity to phosphate, making them ideal candidates for biochar modification. A study conducted by Wu et al. [41] explored rice straw-derived biochar modified with ferrous chloride (Fe(II)) and ferric chloride (Fe(III)). Notably, the Fe(II) biochar displayed superior phosphate adsorption capabilities, attributed to its amorphous state of FeOOH, which has high isoelectric points. The presence of Fe enhances phosphate adsorption through mechanisms such as electrostatic attraction and ligand exchange. Moreover, these field experiments highlighted that chemically modified biochars boosted available P and remarkably decreased leaching in saline-alkaline soils.

Calcium, which is abundant in various waste materials, is another pivotal element in P chemistry. Utilizing marble waste and calcium-rich sepiolite, Deng et al. [78] synthesized Ca/Mg-biochar composites that demonstrated exceptional phosphate adsorption. The mechanism is driven by reactions where Ca or Mg ions in the biochar react with phosphate to form precipitates such as $Ca_5(PO_4)3OH$ and $Mg_3(PO_4)_2$, mitigating phosphate mobility. In a recent study by Tu et al. [79], the research focused on the effectiveness of biochar modified with MgO for P recovery. This study involved the co-pyrolysis of MgO with various raw materials, resulting in different modified biochars: MgO–rice straw, MgO–corn straw, MgO–Camellia oleifera shells, and MgO–garden waste. The results demonstrated a significant improvement in the P adsorption capacities of these modified biochars, with MgO–rice straw displaying the highest capacity. The mechanisms responsible for P adsorption were identified as physical adsorption, precipitation, and surface inner-sphere complexation, with electrostatic attraction playing a limited role.

Additionally, the study found that P adsorbed on these biochars could be released under various pH conditions. MgO–rice straw exhibited modest desorption efficiency, making it a potential candidate for slow-release fertilizers [35]. Extending the exploration to lanthanum, Feng et al. [43] investigated a calcium-modified biochar incorporating sheep manure and oyster shells, showing a limitation in its low-pH adaptability. To counteract this, lanthanum was integrated into biochar, resulting in consistent phosphate adsorption across a wide pH range. The distribution of calcium and lanthanum in the biochar matrix, predominantly on the surface and internal pore structure, respectively, is pivotal for its performance. Another promising avenue for biochar modification is co-pyrolysis, which involves blending biomass with inorganic or organic additives during pyrolysis. For example, combining livestock manure or algae with biomass during pyrolysis allows for the customization of the nutrient profile of the resulting biochar, making it a potent and tailored fertilizer for agricultural use [80]. Therefore, algal-derived biochar is a valuable resource. Rich in nutrients and boasting strong ion-exchange capacity, algal biochar has applications in agriculture, acting as a cost-effective and efficient fertilizer, and in wastewater treatment owing to its porous structure and ion-exchange capabilities [81]. Recognizing the essential role of alkaline functional groups in biochar enables the tailored creation of biochar primed for P adsorption. Modified biochars, enriched with metals such

as Mg, Ca, K, Fe, Zn, Al, and La, present innovative solutions for soil contamination and P sequestration, promoting sustainable agriculture while repurposing waste materials. This amplifies biochar's efficiency and addresses the pressing issue of P mobility in soils.

5.3. Nanotechnology and Its Role in Enhancing P Adsorption

The potential of nanotechnology in the field of environmental sustainability has been captured by its application to biochar. Nanomaterials (NMs), which are central to nanotechnology, exhibit unique attributes, such as large surface areas, superior cation exchangeability, and heightened ion absorption capabilities [82]. Nanocomposite biochars have gained attention by leveraging nanotechnology to introduce nanoparticles into the biochar matrix, such as metal oxides or bio-based nano-compounds. These nanocomposites exhibit targeted functionalities, rendering them effective for precise nutrient release and pollutant remediation [83]. The nuanced differences between NMs and their bulk counterparts can revolutionize how contaminants are addressed, particularly in P adsorption. Yuan et al. [84] demonstrated that owing to their minuscule size and adaptable surface chemistry, nanoscale materials can achieve a more intimate level of interaction with P. When harnessed in biochar, this translates to augmented surface area testing with active sites optimized for P adsorption, leading to enhanced adsorption rates. Research in this domain is dynamic and diverse.

Researchers have made significant efforts to develop nanoscale biochar solutions. For instance, Sun et al. [85] reported a project that resulted in a nano-biochar composite formulated using nanoSiO_2 doping. This composite shone in purifying P-rich waters and proved its poor adsorption capacity, recyclability, and environmental compatibility when pitted against more traditional straw biochar materials. Wu et al. [41] ventured into nanoparticle–biochar integrations with a spotlight on iron oxide. Their rigorous experiments, which utilized rice straw-derived biochar infused with ferrous chloride (Fe(II)) and ferric chloride (Fe(III)), yielded compelling results. Fe(II) biochar has emerged as a frontrunner in phosphate adsorption and has displayed robust resilience against environmental challenges, such as pH shifts and competing anions. This was not just a laboratory victory; the Fe(II) biochar exhibited an 86.4% reduction in leaching, demonstrating its real-world application in mitigating P losses, especially in saline-alkaline soils.

Delving deeper into the realm of P adsorption, Cui et al. [86] demonstrated the advantages of FLO@CSL as a novel adsorbent. This brainchild, which is a $FeLaO_3$-modified sulfomethylated lignin (SL) biochar, hinges on the synergistic affinity of lanthanum (La) and iron (Fe) (hydro) oxides for phosphate. Its standout features include remarkable adsorption capacity and a streamlined magnetic separation process, making it a potential game-changer in wastewater treatment. However, the innovation odyssey continues. Yin et al. [87] investigated the challenge of water eutrophication, shedding light on the crucial role that modified biochars can play. Their extensive experimentation led them to pinpoint Mg–Al-modified biochars as a formidable solution, especially when confronted with complex mixtures, such as the coexistence of NH_4^+, NO_3^-, and PO_4^{3-}. Peng et al. [88] introduced new frontiers by focusing on the agricultural sector. Their work on metal oxide-modified biochars, especially those bolstered by FeAl and MgAl, revealed multifaceted benefits. These ranged from heightened soil P availability and promotion of inorganic P-solubilizing bacteria to a marked reduction in P leaching. Advancements in biochar research were also enriched by Zhang et al. [89] with their nano zero-valent zinc (nZVZ), which aimed to enhance the active sites, thereby improving P adsorption capacity.

Furthermore, Ce^{3+}-enriched ultrafine ceria nanoparticle-loaded biochar exhibited a rapid and efficient phosphate adsorption capacity, which is particularly beneficial owing to the unique characteristics of ceria nanoparticles [90]. In salt-affected soils, nano-biochar amendments have shown the potential to enhance P adsorption due to oxygenated functional groups [91]. Nano zero-valent iron-modified biochar has demonstrated heightened phosphate adsorption capacities, proving especially effective in eutrophication control and potential agricultural applications [12]. Lastly, nano-MgO biochar composites have

been identified as potent adsorbents, with their efficacy amplified when the biochar is co-pyrolyzed with magnesium citrate, showcasing impressive P immobilization [92]. Collectively, these studies highlight nanotechnology's transformative role in amplifying biochar's P adsorption capacity. This synergy promises environmental advancements and paves the way for enhanced agricultural productivity. As we navigate these innovations, ensuring a future where agriculture seamlessly blends productivity with environmental mindfulness is paramount.

6. Biochar in Sustainable Agriculture

Biochar, a carbon-rich material produced from the pyrolysis of biomass, offers a holistic and sustainable solution to various agricultural challenges in addition to traditional soil amendment methods [55]. The conversion of crop residues into biochar can sequester large amounts of CO_2 with substantial potential in specific regions. One of its key advantages is that, when incorporated into agricultural practices, it offers significant carbon sequestration potential at the national level, contributing to climate change mitigation [93]. Studies have demonstrated the capacity of biochar to sequester carbon from the atmosphere, with potential variations based on soil pH levels. Notably, acidic soils tend to release more CO_2 after biochar application than neutral or alkaline soils, emphasizing the need to consider soil pH when assessing carbon sequestration potential [94]. Additionally, the use of biochar in agriculture can mitigate various environmental issues, including marine aquatic biodiversity destruction, soil and water acidification, and eutrophication [95]. The inherent minerals present in biomass significantly influence carbon conversion during pyrolysis and, consequently, the properties of biochar. Removing these minerals before pyrolysis has increased carbon retention in biochar and enhanced its stability. This removal process produces biochar with a higher chemical and thermal oxidation decomposition resistance, making it a more effective carbon sequestration tool [96].

In terms of soil benefits, the porous structure of biochar enhances soil porosity and aggregate stability, leading to improved water dynamics. This enhances water infiltration and retention, making it particularly valuable in arid regions [97]. Additionally, the cation exchange capacity of biochar helps retain essential nutrients, such as ammonium, nitrate, and phosphate, thereby reducing nutrient runoff and its associated ecological impacts [37,87]. Biochar also provides a conducive habitat for beneficial soil microbes, thereby increasing microbial diversity and metabolic activity. This microbial enhancement can further boost soil health and agricultural productivity [37]. Furthermore, biochar is instrumental in immobilizing contaminants, including heavy metals such as Cu^{2+}, Cd^{2+}, and Pb^{2+}, as well as organic pollutants. This action prevents these contaminants from entering the food chain and enhances plant growth. Modified versions of biochar, such as those enhanced with chitosan, demonstrate improved removal of heavy metals from solutions and diminished metal toxicity in soils [98,99]. Economically, although the initial cost of biochar may be higher than that of conventional fertilizers, its long-term impact on soil health and reduced need for recurrent fertilizer applications make it a cost-effective choice. The sustained benefits of a single biochar application on soil health outweigh the costs of routine fertilizer applications. Additionally, the role of biochar in mitigating environmental issues such as nutrient leaching and runoff can result in long-term economic and ecological benefits [100]. As global agriculture shifts towards sustainable practices, biochar's multifaceted benefits become increasingly evident, surpassing traditional soil amendment methods [93]. Biochar is a versatile and sustainable solution that addresses numerous agricultural challenges, from carbon sequestration to soil enhancement, nutrient preservation, bolstered microbial activity, and contaminant immobilization.

6.1. Integration of Advanced Analytical Methods with Cutting-Edge Characterization Techniques and Their Insights

Biochar, derived from the thermal decomposition of organic materials, is a promising solution to various environmental challenges. Its adaptability depends primarily on its

physicochemical properties, which can be modified through specific pyrolysis conditions and feedstock selection. A profound understanding of both its surface attributes and inner configuration is essential for harnessing the full potential of biochar and engineering it for precise applications (Table 2). This calls for emerging advanced spectroscopy methods with state-of-the-art characterization techniques [91]. The relationship between biochar and P, especially their adsorption and desorption behaviors, is better understood because of the development of intricate characterization methodologies. These contemporary analytical instruments have enabled researchers to explore the molecular and microscopic interplay between biochar and P in detail.

Density functional theory: Recent studies have focused on the adsorption of phosphate ($H_2PO_4^-$) in water by metal-modified biochar. Using density functional theory, Yin et al. [101] demonstrated that metal-modified biochar exhibited a stronger molecular-level effect on phosphate adsorption than unmodified variants. In particular, Ca-modified biochar was superior to its Mg-modified counterparts. This study revealed that metal adsorption, primarily through electrostatic attraction, outperforms edge adsorption, which relies on covalent bonding.

Imaging techniques—SEM and EDX: The combined power of scanning electron microscopy (SEM) and energy-dispersive X-ray spectroscopy (EDX) has become indispensable. Wang et al. [90] employed these techniques to obtain high-resolution images of biochar surfaces and performed elemental mapping to locate adsorbed P and elucidate adsorption hotspots on the biochar. Furthermore, they prepared biochar-loaded Ce^{3+}-enriched ultrafine ceria nanoparticles (Ce-BC), which showed significant potential for phosphate removal from water.

Surface chemistry analysis—XPS: X-ray photoelectron spectroscopy (XPS) is a formidable technique for discerning biochar surface chemistry. Identifying the types and concentrations of functional groups involved in P binding is particularly important, as shown by Bolton et al. [102]. Their study elucidated the formation of iron phosphate and revealed that P capture is associated with various mineral phases.

Functional group identification—FTIR: Fourier-transform infrared spectroscopy (FTIR) has become essential for recognizing specific functional groups and chemical bonds on the biochar surface that interact with P. Several studies, including those by Liu et al. [103], Shin et al. [104], and Mahmoud et al. [91], demonstrated the capabilities of FTIR to highlight fundamental adsorption mechanisms and interactions.

Speciation and interaction analysis—NMR: Nuclear magnetic resonance (NMR) spectroscopy, particularly solid-state ^{31}P NMR, offers crucial insights into the nature of P within the biochar matrix. Amin et al. [105] and Sacko et al. [106] employed NMR and other techniques such as ssNMR, XRD, and NEXAFS to elucidate how P binds to biochar and the specifics of these interactions.

The arsenal of advanced characterization techniques has exponentially augmented our understanding of the interplay between biochar and P. By unraveling the underlying mechanisms. These tools can empower researchers to refine biochar properties and set the stage for superior P management strategies in soils.

Table 2. Overview of advanced analytical techniques in biochar research.

Analytical Technique	Principle/Methodology	Benefits in Biochar Research	Challenges/Limitations	References
X-ray Photoelectron Spectroscopy (XPS)	Measures the elemental composition and electronic state of elements	Reveals surface chemistry and potential functional groups	Limited to surface analysis; time-consuming	[107]
Scanning Electron Microscopy (SEM)	Provides detailed images of biochar surfaces using electron beams	Visualizes microstructure and porosity; aids in determining biochar's physical properties	Requires gold or carbon sputter coating for some samples, potentially altering surface	[108]
Fourier-Transform Infrared Spectroscopy (FTIR)	Measures vibrational frequencies to determine chemical compounds	Identifies functional groups and organic components	Limited sensitivity for very low-concentration species	[109]
Nuclear Magnetic Resonance (NMR)	Utilizes nuclear spins in a magnetic field	Offers insights into biochar's carbon types and distribution	Requires high concentrations of samples; relatively expensive	[110]
Thermogravimetric Analysis (TGA)	Monitors weight change in a material as a function of temperature or time	Assesses thermal stability and organic content of biochar	Does not provide specific information on biochar's chemical structure	[111]
Brunauer–Emmett–Teller (BET) Method	Measures gas adsorption on solid surfaces	Evaluates specific surface area, aiding in understanding adsorption capacity	Limited to certain gas–solid systems; does not consider pore geometry	[112]

Overview of key analytical techniques employed in biochar research, detailing their principles, advantages, limitations, and relevance in assessing and understanding biochar structure and properties.

6.2. Role of Artificial Intelligence in Data Analysis and Prediction

Biochar, a carbon-rich derivative obtained by the thermal decomposition of organic materials, has gained significant attention in environmental research. This attention is primarily owing to its potential to offer solutions to some of the pressing environmental challenges. An essential facet of biochar research pertains to its intricate relationship with P, particularly concerning its adsorption and desorption behavior [113]. Understanding the nuances of this relationship requires advanced tools and methodologies. Although useful, traditional analytical methods often grapple with the intricacies of biochar-related datasets. Artificial intelligence (AI), with its sophisticated algorithms, machine learning (ML), and deep learning (DL) capabilities, has revolutionized the domain of biochar research. Notably, AI, when combined with rich historical data, can provide insights into biochar behavior, even predicting the reactions of yet-to-be-produced biochar types with P [114].

Machine learning, a subfield of AI, employs past data to train computational models. For instance, the utility of algorithms, such as neural networks, extreme gradient boosting, and random forests, in predicting biochar behavior, specifically its adsorption patterns, has been documented [113]. Furthermore, advancements in computational chemistry combined with ML have paved the way for the development of biochar as a sustainable alternative to traditional fertilizers. This is exemplified in studies aimed at creating biochar formulations capable of slow and efficient nutrient release, with an emphasis on P [115]. The integration of AI into the optimization of biochar production is particularly noteworthy. Through neural networks, it is now possible to predict the optimal feedstock and pyrolysis

conditions tailored for specific outcomes, effectively transforming a traditional iterative process into a targeted data-driven approach [114]. In wastewater remediation, another realm where biochar holds promise, AI techniques such as ML and DL come into play. These techniques can predict effluent P levels even when data are scarce, facilitating compliance with regulatory standards while potentially reducing costs [116].

6.3. Highlighting More Nuanced AI Applications in Biochar Research

Engineered biochar design using AI: Liu et al. [117] utilized the power of the random forest algorithm to delve into the realm of As adsorption in Fe-modified biochar. Such applications underline the immense potential of AI in aiding the rational design of biochars, specifically tailoring them for targeted contaminant removal, such as arsenic.

Modeling P adsorption: A significant aspect of biochar research is its interaction with P. Tree-based AI algorithms, such as RF, DTs, and XGBoost, have made notable strides. These algorithms, particularly RF, have emerged as pivotal tools for predicting phosphate adsorption patterns and guiding researchers in their quest to design optimal biochar-based adsorbents [118].

Innovative hybrid models: One of the strengths of AI is its adaptability and ability to be integrated with various computational models. This flexibility was displayed in the SVM-ANN ensemble model, which was designed to predict heavy metal sorption efficiency. By considering a plethora of variables ranging from environmental conditions and biochar physicochemical characteristics to contaminant types, AI-driven hybrid models can enhance the accuracy and scope of predictions. Such models are particularly significant for forecasting how biochar behaves under real-world conditions [114].

Optimizing biochar production: The potential of AI is not limited to post-production analyses. Neural networks, another facet of AI, are instrumental in predicting the optimal conditions and raw materials (feedstock) required for biochar production. Through these predictions, the traditional trial-and-error method for biochar production can be streamlined, ensuring that the desired properties of the end product can be achieved with greater efficiency [114].

AI in wastewater treatment: Beyond solid contaminant interactions, biochar shows promise for wastewater remediation. In this sector, ML and DL models are paramount. For instance, scientists leveraging the power of AI have predicted effluent P levels, even in incomplete datasets. Such applications of AI can revolutionize wastewater treatment processes, ensuring that the treated water complies with environmental standards while potentially minimizing treatment costs [116].

Advanced machine learning techniques for yield prediction: The seamless integration of AI with optimization techniques has led to the creation of predictive models, such as the ensemble learning tree (ELT-PSO). Such models have shown exemplary prediction accuracy for biochar yield, thereby minimizing the need for resource-intensive experiments [119].

The potential of AI, particularly in engineered biochar production for efficient P adsorption and desorption, augments its capability to address environmental challenges and ensure more sustainable solutions [120]. Incorporating these advanced techniques and insights ensures that biochar research is comprehensive and resource-efficient. Combining biochar technology with AI provides an enhanced understanding that is vital for effectively addressing current environmental challenges.

7. Practical Implications and Benefits

7.1. Addressing the Environmental and Health Impacts of P Leaching through Sustainable Agricultural Practices

The widespread use of P fertilizers in modern agriculture has led to significant environmental and health challenges. Notably, the leaching of excess P from agricultural terrain into adjacent water systems has myriad adverse ecological consequences [24]. Compounding this issue, intricate edaphic processes often result in the immobilization of P in the

soil, thereby hindering its uptake by plants. Consequently, the efficiency of water-soluble P fertilizers remains a challenge, culminating in profound environmental and public health concerns [24]. Eutrophication of freshwater and marine ecosystems is one of the most important ecological implications of P leaching. This process, exacerbated by agricultural, urban, and industrial activities, results in an excessive influx of nutrients, primarily nitrogen and P, facilitating the uncontrolled proliferation of algal populations. As these algal blooms decay, they deplete dissolved oxygen levels, engendering hypoxic or anoxic conditions. Such environments are calamitous for aquatic life, leading to widespread fish mortality and biodiversity loss. The ramifications of eutrophication are not merely ecological; the economic impact is also substantial, with estimates indicating annual losses of $1 billion for European coastal waters and $2.4 billion for American lakes and streams [22]. Even more disconcerting are certain algal blooms dominated by cyanobacteria and blue-green algae. These blooms produce a spectrum of toxins, collectively termed cyanotoxins, which pose considerable threats to aquatic life and human health. Cyanobacterial harmful algal blooms (CyanoHABs) severely compromise water quality. Ingestion of water or aquatic organisms, such as fish, contaminated with cyanotoxins can have deleterious health effects. Given the global surge in CyanoHAB events primarily attributed to anthropogenic eutrophication and climatic change, there is a pressing need for effective management strategies to safeguard public health and aquatic ecosystem integrity [22,121].

Biochar has emerged as a potential source of sustainable solutions. Owing to its adsorptive properties, biochar serves as an effective P sink and significantly reduces its leaching potential (Figure 5). This assertion is corroborated by empirical studies that have shown the potential of biochar to reduce P leaching by up to 60% [12,122,123]. Beyond the immediate environmental benefits, incorporating biochar into agricultural landscapes reduces the dependency on phosphate fertilizers, thus attenuating the carbon footprint associated with their manufacture and deployment [124]. With strategic measures, including the integration of biochar and a comprehensive grasp of plant physiological processes, we can achieve a harmonious balance that ensures both agricultural productivity and the protection of ecosystems and communities.

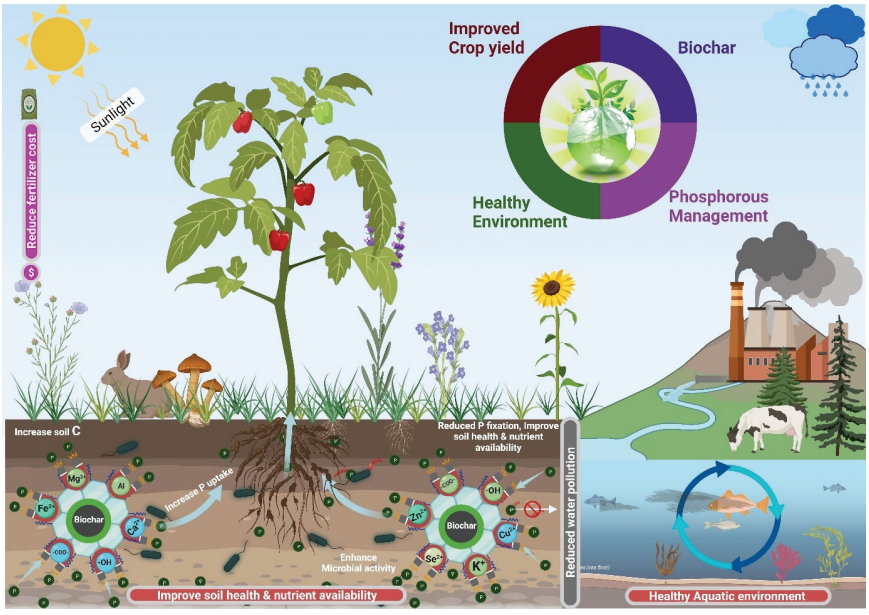

Figure 5. An illustrative overview of the role of biochar in P adsorption and desorption: from enhancing soil nutrient availability and microbial activity to reducing P leaching, leading to improved crop yield, a healthier environment, and mitigated aquatic eutrophication.

7.2. Economic Advantages in Agriculture: The Promise of Biochar

In the ever-changing landscape of agriculture and horticulture, there is an urgent need for solutions that strike a balance between economic feasibility, environmental conservation, and efficiency. Introducing biochar in this milieu can provide significant economic benefits to farmers, agronomists, and horticulturists. One primary advantage of farmers is their potential to reduce costs. The incorporation of biochar can significantly reduce the need for expensive P fertilizers. This is because of the ability of biochar to absorb and gradually release P, thereby ensuring a consistent nutrient source for crops. This reduced reliance on fertilizers could lead to substantial savings, especially for expansive agricultural ventures, as underscored by studies by Sun et al. [81] and Luo et al. [1]. Moreover, the possibility of enhanced crop yields presents a secondary yet paramount benefit. The positive link between biochar use and improved crop outcomes has been well documented, with a notable mention being made by Li et al. [125]. Greater yields inevitably result in heightened revenue for farmers.

For agronomists and horticulturists, these implications extend beyond agricultural output. The nuanced knowledge needed to perfect biochar application, from production to utilization, could spawn specialized consulting services. Such services can guide farmers to customize biochar applications according to specific crop and soil conditions, thereby creating new employment opportunities and research directions, as highlighted by Rogers et al. [126]. Research has also highlighted the potential of combining biochar with other organic materials. For instance, Antonious et al. [127] emphasized the benefits of amalgamating animal manure and other natural substances with biochar. Such synergies can further enhance soil quality and crop yields and reduce costs, making them lucrative for farmers with limited resources. The potential of biochar as a soil revitalizer is also noteworthy, especially in areas with soil degradation. By rejuvenating soil health and its overall structure, biochar ensures sustainable cultivation for prolonged durations, circumventing the requirement for pricey soil amendments or shifting to more fertile terrain. Bista

et al. [128] and Wali et al. [129] highlighted the soil-enhancing capabilities of biochar and its associated benefits for crops.

8. Gaps and Future Directions

8.1. Existing Research Gaps in Biochar Preparation and Modification

Despite the recognized potential of biochar as a sustainable soil amendment, several research gaps persist, especially in its preparation and modification techniques. A notable gap lies in the comprehensive understanding of the influence of diverse feedstocks on biochar physicochemical properties. Although investigations have been made into common feedstocks such as wood and agricultural residues, knowledge of unconventional feedstocks, such as algal biomass and sewage sludge, is limited. In particular, algal biomass is distinct from lignocellulosic biomass because of its unique surface functional groups and the presence of various cations, making it potentially effective for environmental decontamination [130].

Another significant area of research is the optimization of pyrolysis conditions based on specific feedstocks. The current literature often provides generalized pyrolysis conditions, which may not be optimal for all feedstocks. For instance, biochars from animal litter and solid waste show distinct properties compared to those derived from crop residues and wood biomass, even under the same pyrolysis conditions, mainly because of variations in lignin, cellulose, and moisture content in the biomass [47]. The post-production modification of biochar is an emerging research domain with ample room for investigation. Although some studies have investigated acid or alkali activation, the exploration of other potential modification techniques has not been exhaustive. For example, innovative methods to amplify the P adsorption capacity or longevity of biochar have yet to be thoroughly examined. One promising strategy involves the use of zero-valent iron (ZVI) biochar composites modified with $CaCl_2$ to enhance their lifespan and P removal efficacy [131]. Finally, the scalability of biochar preparation and modification techniques remains a challenge. Processes effective at the laboratory scale may not be as efficient when scaled up, hindering the economic feasibility and widespread adoption of biochar use. Although biochar holds immense promise, addressing these research gaps can pave the way for innovative applications and widespread adoption in sustainable agriculture and horticulture.

8.2. Opportunities for Further Innovation and Research

The utilization of biochar in agriculture is on the cusp of significant advancements, and a wide spectrum of research opportunities needs to be explored. One of the most promising research areas is the synergy between biochar application and sustainable agricultural practices. As highlighted by Elkhlifi et al. [132], the interaction of biochar with practices such as agroforestry, conservation tillage, and cover cropping can yield holistic strategies that maximize soil health and environmental benefits. Variances in biochar properties, which depend on factors such as feedstock, pyrolysis conditions, and residence time, require further investigation to optimize their contribution to soil health, microbial activity, nutrient retention, and carbon sequestration.

Another dimension of research, as pointed out by Gillingham et al. [133], is the magnetization of biochar. This novel approach offers a dual solution for waste management: utilizing agricultural waste for magnetic biochar synthesis and facilitating nitrogen pollution management. The potential of magnetic biochar to mitigate nitrogen pollution in soils and recycle it as a fertilizer is particularly compelling, especially considering the widespread environmental and economic concerns surrounding nitrogen runoff. Tan et al. [134] highlighted the intricate relationships between biochar, soil, and microbial communities. The physicochemical properties of biochar play a critical role in shaping microbial interactions, influencing soil fertility and plant growth. Such interactions could be invaluable for the remediation of pollutants, soil enhancement, and bolstering plant resistance against pathogens. With rapid advancements in technology, there is an exciting intersection between biochar research and digital tools. Dehkordi et al. [135] proposed that integrating

high-resolution imaging from UAVs with satellite data could offer deeper insights into the impact of biochar on evapotranspiration across agricultural landscapes. Furthermore, as discussed by Shaikh et al. [136], merging AI, IoT devices, and robotics with traditional agricultural practices could revolutionize biochar applications, offering precise data analysis and optimization opportunities.

Yang et al. [137] introduced the concept of the circular economy in biochar research. It is vital to explore biochar's role in broader systems, such as waste management and energy production, particularly its potential for carbon capture and storage. This could redefine the significance of biochar in both economic and environmental contexts. Finally, given the escalating concerns regarding climate change, Kumar et al. [138] suggested the potential of biochar to bolster soil resilience to extreme weather events. Understanding how biochar can mitigate the impacts of droughts, floods, or heatwaves by enhancing soil properties, such as moisture retention and aeration, could offer strategies to insulate food systems from climatic adversities. For these research opportunities to bear fruit, fostering multidisciplinary collaborations, amplifying funding avenues, and advocating for open-source data sharing is paramount. However, although this quest is challenging, the vision of a resilient and sustainable agricultural future underscores its importance.

8.3. Potential Challenges and Solutions in Biochar Research and Application

Heterogeneity in biochar properties: Biochars exhibit a vast range of physicochemical properties depending on their feedstock and pyrolysis conditions, making it difficult to consistently predict their effects on soils. The intrinsic molecular composition of biochar-derived dissolved black carbon and its interactions with metal ions, which can affect its environmental impact, are not fully understood [139]. Das et al. [140] highlighted the significant influence of pyrolysis temperature and feedstock type on biochar composition, emphasizing the variability in its properties. Similar to soil taxonomy, standardized protocols and classifications for biochar production can help categorize biochars based on their intended use and predictable outcomes. Collaborative databases that incorporate global research can also assist in understanding this variability.

Economic viability: Biochar's high production and transportation costs outweigh its uncertain agricultural benefits, making it a challenge, especially for farmers in developing nations [132,141]. Economies of scale, integrated biochar production within waste management or energy generation systems, and government subsidies can make biochar affordable. The development of low-tech, locally adapted production methods can also be made more accessible to smallholder farmers.

Potential environmental risks: Improper production or application of biochar might result in toxin leaching, alteration of soil pH in a detrimental way, or even harm to aquatic ecosystems. This could be due to the release of harmful components or negative interactions with the environment [142,143]. Rigorous quality checks, biochar production and application guidelines, and continuous monitoring can mitigate these issues. Therefore, educating farmers about the best practices for biochar application is essential.

Limited knowledge transfer: Often, there is a gap between the research findings and their applications by end users. This can lead to suboptimal or misguided biochar use, particularly among farmers with limited education or resources [126]. Bridging the gap between researchers, extension services, and farmers through workshops, field days, and accessible literature can ensure the widespread dissemination of the latest findings and best practices.

Sociocultural acceptance: Introducing new agricultural practices, such as biochar application, can sometimes lead to resistance due to traditional farming methods or a lack of awareness about its benefits in some regions [126]. Participatory research involving farmers in the research process can increase acceptance. Therefore, integrating cultural and social considerations into biochar promotion strategies is crucial.

Despite these challenges, the benefits of biochar and the dedication of the global research community have shone through. As research continues, tailored solutions are emerging, making the integration of biochar into global agriculture more feasible.

9. Conclusions

The potential of biochar for reshaping sustainable agriculture is extensively highlighted in this review. P, a crucial element in agriculture, faces the challenge of fixation in soils with significant environmental and economic repercussions, such as increased greenhouse gas emissions and mounting costs for farmers. Biochar is a promising remedy because of its capacity to adsorb P and minimize its fixation in soils. However, the diversity of biochar properties resulting from different feedstocks and production techniques emphasizes the need for an intricate understanding of uniform results. Progress in biochar modification methods has extended its possibilities, perfecting its attributes for P management. Breakthroughs in analytical tools combining cutting-edge spectroscopy and artificial intelligence have provided comprehensive insights into the interactions of biochar with soil and P. These findings suggest the broad application of biochar derived from P management to enhance soil health and carbon sequestration. By improving soil P availability, crop yields can be increased, and excessive fertilization reduced. This economically benefits farmers and safeguards aquatic ecosystems from P runoff. However, harnessing the full potential of biochar is challenging because of its diverse production and acceptance in traditional agricultural settings. This emphasizes the need for continued research, especially in customizing biochar properties and assessing their long-term implications in diverse soils. The adaptability of modified biochar stands out during this process. Through modification, its characteristics can be tailored to address specific agricultural challenges, making it a potent tool for sustainable farming. However, as we have modified it, caution is necessary to ensure that the environmental integrity of the biochar remains intact. Biochar, especially its modified form, represents hope for a sustainable agricultural future. The insights from this review reinforce the urgency of ongoing research and collaboration, paving the way for a balanced and bountiful agricultural landscape.

Author Contributions: The review was conceptually designed with contributions from all authors. N.A. and L.D. (Lifang Deng) jointly led the literature search and data analysis, contributing equally to the work. Z.H.S., along with providing critical revisions, significantly shaped the intellectual content of the review. B.B. and C.W. were essential for evaluating the relevance of the studies included in the review. L.D. (Lansheng Deng), Y.L., J.L. and S.C. were instrumental in interpreting the research findings and providing key revisions to the manuscript. Z.C., F.H., F.A., R.A. and L.G. contributed to the initial drafting and subsequent critical revisions of the manuscript. P.T. coordinated the review process and provided overall guidance, contributing to the critical review of the manuscript for important intellectual content. All authors engaged in the final drafting of the manuscript, provided comments and insights at various stages, and approved the final version of the manuscript. All authors have read and agreed to the published version of the manuscript.

Funding: We gratefully acknowledge the financial support from the National Natural Science Foundation of China (No. 42377211) and the Basic and Applied Basic Research Foundation of Guangdong Province (No. 2022A1515010941), Scarce and Quality Economic Forest Engineering Technology Research Center (2022GCZX002), Science and Technology Plan projects of Guangzhou (NO. 202206010069), Meizhou Science and Technology Project (NO. 2021A0304001), and the Key-Area Research and Development Program of Guangdong Province (2020B020215003).

Data Availability Statement: No new data were created or analyzed in this study. Data sharing is not applicable in this study.

Acknowledgments: During the preparation of this work, the authors used Paperpal in order to check grammar, sentence structure, and punctuation. After using this tool/service, the authors reviewed and edited the content as needed, and take full responsibility for the content of the publication.

Conflicts of Interest: Author Lin Gong was employed by the company Dongguan Yixiang Liquid Fertilizer Co., Ltd. The authors declare that they have no affiliations with or involvement in

any organization or entity with any financial interest in the subject matter or materials discussed in this manuscript.

References

1. Luo, D.; Wang, L.; Nan, H.; Cao, Y.; Wang, H.; Kumar, T.V.; Wang, C. Phosphorus Adsorption by Functionalized Biochar: A Review. *Environ. Chem. Lett.* **2023**, *21*, 497–524. [CrossRef]
2. Rumi, R.; Maurya, K.; Pandey, M.; Kohli, P.S.; Panchal, P.; Sinha, A.K.; Giri, J. Biotechnological Approaches for Improving Phosphate Uptake and Assimilation in Plants. In *Plant Phosphorus Nutrition*; CRC Press: Boca Raton, FL, USA, 2023; pp. 110–128. [CrossRef]
3. Kolodiazhnyi, O.I.; Kukhar, V.P. Phosphorus Compounds of Natural Origin: Prebiotic, Stereochemistry, Application. *Symmetry* **2021**, *13*, 889. [CrossRef]
4. Barquet, K.; Järnberg, L.; Rosemarin, A.; Macura, B. Identifying Barriers and Opportunities for a Circular Phosphorus Economy in the Baltic Sea Region. *Water Res.* **2020**, *171*, 115433. [CrossRef]
5. Randive, K.; Raut, T.; Jawadand, S. An Overview of the Global Fertilizer Trends and India's Position in 2020. *Miner. Econ.* **2021**, *34*, 371–384. [CrossRef]
6. Filippelli, G.M. Balancing the Global Distribution of Phosphorus with a View Toward Sustainability and Equity. *Glob. Biogeochem. Cycles* **2018**, *32*, 904–908. [CrossRef]
7. Johan, P.D.; Ahmed, O.H.; Omar, L.; Hasbullah, N.A. Phosphorus Transformation in Soils Following Co-Application of Charcoal and Wood Ash. *Agronomy* **2021**, *11*, 2010. [CrossRef]
8. Pierzynski, J.; Hettiarachchi, G.M. Reactions of Phosphorus Fertilizers with and without a Fertilizer Enhancer in Three Acidic Soils with High Phosphorus-Fixing Capacity. *Soil Sci. Soc. Am. J.* **2018**, *82*, 1124–1139. [CrossRef]
9. Haque, S.E. How Effective Are Existing Phosphorus Management Strategies in Mitigating Surface Water Quality Problems in the U.S.? *Sustainability* **2021**, *13*, 6565. [CrossRef]
10. Maharajan, T.; Ceasar, S.A.; Krishna, T.P.A.; Ignacimuthu, S. Management of Phosphorus Nutrient amid Climate Change for Sustainable Agriculture. *J. Environ. Qual.* **2021**, *50*, 1303–1324. [CrossRef]
11. Tian, J.; Ge, F.; Zhang, D.; Deng, S.; Liu, X. Roles of Phosphate Solubilizing Microorganisms from Managing Soil Phosphorus Deficiency to Mediating Biogeochemical p Cycle. *Biology* **2021**, *10*, 158. [CrossRef]
12. Ren, L.; Li, Y.; Wang, K.; Ding, K.; Sha, M.; Cao, Y.; Kong, F.; Wang, S. Recovery of Phosphorus from Eutrophic Water Using Nano Zero-Valent Iron-Modified Biochar and Its Utilization. *Chemosphere* **2021**, *284*, 131391. [CrossRef]
13. Yang, L.; Wu, Y.; Wang, Y.; An, W.; Jin, J.; Sun, K.; Wang, X. Effects of Biochar Addition on the Abundance, Speciation, Availability, and Leaching Loss of Soil Phosphorus. *Sci. Total Environ.* **2021**, *758*, 143657. [CrossRef]
14. Freitas, A.M.; Nair, V.D.; Harris, W.G. Biochar as Influenced by Feedstock Variability: Implications and Opportunities for Phosphorus Management. *Front. Sustain. Food Syst.* **2020**, *4*, 510982. [CrossRef]
15. Li, F.; Liang, X.; Niyungeko, C.; Sun, T.; Liu, F.; Arai, Y. Effects of Biochar Amendments on Soil Phosphorus Transformation in Agricultural Soils. *Adv. Agron.* **2019**, *158*, 131–172.
16. Anae, J.; Ahmad, N.; Kumar, V.; Thakur, V.K.; Gutierrez, T.; Yang, X.J.; Cai, C.; Yang, Z.; Coulon, F. Recent Advances in Biochar Engineering for Soil Contaminated with Complex Chemical Mixtures: Remediation Strategies and Future Perspectives. *Sci. Total Environ.* **2021**, *767*, 144351. [CrossRef]
17. Almanassra, I.W.; Mckay, G.; Kochkodan, V.; Ali Atieh, M.; Al-Ansari, T. A State of the Art Review on Phosphate Removal from Water by Biochars. *Chem. Eng. J.* **2021**, *409*, 128211. [CrossRef]
18. Vikrant, K.; Kim, K.H.; Ok, Y.S.; Tsang, D.C.W.; Tsang, Y.F.; Giri, B.S.; Singh, R.S. Engineered/Designer Biochar for the Removal of Phosphate in Water and Wastewater. *Sci. Total Environ.* **2018**, *616–617*, 1242–1260. [CrossRef]
19. Yang, J.; Zhang, M.; Wang, H.; Xue, J.; Lv, Q.; Pang, G. Efficient Recovery of Phosphate from Aqueous Solution Using Biochar Derived from Co-Pyrolysis of Sewage Sludge with Eggshell. *J. Environ. Chem. Eng.* **2021**, *9*, 105354. [CrossRef]
20. Hong, C.; Lu, S. Does Biochar Affect the Availability and Chemical Fractionation of Phosphate in Soils? *Environ. Sci. Pollut. Res.* **2018**, *25*, 8725–8734. [CrossRef]
21. Wen, Z.; Chen, Y.; Liu, Z.; Meng, J. Biochar and Arbuscular Mycorrhizal Fungi Stimulate Rice Root Growth Strategy and Soil Nutrient Availability. *Eur. J. Soil Biol.* **2022**, *113*, 103448. [CrossRef]
22. DIssanayaka, D.M.S.B.; Ghahremani, M.; Siebers, M.; Wasaki, J.; Plaxton, W.C. Recent Insights into the Metabolic Adaptations of Phosphorus-Deprived Plants. *J. Exp. Bot.* **2021**, *72*, 199–223. [CrossRef]
23. Ali, U.; Lu, S.; Fadlalla, T.; Iqbal, S.; Yue, H.; Yang, B.; Hong, Y.; Wang, X.; Guo, L. The Functions of Phospholipases and Their Hydrolysis Products in Plant Growth, Development and Stress Responses. *Prog. Lipid Res.* **2022**, *86*, 101158. [CrossRef]
24. Bindraban, P.S.; Dimkpa, C.O.; Pandey, R. Exploring Phosphorus Fertilizers and Fertilization Strategies for Improved Human and Environmental Health. *Biol. Fertil. Soils* **2020**, *56*, 299–317. [CrossRef]
25. Zhang, J.; Choi, S.; Fan, J.; Kim, H.J. Biomass and Phosphorus Accumulation and Partitioning of Geranium and Coleus in Response to Phosphorus Availability and Growth Phase. *Agronomy* **2019**, *9*, 813. [CrossRef]
26. Aslam, M.M.; Karanja, J.K.; Yuan, W.; Zhang, Q.; Zhang, J.; Xu, W. Phosphorus Uptake Is Associated with the Rhizosheath Formation of Mature Cluster Roots in White Lupin under Soil Drying and Phosphorus Deficiency. *Plant Physiol. Biochem.* **2021**, *166*, 531–539. [CrossRef]

27. Gong, H.; Meng, F.; Wang, G.; Hartmann, T.E.; Feng, G.; Wu, J.; Jiao, X.; Zhang, F. Toward the Sustainable Use of Mineral Phosphorus Fertilizers for Crop Production in China: From Primary Resource Demand to Final Agricultural Use. *Sci. Total Environ.* **2022**, *804*, 150183. [CrossRef]
28. Kishore, A.; Alvi, M.; Krupnik, T.J. Development of Balanced Nutrient Management Innovations in South Asia: Perspectives from Bangladesh, India, Nepal, and Sri Lanka. *Glob. Food Secur.* **2021**, *28*, 100464. [CrossRef]
29. Rashmi, I.; Roy, T.; Kartika, K.S.; Pal, R.; Coumar, V.; Kala, S.; Shinoji, K.C. Organic and Inorganic Fertilizer Contaminants in Agriculture: Impact on Soil and Water Resources. In *Contaminants in Agriculture: Sources, Impacts and Management*; Springer Nature: Cham, Switzerland, 2020; pp. 3–41.
30. Langhans, C.; Beusen, A.H.W.; Mogollón, J.M.; Bouwman, A.F. Phosphorus for Sustainable Development Goal Target of Doubling Smallholder Productivity. *Nat. Sustain.* **2022**, *5*, 57–63. [CrossRef]
31. Pahalvi, H.N.; Rafiya, L.; Rashid, S.; Nisar, B.; Kamili, A.N. Chemical Fertilizers and Their Impact on Soil Health. In *Microbiota and Biofertilizers, Vol. 2: Ecofriendly Tools for Reclamation of Degraded Soil Environs*; Springer: Cham, Switzerland, 2021. [CrossRef]
32. Dincă, L.C.; Grenni, P.; Onet, C.; Onet, A. Fertilization and Soil Microbial Community: A Review. *Appl. Sci.* **2022**, *12*, 1198. [CrossRef]
33. Tu, P.; Zhang, G.; Cen, Y.; Huang, B.; Li, J.; Li, Y.; Deng, L.; Yuan, H. Phosphate Adsorption and Desorption Characteristics of Mgo-Modified Biochars from Different Raw Materials. *SSRN Electron. J.* **2022**. [CrossRef]
34. Tusar, H.M.; Uddin, M.K.; Mia, S.; Suhi, A.A.; Bin, S.; Wahid, A.; Kasim, S.; Sairi, N.A.; Alam, Z.; Anwar, F. Biochar-Acid Soil Interactions—A Review. *Sustainability* **2023**, *15*, 13366. [CrossRef]
35. Wang, C.; Luo, D.; Zhang, X.; Huang, R.; Cao, Y.; Liu, G.; Zhang, Y.; Wang, H. Biochar-Based Slow-Release of Fertilizers for Sustainable Agriculture: A Mini Review. *Environ. Sci. Ecotechnol.* **2022**, *10*, 100167. [CrossRef]
36. Conz, R.F.; Abbruzzini, T.F.; de Andrade, C.A.; Milori, D.M.B.P.; Cerri, C.E.P. Effect of Pyrolysis Temperature and Feedstock Type on Agricultural Properties and Stability of Biochars. *Agric. Sci.* **2017**, *8*, 914–933. [CrossRef]
37. Pan, S.Y.; Dong, C.D.; Su, J.F.; Wang, P.Y.; Chen, C.W.; Chang, J.S.; Kim, H.; Huang, C.P.; Hung, C.M. The Role of Biochar in Regulating the Carbon, Phosphorus, and Nitrogen Cycles Exemplified by Soil Systems. *Sustainability* **2021**, *13*, 5612. [CrossRef]
38. Jha, P.; Neenu, S.; Rashmi, I.; Meena, B.P.; Jatav, R.C.; Lakaria, B.L.; Biswas, A.K.; Singh, M.; Patra, A.K. Ameliorating Effects of Leucaena Biochar on Soil Acidity and Exchangeable Ions. *Commun. Soil Sci. Plant Anal.* **2016**, *47*, 1252–1262. [CrossRef]
39. Hou, L.; Liang, Q.; Wang, F. Mechanisms That Control the Adsorption–Desorption Behavior of Phosphate on Magnetite Nanoparticles: The Role of Particle Size and Surface Chemistry Characteristics. *RSC Adv.* **2020**, *10*, 2378–2388. [CrossRef] [PubMed]
40. Haddad, K.; Jellali, S.; Jeguirim, M.; Trabelsi, A.B.H.; Limousy, L. Investigations on Phosphorus Recovery from Aqueous Solutions by Biochars Derived from Magnesium-Pretreated Cypress Sawdust. *J. Environ. Manag.* **2018**, *216*, 305–314. [CrossRef]
41. Wu, L.; Zhang, S.; Wang, J.; Ding, X. Phosphorus Retention Using Iron (II/III) Modified Biochar in Saline-Alkaline Soils: Adsorption, Column and Field Tests. *Environ. Pollut.* **2020**, *261*, 114223. [CrossRef]
42. Cui, Q.; Xu, J.; Wang, W.; Tan, L.; Cui, Y.; Wang, T.; Li, G.; She, D.; Zheng, J. Phosphorus Recovery by Core-Shell γ-Al_2O_3/Fe_3O_4 Biochar Composite from Aqueous Phosphate Solutions. *Sci. Total Environ.* **2020**, *729*, 138892. [CrossRef]
43. Feng, Y.; Luo, Y.; He, Q.; Zhao, D.; Zhang, K.; Shen, S.; Wang, F. Performance and Mechanism of a Biochar-Based Ca-La Composite for the Adsorption of Phosphate from Water. *J. Environ. Chem. Eng.* **2021**, *9*, 105267. [CrossRef]
44. Yang, F.; Chen, Y.; Nan, H.; Pei, L.; Huang, Y.; Cao, X.; Xu, X.; Zhao, L. Metal Chloride-Loaded Biochar for Phosphorus Recovery: Noteworthy Roles of Inherent Minerals in Precursor. *Chemosphere* **2021**, *266*, 128991. [CrossRef] [PubMed]
45. Reyhanitabar, A.; Farhadi, E.; Ramezanzadeh, H.; Oustan, S. Effect of Pyrolysis Temperature and Feedstock Sources on Physico-chemical Characteristics of Biochar. *J. Agric. Sci. Technol.* **2020**, *22*, 547–561.
46. Zhou, L.; Xu, D.; Li, Y.; Pan, Q.; Wang, J.; Xue, L.; Howard, A. Phosphorus and Nitrogen Adsorption Capacities of Biochars Derived from Feedstocks at Different Pyrolysis Temperatures. *Water* **2019**, *11*, 1559. [CrossRef]
47. Tomczyk, A.; Sokołowska, Z.; Boguta, P. Biochar Physicochemical Properties: Pyrolysis Temperature and Feedstock Kind Effects. *Rev. Environ. Sci. Biotechnol.* **2020**, *19*, 191–215. [CrossRef]
48. Rodriguez-Franco, C.; Page-Dumroese, D.S. Woody Biochar Potential for Abandoned Mine Land Restoration in the U.S.: A Review. *Biochar* **2021**, *3*, 7–22. [CrossRef]
49. Jellali, S.; Hadroug, S.; Al-Wardy, M.; Al-Nadabi, H.; Nassr, N.; Jeguirim, M. Recent Developments in Metallic-Nanoparticles-Loaded Biochars Synthesis and Use for Phosphorus Recovery from Aqueous Solutions. A Critical Review. *J. Environ. Manag.* **2023**, *342*, 118307. [CrossRef] [PubMed]
50. Roberts, D.A.; Paul, N.A.; Dworjanyn, S.A.; Bird, M.I.; De Nys, R. Biochar from Commercially Cultivated Seaweed for Soil Amelioration. *Sci. Rep.* **2015**, *5*, 9665. [CrossRef]
51. Wondmagegn, S.; Esubalew, M.; Balemual, A.; Mhriet, S.; Nigusu, T.; Adane, W.; Tesfaw, M. Design and Development of a Modified Biomass Charcoal Production Kiln. *Ethiop. Int. J. Eng. Technol.* **2023**, *1*, 12–22. [CrossRef]
52. Garcia-Nunez, J.A.; Pelaez-Samaniego, M.R.; Garcia-Perez, M.E.; Fonts, I.; Abrego, J.; Westerhof, R.J.M.; Garcia-Perez, M. Historical Developments of Pyrolysis Reactors: A Review. *Energy Fuels* **2017**, *31*, 5751–5775. [CrossRef]
53. Tan, H.; Lee, C.T.; Ong, P.Y.; Wong, K.Y.; Bong, C.P.C.; Li, C.; Gao, Y. A Review on the Comparison between Slow Pyrolysis and Fast Pyrolysis on the Quality of Lignocellulosic and Lignin-Based Biochar. *IOP Conf. Ser. Mater. Sci. Eng.* **2021**, *1051*, 012075. [CrossRef]

54. Ercan, B.; Alper, K.; Ucar, S.; Karagoz, S. Comparative Studies of Hydrochars and Biochars Produced from Lignocellulosic Biomass via Hydrothermal Carbonization, Torrefaction and Pyrolysis. *J. Energy Inst.* **2023**, *109*, 101298. [CrossRef]
55. Tenic, E.; Ghogare, R.; Dhingra, A. Biochar—A Panacea for Agriculture or Just Carbon? *Horticulturae* **2020**, *6*, 37. [CrossRef]
56. Sun, D.; Hale, L.; Kar, G.; Soolanayakanahally, R.; Adl, S. Phosphorus Recovery and Reuse by Pyrolysis: Applications for Agriculture and Environment. *Chemosphere* **2018**, *194*, 682–691. [CrossRef]
57. Kumar, A.V.; Muninathan, K.; Arivazhagan, S.; Monish, N.; Ramanan, M.V.; Rao, V.S.; Baskar, G. Investigations on Carbonization Operating Conditions of ANSYS Customized Kiln for Charcoal Production from *Prosopis Juliflora* Biomass and ANN Model Prediction for Optimized Operating Conditions. *Fuel* **2023**, *350*, 128838. [CrossRef]
58. Akanji, M.A.; Al-Swadi, H.A.; Mousa Mousa, M.A.; Usama, M.; Ahmad, M.; Lubis, N.M.A.; Al-Farraj, A.S.F.; Al-Wabel, M.I. Synthesis and Characterization of Clay-Biochar Composites. In *Environmental Applications*; Springer Nature: Singapore, 2023; pp. 91–112. [CrossRef]
59. Shen, Q.; Wu, H. Rapid Pyrolysis of Biochar Prepared from Slow and Fast Pyrolysis: The Effects of Particle Residence Time on Char Properties. *Proc. Combust. Inst.* **2023**, *39*, 3371–3378. [CrossRef]
60. Yang, F.; Sui, L.; Tang, C.; Li, J.; Cheng, K.; Xue, Q. Sustainable Advances on Phosphorus Utilization in Soil via Addition of Biochar and Humic Substances. *Sci. Total Environ.* **2021**, *768*, 145106. [CrossRef]
61. Li, T.; Tong, Z.; Gao, B.; Li, Y.C.; Smyth, A.; Bayabil, H.K. Polyethyleneimine-Modified Biochar for Enhanced Phosphate Adsorption. *Environ. Sci. Pollut. Res.* **2020**, *27*, 7420–7429. [CrossRef]
62. Jung, K.W.; Ahn, K.H. Fabrication of Porosity-Enhanced MgO/Biochar for Removal of Phosphate from Aqueous Solution: Application of a Novel Combined Electrochemical Modification Method. *Bioresour. Technol.* **2016**, *200*, 1029–1032. [CrossRef]
63. Zheng, Q.; Yang, L.; Song, D.; Zhang, S.; Wu, H.; Li, S.; Wang, X. High Adsorption Capacity of Mg–Al-Modified Biochar for Phosphate and Its Potential for Phosphate Interception in Soil. *Chemosphere* **2020**, *259*, 127469. [CrossRef] [PubMed]
64. Biswas, B.; Rahman, T.; Sakhakarmy, M.; Jahromi, H.; Eisa, M.; Baltrusaitis, J.; Lamba, J.; Torbert, A.; Adhikari, S. Phosphorus Adsorption Using Chemical and Metal Chloride Activated Biochars: Isotherms, Kinetics and Mechanism Study. *Heliyon* **2023**, *9*, e19830. [CrossRef] [PubMed]
65. Oginni, O.; Yakaboylu, G.A.; Singh, K.; Sabolsky, E.M.; Unal-Tosun, G.; Jaisi, D.; Khanal, S.; Shah, A. Phosphorus Adsorption Behaviors of MgO Modified Biochars Derived from Waste Woody Biomass Resources. *J. Environ. Chem. Eng.* **2020**, *8*, 103723. [CrossRef]
66. Sachdeva, V.; Hussain, N.; Husk, B.R.; Whalen, J.K. Biochar-Induced Soil Stability Influences Phosphorus Retention in a Temperate Agricultural Soil. *Geoderma* **2019**, *351*, 71–75. [CrossRef]
67. Hafeez, A.; Pan, T.; Tian, J.; Cai, K. Modified Biochars and Their Effects on Soil Quality: A Review. *Environments* **2022**, *9*, 60. [CrossRef]
68. Deng, Y.; Li, M.; Zhang, Z.; Liu, Q.; Jiang, K.; Tian, J.; Zhang, Y.; Ni, F. Comparative Study on Characteristics and Mechanism of Phosphate Adsorption on Mg/Al Modified Biochar. *J. Environ. Chem. Eng.* **2021**, *9*, 105079. [CrossRef]
69. Qin, Y.; Wu, X.; Huang, Q.; Beiyuan, J.; Wang, J.; Liu, J.; Yuan, W.; Nie, C.; Wang, H. Phosphate Removal Mechanisms in Aqueous Solutions by Three Different Fe-Modified Biochars. *Int. J. Environ. Res. Public Health* **2023**, *20*, 326. [CrossRef]
70. Zhang, P.; Xue, B.; Jiao, L.; Meng, X.; Zhang, L.; Li, B.; Sun, H. Preparation of Ball-Milled Phosphorus-Loaded Biochar and Its Highly Effective Remediation for Cd- and Pb-Contaminated Alkaline Soil. *Sci. Total Environ.* **2022**, *813*, 152648. [CrossRef]
71. Yang, Y.; Piao, Y.; Wang, R.; Su, Y.; Qiu, J.; Liu, N. Mechanism of Biochar Functional Groups in the Catalytic Reduction of Tetrachloroethylene by Sulfides. *Environ. Pollut.* **2022**, *300*, 118921. [CrossRef]
72. Aktar, S.; Hossain, M.A.; Rathnayake, N.; Patel, S.; Gasco, G.; Mendez, A.; de Figueiredo, C.; Surapaneni, A.; Shah, K.; Paz-Ferreiro, J. Effects of Temperature and Carrier Gas on Physico-Chemical Properties of Biochar Derived from Biosolids. *J. Anal. Appl. Pyrolysis* **2022**, *164*, 105542. [CrossRef]
73. Han, L.; Zhang, E.; Yang, Y.; Sun, K.; Fang, L. Highly Efficient U(VI) Removal by Chemically Modified Hydrochar and Pyrochar Derived from Animal Manure. *J. Clean. Prod.* **2020**, *264*, 121542. [CrossRef]
74. Zhang, P.; Bing, X.; Jiao, L.; Xiao, H.; Li, B.; Sun, H. Amelioration Effects of Coastal Saline-Alkali Soil by Ball-Milled Red Phosphorus-Loaded Biochar. *Chem. Eng. J.* **2022**, *431*, 133904. [CrossRef]
75. Dai, L.; Lu, Q.; Zhou, H.; Shen, F.; Liu, Z.; Zhu, W.; Huang, H. Tuning Oxygenated Functional Groups on Biochar for Water Pollution Control: A Critical Review. *J. Hazard. Mater.* **2021**, *420*, 126547. [CrossRef]
76. Arbelaez Breton, L.; Mahdi, Z.; Pratt, C.; El Hanandeh, A. Modification of Hardwood Derived Biochar to Improve Phosphorus Adsorption. *Environments* **2021**, *8*, 41. [CrossRef]
77. Liu, L.; Li, Y.; Fan, S. Preparation of KOH and H3PO4 Modified Biochar and Its Application in Methylene Blue Removal from Aqueous Solution. *Processes* **2019**, *7*, 891. [CrossRef]
78. Deng, W.; Zhang, D.; Zheng, X.; Ye, X.; Niu, X.; Lin, Z.; Fu, M.; Zhou, S. Adsorption Recovery of Phosphate from Waste Streams by Ca/Mg-Biochar Synthesis from Marble Waste, Calcium-Rich Sepiolite and Bagasse. *J. Clean. Prod.* **2021**, *288*, 125638. [CrossRef]
79. Tu, P.; Zhang, G.; Cen, Y.; Huang, B.; Li, J.; Li, Y.; Deng, L.; Yuan, H. Enhanced Phosphate Adsorption and Desorption Characteristics of MgO-Modified Biochars Prepared via Direct Co-Pyrolysis of MgO and Raw Materials. *Bioresour. Bioprocess.* **2023**, *10*, 49. [CrossRef]
80. Li, C.; Xie, S.; Wang, Y.; Jiang, R.; Wang, X.; Lv, N.; Pan, X.; Cai, G.; Yu, G.; Wang, Y. Multi-Functional Biochar Preparation and Heavy Metal Immobilization by Co-Pyrolysis of Livestock Feces and Biomass Waste. *Waste Manag.* **2021**, *134*, 241–250. [CrossRef]

81. Sun, J.; Norouzi, O.; Mašek, O. A State-of-the-Art Review on Algae Pyrolysis for Bioenergy and Biochar Production. *Bioresour. Technol.* **2022**, *346*, 126258. [CrossRef]
82. Yadav, A.; Yadav, K.; Ahmad, R.; Abd-Elsalam, K.A. Emerging Frontiers in Nanotechnology for Precision Agriculture: Advancements, Hurdles and Prospects. *Agrochemicals* **2023**, *2*, 220–256. [CrossRef]
83. Kamali, N.; Mehrabadi, A.R.; Mirabi, M.; Zahed, M.A. Synthesis of Vinasse-Dolomite Nanocomposite Biochar via a Novel Developed Functionalization Method to Recover Phosphate as a Potential Fertilizer Substitute. *Front. Environ. Sci. Eng.* **2020**, *14*, 70. [CrossRef]
84. Yuan, J.; Wen, Y.; Ruiz, G.; Sun, W.; Ma, X. Enhanced Phosphorus Removal and Recovery by Metallic Nanoparticles-Modified Biochar. *Nanotechnol. Environ. Eng.* **2020**, *5*, 26. [CrossRef]
85. Sun, E.; Qian, Y.; Jin, H.; Huang, H.; Wu, G.; Chang, Z.; Huang, H. Structure of Straw Biochar/Amino Resin Doping NanoSiO_2 and Its Phosphorus Removal Characteristic. *Nongye Gongcheng Xuebao/Trans. Chin. Soc. Agric. Eng.* **2017**, *33*, 211–218. [CrossRef]
86. Cui, R.; Ma, J.; Jiao, G.; Sun, R. Efficient Removal of Phosphate from Aqueous Media Using Magnetic Bimetallic Lanthanum-iron-Modified Sulfonylmethylated Lignin Biochar. *Int. J. Biol. Macromol.* **2023**, *247*, 125809. [CrossRef]
87. Yin, Q.; Wang, R.; Zhao, Z. Application of Mg–Al-Modified Biochar for Simultaneous Removal of Ammonium, Nitrate, and Phosphate from Eutrophic Water. *J. Clean. Prod.* **2018**, *176*, 230–240. [CrossRef]
88. Peng, Y.; Chen, Q.; Guan, C.Y.; Yang, X.; Jiang, X.; Wei, M.; Tan, J.; Li, X. Metal Oxide Modified Biochars for Fertile Soil Management: Effects on Soil Phosphorus Transformation, Enzyme Activity, Microbe Community, and Plant Growth. *Environ. Res.* **2023**, *231*, 116258. [CrossRef]
89. Zhang, Y.; Zhang, W.; Zhang, H.; He, D. Nano-Zero-Valent Zinc-Modified Municipal Sludge Biochar for Phosphorus Removal. *Molecules* **2023**, *28*, 3231. [CrossRef]
90. Wang, Y.; Xie, X.; Chen, X.; Huang, C.; Yang, S. Biochar-Loaded Ce^{3+}-Enriched Ultra-Fine Ceria Nanoparticles for Phosphate Adsorption. *J. Hazard. Mater.* **2020**, *396*, 122626. [CrossRef] [PubMed]
91. Mahmoud, E.; El Baroudy, A.; Ali, N.; Sleem, M. Spectroscopic Studies on the Phosphorus Adsorption in Salt-Affected Soils with or without Nano-Biochar Additions. *Environ. Res.* **2020**, *184*, 109277. [CrossRef]
92. Zhu, D.; Yang, H.; Chen, X.; Chen, W.; Cai, N.; Chen, Y.; Zhang, S.; Chen, H. Temperature-Dependent Magnesium Citrate Modified Formation of MgO Nanoparticles Biochar Composites with Efficient Phosphate Removal. *Chemosphere* **2021**, *274*, 129904. [CrossRef] [PubMed]
93. Bahuguna, A.; Sharma, S.; Dadarwal, B.K. Biochar as Carbon Sequestration Potential. *Marumegh* **2021**, *6*, 12–14.
94. Sheng, Y.; Zhan, Y.; Zhu, L. Reduced Carbon Sequestration Potential of Biochar in Acidic Soil. *Sci. Total Environ.* **2016**, *572*, 129–137. [CrossRef]
95. Yang, X.; Zhang, S.; Ju, M.; Liu, L. Preparation and Modification of Biochar Materials and Their Application in Soil Remediation. *Appl. Sci.* **2019**, *9*, 1365. [CrossRef]
96. Nan, H.; Yang, F.; Zhao, L.; Mašek, O.; Cao, X.; Xiao, Z. Interaction of Inherent Minerals with Carbon during Biomass Pyrolysis Weakens Biochar Carbon Sequestration Potential. *ACS Sustain. Chem. Eng.* **2019**, *7*, 1591–1599. [CrossRef]
97. Jabborova, D.; Annapurna, K.; Azimov, A.; Tyagi, S.; Pengani, K.R.; Sharma, P.; Vikram, K.V.; Poczai, P.; Nasif, O.; Ansari, M.J.; et al. Co-Inoculation of Biochar and Arbuscular Mycorrhizae for Growth Promotion and Nutrient Fortification in Soybean under Drought Conditions. *Front. Plant Sci.* **2022**, *13*, 947547. [CrossRef]
98. Qi, X.; Yin, H.; Zhu, M.; Yu, X.; Shao, P.; Dang, Z. MgO-Loaded Nitrogen and Phosphorus Self-Doped Biochar: High-Efficient Adsorption of Aquatic Cu^{2+}, Cd^{2+}, and Pb^{2+} and Its Remediation Efficiency on Heavy Metal Contaminated Soil. *Chemosphere* **2022**, *294*, 133733. [CrossRef]
99. Liu, M.; Almatrafi, E.; Zhang, Y.; Xu, P.; Song, B.; Zhou, C.; Zeng, G.; Zhu, Y. A Critical Review of Biochar-Based Materials for the Remediation of Heavy Metal Contaminated Environment: Applications and Practical Evaluations. *Sci. Total Environ.* **2022**, *806*, 150531. [CrossRef]
100. Gu, W.; Wang, Y.; Feng, Z.; Wu, D.; Zhang, H.; Yuan, H.; Sun, Y.; Xiu, L.; Chen, W.; Zhang, W. Long-Term Effects of Biochar Application with Reduced Chemical Fertilizer on Paddy Soil Properties and Japonica Rice Production System. *Front. Environ. Sci.* **2022**, *10*, 902752. [CrossRef]
101. Yin, Q.; Liu, M.; Li, Y.; Li, H.; Wen, Z. Computational Study of Phosphate Adsorption on Mg/Ca Modified Biochar Structure in Aqueous Solution. *Chemosphere* **2021**, *269*, 129374. [CrossRef] [PubMed]
102. Bolton, L.; Joseph, S.; Greenway, M.; Donne, S.; Munroe, P.; Marjo, C.E. Phosphorus Adsorption onto an Enriched Biochar Substrate in Constructed Wetlands Treating Wastewater. *Ecol. Eng. X* **2019**, *1*, 100005. [CrossRef]
103. Liu, L.Y.; Zhang, C.H.; Chen, S.R.; Ma, L.; Li, Y.M.; Lu, Y.F. Phosphate Adsorption Characteristics of $La(OH)_3$-Modified, Canna-Derived Biochar. *Chemosphere* **2022**, *286*, 131773. [CrossRef]
104. Shin, H.; Tiwari, D.; Kim, D.J. Phosphate Adsorption/Desorption Kinetics and P Bioavailability of Mg-Biochar from Ground Coffee Waste. *J. Water Process Eng.* **2020**, *37*, 101484. [CrossRef]
105. Amin, F.R.; Huang, Y.; He, Y.; Zhang, R.; Liu, G.; Chen, C. Biochar Applications and Modern Techniques for Characterization. *Clean. Technol. Environ. Policy* **2016**, *18*, 1457–1473. [CrossRef]
106. Sacko, O.; Whiteman, R.; Kharel, G.; Kumar, S.; Lee, J.W. Sustainable Chemistry: Solubilization of Phosphorus from Insoluble Phosphate Material Hydroxyapatite with Ozonized Biochar. *ACS Sustain. Chem. Eng.* **2020**, *8*, 7068–7077. [CrossRef]

107. Xu, D.Y.; Jin, J.; Yan, Y.; Han, L.F.; Kang, M.J.; Wang, Z.Y.; Zhao, Y.; Sun, K. Characterization of Biochar by X-ray Photoelectron Spectroscopy and 13C Nuclear Magnetic Resonance. *Guang Pu Xue Yu Guang Pu Fen Xi/Spectrosc. Spectr. Anal.* **2014**, *34*, 3415–3418. [CrossRef]
108. Gondim, R.S.; Muniz, C.R.; Lima, C.E.P.; Dos Santos, C.L.A. Explaining the Water-Holding Capacity of Biochar by Scanning Electron Microscope Images. *Rev. Caatinga* **2018**, *31*, 972–979. [CrossRef]
109. Lago, B.C.; Silva, C.A.; Melo, L.C.A.; de Morais, E.G. Predicting Biochar Cation Exchange Capacity Using Fourier Transform Infrared Spectroscopy Combined with Partial Least Square Regression. *Sci. Total Environ.* **2021**, *794*, 148762. [CrossRef]
110. Park, J.; Yoo, S.; Lim, K.H.; Rojas, O.J.; Hubbe, M.A.; Park, S. Impact of Oxidative Carbonization on Structure Development of Loblolly Pine-Derived Biochar Investigated by Nuclear Magnetic Resonance Spectroscopy and X-ray Photoelectron Spectroscopy. *Diam. Relat. Mater.* **2019**, *96*, 140–147. [CrossRef]
111. Malucelli, L.C.; Silvestre, G.F.; Carneiro, J.; Vasconcelos, E.C.; Guiotoku, M.; Maia, C.M.B.F.; Carvalho Filho, M.A.S. Biochar Higher Heating Value Estimative Using Thermogravimetric Analysis. *J. Therm. Anal. Calorim.* **2020**, *139*, 2215–2220. [CrossRef]
112. Pradana, Y.S.; Rochim, N.; Mukaffa, H.S.; Satriawan, H.B.; Hidayat, A.; Budiman, A. Activation of Coconut Shell—Randu Wood Biochar and Its Use as Heterogeneous Catalyst Support for Biodiesel Production. *IOP Conf. Ser. Mater. Sci. Eng.* **2019**, *543*, 012064. [CrossRef]
113. Ukoba, K.; Jen, T.-C. Biochar and Application of Machine Learning: A Review. In *Biochar—Productive Technologies, Properties and Applications*; BoD—Books on Demand: Norderstedt, Germany, 2023.
114. Ke, B.; Nguyen, H.; Bui, X.N.; Bui, H.B.; Nguyen-Thoi, T. Prediction of the Sorption Efficiency of Heavy Metal onto Biochar Using a Robust Combination of Fuzzy C-Means Clustering and Back-Propagation Neural Network. *J. Environ. Manag.* **2021**, *293*, 112808. [CrossRef] [PubMed]
115. Osman, A.I.; Zhang, Y.; Lai, Z.Y.; Rashwan, A.K.; Farghali, M.; Ahmed, A.A.; Liu, Y.; Fang, B.; Chen, Z.; Al-Fatesh, A. Machine Learning and Computational Chemistry to Improve Biochar Fertilizers: A Review. *Environ. Chem. Lett.* **2023**, *6*, 3159–3244. [CrossRef]
116. Xu, Y.; Wang, Z.; Nairat, S.; Zhou, J.; He, Z. Artificial Intelligence-Assisted Prediction of Effluent Phosphorus in a Full-Scale Wastewater Treatment Plant with Missing Phosphorus Input and Removal Data. *ACS ES T Water* **2022**, *3*, 880–889. [CrossRef]
117. Liu, J.; Xu, Z.; Zhang, W. Unraveling the Role of Fe in As(III & V) Removal by Biochar via Machine Learning Exploration. *Sep. Purif. Technol.* **2023**, *311*, 123245. [CrossRef]
118. Wu, Y.; Li, Y.; Jiang, Z.; Xu, Z.; Yang, M.; Ding, J.; Zhang, C. Machine Learning Prediction of Phosphate Adsorption on Six Different Metal-Containing Adsorbents. *ACS ES T Eng.* **2023**, *3*, 1135–1146. [CrossRef]
119. Haq, Z.U.; Ullah, H.; Khan, M.N.A.; Naqvi, S.R.; Ahad, A.; Amin, N.A.S. Comparative Study of Machine Learning Methods Integrated with Genetic Algorithm and Particle Swarm Optimization for Bio-Char Yield Prediction. *Bioresour. Technol.* **2022**, *363*, 128008. [CrossRef]
120. Wong, Y.J.; Arumugasamy, S.K.; Chung, C.H.; Selvarajoo, A.; Sethu, V. Comparative Study of Artificial Neural Network (ANN), Adaptive Neuro-Fuzzy Inference System (ANFIS) and Multiple Linear Regression (MLR) for Modeling of Cu (II) Adsorption from Aqueous Solution Using Biochar Derived from Rambutan (*Nephelium lappaceum*) Peel. *Environ. Monit. Assess.* **2020**, *192*, 31085–31101. [CrossRef] [PubMed]
121. Sultana, S.; Awal, S.; Shaika, N.A.; Khan, S. Cyanobacterial Blooms in Earthen Aquaculture Ponds and Their Impact on Fisheries and Human Health in Bangladesh. *Aquac. Res.* **2022**, *15*, 5129–5141. [CrossRef]
122. Yang, W.; Zhang, X.; Wu, L.; Rensing, C.; Xing, S. Short-Term Application of Magnesium Fertilizer Affected Soil Microbial Biomass, Activity, and Community Structure. *J. Soil Sci. Plant Nutr.* **2021**, *21*, 675–689. [CrossRef]
123. Novais, S.V.; Zenero, M.D.O.; Barreto, M.S.C.; Montes, C.R.; Cerri, C.E.P. Phosphorus Removal from Eutrophic Water Using Modified Biochar. *Sci. Total Environ.* **2018**, *633*, 825–835. [CrossRef]
124. Walling, E.; Vaneeckhaute, C. Greenhouse Gas Emissions from Inorganic and Organic Fertilizer Production and Use: A Review of Emission Factors and Their Variability. *J. Environ. Manag.* **2020**, *276*, 111211. [CrossRef]
125. Li, H.; Yan, T.; Fu, T.; Hao, Y.; Li, J.; Tan, Y.; Li, Z.; Peng, Y.; Chen, X.; Chang, J.; et al. Biochar Combined with Magnesium Fertilizer Improves Cabbage (*Brassica oleraceae* L.) Yield by Modulating Physicochemical Characteristics and the Bacterial Community in Acidic Soil. *Soil Use Manag.* **2023**, *4*, 1422–1436. [CrossRef]
126. Rogers, P.M.; Fridahl, M.; Yanda, P.; Hansson, A.; Pauline, N.; Haikola, S. Socio-Economic Determinants for Biochar Deployment in the Southern Highlands of Tanzania. *Energies* **2022**, *15*, 144. [CrossRef]
127. Antonious, G.F.; Chiluwal, A.; Nepal, A. Chitin, Biochar, and Animal Manures Impact on Eggplant and Green Pepper Yield and Quality. *Agric. Sci.* **2023**, *14*, 368–383. [CrossRef]
128. Bista, P.; Ghimire, R.; Machado, S.; Pritchett, L. Biochar Effects on Soil Properties and Wheat Biomass Vary with Fertility Management. *Agronomy* **2019**, *9*, 623. [CrossRef]
129. Wali, F.; Naveed, M.; Bashir, M.A.; Asif, M.; Ahmad, Z.; Alkahtani, J.; Alwahibi, M.S.; Elshikh, M.S. Formulation of Biochar-Based Phosphorus Fertilizer and Its Impact on Both Soil Properties and Chickpea Growth Performance. *Sustainability* **2020**, *12*, 9528. [CrossRef]
130. Khan, A.A.; Gul, J.; Naqvi, S.R.; Ali, I.; Farooq, W.; Liaqat, R.; AlMohamadi, H.; Štěpanec, L.; Juchelková, D. Recent Progress in Microalgae-Derived Biochar for the Treatment of Textile Industry Wastewater. *Chemosphere* **2022**, *306*, 135565. [CrossRef] [PubMed]

131. Zhang, Q.; Li, J.; Chen, D.; Xiao, W.; Zhao, S.; Ye, X.; Li, H. In Situ Formation of $Ca(OH)_2$ Coating Shell to Extend the Longevity of Zero-Valent Iron Biochar Composite Derived from Fe-Rich Sludge for Aqueous Phosphorus Removal. *Sci. Total Environ.* **2023**, *854*, 158794. [CrossRef]
132. Elkhlifi, Z.; Iftikhar, J.; Sarraf, M.; Ali, B.; Saleem, M.H.; Ibranshahib, I.; Bispo, M.D.; Meili, L.; Ercisli, S.; Torun Kayabasi, E.; et al. Potential Role of Biochar on Capturing Soil Nutrients, Carbon Sequestration and Managing Environmental Challenges: A Review. *Sustainability* **2023**, *15*, 2527. [CrossRef]
133. Gillingham, M.D.; Gomes, R.L.; Ferrari, R.; West, H.M. Sorption, Separation and Recycling of Ammonium in Agricultural Soils: A Viable Application for Magnetic Biochar? *Sci. Total Environ.* **2022**, *812*, 151440. [CrossRef] [PubMed]
134. Tan, S.; Narayanan, M.; Huong, D.T.T.; Ito, N.; Unpaprom, Y.; Pugazhendhi, A.; Chi, N.T.L.; Liu, J. A Perspective on the Interaction between Biochar and Soil Microbes: A Way to Regain Soil Eminence. *Environ. Res.* **2022**, *214*, 113832. [CrossRef]
135. Heidarian Dehkordi, R.; Pelgrum, H.; Meersmans, J. High Spatio-Temporal Monitoring of Century-Old Biochar Effects on Evapotranspiration through the ETLook Model: A Case Study with UAV and Satellite Image Fusion Based on Additive Wavelet Transform (AWT). *GISci. Remote Sens.* **2022**, *59*, 111–141. [CrossRef]
136. Shaikh, T.A.; Rasool, T.; Lone, F.R. Towards Leveraging the Role of Machine Learning and Artificial Intelligence in Precision Agriculture and Smart Farming. *Comput. Electron. Agric.* **2022**, *198*, 107119. [CrossRef]
137. Yang, Q.; Mašek, O.; Zhao, L.; Nan, H.; Yu, S.; Yin, J.; Li, Z.; Cao, X. Country-Level Potential of Carbon Sequestration and Environmental Benefits by Utilizing Crop Residues for Biochar Implementation. *Appl. Energy* **2021**, *282*, 116275. [CrossRef]
138. Kumar, A.; Bhattacharya, T.; Mukherjee, S.; Sarkar, B. A Perspective on Biochar for Repairing Damages in the Soil–Plant System Caused by Climate Change-Driven Extreme Weather Events. *Biochar* **2022**, *4*, 22. [CrossRef]
139. Song, F.; Li, T.; Shi, Q.; Guo, F.; Bai, Y.; Wu, F.; Xing, B. Novel Insights into the Molecular-Level Mechanism Linking the Chemical Diversity and Copper Binding Heterogeneity of Biochar-Derived Dissolved Black Carbon and Dissolved Organic Matter. *Environ. Sci. Technol.* **2021**, *55*, 1624–11636. [CrossRef]
140. Das, S.K.; Ghosh, G.K.; Avasthe, R.K.; Sinha, K. Compositional Heterogeneity of Different Biochar: Effect of Pyrolysis Temperature and Feedstocks. *J. Environ. Manag.* **2021**, *278*, 111501. [CrossRef]
141. Zilberman, D.; Laird, D.; Rainey, C.; Song, J.; Kahn, G. Biochar Supply-Chain and Challenges to Commercialization. *GCB Bioenergy* **2023**, *15*, 7–23. [CrossRef]
142. Xiang, L.; Liu, S.; Ye, S.; Yang, H.; Song, B.; Qin, F.; Shen, M.; Tan, C.; Zeng, G.; Tan, X. Potential Hazards of Biochar: The Negative Environmental Impacts of Biochar Applications. *J. Hazard. Mater.* **2021**, *420*, 126611. [CrossRef]
143. El-Naggar, A.; El-Naggar, A.H.; Shaheen, S.M.; Sarkar, B.; Chang, S.X.; Tsang, D.C.W.; Rinklebe, J.; Ok, Y.S. Biochar Composition-Dependent Impacts on Soil Nutrient Release, Carbon Mineralization, and Potential Environmental Risk: A Review. *J. Environ. Manag.* **2019**, *241*, 458–467. [CrossRef]

land

MDPI

Article

Water-Nutrient Coupling Strategies That Improve the Carbon, Nitrogen Metabolism, and Yield of Cucumber under Sandy Cultivated Land

Xinchao Ma [1,2], Zhanming Tan [1,2,*], Yunxia Cheng [1,2], Tingting Wang [1,2], Man Cao [1,2], Zhengying Xuan [1,2] and Hongbin Du [1,2]

[1] College of Horticulture and Forestry, Tarim University, Aral 843300, China; 120220090@taru.edu.cn (X.M.)
[2] Xinjiang Production & Construction Corps Key Laboratory of Facility Agriculture, Tarim University, Aral 843300, China
* Correspondence: tlmdxtzm@taru.edu.cn

Abstract: The purpose of this study was to explore the carbon and nitrogen metabolism mechanisms of sand-cultivated cucumbers under different deficit irrigation–nitrogen management strategies and provide a theoretical basis for their greenhouse management. This study set up two factors, the deficit irrigation level and the nitrogen application rate, and conducted an experiment on deficit irrigation–nitrogen coupling of sand-cultivated cucumbers using a quadratic saturation D–optimal design. Seven treatments were set up in the experiment, to measure the soluble sugar and protein contents, as well as the activity of key enzymes for carbon and nitrogen metabolism at five different growth stages. The results indicate that the 80% irrigation with 623 kg N hm^{-2} (IN4) treatment significantly improved the soluble sugar, protein, and actual leaf nitrogen contents of cucumber at the five different growth stages and, as a result, achieved higher sucrose synthase (SS) and sucrose phosphate synthase (SPS) activities in the cucumber leaves. Furthermore, such improvements were due to the reduction in oxidative damage of sand–cultivated cucumber at various growth stages. The IN4 and 89% irrigation with 1250 kg N hm^{-2} (IN5) treatments significantly increased the activities of RuBisCO, catalase (CAT), peroxidise (POD), and superoxide dismutase (SOD) at various growth stages of sand-cultivated cucumber. The higher activities of glutamate dehydrogenase (GLDH), glutamate synthase (GOGAT), nitrate reductase (NR), glutamine synthase (GS), acid invertase enzyme (AIE), neutral invertase enzyme (NIE), and better antioxidative enzyme activities were recorded under the IN4 treatments at various growth stages, which effectively improve (69.6%) cucumber yield. The soil properties, carbon and nitrogen metabolism, and antioxidant metabolism were positively correlated with sand-cultivated cucumber yield in a greenhouse. We concluded that the IN4 treatment was the better deficit irrigation–nitrogen management strategy because it considerably improves carbon and nitrogen metabolism, antioxidant enzyme activities, and sand–cultivated cucumber yield in a greenhouse.

Keywords: water–nitrogen coupling; carbon and nitrogen metabolism; antioxidant metabolism; soil properties; sand-cultivated cucumber yield; greenhouse

Citation: Ma, X.; Tan, Z.; Cheng, Y.; Wang, T.; Cao, M.; Xuan, Z.; Du, H. Water-Nutrient Coupling Strategies That Improve the Carbon, Nitrogen Metabolism, and Yield of Cucumber under Sandy Cultivated Land. *Land* **2024**, *13*, 958. https://doi.org/10.3390/land13070958

Academic Editors: Shahzad Ali, Qianmin Jia, Jiahua Zhang and Sajid Ali

Received: 28 May 2024
Revised: 25 June 2024
Accepted: 26 June 2024
Published: 29 June 2024

1. Introduction

For decades, world agriculture has been challenged by water shortages and nitrogen pollution [1]. Blindly increasing the amounts of irrigation and chemical fertilizer applied can improve vegetable yield, but this approach has caused several problems, such as a decline in vegetable quality, secondary soil salinization, and energy waste [2,3]. Therefore, it is an important task facing modern agriculture to reduce the emissions of agricultural pollutants to the minimum while maintaining the production and quality of crops. Improvements in irrigation systems and the optimization of the application of nitrogen fertilizer are effective strategies to solve this problem [4–6]. Over the past decade, accurate and

efficient irrigation and fertilization management has become a major issue in agricultural production [7], particularly in drought and half-drought areas [8]. Ali et al. [9] estimated that, by 2050, drought will seriously affect the growth of more than 50% of crops that can be cultivated. There is rapid progress in the development of economical and efficient fertilization in the greenhouse water-saving stage of fertilizer irrigation and irrigation [10,11]. Therefore, it is necessary to maintain the amount of production of crops and to control the water-saving irrigation nitrogen management measures to increase the production of cucumber under sandy conditions.

Drought stress adversely affects the content of soluble protein (SP) in cucumber leaves, thereby affecting plant sucrose content [11]. Under drought conditions, irrigation promotes plant tissue development and causes a significant increase in nitrogen and SPS content [12]. However, water stress adversely affects the biochemical and physiological processes of plants [13]. The changes in these biochemical and physiological processes also affect plant growth and eventually reduce the production of cucumbers [14]. These results suggest that alternate irrigation strategies can improve the water use efficiency [15] of crops without significantly reducing production and can improve the quality of fruit [16] at the same time. In addition to moisture management, nitrogen nutrition is also an important plant macronutrient, which is an important component of proteins and enzymes and is very important for plant growth, production, and the quality of fruit. Many studies have investigated the combination of irrigation and nitrogen supply [17,18]. Because of the serious waste of resources caused by unreasonable irrigation fertilization, water utilization efficiency is low; groundwater contamination is serious, and the base and production efficiency of soil are low [19,20].

The irrigation nitrogen coupling strategy has a major beneficial effect on the plant–soil system by improving soil structure and permeability to increase the salt leaching rate [21,22], providing essential nutrients for plants [23], and rebuilding microbial activity and populations [24]. Research has shown that, under insufficient irrigation conditions, irrigation mainly improves the quality of cucumber fruits by increasing the content of soluble solids and vitamin C as well as the sugar-to-acid ratio [25]. A lower N supply reduces the quantity and yield of fruits, while it enhances some quality attributes of fruits, manifested by greater hardness and a higher sugar concentration [26].

Thus, oxidative damage adversely affects plant performance [27]. However, crops have developed an advanced antioxidant defense system using enzymes such as superoxide dismutase (SOD), peroxide (POD), and catalase (CAT) [28]. Therefore, it is an important strategy to increase the photosynthetic capacity of plants by raising the activity of SOD, POD, Rubisco, and CAT in the leaves under dry conditions [29]. Water stress may cause a significant decline in the production and quality of vegetable crops [30], which are highly sensitive to water stress. The water–nitrogen binding strategy affects the nutrient absorption of the root system of crops by changing mineral nutrients in the root environment and can affect the overall growth of crops [31]. Within a certain range, improving the water–nitrogen binding strategy can reduce the loss of mineral nutrients and avoid the waste of fertilizer [32], thereby reducing production costs and groundwater pollution and raising the production of crops [33]. Therefore, it is important to understand the response and adaptation to the drought conditions of high-value vegetable crops, to establish effective crop production strategies and to increase the productivity of vegetable crops [34].

Cucumber is one of the most economically relevant vegetable crops in China [35]. In China, cucumber is a vegetable crop commonly seen in agricultural production systems and is a protected vegetable production system. However, strategies for protecting cucumber from oxidative damage and retarding the aging process are important to improve antioxidant defense systems [36]. However, as far as we know, studies have not yet been conducted to understand the response to oxidative stress by drought in a greenhouse of cucumber, soil properties, leaf nitrogen content, and cucumber yield. Therefore, the coordinated effects of irrigation–nitrogen coupling strategies on carbon and nitrogen metabolism mechanisms, antioxidant systems, rubisco activity, nitrogen content, and sand-cultivated

cucumber yields were investigated. The results are predicted to provide some explanations for the increase in cucumber yield by irrigation–nitrogen coupling strategies in a greenhouse.

2. Materials and Methods

2.1. Research Study Area

The experiment was conducted from March to July 2021 at the Horticultural Experiment Station of Tarim University (81°17′ E, 40°32′ N, altitude 990 m) in an energy–saving greenhouse. The cucumber variety "Yushengmei", which was used by local farmers, was planted. The soil physicochemical properties of the research site were Eum–Orthrosols (Chinese Soil Taxonomy), with an organic matter = 6.53 g kg^{-1}, total nitrogen (TN) = 1.29 g kg^{-1}, total phosphorus (TP) = 0.24 g kg^{-1}, total potassium (TK) = 0.46 g kg^{-1}, available nitrogen (AN) = 6.61 mg kg^{-1}, available phosphorus (AP) = 8.01 mg kg^{-1}, available potassium (AK) = 38.34 mg kg^{-1}, nitrate nitrogen = 0.12 mg kg^{-1}, ammonium nitrogen = 3.32 mg kg^{-1}, pH value of 7.49, and EC value of 3.16 μS/cm, respectively. The experiment adopts slot cultivation, with an area of 0.5 × 2.6 m = 1.3 m^2 and a depth of 0.4 m for each cultivation slot. The plant spacing is set at 0.25 m, the large row spacing is 0.6 m, and the small row spacing is 0.3 m. Double–row cultivation is carried out, with 20 cucumbers planted in each plot and 50,000 seedlings preserved per hectare. A total of 7 treatments were set up, each with 3 replicates, for a total of 21 treatments with 420 cucumber plants. We installed a row of protective cultivation tanks on both sides of the greenhouse.

2.2. Experimental Design

The experiment was conducted with two factors: the irrigation level and nitrogen application rate. A quadratic saturation D–optimal design (6–point design with $p = 2$) was adopted, and a treatment IN7 with the highest code value was added. Temperature and humidity are collected with a temperature and humidity RR-9100 logger (Beijing Yugen technology co led., Beijing China) in Figure 1. This treatment was only used as a reference and did not participate in regression analysis to maintain the superiority of the original plan (Table 1).

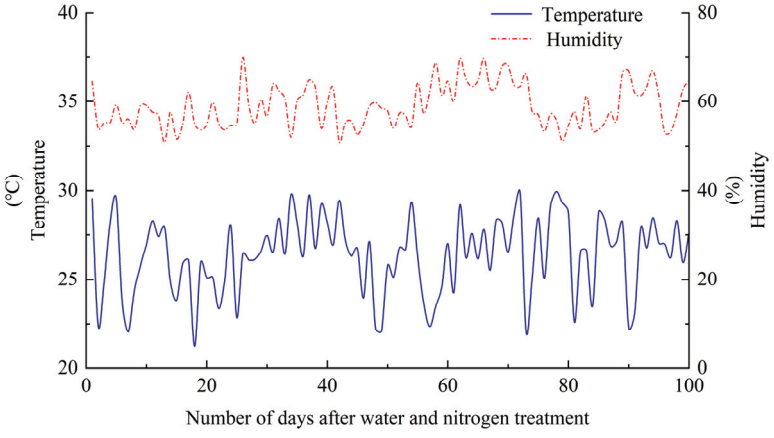

Figure 1. Temperature and humidity at the experimental site.

The irrigation amount is calculated according to Formula (1), with the maximum irrigation limit set at 100% of the field capacity and the minimum value set at 65% of the field capacity; the lower limit of soil moisture is the actual substrate moisture content of each treatment measured at 8:00 a.m. every day. The substrate moisture content is measured in real-time using a DM–300 (Shenzhen Enzi Electronics Co., Shenzhen, China)

soil moisture analyzer, and the soil is regularly collected and calibrated using the drying method. When the soil moisture content approaches or decreases to 60% of the lower limit of irrigation, irrigation is carried out, and fertilizer is applied together with the water.

Table 1. The specific experimental design scheme.

Treatments	Actual Value	
	Irrigation Level (%)	N Application (kg hm^{-2})
IN1	65	150
IN2	100	150
IN3	65	1250
IN4	80	623
IN5	89	1250
IN6	100	917
IN7	100	1250

$$M_{\text{Irrigation}} = r \times p \times h \times \theta f \times \frac{(q_1 - q_2)}{\eta} \quad (1)$$

In the formula, r = soil bulk density, which is 1.61 g cm^3; p = soil moisture ratio, taken as 100%; h = wet layer of irrigation plan, taken as 0.35 m; θf = field water capacity, 14.02%; q_1 and q_2 = represent the upper limit and lower limit of the soil moisture, respectively (expressed as a percentage of relative field water capacity); η = the water use coefficient is 0.9 for drip irrigation.

The elemental fertilizers used in large amounts in the experiment were urea (containing N 46%), potassium dihydrogen phosphate (containing P_2O_5 51%), and potassium sulfate (containing K_2O 50%). Based on the nutrient content in the substrate and the principle of nutrient balance, the amount of phosphorus and potassium fertilizers was set to 290 kg hm^2 and 800 kg hm^2, respectively. Nitrogen, phosphorus, and potassium fertilizers were topdressing with water and applied every 5 days, a total of 20 times. Nitrogen fertilizer was applied in equal amounts each time in each treatment, with 49% phosphorus fertilizer and 21% potassium fertilizer applied in the first 7 times. The remaining phosphorus and potassium fertilizer were applied in equal amounts each time, and trace elements were sprayed in an appropriate amount according to plant growth requirements.

2.3. Data Collection and Measurements

We extracted the fourth functional leaf from top to bottom from five cucumber plants during the seedling stage (20 days after water and nitrogen treatment), flowering stage (35 days after water and nitrogen treatment), initial melon stage (53 days after water and nitrogen treatment), vigorous melon stage (78 days after water and nitrogen treatment), and final melon stage (100 days after water and nitrogen treatment) for the determination of carbon and nitrogen metabolism and related enzyme activities. We measured the total soluble sugar content in leaves using the anthrone method; the soluble protein content was stained using the Coomassie Brilliant Blue G–250 staining method. The activity of key enzymes for carbon and nitrogen metabolism was measured using a plant ELISA kit (Jiangsu Kete Biotechnology Co., Ltd., Yancheng, China), including sucrose phosphate synthase (SPS), sucrose synthase (SS), nitrate reductase (NR), glutamate synthase (GOGAT), glutamate dehydrogenase (GLDH), glutamine synthase (GS), acid invertase enzyme (AIE), and neutral invertase enzyme (NIE). The dry sample of the leaves was crushed through a 0.149 mm mesh sieve and digested using the H_2SO_4–H_2O_2 method. The digested solution was used for the determination of total nitrogen content using a fully automatic SmartChem200 intermittent chemical analyzer (AMS, Rome, Italy).

2.4. Enzyme Extracts Preparation and Antioxidant Enzyme Activities

We took v phosphate buffer (pH 7.8), 0.1 mM EDTA Na_2, and 1% insoluble PVP from 0.5 g of leaf homogenate with the midrib removed. We centrifuged the homogenate at 15,000× *g* for 10 min at 40 °C. After centrifugation, we took the upper supernatant for enzyme determination. According to the technique used by Li [37], the total SOD activity was analyzed at 560 nm. SOD activity is expressed as U g^{-1} FW h^{-1}. According to Amalo et al. [38], the POD activity was calculated using guaiacol at 470nm. POD activity is expressed as U g^{-1} FW min^{-1}. The determination of CAT activity was based on the method proposed by Tan et al. [39]. CAT activity is expressed as U g^{-1} FW min^{-1}.

From the early stage of cucumber fruiting to seedling pulling, the harvested cucumber fruits are directly weighed using a one percent balance. We calculated the individual fruit weight and yield of cucumbers harvested in each community and converted the yield per hectare.

2.5. Statistical Analysis

We analyzed the data using SPSS 18.0 (IBM, San Jose, CA, USA) and analyzed the data obtained from each sampling event separately. Multiple comparisons were tested using Duncan's new multiple-range test. If the *F*–test was significant, we evaluated the mean using the (LSD 0.05) multiple comparison test.

3. Results

3.1. Soluble Sugar, Soluble Protein, and Actual Leaf Nitrogen Contents

The soluble sugar and protein contents of cucumber leaves significantly increased with the increasing drip irrigation and nitrogen application rates at various growth stages (Tables 2 and 3). The soluble sugar content was closely correlated to the protein content and considerably improved the cucumber yield. The soluble sugar and protein contents of leaves were considerably greater from 20 DAT to 78 DAT, whereas they significantly declined from 78 DAT to 100 DAT during the same treatments for the 2021 study year. The mean soluble sugar and protein contents under the IN4 and IN5 treatments considerably increased by 24.6% and 19.7% and 26.1% and 30.1%, respectively, compared to those in the IN1 treatment. During the 2021 study year, soluble sugar and protein contents under the IN4 treatment were significantly higher than the rest of all other treatments at 20, 35, 53, 78, and 100 DAT. However, with respect to the supply of maximum drip irrigation (100%) and nitrogen fertilizer (1250 kg hm^{-2}), there were no significant differences recorded in soluble sugar and protein contents at various growth stages. The drip irrigation considerably affected the soluble sugar and protein contents of leaves at each nitrogen application level during the various growth stages of cucumber.

Table 2. Effects of different treatments on soluble sugar contents and soluble protein contents of cucumber during the 2021 study year.

Treatments	Soluble Sugar Contents (mg g^{-1} FW)					Soluble Protein Contents (mg g^{-1} FW)				
	Days after Treatment (DAT)					Days after Treatment (DAT)				
	20 DAT	35 DAT	53 DAT	78 DAT	100 DAT	20 DAT	35 DAT	53 DAT	78 DAT	100 DAT
IN1	3.5 ± 0.19 b	4.3 ± 0.14 b	5.0 ± 0.11 b	7.7 ± 0.14 b	5.6 ± 0.12 c	17.8 ± 0.27 c	26.0 ± 0.31 d	30.5 ± 0.29 d	38.0 ± 0.35 c	39.6 ± 0.30 c
IN2	2.9 ± 0.15 b	4.2 ± 0.18 b	4.9 ± 0.19 b	7.3 ± 0.15 c	5.4 ± 0.15 c	16.7 ± 0.24 c	21.4 ± 0.33 e	24.9 ± 0.27 e	33.7 ± 0.33 d	31.7 ± 0.29 d
IN3	4.5 ± 0.21 a	5.0 ± 0.22 a	5.9 ± 0.18 b	9.1 ± 0.18 a	6.9 ± 0.19 a	19.3 ± 0.22 b	38.7 ± 0.29 b	41.4 ± 0.22 c	44.3 ± 0.37 b	46.7 ± 0.28 b
IN4	4.7 ± 0.22 a	5.5 ± 0.24 a	6.7 ± 0.23 a	10.3 ± 0.19 a	7.5 ± 0.16 a	20.0 ± 0.19 a	42.5 ± 0.25 a	43.5 ± 0.21 a	46.6 ± 0.38 ab	53.2 ± 0.33 a
IN5	4.9 ± 0.13 a	5.6 ± 0.21 a	6.1 ± 0.26 a	9.1 ± 0.22 a	7.0 ± 0.21 a	23.1 ± 0.28 a	44.7 ± 0.22 a	44.3 ± 0.26 a	50.1 ± 0.39 a	55.4 ± 0.36 a
IN6	4.3 ± 0.11 a	4.9 ± 0.17 b	6.2 ± 0.24 a	9.0 ± 0.21 a	6.6 ± 0.16 b	18.3 ± 0.30 b	33.7 ± 0.21 c	38.2 ± 0.24 b	45.6 ± 0.33 b	44.5 ± 0.39 b
IN7	4.1 ± 0.10 a	4.9 ± 0.19 b	6.1 ± 0.21 a	8.1 ± 0.22 b	6.3 ± 0.22 b	19.4 ± 0.25 b	39.6 ± 0.35 b	37.9 ± 0.28 b	44.9 ± 0.31 b	40.7 ± 0.34 c

Note: IN1: 65% irrigation with 150 kg N hm^{-2}; IN2: 100% irrigation with 150 kg N hm^{-2}; IN3: 65% irrigation with 1250 kg N hm^{-2}; IN4: 80% irrigation with 623 kg N hm^{-2}; IN5: 89% irrigation with 1250 kg N hm^{-2}; IN6: 100% irrigation with 917 kg N hm^{-2}; IN7: 100% irrigation with 1250 kg N hm^{-2}. DAT: days after irrigation water and nitrogen treatments. Values are given as means ± standard deviations, and different lowercase letters indicate significant differences at $p \leq 0.05$ levels in the same line (LSD; $n = 3$).

The IN4 and IN5 treatments had significantly ($p < 0.05$) greater leaf nitrogen contents during various growth stages of cucumber than the rest of all other treatments (Table 3).

There were non-significant differences in leaf nitrogen content at the IN4 and IN5 treatments during various growth stages. Samples from the IN4 treatment had significantly higher leaf nitrogen content than that of all of the other treatments at each growth stage (with the exception of the IN5 treatment). During the 2021 study year, the IN4 and IN5 treatments significantly increased leaf nitrogen content by 27.5% and 33.1% more than that of the IN1 treatment. The leaf nitrogen content significantly increased from 20 DAT to 53 DAT, while the leaf nitrogen content revealed a considerably decreasing trend from 53 DAT to 100 DAT among all the treatments. The leaf nitrogen content considerably improved by 5.5% more in the IN5 treatment than in the IN4 treatment.

Table 3. Effects of different treatments on actual leaf nitrogen content of cucumber during the 2021 study year.

Treatments	Actual Leaf Nitrogen Content (mg g^{-1})				
	Days after Treatment (DAT)				
	20 DAT	35 DAT	53 DAT	78 DAT	100 DAT
IN1	27.2 ± 0.31 e	39.7 ± 0.34 e	37.0 ± 0.30 e	49.5 ± 0.35 c	48.1 ± 0.33 c
IN2	23.4 ± 0.36 f	40.5 ± 0.38 d	36.2 ± 0.31 e	52.9 ± 0.36 b	41.2 ± 0.31 e
IN3	36.7 ± 0.34 d	42.3 ± 0.35 d	48.8 ± 0.34 d	48.5 ± 0.33 c	50.2 ± 0.34 ab
IN4	52.9 ± 0.37 b	58.9 ± 0.32 ab	59.3 ± 0.32 ab	56.7 ± 0.32 a	51.6 ± 0.35 a
IN5	65.0 ± 0.39 a	61.6 ± 0.37 a	63.4 ± 0.35 a	59.9 ± 0.35 a	53.2 ± 0.36 a
IN6	39.4 ± 0.38 c	53.3 ± 0.39 c	54.0 ± 0.37 c	51.1 ± 0.40 b	50.3 ± 0.33 ab
IN7	42.1 ± 0.41 c	54.5 ± 0.40 c	48.3 ± 0.39 d	55.2 ± 0.41 b	44.3 ± 0.31 d

Note: IN1: 65% irrigation with 150 kg N hm^{-2}; IN2: 100% irrigation with 150 kg N hm^{-2}; IN3: 65% irrigation with 1250 kg N hm^{-2}; IN4: 80% irrigation with 623 kg N hm^{-2}; IN5: 89% irrigation with 1250 kg N hm^{-2}; IN6: 100% irrigation with 917 kg N hm^{-2}; IN7: 100% irrigation with 1250 kg N hm^{-2}. DAT: days after irrigation water and nitrogen treatments. Values are given as means ± standard deviations, and different lowercase letters indicate significant differences at $p \leq 0.05$ levels in the same line (LSD; $n = 3$).

3.2. Acid Invertase Enzyme (AIE), Neutral Invertase Enzyme (NIE), and Nitrate Reductase (NR) Activities

Under the IN4 and IN5 treatments, the AIE, NIE, and NR contents of cucumber leaves considerably increased at various growth stages (Table 4 and Figure 2). The AIE, NIE, and NR contents of cucumber leaves improved gradually at 20 to 53 DAT and then decreased from 53 to 100 DAT. Moreover, AIE, NIE, and NR contents rapidly increased from 35 to 53 DAT under both IN4 and IN5 treatments. However, during the 2021 study year, the average of the five different growth stages of cucumber revealed that the IN4 and IN5 treatments had produced considerably more (15.9% and 18.1%) AIE (23.9% and 23.5%) NIE, and (25.8% and 28.8%) NR in the cucumber leaves than that of the IN1 treatment. The AIE, NIE, and NR contents of cucumber leaves were considerably greater in the IN5 treatment, compared with all other treatments at 20, 35, 53, 78, and 100 DAT. During 53 DAT, AIE, NIE, and NR contents of cucumber leaves reached the highest values under the various treatments.

Table 4. Effects of different treatments on acid invertase enzyme activity and neutral invertase enzyme of cucumber during the 2021 study year.

Treatments	Acid Invertase Enzyme (IU g^{-1})					Neutral Invertase Enzyme (IU g^{-1})				
	Days after Treatment (DAT)					Days after Treatment (DAT)				
	20 DAT	35 DAT	53 DAT	78 DAT	100 DAT	20 DAT	35 DAT	53 DAT	78 DAT	100 DAT
IN1	0.514 ± 0.81 d	0.603 ± 0.56 e	0.772 ± 0.53 c	0.769 ± 0.56 c	0.744 ± 0.66 b	0.161 ± 0.55 b	0.190 ± 0.57 c	0.223 ± 0.68 b	0.179 ± 0.62 c	0.284 ± 0.68 b
IN2	0.613 ± 0.69 c	0.721 ± 0.66 c	0.568 ± 0.56 e	0.611 ± 0.59 e	0.687 ± 0.72 c	0.222 ± 0.59 a	0.200 ± 0.59 c	0.146 ± 0.88 d	0.234 ± 0.66 b	0.213 ± 0.71 c
IN3	0.628 ± 0.51 c	0.672 ± 0.76 d	0.821 ± 0.65 b	0.748 ± 0.63 c	0.730 ± 0.63 b	0.147 ± 0.61 b	0.154 ± 0.66 d	0.210 ± 0.64 b	0.168 ± 0.63 c	0.165 ± 0.78 d
IN4	0.790 ± 0.71 a	0.786 ± 0.83 b	0.830 ± 0.44 b	0.810 ± 0.66 a	0.829 ± 0.60 a	0.224 ± 0.69 a	0.275 ± 0.88 a	0.289 ± 0.77 a	0.284 ± 0.69 a	0.290 ± 0.72 a
IN5	0.760 ± 0.49 a	0.862 ± 0.82 a	0.947 ± 0.67 a	0.837 ± 0.69 a	0.846 ± 0.55 a	0.222 ± 0.70 a	0.293 ± 0.56 a	0.252 ± 0.72 a	0.284 ± 0.73 a	0.304 ± 0.81 a
IN6	0.740 ± 0.61 b	0.600 ± 0.49 e	0.660 ± 0.82 d	0.790 ± 0.80 b	0.592 ± 0.58 d	0.153 ± 0.82 b	0.249 ± 0.54 bc	0.199 ± 0.78 c	0.213 ± 0.81 b	0.266 ± 0.91 b
IN7	0.474 ± 0.58 e	0.767 ± 0.58 c	0.677 ± 0.80 d	0.694 ± 0.71 d	0.638 ± 0.49 d	0.233 ± 0.84 a	0.268 ± 0.66 b	0.142 ± 0.80 d	0.216 ± 0.75 b	0.185 ± 0.95 d

Note: IN1: 65% irrigation with 150 kg N hm^{-2}; IN2: 100% irrigation with 150 kg N hm^{-2}; IN3: 65% irrigation with 1250 kg N hm^{-2}; IN4: 80% irrigation with 623 kg N hm^{-2}; IN5: 89% irrigation with 1250 kg N hm^{-2}; IN6: 100% irrigation with 917 kg N hm^{-2}; IN7: 100% irrigation with 1250 kg N hm^{-2}. DAT: days after irrigation water and nitrogen treatments. Values are given as means ± standard deviations, and different lowercase letters indicate significant differences at $p \leq 0.05$ levels in the same line (LSD; $n = 3$).

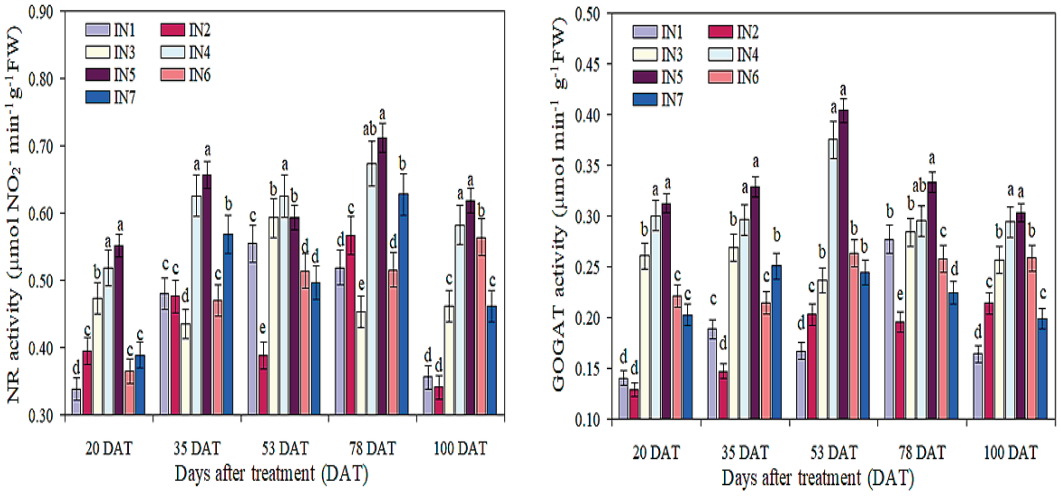

Figure 2. Effects of irrigation water with nitrogen coupling of sand−cultivated cucumbers using a quadratic saturation D−optimal design on nitrate reductase activity and glutamate synthase activity. Note: IN1: 65% irrigation with 150 kg N hm^{-2}; IN2: 100% irrigation with 150 kg N hm^{-2}; IN3: 65% irrigation with 1250 kg N hm^{-2}; IN4: 80% irrigation with 623 kg N hm^{-2}; IN5: 89% irrigation with 1250 kg N hm^{-2}; IN6: 100% irrigation with 917 kg N hm^{-2}; IN7: 100% irrigation with 1250 kg N hm^{-2}. DAT: days after irrigation water and nitrogen treatments. The error bars represent the value of the standard deviation (SD), and different lowercase letters indicate significant differences at $p < 0.05$.

3.3. Glutamate Synthase (GOGAT), Glutamate Dehydrogenase (GLDH), and Glutamine Synthase (GS) Activities

Under the IN4 and IN5 treatments, the GOGAT, GLDH, and GS activities at various growth stages were considerably greater than that of all other treatments (Figures 2 and 3). Under the IN4 and IN5 treatments, the GOGAT, GLDH, and GS activities significantly increased with increasing irrigation (80%) and nitrogen fertilizer (623 kg hm^{-2}) at 20, 35, 53, 78, and 100 DAT. The GOGAT contents, under the IN4 treatment at 20, 35, 53, 78, and 100 DAT, were significantly greater by 53%, 27%, 39%, 6%, and 44%, respectively, and the GLDH contents were significantly greater by 11%, 54%, 2%, 2%, and 50%, and the GS contents were significantly greater by 22%, 3%, 16%, 38%, and 32% than those of the IN1 treatment. The GOGAT contents under the IN5 treatment, at 20, 35, 53, 78, and 100 DAT, were significantly greater by 55%, 43%, 59%, 17%, and 46%, the GLDH contents were significantly greater by 27%, 52%, 13%, 24%, and 51%, and the GS contents were significantly greater by 30%, 1%, 20%, 42%, and 36% than those of the IN1 treatment. During the 53 DAT, GOGAT, GLDH, and GS activities of cucumber leaves reached the highest values under the various treatments.

3.4. Sucrose Phosphate Synthase (SPS) and Sucrose Synthase (SS) Activities

The interactive effect of irrigation with the nitrogen application strategy significantly increased the SPS and SS activities of cucumber leaves (Figure 4). However, there was no considerable variance recorded in the SPS and SS activities under the IN4 and IN5 treatments. The IN4 treatment significantly increased the SPS and SS activities by 16.9% and 9.4% more than those of the IN1 treatment. Under the IN5 treatment, there were significant increases in SPS and SS activities by 21.7% and 11.6% more than those of the IN1 treatment. There were non-significant variances between the IN4 and IN5 treatments. At each drip irrigation with nitrogen application levels, the SPS and SS activities were significantly greater under the IN4 and IN5 treatments, respectively.

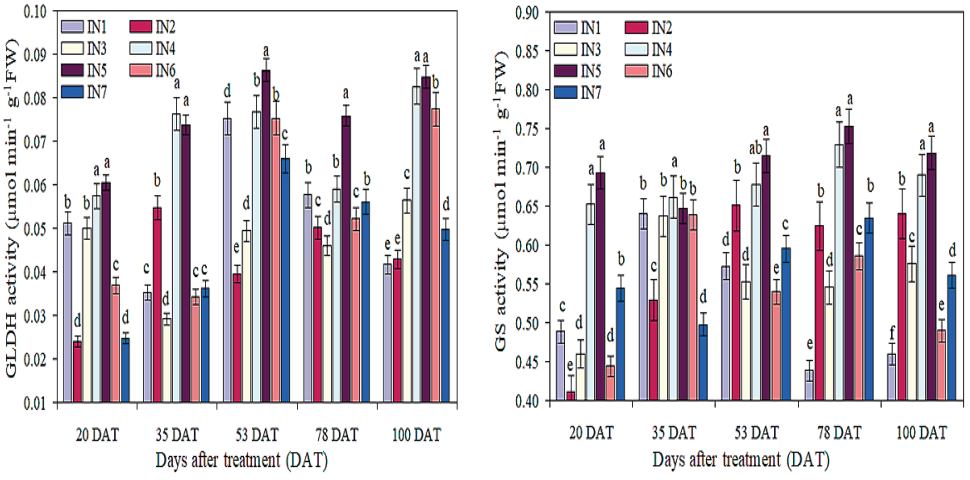

Figure 3. Effects of irrigation water with nitrogen coupling of sand−cultivated cucumbers using a quadratic saturation D−optimal design on glutamate dehydrogenase activity and glutamine synthase activity. Note: IN1: 65% irrigation with 150 kg N hm^{-2}; IN2: 100% irrigation with 150 kg N hm^{-2}; IN3: 65% irrigation with 1250 kg N hm^{-2}; IN4: 80% irrigation with 623 kg N hm^{-2}; IN5: 89% irrigation with 1250 kg N hm^{-2}; IN6: 100% irrigation with 917 kg N hm^{-2}; IN7: 100% irrigation with 1250 kg N hm^{-2}. DAT: days after irrigation water and nitrogen treatments. The error bars represent the value of the standard deviation (SD), and different lowercase letters indicate significant differences at $p < 0.05$.

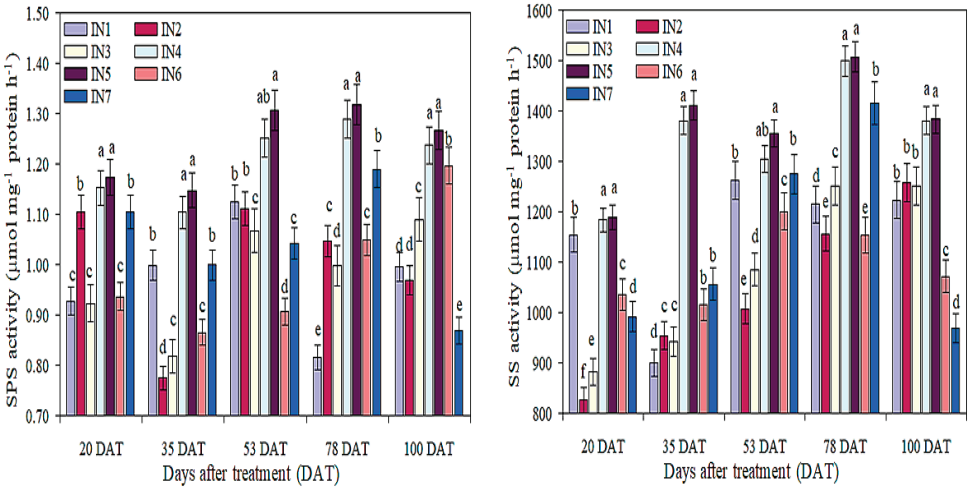

Figure 4. Effects of irrigation water with nitrogen coupling of sand−cultivated cucumbers using a quadratic saturation D−optimal design on sucrose phosphate synthase activity and sucrose synthase activity. Note: IN1: 65% irrigation with 150 kg N hm^{-2}; IN2: 100% irrigation with 150 kg N hm^{-2}; IN3: 65% irrigation with 1250 kg N hm^{-2}; IN4: 80% irrigation with 623 kg N hm^{-2}; IN5: 89% irrigation with 1250 kg N hm^{-2}; IN6: 100% irrigation with 917 kg N hm^{-2}; IN7: 100% irrigation with 1250 kg N hm^{-2}. DAT: days after irrigation water and nitrogen treatments. The error bars represent the value of the standard deviation (SD), and different lowercase letters indicate significant differences at $p < 0.05$.

3.5. CAT, POD, RuBisCO, and SOD Activities

Figure 5 and Table 5 show that, under irrigation and nitrogen fertilizer application, the activities of CAT, POD, RuBisCO, and SOD in cucumber leaves significantly increased at 20, 35, 53, 78, and 100 DAT. Under IN4 and IN5 treatments, the CAT, POD, RuBisCO, and SOD activities of cucumber leaves reached their maximum values at 78 DAT, but there was a non–significant variance between 53 and 78 DAT. Subsequently, the CAT, POD, Rubisco, and SOD activities of cucumber leaves rapidly decreased at 100 DAT, respectively. Furthermore, the difference between IN4 and IN5 treatments was non−significant in all growth stages of cucumber. The activities of CAT, POD, RuBisCO, and SOD in cucumber leaves significantly increased from 20 to 78 DAT, and sharply decreased from 78 to 100 DAT. The effects of IN5 treatment on CAT, POD, RuBisCO, and SOD activities in cucumber leaves at different growth stages were considerably greater than those of the IN1 treatment. The average values of CAT, POD, RuBisCO, and SOD activities in cucumber leaves treated with IN4 and IN5 were significantly higher than those treated with IN1 (16.5%, 25.6%, 18.1%, and 29.4% and 18.1%, 29.4%, 25.7%, and 35.8%, respectively) at five different growth stages. Under conditions of 20, 35, 53, 78, and 100 DAT, the effects of IN4 and IN5 treatments on CAT, POD, RuBisCO, and SOD activities in cucumber leaves were not significant.

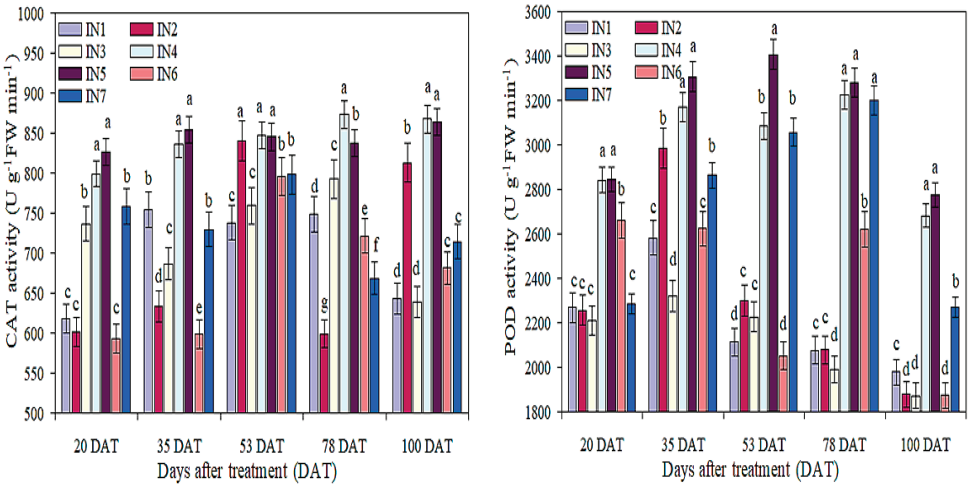

Figure 5. Effects of irrigation water with nitrogen coupling of sand−cultivated cucumbers using a quadratic saturation D−optimal design on catalase activity and peroxidase activity. Note: IN1: 65% irrigation with 150 kg N hm^{-2}; IN2: 100% irrigation with 150 kg N hm^{-2}; IN3: 65% irrigation with 1250 kg N hm^{-2}; IN4: 80% irrigation with 623 kg N hm^{-2}; IN5: 89% irrigation with 1250 kg N hm^{-2}; IN6: 100% irrigation with 917 kg N hm^{-2}; IN7: 100% irrigation with 1250 kg N hm^{-2}. DAT: days after irrigation water and nitrogen treatments. The error bars represent the value of the standard deviation (SD), and different lowercase letters indicate significant differences at $p < 0.05$.

Table 5. Effects of different treatments on the RuBisCO activity and superoxide dismutase activity of cucumber during the 2021 study year.

Treatments	RuBisCO (Ug^{-1} FW h^{-1})					SOD Activity (Ug^{-1} FW h^{-1})				
	Days after Treatment (DAT)					Days after Treatment (DAT)				
	20 DAT	35 DAT	53 DAT	78 DAT	100 DAT	20 DAT	35 DAT	53 DAT	78 DAT	100 DAT
IN1	0.877 ± 0.31 b	0.873 ± 0.33 b	0.831 ± 0.22 d	0.703 ± 0.26 e	0.723 ± 0.33 c	591 ± 0.95 d	457 ± 0.56 e	1171 ± 0.55 b	1032 ± 0.88 d	814 ± 0.61 c
IN2	0.900 ± 0.29 a	0.624 ± 0.31 d	0.896 ± 0.26 b	0.927 ± 0.32 b	0.785 ± 0.31 c	372 ± 0.87 f	726 ± 0.67 c	716 ± 0.63 d	1237 ± 0.91 c	507 ± 0.72 e
IN3	0.801 ± 0.23 c	0.868 ± 0.30 b	0.864 ± 0.30 c	0.756 ± 0.23 d	0.745 ± 0.29 c	814 ± 0.83 c	861 ± 0.63 b	973 ± 0.51 c	1029 ± 0.83 d	865 ± 0.59 c
IN4	0.933 ± 0.33 a	1.043 ± 0.28 a	1.017 ± 0.33 a	1.077 ± 0.22 a	0.823 ± 0.27 b	926 ± 0.75 b	918 ± 0.51 a	1347 ± 0.47 a	1336 ± 0.71 b	1224 ± 0.65 b
IN5	0.941 ± 0.27 a	1.138 ± 0.26 a	1.133 ± 0.28 a	1.146 ± 0.21 a	1.039 ± 0.24 a	1175 ± 0.61 a	941 ± 0.49 a	1351 ± 0.42 a	1415 ± 0.67 a	1445 ± 0.44 a

Table 5. *Cont.*

Treatments	RuBisCO (Ug^{-1} FW h^{-1})					SOD Activity (Ug^{-1} FW h^{-1})				
	Days after Treatment (DAT)					Days after Treatment (DAT)				
	20 DAT	35 DAT	53 DAT	78 DAT	100 DAT	20 DAT	35 DAT	53 DAT	78 DAT	100 DAT
IN6	0.626 ± 0.29 d	0.832 ± 0.23 c	0.922 ± 0.26 b	0.768 ± 0.20 d	0.793 ± 0.23 c	519 ± 0.69 d	695 ± 0.66 d	632 ± 0.39 e	1291 ± 0.77 c	631 ± 0.55 d
IN7	0.916 ± 0.30 a	0.848 ± 0.21 b	1.006 ± 0.22 a	0.841 ± 0.19 c	0.677 ± 0.26 d	493 ± 0.59 e	786 ± 0.72 c	909 ± 0.41 c	745 ± 0.65 e	1202 ± 0.62 b

Note: IN1: 65% irrigation with 150 kg N hm^{-2}; IN2: 100% irrigation with 150 kg N hm^{-2}; IN3: 65% irrigation with 1250 kg N hm^{-2}; IN4: 80% irrigation with 623 kg N hm^{-2}; IN5: 89% irrigation with 1250 kg N hm^{-2}; IN6: 100% irrigation with 917 kg N hm^{-2}; IN7: 100% irrigation with 1250 kg N hm^{-2}. DAT: days after irrigation water and nitrogen treatments. Values are given as means ± standard deviations, and different lowercase letters indicate significant differences at $p \leq 0.05$ levels in the same line (LSD; $n = 3$).

3.6. Cucumber Yield (t hm-2) and Pearson's Correlation Coefficients

The cucumber yield was significantly improved by the interactive effect of irrigation–nitrogen coupling strategies during the 2021 study year (Figure 6). The cucumber yield significantly enhanced with the supply of irrigation and nitrogen fertilizer application, but differences were not significant under the IN4 and IN5 treatments. The cucumber yield was greater under the IN4 and IN5 treatments than under all other treatments. The cucumber yield revealed that, under IN4 and IN5, it produced maximum values of 69.7% and 72.2%, as compared with the IN1 treatment. When compared to the IN2 treatment, the cucumber yield under the IN1, IN3, IN4, IN5, IN6, and IN7 treatments were significantly improved by 14.8%, 67.3%, 74.2%, 75.5%, 73.2%, and 70.9%, respectively. Table 6 displays Pearson's correlation coefficients by using the quadratic saturation D−optimal design of the irrigation water with the nitrogen coupling of sand−cultivated cucumbers. A significant positive correlation was observed between carbon and nitrogen metabolism, antioxidant enzyme activities, and sand–cultivated cucumber yield in a greenhouse.

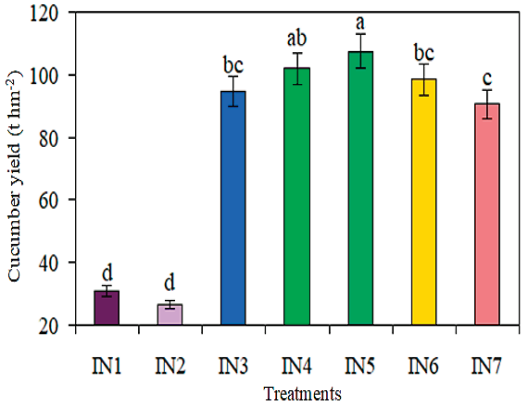

Figure 6. Effects of irrigation water with nitrogen coupling of sand−cultivated cucumbers using a quadratic saturation D−optimal design on cucumber yield (t. hm^{-2}). Note: IN1: 65% irrigation with 150 kg N hm^{-2}; IN2: 100% irrigation with 150 kg N hm^{-2}; IN3: 65% irrigation with 1250 kg N hm^{-2}; IN4: 80% irrigation with 623 kg N hm^{-2}; IN5: 89% irrigation with 1250 kg N hm^{-2}; IN6: 100% irrigation with 917 kg N hm^{-2}; IN7: 100% irrigation with 1250 kg N hm^{-2}. DAT: days after irrigation water and nitrogen treatments. The error bars represent the value of the standard deviation (SD), and different lowercase letters indicate significant differences at $p < 0.05$.

Table 6. Correlation coefficients of irrigation water with nitrogen coupling of sand−cultivated cucumbers using a quadratic saturation D−optimal design.

	AIE	CAT	GLDH	GS	GOGAT	NIE	NR	POD	RUB	SOD	SP	SPS	SSC	SS	TN
CAT	0.945 **														
GLDH	0.921 **	0.872 *													
GS	0.891 **	0.961 **	0.859 *												
GOGAT	0.917 **	0.830 *	0.848 *	0.819 *											
NIE	0.775 *	0.835 *	0.912 **	0.859 *	0.643										
NR	0.940 **	0.950 **	0.919 **	0.926 **	0.921 **	0.852 *									
POD	0.762 *	0.887 **	0.824 *	0.899 **	0.727	0.898 **	0.919 **								
RUB	0.890 **	0.965 **	0.888 **	0.977 **	0.812 *	0.868 *	0.928 **	0.920 **							
SOD	0.988 **	0.972 **	0.909 **	0.917 **	0.904 **	0.779 *	0.948 **	0.809 *	0.934 **						
SP	0.851 *	0.764 *	0.769 *	0.690	0.947 **	0.567	0.891 **	0.699	0.697	0.835 *					
SPS	0.894 **	0.964 **	0.909 **	0.983 **	0.826 **	0.907 **	0.954 **	0.948 **	0.992 **	0.927 **	0.727				
SSC	0.799 **	0.689 **	0.697	0.628	0.877 **	0.538	0.830 *	0.610	0.577	0.744	0.946 **	0.635			
SS	0.889 **	0.895 **	0.932 **	0.806 *	0.716	0.880 **	0.869 **	0.815 *	0.873 *	0.904 **	0.690	0.874 *	0.587		
TN	0.852 *	0.824 *	0.885 *	0.825 *	0.932 **	0.793 *	0.958 **	0.871 *	0.827 *	0.846 *	0.924 **	0.871 *	0.869 *	0.763 *	
Y	0.647	0.556	0.575	0.529	0.850 *	0.405	0.754 *	0.582	0.496	0.614	0.932 **	0.552	0.937 **	0.422	0.863 *

Note: AIE: acid Invertase enzyme; CAT: catalase activity; GLDH: glutamate dehydrogenase activity; GS: glutamine synthase activity; GOGAT: glutamate synthase activity; NIE: neutral invertase enzyme; NR: nitrate reductase activity; POD: peroxidase activity; RUB: RuBisCO; SOD: superoxide dismutase activity; SP: soluble protein content; SPS: sucrose phosphate synthase activity; SSC: soluble sugar content; SS: sucrose synthase activity; TN: total nitrogen content; Y: cucumber yield. * Significant at the 0.05 probability level. ** Significant at the 0.01 probability level.

4. Discussion

The uneven distribution of precipitation causes soil drought and adversely affects soluble sugars and the protein content and antioxidant enzyme activities in cucumber leaves and causes drought-induced plant stress at an important growth stage [40,41]. Studies also show that soluble sugars, proteins, and nitrogen content are sensitive to dry stress [42], and changes in parameters can indicate whether the alternate irrigation mode impairs antioxidant enzyme activity. The higher content of soluble sugars and proteins in cucumber leaves is a sustainable and high−yield result. In the same treatment of the 2021 study year, the soluble sugar and protein content of leaves significantly increased from 20 DAT to 78 DAT, while it significantly decreased from 78 DAT to 100 DAT. Under drought stress, the amount of SP content is low, and the content of sucrose decreases, affecting the grain filling rate and crop yield [43]. Water stress facilitates stomatal closure, thereby affecting the diffusion of CO_2 from the air to the cell, which is the main cause of decreased SP content [44]. The average soluble sugar and protein content of IN4 and IN5 treatments were significantly increased (24.6% and 19.7%) and (26.1% and 30.1%) compared to IN1 treatment, respectively. Thus, carbon and nitrogen metabolism are not only interrelated but also have a certain degree of mutual inhibition [45]. Drip irrigation has a significant impact on the soluble sugar and protein content of cucumber leaves at different growth stages and nitrogen application levels. An earlier study also observed that, compared to traditional planting without using plastic film, wheat flag leaves had higher nitrogen SP contents due to the use of plastic film for drip irrigation [46]. In the 2021 study year, IN4 and IN5 treatments significantly increased leaf nitrogen contents by 27.5% and 33.1% compared to the IN1 treatment. This is consistent with the results of Xu et al. [47]; the decrease in nitrogen application increased the sugar concentration of cucumber, and the excessive application of nitrogen fertilizer was disadvantageous for the absorption of cucumber. Under drought conditions, supplementary irrigation promotes the development of plant tissues, significantly increasing the soluble sugar, protein, and nitrogen content of cucumber leaves [48].

Under the ADI treatment, medium and high levels of nitrogen administration reduced nitrite concentrations in cucumber fruits. Since nitrite reductase is insufficient in the fruit, the nitrite is not able to be reduced to the ammonia nitrogen, and the nitrite that is transported from the leaf accumulates, and it is a negative factor that finally affects the quality [49]. Under the IN4 and IN5 treatments, the AIE, NIE, and NR contents of cucumber leaves significantly increased at different growth stages. The AIE, NIE, and NR contents of cucumber leaves gradually increased at 20–53 DAT and then decreased from 53 to 100 DAT. In addition, under the treatments of IN4 and IN5, the contents of AIE, NIE, and NR rapidly increased from 35 DAT to 53 DAT. However, nitrogen application

treatment improved the photosynthetic performance of leaves, providing more electronic and chemical energy to reduce nitrite in leaves, ultimately reducing the transfer of nitrite from leaves to fruits [50]. However, in the data from the 2021 study year, the average values of five different growth stages of cucumber showed that, compared to the IN1 treatment, the IN4 and IN5 treatments produced significantly more (15.9% and 18.1%) AIE, (23.9% and 23.5%) NIE, and (25.8% and 28.8%) NR in cucumber leaves. During the 53 DAT, the AIE, NIE, and NR contents of cucumber leaves reached their highest values under different treatments. Many of the previous studies focused on the binding of irrigation and fertilization [51] or the IA and irrigation frequency to determine optimal management scheduling [52].

Under the water fertilizer binding action, the soil enzyme activity increases, and the crop root system enhances the absorption of mineral nutrients in the soil [53]. Under the IN4 and IN5 treatments, the GOGAT, GLDH, and GS activities at various growth stages were considerably greater than that of the rest of all other treatments. Under the IN4 and IN5 treatments, the GOGAT, GLDH, and GS activities significantly increased with increasing irrigation (80%) and nitrogen fertilizer (623 kg hm^{-2}) at 20, 35, 53, 78, and 100 DAT. The GOGAT contents under the IN4 treatment at 20, 35, 53, 78, and 100 DAT were significantly greater by 53%, 27%, 39%, 6%, and 44%, respectively, GLDH contents were significantly greater by 11%, 54%, 2%, 2%, and 50%, and the GS contents were significantly greater by 22%, 3%, 16%, 38%, and 32%, respectively, than those of the IN1 treatment. Research shows that the combination of temperature, water, and fertilizer promotes the respiration of soil microbes and root systems [54], enriches soil microbial biomass [55], promotes microbial reproduction and growth, and improves the root system and soil microenvironment [56,57]. The combination of temperature, water, and fertilizer enhances soil enzyme activity and enhances the absorption of mineral nutrients in soil by crop root systems [14].

The interaction between irrigation and nitrogen application strategies significantly improved the SPS and SS activities of cucumber leaves. However, there was no significant difference in SPS and SS activities between IN4 and IN5 treatments. Previous studies have also observed similar trends [34,36,39]. The IN4 treatment significantly increased the SPS and SS activities by 16.9% and 9.4% more than those of the IN1 treatment. At each drip irrigation with nitrogen application levels, the SPS and SS activities were significantly greater under the IN4 and IN5 treatments. As is well known, SPS and SS activities are the first responses of plants to water stress and play a sufficient role in plant stress resistance [22,24]. SPS and SS activities can enhance plants' damage repair abilities by increasing antioxidant activity under drought conditions [28].

Water deficiency is always associated with increased oxidative stress caused by increased ROS accumulation [18,19]. Under the IN4 and IN5 treatments, the CAT, POD, RuBisCO, and SOD activities of cucumber leaves reached their maximum values at 78 DAT, but there was no significant difference between 53 and 78 DAT treatments. Subsequently, the CAT, POD, Rubisco, and SOD activities of cucumber leaves rapidly decreased at 100 DAT, respectively. The difference between the IN4 and IN5 treatments was not remarkable at all growth stages of cucumber. The highest activity of antioxidant enzymes is the response to the decrease in the soil's water storage capacity [10]. Under severe drought conditions, the formation of H_2O_2 and O_2^- in crop leaves markedly increased [33]. In this study, the CAT, POD, RuBisCO, and SOD activities of cucumber leaves significantly increased from 20 to 78 DAT and sharply decreased from 78 to 100 DAT under each irrigation and nitrogen fertilizer application level. The average values of five different growth stages indicate that the average activities of CAT, POD, RuBisCO, and SOD in cucumber leaves treated with IN4 and IN5 are significantly higher than those treated with IN1. Therefore, oxidative damage adversely affects plant performance, PN value, and chlorophyll content [44]. Fotelli et al. [55] confirmed that the SP content and SOD, POD, and CAT activities of wheat flag leaves decreased with the decrease in the irrigation rate and accelerated the senescence rate of late–growing leaves. Irrigation and fertilization affect cucumber growth, development, production, and quality [42,58]. Cucumber plants are highly sensitive to

soil moisture conditions, especially in a greenhouse; therefore, the soil moisture supply has a significant effect on the growth and yield of cucumber [9]. The cucumber yield was highest in the IN4 and IN5 treatments. The results showed that, compared with the IN1 treatment, the IN4 and IN5 treatments had the highest cucumber yield, with 69.7% and 72.2%, respectively.

5. Conclusions

The sandy deficit irrigation with nitrogen management strategies significantly increased the soluble sugar, protein, and actual leaf nitrogen contents and improved soil chemical properties in the root zone of cucumber, thereby improving plant growth and yield. The growth and yield of sand–cultivated cucumber were evaluated comprehensively by using a quadratic saturation D–optimal design. Furthermore, such improvements were due to the reduction in oxidative damage during different growth stages of sand–cultivated cucumber. The IN4 and IN5 treatments significantly increased the activities of RuBisCO, CAT, POD, and SOD during different growth stages of sand–cultivated cucumber. Furthermore, the IN4 treatment attained the highest value at 53 DAT, while also exhibiting significant declines at 100 DAT. The higher activities of NR, GOGAT, GLDH, GS, AIE, NIE, and better antioxidative enzyme activities in the IN4 treatment at various growth stages effectively improved (69.6%) cucumber yield. The soil properties, carbon and nitrogen metabolism, and antioxidant enzyme activities were positively correlated with sand-cultivated cucumber yield in a greenhouse. In conclusion, with respect to global climate change, these results play an important role in guiding deficit irrigation–nitrogen coupling strategies under sand-cultivated cucumber in a greenhouse. Further research is required to test how deficit irrigation–nitrogen coupling strategies influence soil properties and cucumber growth under long–term sand-cultivated conditions.

Author Contributions: Methodology, X.M. and Z.X.; Software, X.M.; Formal analysis, T.W.; Investigation, X.M.; Resources, Y.C.; Data curation, Y.C. and Z.X.; Writing—original draft, Z.T.; Writing—review & editing, X.M., Y.C., M.C., Z.X. and H.D.; Visualization, Z.X.; Supervision, Z.T. and M.C.; Project administration, Z.T. and H.D.; Funding acquisition, Z.T. and M.C. All authors have read and agreed to the published version of the manuscript.

Funding: XPCC Financial Science and Technology Plan Project (2023AB071); Tianshan Talent Training Program (2023TSYCCY0002); Tumushuk Science and Technology Project of the 3rd Division (KY2022GG05), President's Fund Project of Tarim University (TDZKSS202346); Agricultural Key Core Technology Research Project of the Corps (NYHXGG2023AA304).

Data Availability Statement: The raw data supporting the conclusions of this article will be made available by the authors on request.

Conflicts of Interest: The authors declare no conflicts of interest.

References

1. Cheng, M.; Wang, H.; Fan, J.; Zhang, S.; Liao, Z.; Zhang, F.; Wang, Y. A global meta-analysis of yield and water use efficiency of crops, vegetables and fruits under full, deficit and alternate partial root-zone irrigation. *Agric. Water Manag.* **2021**, *248*, 106771. [CrossRef]
2. Du, T.; Kang, S.; Zhang, J.; Davies, W.J. Deficit irrigation and sustainable water-resource strategies in agriculture for China's food security. *J. Exp. Bot.* **2015**, *66*, 2253–2269. [CrossRef]
3. Mutambara, S.; Darkoh, M.B.K.; Atlhopheng, J.R. A comparative review of water management sustainability challenges in smallholder irrigation schemes in Africa and Asia. *Agric. Water Manag.* **2016**, *171*, 63–72. [CrossRef]
4. Wei, Z.H.; Du, T.S.; Li, X.N.; Fang, L.; Liu, F.L. Interactive effects of elevated CO and N fertilization on yield and quality of tomato grown under reduced irrigation regimes. *Front. Plant Sci.* **2018**, *9*, 328. [CrossRef]
5. Liu, H.; Li, H.H.; Ning, H.F.; Zhang, X.X.; Li, S.; Pang, J.; Wang, G.S.; Sun, J.S. Optimizing irrigation frequency and amount to balance yield, fruit quality and water use efficiency of greenhouse tomato. *Agric. Water Manag.* **2019**, *226*, 105787. [CrossRef]
6. Liu, H.J.; Yin, C.Y.; Gao, Z.Z.; Hou, L.Z. Evaluation of cucumber yield, economic benefit and water productivity under different soil matric potentials in solar greenhouses in North China. *Agric. Water Manag.* **2021**, *243*, 106442. [CrossRef]
7. Wang, Q.; Men, L.Z.; Gao, L.H.; Tian, Y.Q. Effect of grafting and gypsum application on cucumber (*Cucumis sativus* L.) growth under saline water irrigation. *Agric. Water Manag.* **2017**, *188*, 79–90. [CrossRef]

8. Chen, W.; Hou, Z.; Wu, L.; Liang, Y.; Wei, C. Evaluating salinity distribution in soil irrigated with saline water in arid regions of northwest China. *Agric. Water Manag.* **2010**, *97*, 2001–2008. [CrossRef]
9. Ali, S.; Xu, Y.; Ma, X.; Ahmad, I.; Kamran, M.; Dong, Z.; Cai, T.; Jia, Q.; Ren, X.; Zhang, P.; et al. Planting models and deficit irrigation strategies to improve wheat production and water use efficiency under simulated rainfall conditions. *Front. Plant Sci.* **2017**, *8*, 1408. [CrossRef]
10. Chen, Z.; Tian, T.; Gao, L.; Tian, Y. Nutrients, heavy metals and phthalate acid esters in solar greenhouse soils in Round-Bohai Bay-Region, China: Impacts of cultivation year and biogeography. *Environ. Sci. Pollut. Res.* **2016**, *23*, 13076–13087. [CrossRef]
11. Cao, C.Y.; Jiang, S.Y.; Zhang, Y.; Zhang, F.X.; Han, X.S. Spatial variability of soil nutrients and microbiological properties after the establishment of leguminous shrub Caragana microphylla Lam. plantation on sand dune in the Horqin Sandy Land of Northeast China. *Ecol. Eng.* **2011**, *37*, 1467–1475. [CrossRef]
12. Cui, Y.; Tian, Z.; Zhang, X.; Muhammad, A.; Han, H.; Jiang, D.; Cao, W.; Dai, T. Effect of water deficit during vegetative growth periods on post-anthesis photosynthetic capacity and grain yield in winter wheat (*Triticum aestivum* L.). *Acta Physiol. Plant.* **2015**, *37*, 196. [CrossRef]
13. Gupta, A.K.; Kaur, K.; Kaur, N. Stem reserve mobilization and sink activity inwheat under drought conditions. *Am. J. Plant Sci.* **2011**, *2*, 70–77. [CrossRef]
14. Sun, Y.; Hu, K.; Fan, Z.; Wei, Y.; Lin, S.; Wang, J. Simulating the fate of nitrogen and optimizing water and nitrogen management of greenhouse tomato in North China using the EU-Rotate_N model. *Agric. Water Manag.* **2013**, *128*, 72–84. [CrossRef]
15. Ran, Y.; Xie, J.; Xu, X.; Li, Y.; Liu, Y.; Zhang, Q.; Li, Z.; Xu, J.; Di, H. Warmer and drier conditions and nitrogen fertilizer application altered methanotroph abundance and methane emissions in a vegetable soil. *Environ. Sci. Pollut. Res.* **2017**, *24*, 2770–2780. [CrossRef] [PubMed]
16. Cao, Q.; Wang, S.Z.; Gao, L.H.; Ren, H.Z.; Chen, Q.Y.; Zhao, J.W.; Wang, Q.; Sui, X.L.; Zhang, Z.X. Effect of alternative furrow irrigation on growth and water us of cucumber in solar greenhouse. *Trans. Chin. Soc. Agric. Eng.* **2010**, *29*, 47–53, (In Chinese with English abstract).
17. Wang, Y.; Jensen, C.R.; Liu, F. Nutritional responses to soil drying and rewetting cycles under partial root-zone drying irrigation. *Agric. Water Manag.* **2017**, *179*, 254–259. [CrossRef]
18. Yu, B.; Yan, S.; Zhou, H.; Dong, R.; Lei, J.; Chen, C.; Cao, B. Overexpression of CsCaM3 improves high temperature tolerance in cucumber. *Front. Plant Sci.* **2018**, *9*, 797. [CrossRef]
19. Fazeli, F.; Ghorbanli, M.; Niknam, V. Effect of drought on biomass, protein content, lipid peroxidation and antioxidant enzymes in two sesame cultivars. *Biol. Plant.* **2007**, *51*, 98–103. [CrossRef]
20. Hou, M.; Jin, Q.; Lu, X.; Li, J.; Zhong, H.; Gao, Y. Growth, water use, and nitrate-15N uptake of greenhouse tomato as influenced by different irrigation patterns, 15N labeled depths, and transplant times. *Front. Plant Sci.* **2017**, *8*, 666. [CrossRef]
21. Lakhdar, A.; Hafsi, C.; Debez, A.; Montemurro, F.; Jedidi, N.; Abdelly, C. Assessing solid waste compost application as a practical approach for salt-affected soil reclamation. *Acta Agric. Scand. Sect. B—Soil Plant Sci.* **2011**, *61*, 284–288. [CrossRef]
22. Lakhdar, A.; Rabhi, M.; Ghnaya, T.; Montemurro, F.; Jedidi, N.; Abdelly, C. Effectiveness of compost use in salt-affected soil. *J. Hazard. Mater.* **2009**, *171*, 29–37. [CrossRef] [PubMed]
23. Lakhdar, A.; Hafsi, C.; Rabhi, M.; Debez, A.; Montemurro, F.; Abdelly, C.; Jedidi, N.; Ouerghi, Z. Application of municipal solid waste compost reduces the negative effects of saline water in *Hordeum maritimum* L. *Bioresour. Technol.* **2008**, *99*, 7160–7167. [CrossRef] [PubMed]
24. Farooq, M.; Wahid, A.; Kobayashi, N.; Fujita, D.; Basra, S.M. Plant drought stress: Effects, mechanisms and management. *Agron. Sustain. Dev.* **2009**, *29*, 185–212. [CrossRef]
25. Farneselli, M.; Benincasa, P.; Tosti, G.; Simonne, E.; Guiducci, M.; Tei, F. High fertigation frequency improves nitrogen uptake and crop performance in processing tomato grown with high nitrogen and water supply. *Agric. Water Manag.* **2015**, *154*, 52–58. [CrossRef]
26. Huang, Y.; Tang, R.; Cao, Q.; Bie, Z. Improving the fruit yield and quality of cucumber by grafting onto the salt tolerant rootstock under NaCl stress. *Sci. Hortic.* **2009**, *122*, 26–31. [CrossRef]
27. Sharma, D.K.; Andersen, S.B.; Ottosen, C.-O.; Rosenqvist, E. Wheat cultivars selected for high Fv/Fm under heat stress maintain high photosynthesis, total chlorophyll, stomatal conductance, transpiration and dry matter. *Physiol. Plant.* **2015**, *153*, 284–298. [CrossRef]
28. Singh, M.C.; Singh, J.P.; Pandey, S.K.; Mahay, D.; Shrivastva, V. Factors affecting the performance of greenhouse cucumber cultivation-a review. *Int. J. Curr. Microbiol. Appl. Sci.* **2017**, *6*, 2304–2323. [CrossRef]
29. Wang, Z.; Liu, Z.; Zhang, Z.; Liu, X. Subsurface drip irrigation scheduling for cucumber (*Cucumis sativus* L.) grown in solar greenhouse based on 20 cm standard pan evaporation in Northeast China. *Sci. Hortic.* **2009**, *123*, 51–57. [CrossRef]
30. Fasina, A.; Awe, G.; Ilori, A.; Babalola, T.; Ogunleye, K. Effect of drip irrigation frequency and N-fertilization on yield and water use efficiency of cucumber (*Cucumis sativus*) in Ado-Ekiti. *Niger. Res. Crop.* **2021**, *22*, 292–300.
31. Blandino, M.; Reyneri, A. Effect of fungicide and foliar fertilizer application to winter wheat at anthesis on flag leaves senescence, grain yield, flour bread-making quality and DON contamination. *Eur. J. Agron.* **2009**, *30*, 275–282. [CrossRef]
32. Tian, Y.; Zhang, X.; Wang, J.; Gao, L. Soil microbial communities associated with the rhizosphere of cucumber under different summer cover crops and residue management: A 4-year field experiment. *Sci. Hortic.* **2013**, *150*, 100–109. [CrossRef]
33. Khan, N.; Bano, A.; Rahman, M.A.; Rathinasabapathi, B.; Babar, M.A. UPLC-HRMS-based untargeted metabolic profiling reveals changes in chickpea (*Cicer arietinum*) metabolome following long-term drought stress. *Plant Cell Environ.* **2019**, *42*, 115–132. [CrossRef] [PubMed]

34. Ren, X.; Jia, Z.; Chen, X. Rainfall concentration for increasing corn production under semiarid climate. *Agr. Water Manag.* **2008**, *95*, 1293–1302. [CrossRef]
35. Reddy, A.R.; Chaitanya, K.V.; Vivekanandan, M. Drought-induced responses of photosynthesis and antioxidant metabolism in higher plants. *J. Plant Physiol.* **2004**, *11*, 15602811. [CrossRef] [PubMed]
36. He, Z.H.; Li, M.L.; Cai, Z.L.; Zhao, R.; Hong, T.T.; Yang, Z.; Zhang, Z. Optimal irrigation and fertilizer amounts based on multi-level fuzzy comprehensive evaluation of yield, growth and fruit quality on cherry tomato. *Agric. Water Manag.* **2021**, *243*, 106360. [CrossRef]
37. Li, H.S. *Principles and Techniques of Plant Physiological Experiment*; Higher Education Press: Beijing, China, 2000; pp. 119–120. (In Chinese)
38. Amalo, K.; Chen, G.X.; Asade, K. Separate assays specific for ascorbate peroxidase and guaiacal peroxidase and for the chloroplastic and cytosolic isozymes of ascorbate peroxidase implants. *Plant Cell Physiol.* **1994**, *35*, 497–504.
39. Tan, W.; Liu, J.; Dai, T.; Jing, Q.; Cao, W.; Jiang, D. Alternations in photosynthesis and antioxidant enzyme activity in winter wheat subjected to post-anthesis water-logging. *Photosynthetica* **2008**, *46*, 21–27. [CrossRef]
40. Wu, Y.; Xi, X.; Tang, X.; Luo, D.; Gu, B.; Lam, S.K.; Vitousek, P.M.; Chen, D. Policy distortions, farm size, and the overuse of agricultural chemicals in China. *Proc. Natl. Acad. Sci. USA* **2018**, *115*, 7010–7015. [CrossRef]
41. Perchlik, M.; Tegeder, M. Leaf amino acid supply affects photosynthetic and plant nitrogen use efficiency under nitrogen stress. *Plant Physiol.* **2018**, *178*, 174–188. [CrossRef]
42. Shi, J.; Yasuor, H.; Yermiyahu, U.; Zuo, Q.; Ben-Gal, A. Dynamic responses of wheat to drought and nitrogen stresses during re-watering cycles. *Agric. Water Manag.* **2014**, *146*, 163–172.
43. Ouyang, Z.; Tian, J.C.; Zhao, C.; Yan, X.F. Coupling model and optimal combination scheme of water, fertilizer, dissolved oxygen and temperature in greenhouse tomato under drip irrigation. *Int. J. Agric. Biol. Eng.* **2021**, *14*, 37–46.
44. Roca, L.F.; Romero, J.; Boh'orquez, J.M.; Alcántara, E.; Fernández-Escobar, R.; Trapero, A. Nitrogen status affects growth, chlorophyll content and infection by Fusicladium oleagineum in olive. *Crop Prot.* **2018**, *109*, 80–85. [CrossRef]
45. Anjum, S.A.; Wang, L.C.; Farooq, M.; Hussain, M.; Xue, L.L.; Zou, C.M. Brassinolide application improves the drought tolerance in maize through modulation of enzymatic antioxidants and leaf gas exchange. *J. Agron. Crop Sci.* **2011**, *197*, 177–185.
46. Kaur, K.; Kaur, N.; Gupta, A.K.; Singh, I. Exploration of the antioxidative defense system to characterize chickpea genotypes showing differential response towards water deficit conditions. *Plant Growth Regul.* **2013**, *70*, 49–60. [CrossRef]
47. Xu, G.; Fan, X.; Miller, A.J. Plant nitrogen assimilation and use efficiency. *Annu. Rev. Plant Biol.* **2012**, *63*, 153–182.
48. Lum, M.S.; Hanafi, M.M.; Rafii, Y.M.; Akmar, A.S.N. Effect of drought stress on growth, proline and antioxidant enzyme activities of upland rice. *J. Anim. Plant Sci.* **2014**, *24*, 1487–1493.
49. Kang, S.Z.; Hao, X.M.; Du, T.S.; Tong, L.; Su, X.L.; Lu, H.N.; Li, X.L.; Huo, Z.L.; Li, S.E.; Ding, R.S. Improving agricultural water productivity to ensure food security in China under changing environment: From research to practice. *Agric. Water Manag.* **2017**, *179*, 5–17. [CrossRef]
50. Valdés, R.; Miralles, J.; Franco, J.A.; Sánchez-Blanco, M.J.; Bañón, S. Using soil bulk electrical conductivity to manage saline irrigation in the production of potted poinsettia. *Sci. Hortic.* **2014**, *170*, 1–7. [CrossRef]
51. Beck, E.H.; Fetitig, S.; Knake, C.; Hartig, K.; Bhattarai, T. Specific and unspecificresponses of plants to cold and drought stress. *J. Biosci.* **2007**, *32*, 501–510.
52. Miller, G.; Suzuki, N.; Ciftci-Yilmaz, S.; Mittler, R. Reactive oxygen species homeostasis and signaling during drought and salinity stresses. *Plant Cell Environ.* **2010**, *33*, 453–467. [CrossRef]
53. Sairam, R.K.; Srivastava, G.C. Water stress tolerance of wheat (*Triticum aestivum* L.): Variations in hydrogen peroxide accumulation and antioxidant activity in tolerant and susceptible genotypes. *J. Agron. Crop Sci.* **2001**, *186*, 63–70. [CrossRef]
54. Yan, M.F.; Zhang, X.S.; Jiang, Y.; Zhou, G.S. Effects of irrigation and plowing on soil carbon dioxide efflux in a poplar plantation chronosequence in northwest China. *Soil Sci. Plant Nutr.* **2011**, *57*, 466–474. [CrossRef]
55. Fotelli, M.N.; Rennenberg, H.; Gessler, A. Effects of drought on the competitive interference of an early successional species (Rubus fruticosus) on *Fagus sylvatica* L. seedlings: N-15 uptake and partitioning, responses of amino acids and other N compounds. *Plant Biol.* **2002**, *4*, 311–320. [CrossRef]
56. Abdalhi, M.A.M.; Cheng, J.L.; Feng, S.Y.; Yi, G. Performance of drip irrigation and nitrogen fertilizer in irrigation water saving and nitrogen use efficiency for waxy maize (*Zea mays* L.) and cucumber (*Cucumis sativus* L.) under solar greenhouse. *Grassl. Sci.* **2016**, *62*, 174–187. [CrossRef]
57. Li, D.; Dong, J.L.; Gruda, N.S.; Li, X.; Duan, Z.Q. Elevated root-zone temperature promotes the growth and alleviates the photosynthetic acclimation of cucumber plants exposed to elevated [CO_2]. Environ. *Exp. Bot.* **2022**, *194*, 104694. [CrossRef]
58. Zhu, Y.; Cai, H.J.; Song, L.B.; Chen, H. Aerated irrigation promotes soil respiration and microorganism abundance around tomato rhizosphere. *Soil Sci. Soc. Am. J.* **2019**, *83*, 1343–1355. [CrossRef]

land

MDPI

Article

Modeling Current and Future Potential Land Distribution Dynamics of Wheat, Rice, and Maize under Climate Change Scenarios Using MaxEnt

Shahzad Ali [1,*], Muhammad Umair [2], Tyan Alice Makanda [3], Siqi Shi [4], Shaik Althaf Hussain [5] and Jian Ni [3]

[1] College of Chemistry and Materials Science, Zhejiang Normal University, Jinhua 321004, China
[2] School of Agriculture and Biology, Shanghai Jiao Tong University, Shanghai 200240, China
[3] College of Life Sciences, Zhejiang Normal University, Jinhua 321004, China
[4] Faculty of Geo-Information Science and Earth Observation (ITC), University of Twente, 7500 AE Enschede, The Netherlands
[5] Department of Zoology, College of Science, King Saud University, P.O. Box 2454, Riyadh 11451, Saudi Arabia
* Correspondence: shahzadali320@aup.edu.pk

Abstract: Accurately predicting changes in the potential distribution of crops resulting from climate change has great significance for adapting to and mitigating the impacts of climate change and ensuring food security. After understanding the spatial and temporal suitability of wheat (*Triticum aestivum*), rice (*Oryza sativa*), and maize (*Zea mays*), as well as the main bioclimatic variables affecting crop growth, we used the MaxEnt model. The accuracy of the MaxEnt was extremely significant, with mean AUC (area under curve) values ranging from 0.876 to 0.916 for all models evaluated. The results showed that for wheat, annual mean temperature (Bio-1) and mean temperature of the coldest quarter (Bio-11) contributed 39.2% and 13.4%, respctively; for rice, precipitation of the warmest quarter (Bio-18) and elevation contributed 34.9% and 19.9%, respectively; and for maize, Bio-1 and precipitation of the driest quarter (Bio-17) contributed 36.3% and 14.3%, respectively. The map drawn indicates that the suitability of wheat, rice, and corn in South Asia may change in the future. Understanding the future distribution of crops can help develop transformative climate change adaptation strategies that consider future crop suitability. The study showed an average significant improvement in high-suitable areas of 8.7%, 30.9%, and 13.1%, for wheat, rice, and maize, respectively; moderate-suitable area increases of 3.9% and 8.6% for wheat and rice, respectively; and a decrease of −8.3% for maize as compared with the current values. The change in the unsuitable areas significantly decreases by −2.5%, −13.5%, and −1.7% for wheat, rice, and maize, respectively, compared to current land suitability. The results of this study are crucial for South Asia as they provide policy-makers with an opportunity to develop appropriate adaptation and mitigation strategies to sustain wheat, rice, and corn production in future climate scenarios.

Keywords: geographic suitability; land suitability dynamics; bioclimatic variables; big data; MaxEnt model; South Asia

Citation: Ali, S.; Umair, M.; Makanda, T.A.; Shi, S.; Hussain, S.A.; Ni, J. Modeling Current and Future Potential Land Distribution Dynamics of Wheat, Rice, and Maize under Climate Change Scenarios Using MaxEnt. *Land* **2024**, *13*, 1156. https://doi.org/10.3390/land13081156

Academic Editor: Nir Krakauer

Received: 19 May 2024
Revised: 17 July 2024
Accepted: 18 July 2024
Published: 28 July 2024

1. Introduction

Global climate change, rising global temperatures, uneven rainfall distribution, and extreme weather, is considered one of the main factors that is affecting global socio-economic development and nature conservation [1,2]. Several studies have revealed that global warming will reduce the crop production of wheat and rice in South Asia, which is a serious threat to food security and sustainable development [3,4]. Climate change is likely to affect the crop distributions [5], which is likely to have a significant influence on global food production. In rural agricultural communities, climate change will greatly affect food and nutritional security [6]. Climate change will alter the existing suitability of regions for specific crops and affect their development, growth, and production [7,8]. Predicting

the potential land suitability of crops is a key issue for accurately assessing the impact of climate change on crop distribution. However, there is relatively little research on the impact of climate change on potential land suitability dynamics.

Land distribution is often seen as a combination of land characteristics and crop demand [9]. The climate conditions, soil quality, water availability, and land characteristics of a region are the most essential factors for a crop land suitability assessment [10]. To assess the potential land suitability of wheat, rice, and corn, it is essential to establish a function to analyze the relationship between land suitability and these factors. In recent years, the latest advances in remote sensing and geographic information technology have made it possible for multiple modeling programs to analyze crop land suitability under climate change [11]. The species distribution model is considered an empirical tool in ecology and natural resource management, and its use in predicting species existence based on the correlation between ecological variables and geographically located species data has been considered important [12]. MaxEnt is one of the most popular niche-based methods for modeling geographical crop distribution [12]. Based on detailed occurrence records and consideration of ecological variables that may affect the target species, the relationship between them can be assessed by using the MaxEnt model [13]. Furthermore, MaxEnt also predicts the spatial and temporal potential species distribution [14,15]. The MaxEnt model has been used to categorize hotspots of potential hazards of invasive species, assess threatened species, predict biodiversity, and identify potential regions for species cultivation in response to climate change [16].

However, global climate change may have considerable influence on future wheat and rice production. For example, it has been proven that rising temperatures can reduce the grain yield of rice and wheat [17]. Furthermore, the intensification of meteorological droughts caused by global warming has had a negative impact on the yield of corn and many other crops [18,19]. In order to meet the global food demand, finding potential suitable areas for wheat, rice, and corn cultivation in the future has become a problem that needs to be addressed [20]. The MaxEnt model involves organizing crops occurrence data, linking these occurrences to land and bioclimatic variables and creating maps that forecast past, present, and future distributions of species [21,22]. They link environmental variables with phylogenetic records to gain a deeper understanding of ecological drivers and help to forecast large-scale agricultural and ecological suitability [23]. The MaxEnt model can handle sparse, irregularly sampled data and small positional errors well. Zheng et al. [24] successfully utilized the MaxEnt model to identify corn-suitable regions in Kenya. Additionally, Bunn et al. [25] drew a land suitability map for rice. Akpoti et al. (2020) [1] drew a recommendation area map to expand wheat crop under the climate change adaptation strategies.

Wheat and rice are important food crops. From the perspective of South Asia, there is an urgent need to narrow the supply–demand gap in order to maintain the supply of wheat and rice in the South Asian market. So far, research on wheat and rice has mainly focused on growth and development [26], production [27], physiological responses [28,29], and farming and management [30]. Thus, it is essential to balance the suitability of wheat and rice, as well as the current and future suitable distribution ranges. This study attempts to address this issue using the MaxEnt model, which uses bioclimatic variables to predict potential planting areas for different crops with occurrence data [31]. This model is the most widely used for predicting land suitability, with a high accuracy [32]. The goal is to optimize the planting layout of wheat, corn, and rice in areas with limited land resources, in order to efficiently generate social, ecological, and economic profits.

Wheat, rice, and corn play important roles in maintaining global food security [33]. Although studies have revealed that the production of these crops can be affected by climate change [34,35], the dynamic changes in the potential land suitability of wheat, rice, and corn caused by climate change have not been studied in South Asia. The purpose of this research is to study the following: (1) What are the main climatic factors that affect the geographical range of wheat, rice, and corn? (2) Which regions are more appropriate for

the growth of wheat, rice, and corn under the current climate conditions? (3) How will the future climate (2020–2100) affect habitats, thereby affecting the potential distribution of wheat, rice, and corn? (4) Determination of the spatial climate suitability changes for wheat, rice, and corn production in South Asia. This research will help decision-makers determine the magnitude of area expansion for wheat, rice, and corn to maintain future regional food security.

2. Materials and Methods

2.1. Study Site and Species Occurrence Record

South Asia includes 8 countries (Figure 1), with a geographic range of 114°09′–122°43′ E and 34°22′–38°23′ N. Areas of study include eight countries such as Afghanistan, Pakistan, India, Nepal, Sri-Lanka, Bangladesh, the Maldives, and Bhutan. This region has a variety of geographic and climatic types, namely dry-land, desert, subtropical and tropical, mountain, alpine, and humid climates. South Asia includes tropical and subtropical regions, with various climate zones in the west, temperate zones in northern India and Nepal, and arid regions in eastern India, Pakistan, and Afghanistan. In this study, we estimated distribution models using public databases collecting current distribution data for wheat, rice, and maize. Global distribution data for wheat, rice, and maize were collected from the GBIF database (GBIF, 2021). In addition, we subsequently reviewed this data set critically from records on the GBIF database and manually removed unreliable and ambiguous records through the "Description of Occurrence" column for unconfirmed species identification. Afterwards, we excluded duplicate records and records with imprecise geographical location definitions (uncertainty greater than 10^4 m) for a more reliable evaluation. After this screening, we obtained a total of 924 records of wheat existence, 1996 records of rice existence, and 332 records of corn existence. Figure 1 shows the general distribution of crop occurrence records. The occurrence records were used to produce present and future distribution models for wheat, rice, and maize species.

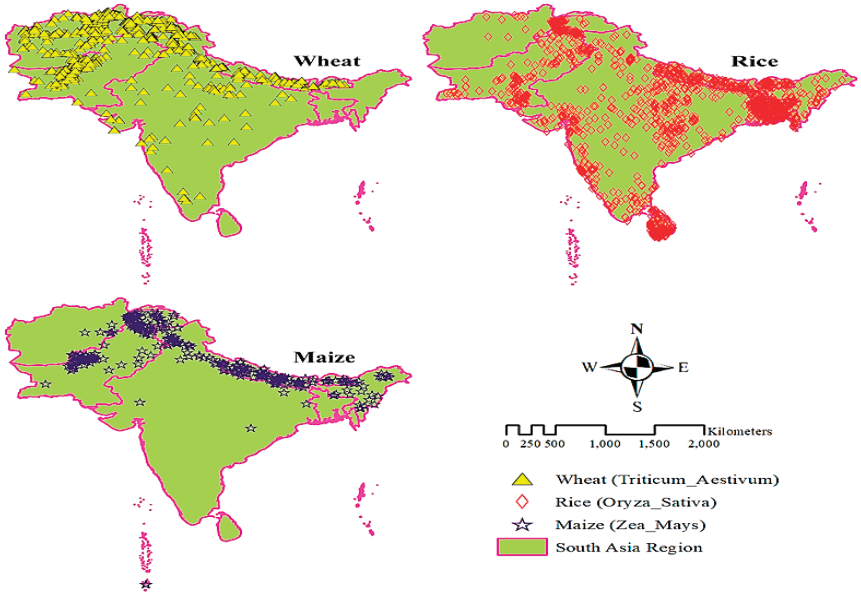

Figure 1. Occurrence points of wheat, rice, and maize in South Asia region. Occurrence points Data were accessed from GBIF.org (https://www.gbif.org/occurrence/search, accessed on 18 May 2024) database. GBIF = Global Biodiversity Information Facility.

2.2. Current Bioclimatic Variables

Climate data for the study area was downloaded from the Worldclim database (version 2.1, www.worldclim.org, accessed on 18 May 2024), which comprises 19 bioclimatic variables, including solar radiation, elevation, wind speed, and water vapor pressure, with global coverage. These variables are derived from the monthly temperature and precipitation values and are frequently used in numerous ecological and biogeographic studies for modeling species distribution [36]. The layers were downloaded at a spatial resolution of 30 s, an equivalence of 1 km^2 (Table 1). With the help of ArcGIS 10.7.1 Esri, all bioclim layers were trimmed to make maps of South Asia. The trimmed layers were then set to the same resolution, extent, and projection and converted to ASCII (asc) to meet the MaxEnt requirements. Additionally, a correlation test was carried out using the SDM toolbox v 2.5 with the Pearson correlation coefficient. To identify highly correlated variables and minimize the effects of multi-collinearity and model overfitting, the person correlation coefficient method was used [36]. The flowchart and processing methodology of the research are shown in Figure 2.

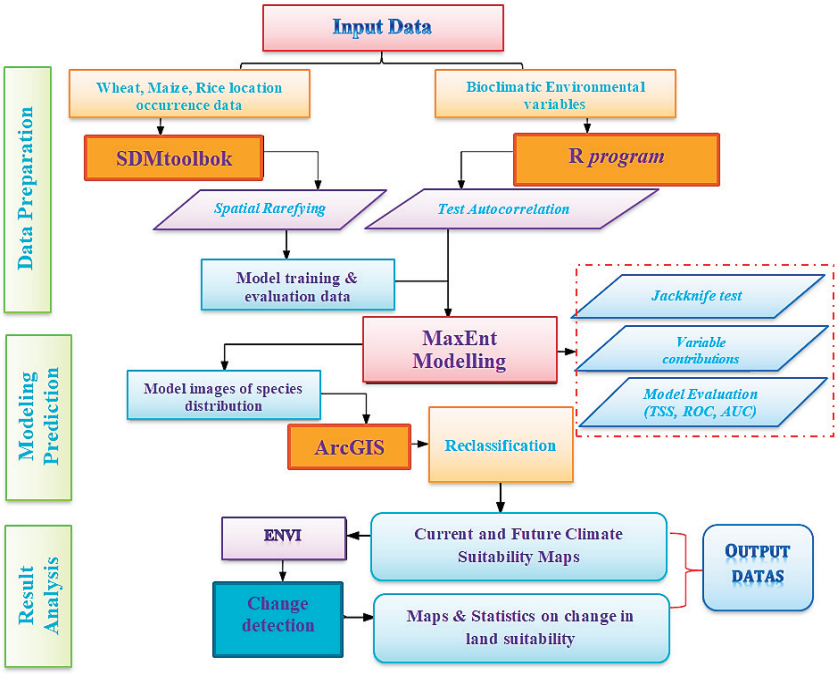

Figure 2. Flowchart summarizing the processing methodology used in this study.

Table 1. Bioclimatic environmental variables used in MaxEnt model.

Variable Code	Description	Unit	Source
Bio1	Annual mean temperature	°C	
Bio2	Mean diurnal range	°C	
Bio3	Isothermality	°C	
Bio4	Temperature seasonality	°C	
Bio5	Maximum temperature of the warmest month	°C	
Bio6	Minimum temperature of the coldest month	°C	
Bio7	Temperature annual range	°C	
Bio8	Mean temperature of the wettest quarter	°C	

Table 1. *Cont.*

Variable Code	Description	Unit	Source
Bio9	Mean temperature of the driest quarter	°C	WorldClim [a,b]
Bio10	Mean temperature of the warmest quarter	°C	
Bio11	Mean temperature of the coldest quarter	°C	
Bio12	Annual precipitation	mm	
Bio13	Precipitation of the wettest month	mm	
Bio14	Precipitation of the driest month	mm	
Bio15	Precipitation seasonality	mm	
Bio16	Precipitation of the wettest quarter	mm	
Bio17	Precipitation of the driest quarter	mm	
Bio18	Precipitation of the warmest quarter	mm	
Bio19	Precipitation of the coldest quarter	mm	
Elev	Elevation	km	
SR	Solar radiation	KJ m^{-2} day^{-1}	
WS	Wind speed	m s^{-1}	
WVP	Water vapor pressure	kPa	

[a] Data for current climate conditions were accessed from WorldClim (https://www.worldclim.org/data/worldclim21.html, accessed on 18 May 2024).[b] Data for future climate projections were accessed from WorldClim (https://www.worldclim.org/data/cmip6/cmip6_clim30s.html, accessed on 18 May 2024).

2.3. Future Climate Change Scenarios

The climate layers for the current projection are representatives of averages for the years 1970–2000. We modeled the future distributions of wheat, rice, and maize to examine differences in their potential habitats under different climate scenarios. This data was derived from the CMIP6. Two global general circulation models (GCMs) namely, HadCM3 and IPSL-CM6A-LR, were used. Global climate model projections portray the future climatic conditions. Hence, making it is possible to understand whether crop suitability in an area will remain the same or not. Each GCM was tested under the shared socioeconomic pathways (SSPs) consisting of five main ACCESS-CM2-SPPs (SSP119, SSP126, SSP245, SSP370, and SSP585). Among them, we use the intermediate shared SSP (SSP585) for four steps: 2021–2040, 2041–2060, 2061–2080, and 2081–2100. The SSPs scenarios belong to the "SSPs socioeconomic family", which stands for "sustainability" [37].

2.4. MaxEnt Model Description

The MaxEnt model version 3.4.4 was used to make the current and future prediction models. The MaxEnt model was selected because it is a widely used SDM that exhibits greater accuracy than other models. The maximum entropy principle does not make any assumptions about the unknown information; it only takes into consideration the known data, and that is, it models species distribution from the information of present species [38]. During the modeling, most of the settings were left at default. The random test percentage was set at 30. This means that 30% of the data was withheld and used for testing, while the remaining 70% was used for model training. It has also been defined as a presence only model that uses predictive data sets to discriminate crop occurrence records [39,40]. Although the underlying prediction of those areas has been systematically sampled from most existing lands, the MaxEnt model is often constructed from spatially based occurrence records [41]. MaxEnt is one of the most popular niche-based methods for modeling geographical crop distributions [42]. This model also offers valuable tools such as jackknife tests, species environment curves, and area under the AUC and ROC curves [43].

2.5. MaxEnt Model Validation and Application

The ROC curve was used to validate the performance of the MaxEnt model. The ROC curves are a standard way to evaluate the MaxEnt model's predictive accuracy [44]. The area of the ROC curve is a threshold independent measure of model performance, called

(AUC) area under the ROC curve [45]. The closer the value is to 1, the greater the probability of a species presence [46,47]. The AUC values greater than 0.9 show very high accuracy, values 0.7–0.9 show high accuracy, and values less than 0.7 show low accuracy [48]. The MaxEnt model predicts 2021–2040, 2041–2060, 2061–2080, and 2081–2100 land suitability for maize, wheat, and rice distribution under different future bioclimatic conditions. During the modeling, most of the settings were left at default, which include auto features, a regularization multiplier of 1, and maximum number of background points of 10,000 [49]. 10 replicates were simulated under the default cross validate run type and used to calculate the mean relative suitability probabilities. The options for response curves and jackknife were also selected. The output from the MaxEnt model is a continuous, unitless scale of environmental suitability ranging from 0 to 1. In order to compare the suitable area, the output models were reclassified using the natural breaks (Jenks) classification method in ArcGIS 10.7.1 Esri. The classification was divided into four classes, which represent areas of 0.0–0.05, not suitable; 0.05–0.33, low suitability; 0.33–0.66, moderate suitability; and 0.66–1.00, high suitable, respectively [50]. The response curves were also used to understand the relationship between crop land suitability and bioclimatic variables in determining the land suitability for wheat, rice, and maize.

3. Results and Discussion

3.1. MaxEnt Model Performance and Jackknife Tests

This study developed a MaxEnt bioclimatic model to examine which bioclimatic variables are more explanatory in the distribution of wheat, rice, and corn species. In this study, the performance of the MaxEnt model was examined based on receiver operating characteristic (ROC) curves and AUC values (Figure 3). The MaxEnt model is an excellent tool for understanding the factors that influence the potential distribution of several crops at different scales [51]. The average AUC values of wheat, rice, and corn after 10 repeated runs were 0.876, 0.882, and 0.916, respectively, which were higher than the 0.70 of the random models, verifying the good simulation results using the test and training datasets of the repeated model. The representativeness of the training samples used in the MaxEnt model may considerably affect the accuracy of land suitability prediction. Firstly, it was selected as the training sample data source [52]. This discovery indicates that the climatic variables selected for the current suitability characteristics of wheat, rice, and corn are excellent. The ROC curve and AUC results indicate that the MaxEnt is highly consistent and can reveal the distribution of wheat, rice, and corn in South Asia. The MaxEnt model performs well in predicting the suitability of wheat, rice, and corn species. A previous study suggested that comparing the performance between different training datasets is appropriate [53].

The impact of each environmental variable on the geographical suitability of wheat, rice, and corn species cultivation was analyzed in the jackknife AUC test. Using fifth percentile proportional sampling [54] and custom interval grouping methods, the AUC values were 0.750 and 0.747, respectively. The jackknife AUC test results showed that the distribution of wheat species is largely controlled by Bio-1, Bio-10, and Bio-11, with altitude and water vapor pressure providing the highest wheat AUC test results (Figure 4). MaxEnt software predicts the potential range of species based on their distribution and environmental variables [55,56]. The precipitation in the driest region (Bio-17) and the warmest region (Bio-18) also contributes more to the wheat model. Based on the jackknife AUC test results, it is worth noting that Bio-2, Bio-7, Bio-12, and altitude contributed to the highest AUC test and provided the determination of rice cultivation (Figure 4). In addition to the precipitation in the driest season (Bio-17) and the warmest season (Bio-18), the contribution to the MaxEnt model of rice is also greater. The suitability of wheat and rice is most important based on precipitation factors, which is consistent with other studies that have identified precipitation as a key determinant of marginal production systems [57,58].

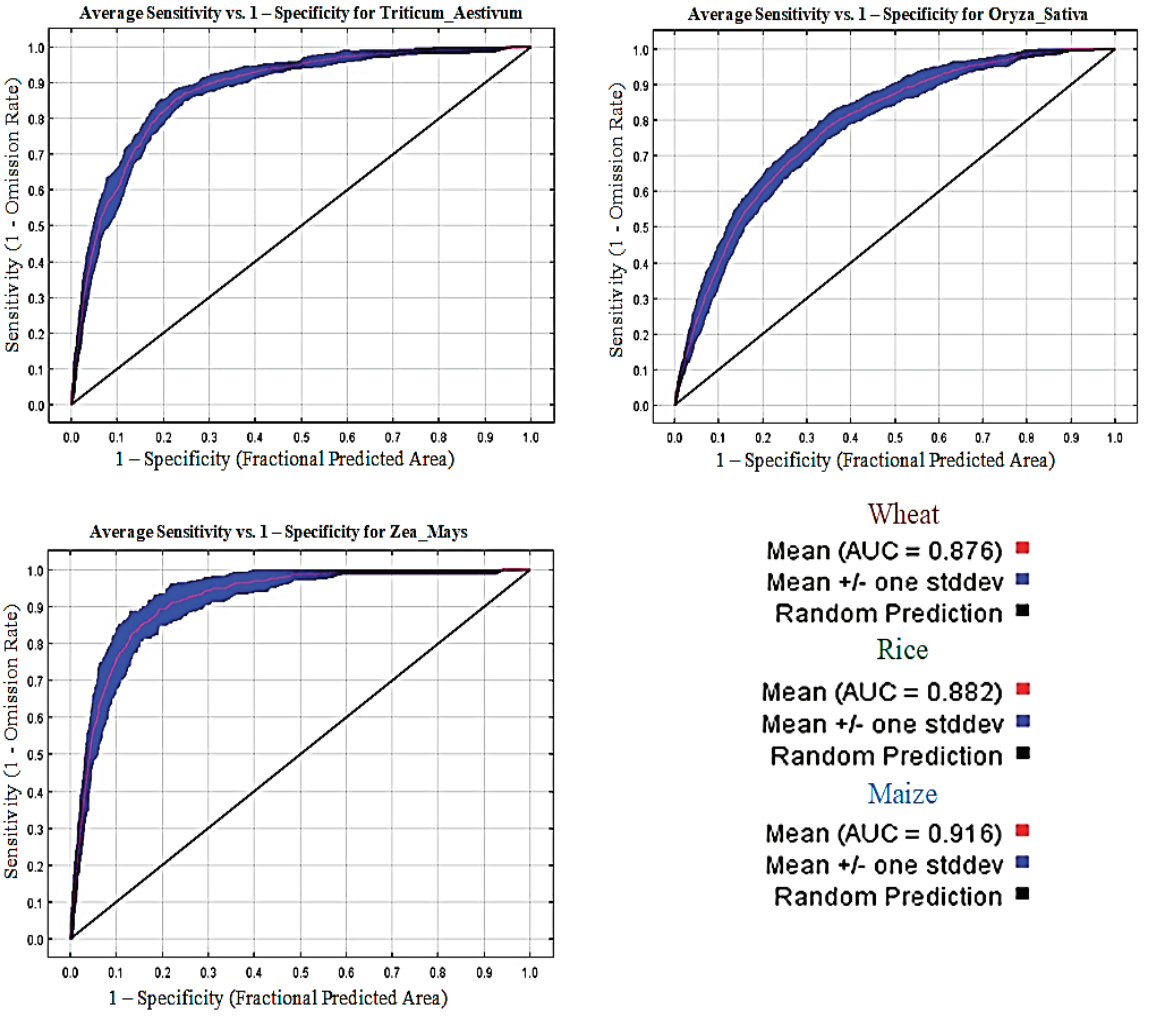

Figure 3. Receiver operating characteristic (ROC) curve and AUC value under the current (1970–2000) period (10 replicated runs).

These environmental bioclimatic variables, acting alone with altitude and water vapor pressure, have a considerable impact on the potential land suitability dynamics of wheat, rice, and corn and indicate that these aspects themselves contain more valuable information than other environmental bioclimatic parameters. The MaxEnt model is an effective tool for generating valuable information related to agricultural plantation management and planting decisions in special areas [59,60]. Jackknife AUC testing showed that the suitability of maize species is largely controlled by Bio-1, Bio-5, Bio-9, and Bio-10, with altitude providing the highest maize AUC test results (Figure 4). The AUC and ROC curves in MaxEnt generally measure the overall model performance at all threshold levels [61].

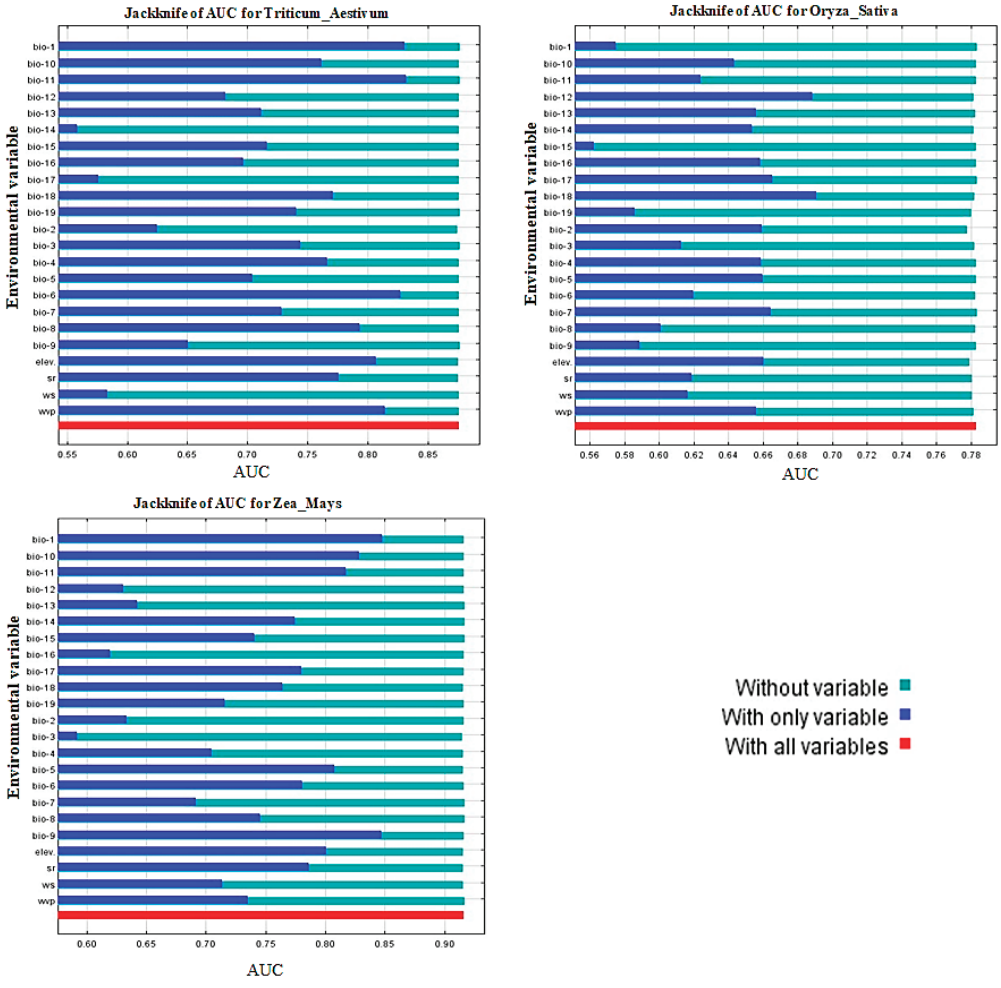

Figure 4. Results of the jackknife AUC test of the MaxEnt model for evaluating the relative importance of bioclimatic environmental variables for wheat, rice, and maize occurrence.

3.2. Contribution and Importance of the Bioclimatic Variables under Different Scenarios

The climate factors that affect the suitability of wheat, rice, and corn production in the region come from six bioclimatic variables selected from each group of highly correlated predictive factors. The jackknife test of this model shows that there are six current (1970–2000) bioclimatic variables, Bio-1, Bio-10, Bio-11, and Bio-18, namely altitude and water vapor pressure, which contribute 39.2%, 5.1%, 13.4%, 6.4%, 5.8%, and 6.3% to the distribution of wheat species (Table 2). In the future, ACCESS-CM2-SPP SSP585 (2021–2040), Bio-1, Bio-11, and Bio-18 contributed 48.5%, 13.8%, and 10.0%, respectively; during the period of 2041–2060, the contribution rates of Bio-1, Bio-11, and Bio-18 were 46.1%, 15.1%, and 8.7%, respectively; during the period of 2061–2080, the contributions of Bio-1, Bio-6, and Bio-18 to the MaxEnt model were 24.2%, 11.7%, and 33.3%, respectively; and during the period of 2081–2100, Bio-1, Bio-11, and Bio-18 were 9.9%, 48.2%, and 8.3%, respectively. It is crucial to determine the main bioclimatic variables that have a considerable impact on crop land distribution in order to predict land suitability [62]. The performance of the MaxEnt model indicates that it is a good model, with an AUC of 0.80 [63].

Table 2. Primary contribution percent and permutation importance of the bioclimatic environmental variables impacting wheat distribution (%). Simulation results of the MaxEnt model.

Bioclimatic Variables	Wheat (Triticum_Aestivum)									
	Current (1970–2000)		SSP585 (2021–2040)		SSP585 (2041–2060)		SSP585 (2061–2080)		SSP585 (2081–2100)	
	Percent Contribution	Permutation Importance (%)	Percent Contribution	Permutation Importance (%)	Percent Contribution	Permutation Importance (%)	Percent Contribution	Permutation Importance (%)	Percent Contribution	Permutation Importance (%)
Bio1	**39.2**	**16.0**	**48.5**	**30.7**	**46.1**	**42.1**	**24.2**	**37.9**	**9.9**	**37.3**
Bio2	1.8	**7.9**	1.9	**3.7**	1.9	**5.1**	1.9	**5.0**	1.7	**4.5**
Bio3	1.0	3.6	0.3	1.2	0.2	0.7	0.2	0.6	0.4	0.9
Bio4	1.9	1.6	1.9	1.0	2.6	1.1	1.9	1.7	1.6	2.5
Bio5	4.7	**11.3**	1.9	**5.6**	2.5	**5.6**	2.0	**3.8**	2.3	**7.8**
Bio6	1.4	0.0	**3.5**	0.2	**5.0**	2.1	**11.7**	1.6	**8.0**	2.3
Bio7	0.5	0.3	0.6	0.4	0.7	0.4	0.4	0.1	0.4	0.3
Bio8	2.2	1.7	3.2	1.6	1.9	1.2	2.4	2.7	4.7	1.4
Bio9	0.2	0.0	0.6	0.4	0.9	1.0	0.6	0.7	0.7	0.3
Bio10	**5.1**	4.0	**7.1**	**4.9**	**7.6**	**6.0**	**6.1**	**4.6**	**6.7**	2.1
Bio11	**13.4**	5.8	**13.8**	**36.3**	**15.1**	**24.1**	**33.3**	**27.4**	**48.2**	**25.9**
Bio12	1.4	2.0	1.3	2.1	1.4	2.0	1.7	2.9	2.2	**2.8**
Bio13	1.0	2.3	0.7	1.5	1.1	1.4	1.1	1.6	0.9	2.0
Bio14	2.3	0.2	**3.5**	1.2	**3.3**	1.2	**3.5**	1.1	**3.4**	2.0
Bio15	0.5	1.0	1.1	1.5	0.8	0.9	0.8	1.4	0.6	1.0
Bio16	0.1	0.8	0.1	0.4	0.1	0.4	0.1	0.4	0.1	0.6
Bio17	0.0	1.6	0.0	0.5	0.0	0.4	0.0	0.2	0.0	0.1
Bio18	**6.4**	5.4	**10.0**	**6.8**	**8.7**	**4.0**	**8.2**	**6.2**	**8.3**	**6.2**
Bio19	0.2	0.8	0.0	0.1	0.0	0.1	0.0	0.1	0.0	0.0
Elevation	**5.8**	5.7								
Solar radiation	2.1	**10.9**								
Wind speed	2.4	**6.8**								
Water vapor pressure	**6.3**	**10.3**								

Here, SSPs = socio-economic pathways; bold: the most influential variable of wheat distribution.

It is expected that surface temperatures will rise throughout the 21st century [64], resulting in a negative impact on global wheat production [65,66]. Under current and future bioclimatic variables, Bio-1, Bio-11, and Bio-18 have the highest ranking importance percentage analysis. For rice, there are currently (1970–2000) six bioclimatic variables Bio-2, Bio-6, Bio-12, Bio-14, Bio-18, and altitude contributing 4.3%, 3.0%, 4.2%, 8.7%, 34.9%, and 19.9% (Table 3). In the future, ACCESS-CM2-SPP SSP585 (2021–2040), Bio-2, Bio-12, and Bio-18 contributed 8.3%, 12.3%, and 47.5%, respectively; during the period of 2041–2060, the contribution rates of Bio-7, Bio-12, and Bio-18 were 7.4%, 10.6%, and 50.6%, respectively; during the period of (2061–2080), the contributions of Bio-4, Bio-12, and Bio-18 to the MaxEnt model were 7.8%, 12.0%, and 49.6%, respectively; and during the period of (2081–2100), Bio-12, Bio-14, and Bio-18 were 22.3%, 6.5%, and 37.6%, respectively. In addition, the temperature and altitude range for rice growth are 20–35 °C and below 1450 m [67], which is consistent with our study results. Under current and future bioclimatic variables, the importance percentage analysis of Bio-2, Bio-12, and Bio-18 rank highest.

We also need to know the influences of climate change to predict the potential suitability of current and future invasive areas in order to develop better prevention strategies. For corn, current bioclimatic variables such as Bio-1, Bio-14, and altitude contribute 36.3%, 14.3%, and 7.1%, respectively (Table 4). The highest percentile importance analysis of corn under current and future bioclimatic variables is Bio-1, Bio-11, and Bio-17, respectively. This result is consistent with previous research findings, which have shown that changes in temperature and day–night range can lead to changes in the distribution of maize plants [68]. The distribution of maize habitats is significantly influenced by temperature [69].

Table 3. Primary contribution percent and permutation importance of the bioclimatic environmental variables impacting rice distribution (%) in the MaxEnt model.

Bioclimatic Variables	Rice (Oryza_Sativa)									
	Current (1970–2000)		SSP585 (2021–2040)		SSP585 (2041–2060)		SSP585 (2061–2080)		SSP585 (2081–2100)	
	Percent Contribution	Permutation Importance (%)	Percent Contribution	Permutation Importance (%)	Percent Contribution	Permutation Importance (%)	Percent Contribution	Permutation Importance (%)	Percent Contribution	Permutation Importance (%)
Bio1	1.9	0.9	0.9	6.6	1.1	5.9	0.8	5.2	0.6	3.2
Bio2	**4.3**	**14.1**	**8.3**	**8.6**	**5.2**	**7.1**	**4.0**	**6.0**	**5.2**	**5.8**
Bio3	2.1	**12.8**	1.5	2.1	2.0	2.6	1.6	1.4	2.6	2.1
Bio4	2.7	1.7	**3.8**	**9.0**	**4.9**	**11.2**	**7.8**	**11.1**	**5.1**	**14.5**
Bio5	0.3	2.3	1.5	0.6	1.0	0.1	1.3	0.1	1.5	0.4
Bio6	**3.0**	**7.1**	**3.6**	**11.8**	**4.3**	**12.6**	3.7	**13.0**	**3.10**	**17.4**
Bio7	1.5	1.2	**6.0**	2.0	**7.4**	2.0	**3.8**	1.9	3.2	2.1
Bio8	0.6	4.0	0.7	3.6	0.6	3.2	0.8	2.9	1.0	3.1
Bio9	1.1	1.8	1.9	2.3	1.2	2.7	2.0	3.0	1.1	2.3
Bio10	0.2	0.7	1.1	**12.4**	1.1	**16.7**	1.8	**23.1**	0.8	**5.9**
Bio11	0.9	2.4	0.5	6.0	0.2	1.0	0.2	2.0	0.4	2.3
Bio12	**4.2**	4.3	**12.3**	**11.2**	**10.6**	**7.0**	**12.0**	**8.6**	**22.3**	4.2
Bio13	0.2	0.3	1.0	0.7	0.4	0.5	0.8	0.7	1.0	4.1
Bio14	**8.7**	4.3	2.4	1.4	2.9	1.4	**4.3**	2.0	**6.5**	4.2
Bio15	1.0	0.8	1.0	0.8	0.8	1.1	0.7	1.0	0.4	0.6
Bio16	0.1	0.1	0.6	1.7	0.5	0.1	0.2	0.1	0.4	0.3
Bio17	2.1	0.2	2.1	4.0	2.1	4.3	1.7	2.4	2.4	5.8
Bio18	**34.9**	**10.4**	**47.5**	**10.3**	**50.6**	**16.0**	**49.6**	**10.8**	**37.6**	**12.7**
Bio19	2.0	4.1	3.4	4.9	3.2	4.5	2.9	4.7	3.9	**8.9**
Elevation	**19.9**	**14.2**								
Solar radiation	2.9	**7.5**								
Wind speed	2.6	3.0								
Water vapor pressure	2.7	1.8								

Here, SSPs = socio-economic pathways; bold: the most influential variable of rice distribution.

Table 4. Primary contribution percent and permutation importance of the bioclimatic environmental variables impacting maize distribution (%) in the MaxEnt model.

Bioclimatic Variables	Maize (Zea_Mays)									
	Current (1970–2000)		SSP585 (2021–2040)		SSP585 (2041–2060)		SSP585 (2061–2080)		SSP585 (2081–2100)	
	Percent Contribution	Permutation Importance (%)	Percent Contribution	Permutation Importance (%)	Percent Contribution	Permutation Importance (%)	Percent Contribution	Permutation Importance (%)	Percent Contribution	Permutation Importance (%)
Bio1	**36.3**	2.0	**50.3**	**14.8**	**52.8**	**10.3**	**51.7**	**13.9**	**50.3**	**10.7**
Bio2	1.8	2.2	2.0	1.8	1.5	2.1	1.4	2.7	1.9	2.8
Bio3	1.3	**7.2**	1.3	3.6	1.2	4.2	1.3	3.5	1.4	3.2
Bio4	1.5	**12.8**	1.8	**9.8**	1.5	**12.7**	1.6	**13.8**	1.2	**13.0**
Bio5	**4.6**	**5.5**	2.8	3.0	2.9	2.1	3.2	2.0	**3.3**	1.5
Bio6	0.9	2.1	1.5	**10.6**	1.2	**8.6**	2.1	**8.0**	2.1	**8.9**
Bio7	0.7	2.0	1.2	1.1	0.7	2.1	0.8	2.0	0.6	2.4
Bio8	0.4	0.3	0.4	0.8	0.4	1.1	0.2	0.4	0.1	0.6
Bio9	2.6	2.0	0.3	2.4	0.2	1.6	0.3	1.6	0.8	2.0
Bio10	4.1	1.7	**5.9**	3.7	**5.1**	**5.6**	**3.5**	4.9	**3.0**	4.2
Bio11	3.1	3.2	**3.4**	**19.0**	**4.6**	**18.6**	**6.7**	**17.2**	**9.6**	**19.0**
Bio12	0.1	0.8	0.3	0.2	0.0	0.1	0.0	0.1	0.0	0.0
Bio13	1.3	0.3	1.2	0.7	0.7	1.3	0.9	1.3	0.7	1.5
Bio14	**8.7**	0.5	**5.8**	0.7	**5.2**	0.7	**5.9**	1.3	2.8	0.8
Bio15	1.2	5.1	1.5	4.3	1.5	3.8	1.4	3.7	0.5	1.6
Bio16	0.1	0.1	0.1	0.2	0.2	0.2	0.0	0.2	0.1	0.6
Bio17	**14.3**	**14.7**	**15.5**	**17.4**	**16.4**	**18.0**	**13.7**	**15.6**	**16.9**	**20.3**
Bio18	2.4	3.9	**4.4**	**4.6**	**3.5**	5.4	**4.4**	**5.9**	**3.6**	**4.9**
Bio19	0.1	2.7	0.3	1.2	0.4	1.6	0.7	2.0	1.2	1.9
Elevation	**7.1**	**16.3**								
Solar radiation	0.5	**9.1**								
Wind speed	**6.5**	5.0								
Water vapor pressure	0.5	0.2								

Here, SSPs = socio-economic pathways; bold: the most influential variable of maize distribution.

3.3. Potential Land Suitability under Current and Future Climate

There is little research on the suitability of crops in South Asia by using regional climate models, but the MaxEnt model is an effective model for potential crop land distribution [70]. The potential geographically suitable habitat distribution of wheat, rice, and corn under current and future conditions is shown in Figure 5. Habitat is divided into four levels on the map. The green-marked areas in Figure 5 represent areas where wheat, rice, and corn are highly suitable for cultivation, as well as areas where crops are currently being grown. The yellow area is expected to be moderately suitable for planting, while the red area is not suitable for planting crops. In addition, for wheat, high suitability land in northern Afghanistan, northwestern Pakistan, northern India, Nepal, and Bhutan is on the rise, while land suitability in Bangladesh, Sri Lanka, and the Maldives is on the decline. A previous study revealed that the global wheat planting area will considerably improve by 2035 [71]. Our findings suggest that environmental changes will considerably alter the overall suitability of wheat planting land. For rice, the northeast of Pakistan and India are highly suitable lands, while Nepal, Bhutan, Bangladesh, and Sri Lanka are highly suitable areas, and rice cultivation is showing an increasing trend. The suitability of rice fields in Afghanistan is decreasing. In addition, India, Thailand, Philippines and Pakistan domestic rice production is insufficient to meet their needs [72]. For corn, the land suitability in northwestern Pakistan, northeastern India, northern Nepal, and Bhutan is higher and showing an increasing trend, while corn cultivation in Afghanistan, Bangladesh, Sri Lanka, the Maldives, and eastern and western India is decreasing. The future climate scenario used in this study has identified the potential changes in suitable habitats for wheat, rice, and corn between current and future climate change (Table 2). Meanwhile, many studies claim that with climate change, drought events will become more frequent and severe [71,73], which may also extremely affect corn suitability [36]. There are significant variances in the potential land suitability of highly and moderately habitats under diverse climate change.

We calculated the suitable habitat area and proportion for each climate scenario in four different periods to further analyze the impact of climate change on the land suitability of wheat, rice, and corn under different scenarios (Table 5). A prerequisite understanding of species distribution is important for species utilization and restoration in ecosystems [38,41]. Under the SSP585 climate scenarios for the study area in 2040, 2060, 2080, and 2100, the suitable high, medium, and low habitats for wheat will significantly increase, while the unsuitable area will significantly decrease. Climate change will raise wheat production in high latitudes, while warm regions may suffer greater [61,65]. It is expected that in the future, the total unsuitable and low-suitable rice area will be significantly reduced compared to the current situation. In the SSP5852040, 2060, 2080, and 2100 scenarios, the high land suitability for rice is expected to significantly rise by 32.3%, 31.8%, 30.2%, and 29.4%, respectively, compared to the current situation. These habitats mainly include the major corn and rice suitability areas in South Asia and provide important commercial food bases [37,74]. For corn, it is expected that in the future, the total area that is not suitable and moderately suitable will be significantly reduced compared to the current situation. In the SSP585 2040, 2060, 2080, and 2100 scenarios, the area of high distribution corn is expected to significantly improve by 12.5%, 11.8%, 15.3%, and 12.8% compared to the current situation, respectively (Figure 6).

Table 5. Changes in land suitability for wheat, rice, and maize under the current and future climatic conditions.

Suitability Index	Climate Scenarios	Time Period	Wheat $\times 10^5$ km^2	Change in Area (%)	Rice $\times 10^5$ km^2	Change in Area (%)	Maize $\times 10^5$ km^2	Change in Area (%)
Unsuitable	Current	1970–2000	5.53		1.35		7.61	
	ACCESS_CM2_ssp585	2021–2040	5.37	−2.92	1.20	−12.22	7.40	−2.83
	ACCESS_CM2_ssp585	2041–2060	5.38	−2.77	1.25	−7.39	7.48	−1.70
	ACCESS_CM2_ssp585	2061–2080	5.42	−2.14	1.18	−14.33	7.53	−1.10
	ACCESS_CM2_ssp585	2081–2100	5.42	−2.01	1.12	−20.18	7.52	−1.24
Low suitable	Current	1970–2000	3.65		5.00		2.06	
	ACCESS_CM2_ssp585	2021–2040	3.72	1.88	4.15	−20.71	2.25	8.61
	ACCESS_CM2_ssp585	2041–2060	3.69	1.00	4.38	−14.24	2.17	5.17
	ACCESS_CM2_ssp585	2061–2080	3.65	0.18	4.40	−13.72	2.13	3.45
	ACCESS_CM2_ssp585	2081–2100	3.66	0.22	4.35	−14.91	2.15	4.06
Moderate suitable	Current	1970–2000	1.27		3.48		0.81	
	ACCESS_CM2_ssp585	2021–2040	1.30	2.02	3.94	11.69	0.76	−7.14
	ACCESS_CM2_ssp585	2041–2060	1.30	2.09	3.66	5.09	0.76	−6.53
	ACCESS_CM2_ssp585	2061–2080	1.36	6.17	3.76	7.43	0.73	−10.71
	ACCESS_CM2_ssp585	2081–2100	1.35	5.45	3.88	10.34	0.75	−8.77
High suitable	Current	1970–2000	0.51		1.14		0.49	
	ACCESS_CM2_ssp585	2021–2040	0.57	10.56	1.68	32.37	0.56	12.53
	ACCESS_CM2_ssp585	2041–2060	0.60	14.26	1.67	31.75	0.55	11.78
	ACCESS_CM2_ssp585	2061–2080	0.54	4.78	1.63	30.22	0.57	15.30
	ACCESS_CM2_ssp585	2081–2100	0.54	5.14	1.61	29.41	0.56	12.83

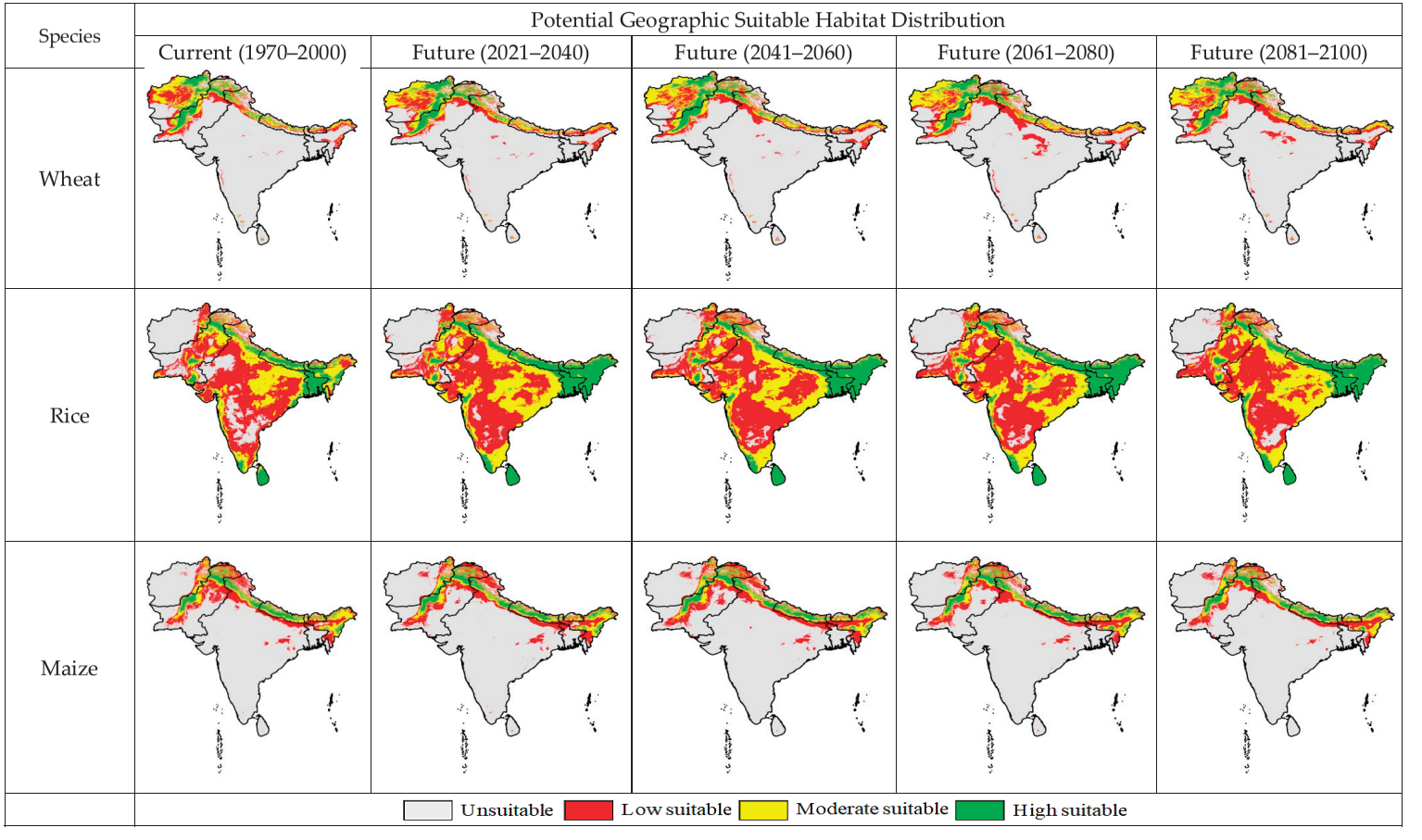

Figure 5. Potential geographic suitable habitat distribution for wheat, rice, and maize production under current (1970–2000) and future (ACCESS_CM2_ssp585, 2021–2040; 2041–2060; 2061–2080; 2081–2100) climate condition scenarios in South Asia.

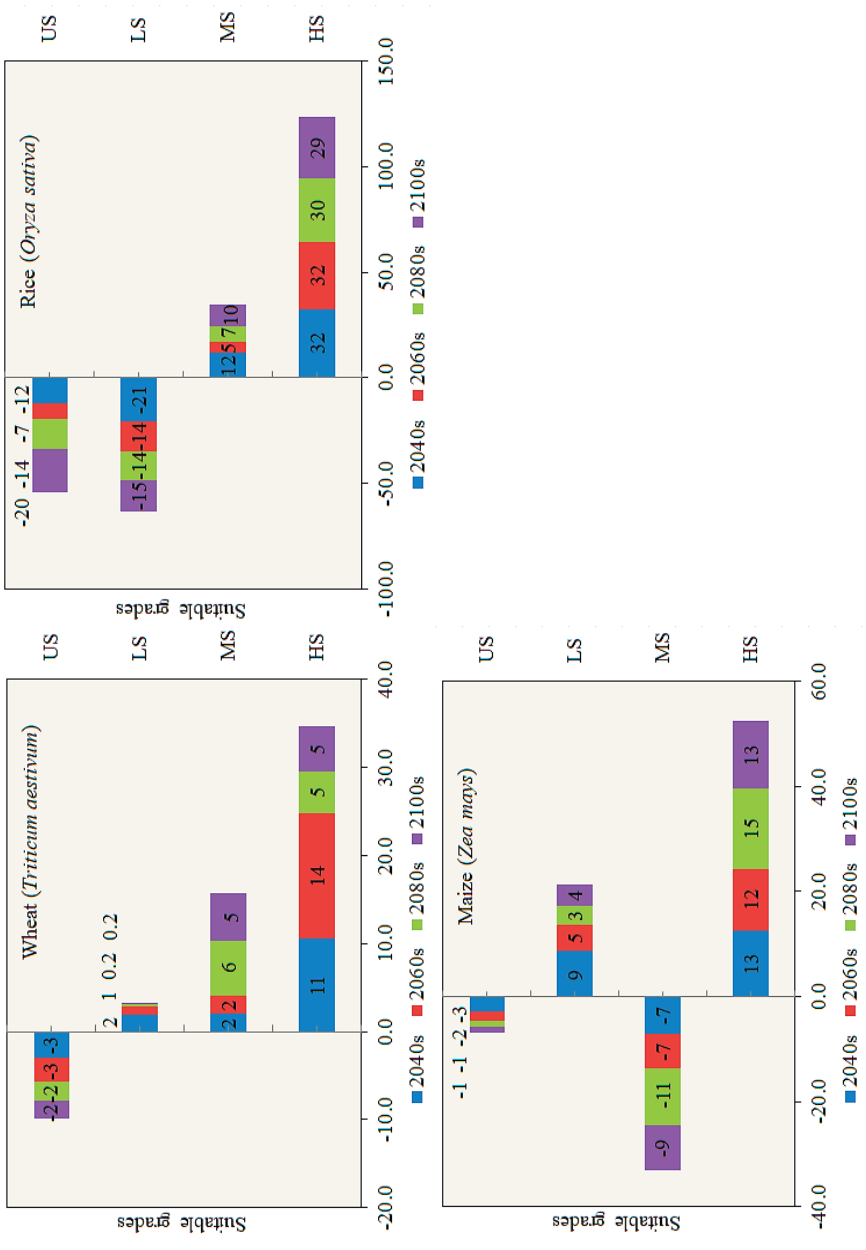

Figure 6. Proportion changes in the potential distribution of wheat, rice, and maize under future (ACCESS_CM2_ssp585, 2021–2040; 2041–2060; 2061–2080; 2081–2100) climate scenarios.

Climate is one of the most significant factors affecting the geographical suitability, vegetation pattern, and community structure of plant species [16]. There is a considerable variance between the climate scenario and the predicted results for the next four periods, which means that the suitable habitats for wheat, rice, and corn will undergo significant changes during the climate scenario and prediction period. The impact of land use transformation will increase the spatial range of unsuitable habitats beyond people's predicted range [23].

3.4. Dominant Environmental Variables

In order to predict land suitability, it is significant to identify the key bioclimatic variables that have an important impact on farmland suitability [33]. The contribution rate of these six bioclimatic variables is as high as 76.2%, indicating that these six factors play an important role in the potential land suitability of wheat. From the response curve, we obtained Bio-01 with the main bioclimatic variables of −20 to 20 °C; Bio-10, −5 to 35 °C; Bio-11, −30 to −5 °C; Bio-18, 0 to 500 mm; altitude, 100 to 2500 km; the water vapor pressure ranges from 0 to 1 kPa (Figure 7). Annual rainfall is the most significant climatic factor affecting plant development, as well as a significant factor affecting seedling survival and growth [39]. In the future, annual rainfall is related to many climatic factors that affect plant physiological and biochemical processes, such as soil moisture, which has been proven to be the main factor affecting plant assimilation rate [44]. The rice curve shows the correlation between bioclimatic variables and the probability of rice existence. According to the response curve of rice, rice prefers Bio-01, 6 to 14 °C; Bio-06, −35 to −5 °C; Bio 12100 to 1200 mm; Bio-14, 0 to 160 mm; Bio-18, 0 to 5000 mm; the altitude ranges from 400 to 7000 km (Figure 7). Temperature and rainfall have the most considerable ecological impact on potential land distribution [30,31]. According to the obtained rice response curve, rice prefers Bio-2 at 4–14 °C; Bio-9, −5 to 25 °C; Bio-12, 600 to 4200 mm; Bio-14, 20 to 220 mm; Bio-17, 80 to 700 mm; and Bio-18, 500 to 2100 mm (Figure 8). These six bioclimatic variables contribute up to 77.5% to maize and play an important role in its potential distribution. A study suggests that in summer, for every degree of warming in the future, corn production may decrease by 16% [26]. From the response curve of corn, we obtained Bio-01 with the main bioclimatic variables ranging from −20 to 20 °C; Bio-05, −5 to 37 °C; Bio-14, 0 to 42 mm; Bio-17, 0 to 200 mm; altitude, 0 to 3000 km; the wind speed ranges from 1 to 1.5 m s^{-1} (Figure 9). Huang et al. [27] study that, compared with rainfall, temperature may have a more considerable impact on species distribution.

3.5. Pearson Correlation Analysis

Bioclimatic variables are based on precipitation and temperature data [19]. Due to these reasons, there is a high correlation between bioclimatic variables. Using highly correlated environmental data for distribution modeling can affect the prediction and distribution process [27,48]. Pearson correlation analyses for wheat, rice, and maize are presented in Tables 6–8. In our study, we identify the highly correlated variables and minimize the effects of model overfitting. For the 19 variables with correlation coefficient values of $p < 0.05$, the Pearson correlation analysis of wheat, rice, and maize showed strong correlations between paired variables. To define which variable has a weaker predictive ability, we pre-ran the model for each variable and calculate the AUC value. In addition, the jackknife tests constructed throughout the MaxEnt model indicate that these variables have little impact on species land suitability.

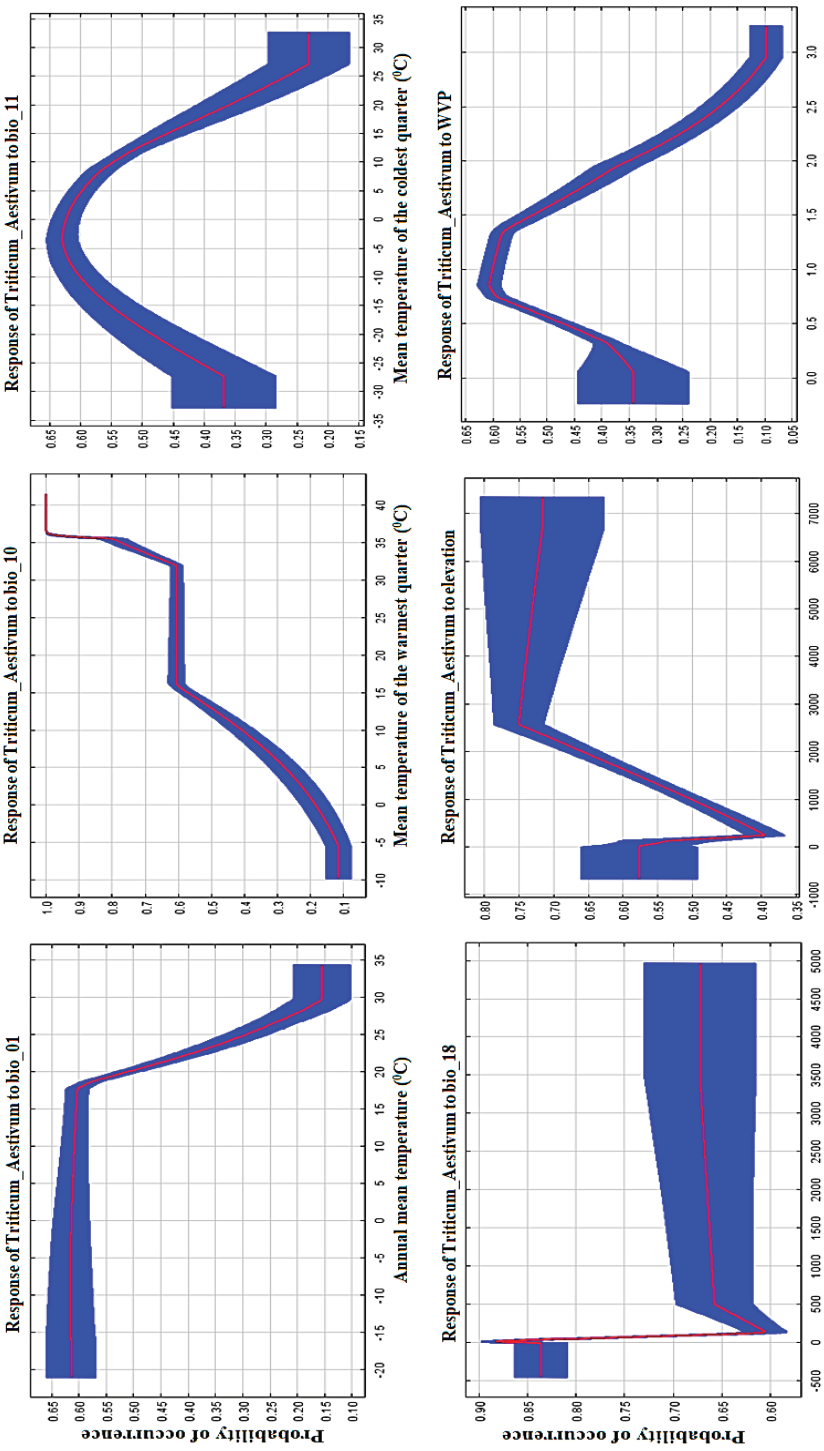

Figure 7. Wheat (*Triticum_Aestivum*) response curves derived from MaxEnt Model showing the influence of bioclimatic environmental variables; Bio_01, Bio_10, Bio_11, Bio_18, elevation, and water vapor pressure in South Asia.

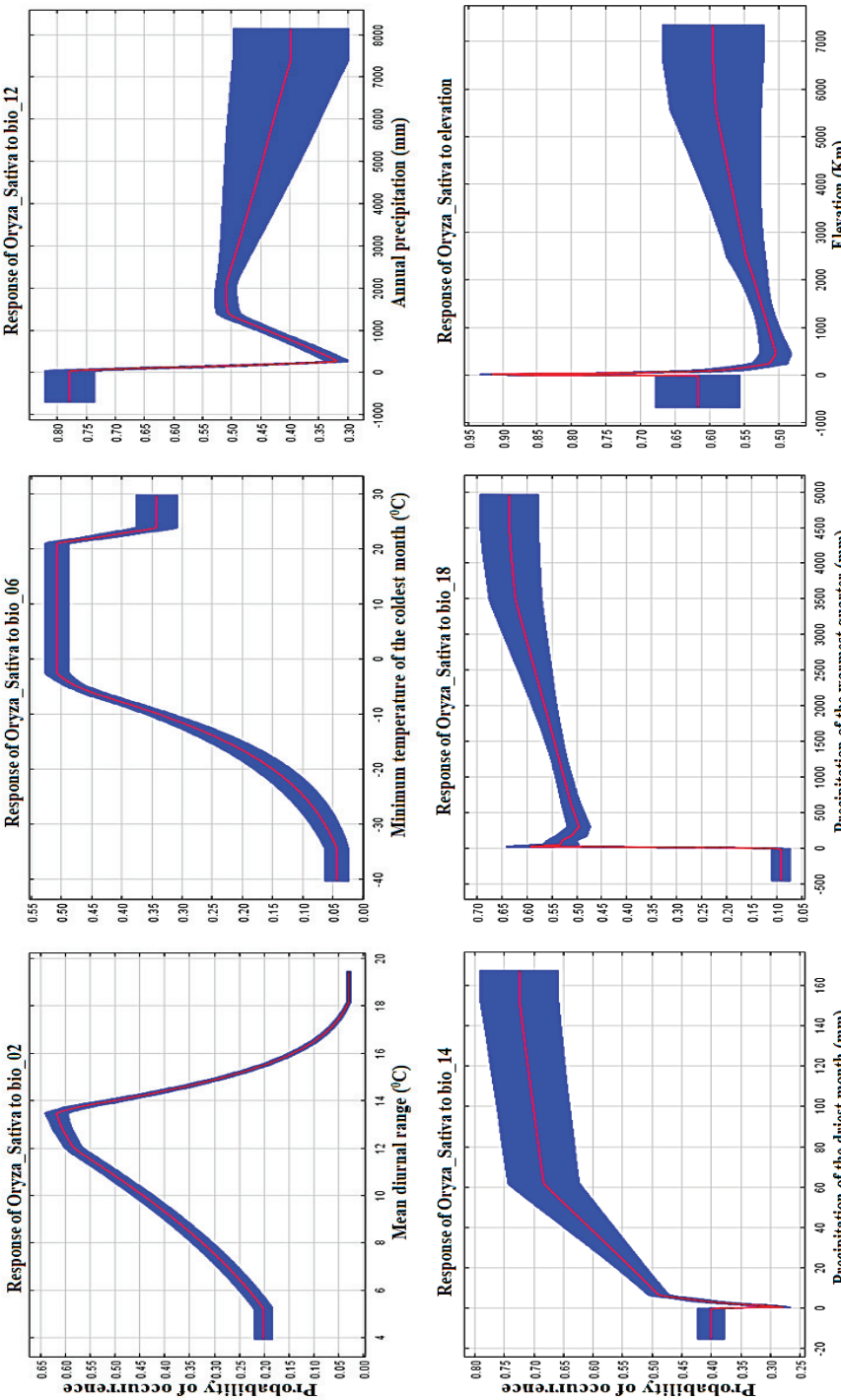

Figure 8. Rice (*Oryza_Sativa*) response curves derived from MaxEnt Model showing the influence of bioclimatic environmental variables; Bio_02, Bio_06, Bio_12, Bio_14, Bio_18, and elevation in South Asia.

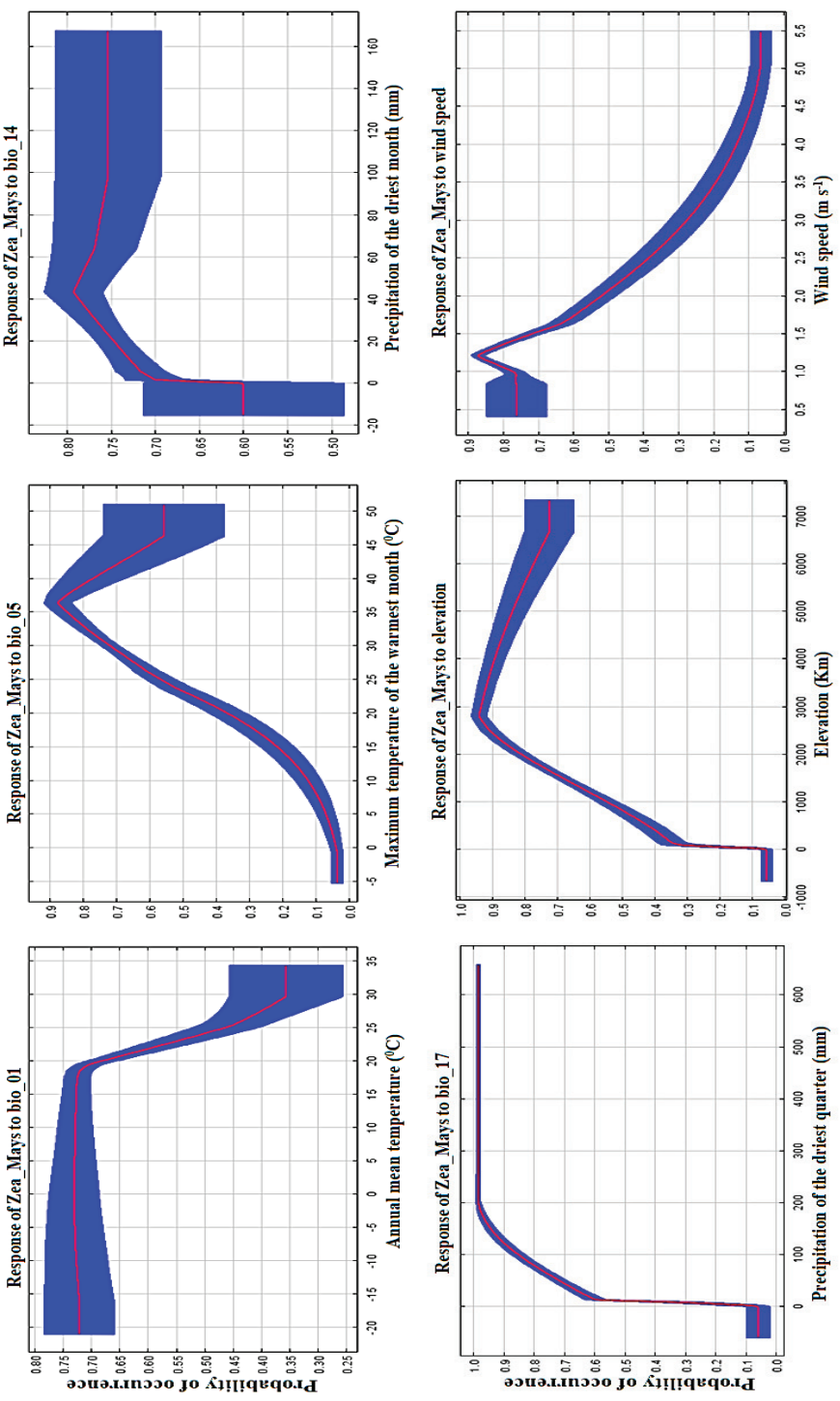

Figure 9. Maize (*Zea_Mays*) response curves derived from MaxEnt Model showing the influence of bioclimatic environmental variables; Bio_01, Bio_05, Bio_14, Bio_17, elevation, and wind speed in South Asia.

Table 6. Wheat correlation analysis results of the bioclimatic environmental variables.

	Bio1	Bio2	Bio3	Bio4	Bio5	Bio6	Bio7	Bio8	Bio9	Bio11	Bio12	Bio13	Bio16	SR
Bio4			**0.551**											
Bio6		**0.604**												
Bio7		**−0.676**												
Bio9								**0.583**						
Bio11		**0.561**				**0.611**		**0.656**						
Bio12								**0.848**		**0.57**				
Bio13					**−0.654**		**0.674**							
Bio14				**−0.562**								**0.638**		
Bio16						**−0.754**								
Bio17				**0.592**				**−0.659**			**−0.625**			
Bio18	**−0.57**	**0.638**												
Elev	**−0.796**													
SR								**0.625**	**0.593**		**0.596**		**0.551**	
WS				**0.61**	**−0.803**									**−0.655**
WVP			**−0.623**						**0.751**					

Bio: bioclimatic environmental variable; bold: strongly correlating ($p < 0.05$); N (replication number): 10.

Table 7. Rice correlation analysis results of the bioclimatic environmental variables.

	Bio1	Bio2	Bio3	Bio4	Bio5	Bio6	Bio7	Bio10	Bio11	Bio13	Bio14	Bio16	Bio17
Bio3	**−0.622**												
Bio4		**0.633**											
Bio9				**−0.557**		**−0.554**							
Bio10	**−0.618**		**0.674**	**−0.686**		**−0.597**							
Bio12					**0.829**		**−0.657**						
Bio13		**0.792**											
Bio14	**−0.89**							**0.687**					
Bio16										**0.638**			
Bio17						**−0.638**					**−0.594**		

Table 7. *Cont.*

	Bio1	Bio2	Bio3	Bio4	Bio5	Bio6	Bio7	Bio10	Bio11	Bio13	Bio14	Bio16	Bio17
Bio18									0.577				
Bio19	0.644											−0.573	
Elev			−0.654					−0.606					
SR						−0.709							0.565
WS											0.709		
WVP	0.767							−0.605			−0.763		

Bio: bioclimatic environmental variable; bold: strongly correlating ($p < 0.05$); N (replication number): 10.

Table 8. Maize correlation analysis results of the bioclimatic environmental variables.

	Bio1	Bio2	Bio3	Bio4	Bio5	Bio6	Bio7	Bio9	Bio10	Bio11	Bio12	Bio18
Bio4	−0.551											
Bio5				−0.653								
Bio8				0.647								
Bio9			0.563			−0.941						
Bio10			−0.765									
Bio11						−0.592						
Bio12	−0.812								0.71			
Bio13						0.71		−0.562		−0.56		
Bio17					0.74		0.717					
Bio18		0.586		0.843	−0.649							
Bio19			−0.561					−0.557	0.659		0.648	
Elev			−0.729				−0.646		0.809		0.79	
WS		−0.581						−0.587				−0.599
WVP		−0.612										

Bio: bioclimatic environmental variable; bold: strongly correlating ($p < 0.05$); N (replication number): 10.

4. Conclusions

This research is the first step towards better understanding the current and future potential land distribution of wheat, rice, and corn production in South Asia. The results showed that for wheat, annual mean temperature (Bio-1) and mean temperature of the coldest quarter (Bio-11) contributed 39.2% and 13.4%, for rice, precipitation of the warmest quarter (Bio-18) and elevation contributed 34.9% and 19.9%, and for maize, Bio-1 and precipitation of the driest quarter (Bio-17) contributed 36.3% and 14.3%, respectively. The map drawn indicates that the suitability of wheat, rice, and corn in South Asia may change in the future. The research revealed, on average, a significant improvement in high suitable area of 8.7%, 30.9%, and 13.1%, for wheat, rice, and maize, respectively; a moderate suitable area increase of 3.9% and 8.6% for wheat and rice, respectively; and a decrease by −8.3% for maize as compared with current values. The change in the unsuitable areas significantly decreased by −2.5%, −13.5%, and −1.7% for wheat, rice, and maize, respectively, compared to the current land suitability. These results indicate that there is a huge potential to increase the present potential planting areas of wheat, rice, and corn to increase crop production in South Asia. In light of our findings, it is our recommendation that further analysis is needed to identify land use changes and determine the effective area of suitable lands that can be targeted for wheat, rice, and corn cultivation in order to ensure sustainable production and mitigate food insecurity. This research can be used as evidence supporting the use of the MaxEnt model for defining potential species distribution areas under current and future climate change and establish policies specific to South Asia's geography and climate.

Author Contributions: Conceptualization, S.A. and J.N.; methodology, S.A., T.A.M. and M.U.; software, T.A.M. and S.A.H.; data curation and validation, S.A.; formal analysis, S.A. and S.S.; field investigation, S.A. and J.N.; writing—original draft, S.A.; writing—review and editing, S.A., S.A.H., S.S., M.U. and J.N.; project administration, S.A. and J.N.; supervision, J.N.; funding acquisition, S.A. and S.A.H. All authors contributed equally. All authors have read and agreed to the published version of the manuscript.

Funding: The authors extend their appreciation to the Researchers Supporting Project number (RSP2024R371), King Saud University, Riyadh, Saudi Arabia; Zhejiang Normal University (ZC304022952), and Shandong Natural Science Youth Project (ZR2020QF281), China.

Data Availability Statement: The data that support the findings of this study are available from the corresponding author upon reasonable request.

Acknowledgments: The authors would like to acknowledge the funding support by the Researchers Supporting Project number (RSP2024R371), King Saud University, Riyadh, Saudi Arabia.

Conflicts of Interest: The authors declare no conflicts of interest.

References

1. Akpoti, K.; Kabo-bah, A.T.; Dossou-Yovo, E.R.; Groen, T.A.; Zwart, S.J. Mapping suitability for rice production in inland valley landscapes in Benin and Togo using environmental niche modeling. *Sci. Total Environ.* **2020**, *709*, 136165. [CrossRef]
2. Angelieri, C.C.; Adams-Hosking, C.; Ferraz, K.M.; de Souza, M.P.; McAlpine, C.A. Using species distribution models to predict potential landscape restoration effects on Puma conservation. *PLoS ONE* **2016**, *11*, e0145232. [CrossRef] [PubMed]
3. Ashoori, A.; Kafash, A.; Varasteh Moradi, H.; Yousefi, M.; Kamyab, H.; Behdarvand, N.; Mohammadi, S. Habitat modeling of the common pheasant *Phasianus colchicus* (Galliformes: Phasianidae) in a highly modified landscape: Application of species distribution models in the study of a poorly documented bird in Iran. *Eur. Zool. J.* **2018**, *85*, 372–380. [CrossRef]
4. Asseng, S.; Ewert, F.; Martre, P.; Rötter, R.P.; Lobell, D.B.; Cammarano, D.; Kimball, B.A.; Ottman, M.J.; Wall, G.W.; White, J.W. Rising temperatures reduce global wheat production. *Nat. Clim. Chang.* **2014**, *5*, 143–147. [CrossRef]
5. Asseng, S.; Foster, I.A.N.; Turner, N.C. The impact of temperature variability on wheat yields. *Glob. Chang. Biol.* **2011**, *17*, 997–1012. [CrossRef]
6. Booth, T.H.; Nix, H.A.; Busby, J.R.; Hutchinson, M.F. BIOCLIM: The first species distribution modelling package, its early applications and relevance to most current MAXENT studies. *Divers. Distrib.* **2014**, *20*, 1–9. [CrossRef]
7. Brown, J.L.; Bennett, J.R.; French, C.M. SDMtoolbox 2.0: The next generation Python-based GIS toolkit for landscape genetic, biogeographic and species distribution model analyses. *PeerJ* **2017**, *5*, e4095. [CrossRef]
8. Bu, K.; Wang, Z.; Zhang, S.; Yang, J. Evaluation of agricultural land suitability for soybean cultivation in the Sanjiang Plain. *Chin. J. Eco-Agric.* **2017**, *25*, 419–428. [CrossRef]

9. Carpenter, G.; Gillison, A.N.; Winter, J. DOMAIN: A flexible modelling procedure for mapping potential distributions of plants and animals. *Biodivers. Conserv.* **1993**, *2*, 667–680. [CrossRef]
10. Chemura, A.; Mudereri, B.T.; Yalew, A.W.; Gornott, C. Climate change and specialty coffee potential in Ethiopia. *Sci. Rep.* **2021**, *11*, 8097. [CrossRef]
11. Chersich, M.F.; Wright, C.Y. Climate change adaptation in South Africa: A case study on the role of the health sector. *Glob. Health* **2019**, *15*, 22. [CrossRef] [PubMed]
12. Duan, J.Q.; Zhou, G.S. Climatic suitability of double rice planting region in China. *Chin. Acad. Meteorol. Sci.* **2012**, *45*, 218–227, (In Chinese with English Abstract). [CrossRef]
13. Elith, J.; Phillips, S.J.; Hastie, T.; Dudík, M.; Chee, Y.E.; Yates, C.J. A statistical explanation of MaxEnt for ecologists. *Divers. Distrib.* **2011**, *17*, 43–57. [CrossRef]
14. Fischer, G.; Shah, M.; Tubiello, F.N.; van Velhuizen, H. Socio-economic and climate change impacts on agriculture: An integrated assessment, 1990–2080. *Philos. Trans. R. Soc. Lond. Ser. B Biol. Sci.* **2005**, *360*, 2067–2083. [CrossRef]
15. Fodor, N.; Challinor, A.; Droutsas, I.; Ramirez-Villegas, J.; Zabel, F.; Koehler, A.-K.; Foyer, C.H. Integrating plant science and crop modeling: Assessment of the impact of climate change on soybean and maize production. *Plant Cell Physiol.* **2017**, *58*, 1833–1847.
16. Fourcade, Y.; Engler, J.O.; Rodder, D.; Secondi, J. Mapping species distributions with MAXENT using a geographically biased sample of presence data: A performance assessment of methods for correcting sampling bias. *PLoS ONE* **2014**, *9*, e97122. [CrossRef]
17. Franklin, J. Species distribution models in conservation biogeography: Developments and challenges. *Divers. Distrib.* **2013**, *19*, 1217–1223. [CrossRef]
18. Gao, Y.; Zhang, A.; Yue, Y.; Wang, J.; Su, P. Predicting shifts in land suitability for maize cultivation worldwide due to climate change: A modeling approach. *Land* **2021**, *10*, 295. [CrossRef]
19. GBIF. 2021. Available online: https://doi.org/10.15468/dl.cjnj2p (accessed on 6 May 2021).
20. Gong, L.; Tian, B.; Li, Y.; Wu, S. Phenological changes of soybean in response to climate conditions in frigid region in China over the past decades. *Int. J. Plant Prod.* **2021**, *15*, 363–375. [CrossRef]
21. Habtemariam, L.T.; Kassa, G.A.; Gandorfer, M. Impact of climate change on farms in smallholder farming systems: Yield impacts, economic implications and distributional effects. *Agric. Syst.* **2017**, *152*, 58–66.
22. He, Q.; Zhou, G. Climatic suitability of potential spring maize cultivation distribution in China. *Acta Ecol. Sin.* **2012**, *32*, 3931–3939. [CrossRef]
23. Hong, D.Y.; Zhou, S.L.; He, X.J.; Yuan, J.H.; Zhang, Y.L.; Cheng, F.Y.; Zeng, X.L.; Wang, Y.; Zhang, X.X. Current status of wild tree peony species with special reference to conservation. *Biodivers. Sci.* **2017**, *25*, 781–793. [CrossRef]
24. Zheng, C.; Wang, Y.C.; Yuan, S.; Xiao, S.; Sun, Y.T.; Huang, J.L.; Peng, S.B. Heavy soil drying during mid-to-late grain filling stage of the main crop to reduce yield loss of the ratoon crop in a mechanized rice ratooning system. *Crop J.* **2022**, *10*, 280–285. [CrossRef]
25. Bunn, C.; Peter, L.; Quaye, A.; Muilerman, S.; Noponen, M.R.A.; Lundy, M. Recommendation domains to scale out climate change adaptation in cocoa production in Ghana. *Clim. Serv.* **2019**, *16*, 100123. [CrossRef]
26. Hou, J.; Geng, T.; Chen, Q.; Chen, C. Impacts of climate warming on growht period and yield of rice in Northeast China during recent two decades. *Chin. J. Appl. Ecol.* **2015**, *26*, 249–259.
27. Huang, C.; Zhang, M.; Zou, J.; Zhu, A.-X.; Chen, X.; Mi, Y.; Wang, Y.; Yang, H.; Li, Y. Changes in land use, climate and the environment during a period of rapid economic development in Jiangsu Province. *China Sci. Total Environ.* **2015**, *536*, 173–181. [PubMed]
28. Ihlow, F.; Dambach, J.; Engler, J.O.; Flecks, M.; Hartmann, T.; Nekum, S.; Rajaei, H.; Rödder, D. On the brink of extinction? How climate change may affect global chelonian species richness and distribution. *Glob. Chang. Biol.* **2012**, *18*, 1520–1530. [CrossRef]
29. Intergovernmental Panel on Climate Change (IPCC). 2023: Sections. In *Climate Change 2023: Synthesis Report. Contribution of Working Groups I, II and III to the Sixth Assessment Report of the Intergovernmental Panel on Climate Change*; Core Writing Team, Lee, H., Romero, J., Eds.; Intergovernmental Panel on Climate Change (IPCC): Geneva, Switzerland, 2023; pp. 35–115. [CrossRef]
30. Kogo, B.K.; Kumar, L.; Koech, R.; Kariyawasam, C.S. Modelling climate suitability for rainfed maize cultivation in Kenya using a maximum entropy (MAXENT) approach. *Agronomy* **2019**, *9*, 727. [CrossRef]
31. Kramer-Schadt, S.; Niedballa, J.; Pilgrim, J.D.; Schroder, B.; Lindenborn, J.; Reinfelder, V.; Stillfried, M.; Heckmann, I.; Scharf, A.K.; Augeri, D.M.; et al. The importance of correcting for sampling bias in MaxEnt species distribution models. *Divers. Distrib.* **2013**, *19*, 1366–1379. [CrossRef]
32. Kulhanek, S.A.; Leung, B.; Ricciardi, A. Using ecological niche models to predict the abundance and impact of invasive species: Application to the common carp. *Ecol. Appl.* **2011**, *21*, 203–213.
33. Li, Y.; Li, M.; Li, C.; Liu, Z. Optimized Maxent Model Predictions of Climate Change Impacts on the Suitable Distribution of *Cunninghamia lanceolata* in China. *Forests* **2020**, *11*, 302. [CrossRef]
34. Liu, B.; Gao, X.; Zheng, K.; Ma, J.; Jiao, Z.; Xiao, J.; Wang, H. The potential distribution and dynamics of important vectors *Culex pipiens pallens* and *Culex pipiens quinquefasciatus* in China under climate change scenarios: An ecological niche modelling approach. *Pest Manag. Sci.* **2020**, *76*, 3096–3107. [PubMed]

35. Liu, B.; Gao, X.; Ma, J.; Jiao, Z.; Xiao, J.; Hayat, M.A.; Wang, H. Modeling the present and future distribution of arbovirus vectors *Aedes aegypti* and *Aedes albopictus* under climate change scenarios in Mainland China. *Sci. Total Environ.* **2019**, *664*, 203–214. [CrossRef]
36. Liu, Z.; Yang, X.; Lv, S.; Wang, J.; Lin, X. Spatio-temporal variations of yield gaps of spring Maize in Northeast China. *Sci. Agric. Sin.* **2017**, *50*, 1606–1616.
37. Lu, F.; Wang, H.; Ma, X.; Peng, H.; Shan, J. Modeling the current land suitability and future dynamics of global soybean cultivation under climate change scenarios. *Field Crops Res.* **2021**, *263*, 108069. [CrossRef]
38. Luo, M.; Wang, H.; Lv, Z. Evaluating the performance of species distribution models Biomod2 and MaxEnt using the giant panda distribution data. *Chin. J. Appl. Ecol.* **2017**, *28*, 4001–4006. [CrossRef]
39. Mabhaudhi, T.; Chimonyo, V.G.P.; Hlahla, S.; Massawe, F.; Mayes, S.; Nhamo, L.; Modi, A.T. Prospects of orphan crops in climate change. *Planta* **2019**, *250*, 695–708. [CrossRef]
40. Mall, R.; Lal, M.; Bhatia, V.; Rathore, L.; Singh, R. Mitigating climate change impact on soybean productivity in India: A simulation study. *Agric. For. Meteorol.* **2004**, *121*, 113–125. [CrossRef]
41. Marcer, A.; Saez, L.; Molowny-Horas, R.; Pons, X.; Pino, J. Using species distribution modelling to disentangle realised versus potential distributions for rare species conservation. *Biol. Conserv.* **2013**, *166*, 221–230. [CrossRef]
42. Massimo, F.; Ma, P.M. Impact on human health of climate changes. *Eur. J. Int. Med.* **2015**, *26*, 1–5.
43. Fan, M.; Shibata, H.; Chen, L. Environmental and economic risks assessment under climate changes for three land uses scenarios analysis across Teshio watershed, northernmost of Japan. *Sci. Total Environ.* **2017**, *599–600*, 451–463.
44. Mohammadi, S.; Ebrahimi, E.; Shahriari Moghadam, M.; Bosso, L. Modelling current and future potential distributions of two desert jerboas under climate change in Iran. *Ecol. Inform.* **2019**, *52*, 7–13. [CrossRef]
45. Montoya, F.; García, C.; Pintos, F.; Otero, A. Effects of irrigation regime on the growth and yield of irrigated soybean in temperate humid climatic conditions. *Agric. Water Manag.* **2017**, *193*, 30–45.
46. Motuma, M.; Suryabhagavan, K.V.; Balakrishnan, M. Land suitability analysis for wheat and sorghum crops in Wogdie District, South Wollo, Ethiopia, using geospatial tools. *Appl. Geomat.* **2016**, *8*, 57–66. [CrossRef]
47. Mustafa, A.; Singh, M.; Sahoo, R.; Ahmed, N.; Khanna, M.; Sarangi, A.; Mishra, A. Land Suitability Analysis for Different Crops: A Multi Criteria Decision Making Approach Using Remote Sensing and GIS. *Researcher* **2011**, *3*, 61–84.
48. Nam, J.; Cho, H.; Kim, J. Effect of plant life cycle on plant settlement in diverse water level. *J. Wetl. Res.* **2015**, *17*, 19–25. [CrossRef]
49. Ncube, B.; Shekede, M.D.; Gwitira, I.; Dube, T. Spatial modelling the effects of climate change on the distribution of *Lantana camara* in Southern Zimbabwe. *Appl. Geogr.* **2020**, *117*, 102172.
50. Nyathi, M.K.; van Halsema, G.E.; Annandale, J.G.; Struik, P.C. Calibration and validation of the AquaCrop model for repeatedly harvested leafy vegetables grown under different irrigation regimes. *Agric. Water Manag.* **2018**, *208*, 107–119. [CrossRef]
51. Ohta, S.; Kimura, A. Impacts of climate changes on the temperature of paddy waters and suitable land for rice cultivation in Japan. *Agric. For. Meteorol.* **2007**, *147*, 186–198. [CrossRef]
52. Ortiz, R.; Sayre, K.D.; Govaerts, B.; Gupta, R.; Subbarao, G.V.; Ban, T.; Hodson, D.; Dixon, J.M.; Iván Ortiz-Monasterio, J.; Reynolds, M. Climate change: Can wheat beat the heat? *Agric. Ecosyst. Environ.* **2008**, *126*, 46–58. [CrossRef]
53. Peterson, A.T.; Soberón, J.; Pearson, R.G.; Anderson, R.P.; Martínez-Meyer, E.; Nakamura, M.; Araújo, M.B. *Ecological Niches and Geographic Distributions (MPB-49)*; Princeton University Press: Princeton, NJ, USA, 2011.
54. Phillips, S.J.; Anderson, R.P.; Schapire, R.E. Maximum entropy modeling of species geographic distributions. *Ecol. Model.* **2006**, *190*, 231–259. [CrossRef]
55. Phillips, S.; Anderson, R.; Dudík, M.; Schapire, R.; Blair, M. Opening the black box: An open-source release of Maxent. *Ecography* **2017**, *40*, 887–893. [CrossRef]
56. Phillips, S.; Dudìk, M. Modeling of species distributions with Maxent: New extensions and a comprehensive evaluation. *Ecography* **2008**, *31*, 161–175. [CrossRef]
57. Qin, A.; Jin, K.; Batsaikhan, M.-E.; Nyamjav, J.; Li, G.; Li, J.; Xue, Y.; Sun, G.; Wu, L.; Indree, T.; et al. Predicting the current and future suitable habitats of the main dietary plants of the Gobi Bear using MaxEnt modeling. *Glob. Ecol. Conserv.* **2020**, *22*, e01032. [CrossRef]
58. Shabani, F.; Kotey, B. Future distribution of cotton and wheat in Australia under potential climate change. *J. Agric. Sci.* **2015**, *154*, 175–185. [CrossRef]
59. Shabani, F.; Kumar, L.; Ahmadi, M. A comparison of absolute performance of different correlative and mechanistic species distribution models in an independent area. *Ecol. Evol.* **2016**, *6*, 5973–5986. [PubMed]
60. Slater, H.; Michael, E. Predicting the current and future potential distributions of lymphatic filariasis in Africa using maximum entropy ecological niche modelling. *PLoS ONE* **2012**, *7*, e32202. [CrossRef]
61. Su, P.; Zhang, A.; Wang, R.; Wang, J.; Gao, Y.; Liu, F. Prediction of future natural suitable areas for rice under representative concentration pathways (Rcps). *Sustainability* **2021**, *13*, 1580. [CrossRef]
62. Swets, J.A. Measuring the accuracy of diagnostic systems. *Science* **1988**, *240*, 1285–1293. [CrossRef]
63. Teichmann, C.; Jacob, D.; Remedio, A.R.; Remke, T.; Buntemeyer, L.; Hoffmann, P.; Kriegsmann, A.; Lierhammer, L.; Bülow, K.; Weber, T.; et al. Assessing mean climate change signals in the global CORDEX-CORE ensemble. *Clim. Dyn.* **2021**, *57*, 1269–1292. [CrossRef]

64. Trenberth, K.E.; Dai, A.; Van Der Schrier, G.; Jones, P.D.; Barichivich, J.; Briffa, K.R.; Sheffield, J. Global warming and changes in drought. *Nat. Clim. Chang.* **2014**, *4*, 17–22. [CrossRef]
65. Walke, N.; Obi Reddy, G.P.; Maji, A.K.; Thayalan, S. GIS-based multicriteria overlay analysis in soil-suitability evaluation for cotton (*Gossypium* spp.): A case study in the black soil region of Central India. *Comput. Geosci.* **2012**, *41*, 108–118. [CrossRef]
66. Wang, L.; Li, Y.; Wang, P.; Wang, X.; Luo, Y.; Wu, H. Assessment of ecological suitability of winter wheat in Jiangsu Province based on the niche—Fitness theory and fuzzy mathematics. *Acta Ecol. Sin.* **2016**, *36*, 4465–4474. [CrossRef]
67. Wang, W.; He, A.; Jiang, G.; Sun, H.; Jiang, M.; Man, J.; Ling, X.; Cui, K.; Huang, J.; Peng, S.; et al. Chapter Four—Ratoon rice technology: A green and resource-efficient way for rice production. *Adv. Agron.* **2020**, *159*, 135–167. [CrossRef]
68. Wisz, M.S.; Hijmans, R.; Li, J.; Peterson, A.T.; Graham, C.; Guisan, A.; NCEAS Predicting Species Distributions Working Group. Effects of sample size on the performance of species distribution models. *Divers. Distrib.* **2008**, *14*, 763–773. [CrossRef]
69. Xu, L.L.; Ren, Z. Relationships between rice growth and climatic factors. *Mod. Agric. Sci. Technol.* **2017**, *18*, 183–185.
70. Yao, H.; Zuo, X.; Zuo, D.; Lin, H.; Huang, X.; Zang, C. Study on soybean potential productivity and food security assessment in China under the influence of the COVID-19 outbreak. *Geogr. Sustain.* **2020**, *1*, 163–171. [CrossRef]
71. Yin, X.; Chen, F. Temporal and spatial changes of global soybean production in 1961–2017. *World Agric.* **2019**, *11*, 65–71.
72. Yue, Y.; Zhang, P.; Shang, Y. The potential global distribution and dynamics of wheat under multiple climate change scenarios. *Sci. Total Environ.* **2019**, *688*, 1308–1318. [CrossRef]
73. Zhang, K.L.; Yao, L.J.; Meng, J.S.; Tao, J. Maxent modeling for predicting the potential geographical distribution of two peony species under climate change. *Sci. Total Environ.* **2018**, *634*, 1326–1334. [CrossRef]
74. Zipper, S.C.; Qiu, J.; Kucharik, C.J. Drought effects on US maize and soybean production: Spatiotemporal patterns and historical changes. *Environ. Res. Lett.* **2016**, *11*, 094021.

land

MDPI

Article

Improving Wheat Yield with Zeolite and Tillage Practices under Rain-Fed Conditions

Mehmood ul Hassan [1], Syed Tanveer Shah [1], Abdul Basit [2], Wafaa M. Hikal [3], Mushtaq Ahmad Khan [1], Waleed Khan [4], Kirill G. Tkachenko [5,*], Faiçal Brini [6] and Hussein A. H. Said-Al Ahl [7,*]

[1] Department of Agriculture, Hazara University, Mansehra 21300, Pakistan; mehmoodarid@gmail.com (M.u.H.); dr.syedtanveershah@hu.edu.pk (S.T.S.); mushtaq@uoswabi.edu.pk (M.A.K.)
[2] Department of Horticultural Science, Kyungpook National University, Daegu 41566, Republic of Korea; abdulbasit97_lily@knu.ac.kr
[3] Department of Biology, Faculty of Science, University of Tabuk, Tabuk 71491, Saudi Arabia; wafaahikal@gmail.com
[4] Laboratory of Crop Production, Department of Applied Biosciences, Kyungpook National University, Daegu 41566, Republic of Korea
[5] Peter the Great Botanical Garden of the V.L. Komarov Botanical Institute, Russian Academy of Sciences, St. Petersburg 197376, Russia
[6] Biotechnology and Plant Improvement Laboratory, Centre of Biotechnology of Sfax, P.O. 1177, Sfax 3018, Tunisia; faical.brini@cbs.rnrt.tn
[7] Medicinal and Aromatic Plants Research Department, Pharmaceutical and Drug Industries Research Institute, National Research Centre (NRC), 33 El-Behouth St. Dokki, Giza 12622, Egypt
* Correspondence: kigatka@gmail.com (K.G.T.); shussein272@yahoo.com (H.A.H.S.-A.A.)

Abstract: Wheat is the most consumed crop worldwide. Zeolite application combined with good tillage practices are good combinations that provide better soil conditions for wheat crops. Zeolite also provides a good layer for carbon to be absorbed into the soil and can retain carbon for hundreds of years. The current study aimed to investigate the effect of tillage practices and zeolite treatments on soil carbon retention and wheat crop productivity. Arranging the treatments implemented according to a factorial randomized block design which includes three replications. Tillage treatments include three levels vis: T_1= 6 tillage practices with the help of cultivator (farmer practice/control), T_2 (minimum tillage), and T_3 (2 cultivation with cultivator + Mold-board plough). The zeolite applications consist of four levels: Z_1 = 0, Z_2 = 5, Z_3 = 10 and Z_4 = 15 t ha^{-1}. The effect of the interaction between zeolite treatments and tillage practices on various factors related to soil and crops such as emission of carbon dioxide (CO_2), dissolved organic carbon, soil organic carbon, and the productivity and components of wheat productivity. Zeolite applied at 10 t ha^{-1} in combination with minimum tillage gave significant differences in terms of CO_2 emission, dissolved organic carbon, and on soil organic carbon. The experimental results showed that minimum CO_2 emission (25.43 and 31.12 (kg CO_2-C ha^{-1} h^{-1}), dissolved organic carbon (4.80 and 4.90 g C kg^{-1}), soil organic carbon (7.88 and 7.97 g C kg^{-1}), plant height (92.14 and 92.97 cm), spike length (11.88 ad 12.11 cm), number of spikelets (20.11 and 20.98), number of tillers (278.65 and 283.93) per unit area, 1000 grain weight (50.74 and 51.54 g), biological yield (8134.87 and 8187.38 kg ha^{-1}) and grain yield (2984.28 and 3028.96 kg ha^{-1}) and harvest index (36.69 and 37.04%) of wheat was observed in zeolite applied at 10 t ha^{-1} with minimum tillage practice ($T_2 \times Z_3$) compared to control and other treatments for both the years, respectively. It is therefore concluded that minimum tillage should be practiced in wheat crops with the application of zeolite at 10 t ha^{-1} to obtain better yield and soil carbon retention under rain-fed conditions.

Keywords: dissolved organic carbon; soil organic carbon; tillage; zeolite; wheat

Citation: Hassan, M.u.; Shah, S.T.; Basit, A.; Hikal, W.M.; Khan, M.A.; Khan, W.; Tkachenko, K.G.; Brini, F.; Said-Al Ahl, H.A.H. Improving Wheat Yield with Zeolite and Tillage Practices under Rain-Fed Conditions. *Land* **2024**, *13*, 1248. https://doi.org/10.3390/land13081248

Academic Editor: Nick B. Comerford

Received: 25 June 2024
Revised: 6 August 2024
Accepted: 8 August 2024
Published: 9 August 2024

1. Introduction

In Pakistan during 2022–2023, wheat was cultivated on 9043 thousand hectares as compared to last year's area of 8977 thousand hectares recorded an increase of 0.7 percent [1]. Wheat contributes to 8.2% of value added in agriculture and 1.9% to GDP. The overall production of wheat stood at 27.634 million tonnes in 2023 compared to 26.208 million tonnes in 2022, which shows a growth of 5.4% in wheat production. Wheat is an annual grass that can attain a height of $\frac{1}{2}$ to 1 $\frac{1}{4}$ meters with the characteristic of long stalks and spikes formed with many kernels [2]. Due to wheat's high nutritional value and better grain quality, it is grown all over the world, along with maize and rice. It is used in the production of many items of food like bread, biscuits, feeds, and confectionery. This crop is mainly grown under irrigated conditions with a water requirement ranging from about 18 to 22 inches per acre. In human nutrition, wheat is one of the best sources of carbohydrates. Pakistan ranked tenth among the top wheat-producing countries. However, wheat production in Pakistan is limited to only 25–35% and has not exceeded. This may be due to some adverse factors such as less availability of water, uncertain climates, more emission of carbon from the soil, and availability of proper fertile land [3], which badly affects wheat yield and productivity. Wheat production can be enhanced to a great extent by the use of good inputs, advanced production techniques, and appropriate tillage technologies. Because of these factors yield of wheat is affected, as they affect the chemical and physical properties of the soil and water [4]. Tillage practices play a very crucial role in crop production. It adds up to 20% among different production factors of wheat [5]. Soil is deteriorating day by day due to the use of repetitive and unwanted conventional tillage practices. Therefore, there is a need to promote proper utilization of water in wheat cultivation, control the soil erosion process, and enhance crop productivity with an emphasis on shifting to reduced and zero-tillage [6]. Because of the benefits from zero tillage, i.e., more yield, cost-effectiveness, and significant savings in water, soil quality, and inputs, nowadays research work on zero tillage technology has been under serious consideration. It enables farmers to sow wheat at the proper time with good crop establishment. Zero and minimum tillage practices can reduce the expenditure of water and to buildup of seedbeds by about 30% [7]. Zero and minimum tillage practices can give better results than other tillage operations as these are less costly compared to other tillage systems [8]. Deep tillage has several disadvantages because it can break up the tiller bed, increase surface run-off, and deep leaching of nutrients that become unavailable to plants [9]. Recently, along with the use of less tillage practices zeolite is now mostly used in agriculture practices as a source of inorganic soil amendment. It reduces nitrogen leaching, enhances nitrogen use efficiency, and improves crop productivity. Zeolites have many properties that can improve crop productivity, these include crystalline nature with hydrated alumino-silicates, having the characteristics of high cation exchange capacity and water holding capacity [10]. The other advantages of zeolite include that it has the ability to provide plant nutrients especially NH4+ which has been used to enhance soil nitrogen retention and nitrogen availability to plants [11]. Zeolites have been found to increase nitrogen use efficiency and enhance the productivity of many crops such as spinach [12], canola [13], corn, rice, and wheat [14]. There is now much research about the effects of zeolite application on agronomic characteristics of wheat under irrigated conditions, but few of these studies have examined its effect on wheat under rain-fed conditions. In addition, zeolite could also increase water use efficiency by improving soil water retention capacity and water availability to plants using it under water shortage conditions [15]. Natural zeolites have the ability to enhance crop water use efficiency and to also control nutrient leaching [16]. Application of zeolite at a rate of 8 g/kg significantly enhanced the water use efficiency (WUE) of cereal crops and obtained the highest value [17]. Zeolite dosage at 90 t/hm2 and irrigation levels at 100% ET obtained the highest WUE of wheat, maize, strawberry, and common bean [18]. Due to the ability of zeolite to retain water in itself and thus, increase water availability to the plant under water stress conditions [19].

Combining zeolite application with appropriate tillage combinations can reduce irrigation water and nitrogen loss and enhance cereal grain yield [18].

The aim of this research was to investigate whether zeolite application and different tillage practices affect the soil carbon content and wheat productivity. Therefore, the current research hypothesis was to study the effect of zeolite concentrations and tillage practices under field conditions to improve soil carbon content, yield, and yield-related attributes of wheat.

2. Materials and Methods

A two-year field trial was conducted from June 2021 to May 2023 at the Agriculture Research Farm, Hazara University Mansehra, Pakistan to study the effect of different tillage practices and zeolite doses on wheat (*Triticum aestivum* L.) yield and soil carbon. Previously, the field was fallow, i.e., no crop was sown on it. Moreover, no fertilizer and tillage were applied in the field. The soil of the study area was clay loam with pH ranging from 7 to 8. A randomized factorial block design consisting of two factors with three replicates and an area of 5×8 m^2 was used. The first factor of the experiment was three levels of tillage practices; T_1: Control or farmer practice (6 cultivations with cultivator), T_2: minimum tillage (2 tillage practices) with cultivator, and T_3: 1 Mold-board plough + 2 cultivations with cultivator and the second factor was the provision of zeolite consist of four levels. The zeolite dosages consist of four levels: $Z_1 = 0$, $Z_2 = 05$, $Z_3 = 10$, and $Z_4 = 15$ t ha^{-1}. Wheat was planted using seeds at a seed rate of 120 kg ha^{-1} leaving a distance of 12 cm between rows. NPK fertilizer was applied at a rate of 35–40–20 kg ha^{-1} from sources of urea, diammonium phosphate, and potassium sulphate, respectively. Sowing was performed using a seed drill. All fertilizers were applied as a base dose at the time of planting and no fertilizers were applied during the entire wheat growth period. Zeolite was applied before the onset of monsoon rains so that proper mixing was possible, and no subsequent doses of zeolite were applied during the wheat growing season. Tillage practices especially minimum tillage and the use of mold-board plough during monsoon were chosen because, in rain-fed areas, farmers use conventional techniques, which results in lower yields. Here, the concept of minimum tillage practices was introduced in these areas so that farmers can obtain maximum yield with smart use of water, which is lost using conventional tillage. Zeolite doses were chosen on the basis of the soil condition of rain-fed areas due to their role in improving soil physical and chemical structure. Moreover, these zeolite doses also suit the soil of these areas. Tillage treatment T_1 involves performing 6 cultivations using a cultivator. A plank was used to level the ground after each ploughing. In the tillage treatment, two tillage operations were carried out before the onset of monsoon whereas, other four tillage practices were carried out before planting the crop. In T_2 only two cultivator-assisted tillage practices were used before planting. In tillage treatment, T3, one tillage practice was carried out using a plow before the onset of monsoon and two more tillage practices were carried out using a cultivator before wheat planting.

2.1. Soil Sampling

Three random soil samples were taken at a depth of 0–15 cm after each tillage practice and before sowing the wheat during the two years of the study from each treatment in three different locations and a composite sample was taken after that. After collecting the samples, they were placed for 48 h at 105 °C to dry and then sieved through a 2 mm stainless steel sieve and stored in glass jars. Soil samples were collected to calculate soil organic carbon, dissolved organic carbon, and carbon emission.

2.2. Carbon Emission

Soil CO_2 emission was measured using the static chamber method through CO_2 meter (Lutron GC-2028, Lutron manufacturer, Taipei, Taiwan). The fiber chamber rim was fixed in a collar groove that was used in the field according to random determination of the gas

flow. After 30 days, the gas percentage was measured. It was noted by transformation in headspace concentration over a specific duration using the formula:

$$Flux = \frac{(dGas/dt) \times 10^{-6} \times (Vchanmber \times P \times 100 \times MW)}{R \times T \times A \times 10^{-6}}$$

$dGas/dt$ refers to the change in concentration over time and measured in ppm h^{-1}; *Vchamber* is the volume of the chamber, P is atmospheric pressure, MW is the molecular weight, R is a gas constant, 8314 J mol^{-1} K^{-1}, T is the required temperature taken in Kelvin and A is the chamber area. The flux of CO_2 gas was taken by a hectare and converted into kg CO_2-C ha^{-1} h^{-1} [20].

2.3. Dissolved Organic Carbon

Dissolved Organic Carbon (DOC) was calculated by taking 2 g of soil material and shaking it in 20 mL of distilled water for 24 h and dissolved C was analyzed on a total organic carbon (TOC) analyzer [21].

2.4. Soil Organic Carbon

Soil organic carbon (SOC) was measured by taking 1 g of soil into a 500 mL beaker. Then, ten mL of 1 N potassium dichromate solution and 20 mL of concentrate H_2SO_4 was added into the beaker and stirred to mix the suspension. The suspension was then set for 30 min. Then, 200 mL of distilled water was added after adding 10 mL of H_3PO_3 to the suspension. Then, 10 drops of diphenylamine indicator were added, and the solution was titrated with 0.5 N solution of ferrous ammonium sulphate until the color changed from blue to sharp green [22]. Percentage of total organic carbon (w/w) = 1.334 × oxidizable organic Carbon.

2.5. Plant Data Collection and Analysis

Wheat plant height was measured by taking 10 plants randomly from each plot and the average was determined. The length of the spike, the number of spikelets per spike, and 1000 grain weight were determined by randomly selecting 10 plants from each plot. The Number of tillers per unit area was calculated by placing the quadrat of 1 m^2 at different places of each plot. Biological yield was taken by taking the weight of above-ground biomass of all wheat plants from each plot and then taking the total biomass. Grain yield was taken by removing grains from each spike in kg ha^{-1}. The harvest index (*HI*) was determined as a percentage by dividing the grain yield of the wheat crop by the biological yield and then multiplying it by 100.

$$HI(\%) = \frac{Grain\ yield}{Biological\ yield} * 100$$

The data was analyzed statistically to learn the difference between the treatments by using SPSS software v. 1.7. The least significant difference within treatment was calculated at $p \leq 0.05$.

3. Results

Regarding the means for soil carbon emission, tillage practices and zeolite treatments significantly ($p \leq 0.05$) affected soil carbon emission. Tillage practice T_1 (Control) and zeolite treatment Z1 (0 t ha^{-1}) during the first study year recorded a CO_2 emission of 49.22 kg CO_2-C ha^{-1} h^{-1} while 52.24 kg CO_2-C ha^{-1} h^{-1} during the second year, which was the maximum among all treatments (Figure 1A,D). The interaction between T_2 (minimum tillage) practice and Z3 zeolite treatment (10 t ha^{-1}) revealed the lowest CO_2 emission which was about 26.47 kg CO_2-C ha^{-1} h^{-1} during the first year and 32.67 kg CO_2-C ha^{-1} h^{-1} during the second year (Figure 1A,D).

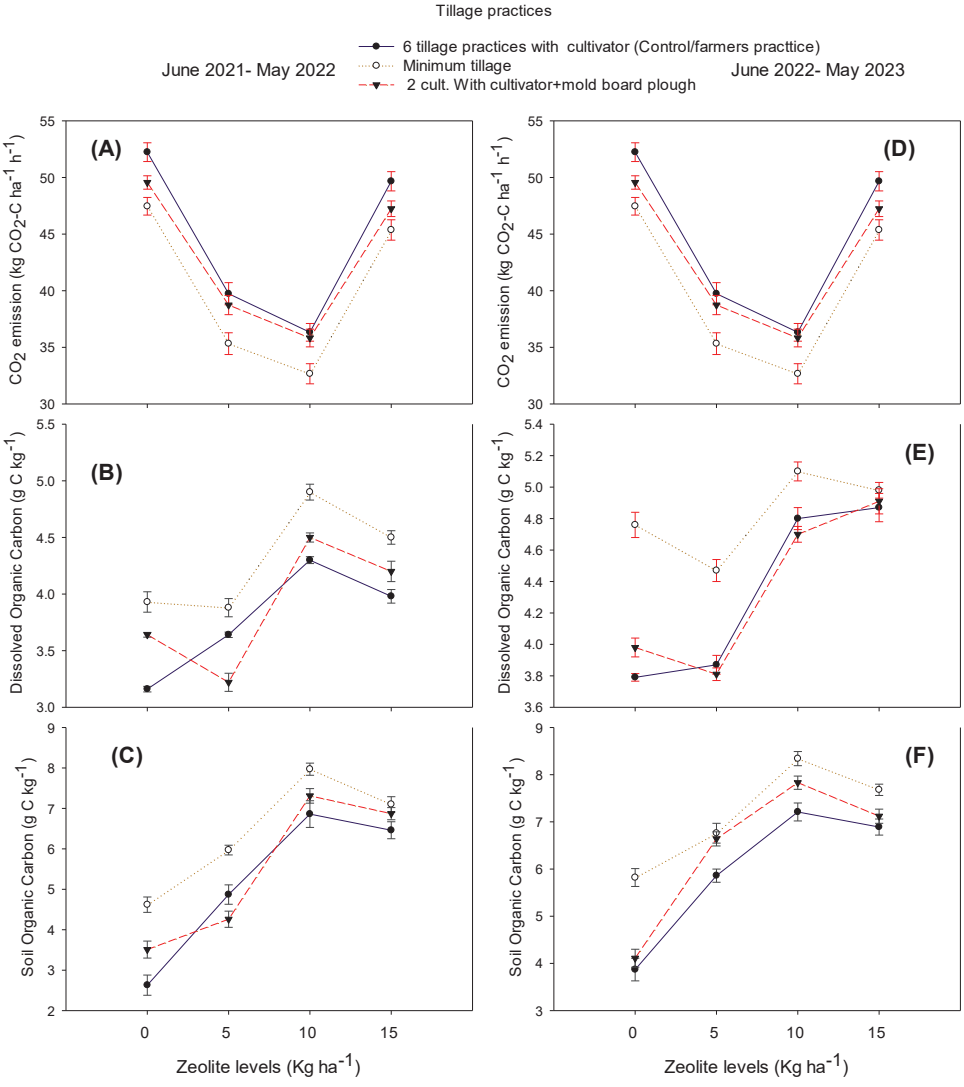

Figure 1. Effect of tillage operations and zeolite levels on CO_2 emission (**A**,**D**), dissolved organic carbon (**B**,**E**), and Soil organic carbon (**C**,**F**).

Dissolved organic carbon was also significantly ($p \leq 0.05$) affected by zeolite and tillage practices interaction. The data regarding dissolved organic carbon (DOC) showed that the lowest DOC found in $T_1 \times Z_1$, i.e., no zeolite and zero tillage which was about 3.16 g C kg^{-1} during the first year and 3.79 g C kg^{-1} during the second year, whereas wheat crops in minimum tillage practices supplied with 10 t ha^{-1} recorded the highest DOC 4.9 g C kg^{-1} during the first year and 5.1 g C kg^{-1} during the second year (Figure 1B,E). The interaction between $T_2 \times Z_1$ and $T_2 \times Z_2$ gave the nominal values (Figure 1B,E).

Significant ($p \leq 0.05$) differences were observed for soil organic carbon. Data on soil organic carbon (SOC) revealed that $T_1 \times Z_1$, i.e., control treatment gave SOC (2.63 g C kg^{-1}) during the first year and 3.87 g C kg^{-1} during the second year (Figure 1C,F). Interaction of $T_2 \times Z_3$ gave 7.97 g C kg^{-1} SOC during the first year and 8.34 g C kg^{-1} during the second

year. Interaction of $T_2 \times Z_3$ gave statistically ($p \leq 0.05$) higher SOC (69.36%) than $T_1 \times Z_1$ (Figure 1C,F).

Wheat productivity indicators were also analyzed to determine the effect of tillage practices and different zeolite doses and showed significant ($p \leq 0.05$) for the growth and yield attributes of wheat. The data revealed that maximum plant height (92.14 and 92.97 cm) was observed in wheat crops with minimum tillage practice and zeolite at 10 t ha^{-1} during the 1st year and 2nd year growing season, respectively, which was statistically different ($p \leq 0.05$) from the rest of the treatments followed by $T_2 \times Z_3$ interaction. The lowest SOC (80.12 and 80.98 cm) was obtained in $T_1 \times Z_1$ during the 1st and 2nd year of study, respectively (Figure 2A,E). $T_1 \times Z_1$ and $T_1 \times Z_4$ interaction gave results that are statistically at par ($p \leq 0.05$) similar to each other. Interaction of $T_2 \times B_3$ gave 12.45% more plant height as compared to $T_1 \times Z_1$ (Figure 2A,E). During both years, the maximum spike length (11.98 and 12.11 cm) was observed in $T_2 \times Z_3$ while the minimum spike length (8.112 and 8.87 cm) was observed in $T_1 \times Z_1$, (Figure 2B,F). On a percentage basis, $T_2 \times Z_3$ gave 42.43% greater height length than $T_1 \times Z_1$. The results for the number of tillers revealed that during both study years, the minimum number of tillers (215.32 and 217.27) per unit area resulted from the $T_1 \times Z_1$ interaction while the interaction of minimum tillage with 10 t ha^{-1} zeolite concentrations produced significantly ($p \leq 0.05$) higher number of tillers (278.65 and 283.93) per unit area for 1st and 2nd year of study, respectively, (Figure 2C,G). During both years, $T_2 \times Z_3$ showed an increase in tillering by 30.44% per unit area as compared to $T_1 \times Z_1$.

The number of spikelets/spike was significantly ($p \leq 0.05$) affected by tillage practices and zeolite interaction. During both years of study, $T_2 \times Z_3$ recorded the highest (20.11 and 20.98 spikelets/spike whereas minimum spikelets/spike (16.27 and 16.97) was obtained from wheat plants in the control treatment, i.e., $T_1 \times Z_1$ (Figure 2D,H). The $T_2 \times Z_3$ interaction gave 23.98% more spikelets/spike than $T_1 \times Z_1$. The combination of tillage practices and zeolite concentration had a significant ($p \leq 0.05$) effect on 1000-grain weight. The maximum value of 1000 grain weight (50.74 and 51.54 g) was observed during both years of the study when minimum tillage was practiced in wheat fields and 10 t ha^{-1} of zeolite concentrations. The minimum value is given by $T_1 \times Z_1$, which was 41.62 g (Figure 3A,E). The mean percentage difference between these two reactions was 26.02%. Significant ($p \leq 0.05$) variation was recorded for the biological yield of wheat crops with the combined effect of tillage practices and zeolite concentrations. It is evident from Figure 3B,F that during both the study years, the $T_2 \times Z_3$ interaction gave the maximum biological yield (8134.87 and 8178.31 kg ha^{-1}) which was statistically ($p \leq 0.05$) different from the other treatments. Minimum biological yield (7398.35 and 7483.29 kg ha^{-1}) was observed in $T_1 \times B_1$, i.e., control treatment (Figure 3B,F). The $T_2 \times Z_3$ reaction gave a 9.52% greater biological yield compared to the $T_1 \times Z_1$.

The results for grain yield showed significant differences sown under different tillage practices and zeolite concentrations. Wheat crop is grown under minimum tillage and 10 t ha^{-1} significantly ($p \leq 0.05$) increased grain yield (2754.98 and 2863.39 kg ha^{-1}) in both years, respectively, whereas, minimum grain yield (2438.39 and 2576.22 kg ha^{-1}) was recorded in the control treatment, i.e., $T_1 \times Z_1$ (Figure 3C,G). The values of $T_1 \times Z_2$ and $T_1 \times Z_3$ interactions were found to be statistically similar ($p \leq 0.05$) to each other (Figure 3C,G). The harvest index was significantly affected by tillage practice and zeolite concentrations. The data revealed that the maximum harvest index (36.69 and 37.54%) during the two years of the study was observed at $T_2 \times Z_3$ while the minimum harvest index (32.96 and 34.43%) was given by $T_1 \times Z_1$ (Figure 3D,H). During both years of the study, the harvest index recorded in $T_1 \times Z_1$ was statistically ($p \leq 0.05$) at par with $T_1 \times Z_4$ interactions (Figure 3D,H).

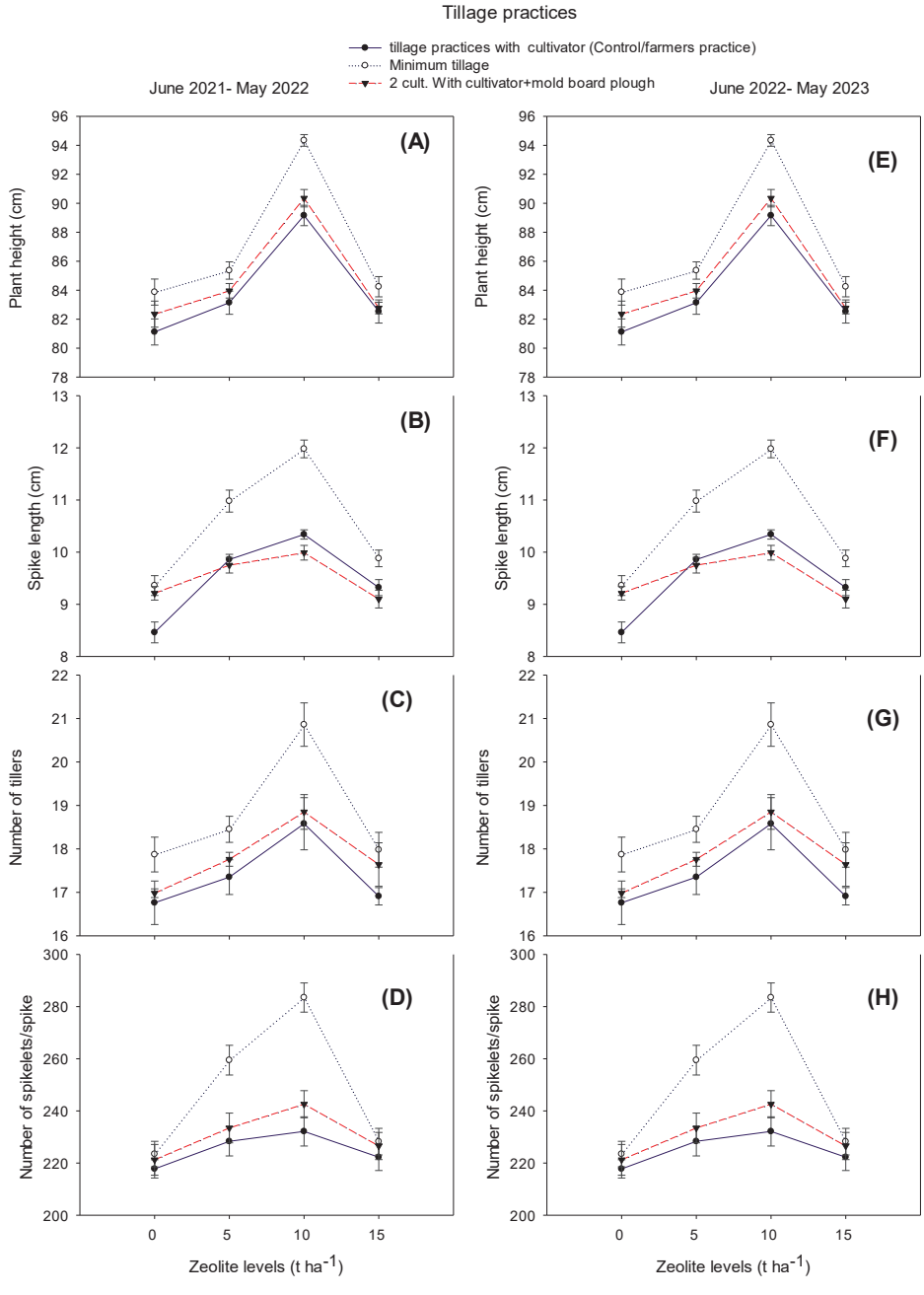

Figure 2. Effect of tillage operations and zeolite levels on plant height (**A**,**E**), spike length (**B**,**F**), number of tillers (**C**,**G**), and number of spikelets/spike (**D**,**H**).

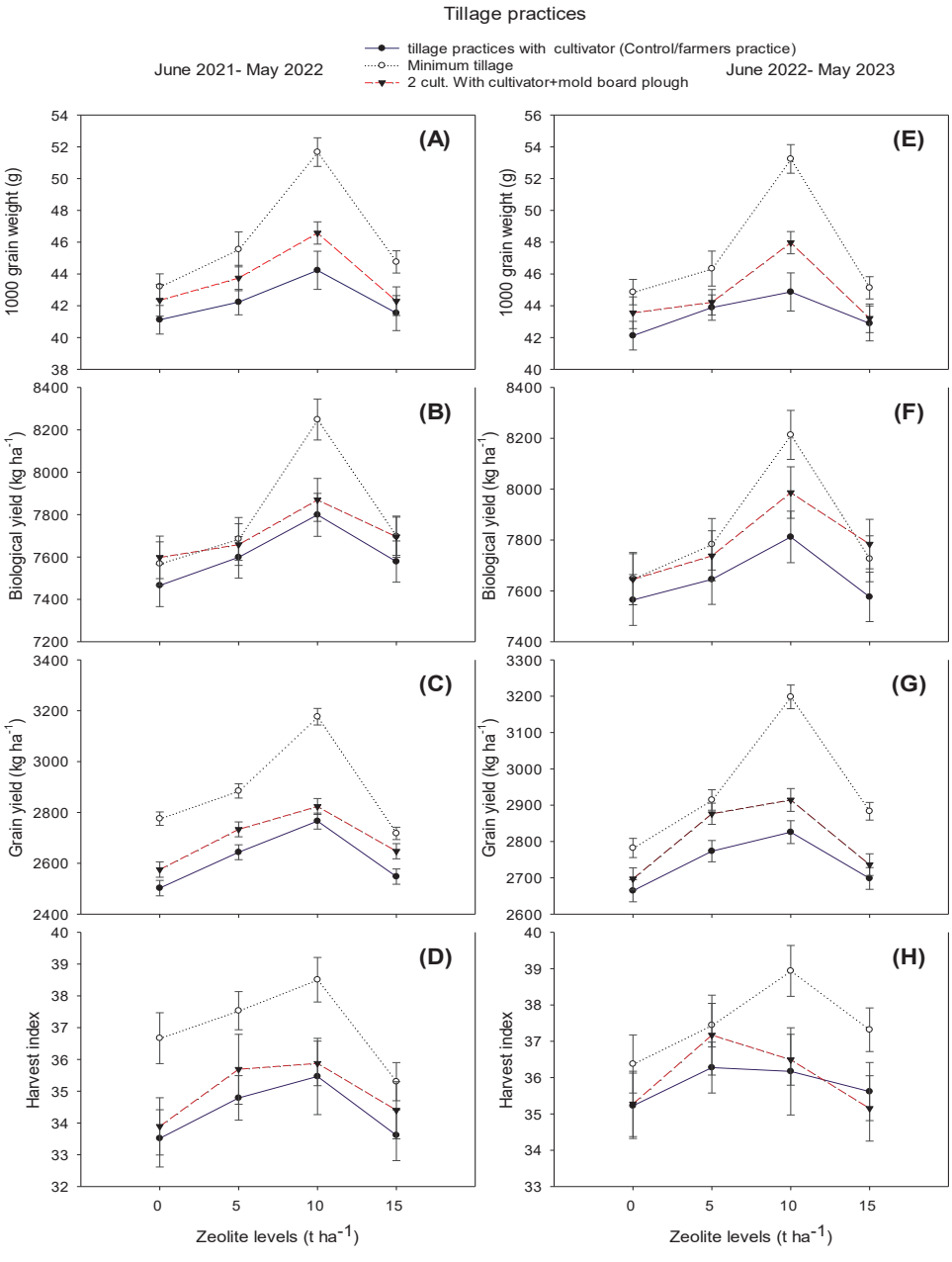

Figure 3. Effect of tillage operations and zeolite levels on 1000 grain weight (**A**,**E**), biological yield (**B**,**F**), grain yield (**C**,**G**), and harvest index (**D**,**H**).

3.1. Correlation Analysis

The heat map displays correlation coefficients between agricultural traits. Significant positive correlations were observed between plant height (PH) and spike length (SL), suggesting a potential link in growth traits. A similarly strong positive relationship exists between biological yield (BY) and grain yield (GY), meaning that increases in total plant

biomass are closely related to harvestable grain production. Conversely, harvest index (HI), correlates poorly with both morphological and production traits, indicating that the efficiency of biomass conversion to grain is governed by mechanisms that largely depend on plant size and total production (Figure 4).

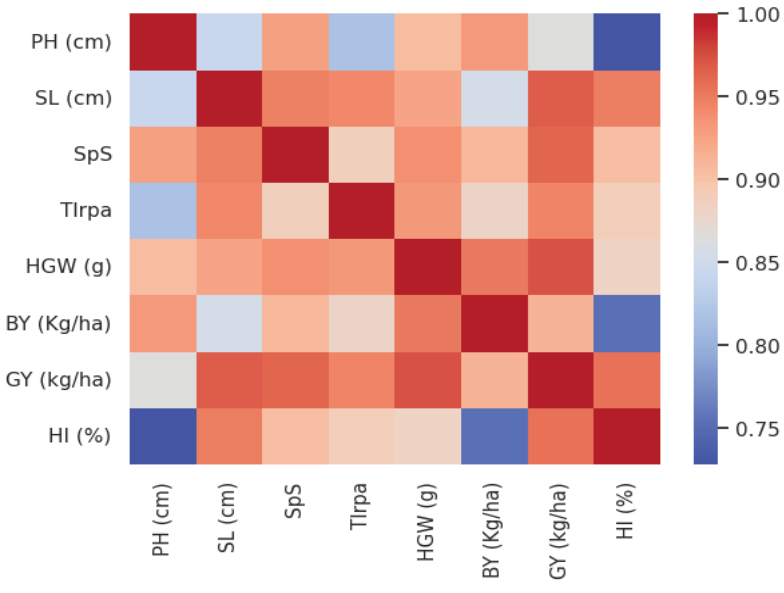

Figure 4. Heat map Correlation of Agronomic Traits in Plant Germplasm. The heatmap details the Pearson correlation coefficients among selected traits with strong correlations shown in red and weak correlations in blue ranging from −1 (perfect negative correlation, displayed in blue) to +1 (perfect positive correlation, displayed in red).

3.2. Principal Component Analysis

The Principal Component Analysis (PCA) biplot depicts the relationship between different agronomic traits and the first two principal components explain the cumulative variance of 95.92%, with PC1 accounting for 91.58% and PC2 for 4.34%. Vectors represent individual traits, and their direction and length indicate their contribution and association with the respective principal components. The biplots show that plant height (PH) and biological yield (BY) are closely related to PC1, indicating that they contribute significantly to the variance along this principal component. Likewise, spike length (SL) and harvest index (HI) display a positive correlation with PC1, although HI also extends to the PC2 axis, implying a multidimensional effect on the data structure. The 1000-grain weight (HGW) vector is negatively correlated with PC1, indicating that as PH and BY increase, HGW decreases, which may indicate a trade-off between these traits in the population studied. The spike sphericity (SpS) aligns closely with the HGW, reinforcing a possible inverse relationship with the PH and BY traits (Figure 5).

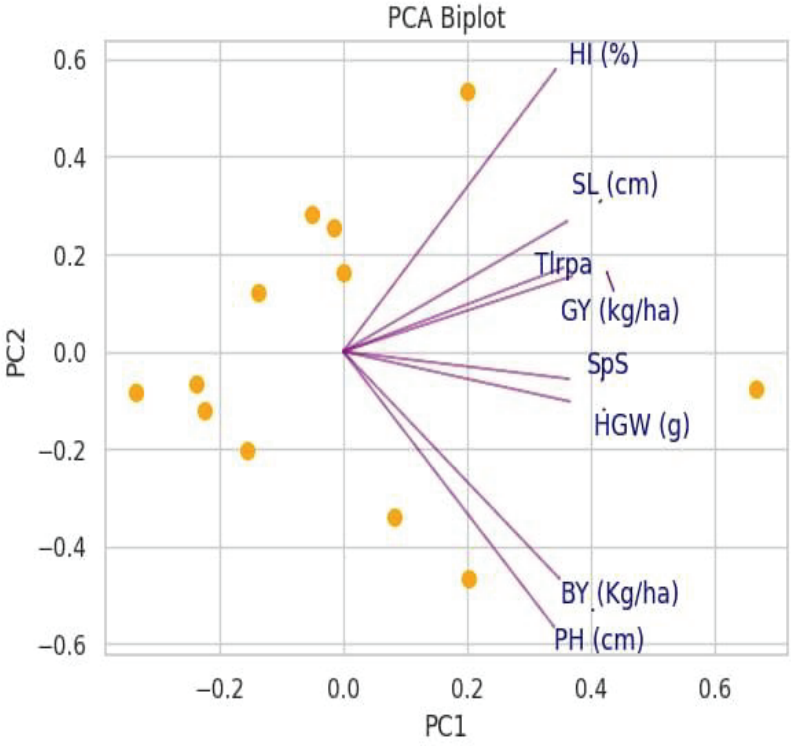

Figure 5. Principal components PC1 (91.58%) and PC2 (4.34%) are plotted, with trait vectors such as plant height, biological yield, and harvest index indicating their respective influences on the explained variance. Data points represent individual samples positioned relative to the principal components and trait vectors, highlighting the principal correlations within the dataset.

4. Discussion

Due to climate change, not only the air environment but also the soil environment is being polluted, especially by cutting trees, using heavy tillage practices, and using inappropriate inputs to enhance crop productivity. By doing all these practices the soil structure is being demolished day by day and a large amount of carbon is emitted from the soil which is very dangerous for the soil microorganisms as well as for the open environment [23]. The same results were obtained in the present experiment where soil carbon emission was higher in tillage practice T_1 (Control), which was an agricultural practice, and this may be due to soil disturbance through the use of a large number of tillage practices causing degradation and carbon emission from the soil. The T_2 Tillage treatment combined with the Z_3 zeolite treatment (10 t ha^{-1}) gave more dissolved organic carbon (DOC), i.e., (4.8 and 4.9 g C Kg^{-1}), which may be due to fewer tillage practices conserving soil carbon and the zeolite captured this carbon in a better way compared to the control treatment. Peng et al. [24] also described that fewer tillage practices and the use of an appropriate amount of zeolite cause less soil damage and prevent carbon emission. Deep and intensive tillage practices and less or no use of zeolite can reduce soil-dissolved organic carbon (DOC) [25]. This may be the reason why the interaction in the present study ($T_1 \times Z_1$), i.e., more tillage practices and no use of zeolite did not conserve soil carbon as zeolite can retain moisture and nutrients in the soil. Higher soil organic carbon (SOC) contents (7.88 and 7.97 g C Kg^{-1}) were found in the T_2 (minimum tillage) and Z_3 (10 t ha^{-1}) reaction compared to other tillage practices and zeolite doses, which may be due to reduced soil disturbance and use of appropriate material. Zeolite captures carbon due to its porous

nature. Darko et al. [26] also described that soil carbon contents are higher where tillage practices are lower and zeolite is frequent. Soils with extensive use of tillage practices have poor structure and greater loss of soil organic carbon [27].

Yield and yield parameters also gave significant differences using tillage and zeolite in our experiment. Wheat plant height was maximum (92.14 and 92.97 cm) in the $T_2 \times Z_3$ interaction compared to the rest of the tillage practices and zeolite doses, and this may be due to the minimum tillage practice, which conserves soil moisture contents that may be lost due to heavy tillage practices. Zeolite dose (10 t ha^{-1}) also provided the proper amount of carbon and minerals to the plants, allowing them to gain maximum height. Qi et al. [28] also reported that by using minimum tillage practices along with using proper zeolite dosages can conserve soil moisture and enhance soil porosity, which helps in better growth of plants. Gao [29] described that conventional tillage practices, poor application of nutrients, and carbon capture sources such as zeolite led to land degradation and poor crop stand. The spike length results showed that conventional tillage T_1 and no application of zeolite Z_1 produced retarded spike length while the interaction $T_2 \times Z_3$ showed better spike length (11.88 and 12.11 cm) where minimum tillage practices were used and zeolite dosage at 15 t ha^{-1} was applied as compared to the rest of tillage and zeolite interactions. Similar results were also described by Aghaalikhani et al. [30] who reported that using less tillage and material that enhances soil porosity can improve spike length as a parameter related to good plant growth, which is possible when soil is porous to access air and nutrients. The $T_2 \times Z_3$ interaction gave the highest number of spikelets/spike (20.11 and 20.98) and minimum found in $T_1 \times Z_1$, this may be due to heavy tillage practices which lose soil moisture and become unavailable to the plants. Chen et al. [31] also discussed that if heavy tillage practices were used frequently and no use of zeolite and other materials that became the soil porous then soil degradation may occur, which causes poor plant growth. The number of tillers per unit area was calculated and found that $T_1 \times Z_1$ gave the minimum number of tillers per unit area as compared to the other interaction. Tillers depend on soil fertility, nutrient availability, and healthy plant stand, which was poor in $T_1 \times Z_1$.

Deep and frequent tillage practices and poor amounts of zeolite reduced soil moisture and nutrient contents, which is the reason for poor plant establishment and ultimately tiller number [32]. The $T_2 \times Z_3$ interaction produced a maximum 1000-grain weight (50.74 and 51.54 g) compared to other interactions, which might be due to the zeolite enhancing soil organic carbon and nutrients and the minimum number of tillage practices conserved moisture, providing the crop with better stability and ultimately better grain yield. El-Porai et al. [33] also described that less soil disturbance and a proper amount of zeolite can yield better gains, but if excessive amounts of tillage and zeolite were applied soil nutrients may escape, and the crop does not obtain benefit from them. The upper ground portion has also been considered as a biological yield of wheat crops. This mainly depends on soil health and better crop stand [34]. The proper amount of zeolite application is very essential to achieve good yield because if an excessive amount is applied it may affect the roots of the plant causing less biological production [35]. The results of the present experiment also showed that the $T_2 \times Z_3$ interaction gave maximum biological yield (8134.87 and 8178.38 kg ha^{-1}) compared to the rest of the interactions, which might be due to improper application of zeolite and tillage practices. The wheat grain yield was taken when the plants were completely dried. The grain yield of the crop will be better if the crop plants are healthy and this is only possible if the nutrients and moisture are at the required level [36]. Wheat grain yield (2984.28 and 3028.96 Kg ha^{-1}) was higher in $T_2 \times Z_3$, which may be due to improved moisture level due to less soil disturbance and the effect of zeolite which makes the soil porous for better crop growth. The $T_1 \times Z_1$ reaction provides poor grain yield, which might be due to poor soil moisture and inappropriate zeolite management. The harvest index (HI) was also calculated by dividing the economic yield of wheat by the biological yield and then multiplying it by 100 to obtain the values in percentage. The results showed that the $T_2 \times Z_3$ interaction gave the maximum values of HI, and this may be due to the improvement of biological and grain yield. Improved moisture conservation

and nutrient retention due to zeolite management during monsoon gave a better harvest index as compared to the rest of the treatments, which caused loss of moisture and nutrients. Poor HI may be obtained due to deep tillage practices that cause nutrient leakage and lead to poor biological yield and grain production [37]. Kima et al. [38] also reported that zeolite should be applied in appropriate amounts with a combination of best tillage practices, it will not pose a risk to soil nutrients and can enhance crop productivity to a great extent.

5. Conclusions

The results of our current study, which was performed in rain-fed conditions showed that the interaction of tillage with zeolite doses played a significant role in soil carbon content and wheat yield. Soil carbon contents play a crucial role in crop growth. Excess carbon emission from the soil by using heavy tillage, i.e., mold-board plough not only creates a hard pan in the soil but also pollutes the environment compared to minimum tillage practices. Several tillage practices have been applied to reduce soil carbon emissions and enhance wheat productivity. The results of our experiment indicate that if minimum tillage (2 tillage with a cultivator) is used combined with the application of zeolite (10 t ha^{-1}), we can reduce carbon loss from the soil and enhance wheat productivity. By using these tillage practices and zeolite doses in rain-fed areas farmers socio-economic conditions can be improved. This is because these practices can enhance the productivity of wheat globally to a large extent. Furthermore, there is a need for a more comprehensive study on the long-term impacts of zeolite application and minimum tillage on different soil types of rain-fed as well as on irrigated lands under different climatic conditions.

Author Contributions: Conceptualization, M.u.H., A.B. and M.A.K.; methodology, M.u.H., A.B., and S.T.S.; software, M.u.H., W.M.H., A.B. and F.B.; validation, K.G.T., H.A.H.S.-A.A. and S.T.S.; formal analysis, M.u.H., A.B., M.A.K. and S.T.S.; investigation, H.A.H.S.-A.A., W.K. and W.M.H.; resources, K.G.T., H.A.H.S.-A.A.,W.M.H., M.u.H. and A.B.; data curation, M.u.H., A.B., M.A.K., W.M.H. and K.G.T.; writing—original draft preparation, W.K., M.u.H., A.B., S.T.S. and W.M.H.; writing—review and editing, K.G.T.; H.A.H.S.-A.A., W.K., A.B., F.B. and M.A.K.; visualization, W.M.H., A.B. and H.A.H.S.-A.A.; supervision, H.A.H.S.-A.A. and M.A.K. All authors have read and agreed to the published version of the manuscript.

Funding: This research received no external funding.

Data Availability Statement: No new data were created or analyzed in this study. Data sharing is not applicable to this article.

Conflicts of Interest: The authors declare no conflicts of interest.

References

1. GOP. *Economic Survey of Pakistan*; Finance and Economic Affairs Division: Islamabad, Pakistan, 2022.
2. Abu, M.S. Comparative evaluation of cassava composite flours and bread. *Asian J. Nat. Prodt. Biochem.* **2023**, *21*, 13–17. [CrossRef]
3. Ryan, J.; Masri, S.; Ibrikci, H.; Singh, M.; Pala, M.; Harris, H.C. Implications of cereal-based crop rotations, nitrogen fertilization, and stubble grazing on soil organic matter in a Mediterranean-type environment. *Turk. J. Agric. For.* **2008**, *32*, 289–297.
4. Bonfil, D.J.; Mufradi, I.; Klitman, S.; Asido, S. Wheat grain yield and soil profile water distribution in a no-till arid environment. *Agron. J.* **1999**, *91*, 368–373. [CrossRef]
5. Sharma, P.; Abrol, V.; Sharma, K.R.; Sharma, N.; Phogat, V.K.; Vikas, V. Impact of conservation tillage on soil organic carbon and physical properties–a review. *Int. J. Bio-Resour. Stress Manag.* **2016**, *7*, 151–161. [CrossRef]
6. Ullah, I.; Muhammad, D.; Mussarat, M.; Khan, S.; Adnan, M.; Fahad, S.; Ismail, M.; Mian, I.A.; Ali, A.; Saleem, M.H.; et al. Comparative effects of biochar and NPK on wheat crops under different management systems. *Crop. Pasture Sci.* **2022**, *74*, 31–40. [CrossRef]
7. Singh, S.; Prasanna, R.; Pranaw, K. *Bioinoculants: Biological Option for Mitigating global Climate Change*; Springer Nature: Berlin/Heidelberg, Germany, 2023.
8. Singh, O.P.; Singh, P.K. Environmental and socio-economic impact of zero-tillage in indo-gangatic plain of uttar pradesh, India. *Int. J. Agric. Stat. Sci.* **2020**, *16*, 589.
9. Higashida, S.; Yamagami, M. Effects of deep plowing with concomitant application of farm yard manure on the productivity of arable crops. *Bull. Hokkaido Prefect. Agric. Exp. Stat.* **2003**, *84*, 55–64.

10. Sfechiș, S.; Vidican, R.; Sandor, M.; Stoian, V.; Sandor, V.; Muste, B. Using assessment of zeolite amendments in agriculture. *ProEnvironment* **2015**, *8*, 21.
11. Abdi, G.H.; Khosh-Khui, M.; Eshghi, S. Effects of natural zeolite on growth and flowering of strawberry (*Fragaria* × *ananassa* Duch.). *Int. J. Agric. Res.* **2010**, *5*, 799–804.
12. Li, Z.; Zhang, Y.; Li, Y. Zeolite as slow-release fertilizer on spinach yields and quality in a greenhouse test. *J. Plant Nutr.* **2013**, *36*, 1496–1505. [CrossRef]
13. Bybordi, A.; Elnaz, E. Growth, yield and quality components of canola fertilized with urea and zeolite. *Commun. Soil Sci. Plant Anal.* **2013**, *44*, 2896–2915. [CrossRef]
14. Bernardi, A.C.d.C.; de Souza, G.B.; Polidoro, J.C.; Paiva, P.R.P.; Monte, M.B.d.M. Yield, quality components, and nitrogen levels of silage corn fertilized with urea and zeolite. *Commun. Soil Sci. Plant Anal.* **2011**, *42*, 1266–1275. [CrossRef]
15. Xiubin, H.E.; Zhanbin, H. Zeolite application for enhancing water infiltration and retention in loess soil. *Resour. Conserv. Recycl.* **2001**, *34*, 45–52. [CrossRef]
16. Gholamhoseini, M.; Ghalavand, A.; Khodaei-Joghan, A.; Dolatabadian, A.; Zakikhani, H.; Farmanbar, E. Zeolite-amended cattle manure effects on sunflower yield, seed quality, water use efficiency and nutrient leaching. *Soil Tillage Res.* **2013**, *126*, 193–202. [CrossRef]
17. Hazrati, S.; Tahmasebi-Sarvestani, Z.; Mokhtassi-Bidgoli, A.; Modarres-Sanavy, S.A.M.; Mohammadi, H.; Nicola, S. Effects of zeolite and water stress on growth, yield and chemical compositions of *Aloe vera* L. *Agric. Water Manag.* **2017**, *181*, 66–72. [CrossRef]
18. Ozbahce, A.; Tari, A.F.; Gönülal, E.; Simsekli, N.; Padem, H. The effect of zeolite applications on yield components and nutrient uptake of common bean under water stress. *Arch. Agron. Soil Sci.* **2015**, *61*, 615–626. [CrossRef]
19. Zahedi, H.; Noormohammadi, G.; Rad, A.S.; Habibi, D.; Boojar, M.M.A. The effects of zeolite and foliar applications of selenium on growth, yield and yield components of three canola cultivars under drought stress. *World App. Sci. J.* **2009**, *7*, 255–262. [CrossRef]
20. Zhang, M.; Hanna, M.; Li, J.; Butcher, S.; Dai, H.; Xiao, W. Creation of a hyperpermeable yeast strain to genotoxic agents through combined inactivation of PDR and CWP genes. *Toxicol. Sci.* **2010**, *113*, 401–411. [CrossRef]
21. Muhammad, A.; Amjad, A.; Parimala, G.S.; Arockiam, J.; Saqi, B.; Qaiser, H.; Fazli, W.; Esmat, F.A.; Hamada, A.; Ronghua, L.; et al. Effects of sheep bone biochar on soil quality, maize growth, and fractionation and phyto-availability of Cd and Zn in a mining-contaminated soil. *Chemosphere* **2021**, *282*, 10–16. [CrossRef]
22. Nelson, D.A.; Sommers, L. Total carbon, organic carbon, and organic matter. *Met. Soil Anal. Part 2 Chem. Microbiol. Prop.* **1983**, *9*, 539–579.
23. Spiertz, J.H.J. Nitrogen, sustainable agriculture and food security: A review. *Sustain. Agric.* **2010**, *30*, 43–55. [CrossRef]
24. Peng, S.; Buresh, R.J.; Huang, J.; Zhong, X.; Zou, Y.; Yang, J.; Dobermann, A. Improving nitrogen fertilization in rice by site specific N management. A review. *Agron. Sustain. Dev.* **2010**, *30*, 649–656. [CrossRef]
25. Mahajan, G.; Chauhan, B.S.; Timsina, J.; Singh, P.P.; Singh, K. Crop performance and water-and nitrogen-use efficiencies in dry-seeded rice in response to irrigation and fertilizer amounts in northwest India. *Field Crops Res.* **2012**, *134*, 59–70. [CrossRef]
26. Darko, R.O.; Shouqi, Y.; Junping, L.; Haofang, Y.; Xingye, Z. Overview of advances in improving uniformity and water use efficiency of sprinkler irrigation. *Int. J. Agric. Biol. Eng.* **2017**, *10*, 1–15.
27. Ahmed, O.H.; Sumalatha, G.; Muhamad, A.N. Use of zeolite in maize (*Zea mays*) cultivation on nitrogen, potassium and phosphorus uptake and use efficiency. *Int. J. Phys. Sci.* **2010**, *5*, 2393–2401.
28. Qi, W.; Guimin, X.; Taotao, C.; Daocai, C.; Ye, J.; Dehuan, S. Impacts of nitrogen and zeolite managements on yield and physicochemical properties of rice grain. *Int. J. Agric. Biol. Eng.* **2016**, *9*, 93–100.
29. Gao, P.; Liu, Y.; Wang, Y.; Liu, X.; Wang, Z.; Ma, L.Q. Spatial and temporal changes of P and Ca distribution and fractionation in soil and sediment in a karst farmland-wetland system. *Chemosphere* **2019**, *220*, 644–650. [CrossRef]
30. Aghaalikhani, M.; Gholamhoseini, M.; Dolatabadian, A.; Khodaei-Joghan, A.; Sadat Asilan, K. Zeolite influences on nitrate leaching, nitrogen-use efficiency, yield and yield components of canola in sandy soil. *Arch. Agron. Soil Sci.* **2012**, *58*, 1149–1169. [CrossRef]
31. Chen, T.; Sun, D.; Zhang, X.; Wu, Q.; Zheng, J.; Chi, D. Impact of water-nitrogen coupling on grain yield, water and nitrogen usage in zeolite-amended paddy field under alternate wetting and drying irrigation. *Trans. Chin. Soc. Agric. Eng.* **2016**, *32*, 154–162.
32. Ranjan, S.; Dasgupta, N.; Singh, S.; Gandhi, M. Toxicity and regulations of food nanomaterials. *Environ. Chem. Lett.* **2019**, *17*, 929–944. [CrossRef]
33. El-Porai, E.S.; Salama, A.E.; Sharaf, A.M.; Hegazy, A.I.; Gadallah, M.G.E. Effect of different milling processes on Egyptian wheat flour properties and pan bread quality. *Ann. Agric. Sci.* **2013**, *58*, 51–59. [CrossRef]
34. Neylon, E.; Arendt, E.K.; Zannini, E.; Sahin, A.W. Fermentation as a tool to revitalize brewers' spent grain and elevate techno-functional properties and nutritional value in high fibre bread. *Foods* **2021**, *10*, 1639. [CrossRef] [PubMed]
35. Buteler, M.; Gitto, J.G.; Stadler, T. Enhancing the potential use of microparticulate insecticides through removal of particles from raw grain. *J. Stored Prod. Res.* **2020**, *89*, 101707. [CrossRef]
36. Bodroza-Solarov, M.; Rajic, N.; Pezo, L.; Kojic, J.; Krulj, J.; Filipcev, B.; Jevtic-Mucibabic, R. The rheological properties of wheat dough containing zeolite residue. *Chem. Ind. Chem. Eng. Q.* **2020**, *26*, 377–384. [CrossRef]

37. Van Den Noortgate, H.; Sree, S.P.; Ostyn, N.; Lagrain, B.; Roeffaers, M.; Wenseleers, T.; Martens, J.A. Material properties determining insecticidal activity of activated carbon on the pharaoh ant (*Monomorium pharaonis*). *J. Pest Sci.* **2019**, *92*, 643–652. [CrossRef]
38. Kima, A.S.; Chung, W.G.; Wang, Y.M. Improving irrigated lowland rice water use efficiency under saturated soil culture for adoption in tropical climate conditions. *Water* **2014**, *6*, 2830–2846. [CrossRef]

land

MDPI

Article

Climate-Smart Drip Irrigation with Fertilizer Coupling Strategies to Improve Tomato Yield, Quality, Resources Use Efficiency and Mitigate Greenhouse Gases Emissions

Xinchao Ma [1,†], Yanchao Yang [1,†], Zhanming Tan [1,2,*], Yunxia Cheng [1], Tingting Wang [1], Liyu Yang [1], Tao He [1] and Shuang Liang [1]

[1] Key Laboratory of Protected Agriculture of Southern Xinjiang/National and Local Joint Engineering Laboratory of High Efficiency and High Quality Cultivation and Deep Processing Technology of Characteristic Fruit Trees in Southern Xinjiang/College of Horticulture and Forestry Sciences, Tarim University, Alar 843300, China
[2] Aksu Naida Agricultural Technology Co., Ltd., Aksu 843000, China
* Correspondence: tlmdxtzm@taru.edu.cn; Tel.: +86-159-0997-6635
† These authors contributed equally to this work.

Abstract: Background: Integrated water and fertilizer management is important for promoting the sustainable development of agriculture. Climate-smart drip irrigation with fertilizer coupling strategies plays an important role to mitigate greenhouse gas emissions, ensuring food production, and alleviating water scarcity and excessive use of fertilizers. **Methods:** The greenhouse experiment consists of three drip irrigation treatments which include D1: drip irrigation (100 mm); D2: drip irrigation (200 mm); D3: drip irrigation (300 mm) under three different fertilizer management practices N1: nitrogen level (150 kg N ha^{-1}); N2: nitrogen level (300 kg N ha^{-1}); N3: nitrogen level (450 kg N ha^{-1}). **Results:** The results showed that significantly improved soil moisture contents, quality and tomato yield, while reduced (38.6%) greenhouse gas intensity (GHGI) under the D3N3 treatment. The D2 and D3 drip irrigation treatments with 450 kg nitrogen ha^{-1} considerably improved NH_4^+-N contents, and NO_3^--N contents at the fruit formation stage. The improve in net primary productivity (NPP), net ecosystem productivity (NEP), evapotranspiration (ET), and ecosystem crop water productivity (CWP_{eco}) through D3N3 treatment is higher. The D3N3 treatment improved (28.2%) the net global warming potential (GWP), but reduced GHGI, due to improved (18.4%) tomato yield. The D3N3 treatment had significantly greater irrigation water productivity (IWP) (42.8%), total soluble sugar (TSS) (32.9%), vitamin C content (VC) (39.2%), soluble sugar content (SSC) (44.2%), lycopene content (41.3%) and nitrogen use efficiency (NUE) (52.4%), as compared to D1N1 treatment. **Conclusions:** Therefore, in greenhouse experiments, the D3N3 may be an effective water-saving and fertilizer management approach, which can improve WUE, tomato yield, and quality while reducing the effect of global warming.

Keywords: coupling of drip irrigation and fertilizer; tomato production; greenhouse gas emissions; nutrients update; irrigation water productivity; tomato quality

Citation: Ma, X.; Yang, Y.; Tan, Z.; Cheng, Y.; Wang, T.; Yang, L.; He, T.; Liang, S. Climate-Smart Drip Irrigation with Fertilizer Coupling Strategies to Improve Tomato Yield, Quality, Resources Use Efficiency and Mitigate Greenhouse Gases Emissions. *Land* **2024**, *13*, 1872. https://doi.org/10.3390/land13111872

Academic Editor: Krish Jayachandran

Received: 11 October 2024
Revised: 1 November 2024
Accepted: 5 November 2024
Published: 8 November 2024

1. Introduction

Tomato (*Solanum lycopersicum* L.) is rich in carotene, vitamins C, and B, with great nutritious values. Xinjiang is the most essential tomato-producing region in China, including a planting area of more than 1 million hectare [1]. In recent years, the cultivation area of greenhouse tomatoes in Xinjiang, China, has gradually expanded, but the development of the greenhouse tomato industry has been considerably limited. Precise water and fertilizer coupling technology may be able to overcome this urgent problem to improve the quality of tomatoes while increasing their ability to withstand storage. Water and fertilizer coupling technology [2] is based on varying water conditions, irrigation and fertilization durations,

quantities, and modes of coordination, promoting soil water absorption range, using deeper soil water, and enhancing crop transpiration and photosynthesis. Li [3] demonstrated that the ratio of water and fertilizer had a significant influence on the quality and yield index of tomatoes. Yao et al. [4] indicated that sugar, as an energy substance and signal molecule, regulates fruit sweetness and physiological processes, such as ripening, senescence, and responses to stress. Currently, there are few reports on the integration use of drip irrigation and nitrogen coupling on tomato quality and yield. Nitrogen is an important element for chlorophyll, enzymes, proteins, and vitamins; it plays a crucial role in keeping crop life activities and improving yield and quality [5]. Insufficient nitrogen application can limit plant growth, while excessive nitrogen application can delay ripening, deteriorate since tomato quality, and increase nitrate leaching [6,7].

Many countries and regions around the world are facing a food shortage crisis due to conflicts, extreme weather, and insufficient water resources. As a shallow-rooted crop, tomatoes are sensitive to water and nutrient stress at all growth stages [8–10]. Water is a key factor affecting crop nutrient absorption. Only when soil nutrients are dissolved in water can crops absorb and utilize them [11–13]. Compared with traditional flood irrigation and furrow irrigation, drip irrigation saves a large amount of irrigation water, delivers irrigation water directly to the root zone of plants, and effectively improves water productivity [14–16]. Drip irrigation combined with nutrient management approach can significantly reduce the use of chemical fertilizers, inhibit the leaching of nutrients and fertilizers below the root zone, improve nitrogen use efficiency (NUE), crop yield, and minimize the effect of chemical fertilizers on the soil ecology [17,18]. However, the response of tomato production and irrigation water productivity varies depending on the climatic conditions of the research site and the characteristics of the drip irrigated soil [19]. Unfortunately, in recent years, the disadvantages of drip irrigation and fertilization have gradually become apparent, particularly in low organic carbon content with poor soils, which can lead to soil compaction [20]. The current drip irrigation fertigation model relies heavily on the application of soluble inorganic fertilizers rather than the application of organic fertilizers [14]. Some studies have reported that partial replacement of chemical fertilizers with organic fertilizers under drip irrigation can raise the nutritional contents of the soil and improve crop yields [13]. Hence, there is an urgent need to further optimize the drip irrgation regime for a better greenhouse tomato production.

China leads the world in tomato cultivation area more than 1 million hectares and tomato production of 56 million tons per year [21,22]. Tomatoes are generally grown in open fields and greenhouse environments [23]. Over the past few decades, solar greenhouses have become the mainstream of vegetable cultivation in China. This is because they not only have the potential to produce high-quality vegetables and high profits during the off-season but also can resist climate change [24,25]. Therefore, the development of a sustainable greenhouse production system is essential for better crop growth and stable high tomato yields. Water wastage is still a serious issue, and large amounts of soil are lost to deep soil through evaporation, while the crop utilization rate is low [26]. In addition, unnecessary nitrogen and drip irrigation water to reduce the risk of yield decline have led to resource waste and ecological damage, such as leaching nutrients in groundwater [24,27]. Furthermore, nutrient management can improve fruit quality and crop yield [28,29]. Du et al. [30] reported that irrigation in greenhouse systems had significantly improved crop productivity. While, Zhu et al. [31] also reported that the sugar-acid ratio, lycopene, vitamin C, and soluble sugar of tomato fruits under subsurface drip irrigation were higher. A study by Chen et al. [28] also reported that the carbon footprint of integrated irrigation and fertilization management was significantly higher than that of conventional irrigation.

Greenhouse cultivation has become the main method of vegetable production in China, providing a stable supply in different seasons and meeting the growing demand for vegetables [32,33]. The worsening of global water shortages has led to increased attention to irrigation methods that maximize water-use efficiency [34,35]. Drip irrigation is the most effective water-saving irrigation technology [36]. Excessive irrigation and fertilization

reduce water and nutrient utilization, leading to a series of environmental problems and nutrient leakage [37,38]. Because greenhouse vegetables have a short growth cycle and a large demand for water and nutrients to increase yields, with little consideration of the effect of water and nitrogen application on ecological pollution [39]. Irrigation volume can have a significant impact on soil moisture and nitrogen distribution, thereby affecting greenhouse gas emissions. Excessive nitrogen fertilizer application leads to increased CO_2 and N_2O emissions [27]. High temperature and humidity in greenhouses accelerate soil nitrogen cycling, thereby increasing greenhouse gas emissions [40]. Therefore, scientific management of water and nitrogen can ensure crop yield and reduce nitrogen leaching and greenhouse gas emissions while avoiding excessive water and nitrogen application [41]. However, there is an obvious lack of research on how to coordinate and control irrigation and nitrogen fertilizer application to achieve synergistic improvements in the tomato growth cycle and production, quality, efficiency improvements, and emission reductions. The results of this study are expected to extend our understanding of the integrated effects of drip irrigation and nitrogen application on tomato yield, quality, water and nitrogen use efficiency, and net greenhouse gas emissions, and have potential application value in precision irrigation management for high yield, providing effective guidance for the water and fertilizer management of local greenhouse tomato production.

2. Materials and Methods

2.1. Site Description

The research was performed in a multi-span greenhouse at the Horticultural Experimental Station of Tarim University (81°16′ E, 40°33′ N) during the 2021 study year. The tested tomato variety was 'Qinshulingyue'. The experiment was conducted under trough cultivation in the north-south direction, using an individual plant spacing of 0.35 m and row spacing of 1.1 m, in an area of 7.5 m^2. Drip irrigation was accomplished using a reliable water source, water pump, water meter, fertilizer barrel (electric sprayer), water pipeline, dripper, drip pipe, and other systems. The dripper exhibited a pressure-compensated flow rate of 2 L per hour, with a dripper spacing of 35 cm. The chemical properties of greenhouse soil are shown in Table 1.

Table 1. The soil properties of greenhouse of the soil layers (0–20 cm).

Year	pH	SOM (g kg^{-1})	TN (g kg^{-1})	TP (g kg^{-1})	TK (g kg^{-1})	AP (mg kg^{-1})	AK (mg kg^{-1})
2021	8.11	15.29	1.04	1.06	16.28	18.91	163.59

2.2. Greenhouse Research Management

The randomize complete block design (RCBD) was used with four replications. Each plot area has 7.5 m^2. It includes nine treatments: D1N1: drip irrigation (100 mm) with nitrogen level (150 kg ha^{-1}); D1N2: drip irrigation (100 mm) with nitrogen level (300 kg ha^{-1}); D1N3: drip irrigation (100 mm) with nitrogen level (450 kg ha^{-1}); D2N1: drip irrigation (200 mm) with nitrogen level (150 kg ha^{-1}); D2N2: drip irrigation (200 mm) with nitrogen level (300 kg ha^{-1}); D2N3: drip irrigation (200 mm) with nitrogen level (450 kg ha^{-1}); D3N1: drip irrigation (300 mm) with nitrogen level (150 kg ha^{-1}); D3N2: drip irrigation (300 mm) with nitrogen level (300 kg ha^{-1}); D3N3: drip irrigation (300 mm) with nitrogen level (450 kg ha^{-1}). The 40% nitrogen was supplied at the sowing stage, (30%) at the vegetative growth stage and (30%) at the flowering stage. The recommended doses of P and K were applied one day before sowing. During growing season weeds were controlled manually.

2.3. Sampling and Measurements

2.3.1. Soil Water Content

Soil moisture content (SWC) was monitored at EGS: early growth stage, VGS: vegetative growth stage, FS: flowering stage, FFS: fruit formation stage, and RS: ripening stage in 2021. A TDR meter was used to measure the water content at 20 cm intervals at soil depths from 0 to 100 cm.

Evapotranspiration (ET) was calculated seasonally:

$$\mathrm{ET} = \mathrm{R} + \Delta\mathrm{SWS} \tag{1}$$

2.3.2. Gas Sampling and Analysis

CO_2 and N_2O emissions were measured at GS: germination stage, EGS: early growth stage, VGS: vegetative growth stage, FS: flowering stage, FFS: fruit formation stage, and RS: ripening stage. All stainless steel chambers for gas chromatography were equipped with fans to complete the gas mixing. GHG concentrations were analyzed within 72 h of gas sampling using an Agilent 7890A gas chromatograph (Agilent, Santa Clara, CA, USA).

Gas emission rates were calculated according to [40]:

$$\text{Gas emission rate } \left(\mathrm{mgm^{-2}h^{-1}}\right) = \Delta c/\Delta \mathrm{t} \times \mathrm{V/A} \times \rho \times 273/\mathrm{T} \tag{2}$$

The seasonal gas flow rate was calculated using the following equation [41]:

$$\text{Seasonal flux } \left(\mathrm{kgha^{-1}}\right) = \sum_i^{\mathrm{n}} \left(\mathrm{R_i} \times D_i\right) \tag{3}$$

Net GWP was calculated by using the following equation [42]:

$$\begin{aligned} &\mathrm{NetGWP}\left(\mathrm{kgCO_2 - eqha.^{-1}}\right) = \mathrm{CH_4flux25} \\ &+\mathrm{N_2Oflux298} - \Delta\mathrm{SOC44/12} \end{aligned} \tag{4}$$

The GHGI was calculated by using net GWP per tomato yield [43]:

$$\text{GHGI (kg } \mathrm{CO_2}\text{-eq kg}^{-1} \text{ yield)} = \text{Net GWP/tomato yield} \tag{5}$$

To analysed the net ecosystem carbon budget (NECB) using the variations in total carbon input and total carbon output [44,45].

$$\begin{aligned} \mathrm{NECB} &= \sum \mathrm{Cinput} - \sum \mathrm{Coutput} \\ &= (\mathrm{NPP} + \mathrm{biomass} + \mathrm{urea}) \\ &-(\mathrm{harvested\ Cremoval} + \mathrm{respired\ Closs}) \end{aligned} \tag{6}$$

Soil samples were mixed with 1 M KCL at a soil-to-solution ratio of 1:10 and then filtered to produce extracts, and the concentrations of NH_4^+-N and NO_3^--N contents were measured by colorimetry using a continuous flow analyzer [46].

2.3.3. Calculation of Net Primary Productivity (NPP), and Net Ecosystem Productivity (NEP)

The net ecosystem productivity NEP of CO_2 was calculated by Zhang et al. [47].

$$\mathrm{NEP} = \mathrm{R_H} - \mathrm{NPP} \tag{7}$$

Then NPP was calculated by using the below equation [48,49].

$$\mathrm{NPP} = 0.446\mathrm{W_{max}} - 0.00067 \tag{8}$$

Ecosystem crop water productivity is calculated by the following equation [50].

$$CWPeco = NEP/ET \quad (9)$$

The irrigation water productivity (IWP) was determined as equation.

$$IWP = Y_1 - Y_2/I \quad (10)$$

where Y (kg ha^{-1}) is the tomato yield; I is the deficit irrigation; Y_1 (kg ha^{-1}) is the tomato yield of irrigated plot; Y_2 (kg ha^{-1}) is the tomato yield of un-irrigated plot.

N use efficiency (NUE) was determined as the ratio of tomato yield to the total N uptake [51].

The content of soluble sugar was determined via anthrone colorimetry. Each sample was examined three times in parallel. The soluble sugar content was calculated from the standard curve, in units of %.

The lycopene content was calculated according to a value obtained using a colorimeter. The method was adapted to rapidly detect the lycopene content with a colorimeter [52]. A CR-400/410 colorimeter(Konica Minolta, Tokyo, Japan) was utilized. Specifically, three fruits were obtained from each group, and each fruit was measured three times, yielding three consecutive values. Chroma was measured using L, a, and b values and substituted into the formula, O (lycopene content) = 3.004X − 35.003, where X represents the Chroma value, and the lycopene content is expressed as $\mu g \cdot g^{-1}$.

Vitamin C content was measured using the 2,6-dichlorophenol indophenol sodium method [53]. Each sample was measured in triplicate, and vitamin C levels were calculated from the standard curve, with the unit of measurement being mg kg^{-1}.

2.3.4. Data Processing

Analysis of variance (ANOVA) was performed using SPSS 13.0 (SPSS Inc., Chicago, IL, USA). Data from each sampling event were analyzed separately. Means among treatments were compared based on the least significant difference test (LSD 0.05). Significance level was set at $p < 0.05$. All graphs were generated in this study using Origin 2021 software. In this experiment, Microsoft Excel 2020 was used for counting and sorting the data analysis.

3. Results

3.1. Soil Water Contents and ET Rate

In the greenhouse study, SWC at soil depths of 1–100 cm was regularly measured at various growth stages of tomato. The climate-smart drip irrigation and fertilizer coupling strategy significantly increased SWC compared to control plots (Figure 1). There were significant ($p < 0.05$) variances in SWC at each growth stage, and the treatment order was as follows: D3N3 > D2N3 > D3N2 > D2N2 > D1N3 > D3N1 > D2N1 > D1N2 > D1N1 treatment. In the greenhouse study, SWC at sowing was not significantly different between treatments. At each growth stage, SWC treated with D3N3 and D2N3 was considerably greater as compared with the rest of all other treatments. During the greenhouse trial, SWC increased significantly for all treatments from the early growth stage to the flowering stage and decreased considerably from flowering to the mature stage.

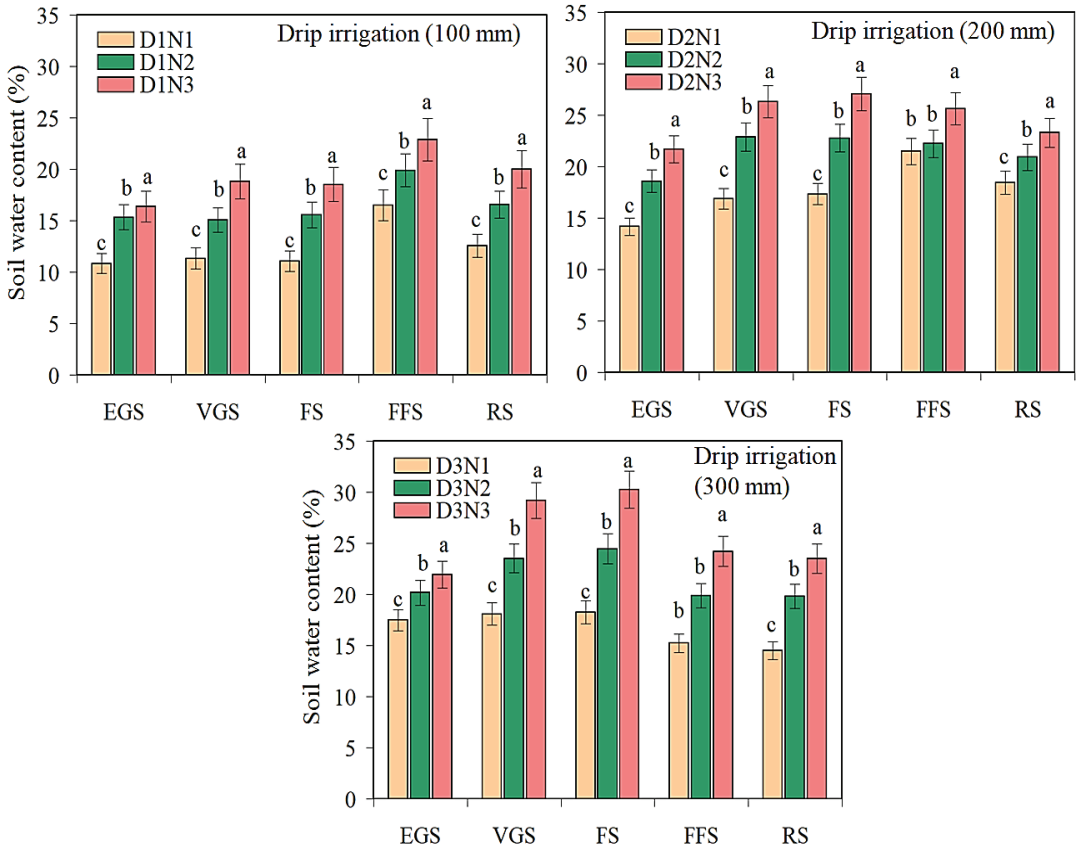

Figure 1. Effects of different drip irrigation and fertilizer coupling strategies on soil water content (%) at the depth of 0–100 cm soil layers during 2021. Note: D1N1: drip-irrigation (100 mm) with nitrogen level (150 kg ha^{-1}); D1N2: drip-irrigation (100 mm) with nitrogen level (300 kg ha^{-1}); D1N3: drip-irrigation (100 mm) with nitrogen level (450 kg ha^{-1}); D2N1: drip-irrigation (200 mm) with nitrogen level (150 kg ha^{-1}); D2N2: drip-irrigation (200 mm) with nitrogen level (300 kg ha^{-1}); D2N3: drip-irrigation (200 mm) with nitrogen level (450 kg ha^{-1}); D3N1: drip-irrigation (300 mm) with nitrogen level (150 kg ha^{-1}); D3N2: drip-irrigation (300 mm) with nitrogen level (300 kg ha^{-1}); D3N3: drip-irrigation (300 mm) with nitrogen level (450 kg ha^{-1}). EGS: early growth stage; VGS: vegetative growth stage; FS: flowering stage; FFS: fruit formation stage; RS: ripening stage. Values are given as means, and different lowercase letters indicate significant differences at $p \leq 0.05$ levels in the same line (Duncan's multiple range test).

There is a positive correlation between tomato ET and drip irrigation nitrogen fertilizer coupling management method. Compared with the D3N1 and D2N1 treatments, the D3N3 and D3N2 treatments with different drip irrigation and nitrogen fertilizer coupling management had higher ET rates due to strong transpiration (Table 2). The results showed that the ET of D1N1 was considerably higher than that of D2N1 and D3N1 treatments. Compared with the D3N3 treatment, the D3N2 treatment significantly reduced ET by 0.6%, and the D2N3 treatment significantly reduced ET by 3.9%.

Table 2. CO_2 emissions, NPP, NEP, evapotranspiration (ET) and CWP as affected by various treatments [a].

Treatments	CO_2-C (kg CO_2 ha^{-1})	NPP (kg CO_2 ha^{-1})	NEP (kg CO_2 ha^{-1})	ET (mm)	CWPeco (kg CO_2 ha^{-1} mm^{-1})
D1N1	3375 a	5859 f	1637 g	348.8 c	6.1 b
D1N2	3163 c	6098 e	2240 e	359.7 c	6.8 b
D1N3	2950 e	6336 c	2743 c	364.7 b	7.5 a
D2N1	3278 b	5646 f	1729 f	354.9 c	4.9 c
D2N2	3041 d	6062 e	2309 e	361.1 b	6.4 b
D2N3	2805 f	6478 b	2889 b	368.8 b	7.8 a
D3N1	3079 d	5691 f	1872 f	376.6 b	5.0 c
D3N2	2900 e	6119 d	2535 d	381.6 a	6.6 b
D3N3	2722 g	6546 a	3198 a	383.9 a	8.3 a

[a] D1N1: drip-irrigation (100 mm) with nitrogen level (150 kg ha^{-1}); D1N2: drip-irrigation (100 mm) with nitrogen level (300 kg ha^{-1}); D1N3: drip-irrigation (100 mm) with nitrogen level (450 kg ha^{-1}); D2N1: drip-irrigation (200 mm) with nitrogen level (150 kg ha^{-1}); D2N2: drip-irrigation (200 mm) with nitrogen level (300 kg ha^{-1}); D2N3: drip-irrigation (200 mm) with nitrogen level (450 kg ha^{-1}); D3N1: drip-irrigation (300 mm) with nitrogen level (150 kg ha^{-1}); D3N2: drip-irrigation (300 mm) with nitrogen level (300 kg ha^{-1}); D3N3: drip-irrigation (300 mm) with nitrogen level (450 kg ha^{-1}). Values are given as means, and different lowercase letters indicate significant differences at $p \leq 0.05$ levels in the same line (Duncan's multiple range test).

3.2. Soil NO_3^- and NH_4^+ Contents

Nitrogen such as NO_3^- and NH_4^+ is uptake by the roots and transported to the shoots by the xylem. Different climate-smart drip irrigation and fertilizer coupling strategies significantly changed the NO_3^- and NH_4^+ contents in the shoots (Figures 2 and 3). At each growth stage, the NO_3^- and NH_4^+ contents of the D3N3 treatment were considerably greater than those of all other treatments. At the V7, flowering and grain-filling stages, the NH_4^+ content under 300 mm drip irrigation with 450 kg ha^{-1} nitrogen application level was considerably greater than that in the D3N1 treatment, while the D3N3 and D3N2 treatments had higher concentrations in GS, EGS, FS, FFS, and RS. There is not much difference between stages. Therefore, in the GS, EGS, FS, FFS, and RS stages, the NO_3^- transport rate of the D3N3 treatment was significantly higher than that of the D1N1 treatment. Furthermore, the NO_3^- and NH_4^+ transport rates in D3N3 and D3N2 treatments were considerably greater as compared with the rest of all treatments.

3.3. Greenhouse Gas Emissions

A greenhouse study found that CO_2 emission was positive and qualified three variations (Figure 4). Irrespective of the various climate-smart drip irrigation with fertilizer coupling strategies, CO_2 is minimum during the early growth stage, but enhanced significantly during the fruit formation stage and reaches the highest during the fruit formation stage. Compared with the D1N1 treatment, D3N3, and D3N2 treatments considerably changed the CO_2; while the emissions of the D3N3 treatment were considerably more than that of the D1N3 treatment. Different drip irrigation with fertilizer coupling strategies at all growth stages have significant effect on N_2O content. N_2O showed two peaks during the vegetative growth period and fruit formation period, and the N_2O emission in the D1N1 was considerably lower than the other treatments (Figure 5). N_2O emissions under D3N3 and D3N2 treatments were considerably greater than those under D2N1 and D3N1. Under various coupling strategies of drip irrigation and fertilization, N_2O emissions in different growth periods have significant effects.

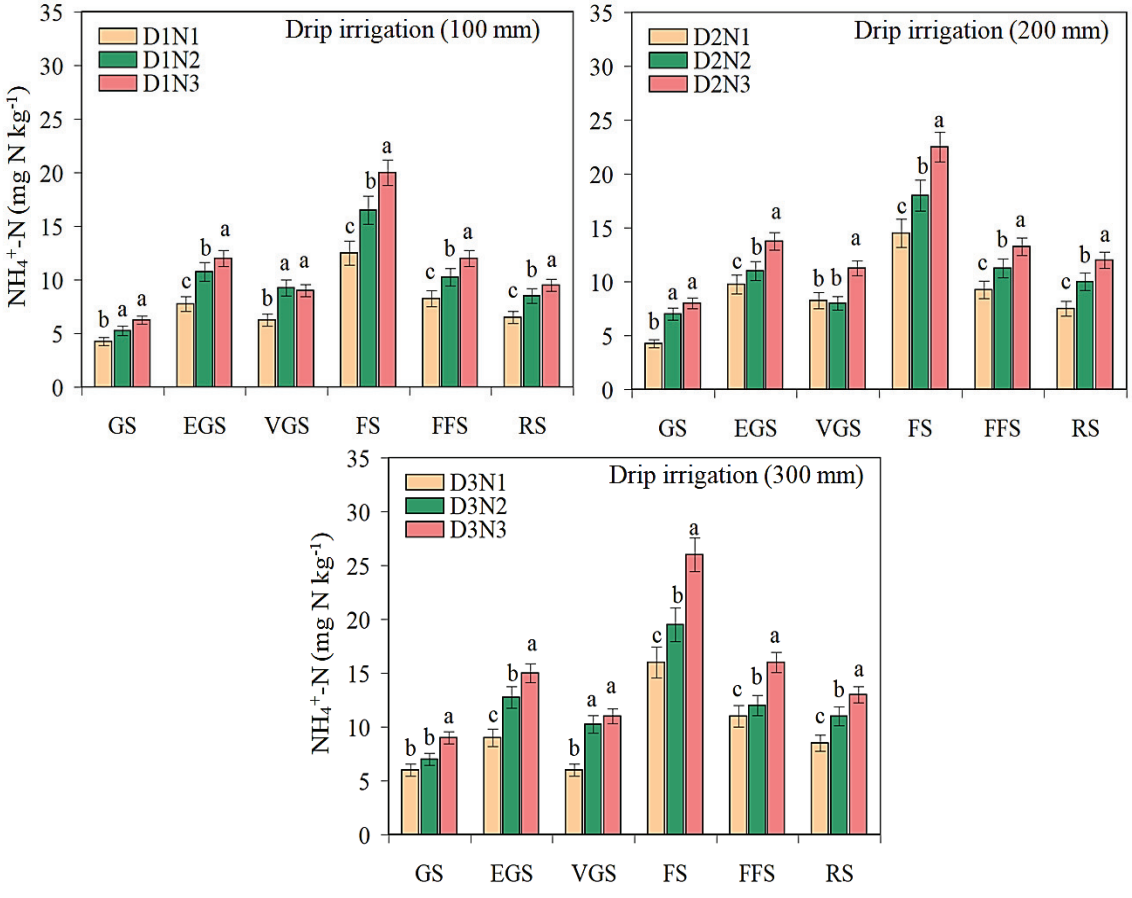

Figure 2. Effects of different drip irrigation and fertilizer coupling strategies on NH_4^+-N contents at different growth stages of tomato during 2021. Note: D1N1: drip-irrigation (100 mm) with nitrogen level (150 kg ha^{-1}); D1N2: drip-irrigation (100 mm) with nitrogen level (300 kg ha^{-1}); D1N3: drip-irrigation (100 mm) with nitrogen level (450 kg ha^{-1}); D2N1: drip-irrigation (200 mm) with nitrogen level (150 kg ha^{-1}); D2N2: drip-irrigation (200 mm) with nitrogen level (300 kg ha^{-1}); D2N3: drip-irrigation (200 mm) with nitrogen level (450 kg ha^{-1}); D3N1: drip-irrigation (300 mm) with nitrogen level (150 kg ha^{-1}); D3N2: drip-irrigation (300 mm) with nitrogen level (300 kg ha^{-1}); D3N3: drip-irrigation (300 mm) with nitrogen level (450 kg ha^{-1}). GS: germination stage; EGS: early growth stage; VGS: vegetative growth stage; FS: flowering stage; FFS: fruit formation stage; RS: ripening stage. Vertical bars represent the LSD at $p = 0.05$ (n = 3). Values are given as means, and different lowercase letters indicate significant differences at $p \leq 0.05$ levels in the same line (Duncan's multiple range test).

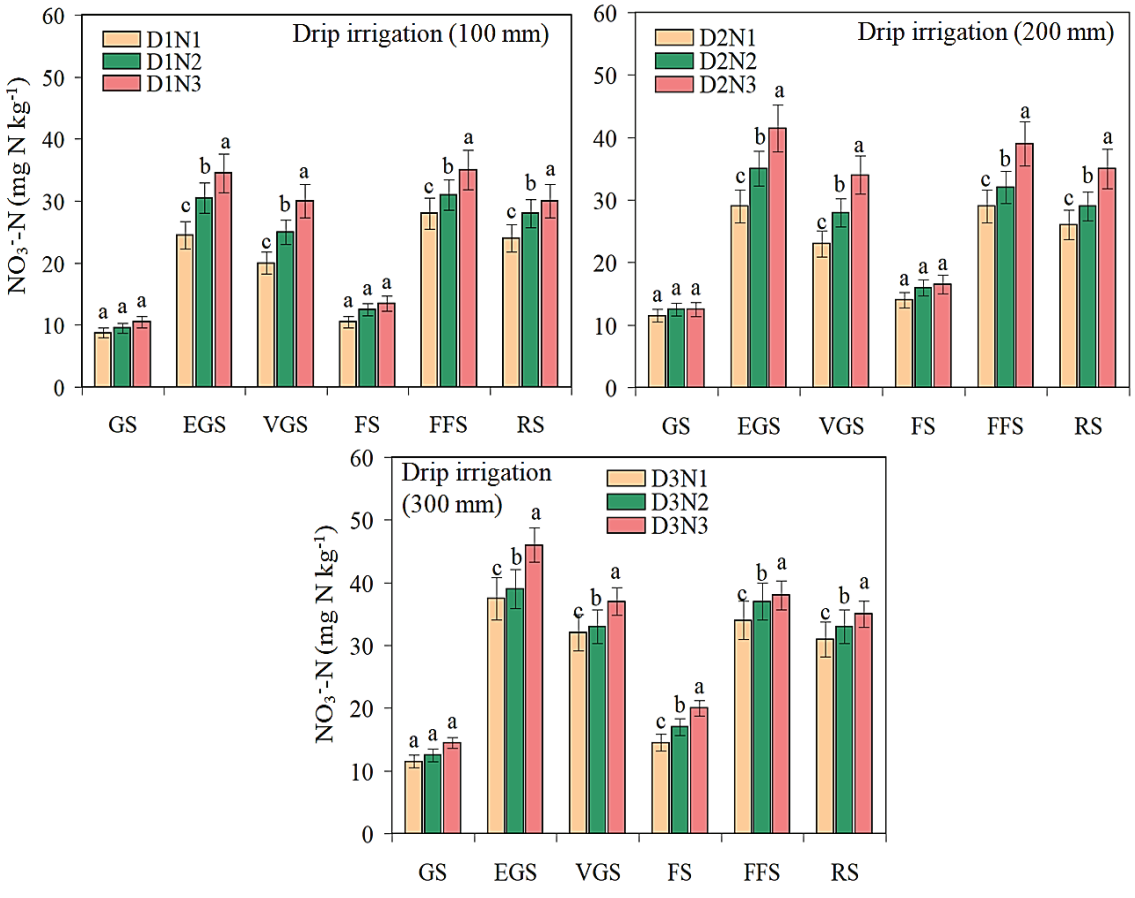

Figure 3. Effects of various drip irrigation and fertilizer coupling strategies on NO_3^--N contents at different growth stages of tomato during 2021. Note: D1N1: drip-irrigation (100 mm) with nitrogen level (150 kg ha^{-1}); D1N2: drip-irrigation (100 mm) with nitrogen level (300 kg ha^{-1}); D1N3: drip-irrigation (100 mm) with nitrogen level (450 kg ha^{-1}); D2N1: drip-irrigation (200 mm) with nitrogen level (150 kg ha^{-1}); D2N2: drip-irrigation (200 mm) with nitrogen level (300 kg ha^{-1}); D2N3: drip-irrigation (200 mm) with nitrogen level (450 kg ha^{-1}); D3N1: drip-irrigation (300 mm) with nitrogen level (150 kg ha^{-1}); D3N2: drip-irrigation (300 mm) with nitrogen level (300 kg ha^{-1}); D3N3: drip-irrigation (300 mm) with nitrogen level (450 kg ha^{-1}). GS: germination stage; EGS: early growth stage; VGS: vegetative growth stage; FS: flowering stage; FFS: fruit formation stage; RS: ripening stage. Vertical bars represent the LSD at $p = 0.05$ (n = 3). Values are given as means, and different lowercase letters indicate significant differences at $p \leq 0.05$ levels in the same line (Duncan's multiple range test).

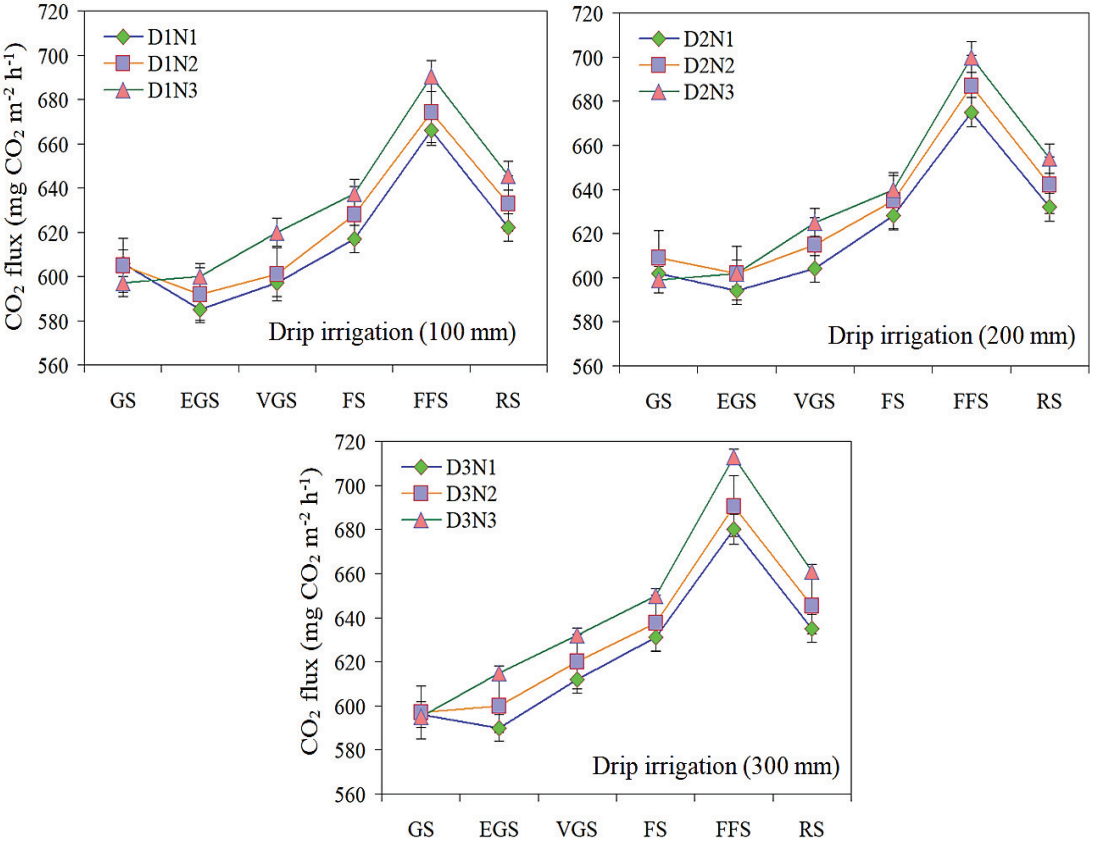

Figure 4. Effects of different drip irrigation and fertilizer coupling strategies on CO_2 emission at different growth stages of tomato during 2021. Note: D1N1: drip-irrigation (100 mm) with nitrogen level (150 kg ha^{-1}); D1N2: drip-irrigation (100 mm) with nitrogen level (300 kg ha^{-1}); D1N3: drip-irrigation (100 mm) with nitrogen level (450 kg ha^{-1}); D2N1: drip-irrigation (200 mm) with nitrogen level (150 kg ha^{-1}); D2N2: drip-irrigation (200 mm) with nitrogen level (300 kg ha^{-1}); D2N3: drip-irrigation (200 mm) with nitrogen level (450 kg ha^{-1}); D3N1: drip-irrigation (300 mm) with nitrogen level (150 kg ha^{-1}); D3N2: drip-irrigation (300 mm) with nitrogen level (300 kg ha^{-1}); D3N3: drip-irrigation (300 mm) with nitrogen level (450 kg ha^{-1}). GS: germination stage; EGS: early growth stage; VGS: vegetative growth stage; FS: flowering stage; FFS: fruit formation stage; RS: ripening stage.

3.4. NPP, NEP, Multilevel Crop Water Productivity

Table 2 shows the annual range from 3375 to 2722 kg CO_2 ha^{-1}. There was no significant variance in annual NPP between the D1N2 and D2N2 treatments since the total biomass values for all treatments were very close. However, greenhouse studies showed that the D3N3 had greater annual NPP values than all the remaining treatments. In a tomato greenhouse experiment, a climate-smart drip irrigation and fertilizer coupling strategy had a considerable effect on the NEP between NPP and total CO_2 flux. Annual NEP ranged from 1637 to 3198 kg CO_2 ha^{-1}. Annual NEP increased significantly for D3N2 and D3N3 treatments compared to all remaining treatments. When it comes to CWPeco, there are considerable differences between climate-smart drip irrigation and fertilizer coupling strategies. The average CWPeco values for the nine treatments ranged from 8.3 to 4.9 kg CO_2 ha^{-1} mm^{-1}. Overall, the CWPeaco values for the D3N3 treatment are quite high compared to all the remaining treatments.

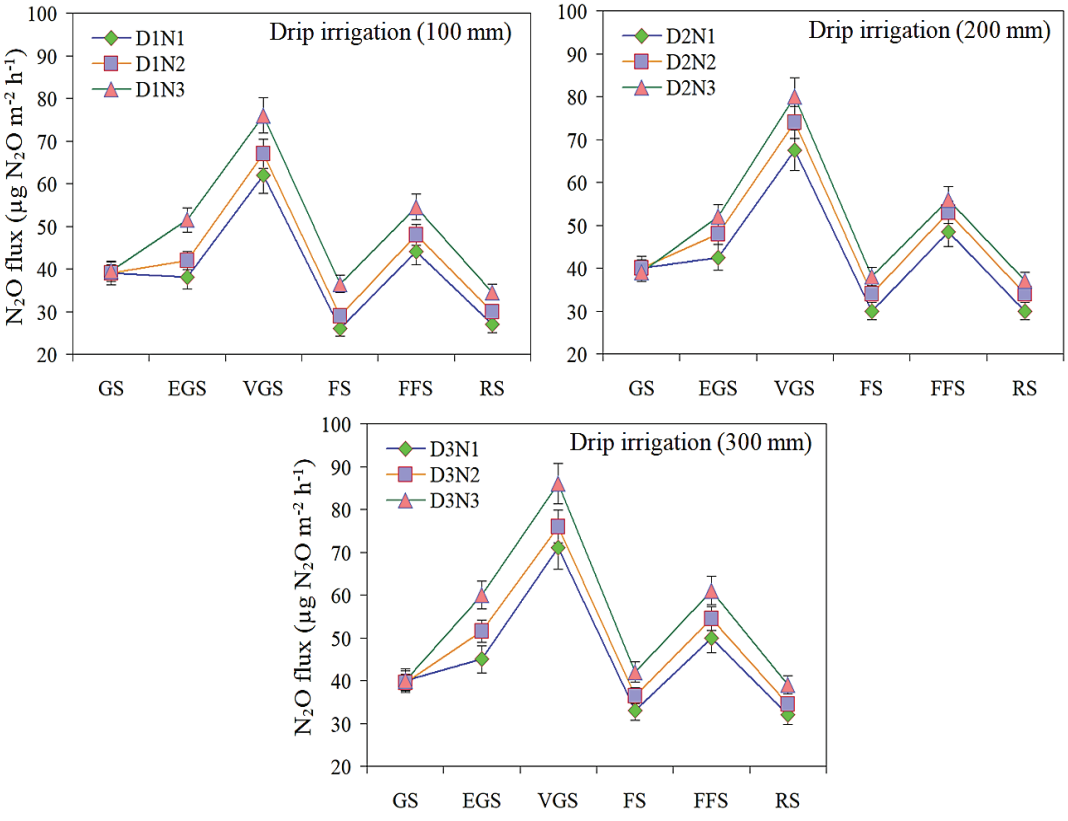

Figure 5. Effects of different drip irrigation and fertilizer coupling strategies on N_2O emission at different growth stages of tomato during 2021. Note: D1N1: drip-irrigation (100 mm) with nitrogen level (150 kg ha^{-1}); D1N2: drip-irrigation (100 mm) with nitrogen level (300 kg ha^{-1}); D1N3: drip-irrigation (100 mm) with nitrogen level (450 kg ha^{-1}); D2N1: drip-irrigation (200 mm) with nitrogen level (150 kg ha^{-1}); D2N2: drip-irrigation (200 mm) with nitrogen level (300 kg ha^{-1}); D2N3: drip-irrigation (200 mm) with nitrogen level (450 kg ha^{-1}); D3N1: drip-irrigation (300 mm) with nitrogen level (150 kg ha^{-1}); D3N2: drip-irrigation (300 mm) with nitrogen level (300 kg ha^{-1}); D3N3: drip-irrigation (300 mm) with nitrogen level (450 kg ha^{-1}). GS: germination stage; EGS: early growth stage; VGS: vegetative growth stage; FS: flowering stage; FFS: fruit formation stage; RS: ripening stage.

3.5. GHGI and GWP

To evaluate the effect of D3N2 and D3N3 treatments on global warming, the net GWP was calculated by considering the GWP values of each greenhouse gas emission and the change in soil carbon stock (Table 3). Irrespective of the drip irrigation and fertilization strategy, the net GWP is highly dependent on the depletion of soil carbon pools. In the D3N3, the net GWP was 19.2 Mg CO_2-eq. ha^{-1} soil carbon consumption and N_2O emission. Although a small amount of CH_4 (approximately 83.9 kg CO_2-eq. ha^{-1}) is utilized during cultivation, its contribution to the net GWP reduction is negligible. Compared with the D1N1 treatment, the net GWP was significantly increased by 33.8% in the D3N3 treatment, which was mostly due to the significantly improved consumption of soil carbon pools. However, the N3 treatment under various drip irrigation conditions had higher net GWP values compared to the control. In the two combined drip and fertilization irrigation strategies, the D3N3 treatment had a significant impact on GHGI (net GWP per unit yield). Compared to D1N1 treatment, D3N3 treatment significantly reduced GHGI 1.97 kg CO_2-

eq. ha^{-1} due to a significant increase in tomato yield. The D2N3 treatment significantly reduced the GHGI by 1.57 kg CO_2-eq. ha^{-1} than the D2N1 treatment. The decline in GHGI is primarily driven by increased greenhouse gas emissions rather than increased depletion of soil carbon pools.

Table 3. Characteristics of seasonal greenhouse gas fluxes, global warming potential (GWP) and greenhouse gas intensity (GHGI) in tomato crop under irrigation and fertilizer coupling strategies.

Treatments	GHG Flux (kg ha^{-1})			GWP (kg CO_2-eq ha^{-1})				GHGI
	CH_4	N_2O	NECB	CH_4	N_2O	NECB	Net	(kg CO_2-eq kg^{-1})
D1N1	1.18 c	3.91 c	−2429 i	21.7 g	1149 f	−8816 g	10263 g	2.07 b
D1N2	2.08 b	4.61 b	−3322 h	45.7 e	1340 d	−12081 f	13780 f	1.67 c
D1N3	2.18 b	5.21 a	−4133 c	51.1 d	1549 b	−15055 c	17047 b	1.07 c
D2N1	1.38 c	4.21 b	−3495 g	31.0 f	1221 e	−12723 f	14986 e	2.41 b
D2N2	2.28 b	4.91 b	−3548 f	61.4 c	1400 c	−13112 e	14666 e	2.27 b
D2N3	2.48 b	5.51 a	−4656 b	64.3 c	1612 a	−16983 b	19022 a	1.57 c
D3N1	1.58 c	4.61 b	−3698 e	31.8 f	1340 d	−13472 e	15029 d	3.37 a
D3N2	2.98 b	5.03 a	−4032 d	72.7 b	1519 b	−14683 d	16469 c	2.47 b
D3N3	3.38 a	5.91 a	−4820 a	83.9 a	1686 a	−17573 a	19272 a	1.97 c

D1N1: drip-irrigation (100 mm) with nitrogen level (150 kg ha^{-1}); D1N2: drip-irrigation (100 mm) with nitrogen level (300 kg ha^{-1}); D1N3: drip-irrigation (100 mm) with nitrogen level (450 kg ha^{-1}); D2N1: drip-irrigation (200 mm) with nitrogen level (150 kg ha^{-1}); D2N2: drip-irrigation (200 mm) with nitrogen level (300 kg ha^{-1}); D2N3: drip-irrigation (200 mm) with nitrogen level (450 kg ha^{-1}); D3N1: drip-irrigation (300 mm) with nitrogen level (150 kg ha^{-1}); D3N2: drip-irrigation (300 mm) with nitrogen level (300 kg ha^{-1}); D3N3: drip-irrigation (300 mm) with nitrogen level (450 kg ha^{-1}). Values are given as means, and different lowercase letters indicate significant differences at $p \leq 0.05$ levels in the same line (Duncan's multiple range test).

3.6. Tomato Yield and Fruit Quality

The combined climate-smart drip irrigation and fertilization strategy significantly affected tomato fruit quality, including SSC, VC, TSS, and lycopene values. These parameters were also considerably affected by nitrogen levels (Table 4). SSC, VC, TSS, and lycopene values in D3N2 and D3N3 treatments were significantly higher than all other treatments, respectively. Table 4 shows that with increasing levels of drip irrigation and fertilization, IWP and NUE values increased significantly, as did tomato yield. Meanwhile, all tomato fruit quality parameters improved considerably with improving levels of drip irrigation and fertilization. The tomato yield under the D3N3, D3N2, D3N1, D2N3, D2N2, D2N1, D1N3, D1N2, and D1N1 treatments was 7.7 t ha^{-1}, 5.8 t ha^{-1}, 2.7 t ha^{-1}, 5.1 t ha^{-1}, 3.5 t ha^{-1}, 0.3 t ha^{-1}, 3.0 t ha^{-1}, and 1.3 t ha^{-1} greater, than that of D1N1 treatment, respectively.

Table 4. Effects of various irrigation and fertilizer coupling strategies on tomato yield, irrigation water productivity (IWP), and quality of tomato plants in greenhouse.

Treatments	Tomato Yield (t ha^{-1})	IWP (kg mm^{-1})	TSS (%)	VC (mg 100 g^{-1})	SSC (%)	Lycopene (ug g^{-1})	NUE kg kg^{-1})
D1N1	59.8 h	--	4.9 d	3.1 c	2.9 c	35.1 f	--
D1N2	62.1 f	--	5.1 c	3.3 c	3.1 c	39.2 e	10.8 d
D1N3	63.8 e	--	5.9 c	3.8 c	3.6 c	44.6 d	13.6 c
D2N1	61.1 g	1.9 d	5.1 c	3.6 c	3.8 c	41.2 d	--
D2N2	65.3 d	13.8 b	5.8 c	4.1 b	4.3 b	47.5 c	26.7 a
D2N3	70.9 c	13.1 b	6.7 b	4.6 b	4.8 b	52.6 b	21.8 b
D3N1	63.5 e	8.7 c	5.6 c	4.0 b	4.1 b	46.7 c	--
D3N2	76.6 b	14.5 a	6.2 b	4.4 b	4.6 b	54.1 b	25.8 a
D3N3	82.5 a	15.2 a	7.3 a	5.1 a	5.2 a	59.8 a	22.7 b

D1N1: drip-irrigation (100 mm) with nitrogen level (150 kg ha^{-1}); D1N2: drip-irrigation (100 mm) with nitrogen level (300 kg ha^{-1}); D1N3: drip-irrigation (100 mm) with nitrogen level (450 kg ha^{-1}); D2N1: drip-irrigation (200 mm) with nitrogen level (150 kg ha^{-1}); D2N2: drip-irrigation (200 mm) with nitrogen level (300 kg ha^{-1}); D2N3: drip-irrigation (200 mm) with nitrogen level (450 kg ha^{-1}); D3N1: drip-irrigation (300 mm) with nitrogen level (150 kg ha^{-1}); D3N2: drip-irrigation (300 mm) with nitrogen level (300 kg ha^{-1}); D3N3: drip-irrigation (300 mm) with nitrogen level (450 kg ha^{-1}). Values are given as means, and different lowercase letters indicate significant differences at $p \leq 0.05$ levels in the same line (Duncan's multiple range test).

4. Discussion

An optimum soil environment can efficiently promote the growth process of greenhouse tomatoes, thereby improving tomato production [53,54]. In this study, SWC was frequently measured at soil depths of 1–100 cm at different growth stages of tomatoes in a greenhouse study. In the greenhouse study, SWC in the D3N3 and D2N3 treatments was significantly higher than all other treatments at different growth stages. Deficit irrigation with various nitrogen application methods is widely used as a useful agricultural practice to improve soil moisture conditions and increase tomato yields [55]. However, covering with various nitrogen fertilizer applications considerably increases greenhouse gas emissions [56] and depletes soil carbon pools [57,58]. The effects of plastic film mulching and various nitrogen fertilizer applications increasing crop yields are still under debate. Soil moisture content significantly improved from the early growth stage to the flowering stage and significantly decreased from the flowering stage to the maturity stage. Tomato ET was positively correlated with the management strategy of drip irrigation combined with nitrogen fertilizer. Jiang et al. [59] showed that mulching can effectively increase the amount of precipitation in the soil, which reduces soil evaporation and increases leaf transpiration rate [60]. Under the D3N3 and D3N2 with different combination management of drip irrigation and nitrogen fertilizer had higher ET rates due to stronger transpiration. Compared with the D3N3 treatment, the D3N2 considerably decreased ET by 0.6%, and the D2N3 treatment significantly reduced ET by 3.9%. RF technology can increase soil moisture content by retaining a small amount of rainwater, decreasing soil evaporation and infiltration rainfall [61].

This may be due to growth inhibiting ammonia-oxidizing bacteria and related enzymes, effectively slowing down the oxidation of NH_4^+-N and NO_3^--N contents [62,63]. By controlling the rapid transformation of soil nitrogen and maintaining high soil NH_4^+-N, it can effectively reduce the accumulation and leaching loss of NO_3^--N, and reduce N_2O emissions [64,65]. Nearly all nitrogen, including NH_4^+-N and NO_3^--N contents, is absorbed by the roots and transported to the shoots through the xylem. Different climate-smart drip irrigation and fertilizer coupling strategies can significantly change the NH_4^+-N and NO_3^--N contents in the shoots [66]. In our study, the $NH4^+$ content under drip irrigation (300 mm) and nitrogen level (450 kg N ha^{-1}) was considerably greater at the V7, flowering, and ripening stages. The NO_3^--N transport rate in the D3N3 was considerably greater. High NO_3^--N content can significantly encourage fruit growth and delay the ripening time of tomatoes [54,67], which is consistent with the fact that the rate of tomatoes under N1 and N2 was higher than that under N3.

Increased soil temperature under low radiation can stimulate microbial activity [68], thus explaining the increase in CO_2 flux. No matter which climate-smart drip irrigation and fertilizer coupling strategy is adopted, CO_2 is lowest in the early growth period, significantly enhanced in the fruit formation period, and reaches the highest level in the fruit formation period, which is consistent with the research results of Liu et al. [64]. Manna et al. [62] also reported that irrigation is more active in destroying early N_2O emissions in tomatoes. Another study reported that adding nitrogen can also reduce soil N_2O emissions by 39% [60,69]. Under the D3N3 and D3N2 had considerable changes in CO_2. Meanwhile, the emissions in the D3N3 were considerably maximum. Different drip irrigation and fertilizer combination strategies in each growth stage have a significant effect on N_2O content, with two N_2O peaks appearing during the vegetative growth and fruit formation stages. N_2O is generally produced by nitrification and denitrification in soil microbes [70,71]. Jiang et al. [59] confirmed that soil cover materials have a significant effect on N_2O emissions in a long-term fertility experiment. Additionally, larger tomato plants may increase nitrogen uptake, potentially reducing soil N_2O emissions [52,72].

GHGI may be an indicator of the GWP in the agronomic sector and crop production [56]. The rise in GHGI is mostly due to a significant decrease in soil carbon stocks, not an increase in GHGI. Current studies have shown that GHGI can be effectively reduced by increasing crop yields [73]. Greenhouse studies showed that the D3N3 had higher annual

NPP values than all the remaining treatments. In the tomato greenhouse experiment, a combined climate-smart drip irrigation and fertilizer strategy had a considerable effect on NEP between NPP and total CO_2 fluxes. The D3N2 and D3N3 treatments had a significant increase in annual NEP compared to all other treatments. The average CWPeco values of the nine treatments ranged from 8.3 to 4.9 kg CO_2 ha^{-1} mm^{-1}. Current studies have shown that GHGI can be effectively reduced by increasing tomato yields [56,62]. Compared with the D1N1 treatment, the net GWP was considerably increased by 33.8% in the D3N3 treatment, which was mainly due to a significantly increased consumption of soil carbon pools. When a large amount of carbon is removed, soil carbon stocks are reduced [74]. Mulching significantly increased the GWP which is calculated by adding CH_4 and NO_2 fluxes and NECB to CO_2 equivalents [67,69]. However the GWP values of the N3 under different drip irrigation conditions. The D3N3 treatment significantly improved tomato yields, which reduced GHGI by 1.979 kg CO_2 eq. ha^{-1}. The decline in GHGI is driven primarily by increased greenhouse gas emissions rather than a significant decline in soil carbon stocks. GHGI can be used as an index to assess the influence of the farming sector on GWP and crop yields [69,75].

Therefore, different irrigation and nitrogen levels can efficiently increase tomato fruit quality. Wu et al. [76] reported the impact of nitrogen application on tomato quality. A climate-smart drip irrigation and fertilizer combination strategy had a significant effect on tomato fruit quality, including SSC, VC, TSS, and lycopene values. While, over-irrigation can reduce the nutritional value of the fruit through dilution, thereby negatively affecting related quality indicators [77,78]. The results showed that the values of SSC, VC, TSS, and lycopene under D3N2 and D3N3 treatments were significantly higher than all other treatments. However, excessive fertilization can cause soil detachment, which can negatively affect tomato growth and fruit quality [79,80]. The tomato yield was significantly positively correlated with the tomato quality, soil chemical properties, and resource use efficiencies (Table 5). In the present study, Table 4 shows that as drip irrigation and fertilization levels increased, IWP and NUE values increased significantly and tomato yield also increased. Tomato yield in the D3N3 treatment was 7.7 t/ha higher than that in the D1N1 treatment. Therefore, the results provide a scientific reference for future studies on the impacts of climate-smart drip irrigation with fertilizer coupling strategies on the quality and yield of greenhouse tomatoes.

Table 5. Correlation coefficients of tomato yield, quality and resourece use efficienies.

	CWPeco	ET	GHGI	Lycopene	N_2O	NEP	NH_4^+	NO_3^-	NPP	SSC	TSS	TY	VC	CO_2
ET	0.3762													
GHGI	−0.7806 *	0.2500												
Lycopene	0.5083	0.8885 *	0.0509											
N_2O	0.6885 *	0.7995 *	−0.2330	0.9389 **										
NEP	0.9575 **	0.5132	−0.6301 *	0.6720 *	0.8069 *									
NH_4^+	0.7715 *	0.7106 *	−0.3342	0.9077 **	0.9522 **	0.8909 **								
NO_3^-	0.5839	0.9124 **	−0.0200	0.9655 **	0.9407 **	0.7075 *	0.8894 *							
NPP	0.9641 *	0.4509	−0.6844 *	0.6462 *	0.7984 *	0.9890 **	0.8804 *	0.6918 *						
SSC	0.3623	0.7977 *	0.1469	0.9683 **	0.8739 *	0.5419	0.8427 *	0.9123 **	0.5356					
TSS	0.6856 *	0.7879 *	−0.1851	0.9528 **	0.9637 **	0.8263 *	0.9601 **	0.9457 **	0.8119 *	0.9084 **				
TY	0.6234 *	0.9006 **	−0.0402	0.9726 **	0.9336 **	0.7737 *	0.9189 **	0.9549 **	0.7319 *	0.8932 *	0.9586 **			
VC	0.4972	0.8363 *	0.0343	0.9891 **	0.9358 **	0.6703 *	0.9087 **	0.9544 **	0.6547 *	0.9822 **	0.9674 **	0.9503 **		
CO_2	0.6904 *	0.7142 *	−0.2764	0.9254 **	0.9850 **	0.8167 *	0.9672 **	0.9080 **	0.8229 *	0.8878 **	0.9669 **	0.9073 **	0.9384 **	
SWC	0.5890	0.7041 *	−0.1708	0.9358 **	0.9343 **	0.7116 *	0.9377 **	0.9075 **	0.7304 *	0.9411 **	0.9339 **	0.8745 *	0.9496 **	0.9630 **

* Significant at the 0.05 probability level (n = 12). ** Significant at the 0.01 probability level (n = 12).

5. Conclusions

This study investigates the impacts of various drip irrigation and nutrient management strategies on greenhouse tomato quality and yield, including total soluble sugars, vitamin C content, soluble sugars, lycopene content, and nitrogen use efficiency (NUE), to comprehensively evaluate tomato fruit quality maintenance after storage under various

drip irrigation and fertilizer treatments. The results indicated that D3N3 treatment significantly reduced (38.6%) greenhouse gas intensity (GHGI) and improved tomato yield, quality, and soil moisture status. D2 and D3 drip irrigation with nitrogen addition of 220 kg ha^{-1} improved the soil environment and significantly increased soil moisture content, CO_2 emissions, N_2O emissions, NO_3^--N, and NH_4^+-N contents at the fruit formation period. The improvement effect of D3N3 treatment on net primary productivity (NPP), net ecosystem productivity (NEP), evapotranspiration (ET), and ecosystem crop water productivity (CWPeco) was higher than other treatments. D3N3 treatment increased net global warming potential (GWP) (28.2%) but decreased GHGI due to an increase in tomato yield (18.4%). D3N3 treatment resulted in higher irrigation water productivity (IWP) (42.8%), TSS (32.9%), vitamin C content (VC) (39.2%), SSC (44.2%), lycopene content (41.3%), and nitrogen use efficiency (NUE) (52.4%), compared with all other treatments had a positive impact on the environment. Therefore, in greenhouse experiments, the D3N3 may be an effective water-saving and fertilizer management approach, which can improve water use efficiency (WUE), tomato yield, and quality while reducing the effect of global warming.

Author Contributions: Conceptualization, Z.T. and X.M.; methodology, Y.Y.; software, T.W.; validation, T.H., S.L. and L.Y.; formal analysis, X.M.; investigation, Y.Y.; resources, L.Y.; data curation, T.W.; writing—original draft preparation, Y.Y.; writing—review and editing, X.M.; visualization, Y.C.; supervision, Z.T.; project administration, Z.T.; funding acquisition, Y.Y. All authors have read and agreed to the published version of the manuscript.

Funding: This research was financially supported by the XPCC Financial Science and Technology Plan Project (2023AB071); the Tianshan Talent Training Program (2023TSYCCY0002); the Key core agricultural technology research and development projects of the XPCC (NYHXGG2023AA311), the First Division Aral City Financial Science and Technology Plan Project (2024NY04).

Data Availability Statement: The data that support the findings of this study are available from the corresponding author upon reasonable request.

Conflicts of Interest: Zhanming Tan was employed by Aksu Naida Agricultural Technology Co., Ltd. The authors declare no conflicts of interest.

References

1. Jamir, A.; Khawlhring, C. Effects of Different Post-harvest Treatments on Physico-Chemical Attributes and Shelf Life of Tomato Fruits. *Sci. Technol. J.* **2017**, *5*, 63–66. [CrossRef]
2. Li, J.; Pan, T.; Wang, L.; Du, Q.; Chang, Y.; Zhang, D.; Liu, Y. Effects of water-fertilizer coupling on tomato photosynthesis, yield and water use efficiency. *Trans. Chin. Soc. Agric. Eng.* **2014**, *30*, 82–90.
3. Li, Y.J. Effect of drip irrigation criteria on yield and quality of muskmelon grown in greenhouse conditions. *Agric. Water Manag.* **2012**, *109*, 30–35. [CrossRef]
4. Yao, S.X.; Cao, Q.; Xie, J.; Deng, L.L.; Zeng, K.F. Alteration of sugar and organic acid metabolism in postharvest granulation of Ponkan fruit revealed by transcriptome profiling. *Postharvest Biol. Technol.* **2018**, *139*, 2–11. [CrossRef]
5. Srek, P.; Hejcman, M.; Kunzova, E. Multivariate analysis of relationship between potato (*Solanum tuberosum* L.) yield, amount of applied elements, their concentrations in tubers and uptake in a long-term fertilizer experiment. *Field Crop. Res.* **2010**, *118*, 183–193. [CrossRef]
6. Zhou, H. Study on Differences Expression of *Triticum aestivum* Protein and mRNA in Different Concentration of Nitrogen In Vitro Cultivatio. Master's Thesis, Shihezi University, Shihezi, China, 2006. (In Chinese with English Abstract).
7. Li, W. Impact of Irigation Management on Greenhouse Soil Microbial Characteristics. Master's Thesis, Shenyang Agricultural University, Shenyang, China, 2017. (In Chinese with English Abstract).
8. Nurmanov, Y.T.; Chernenok, V.G.; Kuzdanova, R.S. Potato in response to nitrogen nutrition regime and nitrogen fertilization. *Field Crop. Res.* **2019**, *231*, 115–121. [CrossRef]
9. Garg, N.; Choudhary, O.P.; Thaman, S.; Sharma, V.; Singh, H.; Vashistha, M.; Sekhon, K.S.; Sharda, R.; Dhaliwa, M.S. Effects of irrigation water quality and NPKfertigation levels on plant growth, yield and tuber size of potatoes in a sandy loam alluvial soil of semi-arid region of Indian Punjab. *Agric. Water Manag.* **2022**, *266*, 107604. [CrossRef]
10. Ierna, A.; Mauromicale, G. How irrigation water saving strategy can affect tuber growth and nutritional composition of potato. *Sci. Hortic.* **2022**, *299*, 111034. [CrossRef]
11. Guo, S.; Qi, Y.; Dong, Y.; Peng, Q.; Liu, X.; Sun, L.; Jia, J.; He, Y.; Cao, S.; Yan, Z. Response of production and emission of CO_2 and N_2O of agricultural soil to drip irrigation. *China Envi. Sci.* **2014**, *34*, 2757–2763. [CrossRef]

12. Xing, Y.; Zhang, F.; Wu, L.; Fan, J.; Zhang, Y.; Li, J. Determination of optimal amount of irigation and ferilizer under drip fertigated system based on tomato yield, quality, water and fertilizer use efficiency. *Trans. Chin. Soc. Agric. Eng.* **2015**, *31*, 110–121. [CrossRef]
13. Er, C.; Lin, T.; Xia, W.; Zhang, H.; Xu, G.; Tang, Q. Coupling effects of irrigation and nitrogen levels on yield, water distribution and nitrate nitrogen residue of machine-harvested cotton. *Acta Agron. Sin.* **2022**, *48*, 497–510. [CrossRef]
14. Tao, R.; Wakelin, S.A.; Liang, Y.; Chu, G. Organic fertilization enhances cotton productivity, nitrogen use efficiency, and soil nitrogen fertility under drip irrigated field. *Agron. J.* **2017**, *109*, 2889–2897. [CrossRef]
15. Yao, Z.; Yan, G.; Wang, R.; Zheng, X.; Liu, C.; Butterbach-Bahl, K. Drip irrigation or reduced N-fertilizer rate can mitigate the high annual N_2O+NO fluxes from Chinese intensive greenhouse vegetable systems. *Atmos. Environ.* **2019**, *212*, 183–193. [CrossRef]
16. Lu, J.; Shao, G.; Cui, J.; Wang, X.; Keabetswe, L. Yield, fruit quality and water use efficiency of tomato for processing under regulated deficit irrigation: A metaanalysis. *Agric. Water Manag.* **2019**, *222*, 301–312. [CrossRef]
17. Liu, C.; Wang, R.; Wang, W.; Hu, X.; Cheng, Y.; Liu, F. Effect of fertilizer solution concentrations on filter clogging in drip fertigation systems. *Agric. Water Manag.* **2021**, *250*, 106829. [CrossRef]
18. Zhang, J.; Cao, Z.; Dai, H.; Zhang, Z.; Miao, M. Yield, nitrogen uptake and nitrogen leaching of sensor-based fertigation-cultured tomato in a shallow groundwater region: Effect of shallow groundwater on tomato. *Irrig. J. Agr. Sci.* **2020**, *12*, 10. [CrossRef]
19. Zhang, H.; Xiong, Y.; Huang, G.; Xu, X.; Huang, Q. Effects of water stress on processing tomatoes yield, quality and water use effciency with plastic mulched drip irrigation in sandy soil of the Hetao Irrigation District. *Agric. Water Manag.* **2017**, *179*, 205–214. [CrossRef]
20. Li, Y.; Wang, L.; Xue, X.; Guo, W.; Xu, F.; Li, Y.; Sun, W.; Chen, F. Comparison of drip fertigation and negative pressure fertigation on soil water dynamics and water use efficiency of greenhouse tomato grown in the North China Plain. *Agric. Water Manag.* **2017**, *184*, 1–8. [CrossRef]
21. Zhao, Y.; Lv, H.; Qasim, W.; Wan, L.; Wang, Y.; Lian, X.; Liu, Y.; Hu, J.; Wang, Z.; Li, G.; et al. Drip fertigation with straw incorporation significantly reduces N_2O emission and N leaching while maintaining high vegetable yields in solar greenhouse production. *Environ. Pollut.* **2021**, *273*, 116521. [CrossRef]
22. FAO. FAOSTAT-FAO's Online Statistical Database. FAO: Rome, Italy, 2022. Available online: https://www.fao.org/faostat/zh/#data/QCL (accessed on 7 October 2022).
23. Chand, J.; Hewa, G.; Hassanli, A.; Myers, B. Evaluation of deficit irrigation and water quality on production and water productivity of tomato in greenhouse. *Agriculture* **2020**, *10*, 297. [CrossRef]
24. Lv, H.; Lin, S.; Wang, Y.; Lian, X.; Zhao, Y.; Li, Y.; Du, J.; Wang, Z.; Wang, J.; ButterbachBahl, K. Drip fertigation significantly reduces nitrogen leaching in solar greenhouse vegetable production system. *Environ. Pollut.* **2019**, *245*, 694–701. [CrossRef] [PubMed]
25. Huang, Y.; Yang, Y.-R.; Yu, J.-X.; Huang, J.-X.; Kang, Y.-F.; Du, Y.-R.; Tian, G.-Y. Interaction of the Coupled Effects of Irrigation Mode and Nitrogen Fertilizer Format on Tomato Production. *Water* **2023**, *15*, 1546. [CrossRef]
26. Al-Ghobari, H.M.; Dewidar, A.Z. Integrating deficit irrigation into surface and subsurface drip irrigation as a strategy to save water in arid regions. *Agric. Water Manag.* **2018**, *209*, 55–61. [CrossRef]
27. Li, Y.K.; Xue, X.Z.; Xu, F.; Guo, W.Z.; Duan, M.J.; Lin, S.; Li, Y.L.; Wang, Z. Negative-pressure irrigation improves water and fertilizer use efficiencies and fruit yield of greenhouse tomato on the North China Plain. *Irrig. Drain.* **2021**, *70*, 1027–1038. [CrossRef]
28. Chen, X.Z.; Thorp, K.R.; van Oel, P.R.; Xu, Z.C.; Zhou, B.; Li, Y.K. Environmental impact assessment of water-saving irrigation systems across 60 irrigation construction projects in northern China. *J. Clean. Prod.* **2020**, *245*, 118883. [CrossRef]
29. Pendergast, L.; Bhattarai, S.P.; Midmore, D.J. Evaluation of aerated subsurface drip irrigation on yield, dry weight partitioning and water use efficiency of a broadacre chickpea (*Cicer arietinum*, L.) in a vertosol. *Agric. Water Manag.* **2019**, *217*, 38–46. [CrossRef]
30. Du, Y.D.; Gu, X.B.; Wang, J.W.; Niu, W.Q. Yield and gas exchange of greenhouse tomato at different nitrogen levels under aerated irrigation. *Sci. Total Environ.* **2019**, *668*, 1156–1164. [CrossRef]
31. Zhu, Y.; Cai, H.; Song, L.; Chen, H. Impacts of oxygation on plant growth, yield and fruit quality of tomato. *Trans. Chin. Soc. Agric. Mach.* **2017**, *48*, 199–211.
32. Chang, T.; Zhang, Y.; Zhang, Z.; Shao, X.; Wang, W.; Zhang, J.; Yang, X.; Xu, H. Effects of irrigation regimes on soil NO_3-N, electrical conductivity and crop yield in plastic greenhouse. *Int. J. Agric. Biol. Eng.* **2019**, *12*, 109–115. [CrossRef]
33. Wang, L.; Zhou, C. Determination of calculated method for necessary ventilation rate and its determination analysis of parameter value. *Trans. Chin. Soc. Agric. Eng.* **2017**, *33*, 190–198.
34. Mattar, M.A.; Zin El-Abedin, T.K.; Alazba, A.A.; Al-Ghobari, H.M. Soil water status and growth of tomato with partial root-zone drying and deficit drip irrigation techniques. *Irrig. Sci.* **2020**, *38*, 163–176. [CrossRef]
35. Hvistendahl, M. China's push to add by subtracting fertilizer. *Science* **2010**, *327*, 801. [CrossRef] [PubMed]
36. Min, J.; Zhang, H.L.; Shi, W.M. Optimizing nitrogen input to reduce nitrate leaching loss in greenhouse vegetable production. *Agric. Water Manag.* **2012**, *111*, 53–59. [CrossRef]
37. Fan, Z.B.; Lin, S.; Zhang, X.M.; Jiang, Z.M.; Yang, K.C.; Jian, D.D.; Chen, Y.Z.; Li, J.L.; Chen, Q.; Wang, J.G. Conventional flooding irrigation causes an overuse of nitrogen fertilizer and low nitrogen use efficiency in intensively used solar greenhouse vegetable production. *Agric. Water Manag.* **2014**, *144*, 11–19. [CrossRef]
38. Mancinelli, R.; Marinari, S.; Brunetti, P.; Radicetti, E.; Campiglia, E. Organic mulching, irrigation and fertilization affect soil CO2 emission and C storage in tomato crop in the Mediterranean environment. *Soil Tillage Res.* **2015**, *152*, 39–51. [CrossRef]

39. Vega-Mas, I.; Marino, D.; Sánchez-Zabala, J.; González-Murua, C.; Estavillo, J.M.; González-Moro, M.B. CO_2 enrichment modulates ammonium nutrition in tomato adjusting carbon and nitrogen metabolism to stomatal conductance. *Plant Sci.* **2015**, *241*, 32–44. [CrossRef]
40. Rolston, D.E. Gas flux. In *Methods of Soil Analysis, Part 1, Physical and Mineralogical Methods*, 2nd ed.; Agronomy Monographs Klute, A., Ed.; American Society of Agronomy: Madison, WI, USA, 1986; Volume 9, pp. 1103–1119.
41. Singh, S.; Singh, J.S.; Kashyap, A.K. Methane flux from irrigated rice fields in relation to crop growth and N-fertilization. *Soil Biol. Biochem.* **1999**, *31*, 1219–1228. [CrossRef]
42. IPCC. *Climate Change 2007. Mitigation Contribution of Working Group III to the Fourth Assessment Report of the Intergovernmental Panel on Climate Change*; Metz, B., Davidson, O.R., Bosch, P.R., Dave, R., Meyer, L.A., Eds.; Cambridge University Press: Cambridge, UK; New York, NY, USA.
43. Li, C.; Salas, W.; DeAngelo, B.; Rose, S. Assessing alternatives for mitigating net greenhouse gas emissions and increasing yields from rice production in China over the next twenty years. *J. Environ. Qual.* **2006**, *35*, 1554. [CrossRef]
44. Ma, Y.C.; Kong, X.W.; Yang, B.; Zhang, X.L.; Yan, X.Y.; Yang, J.C.; Xiong, Z.Q. Net global warming potential and greenhouse gas intensity of annual rice-wheat rotations with integrated soil-crop system management. *Agric. Ecosyst. Environ.* **2013**, *164*, 209–219. [CrossRef]
45. Hwang, H.Y.; Kim, G.W.; Kim, S.Y.; Mozammel Haque, M.; Khan, M.I.; Kim, P.J. Effect of cover cropping on the net global warming potential of rice paddy soil. *Geoderma* **2017**, *292*, 49–58. [CrossRef]
46. Sainju, U.M.; Stevens, W.B.; Caesar-Tonthat, T.; Liebig, M.A. Soil greenhouse gas emissions affected by irrigation, tillage, crop rotation, and nitrogen fertilization. *J. Environ. Qual.* **2012**, *41*, 1774–1786. [CrossRef] [PubMed]
47. Zhang, K.; Zheng, H.; Chen, F.; Li, R.; Yang, M.; Ouyang, Z.; Lan, J.; Xiang, X. Impact of nitrogen fertilization on soil-Atmosphere greenhouse gas exchanges in eucalypt plantations with different soil characteristics in southern China. *PLoS ONE* **2017**, *12*, e0172142. [CrossRef] [PubMed]
48. Raut, N.; Sitaula, B.K.; Bakken, L.R.; Bajracharya, R.M.; Dörsch, P. Higher N_2O emission by intensified crop production in South Asia. *Glob. Ecol. Conserv.* **2017**, *4*, 176–184. [CrossRef]
49. Oertel, C.; Matschullat, J.; Zurba, K.; Zimmermann, F.; Erasmi, S. Greenhouse gas emissions from soils—A review. *Geochemistry* **2016**, *76*, 327–352. [CrossRef]
50. Gong, W.; Yan, X.Y.; Wang, J.Y.; Hu, T.X.; Gong, Y.B. Long-term manuring and fertilization effects on soil organic carbon pools under a wheat–maize cropping system in North China Plain. *Plant Soil* **2009**, *314*, 67–76. [CrossRef]
51. Guo, Y.J.; Di, H.J.; Cameron, K.C.; Li, B.; Podolyan, A.; Moir, J.L.; Monaghan, R.M.; Smith, L.C.; O'Callaghan, M.; Bowatte, S.; et al. Effect of 7-year application of anitrification inhibitor, dicyandiamide (DCD), on soil microbial biomass, protease and deaminase activities, and the abundance of bacteria and archaea in pasture soils. *Soils Sediments* **2013**, *13*, 753–759. [CrossRef]
52. Hasan, Y.; Taner, B. Color and Lycopene Content of Tomato Puree Affected by Electroplasmolysis. *Int. J. Food Prop.* **2007**, *10*, 489–495.
53. Murphy, J.; Riley, J.P. A modified single solution method for the determination of phosphate in natural waters. *Anal. Chim. Acta* **1962**, *27*, 31–36. [CrossRef]
54. Ahmed, A.K.A.; Shi, X.; Hua, L.; Manzueta, L.; Qing, W.; Marhaba, T.; Zhang, W. Influences of air, oxygen, nitrogen, and carbon dioxide nanobubbles on seed germination and plant growth. *J. Agric. Food Chem.* **2018**, *66*, 5117–5124. [CrossRef]
55. Zhang, Z.; Yang, R.; Sun, J.; Li, Y.; Geng, Y.; Pan, Y.; Zhang, Z. Root-zone aeration improves fruit yield and quality of tomato by enhancement of leaf photosynthetic performance. *Agric. Water Manag.* **2024**, *291*, 108639. [CrossRef]
56. Li, J.; Yu, X.; Wang, X.; Zhang, J.; Jiao, X.; Huang, Q. Optimization of fertigation scheduling for drip-irrigated watermelon based on its yield, quality and fertilizer and water use efficiency. *Trans. Chin. Soc. Agric. Eng.* **2020**, *36*, 75–83. [CrossRef]
57. Cuello, J.P.; Hwang, H.Y.; Gutierrez, J.; Kim, S.Y.; Kim, P.J. Impact of plastic film mulching on increasing greenhouse gas emissions in temperate upland soil during maize cultivation. *Appl. Soil Ecol.* **2015**, *91*, 48–57. [CrossRef]
58. Feng, Y.; Cui, N.B.; Gong, D.Z.; Wang, H.B.; Hao, W.P.; Mei, X.R. Estimating rain-fed spring maize evapotranspiration using modified dual crop coefficient approach based on leaf area index. *Trans. Chin. Soc. Agric. Eng.* **2016**, *32*, 90–98, (In Chinese with English Abstract).
59. Liu, H.; Li, H.; Ning, H.; Zhang, X.; Li, S.; Pang, J.; Wang, G.; Sun, J. Optimizing irrigation frequency and amount to balance yield, fruit quality and water use efficiency of greenhouse tomato. *Agric. Water Manag.* **2019**, *226*, 105787. [CrossRef]
60. Jiang, Y.; Huang, X.M.; Zhang, X.; Zhang, X.Y.; Zhang, Y.; Zheng, C.Y.; Deng, A.X.; Zhang, J.; Wu, L.H.; Hu, S.J.; et al. Optimizing Rice Plant Photosynthate Allocation Reduces N_2O Emissions from Paddy Fields. *Sci. Rep.* **2016**, *6*, 29333. [CrossRef]
61. Zhiguo, L.; Kun, L.; Yuqing, W.; Bo, Z.; Zhibo, Y. Multi-scale engineering properties of tomato fruits related to harvesting, simulation and textural evaluation. *LWT-Food Sci. Technol.* **2015**, *61*, 444–451.
62. Mosier, A.R.; Halvorson, A.D.; Reule, C.A.; Liu, X.J. Net global warming potential and greenhouse gas intensity in irrigated cropping systems in northeastern Colorado. *J. Environ. Qual.* **2006**, *35*, 1584–1598. [CrossRef]
63. Manna, M.C.; Swarup, A.; Wanjari, R.H.; Ravankar, H.N. Long-term effect of NPK fertiliser and manure on soil fertility and a sorghum–wheat farming system. *Aust. J. Exp. Agric.* **2007**, *47*, 700–711. [CrossRef]
64. Di, H.J.; Cameron, K.C.; Shen, J.P.; He, J.Z.; Winefield, C.S. Alysimeter study of nitrate leaching from grazed grassland as affected by a nitrification inhibitor, dicyandiamide, and relationships with ammonia oxidizing bacteria and archaea. *Soil Use Manag.* **2009**, *25*, 454–461. [CrossRef]

65. Liu, C.; Zheng, X.; Zhou, Z.; Han, S.; Wang, Y.; Wang, K.; Liang, W.; Li, M.; Chen, D.; Yang, Z. Nitrous oxide and nitric oxide emissions from an irrigated cotton field in northern China. *Plant Soil* **2010**, *332*, 123–134. [CrossRef]
66. Ghimire, R.; Lamichhane, S.; Acharya, B.S.; Bista, P.; Sainju, U.M. Tillage, crop residue, and nutrient management effects on soil organic carbon in rice-based cropping systems: A review. *J. Integr. Agric.* **2017**, *16*, 1–15. [CrossRef]
67. IPCC. *Climate Change 2013: The Physical Science Basis. Contribution of Working Group I to the Fifth Assessment Report of the Intergovernmental Panel on Climate Change*; Stocker, T.F., Qin, D., Plattner, G.K., Tignor, M.M.B., Allen, S.K., Boschung, J., Nauels, A., Xia, Y., Bex, V., Midgley, P.M., Eds.; Cambridge University Press: Cambridge, UK; New York, NY, USA, 2013.
68. Wang, G.; Yueping, L.; Qian, Z.; Shiva, K.J.; Yang, G.; Xiaojun, S.; Jingsheng, S.; Aiwang, D. Mitigated CH_4 and N_2O emissions and improved irrigation water use efficiency in winter wheat field with surface drip irrigation in the North China Plain. *Agric. Water Manag.* **2016**, *163*, 403–407. [CrossRef]
69. Romero, P.; Rose, J.K.C. A relationship between tomato fruit softening, cuticle properties and water availability. *Food Chem.* **2019**, *295*, 300–310. [CrossRef]
70. Li, Q.; Li, H.; Zhang, L.; Zhang, S.; Chen, Y. Mulching improves yield and water-use efficiency of potato cropping in China: A meta-analysis. *Field Crops Res.* **2018**, *221*, 50–60. [CrossRef]
71. Distefano, M.; Arena, E.; Mauro, R.P.; Brighina, S.; Leonardi, C.; Fallico, B.; Giuffrida, F. Effects of Genotype, Storage Temperature and Time on Quality and Compositional Traits of Cherry Tomato. *Foods* **2020**, *9*, 1729. [CrossRef]
72. Fierer, N.; Schimel, J.P. A proposed mechanism for the pulse in carbon dioxide production commonly observed following the rapid rewetting of a dry soil. *Soil Sci. Soc. Am. J.* **2003**, *67*, 798–805. [CrossRef]
73. Çolak, Y.B.; Yazar, A.; Gonen, E.; Eroglu, E.Ç. Yield and quality response of surface and subsurface drip-irrigated eggplant and comparison of net returns. *Agric. Water Manag.* **2018**, *206*, 165–175. [CrossRef]
74. Abdallah, M.; Osborne, B.; Lanigan, G.; Forristal, D.; Williams, M.; Smith, P.; Jones, M.B. Conservation tillage systems: A review of its consequences for greenhouse gas emissions. *Soil Use Manag.* **2013**, *29*, 199–209. [CrossRef]
75. Badalucco, L.; Grego, S.; Dell'Orco, S.; Nannipieri, P. Effect of liming on some chemical, biochemical, and microbiological properties of acid soils under spruce (*Picea abies* L.). *Biol. Fertil. Soils* **1992**, *14*, 76–83. [CrossRef]
76. Piao, S.; Ciais, P.; Huang, Y.; Shen, Z.; Peng, S.; Li, J.; Zhou, L.; Liu, H.; Ma, Y.; Ding, Y. The impacts of climate change on water resources and agriculture in China. *Nature* **2010**, *467*, 43–51. [CrossRef]
77. Wu, Y.; Yan, S.; Fan, J.; Zhang, F.; Zheng, J.; Guo, J.; Xiang, Y. Combined application of soluble organic and chemical fertilizers in drip fertigation improves nitrogen use efficiency and enhances tomato yield and quality. *J. Sci. Food Agric.* **2020**, *100*, 5422–5433. [CrossRef] [PubMed]
78. Gong, X.; Li, X.; Qiu, R.; Bo, G.; Ping, Y.; Xin, Q.; Ge, J. Ventilation and irrigation management strategy for tomato cultivated in greenhouses. *Agric. Water Manag.* **2022**, *273*, 107908. [CrossRef]
79. Ouyang, Z.; Tian, J.; Yan, X.; Shen, H. Effects of different concentrations of dissolved oxygen on the growth, photosynthesis, yield and quality of greenhouse tomatoes and changes in soil microorganisms. *Agric. Water Manag.* **2021**, *245*, 106579. [CrossRef]
80. Wang, J.; Zhu, B.; Zhang, J.; Müller, C.; Cai, Z. Mechanisms of soil N dynamics following long-term application of organic fertilizers to subtropical rain-fed purple soil in China. *Soil Biol. Biochem.* **2015**, *91*, 222–231. [CrossRef]

MDPI AG
Grosspeteranlage 5
4052 Basel
Switzerland
Tel.: +41 61 683 77 34

Land Editorial Office
E-mail: land@mdpi.com
www.mdpi.com/journal/land

Academic Open
Access Publishing

mdpi.com

ISBN 978-3-7258-2964-4